LABORATORY STUDY AND FIELD INVESTIGATION OF SCOUR AROUND BRIDGE PIER IN BANGLADESH

By

M R Kabir[1], I M Faisa[2]l, Fahmida Khatun[1]

ABSTRACT

The parameters affecting scour around a bridge pier include flow, approach depth, shape of the pier, angle of attack and mean particle size of the bed material. However, empirical equations of Lacey, Inglis, Blench, Laursen and Shen do not explicitly include all these parameters. As a result, field application of these equations has been difficult and not satisfactory in terms of the accuracy of prediction. This paper examines the commonly used empirical equations for scour depth estimation in the light of some laboratory experiments and field data. It has been observed during the laboratory investigation that the shape of the pier and mean particle size has significant effect on the scour depth predicted by these equations. For example, the minimum scour was observed around a sharp-nose pier (most streamlined) and the maximum scour was observed around a rectangular pier. Also, scour depth increased with the decrease of mean particle size and increase of the angle of attack, particularly beyond 20 degrees. Moreover, when predictions are compared with the actual data collected from a few major sites, it is observed that no method appears to be satisfactory in correctly predicting the scour depth. Perhaps because of this uncertainty, design engineers prefer to use equations of Lacey and Laursen, which significantly over-predict the scour depth, thereby allow the engineers to remain on the safe side. It is recommended that more data on the scour depth should be collected from different parts of Bangladesh and these should be used to verify and re-calibrate the empirical equations used for scour depth estimation.

INTRODUCTION

Scour around any obstruction is the lowering of a portion of the riverbed below its natural level due to the large-scale eddy or vortex formation. Knowledge of maximum scour depth under bridge piers for different types of bed materials is essential for designing bridge foundations.

Laboratory experiments and model studies have been carried out to estimate the scour depth as a function of various flow parameters and pier geometry. However, these equations are limited in scope as the three dimensional flow conditions cannot be adequately simulated in the laboratory. Factors affecting the scour depth include the shape and size of the pier. angle of attack, flow depth, velocity, size and gradation of bed materials, slope, and fluid properties. As a result, when applied to a particular structure, the scour depths predicted by the empirical equations may significantly differ from the observed one.

[1] Dept. of Water Resources Engineering, Bangladesh University of Engineering and Technology, Dhaka-1000, Bangladesh.
[2] Dept. of Environmental Studies, North South University, 12 Kemal Ataturk Avenue, Banani, Dhaka-1000, Bangladesh

Lacey, Inglis, Blench, Laursen and Shen-et-al (Garde and Raju, 1985) have proposed empirical equations which are widely used for scour depth estimation. In this study, these equations have been tested based on both laboratory and field data. Laboratory experiments have been conducted at Bangladesh University of Engineering and Technology (BUET) and River Research Institute (RRI). Field data have been collected for two important sites - Hardinge Bridge (constructed in 1912) and East-west Inter-connector (constructed in 1982). The design criteria for the scour depth calculation practiced by Roads and Highways (R&H) department have been evaluated for Bangabandhu Bridge (Jamuna Multipurpose Bridge), Meghna Bridge, Meghna-Gumti Bridge, Kushiara Bridge, and Shambhugonj Bridge. Finally a few recommendations have been made based on the study findings.

LABORATORY INVESTIGATION

Laboratory investigations have been carried out at BUET and RRI to determine the effect of various flow parameters, pier geometry and bed materials on the scour depth. Different flows ranging from 0.00368 to 0.384 cumec have been used along with four different pier shapes (rectangular, circular, round-nose and sharp-nose). Bed materials having mean particle size ranging from 0.08mm to 0.94mm have been used. The discharge values have been determined from the physical modeling requirements and limitation of the laboratory setups. Mean diameters of the bed material have been primarily selected based on the actual size of the bed materials found in the rivers of Bangladesh. Outlines of the experimental setups are provided below.

Experimental Setup

BUET: The experiments have been conducted in a re-circulating flow visualization tank with 4.0m length, 0.6m width and 0.2m depth. The flume bed was filled up with 9cm depth of sand with zero initial slope. The scour depth has been observed for rectangular, circular, round-nose and sharp-nose piers. Three mean bed material sizes of 0.19mm, 0.4mm and 0.94 mm have been used along with four different discharges ranging from 0.00368 cumec to 0.0068 cumec.

RRI: The experimental channel had a length, width and depth of 19.15m, 3.52m and 0.25m respectively. A sand layer of 1m depth with a bed slope of 0.00028 has been used for constructing the movable bed of the channel. The mean bed material size of 0.23mm has been used and the discharge has been varied between 0.035 cumec to 0.141 cumec. Another five laboratory test runs of Paksey Bridge pile configuration have been conducted by placing two pier groups on bed material of mean size 0.08mm. The discharge, velocity and flow depth for this model were 0.384 cumec, 0.53 m/s and 0.34m respectively. The scale of the model was 1:90. All piers had a circular shape.

Experimental results

It can be shown through dimensional analysis that the depth of scour around a bridge pier is a function of a number of parameters as shown in Equation 1 below (Kabir, 1984).

$$\frac{d_t}{b} = f\left(\frac{l}{b}, \frac{Y}{b}, \frac{d_{50}}{Y}, F_p, F\right) \quad [1]$$

where, d_t is the depth of scour, b is the pier width, l is the pier length, Y is the depth of approach flow, d_{50} is the mean particle size, F_p is the particle Froude number and F is the Froude number.

In this study, the effects of Y/b, Fp and F on the scour depth have been investigated as the empirical equations considered in this study use these parameters for predicting the scour depth.

Effect of Froude number

The relative scour depth, d_t/b has been plotted against the Froude number for different l/b ratio and d_{50} in Figure 1. It is seen from the plot that the relative scour depth increases with the increase in Froude number. Since the Froude number is a linear function of approach velocity, V, it can be said that for a given approach depth, sour depth is directly proportional to the approach velocity. The positive relationship between the scour depth and the Froude number has been used in various empirical equations as suggested by Shen et. al., Chitale and Bata (Kabir, 1984). Moreover, the scour depth increases as the bed material becomes finer.

Effect of Approach Depth

The variation of d_t/b with respect to the relative approach depth, Y/b for different l/b ratio and d_{50} is shown in Figure 2. Here, the relative scour depth shown a linearly increasing relationship with the relative approach depth. The scour depth changes with the approach depth at an average rate of 1.95, which shows only minor variation for different pier shapes and bed materials. Laursen has estimated this rate as 2.0 (Garde and Raju, 1985), which is in close agreement with the rate of 1.95 found in this study.

Effect of Pier Shape

Figure 3 shows the scour pattern around piers of four different shapes. The same l/b ratio has been maintained for the rectangular, round-nose and sharp-nose piers. Among these, the sharp-nosed pier had the minimum scour and the rectangular pier had the maximum scour. The pattern of scour around the pier is similar for the rectangular and round-nose shapes. However, the location of maximum scour depth is near the upstream edge for all the piers. The effect of pier shape has been incorporated in the scour depth estimation in a simplified form through the width of the pier. However, it is generally observed that streamlining the nose of the pier can reduce the scour depth.

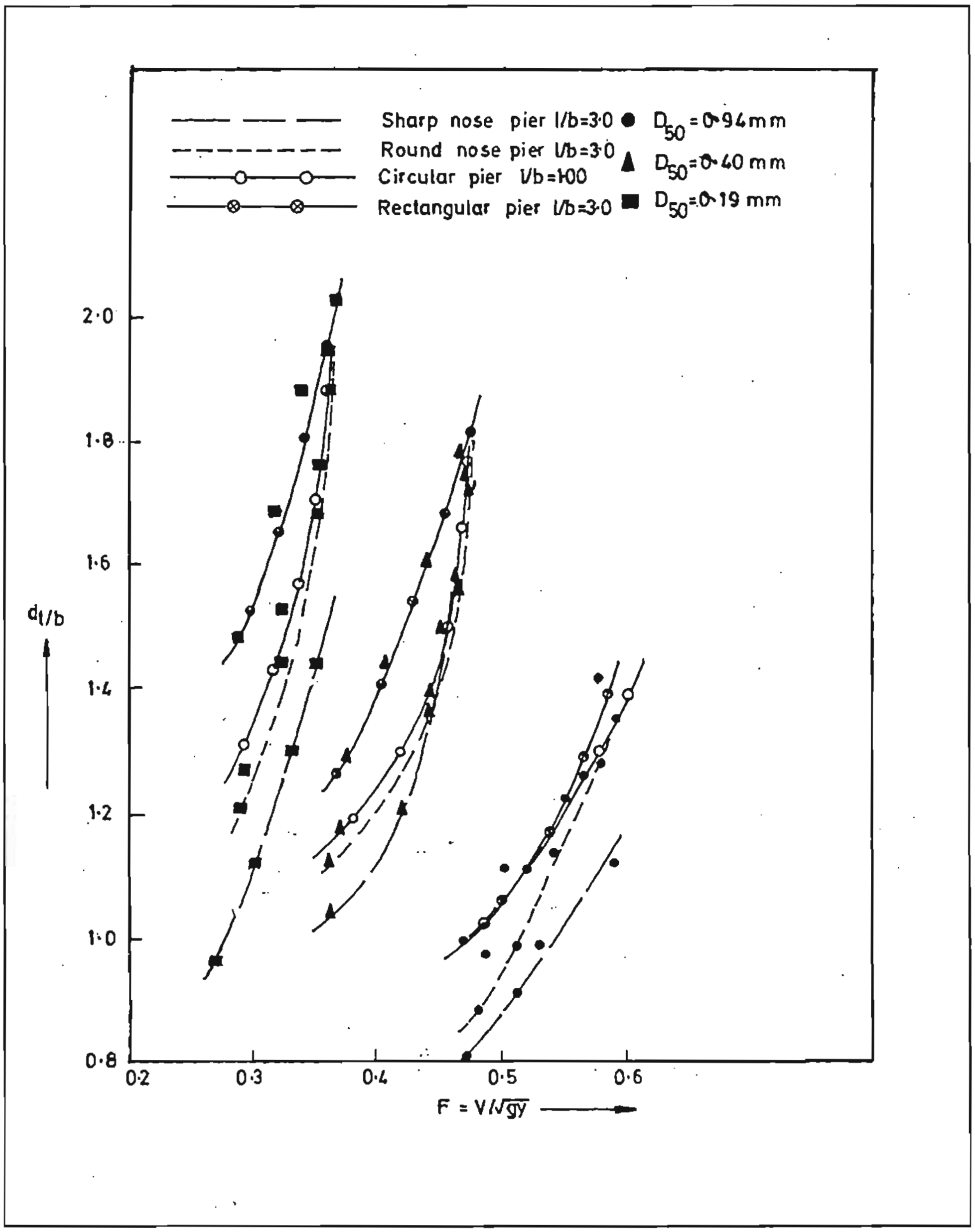

Fig. 1 Relative scour depth versus Froude number

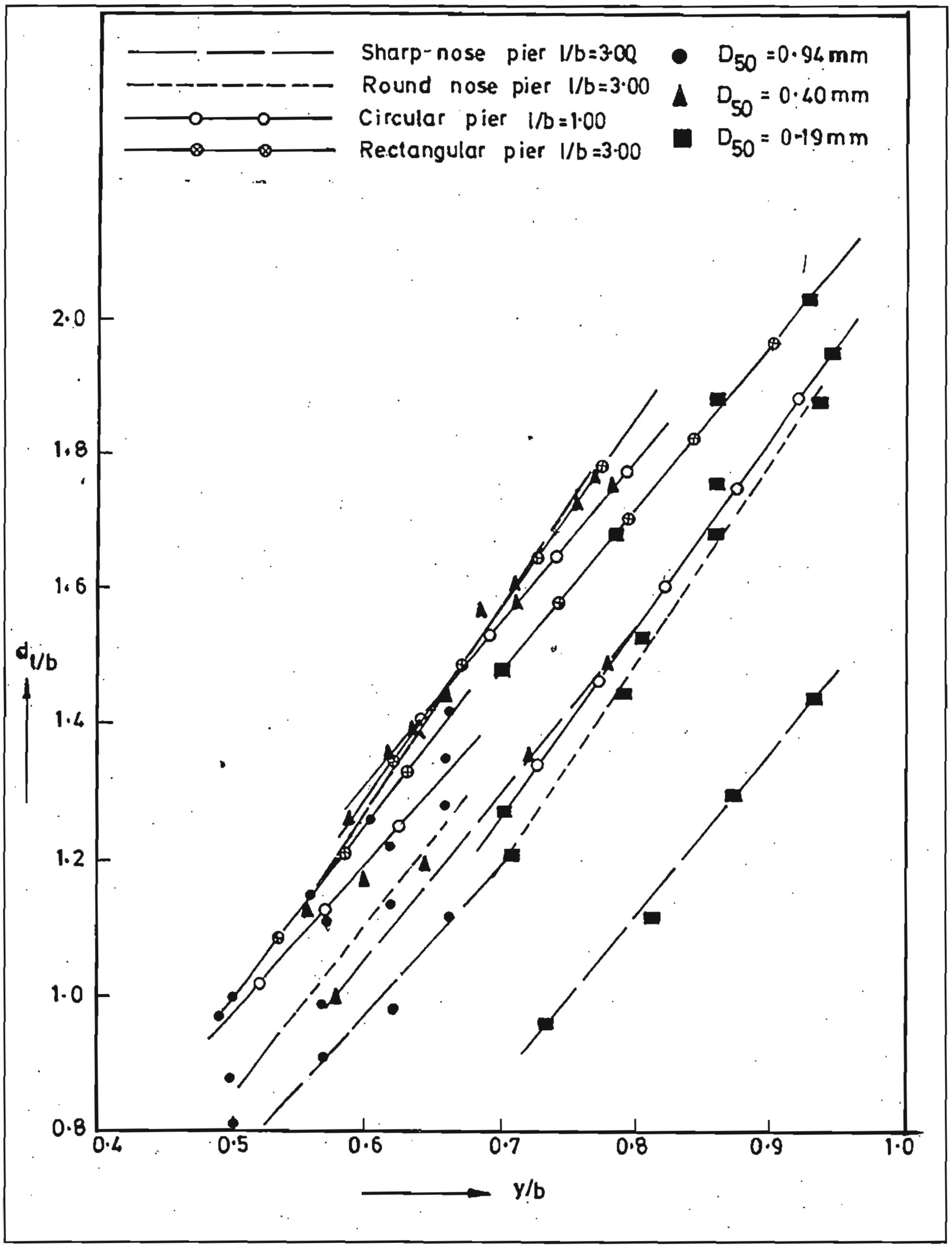

Fig. 2 Relative scour depth versus relative approach depth

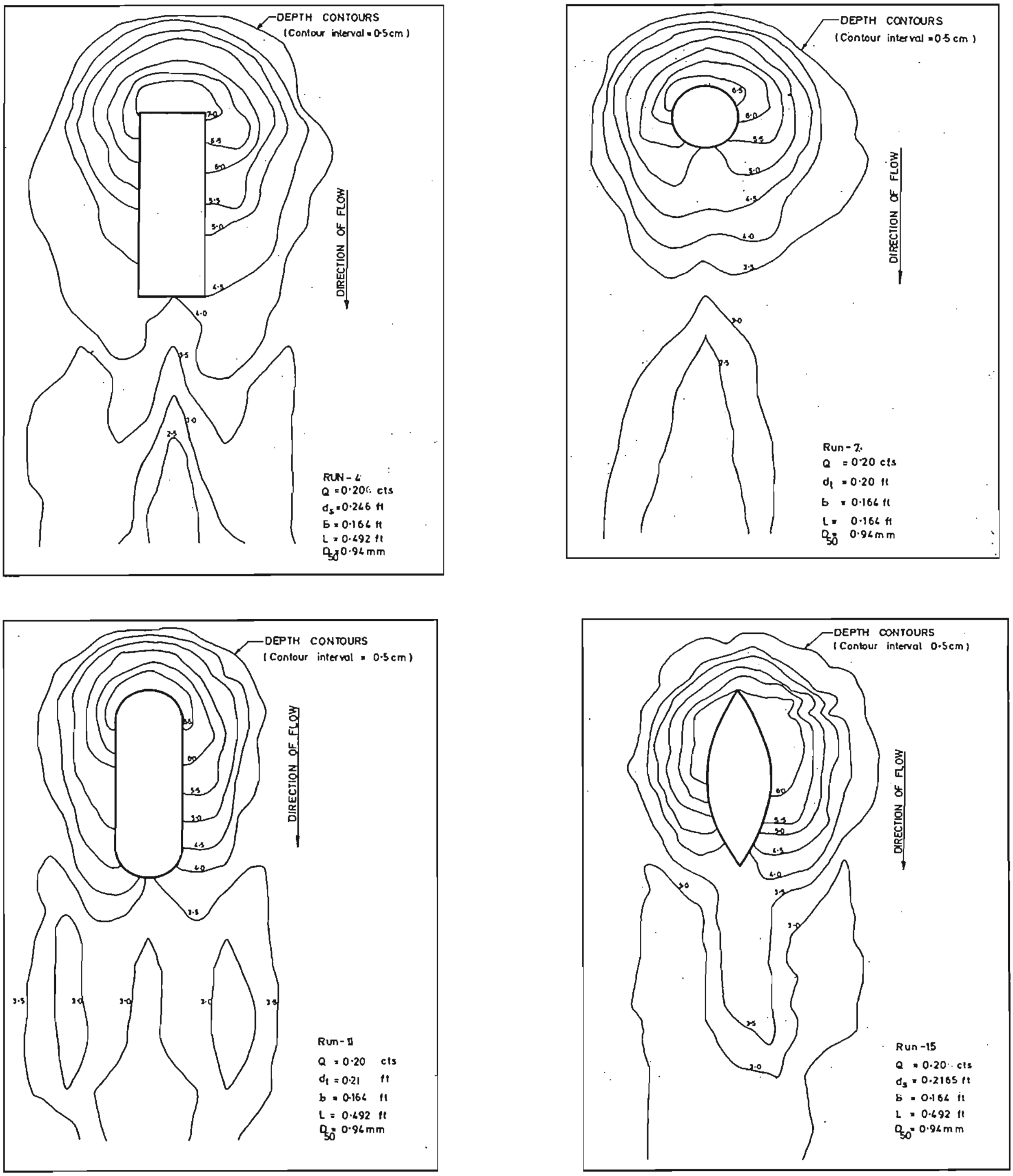

Fig. 3 Scour around bridge piers of different shapes

Effect of Angle of Attack

The scour depth is related to the projected width, which changes with the angle of attack. It is seen from Figure 4 that with the increasing angle of attack, the location of maximum scour depth moves along the exposed side of the pier from the front to the rear end. The depth of scour gradually increases with the angle of attack, but beyond 20° the effect may be very pronounced (Anwaruzzaman, 1998). As the angle of attack increases from 0° to 30°, the scour depth increased by about 20%, which is practically the same as suggested by Laursen's design curves (Raudkivi, 1990).

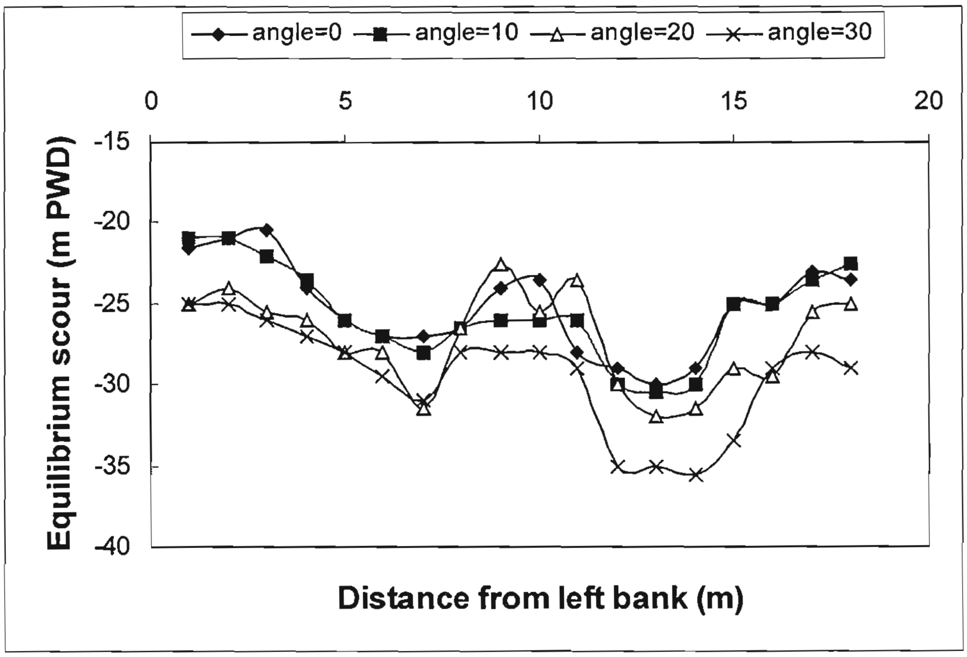

Fig. 4 Effect of angle of attack on scour depth

Performance evaluation based on the laboratory investigation

The observed scour depths in the laboratory have been compared with the predicted scour depths by various formulae such as Inglis, Blench, Shen et al., Lacey and Laursen. The comparison for the round-nose and circular piers (these two shapes are most commonly found in Bangladesh) are shown in Table 1.

Table 1 Comparison of observed and predicted scour for round-nose and circular piers

Equation	Experimental Result					
	Round-nose			Circular pier		
	D_{50}=0.94 mm	D_{50}=0.40 mm	D_{50}=0.19 mm	D_{50}=0.94 mm	D_{50}=0.40 mm	D_{50}=0.19 mm
Inglis	Under predicted	Highly under predicted	Highly under predicted	Under predicted	Highly under predicted	Highly under predicted
Blench	Slightly over Predicted	Slightly under Predicted	Good correlation	Good correlation	Slightly under Predicted	Good correlation
Shen-et-al	Highly over predicted	Over predicted	Over predicted	Over predicted	Highly over predicted	Slightly over predicted
Lacey	Over predicted	Slightly over predicted	Slightly over predicted	Highly over predicted	Over predicted	Highly over predicted
Laursen	Highly over predicted	Highly over predicted	Highly over predicted	Highly over predicted	Highly over predicted	Highly over predicted

From Table 1, it can be seen that Blench formula has made better predictions compared to other formulae. However, it should be noted that all the empirical equations are very sensitive to the mean particle size of the bed material and shape of the pier. The effect of mean particle size for Shen's equation for four different discharges is shown in Figure 5. It is clear that the scour depth changes inversely with the mean particle size. Similarly, the effect of pier shape for Shen's equation is shown in Figure 6. The scour depth is maximum for the rectangular pier and minimum for the sharp-nose pier. Thus, it is expected that scour predictions from empirical equations are likely to deviate from the actual ones. It may be possible to recalibrate these equations for different particle size and pier shapes to improve the accuracy of prediction.

FIELD INVESTIGATION

Secondary data for the years 1976 through 1978 have been collected for one of the mid-stream round-nose piers of the Hardinge Bridge and six caissons of the East-west Inter-connector to evaluate the performance of different empirical equations. Hardinge Bridge is an $1^1/_8$ mile long railway bridge which links between the Pakshey (Pabna) and Bheramara (Kushtia) over the river Padma. The mean size of the bed material was 0.14mm. The East- west Inter-connector, which is part of the national power grid, crossed the river Jamuna approximately in between Aricha and Nagarbari. It consists of eleven circular caissons of which six are located in the main river. The median size of bed material is 0.19 mm.

Data was provided by the Railway Department (Hardinge Bridge) and the Power Development Board (East-west Inter-connector).

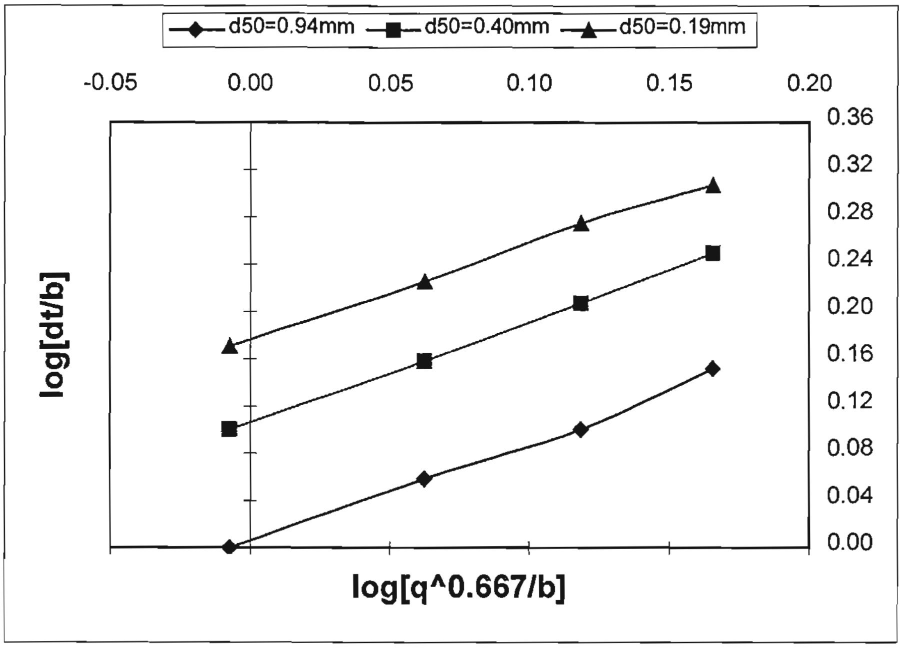

Fig. 5 Effect of mean particle size on scour depth

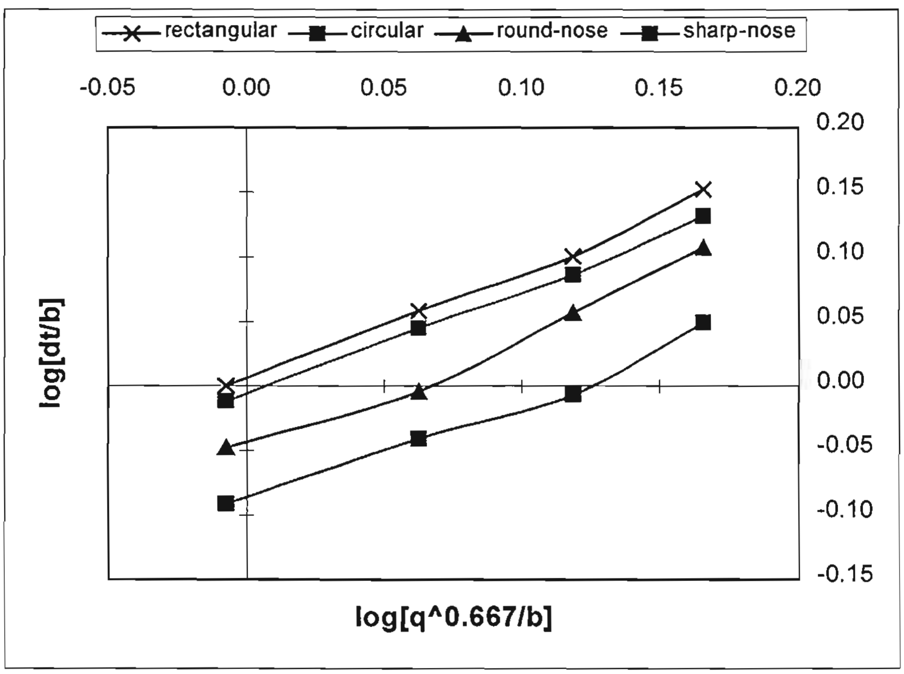

Fig. 6 Effect of pier shape on scour depth

Observations from the field Investigation

In general, there is an inverse relationship between the scour depth and the water level or flow. During low flow months between January and April, the scour depth is minimum and it remains fairly unchanged. After that, the flow gradually increases with consequent increase of the scour depth. The flow and the scour depth are the highest in the months of July through September. Figure 7 shows this monthly variation of water level and scour depth for a caisson of the East-west Inter-connector.

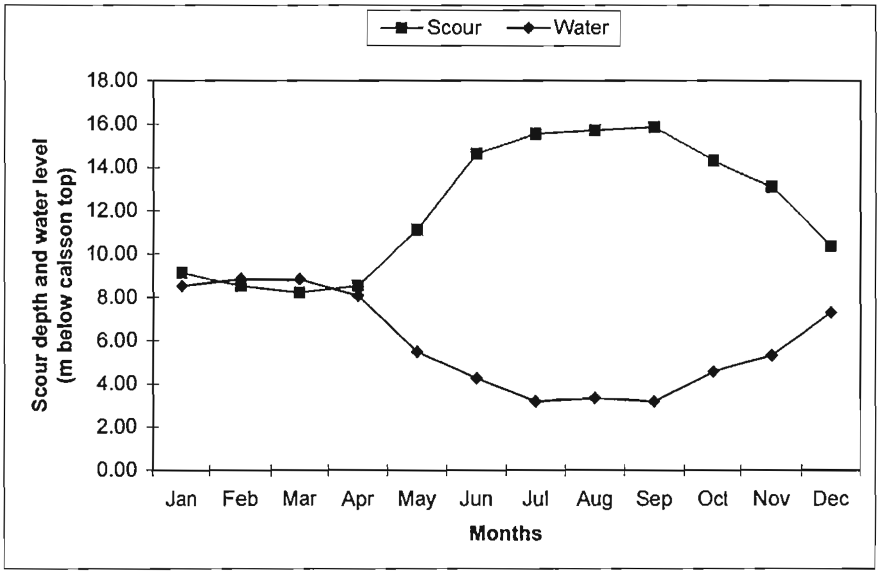

Fig. 7 Monthly scour depth at a caisson of East-west Inter-connector

To determine the efficacy of the empirical equations, the scour data of the Hardinge bridge and East-west Inter-connector have been used to estimate the coefficients of the empirical equations. The estimated and proposed equations of Inglis and Blench are shown in Table 2, other equations are not included due to poor performance.

Table 2 Estimated and proposed empirical equations

Investigator	**Equations (FPS System)**	**Hardinge Bridge**	**East-West Inter-connector**
Inglis	$d_t/b=1.7*(q^{2/3}/b)^{0.78}$	$d_t/b=1.34(q^{2/3}/b)^{1.07}$ $R^2=0.81$	$d_t/b=1.23(q^{2/3}/b)^{0.53}$ $R^2=0.5184$
Blench	$d_t/y=1.8*(b/y)^{0.25}$	$d_t/y=1.82(b/y)^{0.75}$ $R^2=0.9801$	$d_t/y=1.38(b/y)^{0.312}$ $R^2=0.6724$

As can be seen from Table 2, Blench has a higher regression coefficient than the same of Inglis. The original Blench equation seems to under predict the scour depth at Hardinge Bridge, which may explain why design engineers prefer Lacey and Laursen. Both these equations over predict the scour depth and allow the designers to be on the conservative side. However, the nature of bias is not clear for East-west Inter-connector. Inglis performed well at the Hardinge Bridge but showed a weak correlation at the East-west Inter-connector. In short, more and reliable data are required to make conclusive comments on the effectiveness of empirical equations for scour depth prediction.

DESIGN CRITERIA OF SOME MAJOR BRIDGES OF BANGLADESH

Hydraulic and hydrologic studies are carried out to design a bridge which include determination of the design discharge, high and low water levels, and the scour depth around piers and abutments. For the design discharge and water levels, a 100-year recurrence interval is normally adopted. The design scour is estimated as the sum of general scour, constriction scour, bend scour, confluence scour, and local scour. Empirical equations used for scour depth estimation incorporate all these forms of scours through a number of parameters and multiplying factors. The commonly used parameters are: design discharge, approach depth, median size of the bed material, approach velocity, width of the channel, and width of the pier.

In Bangladesh, bridges and culverts are built by two government organizations, namely Local Government and Engineering department (LGED) and Roads and Highways (R&H). The former normally designs small bridges and culverts and uses Lacey's equation for calculating the scour depth (LGED, 1998). The latter is engaged in construction of large bridges and uses Lacey, Laursen, and Poona equations for the estimating the scour depth.

Table 3 Design features of some major bridges of Bangladesh

Bridge	Characteristics of the river	Location	Bridge type	Bridge length	Max^{m} span length	Bridge width	Design scour depth	Empirical equation used
Jamuna Bridge	Braided, river course is shifting	Sirajgonj	Prestressed concrete box girder	4.8 km	100 m	18.5 m	42.7 m	Based on physical model
Meghna Bridge	River course is shifting	Meghna ferry ghat	Cast-insitu prestressed concrete box girder	930m	87m	9.2m	11.0m (PWD)	Laursen
Meghna-Gumti Bridge	No major shifting of river	Meghna-Gumti ferry ghat	Cast-insitu prestressed concrete box girder	1.48 km	90m	9.2m	12.30m (PWD)	Lacey
Kushiara Bridge	No major shifting of river	Fenchuganj railway bridge	Cast-insitu prestressed concrete box girder	286m	84m	9.2m	6.7m (PWD)	Lacey
Shambhu ganj Bridge	No major shifting of river	Mymensingh railway bridge	Prestressed beam (t-girder)	400m	40m	9.2m	7.9m (PWD)	Laursen

Although Lacey and Laursen normally over predicts the depth of the scour, organization involved in bridge design in Bangladesh use these equations for added safety. If Blench equation was used instead, considerable cost saving could be made.

CONCLUSION

The analysis of laboratory and field data on scour around bridge piers for different shapes, bed materials and flow conditions leads to the following conclusions.

i. The maximum depth and extent of scour developed in case of rectangular pier followed by circular, round-nose and sharp-nose piers.

ii. The maximum scour depth may occur either at the upstream or at the downstream of the pier depending on the shape of pier and flow conditions.

iii. The scour depth is higher in case of finer bed material and it gradually decreases as the bed material becomes coarse.

iv. Angle of attack has a considerable impact on the scour depth beyond 20^0.

v. Scour predicted by Blench shows better correlation with the laboratory and field data.

In Bangladesh, Lacey and Laursen equations are generally used in bridge design although they over predict the scour depth. This is due to a number of reasons. One, the designers want to err on the safe side. Two, estimated scour is seldom monitored after construction of the bridge and no feedback is generated that can be used to economize construction of future bridges. Moreover, soil type at the bridge site may dictate the foundation depth. In such cases, the scour depth calculation may become of secondary importance.

In the light of the above, it is recommended that more data on the scour depth should be collected from different parts of Bangladesh and these should be used to verify and re-calibrate the empirical equations used for scour depth estimation. Finally, these information should be part of a national bridge design manual that can be jointly prepared by the organizations currently involved in major bridge construction in Bangladesh.

REFERENCES

1. Anwaruzzaman, S. M., 1998, "Evaluation of Selected Local Scour Formulae around Piers and Groynes", M.Eng. Thesis, Department of Water Resources Engineering, BUET, Dhaka.

2. Garde, R. J. and Raju, R., 1985, "Mechanics of Sediment Transportation and Alluvial Stream Problems", Wiley Eastern Ltd., New Delhi, India.

3. JMBA, 1989, "Feasibility Report, Vol. 2, Annex-D", Jamuna Bridge Project, Phase II Study, Rendel Palmer and Tritton, NEDECO, Bangladesh Consultants Limited, UNDP/ World Bank, Government of Bangladesh.

4. Kabir, M.R., 1984, "An Investigation of Local Scour around Bridge Piers", M.Sc. Thesis, Department of Water Resources Engineering, BUET, Dhaka, Bangladesh.

5. LGED, 1998, "Road Structures Manual, Part A," Local Government and Engineering Department, Agargaon, Dhaka, Bangladesh.

6.Raudkivi, A. J., 1990, "Loose Boundary Hydraulics (3rd ed.)", Pergamon Press, Oxford, England.

SCOUR DEPTH - PREDICTION AND PRACTICE

By

Dr. B.R.Phani Kumar[1]

ABSTRACT

Many bridges have failed because of improper estimation of scour depth. For prediction of scour depth, several empirical equations have been developed. Scour depth is arrived at according to these equations as a function of so many parameters like silt factor. In spite of these innovative methods of prediction of scour depth, bridge piers have been subjected to undermining. Hence, continuous filed monitoring and experience based on previous failures is also necessary. This paper discusses various empirical correlations for scour depth and also some practical considerations for determining the depth of the foundation in terms of scour depth.

INTRODUCTION

Scour or removal of soil particles by flowing water from around the bridge piers has an undermining effect and has caused many a bridge failure. A pier or an abutment is an obstruction to the flowing water of a meandering stream, and modifies the flow pattern in its vicinity. The main current gets deflected, and a spiral flow is formed with a downward direction. This bottom spiral flow removes the particles from the bed and causes scour. The base of the pier should be placed below the scour depth to avoid scour.

Undermining of piers has taken place mainly because of the fact that the maximum depth of scour could not be estimated correctly. If the scour depth is predicted to some precision and the base of pier is laid below scour depth, failure of bridges can be avoided. Scour depth is predicted with the help of many empirical equations and theoretical correlations suggested by different researchers.

THEORETICAL CORRELATIONS

The equations for scour depth developed in terms of various parameters are either empirical relationships based on local observations or theoretical relationships based on analysis. The parameters that have been considered for the development of equations for prediction of scour depth are the width of the stream, depth of the flow, drag coefficient of sediment particles, silt factor, bed factor etc. A review of some of these theories follows:

---

[1] Dr. B.R. Phani Kumar, Department of Civil Engineering, JNTU College of Engineering, Kakinada-533 003, INDIA

Laursen (1963) conducted a number of experiments on scour phenomenon and the factors affecting it. He maintains that the rate of scour will be equal to the difference of the capacity of transport of sediment out of the scoured area and the rate of supply of sediment to that area. He also found that when the rate of sediment becomes equal to the rate of supply, scouring stops. This depth is called equilibrium depth of scour.

Garde (1961) applied the dimensional analysis to the problem of scour and, based on the widths of constricted and unconstricted sections, he proposed that the depth of scour (d_s) below river bed can be obtained from the equation:

$$[(D+d_s)/D] = (K/\propto) . F^n,$$

where $\propto$ is a constant equal to the ratio of the width of construction section to that of the unconstricted section, F is Froude number, and K and n are the functions of average drag coefficients of sediment particles.

Straub (1942) treated the bridge as a long construction. He applied the flow and transport equations at the constricted and the unconstricted sections, and obtained the following equation for predicting scour depth.

$$(D+d_s)/D = [B/b]^{0.642}$$

where D is the depth of flow in the river,
d_s is the depth of scour below river bed,
B is the total unconstricted width of the river, and
b is the width of the constricted section.

Venkatadri et al (1965) developed an equation based on the concept of equilibrium depth of scour. They conducted a series of experiments using different shapes of piers. They observed that deflection of streamlines around any obstruction is one of the main causes of scour. The equation for scour depth proposed by them is,

$$d_2/d_1 = (1+CF^2)$$

where d_2 is the depth of scour below the water surface,
d_1 is the depth of flow in the stream,
F is the Froude number, and
C is a constant, which depends on the shape of the pier.

The scour depth predicted from this equation has been found to tally with the observed experimental value.

In spite of these different analytical approaches, many bridges have failed. This calls for rigorous practice, which involves constant field monitoring and previous experience.

PRACTICAL CONSIDERATIONS

The practical considerations for the determination of scour depth need to the taken into account for the safety of the bridge piers. The factors determining the depth of the foundation are the safety against the maximum scour, the minimum grip below scour level required to resist over-turning, sliding of well and the permissible foundation pressures.

In India, the practice is to choose a preliminary value of the depth of foundations according to the Indian Roads congress code of practice for Bridges. Generally, one - third of the maximum anticipated scour below the highest flood level (HFL) is provided as the minimum grip length. Thus, the code recommends that the depth of the foundation be 1.33 times the designed HFL. The maximum depth of scour is taken as twice the normal depth of scour.

Terzaghi and Peck (1962) report of failure of two bridge piers. One pier had its base placed in a bed containing boulders of large size. In another case, the base of the pier was established deep into a gravel stratum. Yet, during seasons of high water, the piers failed due to scour. Hence, it is advisable that the base of the foundation be established at a depth below low-water channel equal to not less than four times the highest flood level.

CONCLUSION

Scour depth can be predicted to a reasonable precision with the help of empirical or theoretical correlations involving parameters like silt factor, bed factor, depth of flow etc. which affect the intensity of scour. As bridges continue to fail in spite of the theoretical precision, reliable forecasts of scour need to be given based on experience. A large factor of safety helps because of the uncertainty involved in the prediction of scour depth. It is advisable to follow the local standard code of practice.

REFERENCES

1. Grade R.J., 1961, "Local Bed Variation at Bridge Piers in Alluvial Channels", Research Journal, University of Rooskee, Roorkee, India.
2. Laursen E.M., 1963, "A Generalized Model Study of Scour around Bridge Piers and Abutments", Proceedings of Minnesota International Hydraulics convention, Minnesota, USA.
3. Standard specifications and Code of Practice for Bridges, Section 1: General Features of Design, Section 2: Loads and Stresses, Indian Roads Congress, New Delhi, India.
4. Straub L.G., 1942, "Mechanics of Rivers", Physics of the Earth, Part IX, Hydrology, McGraw - Hill Book Company, New York, USA.
5. Terzaghi K., Peck R.B., 1962, "Soil Mechanics in Engineering Practice", Asia Publishing House, New Delhi, India.
6. Venkatadri C., Rao G.M., Hussian S.T., Asthana K.C., 1956, "Scour around Bridge Piers and Abustments", Journal of Central Board of Irrigation and Power, Vol.22, No.1, New Delhi, India.

THE SRICOS METHOD: A SUMMARY

by

Jean-Louis Briaud[1], H. C. Chen[2], Kiseok Kwak[3]

ABSTRACT

In the USA, the scour depth around a bridge pier is currently calculated using the HEC-18 equation. This equation was developed for piers founded in sand and there is a sense that in clay the depth of scour is not as large. The purpose of this study was to develop a method for clays, silts, and dirty sands. The SRICOS method (http://tti.tamu.edu/geotech/scour) was developed on the basis of flume tests, numerical testing, and erosion testing of the soil. A new apparatus called the EFA (Erosion Function Apparatus) was built for engineers to test the soil for erodibility in the laboratory.

The output of the simple SRICOS method is a scour depth after a given time. If a hydrograph is used as input, the extended SRICOS method can be used and results in a scour depth versus time curve.

[1] Spencer J. Buchanan Professor, Dept. of Civil Engineering, Texas A&M University, College Station, Texas 77843-3136, USA (briaud@tamu.edu)

[2] Associate professor, Dept of Civil Engineering, Texas A&M University, College Station, Texas 77843-3136, USA.

[3] Ph.D. Student, Department of Civil Engineering, Texas A&M University, College Station, Texas 77843-3136, USA

In the case of cohesive soils the scour rate can be thousands of times slower than in the case of cohesionless soils. Cohesive soils include silts and clays. According to the unified soil classification system, silts and clays are soils which have more than 50% by weight of particles passing the 0.075mm sieve opening. Silt size particles are between 0.075mm and 0.002mm and clay size particles are smaller than 0.002mm. Cohesive soils are not classified by grain size but instead by their degree of plasticity which is measured by the Atterberg limits.

Because cohesive soils scour so much slower than cohesionless soils, it is necessary to include the scour rate in the calculations. Indeed, while one flood may be sufficient to create the maximum scour depth z_{max} in cohesionless soils, the final scour depth after many years of flood history at a bridge in cohesive soil may only be a fraction of z_{max}. The scour rate effect in cohesive soils is measured by the erosion rate versus shear stress curve which can be used to calculate the reduction in scour depth in the case of cohesive soils. The erosion rate $\dot{z}$ is defined as the depth of soil scoured per unit of time and is conveniently quoted in mm/hr. The shear stress τ is the shear stress imposed at the water soil interface and is given in N/m².

The $\dot{z}$ vs. τ curve is a measure of the erodibility of the soil (Figure 1). Typically the erosion rate $\dot{z}$ is zero until the critical shear stress τ_c is reached and then $\dot{z}$ increases as τ increases. The $\dot{z}$ vs. τ curve can be measured with the EFA (patent pending) (Erosion Function Apparatus) (http://tti.tamu.edu/geotech/sour) (Briaud et al., 1999(a)). In the EFA (Figure 1) a soil sample is eroded by water flowing over it. The sample is collected from the site in a standard thin wall steel tube, placed through the bottom of a rectangular cross section pipe, and a 1mm protrusion is eroded over time.

Once the $\dot{z}$ vs. τ curve is obtained the method to predict the pier scour depth as a function of time proceeds as follows. First the maximum shear stress τ_{max} around the bridge pier is calculated (Briaud et al, 1999)(a)):

$$\tau_{max} = 0.094\, \rho v^2 \left(\frac{1}{\log \mathrm{Re}} - \frac{1}{10} \right) \tag{1}$$

where ρ is the density of water, v the mean approach velocity, and Re the pier Reynolds number. Second the initial scour rate $\dot{z}_i$ corresponding to τ_{max} is read on the $\dot{z}$ vs. τ curve. Third the maximum depth of scour z_{max} is calculated (Briaud et al., 1999)(a)):

$$z_{max}(mm) = 0.18\, \mathrm{Re}^{0.635} \tag{2}$$

where Re is the pier Reynolds number. Note that equation (2) gives a value of z_{max} which is very close to the one for cohesionless soils. Indeed it was found that the maximum depth of scour in clays and in sands where approximately the same in flume experiments. In those same experiments however it was found that the scour hole in clay developed to the side and in the back of the pier and not in the front of the pier. This indicates that for scour in clay the front of the pier may not be the best place to install monitoring equipment. Fourth, the equivalent time t_{eq} is calculated. The time t_{eq} is defined as the time over which the design velocity v_{des} would have to be applied for the depth of scour z to be equal to the depth of scour reached after the hydrograph spanning the design life of the bridge t_{life} has been applied. The time t_{eq} is calculated as (Briaud et al., 1999)(b)):

$$t_{eq}(hrs) = 73\, \left(t_{life}(years)\right)^{0.126} \left(v_{des}(m/s)\right)^{1.706} \left(\dot{z}_i(mm/hr)\right)^{-0.20} \tag{3}$$

Fifth, the scour depth z versus time t curve is given by:

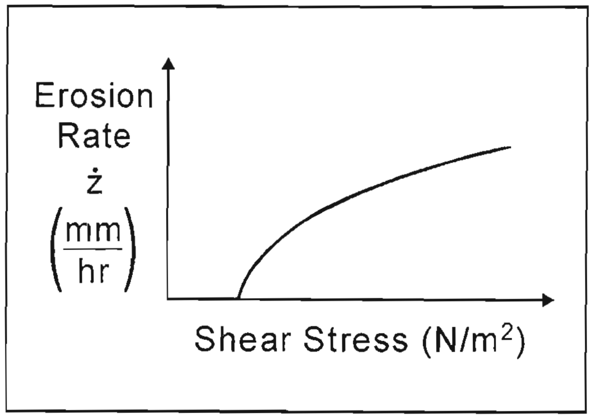

(b)

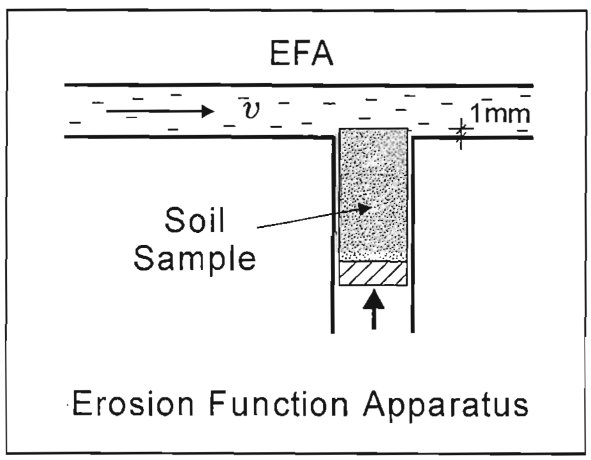

(a)

Fig. 1 – The EFA: (a) Diagram of the Apparatus, (b) Result of an EFA tests

$$z = \frac{t}{\frac{1}{\dot{z}_i} + \frac{t}{z_{\max}}} \tag{4}$$

and the depth of scour at the end of the design life of the bridge is calculated by using equation (4) with the t_{eq}, $z_{\max}$, and $\dot{z}_i$ values obtained from equation (3) and (2) and from the erodibility curve respectively. The following example illustrates the procedure.

A bridge is to be built in a cohesive soil. The diameter of the bridge pier is 2m, the water depth is 5m , the design velocity is 3m/s and the design life of the bridge is 75 years (Figure 2).

The erodibility curve has been measured by testing a soil sample from the site in the EFA and gave the curve shown on Figure 2. The maximum shear stress around the pier before scour begins is calculated:

$$\tau_{\max} = 0.094 \times 1000 \times 3^2 \left(\frac{1}{\log \frac{3 \times 2}{10^{-6}}} - \frac{1}{10} \right) = 40\, N/m^2$$

The initial rate of scour $\dot{z}_i$ is read on the $\dot{z}$ vs. τ curve for the $\tau_{\max}$ value.

$$\dot{z}_i = 6mm/hr.$$

Then the maximum depth of scour is calculated:

$$z_{\max} = 0.18 \times \left(\frac{3 \times 2}{10^{-6}} \right)^{0.635} = 3626mm$$

The equivalent time t_{eq} is given by:

$$t_{eq} = 73 \times 75^{0.126} \times 3^{1.706} \times 6^{-0.20} = 573\ hrs = 24\ days$$

The depth of scour after 75 years of flow around that bridge pier is calculated as:

$$z = \frac{24 \times 24}{\frac{1}{6} + \frac{24 \times 24}{3626}} = 1765mm$$

In this case the scour depth after 75 years (1765mm) is approximately 50% of the maximum scour depth (3626mm).

It is also possible to make predictions by applying a detailed velocity history over the design life of the bridge if one is available. This requires the use of the SRICOS computer program which can also consider the case of a layered soil system (Briaud et al., 1999)(b)). An example of results for a run using the SRICOS program is shown in Figure 3.

CONCLUSIONS

A method called SRICOS is presented for bridges over water with piers founded in cohesive soils (clays, silts, dirty sands). The method is used to predict pier scour as a function of time.

Problem: Maximum flood velocity = 3 m/s
Bridge design life = 75 years
Pier diameter = 2 m
Water depth = 5 m
What is the depth of scour after 75 years?

Solution: S-SRICOS Method

1. Results of EFA tests gave the $\dot{z}$ vs τ curve shown.
2. Maximum hydraulic shear stress around the pier is:

$$\tau_{max} = 0.094\ \rho v^2 \left(\frac{1}{logRe} - \frac{1}{10} \right) = 40\ N/m^2$$

3. The initial rate of scour $\dot{z}_i$ is read on the EFA curve at $\tau = \tau_{max}$. $\dot{z}_i = 6$ mm/hr
4. The maximum depth of scour z_{max} is

$$z_{max} = 0.18\ Re^{0.635} = 3626\ mm$$

5. Equivalent time

$$t_e = 73 (t_{hydro})^{0.126} (v_{max})^{1.706} (\dot{z}_i)^{-0.2} = 573\ hrs.$$

6. The equation for the $z(t)$ curve is

$$z = \frac{t}{\frac{1}{\dot{z}_i} + \frac{t}{z_{max}}} = 1765\ mm\ \text{after 75 years}$$

$z_{75\ years}$ is 49% of z_{max}

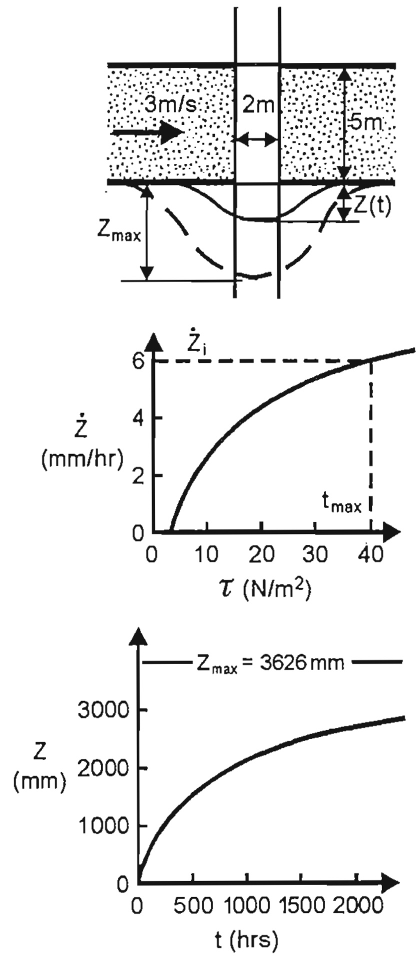

Fig. 2 - Example of scour calculations by the S-SRICOS method.

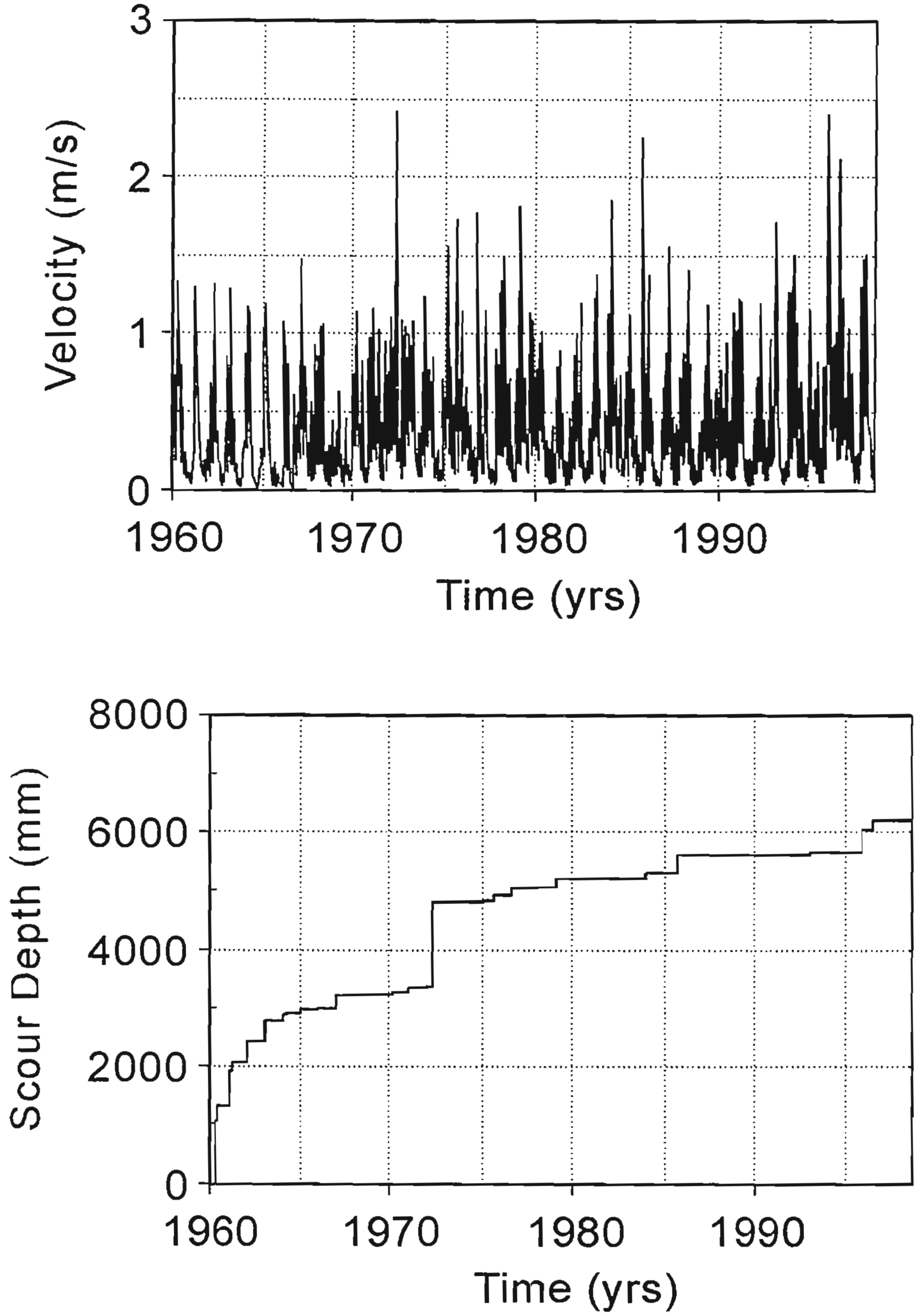

Fig. 3 – Velocity Hydrograph and Predicted Scour Depth vs. Time Curve for Pier 1E of the Existing Woodrow Wilson Bridge in Washington D.C.

ACKNOWLEDGEMENTS

The SRICOS method was initially developed under sponsorship by the Texas Department of Transportation. It is being further developed under sponsorship by the National Cooperative Highway Research Program.

REFERENCES

- Briaud, J.-L., Ting, F.C.K., Chen, H.C., Gudavalli, R., Perugu, S., Wei, G., 1999 (a), "SRICOS: Prediction of Scour Rate in Cohesive Soils at Bridge Piers", Journal of Geotechnical and Geoenvironmental Engineering, Vol. 125, No. 4, April 1999, pp. 237-246, American Society of Civil Engineers, Reston, Virginia, USA.
- Briaud, J.-L., Ting, F.C.K., Chen, H.C., Gudavalli, R., Kwak, K., Philogene, B., Han, S.W., Perugu, S., Wei, G.,Nurtjahyo, P., Cao, Y., Li, Y., 1999(b), "SRICOS: Prediction of Scour Rate at Bridge Piers", Report 2937-F to the Texas Department of Transportation, Texas A&M University, Civil Engineering, College Station, TX 77843-3136, USA.

PREDICTION OF BED LIQUEFACTION AND LOCAL SCOUR AROUND A BRIDGE PIER UNDER ABRUPT WATER PRESSURE CHANGE

By

Md. Faruque Mia [1], Hiroshi Nago [2]

ABSTRACT

A large number of bridges are collapsed especially under sudden attack of flood flows or storm waves. Most of the failures are reported due to scour. During such natural conditions, river water level rises very quickly, many reaches flood stages, and decreases suddenly. The rapid change in the depth of flow from a high stage to a low stage results a sudden change of water pressure variation near the structures and causes excess pore pressure development into the sand bed. Thus the dynamic stability of the bed material around the bridge pier is also related to the failure of the bridges.

This paper describes experimental results carried out in a laboratory channel, to predict the bed liquefaction and its influence on the local scour development around a circular bridge pier under abrupt water pressure change. Several experiments were performed to investigate the variation of scour depth for clear-water steady flow and instantaneous local scour depth due to abrupt water pressure change. This paper deals with the distribution of pore water pressure, effective stresses and local scour around a circular bridge pier. The results of the investigations show that, the sediment bed is liquefied by an increase of the excess pore water pressure development under abrupt water pressure change and the equilibrium local scour depth increases considerably at a stage of liquefaction occur.

---

[1] Graduate Student, The Graduate School of Natural Science and Technology, Okayama University, Okayama-shi 700-8530, Japan.

[2] Professor, Dept. of Civil and Environmental Engineering, Okayama University, Okayama-shi 700-8530, Japan.

INTRODUCTION

Failure of bridges due to scouring at piers is a common occurrence especially during flood flows or storm waves. These types of scour that may affect bridges can be classified as local scour, localized scour and degradational scour. The special attention of this paper is the local scour which can be defined as the removal of sediment due to the interference with flow by the piers. It can occur in one of two ways: (1) clear-water scour and (2) live-bed scour. Clear-water scour occurs when the bed material upstream of the scour area is at rest and live bed scour can be referred to as general bed load transport by the flow. The ratio U/U_c is a measure of flow intensity and determines whether or not the initiation of particle movement occurs. For $U/U_c \leq 1$, clear water scour conditions pertain and for $U/U_c > 1$, live bed scour occurs. Where U is the mean flow velocity and U_c is the critical flow velocity. In Fig.1 qualitative diagrams are shown to differentiate between the development of clear-water scour and live bed scour depths with time and approach velocity. For live bed conditions the scour depth increases rapidly with time and then fluctuates against a mean value, which is referred to as equilibrium scour depth. This is always less than the maximum scour depth developed for clear-water conditions.

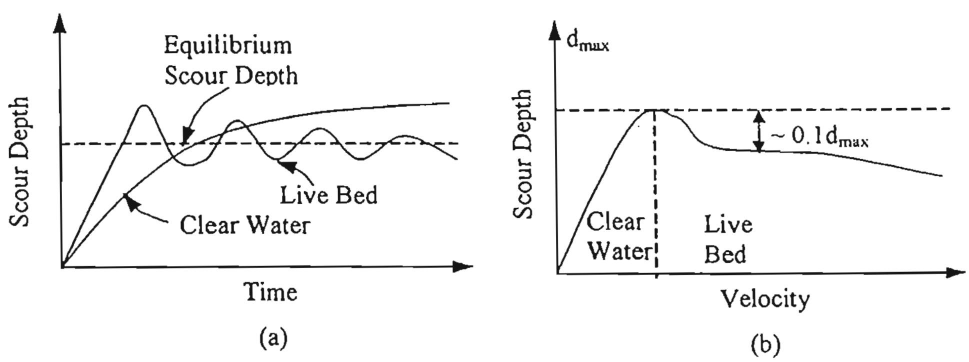

Fig.1. Scour depth as a function of : (a) Time, and (b) Approach Velocity

The factors mainly flow velocity, flow depth, sediment size, sediment gradation, pier shape, and pier alignment are considered by Melville and Sutherland (1988), U.S. Department of Transportation (1993), Hancu (1971), Laursen and Toch (1956), Shen et al. (1969), Breusers et al. (1977), and Jain and Fischer (1979) to develop the equation for local scour depth mainly due to steady flow. Whereas, there is no generally accepted method for estimating the scour due to combined wave and current flows. A few number of studies are attempted for scouring during unsteady flow by Saito et al. (1990), Kawata and Tsuchiya (1988), and Sumer et al. (1992). However, many hydraulic structures such as platforms, bridges, subsea templates, and so on collapse due to scouring under sudden attack of flood flows or storm waves. A rapid change in the depth of flow from a high stage to a low stage will result in a steep depression in the water surface. Such a phenomenon is generally caused by an abrupt change in the channel slope or cross-section and is known as a hydraulic drop. This phenomenon creates sudden change of water pressure variation near the structures and causes excess pore pressure development into the sand bed.

To make safe design for the occurrence of scour, one must be able to predict realistically maximum depth of scour hole. The mechanisms of environmental forcing (waves, currents, etc), the dynamic behavior of bed material and soil characteristics are to be very important considerations for the engineers to enable accurate design for the maximum scour depth. If shear stresses are exerted on loosely packed sand which can be defined as the porosity (percentage of voids) of the sand is higher than a critical value, the sediment particles tend adopt a denser packing. As the pores are filled with water, over-pressure occurs in the pore water, diminishing the effective stresses and thus reducing the frictional resistance. The authors earlier expected that under sudden water pressure variation, the bed layer will decrease the effective stress, that is, liquefaction will occur by an increase of excess pore water pressure. The amount of sediment will remove from the scour hole more than that of the amount of sediment transports from the upstream into the scour hole. As a result, the equilibrium local scour around the pier reached for steady state flow will increase instantaneously at a stage of the occurrence of liquefaction due to abrupt water pressure change.

Nago (1981) studied the influence of the properties of the oscillating water pressure and the sand layer on the characteristics of the liquefaction for the explanation of the local scouring mechanism around the hydraulic structures. Nago and Maeno (1986) stated that the strength of the sand bed decreases notably and the unstable zone will occur during the crest or the trough being in front of the structures. Zen and Yamakazi (1993) defined that the pressures due to the surface waves are transmitted into the sand bed and they give rise to horizontal and vertical pressure gradients, which encourage liquefaction. Sakai et al. (1992) suggested that an important mechanism that makes the bed surface layers more susceptible to erosion is bed liquefaction. According to Zen and Yamakazi (1993), liquefaction is considered to be important for estimating scour at, and hence the stability of, coastal structures (Scour at marine structures (1998)). A bed is called in liquefied state when the effective stress of it becomes zero (Nago, 1981). An increase in the excess pore pressure under variation in the water pressure produces a decrease in the effective stress of the bed material (Nago, Maeno, 1987). In the state of sand bed liquefaction, it is expected that the liquefied sand will remove easily by the flow tangential to the surface, and the sand layer will be scoured successively (Nago 1981). A few laboratory experiments were done by Nago et al. (1984) to investigate the effect of water pressure variation on the scour around bridge pier. Mia and Nago (1999) studied dynamic behavior of bed material around a circular bridge pier under abrupt change of water pressure. They mentioned in their study that the failure of structures during flood flows due to scouring can be considered close relation to the dynamic behavior of bed material around the structures under water pressure change.

The determination of the decrease in the effective stress, that is, formation of liquefaction, is considered to be very important for the design of hydraulic structures under variation in the water pressure. The predicted **"bed liquefaction"** can be considered as one of the most important factors for the design of local scour depth to prevent the failure of the hydraulic structures. In this paper, we discussed the fundamental characteristics of the pore water pressure distribution, decrease in the effective stress, that is, liquefaction and their effect in the development of local scour around a circular bridge pier under abrupt water pressure change using a laboratory model. The results show that, the sediment bed is liquefied by an increase of excess pore water pressure and the equilibrium local scour reached for steady flow increases considerably at a stage of liquefaction occur under abrupt water pressure change.

EXPERIMENTAL SET UP

The experiments to study the prediction of bed liquefaction and local scour around a circular bridge pier model were conducted in a flume 1600cm long, 60cm wide and 40cm deep, located in the Hydraulics Laboratory of Okayama University, Japan. Fig.2 shows the side view and plan view of the channel with working section. Water was conveyed to the flume from an elevated tank by a pipe through an approach channel to measure the discharge by means of a sharp crested weir. The flow rate in the flume was adjusted by controlling a valve in the pipe. Then the corresponding head over the sharp crested weir

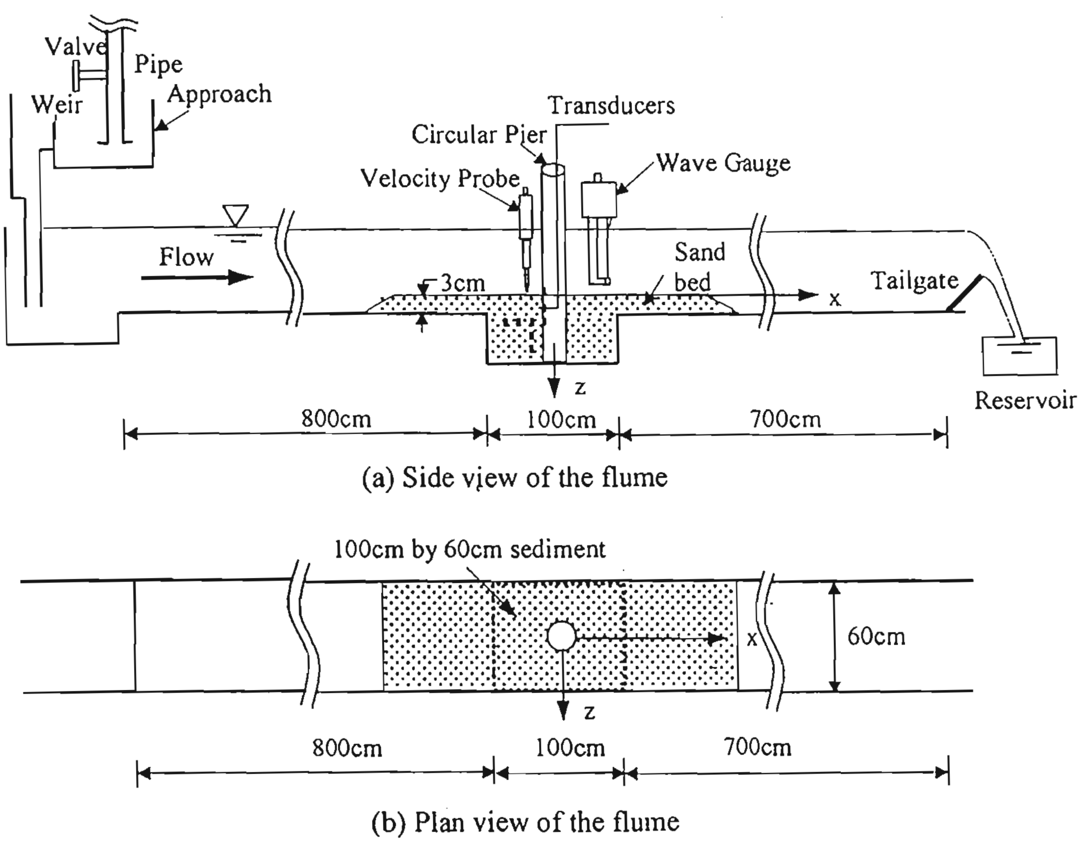

Fig.2. Schematic diagram and definition sketches of the experimental flume

was measured for the supplied discharge value. The depth of water was being changed by controlling the tailgate. The working section, 100cm long, 60cm wide and 57cm deep was located 800cm downstream from the entrance of the flume where the pier was located. This section was filled with the sediment of mean particle size 0.25mm below the bed level and the bed was flattened with the same size of the sediment used in the test section. Before the start of the experiments for the variation of scour depth measurement with time, the working section and the bed was made level. The pier was placed centrally and vertically in the working section. Then the leveled area around the pier was covered with 3-mm thick acrylic sheet. The valve was slowly adjusted without causing any disturbance to the bed material until the desired discharge was reached to the flume, and the required depth was obtained by controlling the tailgate. The steady flow conditions were adjusted slowly at least by 5 minutes. When the expected flow conditions were established the acrylic sheet was removed very carefully that ensures no scouring occurred around the pier due to this operation. The scour depths were recorded from a reading scale attached to the wall of the pier relative to the initial bed against time. A total of eight transducers were connected to the amplifier to record the digital data of pore pressure around the bridge pier. Three were set directly to the wall of the pier vertically at a distance of 4.5cm apart, three were set horizontally at a distance of 3cm apart each at a depth of 9cm from the top of the sediment recess and the rest two were set vertically at distance of 3.5cm apart each at 3cm away from the upstream of the pier (Fig.2). The average of at least 9,000 samples processed by a computerized data acquisition system at 50 Hz was taken by a digital recorder at each measured point.

The experimental conditions can be summarized as the following steps:

(a) At first, steady flow conditions of clear-water were established and the scour depths (d_s) were recorded against time.
(b) To investigate the effect of pore pressure and the effective stress in the bed material around the pier, the depth of flow was risen relative to the normal depth.
(c) The sudden drops were allowed at a stage when the equilibrium local scour around the pier was almost reached.
(d) In order to investigate the effect of pressure drop size, the experiments were conducted with sudden pressure drops of different variations.
(e) Excess local scour over clear-water steady flow was observed and data for pore water pressure were recorded.
(f) Uniform bed materials were used with the mean particle size of 0.25 mm and the porosity was assumed as 0.40.
(g) The size of the pier was used 6.0 cm in diameter (D).
(h) Sand was placed as a 3-cm thick layer in the flume bed with a bed slope of 0.002.

CONCEPT OF PORE PRESSURE AND SCENARIO OF THE OCCURRENCE OF SCOUR

When the water level is subjected to a rapid change against initial water level in accordance with wave propagation, a total stress variation is introduced in the underlying

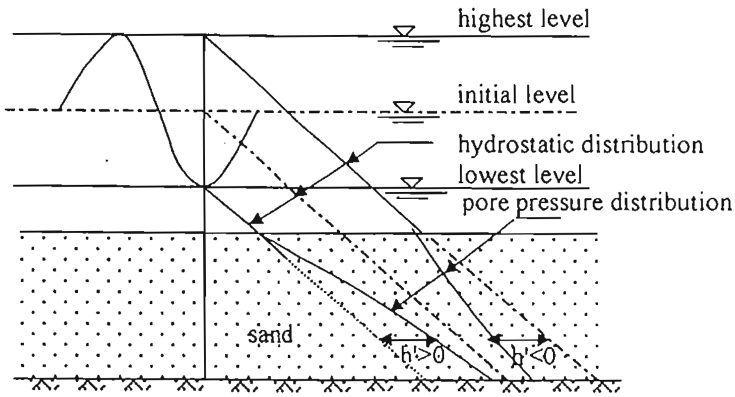

Fig.3. Key sketch for the definitions of pore water pressure

sediment bed. Fig.3 shows the concept of the pore pressure change from the initial state of the hydrostatic pressure in the sand bed. Under certain conditions the effective stress may become equal to zero due to the increase of pore pressure, that is; liquefaction will occur. The liquefied or weakened sand near the surface is removed easily by the shear stress of flow and the scour around the structures placed in such conditions will progress much more than that of the steady state flow (Nago and Mia, 1999) and that can cause instability of the foundation structures. Fig.4 shows the schematic phases for the scenario of the occurrence of scour under abrupt pressure change.

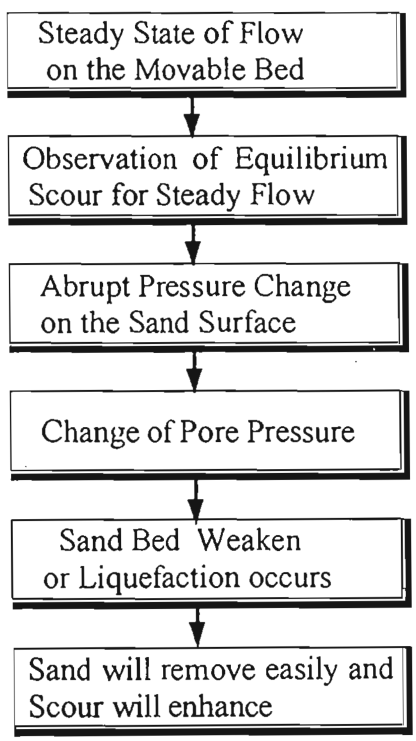

Fig.4. Scenario of the occurrence of scour under abrupt water pressure change

LIQUEFACTION CRITERIA

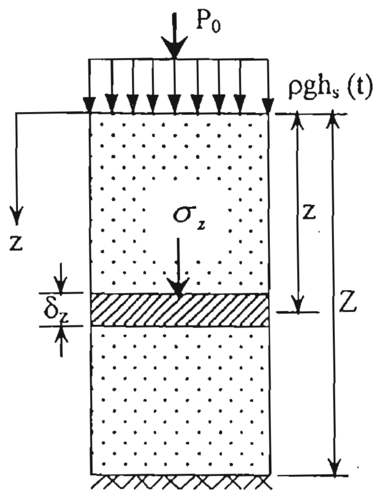

Fig.5. Sand layer under water pressure variation

The pore pressure and the effective stress in the sand bed can be analyzed by the method used to analyze ground water problems in an elastic acquifer (Rouse, 1950). That is, it is assumed that the sand and the water are compressible and then that the density of water, the porosity of the sand and the thickness of the layer are variable. The void in the layer is occupied by the water and the air. Then, it is assumed that the porosity λ is composed of the part for the water λ_w and the part of the air λ_a. Here, the experimental explanation of the sand bed behavior under water pressure variation is expressed by using the following equations.

The relation between the effective stress and the pore water pressure can be equated to the downward acting force of water pressure variation and the weight of constituents of sand on the plane of contact of bed (Nago, 1981). Considering a sand layer at depth z of a saturated sand column of height Z as shown in Fig.5, it can be expressed that,

$$\sigma_z + \rho gh = \gamma_s z + \rho gh_s \tag{1}$$

The pore water pressure ρgh and the weight of the sand column above the plane of contact $\gamma_s z$ can be expressed as follows:

$$\rho gh = \rho g\left(h_s + z + h'\right) \tag{2}$$

$$\gamma_s z = \rho_s gz\left(1-\lambda\right) + \rho gz\lambda_w \tag{3}$$

where, σ_z : effective stress

h : pore water pressure in head (variation from hydrostatic pressure relative to mean water level)
$\rho_s g$: weight of unit volume of the individual sand grain
h_s : variation of water pressure acting on the surface of the bed relative to the initial water level
h' : excess pore water pressure
z : depth of the sand layer measured from top of the sand surface as datum
ρ_s : density of sand
ρ : density of water
g : gravity due to acceleration
λ_w : porosity of water part
λ : porosity of the sand column
($\lambda = \lambda_w + \lambda_a$, λ_a: porosity of air part)

Substituting equations (2) and (3) into equation (1), and assuming $\lambda_w \cong \lambda$,

$$\sigma_z + \rho g h' = (\rho_s - \rho) g z (1 - \lambda) = \text{constant} \tag{4}$$

Thus, the liquefaction state can be expressed by:

$$\frac{\sigma_z}{(\rho_s - \rho) g z (1 - \lambda)} = 1 - \frac{\rho g h'}{(\rho_s - \rho) g z (1 - \lambda)} = 0 \tag{5}$$

EXPERIMENTAL DETAILS

The Shields diagram was used to determine critical shear velocity, u_{*c}, against mean grain size, d_{50}. The relation between critical shear velocity and mean grain size can be expressed as:

$$u_{*c} = 0.03 d_{50}^{1/2} \tag{6}$$

where, u_{*c} is in m/s, and d_{50} is in mm.

Critical shear velocity can be converted into critical mean flow velocity (U_c) by using the following logarithmic expression of the velocity profile:

$$\frac{U_c}{u_{*c}} = 5.75 \log\left(5.53 \frac{h_0}{d_{50}}\right) \tag{7}$$

where, h_0 = flow depth.

Table 1 Experimental conditions and results of scour depth under abrupt pressure change

Ex. No.	Initial depth (h_0) (cm)	U/U_c	Equilibrium scour due to steady flow (d_s) (cm)	Pressure size ($H-h_0$) (cm)	Increased Scour depth (d_{si}) (%)	Maximum scour depth (d_{smax}) (cm)
A1	20	1.060	7.1	10	9.9	7.8
			7.4	15	12.2	8.3
A2	20	0.928	7.1	10	9.9	7.8
			7.3	15	9.6	8.0
A3	20	0.795	6.5	15	16.9	7.6
A4	15	0.914	7.3	10	9.6	8.0
			7.2	15	13.9	8.2
A5	16	0.850	6.6	11	13.6	7.5
			6.8	15	17.6	8.0
A6	15	0.914	7.2	12	13.9	8.2
			7.2	16	16.7	8.4

Table1 shows the experimental details. Each of the experiments was run for clear-water steady flow to confirm the maximum equilibrium local scour depth. When equilibrium scour depth was reached, the water level was risen from the initial stage to a high stage and then it was allowed to drop from the high stage to the initial stage. The scour depth and pore water pressure measurements were recorded carefully during the application of abrupt pressure change.

EXPERIMENTAL RESULTS AND DISCUSSIONS

The results corresponding to Fig.6-11 of 16cm abrupt pressure change for experiment no. A6 has been chosen for the discussions. Fig.12-17 are the results of 11cm pressure change for experiment no. A5. The models of the pressure sensors for both the cases were shown in Fig.6 and in Fig.12 respectively. The experiments for the other conditions also confirmed the similar results. Fig.7 shows water surface variation relative to the initial water level (h_0) of the steady flow with time. Fig.8 expresses the time history of the distribution of pore water pressure at each level of sand surface. Fig.10 is the scour depth variation with time for clear-water steady flow. The position of the circle drawn in Fig.10 expresses the excess development of the scour depth to that of the steady flow for the abrupt change of water pressure. This is happened due to the increase of the excess pore water pressure and the formation of liquefaction into the sand bed. Fig.9 represents the effective stresses corresponding to each layer. The near surface level of Pt.3 indicates that the effective stress decreased as to zero; that is, the layer is fully liquefied and susceptible

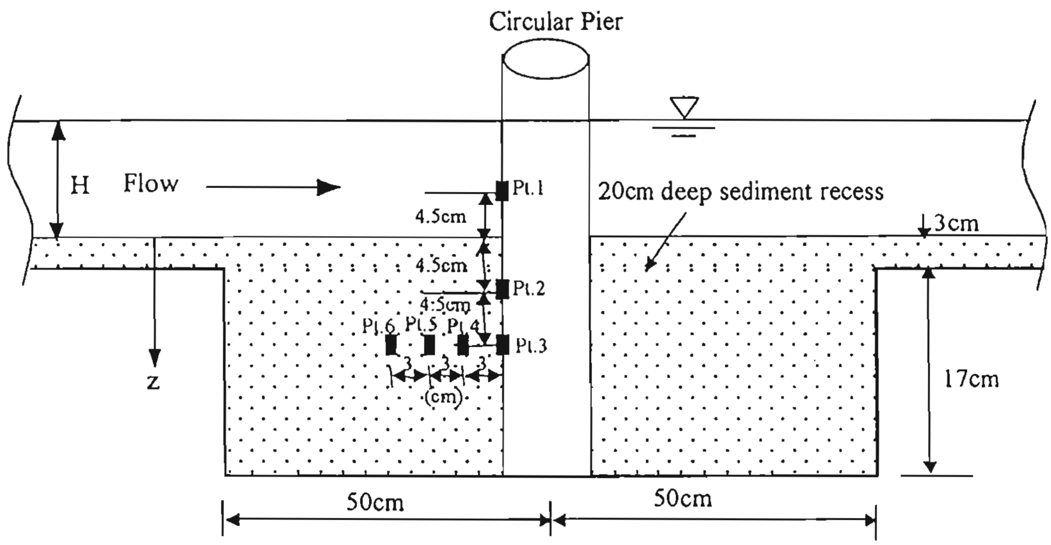

Fig.6. Location of sensors for pore pressure measurement

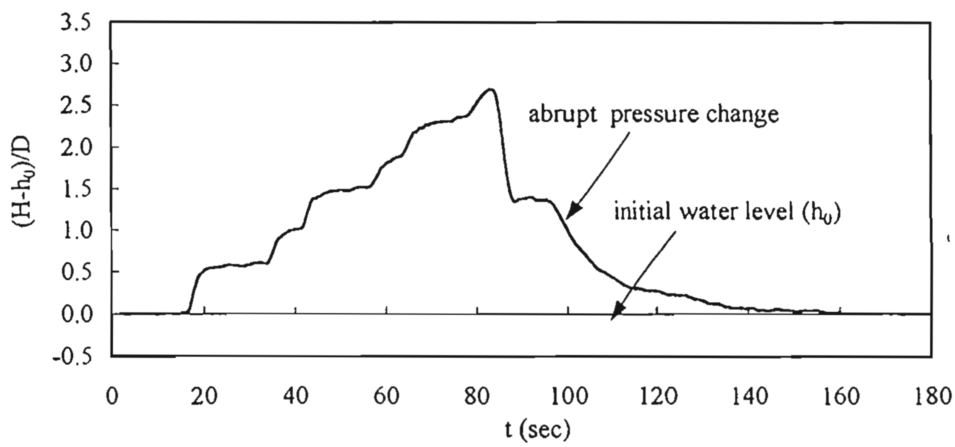

Fig.7. Variation of water surface profile

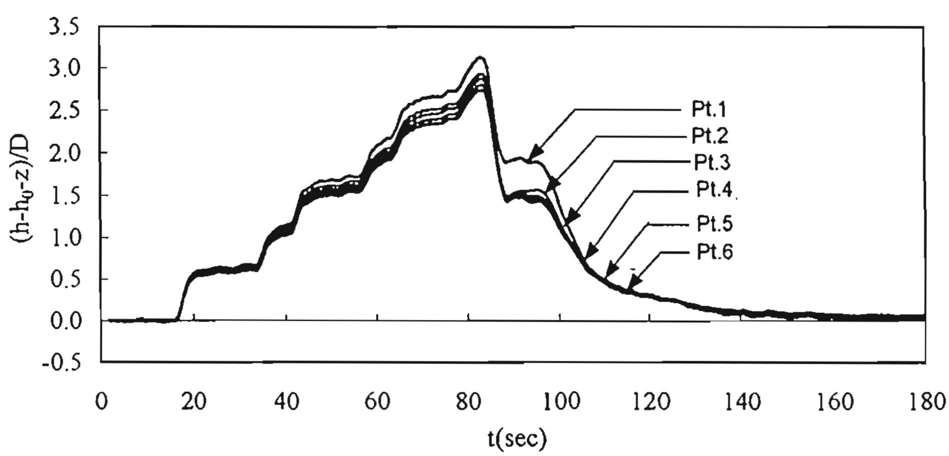

Fig.8. Pore water pressure variation

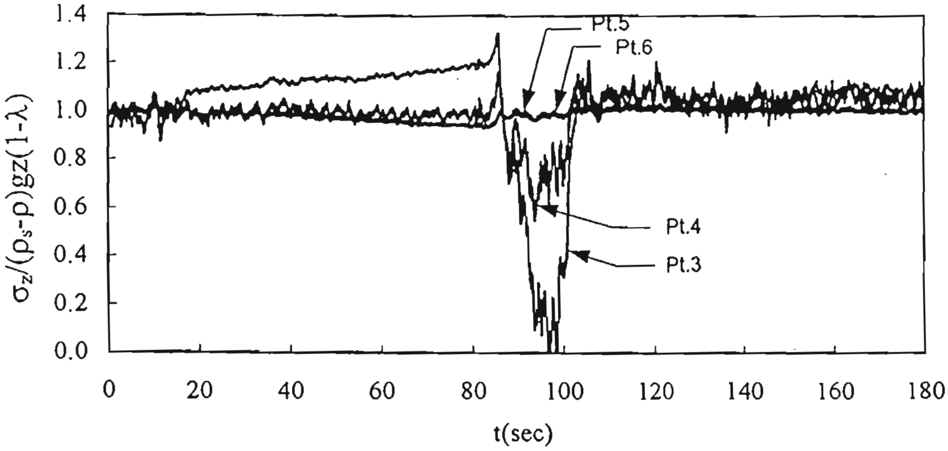

Fig.9. Effective stress

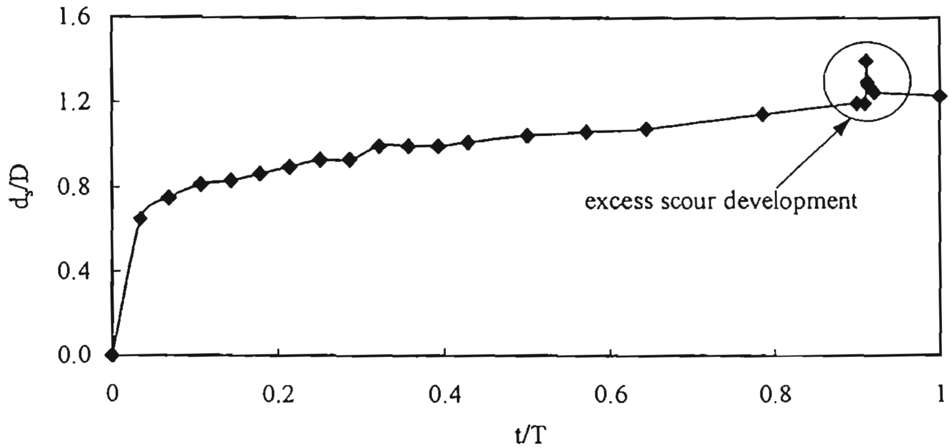

Fig.10. Variation of scour depth with time

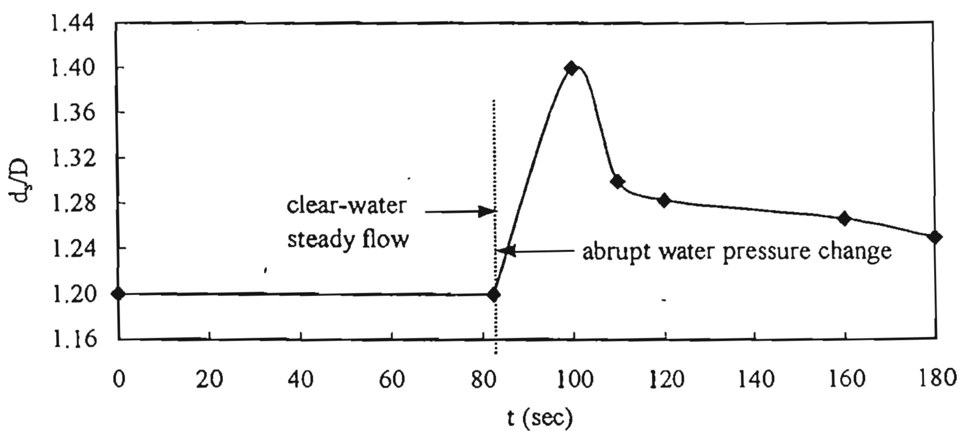

Fig.11. Excess scour developed due to abrupt pressure change

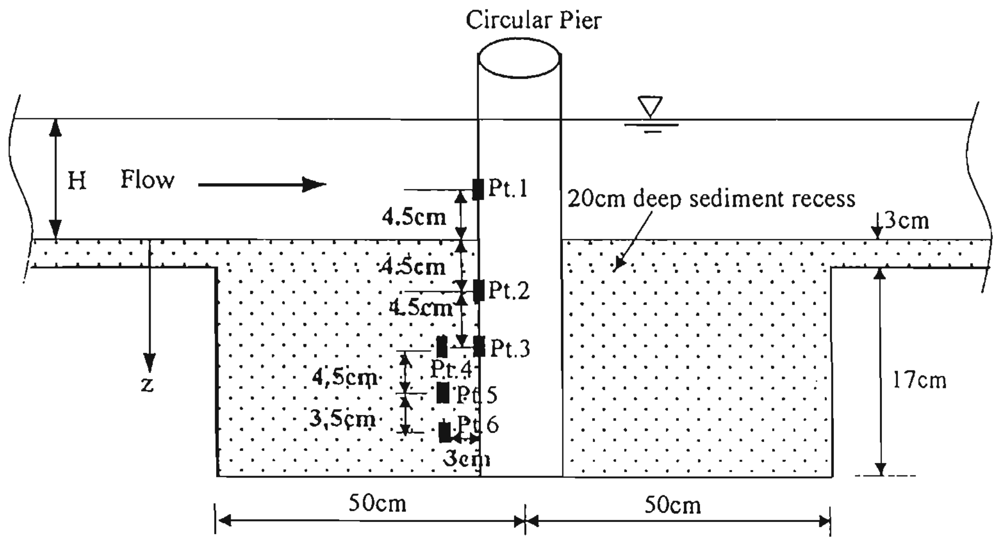

Fig.12. Location of sensors for pore pressure measurement

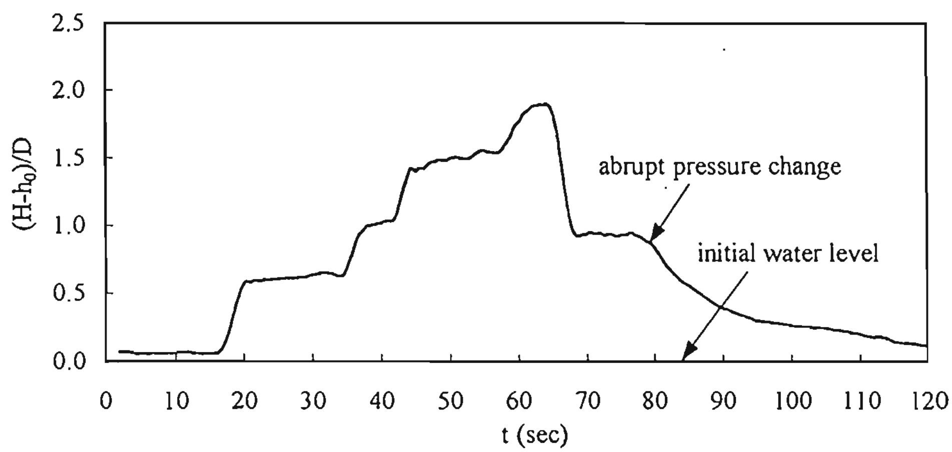

Fig.13. Variation of water surface profile

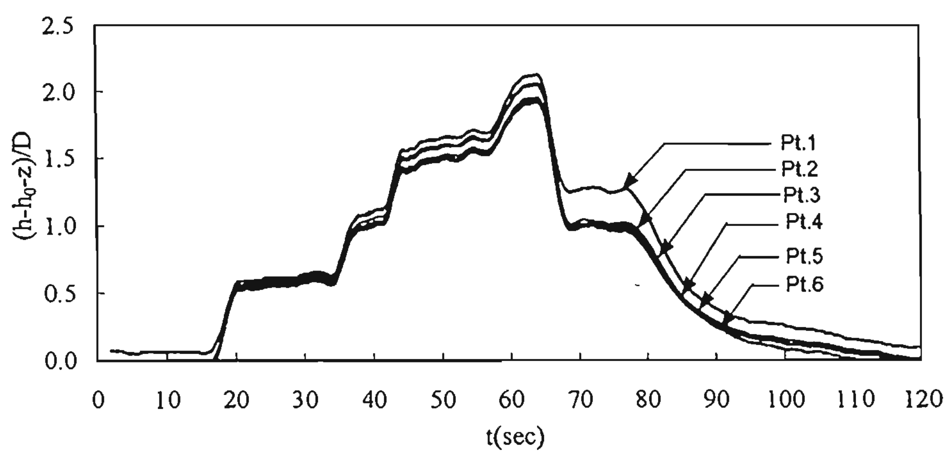

Fig.14. Pore water pressure variation

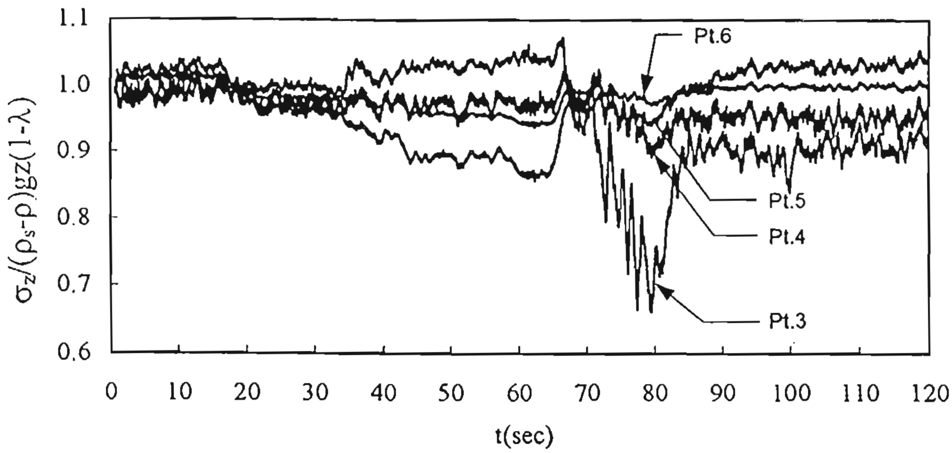

Fig.15. Effective stress

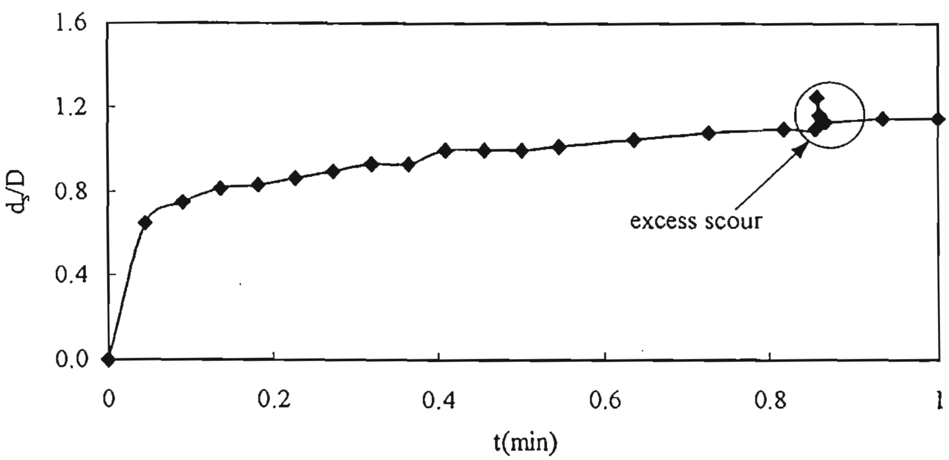

Fig.16. Variation of scour depth with time

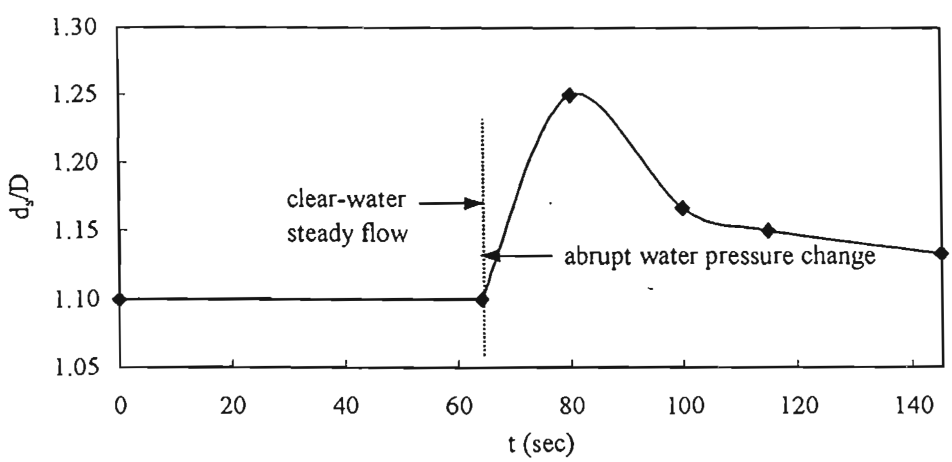

Fig.17. Excess scour developed due to abrupt pressue change

to scour depth enhancement. Pt.4 is considered just 3cm away upstream of the pier. The sand layer of Pt.4 also indicates a factor of effective stress less than 1, that is, partial liquefaction occurred. The results assure a lack of stability of the bed layer around the pier. Fig.11 represents the excess development of local scour depth due to abrupt change of water pressure to that of steady flow. It is cleared from Fig.9 and Fig.11 (Fig.15 and Fig.17) that the developed excess scour depth is maximum at a stage of the effective stress being reduced.

CONCLUSIONS

The effective stresses in the bed layer was decreased, that is, the sediment bed was either fully liquefied or partially liquefied by the application of abrupt water pressure change. As a result, a quick removal of sediment was found to transport. The scour depths around the pier were increased by an amount about 10%-18% for the cases studied. The excess scour depths always found maximum at a stage of considerably reduced effective stress under the application of abrupt water pressure change.

ACKNOWLEDGEMENT

This research was supported by a Grant-in-Aid for Scientific Research (C) (1998, 1999, No.10650508) from the Japanese Ministry of Education, Science, Sports and Culture. We are grateful for this support.

REFERENCES

1. Breusers, H. N. C., Nicollet, G., Shen, H. W., 1977, " Local scour around cylindrical piers," Journal of Hydraulic Research, Vol.15(3), pp.211-252.
2. Hancu, S., 1971, "Sur le calcul des affouillements locaux dams la zone des piles de ponts," Proceeding of the 14th IAHR Congress, Vol.3, pp.299-313.
3. Jain, S. C., Fischer, E. E.,1979, "Scour around circular bridge piers at high Froude numbers," FhwA-RD-79-104.
4. Kawata, Y., Tsuchiya, Y., 1988, "Local scour around cylindrical piles due to waves and currents combined," Proceeding of the 21st International Conference on Coastal Engineering, Vol.2, pp-1310-1322.
5. Laursen, E. M., Toch, A., 1956, "Scour around bridge piers and abutments," Bulletin number 4, Iowa Highways Research Board.
6. Melville, B. W., Sutherland, A. J., 1988, "Design method of local scour at bridge piers," Journal of Hydraulic Engineering, American Society of Civil Engineers, Vol.114(10), pp.1210-1226.
7. Mia, M. F., Nago, H., 1999, "Dynamic behavior of bed material around bridge pier under abrupt change of water pressure," Proceeding, Abstract Volume, Paper on CD-ROM, XXVIII IAHR Congress.

8. Nago, H., 1981, "Liquefaction of highly saturated sand layer under oscillating water pressure," Memoirs of the School of Engineering, Okayama University, Japan, Vol.16(1), pp.91-104.
9. Nago, H., Maeno, S., 1984, "Effect of water pressure variation on the scour around bridge pier," Annual Meeting, Chugoku Region, Japan Society of Civil Engineers, pp.16-17.
10. Nago, H., Maeno, S., 1986, "Dynamic behavior of sand bed around structure under wave motion," Memoirs of the School of Engineering, Okayama University, Japan, Vol.21(1), pp.81-91.
11. Nago, H., Maeno, S., 1987, "Pore pressure and effective stress in a highly saturated sand bed under water pressure variation on its surface," Natural Disaster Science, Vol.9(1), pp.23-35.
12. Nago, H., Mia, M. F., 1999, "Sand bed liquefaction and sediment transport under water pressure variation," International Symposium on Water Environment, Journal of the Faculty of Environmental Science and Technology, Okayama University (Special Edition), pp.17-21.
13. Rouse, H., 1950, "Engineering Hydraulics," Jhon Willey & Sons, New York, pp.326-331.
14. Saito, E., Sata, S., Shibayama, T., 1990, "Local scour around a large circular cylinder due to wave action," Proceeding of the 22nd International Conference, Coastal Engineering, Delft.
15. Sakai, T., Hatanaka, K. Mase, H., 1992, "Wave-induced stresses in sea bed and its momentary liquefaction," Proceeding of the American Society of Civil Engineers, Vol.118, (WW2), pp.202-206.
16. Shen, H. W., Schneider, V. R., Karaki, S., 1969, "Local scour around bridge piers," Proceeding of the American Society of Civil Engineers, Vol.95(6), pp.1919-1940.
17. Sumer, B. M., Fredose, J., Christiansen, N., 1992, "Scour around vertical pile in waves," Proceeding of the American Society of Civil Engineers, Vol.118(1), pp.15-31.
18. U.S. Department of Transportation., 1993, "Evaluating scour at bridges," Hydraulic Engineering, Circular No. 18, Rep. No. FHwA-IP-90-017.
19. Whitehouse, R. J. S., 1998, "Scour at marine structures," A manual for practical applications, Thomas Telford Ltd., pp.30.
20. Zen, K., Yamakazi, H., 1993, "Wave-induced liquefaction in a permeable sea bed," Report of the Port and Harbour, Research Institute, Japan, Vol.6, pp.155-192.

SCOUR OF ROCK AND OTHER EARTH MATERIALS AT BRIDGE PIER FOUNDATIONS

By

George W. Annandale[1], Steven P. Smith[2] and Tamara Butler[3]

ABSTRACT

Bridge foundations must be designed to withstand the effects of scour from extreme flood events that could potentially occur during the structure's life. Many equations are available to assist in the prediction of scour at bridge crossings but until recently, few accounted for the effects of gradation and none for the effects of cohesion and consolidation. No quantitative procedure for predicting bridge pier scour in rock has previously been available to practicing engineers.

Recognizing this need the United States Transportation Research Board Committee on Hydraulics, Hydrology and Water Quality identified scour in erodible rock and consolidated materials as one of its top three hydraulic problems. One of the methods that have been developed to address this need (Smith et al. 1997) is based on the Erodibility Index Method (Annandale 1995). The Erodibility Index Method is a semi-empirical method that can be used to estimate the erodibility of any earth material, including cohesionless granular soil (sand, gravel and cobbles), cohesive soil, and jointed and fractured rock.

This paper summarizes the Erodibility Index Method and explains how it is used to calculate the depth of scour around bridge piers. Application of the method is demonstrated by means of a case study.

INTRODUCTION

This paper introduces concepts that can be used to explain the scour resistance of complex earth materials such as rock, slickensided and cohesive clays, and also non-cohesive granular material. A semi-empirical approach that can be used to quantify the relative ability of these earth materials to resist scour is presented, concomitantly with a method that can be used to calculate the depth of scour around bridge piers.

The first bridge pier scour analysis using the Erodibility Index Method was conducted for the Northumberland Strait Bridge (Anglio et al. 1996) (Figure 1). This analysis entailed verification of the Erodibility Index Method by using material properties and estimates of the erosive power of water that caused scour in rock around one of the bridge piers. Laboratory

---

[1] Director Water Resource Engineering, Golder Associates Inc., 44 Union Blvd, Suite 300, Lakewood, Colorado 80228.
[2] Hydraulic Design Manager, URS Greiner Woodward Clyde, 4582 South Ulster Street, Denver, Colorado 80237.
[3] Engineer, Golder Associates Inc., 44 Union Blvd, Suite 300, Lakewood, Colorado 80228.

studies were conducted to quantify the relative magnitude of the erosive power of water around the bridge piers. The verified relationship and estimates of the relative magnitude of the erosive power of water for design conditions were used to predict the likelihood of scour at other bridge piers and to design countermeasures.

Subsequent research on the application of the Erodibility Index Method resulted in a method to calculate the depth of scour at bridge pier foundations. This paper summarizes the Erodibility Index Method, conceptually explains how to apply the method to calculate scour depth around bridge piers, and presents a case study.

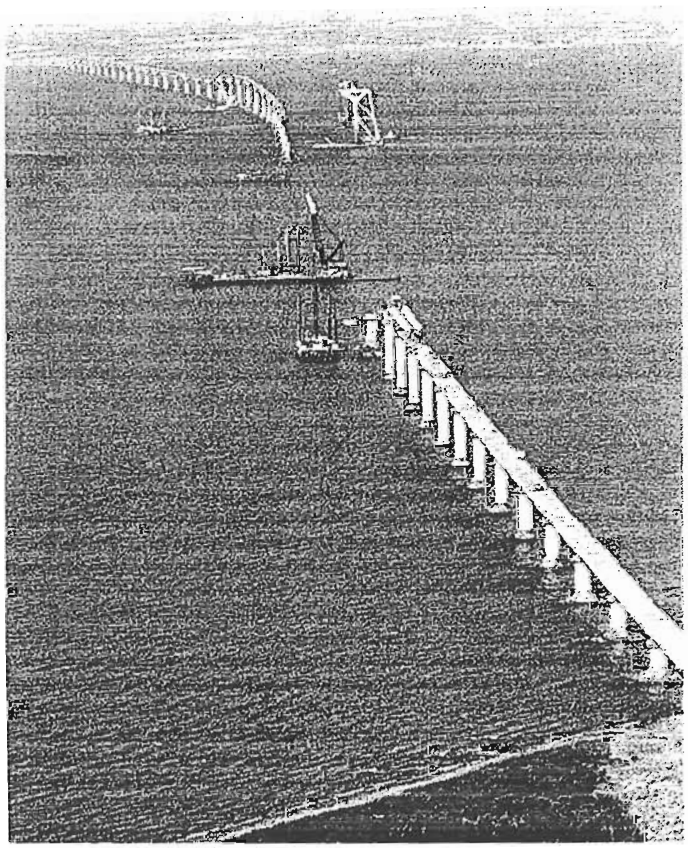

Fig. 1 Northumberland Strait Bridge

ERODIBILITY INDEX METHOD

Development of methods that can be used to predict initiation of scour is challenging, and has been the subject of research for many years (e.g. Shields 1936, Hjulstrom 1935, Yang 1973). However, available methods are often limited in their application because they either oversimplify the complexity of the hydraulic processes or they oversimplify the complexity of factors determining the relative ability of earth material to resist scour.

Successful scour models capture the complexity of the behavior of earth materials as well as the essence of the principal processes that quantify the relative magnitude of the erosive power of water. Assumptions that small-scale processes govern the erosion of earth material often referred to as 'grain-by-grain' removal, can misrepresent actual scour processes because natural earth materials are seldom uniform. The non-uniformity of earth materials is a factor that should be acknowledged when assessing its relative ability to resist erosion. This implies that sole reliance on test results of one parameter, such as undrained shear strength or particle size, can potentially lead to incorrect assessment of the relative ability of earth material to resist scour. Experience has shown that large-scale processes often dominate the scour process (e.g. Annandale 1995; Annandale, et al. 1998; Cohen and Von Thun 1994), and that larger units of earth material may scour prior to grain-by-grain removal. This applies to cases of scour of jointed and fractured rock, and to scour of fissured and slickensided clays. The joints in these materials are often weaker than the crystalline bonds between rock particles or the electromagnetic bonds created by the Van der Waals forces between clay particles. Failure during the scour process in such cases often proceed along the discontinuities before the clay or rock blocks, delineated by these discontinuities, break.

The Erodibility Index Method empirically incorporates the principal factors that determine the relative ability of earth material to resist erosion. Conceptual sketches representing the scour process in four material types are presented in Figure 2. Figure 2(a) represents a granular material and Figure 2(b) a uniform cohesive soil. A schematic representation of scour in slickensided or fissured clay is presented in Figure 2(c), whereas the same for jointed and fractured rock is presented in Figure 2(d).

Plucking and cyclic loading introduced by turbulence, most probably the dominant processes in scour of earth materials (Briaud, et al. 1999), act in addition to shear stress to scour earth material. Materials mainly held together by gravity bonds scour principally because of fluctuating forces developing over individual particles, as would be the case for cohesionless granular soil (Figure 2(a)). The fluctuating forces pluck the soil particles out of their positions of rest. In the case of uniform cohesive soil, the cyclic loading introduced by the plucking forces weakens the soil, resulting in scour as the soil gradually yields (Figure 2(b)).

Consideration of the scour process in more complex materials, such as slickensided or fissured clays, or jointed and fractured rock, indicate that the role of fluctuating pressure is very important. A conceptual model for the scour process in these materials entails the following. When water flows over, say, rock (Figure 2(d)), some of the water penetrates the joints and fractures. The pressure caused by the presence of the water between the rock blocks is equal to hydrostatic pressure, determined by the difference between the elevation within the joint and the elevation of the water surface above the joint. Water flowing over the rock is turbulent, resulting in pressure fluctuations at the interface between the rock and the water. The balance between the hydrostatic pressure within the rock fractures and joints, and the fluctuating pressures at the interface results in net fluctuating forces acting on the blocks of rock. The fluctuating pressures move the blocks from their positions of rest, and finally dislodge them. Once dislodged, the water can displace the rock, provided it has enough power. This same concept is applicable to fissured or slickensided cohesive soils, conceptually shown in Figure 2(c). Failure is likely to occur along the fractures and joints in the rock, and along the fissures and slickensides in the clay, before failure of the blocks of rock or clumps of clay themselves occur.

Material Resistance

When scour in a complex earth material such as rock is considered, the relative ability of such earth materials to resist erosion is defined by multiple parameters. Material properties that determine scour resistance of rock include intact material strength, block size, shear strength between blocks of rock, and the relative shape and orientation of the rock blocks. By making use of parameters that represent the relative role of each of these properties to resist erosion it is possible to define a geo-mechanical index that quantifies the relative ability of earth material to resist erosion. Research (Annandale 1995) has shown that the relative ability of other earth materials to resist erosion, such cohesionless silt, sand, gravel and cobbles, and cohesive earth materials, can also be quantified with the same set of parameters as used for rock. The Erodibility Index, which is identical to Kirsten's Excavatability Index (Kirsten 1982) is defined by the equation

$$K = M_s \cdot K_b \cdot K_d \cdot J_s \tag{1}$$

Where M_s = intact material strength number; K_b = block or particle size number; K_d = discontinuity or inter-particle bond shear strength number; and J_s = relative shape and orientation number. Tables and methods to quantify the constituent parameters are presented in Annandale (1995), Kirsten (1982) and the National Engineering Handbook (NRCS 1997).

Erosive Power of Water

The Erodibility Index Method uses stream power, which is equivalent to the rate of energy dissipation in flowing water, to represent the erosive power of water. (These terms are used interchangeably in this paper). By making use of this variable it is possible to quantify the relative magnitude of pressure fluctuations, which play an important role in initiating sediment motion and maintaining sediment transport. In order to support the hypothesis that the rate of energy dissipation can be used to represent the relative magnitude of pressure fluctuations, Annandale (1995) analyzed observations by Fiorotto and Rinaldo (1992) who measured pressure fluctuations under hydraulic jumps. The results of the analysis indicated that the standard deviation of pressure fluctuations is directly proportional to the rate of energy dissipation (Figure 3). This finding supports the use of stream power to quantify the relative magnitude of the erosive power of water. Increases in stream power are related to increases in fluctuating pressures, which form the basis of the conceptual model of the erosion process schematized in Figure 2. A method that can be used to determine the magnitude of the rate of energy dissipation around bridge piers are presented further on in this paper.

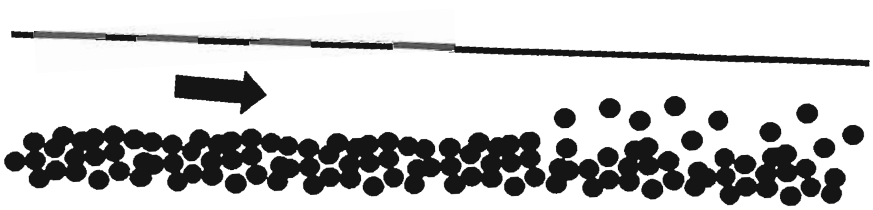

(a) Cohesionless, granular soil.

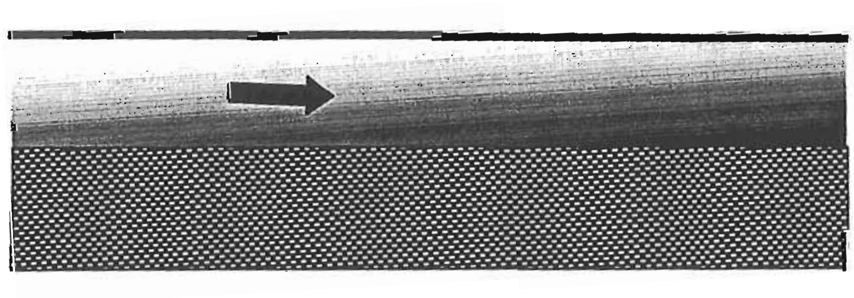

(b) Uniform, cohesive soil.

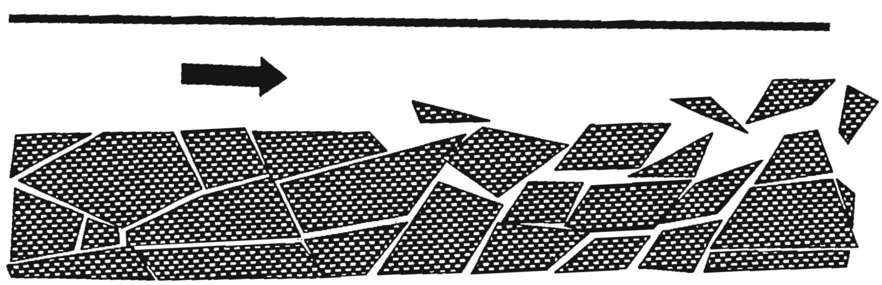

(c) Slickensided clay.

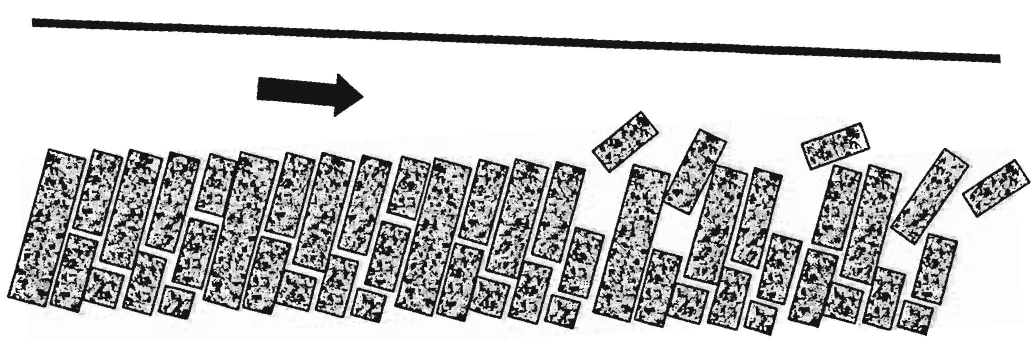

(d) Jointed and fractured rock.

Fig. 2 Conceptual representation of erosion for a number of earth material types.

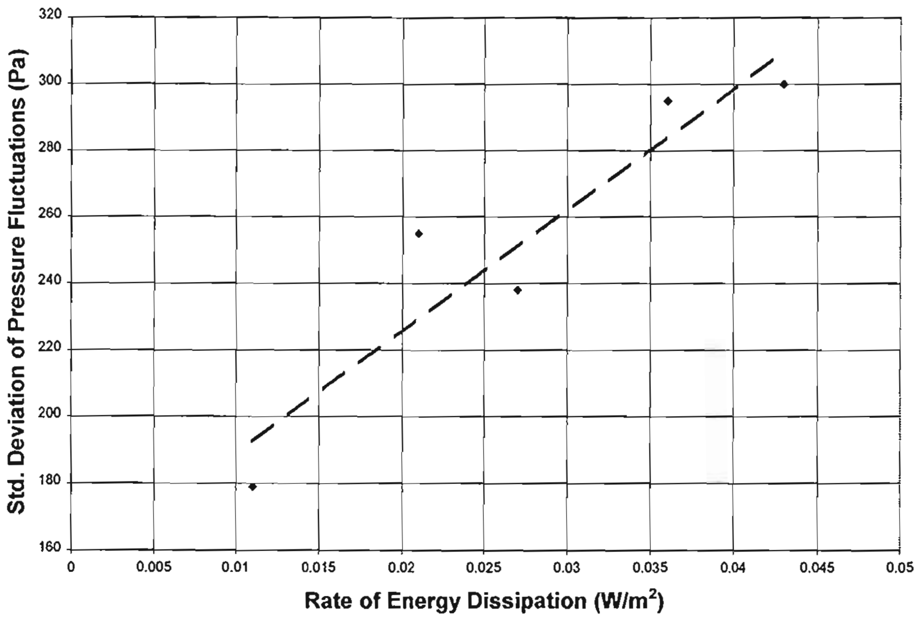

Fig. 3 Relationship between the rate of energy dissipation and standard deviation of pressure fluctuations (Annandale 1995).

Erosion Threshold

The correlation between stream power (p) and a mathematical function ($f(K)$) that represents an earth material's relative ability to resist erosion can, at the erosion threshold, be expressed by the relationship:

$$P = f(K) \tag{2}$$

If $p > f(K)$, the erosion threshold is exceeded, and the earth material is expected to erode. Conversely, if $p < f(K)$, the erosion threshold is not exceeded, and the earth material is expected not to erode. The function $f(K)$ represents the Erodibility Index as defined by equation (1).

Annandale (1995) established a relationship between stream power and the Erodibility Index by analyzing published data pertaining to the erosion threshold of cohesionless granular material and field data pertaining to the scour of rock, cohesive soils and vegetated soils. The published data that was used include data by Tison (1953), Gilbert (1914), Kramer (1935), U.S. Army Corps of Engineers, Waterways Experiment Station (WES, 1935) and Vanoni (1964). The field data pertaining to the erosion of cohesive soil, vegetated soil and rock was obtained from the Agricultural Research Service (1984 and 1991), Cohen and Von Thun (1994) and van Schalkwyk (1992).

Figure 4 shows the result of the analysis of field data pertaining to scour of cohesive material, vegetated soil, and fractured and jointed rock. Two data types are plotted on the graph, consisting of events where scour occurred and events where scour did not occur. The dotted line indicates the approximate location of the erosion threshold.

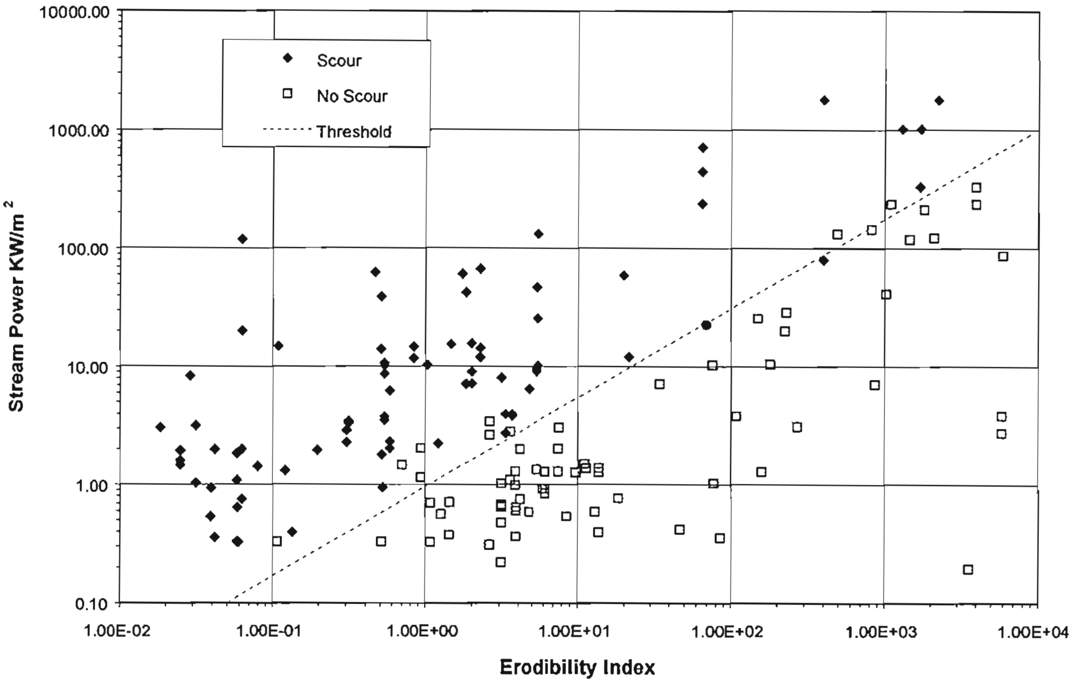

$\lg P = \frac{3}{4} \lg K_h$

Fig. 4 Erosion threshold for higher values of the Erodibility Index (Annandale 1995).

Figure 5 contains the results of the analysis of erosion threshold data for cohesionless granular material ranging from silt to sand, gravel and cobbles. The results plotted on this graph represent the relationship between stream power and the Erodibility Index at the threshold of erosion. Because the relationship is located at the threshold of erosion, the scatter is less than that on Figure 4.

If all the data is plotted on one graph (Figure 6) the erosion threshold on Figure 5 connects with the erosion threshold on Figure 4 (the dotted line). The dotted line of Figure 4 is not shown on Figure 6, due to scale difficulties, but is located at the lower boundary defined by the set of points in the upper right hand part of the figure that represent scour events. It is concluded that the erosion threshold line, as defined by the relationship between stream power and the Erodibility Index, forms a continuous curve for the whole range of earth materials. The earth material represented on Figure 6 ranges from silt (at the lower end of the figure) to hard, intact rock (at the upper end of the figure). The erosion threshold lines presented in Figures 4 through 6 can be used to determine the erodibility of earth materials and to calculate the extent (depth) of scour. The methods used to achieve these objectives are conceptually discussed in what follows.

? linear

Determination of Erodibility

The erodibility of earth materials is determined by plotting the Erodibility Index for a given earth material and the magnitude of the stream power on Figures 4, 5 or 6. If the plotted point is located above the erosion threshold line erosion is expected to occur and if it is located below the threshold line erosion is not expected to occur (Figure 7).

$\approx \quad \lg P = \lg K_b \cdot \frac{5}{11}$

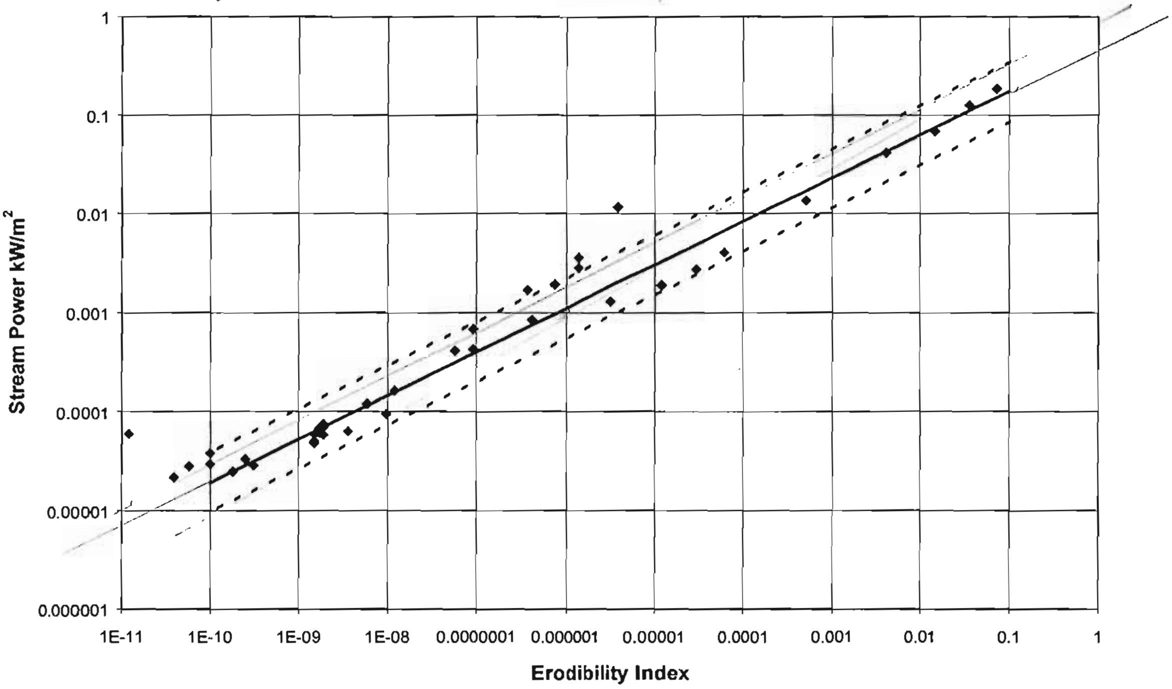

Fig. 5 Erosion threshold for lower values of the Erodibility Index (Annandale 1995).

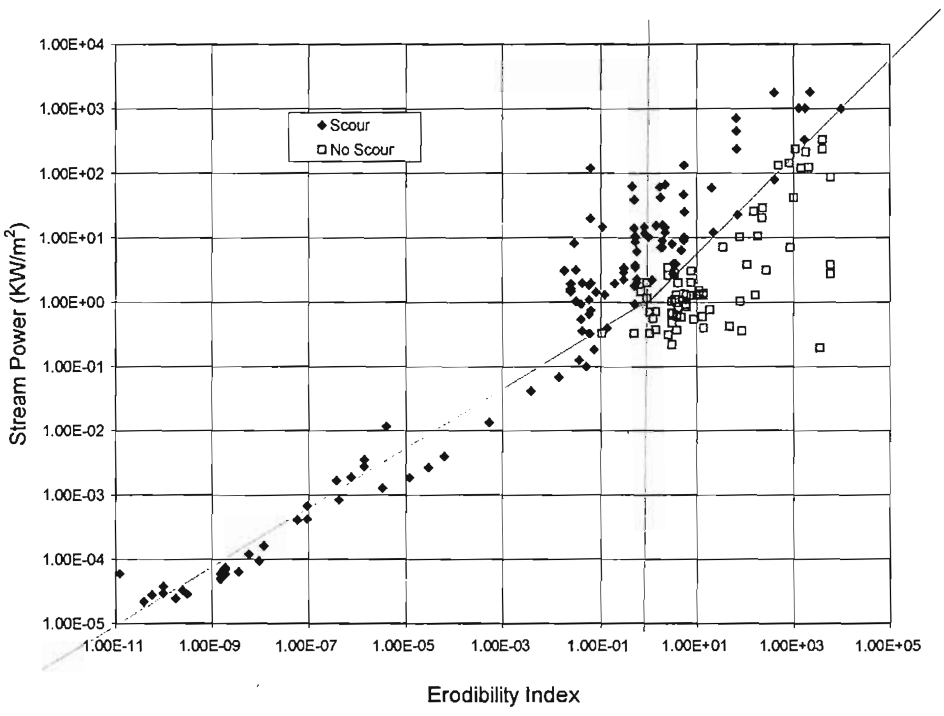

Fig. 6 Erosion threshold for the entire range of earth materials, ranging from silt to intact, massive rock – combining Figures 4 and 5 (Annandale 1995).

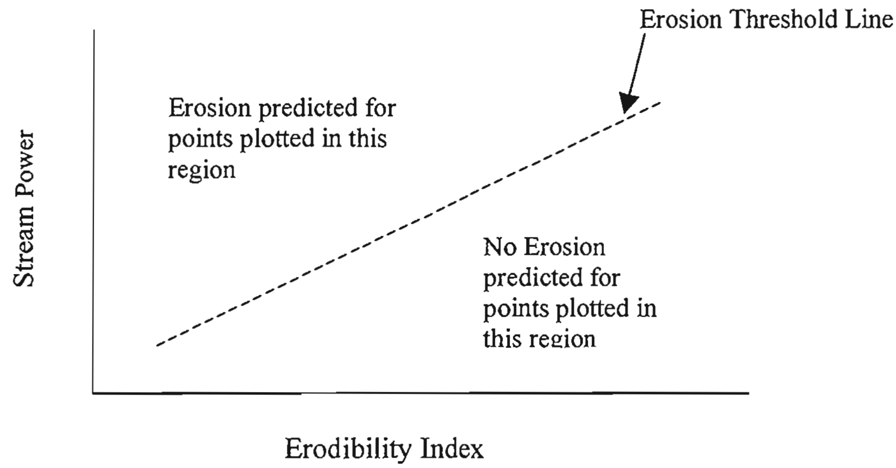

Fig. 7 Determination of erodibility of earth materials.

Determination of Extent of Scour

The extent (depth) of scour is determined by comparing the stream power that is *available* to cause scour with the stream power that is *required* to scour the earth material under consideration. The available stream power represents the erosive power of the water discharging over the earth material, whereas the required stream power is the stream power that is required by the earth material for scour to commence. If the available stream power is exactly equal to the required stream power, the material is at the threshold of erosion. In cases where the available stream power exceeds the required stream power, the material will scour. Otherwise, it will remain intact.

Figure 8 shows how the available and required stream power, both plotted as a function of elevation beneath the riverbed, are compared to determine the extent of scour. Scour will occur when the available stream power exceeds the required stream power. Once the maximum scour elevation is reached the available stream power is less than the required stream power, and scour ceases.

The required stream power is determined by first indexing a geologic core or borehole data. The values of the Erodibility Index thus determined will vary as a function of elevation, dependent on the variation in material properties. Once the index values at various elevations are known, the required stream power is determined from Figure 4 or 5, as conceptually shown in Figure 9. Figure 9 indicates that the stream power required to scour a particular earth material is determined by entering the erosion threshold graph on the abscissa, with the Erodibility Index known, moving vertically to the erosion threshold line, and reading the required stream power on the ordinate. Figure 10 illustrates that the process is repeated as a function of elevation below the riverbed. The values of the required stream power is then plotted as a function of elevation.

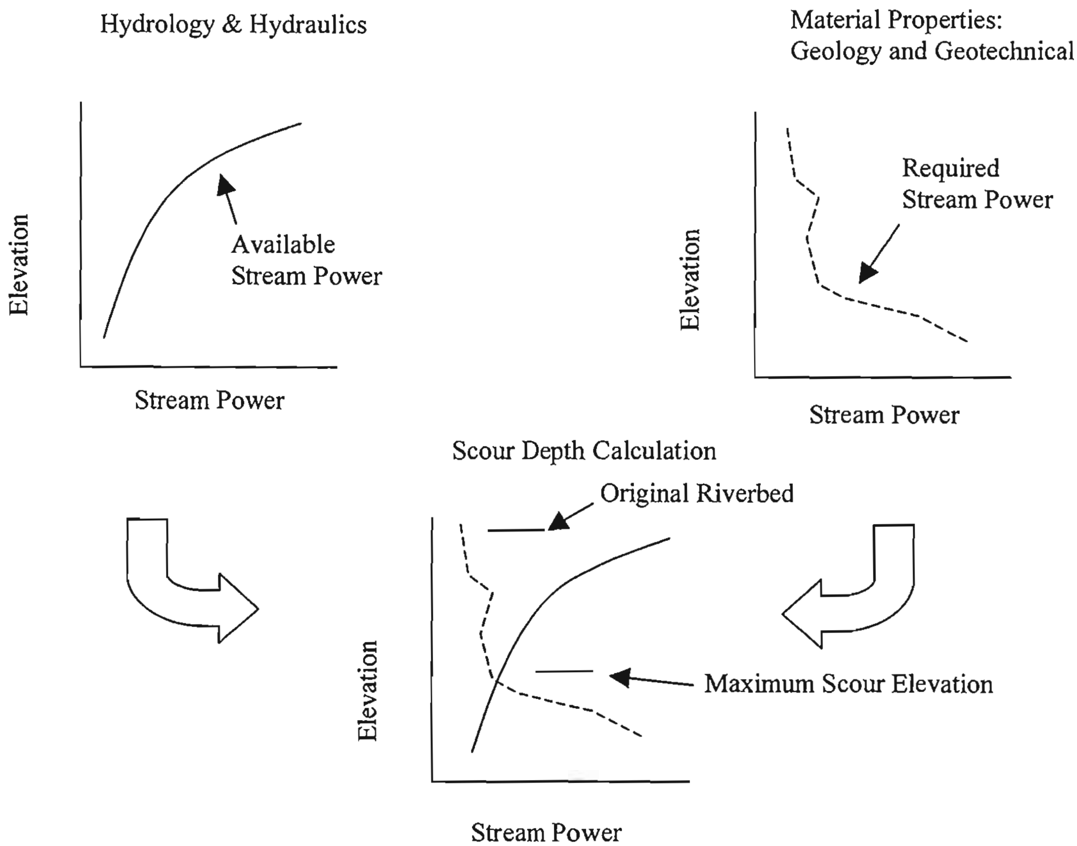

Fig. 8 Determination of the extent of scour by comparing available and required stream power.

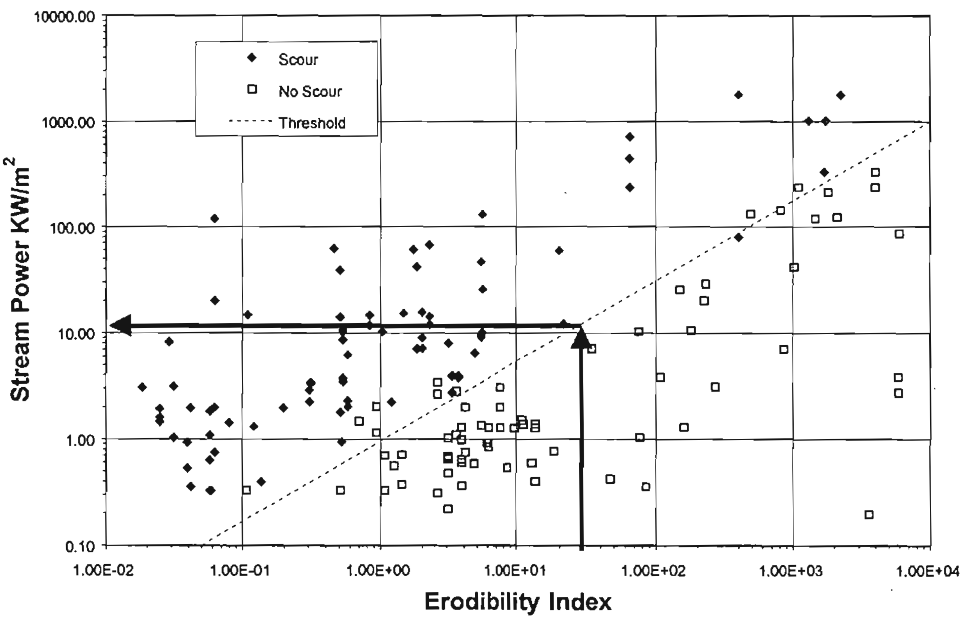

Fig. 9 Determination of stream power that is required to scour earth material once the value of the Erodibility Index is known.

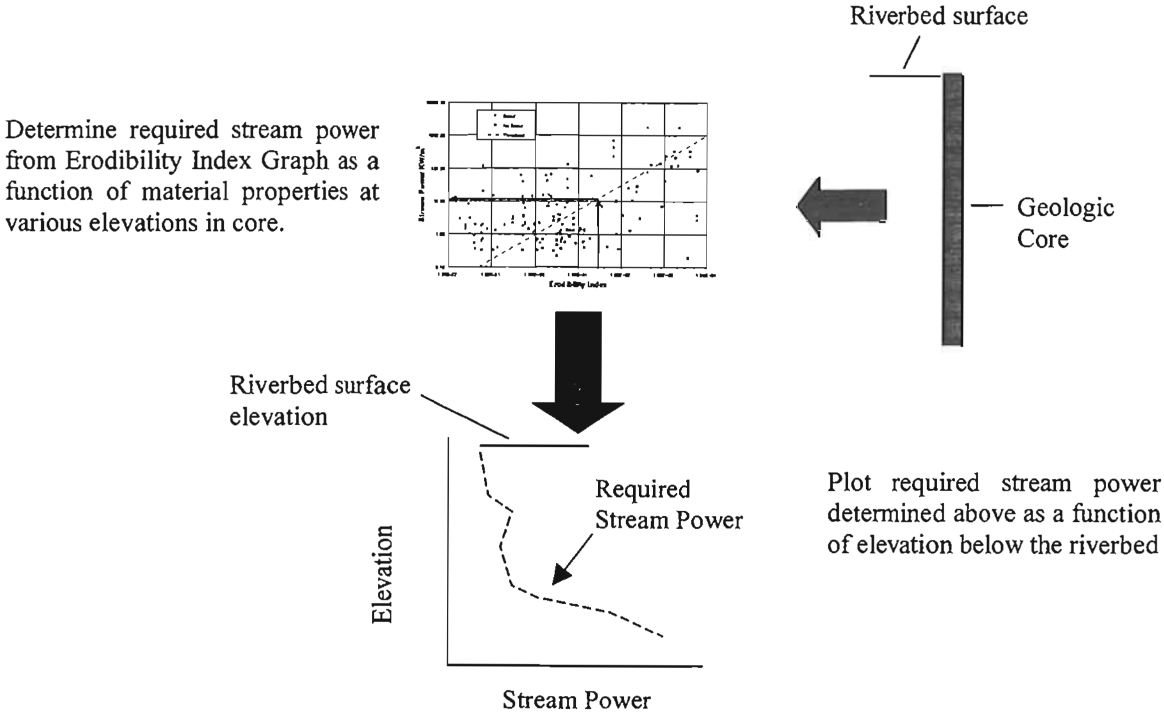

Fig. 10 Development of a relationship between the required stream power and elevation below a riverbed.

EROSIVE POWER AROUND BRIDGE PIERS

As water flows around bridge piers very complex flow patterns develop that increase its turbulence intensity and erosive power. The increase in erosive power of water causes scour around bridge piers that has resulted in the failure of bridges. Research conducted by the FHWA (Smith et al. 1997) concluded that the erosive power of water around bridge piers decrease as scour holes increase in depth. This finding has significant implications because earth material often increases in strength as a function of elevation below a riverbed. Concurrent decrease in the magnitude of the erosive power of water and increase in earth material strength causes scour holes around bridge piers to have finite depths. The maximum scour depth occurs at the elevation where the erosive power of water is less than the erosive power that is required to cause scour of the earth material at that elevation.

Estimates of the magnitude of the erosive power of water as a function of scour hole depth can be made by means of physical hydraulic model studies, three-dimensional computer simulation or graphs that are based on the results of the FHWA research (Smith et al. 1997). Figure 11 shows the change in stream power around bridge piers as scour holes increases in depth. The stream power is expressed in dimensionless form as the ratio P/P_a, and scour depth as the dimensionless ratio y_s/y_{max}. P_a is the magnitude of the approach stream power in the river upstream of the pier and P is the magnitude of variable stream power at the base of the scour hole as it increases in depth. The variable y_{max} represents the maximum scour depth for given flow conditions that can develop around a bridge pier without regard to scour resistance offered by earth material, whereas y_s represents variable scour depth ($y_s \leq y_{max}$).

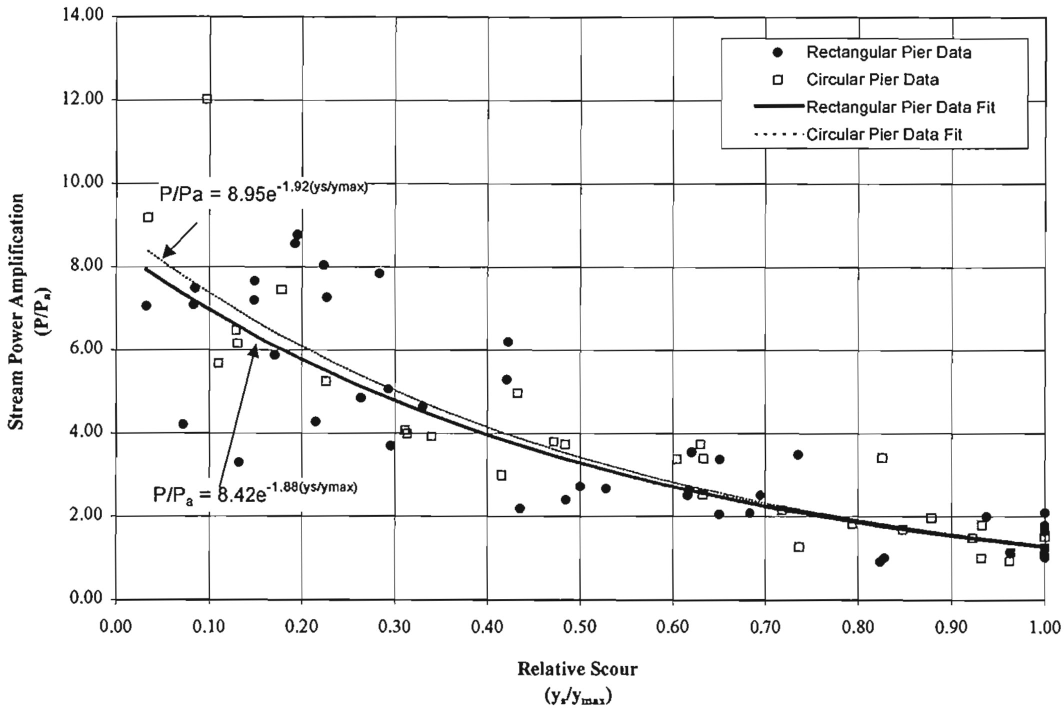

Fig. 11 Dimensionless stream power at the base of a scour hole versus dimensionless scour hole depth from FHWA.

Quantification of the axes of Figure 11 requires estimates of the approach stream power (P_a) and the maximum scour depth (y_{max}). The equation that is used to calculate the approach stream power is based on the equation derived by Bagnold (1966),

$$P_a = \tau v \tag{3}$$

where P_a = approach stream power per unit area of the bed (W/m^2), τ = shear stress on the bed (N/m^2) and v = velocity (m/s).

By writing shear stress τ as a function of the unit weight of water, flow depth and energy slope, approach stream power can also be expressed as:

$$P_a = \gamma \, d \, s \, v \tag{4}$$

where d = flow depth (m), γ = unit weight of water (N/m^3), s = dimensionless energy slope (or bed slope in the case of uniform, steady flow), and v = velocity (m/s).

An estimate of y_{max} can be obtained by making use of the bridge pier scour equation in HEC-18 (FHWA 1995), which is based on an envelope curve embracing a large number of bridge pier scour experiments. This equation (presented below) is considered to provide a conservative estimate of scour depth.

$$\frac{y_s}{y_1} = 2.0 \cdot K_1 \cdot K_2 \cdot K_3 \cdot \left(\frac{a}{y_1} \right)^{0.65} Fr_1^{\ 0.43} \tag{5}$$

L kommt nicht vor!

where y_s = scour depth (ft), y_1 = flow depth directly upstream of the pier (ft), K_1 = correction factor for pier nose shape, K_2 = correction factor for angle of attack of flow, K_3 = correction factor for bed condition, a = pier width (ft), L = length of pier (ft), Fr_1 = Froude Number = $V_1/(gy_1)^{1/2}$, and V_1 = mean velocity of flow directly upstream of the pier (ft/s).

With y_{max} assumed to be the maximum scour, the scour depth estimated with the Erodibility Index Method can never exceed this value. The range of scour depth estimates for this method is therefore $0 \leq y_s \leq y_{max}$.

CASE STUDY: WOODROW WILSON BRIDGE

The Woodrow Wilson Bridge over the Potomac River is an essential part of local, regional and national transportation systems (Figure 12). The Bridge carries six lanes of Capital Beltway traffic between Alexandria, Virginia and Oxon Hill, Maryland and is the last river crossing for approximately 50 miles down river. Congestion and the frequency of drawbridge openings for marine traffic cause traffic delay at the bridge. The Woodrow Wilson Bridge is one of a few on the Interstate highway system that contains a movable span. Under current Coast Guard regulations, the 50-foot high drawbridge opens approximately 240 times per year to allow for the passage of marine traffic traveling the Potomac River.

The five-mile section of the Beltway within the project area serves as a systematic link for local traffic on major north-south roadways feeding into interchanges at Telegraph Road, US Route1, I-295 and MD 210. Furthermore, the eastern half of the Beltway, including the Woodrow Wilson Bridge, is designated as I-95 and constitutes a critical link in the Maine to Florida interstate route. Because the adjacent section of the hectic Beltway is eight lanes wide, the current six-lane Woodrow Wilson Bridge represents a severe bottleneck on the highway system.

Furthermore, the existing Woodrow Wilson Bridge cannot last much beyond 2004 without major structural rehabilitation. The inspections and repair activities at the Bridge would result in extended traffic delays and increased costs. Replacing the Bridge before 2004 will greatly reduce traffic delays in the area.

In 1992, a Coordination Committee of affected jurisdictions from Maryland, Virginia, and the District of Columbia and local, regional, state and federal governments began investigating solutions to the traffic problems at Woodrow Wilson Bridge. The Committee approved a "Preferred Alternative" in 1996, which featured a facility with side-by-side, movable span, twin bridges with a 70-foot navigational clearance. The new twin bridges will carry 10 lanes of traffic plus two future High Occupancy Vehicle (HOV) lanes. The new Bridge design will clear the river by 70 ft, which will reduce the number of openings by more than two-thirds, thus decreasing traffic delays.

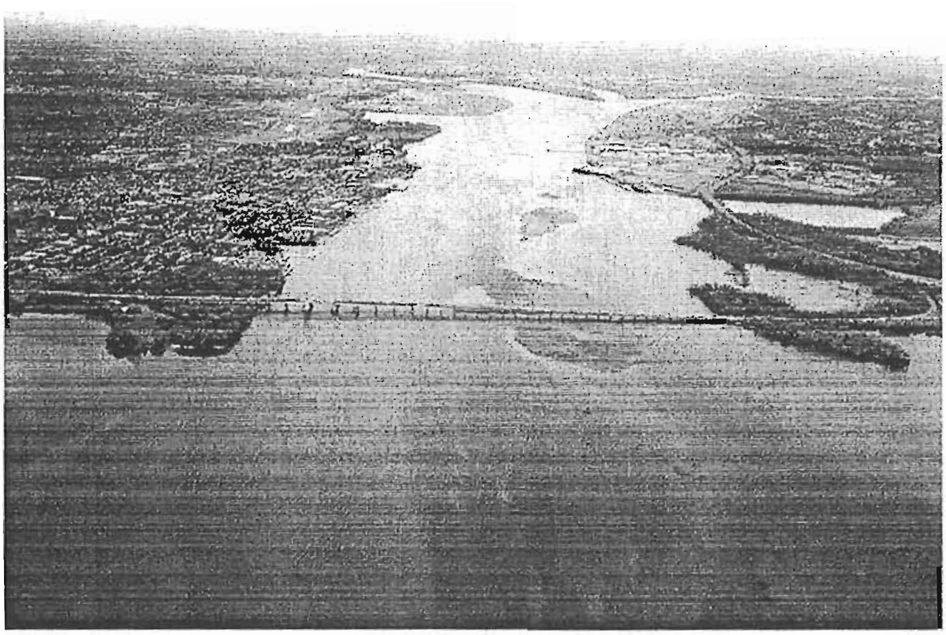

Fig. 12 Potomac River and the existing Woodrow Wilson bridge. Virginia is on the left side of the bridge; Maryland is on the right side of the bridge.

This case study summarizes the procedure followed to estimate scour with the Erodibility Index Method at the proposed Woodrow Wilson Bridges. The analysis entailed assessment of riverbed material properties, hydraulic analysis and scour analysis as outlined in this paper. Potential scour depths for the 100-year and 500-year floods were calculated for each of the proposed bridge piers (see Figure 13 for schematic of bridge pier layout). Factors of safety against scour were also calculated.

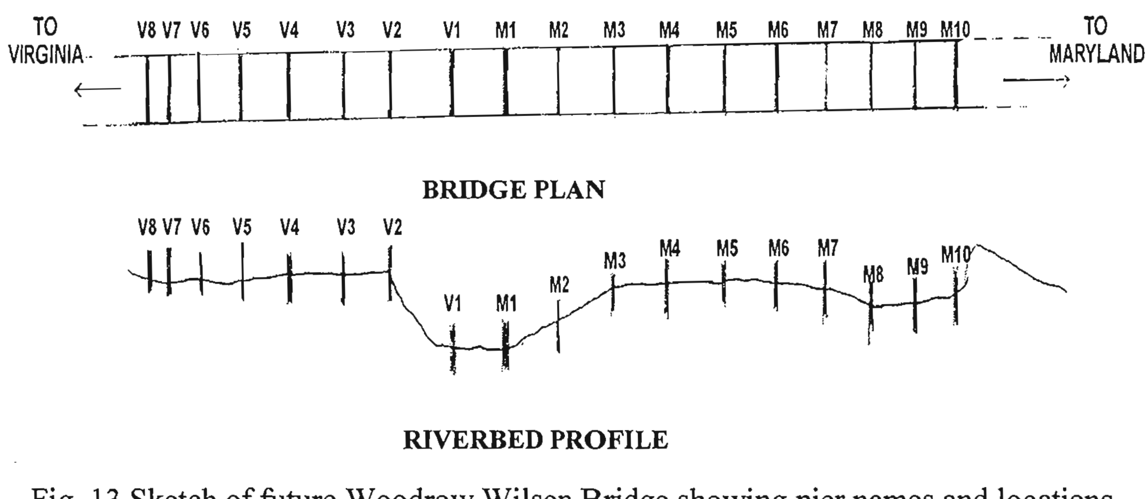

Fig. 13 Sketch of future Woodrow Wilson Bridge showing pier names and locations.

Riverbed Material Properties and Required Stream Power

Borehole logs, and shear strength and Dilatometer test results were used to calculate the Erodibility Index of the riverbed. Boreholes, drilled near all of the proposed bridge piers, provided soil property information through descriptions and blow counts. Soil profiles near piers V1 and M1 through M5 have a thick layer of very soft to soft gray to brown silty clay, with some sand and gravel. Below is a layer of Pleistocene era terrace deposits, which are gray and brown, dense to very dense sand with silt, gravel and clay lenses. Finally, the Cretaceous period Potomac group consists of hard gray clay. Soil profiles near piers M6 through M10 and V2 have a thinner layer of soft to very soft alluvial clay, followed by a thin layer of alluvial deposits that consist of loose medium dense brown silty sand. The Pleistocene terrace deposits and Cretaceous Potomac group deposits follow. Dilatometer test results were used to estimate the undrained shear strength of the soil and the residual angle of friction. The shear strength test results were used to confirm the estimates made with the Dilatometer test results.

Estimates of parameter values for the intact material strength number (M_s), the block or particle size number (K_b), the discontinuity or inter-particle bond shear strength number (K_d) and the relative shape and orientation number (J_s) were required to estimate the Erodibility Index. Estimation of each of these for the Woodrow Wilson Bridge are summarized in what follows.

Intact Material Strength Number (M_s)

In-situ Dilatometer Test (DMT) results were used to determine a relationship between depth and undrained shear strength of the very soft to soft clay material. A relationship was developed for the soft clay deposits, which begins at the riverbed surface and extends to various depths throughout the bridge cross-section of the riverbed. The soft and very soft alluvial deposits layer was estimated to have a cohesive intercept of 3.5 kPa and a residual angle of friction, ϕ, is 8.1°. The simplified relationship between undrained shear strength and depth below the original ground surface is:

$$Su = 3.5 + 1.42 \cdot H, \tag{6}$$

where: Su = undrained shear strength of soft and very soft alluvial deposits (kPa) and H = depth to the point in question from the original ground surface (m).

For borehole depths where the very soft to soft clay was found, equation (6) was used to calculate the undrained shear strength. The intact material strength number for cohesive soils can be calculated with the following equation (NRCS 1997),

$$M_s = 0.78 \cdot (UCS)^{1.09} = 0.78 \cdot (2 \cdot Su)^{1.09}, \tag{7}$$

where: *UCS* = unconfined compressive strength (MPa), which must be less than 10 MPa for this equation to be valid.

The intact material strength number for non-cohesive granular material was based on SPT blow counts and values from Table A-1 in Annandale (1995).

For pier M10 column (4) of Table 1 shows the value of Su (kPa) or the SPT blow count, whichever is applicable according to the log, at various depths below the riverbed surface. Note that Su values appear as decimal numbers; blow counts appear as whole numbers. Column (5) of Table 1 shows the estimated values of M_s.

Block or Particle Size Number

The borehole log material descriptions were used to determine the particle/block size number, K_b. K_b was assigned a value of one for all materials except the hard clay. The hard clay of the cretaceous period Potomac group was assigned a value of 100. The reason for using K_b = 100 for the cretaceous period clay is that the clay is so hard that it can be viewed as soft intact rock according to tables in Annandale (1995). K_b determinations for pier M10 are shown in column (6) of Table 1.

Discontinuity or Inter-particle Bond Shear Strength Number

The shear strength number, K_d, was calculated using the following equation (Annandale 1995):

$$K_d = \tan(\phi), \tag{8}$$

where ϕ = 8.1° for the very soft to soft clay material, but = 30° for all other materials. K_d values with depth for pier M10 are shown in Table 1 column (7).

Relative Shape and Orientation Number

A value of one was assigned to the ground structure number, J_s, in all cases (Annandale 1995). J_s is shown in column (8) of Table 1.

Erodibility Index and Required Power

Erodibility Index (EI), the product of Ms, Kb, Kd, and Ks, is shown in Table 1 column (9). The power required to scour the Potomac River's bed material was determined using Annandale's (1995) erosion threshold (Wittler, et al. 1998) for low strength materials (as a conservative approach):

$$pR = 0.48 \cdot EI^{0.44} \tag{9}$$

where: pR = power required to scour granular material (kW/m^2). Required stream power is calculated in Table 1 column (10) for pier M10.

Table 1 Pier M10 calculations for available and required stream power for scour determination.

										100-Year Flood					500-Year Flood				
(1)	(2)	(3)	(4)	(5)	(6)	(7)	(8)	(9)	(10)	(11)	(12)	(13)	(14)	(15)	(16)	(17)	(18)	(19)	(20)
Depth (ft)	Elevation (ft)	Depth, H (m)	Su (kPa) OR SPT	Ms	Kb	Kd	Js	El	Required Stream Power (KW/m^2)	Dimension-less scour depth	Relative Stream Power	Available Stream Power (KW/m2)	P_R/P_A	Scour (Y/N)?	Dimension-less scour depth	Relative Stream Power	Available Stream Power (KW/m2)	Scour (Y/N)?	P_R/P_A
0	-2.39	0	3.5	0.003	1	0.142	1	0.000	0.017	0					0				
1	-3.39	0.305	3.933	0.004	1	0.142	1	0.001	0.018	0.018	8.15	0.0784	0.23	yes	0.016	14.12	0.3381	yes	0.05
2	-4.39	0.610	4.366	0.004	1	0.142	1	0.001	0.019	0.036	7.88	0.0758	0.25	yes	0.032	13.55	0.3247	yes	0.06
3	-5.39	0.914	4.798	0.005	1	0.142	1	0.001	0.020	0.054	7.62	0.0733	0.27	yes	0.047	13.02	0.3118	yes	0.06
4	-6.39	1.219	5.231	0.005	1	0.142	1	0.001	0.020	0.071	7.36	0.0709	0.29	yes	0.063	12.50	0.2994	yes	0.07
5	-7.39	1.524	5.664	0.006	1	0.142	1	0.001	0.021	0.089	7.12	0.0685	0.31	yes	0.079	12.00	0.2875	yes	0.07
6	-8.39	1.829	6.097	0.006	1	0.142	1	0.001	0.022	0.107	6.88	0.0662	0.33	yes	0.095	11.52	0.2760	yes	0.08
7	-9.39	2.134	6.530	0.007	1	0.142	1	0.001	0.023	0.125	6.66	0.0641	0.36	yes	0.111	11.06	0.2650	yes	0.09
8	-10.39	2.438	6.963	0.007	1	0.142	1	0.001	0.023	0.143	6.44	0.0619	0.38	yes	0.126	10.62	0.2545	yes	0.09
9	-11.39	2.743	7.395	0.008	1	0.142	1	0.001	0.024	0.161	6.22	0.0599	0.40	yes	0.142	10.20	0.2444	yes	0.10
10	-12.39	3.048	7.828	0.008	1	0.142	1	0.001	0.025	0.179	6.02	0.0579	0.43	yes	0.158	9.80	0.2347	yes	0.11
11	-13.39	3.353	8.261	0.009	1	0.142	1	0.001	0.026	0.196	5.82	0.0560	0.46	yes	0.174	9.41	0.2253	yes	0.11
12	-14.39	3.658	8.694	0.009	1	0.142	1	0.001	0.026	0.214	5.62	0.0541	0.48	yes	0.190	9.03	0.2164	yes	0.12
13	-15.39	3.962	9.127	0.010	1	0.142	1	0.001	0.027	0.232	5.44	0.0523	0.51	yes	0.205	8.67	0.2077	yes	0.13
14	-16.39	4.267	9.559	0.010	1	0.142	1	0.001	0.027	0.250	5.26	0.0506	0.54	yes	0.221	8.33	0.1995	yes	0.14
15	-17.39	4.572	2	0.01	1	0.577	1	0.007	0.053	0.268	5.08	0.0489	1.08	no	0.237	8.00	0.1915	yes	0.28
16	-18.39	4.877	2	0.01	1	0.577	1	0.007	0.053	0.286	4.92	0.0473	1.12	no	0.253	7.68	0.1839	yes	0.29
17	-19.39	5.182	2	0.01	1	0.577	1	0.007	0.053	0.304	4.75	0.0457	1.16	no	0.269	7.37	0.1766	yes	0.30
18	-20.39	5.486	2	0.01	1	0.577	1	0.007	0.053	0.321	4.60	0.0442	1.20	no	0.284	7.08	0.1696	yes	0.31
19	-21.39	5.791	2	0.01	1	0.577	1	0.007	0.053	0.339	4.44	0.0428	1.24	no	0.300	6.80	0.1628	yes	0.33
20	-22.39	6.096	1	0.01	1	0.577	1	0.003	0.040	0.357	4.30	0.0414	0.96	yes	0.316	6.53	0.1564	yes	0.25
21	-23.39	6.401	1	0.01	1	0.577	1	0.003	0.040	0.375	4.15	0.0400	0.99	yes	0.332	6.27	0.1501	yes	0.26
22	-24.39	6.706	1	0.01	1	0.577	1	0.003	0.040	0.393	4.02	0.0387	1.03	no	0.348	6.02	0.1442	yes	0.28
23	-25.39	7.010	1	0.01	1	0.577	1	0.003	0.040	0.411	3.88	0.0374	1.06	no	0.363	5.78	0.1384	yes	0.29
24	-26.39	7.315	1	0.01	1	0.577	1	0.003	0.040	0.429	3.76	0.0361	1.10	no	0.379	5.55	0.1329	yes	0.30
25	-27.39	7.620	20	0.07	1	0.577	1	0.042	0.119	0.446	3.63	0.0349	3.40	no	0.395	5.33	0.1276	yes	0.93
26	-28.39	7.925	20	0.07	1	0.577	1	0.042	0.119	0.464	3.51	0.0338	3.52	no	0.411	5.12	0.1226	yes	0.97
27	-29.39	8.230	20	0.07	1	0.577	1	0.042	0.119	0.482	3.40	0.0327	3.64	no	0.427	4.91	0.1177	no	1.01
28	-30.39	8.534	20	0.07	1	0.577	1	0.042	0.119	0.500	3.28	0.0316	3.76	no	0.442	4.72	0.1130	no	1.05
29	-31.39	8.839	20	0.07	1	0.577	1	0.042	0.119	0.518	3.17	0.0305	3.89	no	0.458	4.53	0.1085	no	1.10
30	-32.39	9.144	14	0.06	1	0.577	1	0.033	0.107	0.536	3.07	0.0295	3.62	no	0.474	4.35	0.1042	no	1.03
31	-33.39	9.449	14	0.06	1	0.577	1	0.033	0.107	0.554	2.97	0.0286	3.75	no	0.490	4.18	0.1000	no	1.07

Available Stream Power

The available stream power at each proposed bridge pier was determined with HEC-RAS model results. The available power around the bridge piers was expressed as a function of scour hole depth and quantified through a three-step process using the available data.

First, the available stream power of the Potomac River at a point upstream of the proposed bridge was calculated for each proposed pier using:

$$P_a = \gamma \cdot v \cdot d \cdot s, \tag{4}$$

where P_a = available stream power in the river upstream of a bridge pier (kW/m^2); γ = unit weight of water (kN/m^3); v = velocity of water (m/s); d = flow depth (m); and s = energy slope of flow in the river. Data for approach velocity, depth of flow, and energy slope in the Potomac River were obtained from the HEC-RAS model for a river section approximately 5 ft upstream of the proposed Woodrow Wilson Bridge. The HEC-RAS model was designed to calculate a velocity distribution across the river cross-section, thus allowing velocity upstream of each proposed pier to be approximated. The number of HEC-RAS model flow tubes affected the velocity calculated at the piers; thus the number of tubes was varied to achieve maximum velocities at the bridge piers. A schematic of velocity across the upstream section is shown in Figure 14. Available stream power upstream of the bridge was calculated for the HEC-RAS data for the 100-year and 500-year floods. Hydraulic data and resulting available stream power are presented in Table 2 for pier M10.

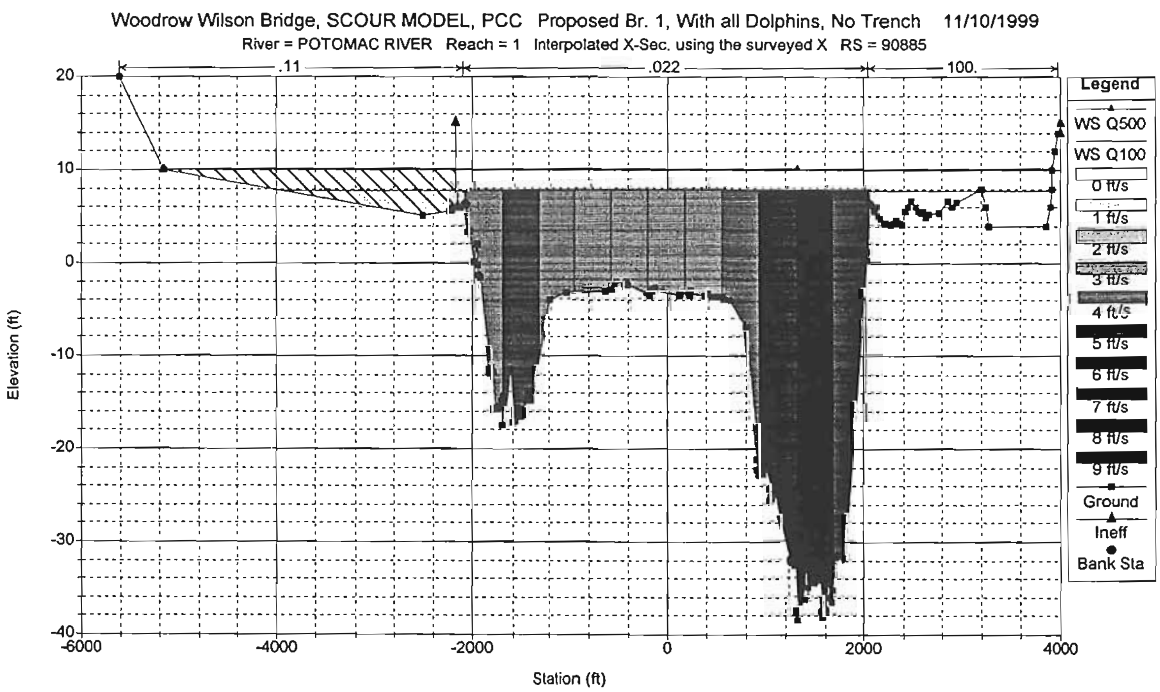

Fig. 14 Velocity distribution from HEC-RAS model of Potomac River at cross-section approximately 5 miles upstream of the proposed bridges.

Table 2 Pier M10 Hydraulic Data.

Hydraulic Variable	100-Year Flood	500-Year Flood	
Upstream Velocity	3.98 fps =1.21 m/s	5.49 fps = 1.67 m/s	v
Water Surface Elev.	10.86 ft = 3.31 m	14.69 ft = 4.48 m	
Ground Surface Elev.	-2.39 ft = -0.73 m	-2.39 ft = -0.73 m	
Flow Depth	13.25 ft = 4.04 m	17.08 ft = 5.21 m	d
Gamma	9.82 kN/m^3	9.82 kN/m^3	γ
Energy Slope	0.0002	0.00028	s
Upstream Stream Power	0.010 kW/m^2	0.024 kW/m^2	P_a
HEC-18 Scour Depth	56.0 ft = 17.1 m	63.3 ft = 19.3 m	

In the second step, a relationship between dimensionless stream power at the base of a scour hole and dimensionless scour hole depth was determined using Figure 11. The stream power is expressed in dimensionless form on the ordinate of the graph as the ratio P/Pa and scour depth as the ratio ys/ymax. Pa is the magnitude of the stream power in the river upstream of the pier as determined by equation (4), and P is the magnitude of the stream power at the base of the scour hole as it increases in depth. The variable ymax represents the maximum scour depth that can develop around a bridge pier under given flow conditions, whereas ys represents variable scour depth (ys < ymax). The maximum depth was assumed to be that calculated by HEC-18.

The equations used to make Figure 11 dimensional are:

$$\text{Rectangular Piers: } P/P_a = 8.42 \cdot e^{-1.88 \cdot (y_s / y_{max})}, \tag{9a}$$

$$\text{Circular Dolphins: } P/P_a = 8.95 \cdot e^{-1.92 \cdot (y_s / y_{max})}, \tag{9b}$$

The dimensionless scour depths for pier M10 are shown in Table 1 columns (11) and (16) for the 100- and 500-year floods, respectively. Columns (12) and (17) of Table 1 show 100- and 500-year flood relative stream power calculations using equation (9a) for pier M10.

In step three, the available stream power at a given scour depth, P (subsequently referred to as pA), is the product of P_a from step one and P/P_a from step two. The pA calculations for pier M10 are shown in Table 1 columns (13) and (18) for the 100- and 500-year floods, respectively.

Results and Discussion for example pier M10

The scour elevation at pier M10 was determined by comparing the stream power that is available to cause scour, pA, and the stream power that is required to scour the riverbed material, pR. Scour is expected to occur until pA is less than pR. Available power and required power are shown versus elevation in Figure 15. Table 1 columns (15) and (19) for the 100- and 500-year floods, respectively, show whether scour is expected to occur at a given elevation. For the 100-year flood, scour is expected to occur to a depth of 15 feet, which is an elevation of -17.4 feet. The calculated scour depth for the 500-year flood is 27 feet (elevation of -29.4 feet). The Erodibility Index Method predicted scour elevations at Pier M10 are 41 feet and 36 feet shallower than the HEC-18 predictions for the 100- and 500-year floods, respectively

The factor of safety quantifies the ability of the earth material to withstand the erosive power of the river at potential scour depths. The factor of safety was calculated as the required stream power divided by the available stream power in columns (14) and (20) of Table 1 for pier M10. The factor of safety at the base of the expected 100-year flood scour hole is approximately 1.

The variation in the factors of safety with depth, as seen in Table 1 are dictated by the relationship between the variation in material properties as a function of elevation below the riverbed and changes in the available stream power. To be conservative in the bridge pier design, Maryland State Highway Department is designing pier M10's foundation at the elevation where the 500-year flood factor of safety is greater than 5.0; this elevation is –38.4 with a factor of safety of 18.3.

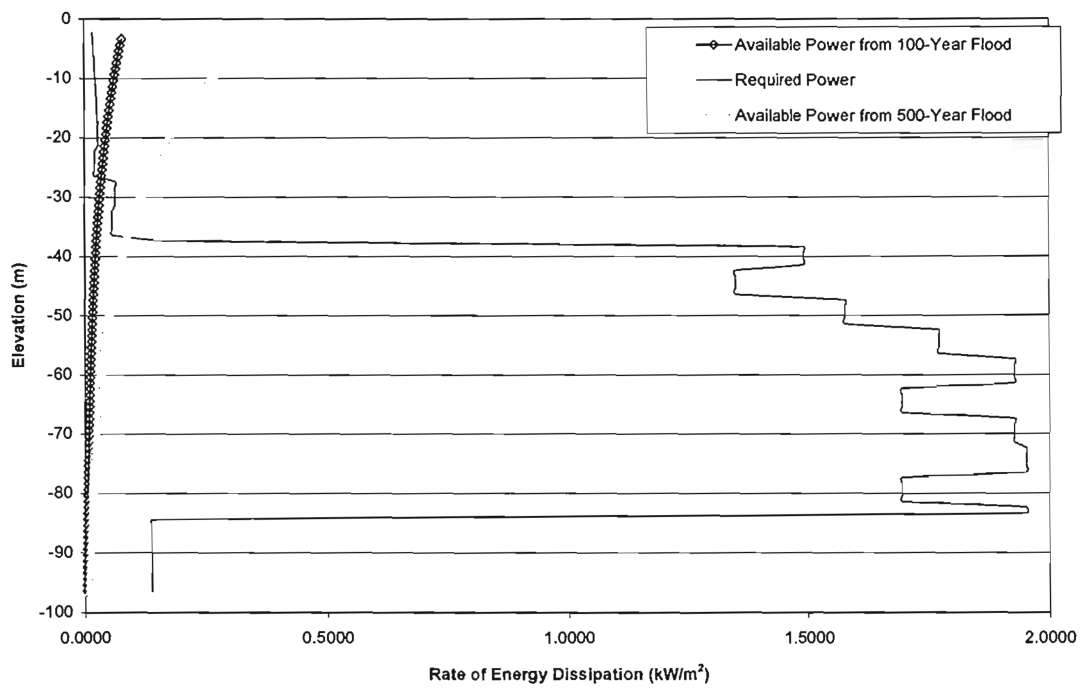

Fig. 15 Available Stream Power And Power Required At Pier M10.

CONCLUSION

A semi-empirical approach, known as the Erodibility Index Method is conceptually presented in this paper. Detail pertaining to the application of this method to determine erosion thresholds for earth materials can be found in Annandale (1995). The method defines an erosion threshold for all earth materials, including rock and cohesive and non-cohesive granular material and has been applied successfully to predict the onset of scour of rock around bridge piers (Anglio, et al. 1996).

A method that can be used to predict the extent of scour by comparing the stream power that is required to scour earth material with the stream power that is available around bridge piers is also presented. The method requires indexing of the earth material underlying the riverbed, and determination of the required stream power by making use of the erosion threshold line defined by the Erodibility Index Method. In addition it also requires quantification of the stream power that is available to cause scour. This is determined by making use of dimensionless graphs that define the change in stream power as a function of scour hole development (Smith, et al. 1997). A case study that illustrates application of the method to calculate scour around bridge piers is presented.

REFERENCES

1. Anglio, C.D., Nairn, R.B., Cornett, A.M., Dunaszegi, L., Turnham, J. and Annandale, G.W., 1996, Bridge Pier Scour Assessment for the Northumberland Strait Crossing, Coastal Engineering 1996, *Proceedings of the Twenty-fifth International Conference held in Orlando*, Florida, September 2-6, 1996, Billy L. Edge, Editor.

2. Annandale, G. W., Wittler, R. J., Ruff, J. F. and Lewis, T. M., 1998, Prototype Validation of Erodibility Index for Scour in Fractured Rock Media, Proceedings of the Water Resources Conference, American Society of Civil Engineers, Memphis, Tennessee, August.

3. Annandale, G.W., 1995, "*Erodibility.*" Journal of Hydraulic Research, Vol. 33, No. 4, pp. 471-494.

4. Briaud, J-L, Ting, F.C.K., Chen, H.C., Gudavalli, R. Perugu, S. and Wei, G., 1999, SRICOS: Prediction of Scour Rate in Cohesive Soils at Bridge Piers, Journal of Geotechnical and Geoenvironmental Engineering, American Society of Civil Engineers, Vol. 125, No. 4.

5. Cohen, E. and Von Thun, J. L., 1994, Dam Safety Assessment of the Erosion Potential of the Service Spillway at Bartlett Dam, *Proc. International Commission on Large Dams*, Durban, South Africa, pp. 1365-1378.

6. Federal Highway Administration, 1995, Evaluating Scour at Bridges, Third Edition, Hydraulic Engineering Circular 18 (HEC-18), Publication No. FHWA-IP-90-017, US Department of Transportation, 400 Seventh Street, Washington D.C. 20590.

7. Hjulstrom, F., 1935, The Morphological Activity of Rivers, Bulletin of the Geological Institute, Uppsala, Vol. 25, chapter 3.

8. Kirsten, H.A.D., 1982, A classification system for excavation in natural materials, *The Civil Engineer in South Africa*, July, pp. 292-308.

9. Shields, A., 1936, Application of Similarity Principles and Turbulence Research to Bed-Load Movement (in German), Mitteilungen der Preuss. Versuchsanstalt fur Wasserbau und Schiffbau, Berlin, No. 26.

10. Smith, S. P., Annandale, G. W., Johnson, P. A., Jones, J. S. and Umbrell, E. R., 1997, "Pier Scour in Resistant Material: Current Research on Erosive Power", Proceedings of Managing Water: Coping with Scarcity and Abundance, 27th Congress of the International Association of Hydraulic Research, San Francisco, California, pp. 160-165.

11. U.S. Natural Resources Conservation Service (NRCS), 1997, *Field procedures guide for the headcut erodibility index*, Chapter 52, in "Part 628 : Dams" of the National Engineering Handbook. Washington D.C. : U.S. Department of Agriculture.

12. Wittler, R.J., Annandale, G.W., Abt, S.R., Ruff, J.F., 1998, "New Technology for Estimating Plunge Pool or Spillway Scour." *Proceedings of the 1998 Annual Conference of the Association of State Dam Safety Officials*. October 11-14, Las Vegas, NV.

13. Yang, C. T., 1973, Incipient Motion and Sediment Transport, Journal of the Hydraulics Division, ASCE, Vol. 99, No. HY10, Proceedings Paper 10067, pp. 1679-1704.

SIZING RIPRAP TO PROTECT AGAINST LOCAL SCOURING AT BRIDGE PIERS

by

Christine S. Lauchlan[1], Bruce W. Melville[2], Stephen E. Coleman[3]

ABSTRACT

As flow passes around a pier, strong vortex motion is initiated. This condition can result in bed sediment being entrained and a scour hole forming at the base of the pier. The scour hole may develop to such an extent that the foundations of the pier are undermined and failure of the bridge structure occurs. A wide range of countermeasures has been employed to inhibit the formation of local scour holes. The most common technique is to apply some form of armouring device to the bed, such as rock riprap stones. Armour protection provides a physical barrier to withstand the erosive power of the flow. The problem associated with using riprap as a countermeasure lies in determining the actual size of stone required for the likely flow conditions. This paper summarises a number of proposed riprap sizing criteria and compares their predictions for various flow situations. The equations discussed have been developed from numerous sources, including bank and channel protection methods, threshold of motion criteria, and empirical results from laboratory experiments. In order to compare the equations from such varied sources, the equations are reduced to a common form. Comparison of the sizing methods indicates a wide range of predicted riprap sizes for any given flow condition. Equations based on threshold of motion criteria for sediment upstream of the pier are found to under-predict riprap sizes, while many of the empirically based formulae are strongly dependent on experimentally derived coefficients. However, a number of procedures produce results consistent with riprap sizes assessed in model studies. The equations developed by Richardson and Davis (1995) and Lauchlan (1999) are recommended as they provide a cautious yet realistic estimate of riprap sizes required. Further laboratory testing and field studies of these equations are required to ensure confidence in riprap countermeasures as a long term pier scour solution.

INTRODUCTION

Riprap is the most commonly used pier scour countermeasure. It consists of large rocks placed around a pier in order to armour the sediment bed. This armouring prevents the strong vortex motion at the front of the pier from entraining bed sediment and forming a scour hole.

The ability of the riprap layer to provide scour protection is a function of the stone size and the configuration of the layer. Both aspects influence the likely response of the layer to shear failure, winnowing failure, edge failure and bed-form destabilisation. Layer configuration aspects of riprap performance are not discussed here. For a summary of design criteria for riprap layer configuration see Melville and Coleman (2000).

[1] Postdoctoral Fellow, Delft University of Technology, Faculty of Civil Engineering and Earth Sciences, Delft, the Netherlands

[2] Associate Professor, Dept. of Civil and Resource Engineering, The University of Auckland, Auckland New Zealand

[3] Senior Lecturer, Dept. of Civil and Resource Engineering, The University of Auckland, Auckland, New Zealand

The size of the stones is a critical factor in terms of shear failure. Shear failure occurs when the flow velocity is high enough to entrain the riprap stones. If the riprap is incorrectly sized, the stones will be plucked from the bed and moved downstream of the pier before the design velocity is reached.

Stone size also influences winnowing, as the larger the stones the greater the gaps between adjacent stones and the easier it is for bed material to be winnowed from beneath them. If the riprap layer is two to three stone diameters thick, the effect of this form of failure is minimal. A layer three stone diameters thick is likely to experience significant winnowing only after disintegration of the riprap layer by the other failure mechanisms has occurred.

Edge failure and bed-form destabilisation are largely a function of the bed features in the flow. Large dunes with deep troughs cause greater undercutting at the edges of the riprap layer and have greater ability to destabilise the layer. However, increasing stone size requires increasing bed-form size to cause the same level of damage for a particular layer configuration.

This paper summarises a number of riprap size prediction equations and compares them over a range of flow conditions. The equations range from those developed for bank and channel protection measures to the results of small-scale laboratory studies of bridge piers. It is shown that there is a wide scatter of predicted riprap sizes for given flow conditions. Those equations providing the most realistic results are identified. Further laboratory and field tests are required to confirm these results.

COMPARISON OF RIPRAP SIZE PREDICTION EQUATIONS

Riprap size criteria are based on a number of different approaches. The starting point for many is the riprap sizing criterion for the general water environment. Many of the pier riprap sizing equations are modified forms of original bank or channel protection equations. Two equations originating from channel protection methods are discussed here.

One of the earliest methods of sizing riprap was introduced by Isbash (1935). He defined a 'stability number' criterion to quantify the stability of rock dumped onto a flat bed in flowing waters. The stability number criterion proposed by Isbash is:

$$N_{sc} = 2E^2 \tag{1}$$

where N_{sc} is a dimensionless stability factor for the riprap stone, given by

$$N_{sc} = \frac{U_{cr}^2}{g(S_r - 1)d_{r50}} \tag{2}$$

d_{r50} = the mean riprap size, U_{cr} = the critical velocity for entrainment of the riprap stones, S_r = the specific gravity of the riprap, g is gravitational acceleration, and E is an empirical constant.

Isbash proposed values for the parameter E of 0.86 for loosely placed stones in flowing water, and 1.2 for those that have embedded. If a value of 1.2 is substituted into (2) it produces

$$d_{r50} = \frac{0.347U_{cr}^2}{(S_r - 1)g} \tag{3}$$

An alternative equation was provided by Farraday and Charlton (1983) who considered the sizing of riprap for the general water environment with an additional coefficient to account for flow changes in certain situations. They produced the equation

$$\frac{d_{r50}}{y_o} = C^* Fr^3 \tag{4}$$

where C* is a coefficient determined from laboratory and field-testing, y_o is the average flow depth, and Fr is the flow Froude number. At bridge piers, they suggested using a safety factor of 2 and a corresponding C* value of 0.28. The form of equation (4), a Froude number multiplied by a coefficient, is a useful way of expressing many riprap equations. This method has an advantage over the stability number formulae as the riprap size can be calculated directly for the given flow conditions.

Alternatively, small-scale experimental results have also been used to develop stone size criteria specific to bridge-pier riprap. Lauchlan (1999) provides a summary of a large number of pier riprap size prediction equations. Here we will discuss a number of the equations and compare their results.

Breusers et al. (1977) provide riprap-sizing criteria based on previous pier scour experiments by Carstens (1966), Hancu (1971) and Nicollet and Ramette (1971). It was determined that for given sediment, scouring begins at half the critical velocity, irrespective of the pier diameter. Breusers et al. (1977) suggest that the riprap should therefore be sized so that the critical velocity of the stones is twice the maximum mean velocity of the flow. The resulting equation is provided below, where U_{max} is the maximum mean flow velocity. The formula is based on Isbash (1935) using E = 0.85.

$$d_{r50} = 2.83\frac{U_{max}^2}{(S_r - 1)g} \tag{5}$$

The Isbash (1935) equation was also rearranged by Richardson and Davis (1995) to give equation (6), where U = mean flow velocity. The 'K' factor is introduced to account for velocity changes associated with different pier shapes (Table 1).

$$d_{r50} = \frac{0.692(KU)^2}{(S_r - 1)2g} \tag{6}$$

Quazi and Peterson (1974) conducted an early experimental riprap study. They undertook a series of small-scale experiments with a riprap layer placed around a round-nosed pier, and lying flush with the bed. They developed the following relation.

$$N_{sc} = 1.14\left(\frac{d_{r50}}{y_o}\right)^{-0.20} \tag{7}$$

Also based on experimental results is the equation of Croad (1997), which is in the same form as (7), but with the addition of a pier shape factor, A.

$$N_{sc} = 2.1A\left(\frac{y_o}{d_{r50}}\right)^{1/6} \tag{8}$$

Croad suggested that the riprap formula should be compared to an embedment criterion such as that developed by Ettema (1980).

Breusers and Raudkivi (1991) developed a sizing formula based on the Manning and Strickler formulae and the idea of a critical velocity for sediment scouring as suggested by Breusers et al. (1977). Their equation states

$$U = 4.8(S_r - 1)^{0.5} d_{r50}^{1/3} y_o^{1/6} \tag{9}$$

where U is the flow velocity.

Similarly, Chiew (1995) provides a variation of this approach based on a slightly lower critical velocity for scouring and also including factors to account for sediment size (K_d) and flow depth (K_y) variations. Definitions of both factors are given in Table 1, the equation of Chiew (1995) being

$$N_{sc} = \frac{0.296}{K_y^2 K_d^2}\left(\frac{d_{r50}}{y_o}\right)^{-0.33} \tag{10}$$

Parola (1995) offers a design approach that considers cylindrical and rectangular piers separately. For a rectangular pier, the stability number is determined by the riprap size ratio, Table 1. For a cylindrical or round-nosed pier, a stability number of 1.4 is proposed, with N_{sc} = 1.6 for velocities greater than 1 m/s.

Finally, Lauchlan (1999) developed a riprap sizing formula based on a large number of small-scale riprap experiments. The equation is in the Froude number form and includes a factor to account for the placement depth of the riprap layer Y relative to the sediment bed level. The inclusion of this factor is due to the importance of placement level on the riprap failure mechanisms, Lauchlan (1999).

$$\frac{d_{r50}}{y_o} = 0.3Fr^{1.2}\left(1 - \frac{Y}{y_o}\right)^{2.75} \tag{11}$$

Equation (11) defines failure as having occurred only after more than 20% of the unprotected scour depth has occurred in the riprap later.

COMPARISON

The equations mentioned have been chosen for this discussion as most of them can be written in the Froude number form. A summary of the equations is provided in Table 1.

Figure 1 shows how the predicted riprap size varies with flow conditions for most of the different size prediction equations discussed. The equations are plotted for circular piers and specific gravity, S_r = 2.65. Chiew (1995) is plotted for three different values of b/d_{r50}, Table 1. Lauchlan (1999) is plotted for riprap placed flush with the bed, i.e. Y = 0.

It is apparent that for any particular flow, the predicted riprap size can vary significantly depending on the equation chosen. For example, for a Froude number of 0.4, Breusers et al (1977) predicts a riprap size (d_{r50}/y_o) greater than 0.2, Lauchlan (1999) predicts 0.1, Parola (1995) and Richardson and Davis (1995) predict about 0.075, Faraday and Charlton (1983) give

Table 1 - Equations for Sizing Riprap at Bridge Piers

Reference	Original Form of Equation	Equation Used for Comparison	Symbols
Isbash (1935)	$N_{sc} = 2E^2 = \frac{U_{cr}^2}{g(S_r - 1)d_{r50}}$	$\frac{d_{r50}}{y_o} = \frac{0.347}{(S_r - 1)} Fr^2$	N_{sc} = Critical stability number = $U_{cr}^2/[g[S_r-1)d_{r50}]$ Fr = Froude No. of the approach flow E = 1.2 for riprap situation U_{cr} = critical flow velocity S_r = specific gravity of the riprap stones y_o = mean approach flow depth
Quazi & Peterson (1974)	$N_{sc} = 1.14\left(\frac{d_{r50}}{y_o}\right)^{-0.20}$	$\frac{d_{r50}}{y_o} = \frac{0.85}{(S_r - 1)^{1.25}} Fr^{2.5}$	
Breusers et al (1977)	$U_{cr} = 0.85\sqrt{2g(S_r - 1)d_{r50}}$	$\frac{d_{r50}}{y_o} = \frac{2.83}{(S_r - 1)} Fr^2$	
Breusers & Raudkivi (1991)	$U = 4.8(S_r - 1)^{0.5} d_{r50}{}^{1/3} y_o{}^{1/6}$	$\frac{d_{r50}}{y_o} = \frac{0.278}{(S_r - 1)^{1.5}} Fr^3$	U = flow velocity
Chiew (1995)	$d_{r50} > \frac{U^3}{10.47\sqrt{y_o}}$	$\frac{d_{r50}}{y_o} = \frac{6.21 K_y^3 K_d^3}{(S_r - 1)^{1.5}} Fr^3$	K_y = flow depth factor, K_d = sediment size factor. $K_y = 0.783\left(\frac{y_o}{b}\right)^{0.322} - 0.106$ $0 \le \left(\frac{y_o}{b}\right) < 3$ $K_y = 1$ $\left(\frac{y_o}{b}\right) \ge 3$ $K_d = 0.398\ln\left(\frac{b}{d_{r50}}\right) - 0.034\left[\ln\left(\frac{b}{d_{r50}}\right)\right]^2$ $1 \le \left(\frac{b}{d_{r50}}\right) < 50$ $K_d = 1$ $\left(\frac{b}{d_{r50}}\right) \ge 50$ b = pier width

Reference	Original Form of Equation	Equation Used for Comparison	Symbols
Croad (1997)	$N_{sc} = 2.1A\left(\frac{y_o}{d_{r50}}\right)^{1/6}$	$\left(\frac{d_{r50}}{y_o}\right)^{5/6} = \frac{0.476Fr^2}{A(S_r - 1)}$	A = acceleration factor for bridge piers; A = 0.45 (circular and slab piers), A = 0.35 (square and sharp-edged piers)
Farraday and Charlton (1983)	$\frac{d_{r50}}{y_o} = C^* Fr^3$	$\frac{d_{r50}}{y_o} = 0.547Fr^3$	C^* = 0.28, coefficient to account for the presence of the bridge pier (adopting a safety factor of 2).
Lauchlan (1999)		$\frac{d_{r50}}{y_o} = 0.3Fr^{1.2}\left(1 - \frac{Y}{y_o}\right)^{2.75}$	Y = riprap placement level with respect to the average bed level; Y= 0 for riprap placed flush with the sediment bed
Parola (1995)	Rectangular Pier: $N_{sc} = 1.2$ $4 < \frac{b_p}{d_{r50}} < 7$ $N_{sc} = 1.0$ $7 < \frac{b_p}{d_{r50}} < 14$ $N_{sc} = 0.8$ $20 < \frac{b_p}{d_{r50}} < 33$	$\frac{d_{r50}}{y_o} = \frac{f_1 f_3}{(S_r - 1)} Fr^2$	b_p is the projected width of the pier f_1 = pier shape factor; f_1 = 1.0 (rectangular), 0.71 (round nose if aligned) f_3 = pier size factor (rectangular pier only)= $f(b_p/d_{r50})$, where $f_3 = 0.83$, $4<(b_p/d_{r50})<7$ $f_3 = 1.0$, $7<(b_p/d_{r50})<14$ $f_3 = 1.25$, $20<(b_p/d_{r50})<33$
	Round Nosed Pier: $N_{sc} = 1.4$	$\frac{d_{r50}}{y_o} = \frac{0.71}{(S_r - 1)} Fr^2$	
Richardson and Davis (1995)	$d_{r50} = \frac{0.692(KU)^2}{(S_r - 1)2g}$	$\frac{d_{r50}}{y_o} = \frac{0.346 f_1^2 f_2^2}{(S_r - 1)} Fr^2$	f_1 = factor for pier shape; f_1 = 1.5 (round-nose), 1.7 (rectangular-nosed) f_2 = factor ranging from 0.9 for a pier near the bank in a straight reach to 1.7 for a pier in the main current at a bend

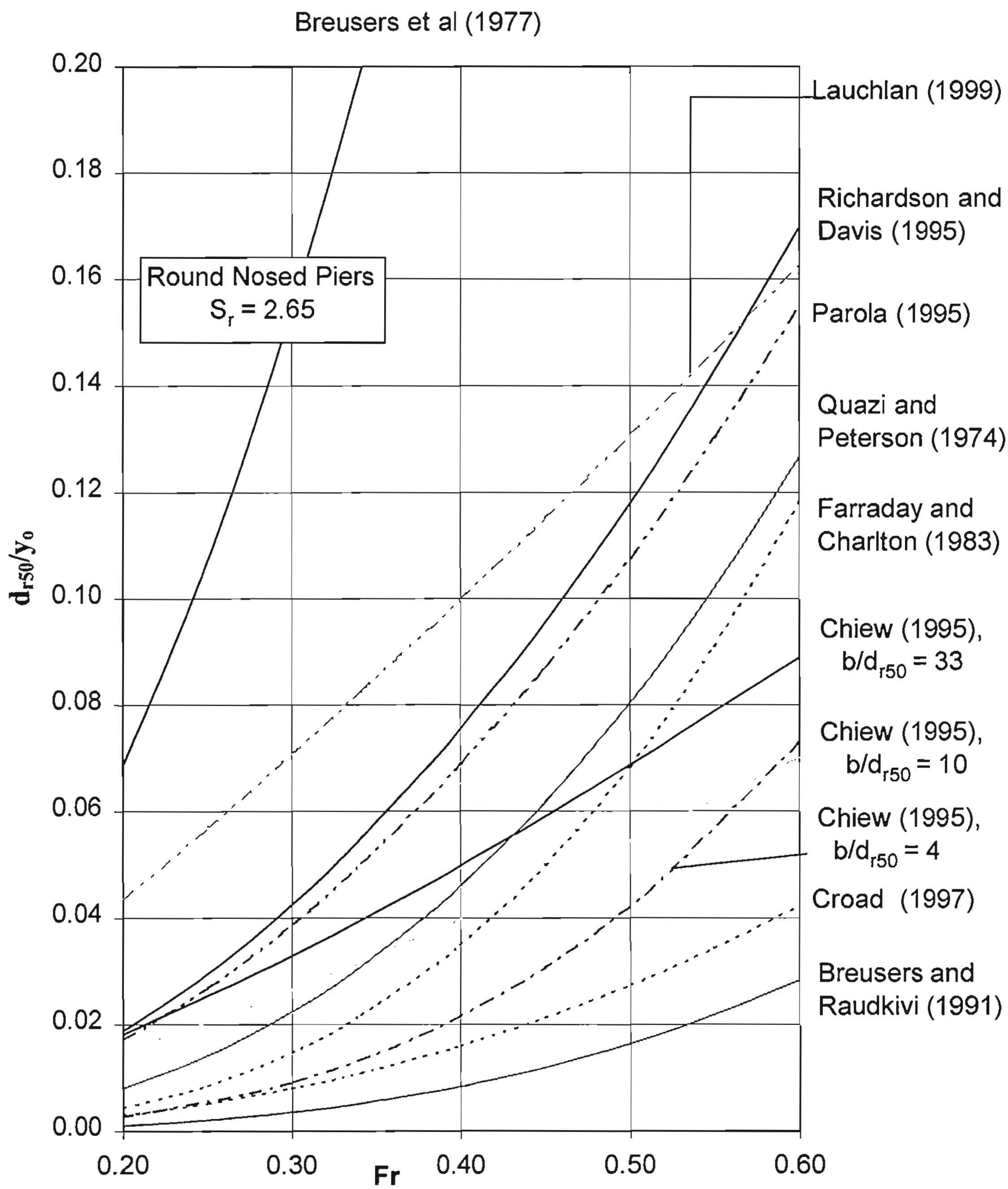

Figure 1 - Comparison of Equations for Sizing Riprap at Bridge Piers.

0.035, while Breusers and Raudkivi (1991) give 0.009. In order to chose the most appropriate equation, the reasons for these differences must be assessed.

Breusers et al. (1977) produces a significantly larger riprap size than the remaining equations. For this equation the numerical value of the coefficient is greater than 2. The other equations have coefficients less than 1.

Conversely, equations based on threshold of motion type criteria tend to lead to rather low d_{r50} values. For example, Breusers and Raudkivi (1991), Croad (1997), and Chiew (1995) for $b/d_{r50} = 4$, produce very small riprap sizes. The reason for this may be that the threshold of motion approach to riprap stability is not only affected by the choice of critical condition, which varies substantially with the exposure of stones, but also by the shape of the stones. The drag coefficient varies with the shape and roughness of the stones and the asymmetric shape of rocks also introduces an unknown lift force effect, Raudkivi (1990). Therefore any equation based on this criterion should also be able to adapt to changing embedment levels and stone shape factors.

Given the lack of consistency amongst the methods, it is prudent to select a method that leads to conservatively large riprap relative to the other remaining methods. On this basis, the methods of Richardson and Davis (1995) and Lauchlan (1999) are recommended for selecting suitable riprap for bridge pier protection, Melville and Coleman (2000). These methods were used to assess riprap size requirements for the Hutt Estuary Bridge (Melville and Lauchlan, 1998) and provided good agreement with model study results (Lauchlan, Melville and Coleman, 2000).

In order to improve confidence in the use of riprap size prediction formulae it is necessary to compare these equations to field results. Also, additional laboratory work could include assessing riprap layer performance under unsteady flow conditions.

CONCLUSIONS

1. Riprap failure mechanisms are affected by riprap size. Shear failure can be eliminated by correctly sized stones.
2. There is a lack of consistency amongst existing riprap size prediction equations, and a conservative approach following the method of Richardson and Davis (1995) or that of Lauchlan (1999) is recommended as appropriate under most situations.
3. Further laboratory and field studies are required to improve confidence in the prediction methods.

Ab Stability = f(sublayers) ?

REFERENCES

1. Breusers, H. N. C., and Nicollet, G., and Shen, H. W. (1977). "Local Scour Around Cylindrical Bridge Piers." *Journal of Hydraulic Research,* 15(3), 211-250.
2. Breusers, H. N. C.,and Raudkivi, A. J. (1991). *Scouring,* A. A. Balkema, Rotterdam; Brookfield.
3. Carstens, M. R. (1966). "Similarity Laws for Localised Scour." *Journal of the Hydraulics Division,* 92(HY3), 13-36.

4. Chiew, Y. M. (1995). "Mechanics of Riprap Failure at Bridge Piers." *Journal of Hydraulic Engineering*, 121(9), 635-643.
5. Croad, R. N. (1997). "Protection from Scour of Bridge Piers Using Riprap." *No.PR3-0071*, Works Consultancy Services Ltd, Central Laboratories, Lower Hutt.
6. Ettema, R. (1980). "Scour at Bridge Piers," PhD, The University of Auckland, Auckland, New Zealand.
7. Farraday, R. V., and Charlton, F. G. (1983). "Bank Protection and River Training." Hydraulic Factors in Bridge Design, HR Wallingford, Wallingford, 55-65.
8. Hancu, S. (1971) "Sur le calcul des affouillements locaux dams la zone des piles des ponts." *14th International Association of Hydraulic Research Congress*, Paris, France.
9. Isbash, S. V. (1935). "Construction of Dams by Dumping Stones in Flowing Water (Translated by A. Dorijkow).", U.S Army Engineer, Eastport.
10. Lauchlan, C.S (1999). "Pier Scour Countermeasures," PhD, The University of Auckland, Auckland.
11. Lauchlan, C.S., Melville, B.W., and Coleman, S.E. (2000). "Protection of the Hutt Estuary Bridge Against Local Scour." International Symposium on Scour of Foundations, Melbourne, Australia, November, 2000
12. Melville, B. W., and Coleman, S. E. (2000). *Bridge Scour*, Water Resources Publications, Colorado, USA: 550pp
13. Melville, B.W., and Lauchlan, C.S. (1998) "Hutt Estuary Bridge Physical Model Study of Scour at Bridge Piers." Auckland Uniservices Limited, Auckland
14. Nicollet, G., and Ramette, M. (1971) "Affouillements au voisinage de piles des pont cylindriques circulaires." *14th International Association of Hydraulic Research Congress*, Paris, France.
15. Parola, A. C. (1995). "Boundary Stress and Stability of Riprap at Bridge Piers." River, Coastal and Shoreline Protection: Erosion Control using Riprap and Armourstone, C. R. Thorne, S. R. Abt, F. B. J. Barends, S. T. Maynord, and K. W. Pilarczyk, eds., John Wiley & Sons, 149-159.
16. Quazi, M. E., and Peterson, A. W. (1974). "A Method for Bridge Pier Riprap Design." *First Canadian Hydraulics Conference,* Edmonton, Canad, 96-106.
17. Raudkivi, A. J. (1990). *Loose Boundary Hydraulics*, Pergamon Press, Oxford.
18. Richardson, E. V., and Davis, S. R. (1995). "Evaluating Scour at Bridges." *FHWA-IP-90-017*, Fairbank Turner Highway Research Centre, McLean, Virginia.

TOTAL SCOUR DEPTH AT BRIDGE ABUTMENTS

By

Stephen E. Coleman[1], Bruce W. Melville[2], Christine S. Lauchlan[3]

ABSTRACT

The scour depth at a bridge foundation is the combination of general scour occurring irrespective of the existence of the bridge, and localised scour arising due to the bridge presence. General-scour depths arise from the effects of general degradation, the presence of the channel thalweg, bend scour, confluence scour, and the presence of bed-forms. Localised scour takes the form of contraction scour, due to flow convergence as it passes through the bridge site, and local scour due to the local interaction of the flow with the bridge foundations (abutments and piers). The expected scour depth at a given bridge foundation can be severely underestimated if the combination of the full range of possible scour components is not considered for the foundation. In this paper, an overall methodology for the quantitative prediction of total scour depths at bridge abutments is presented, together with a summary of expressions enabling calculation of the various components of general and localised scour. The presented methodology highlights the range of variables to be considered in the assessment of total scour. The methodology is also applicable to the determination of total scour depths at piers if expressions for local scour at a pier are substituted for the local-abutment-scour expressions given herein (Coleman and Melville, 2000). Work remains to strengthen the methodology, particularly in regard to general scour estimates, by expanding the prediction expressions to cover the ranges of sediments, flows, bridge geometries and river morphologies occurring at bridge sites.

METHODOLOGY FOR THE PREDICTION OF TOTAL SCOUR DEPTHS AT ABUTMENTS

Figure 1 gives an overall methodology for the quantitative prediction of scour depths, whereby flow depths are successively determined for the effects of degradation, contraction scour, the

[1] Senior Lecturer, Department of Civil and Resource Engineering, The University of Auckland, Auckland, New Zealand.
[2] Associate Professor, Department of Civil and Resource Engineering, The University of Auckland, Auckland, New Zealand.
[3] Postdoctoral Fellow, Delft University of Technology, Faculty of Civil Engineering and Earth Sciences, Delft, the Netherlands.

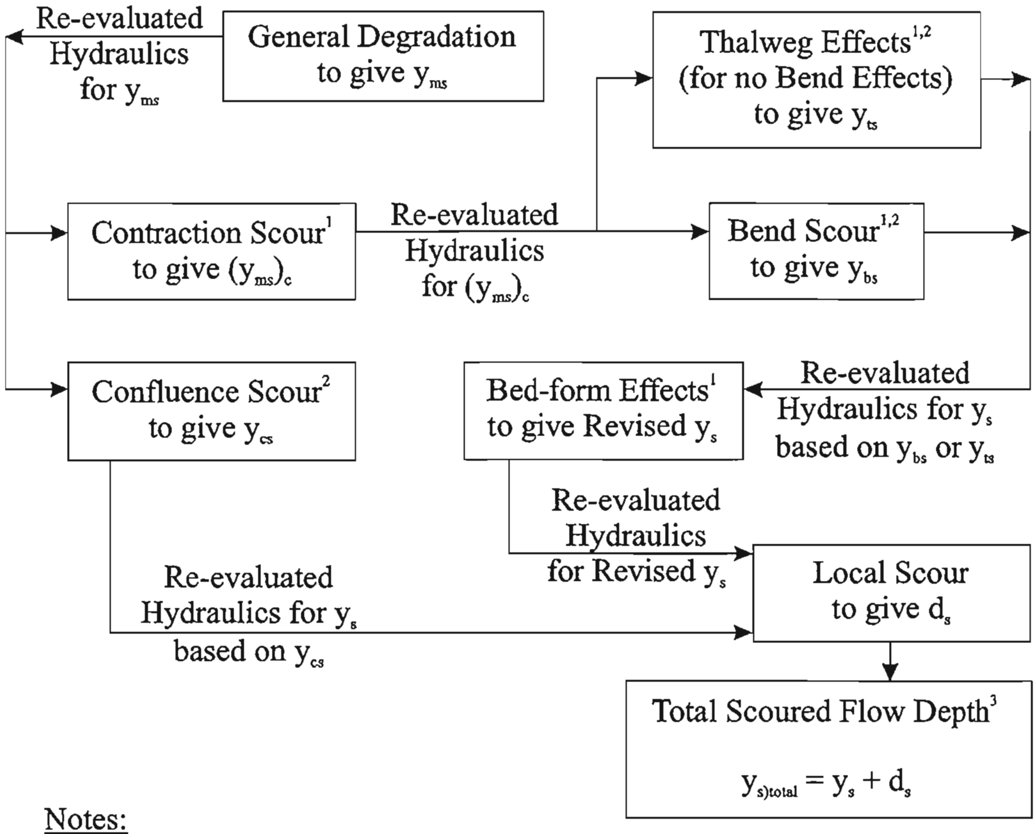

Notes:
1. Not where y_{ms} has been calculated using the method of Holmes (1974).
2. Allow for varying position of the thalweg, bend or confluence.
3. Allow for regions of local scour overlap.

Fig. 1 Methodology for Quantitative Prediction of Total Scour Depth.

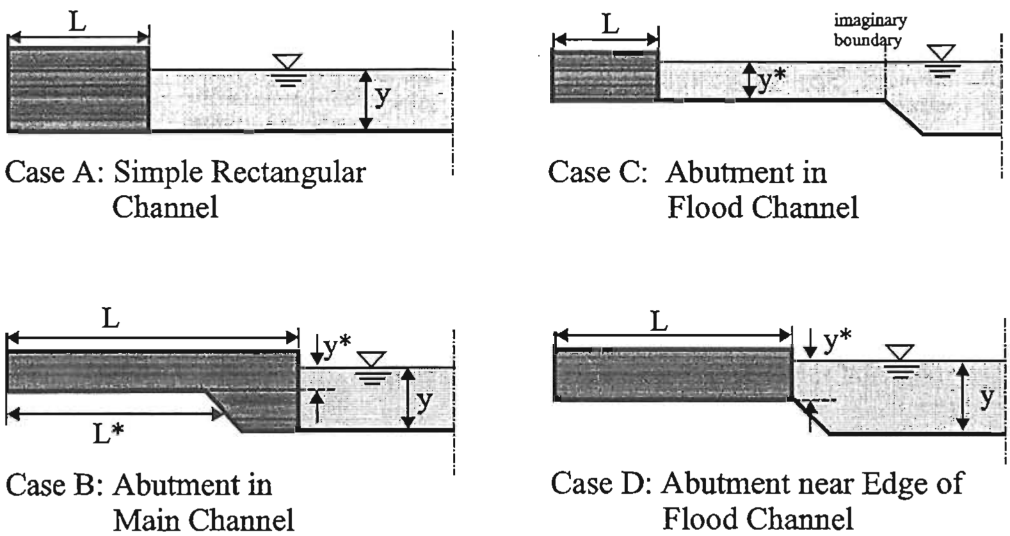

Fig. 2 Cases of Local Scour at Abutments in Compound Channels.

channel thalweg, bend scour, bed forms, and confluence scour. The resulting flow depth for general and contraction scour y_s is combined with the local scour depth at a foundation d_s to give the total scour depth at the foundation (Figure 1), namely

$$y_s)_{total} = y_s + d_s \quad (1)$$

A summary of expressions for the determination of the various scour-depth components at bridge abutments is given below, where symbol definitions are given at the end of the paper. Additional expressions for local pier scour and lateral erosion are given in Melville and Coleman (2000). Use of any scour formulae must ensure that the expressions are relevant to the characteristics (flows, channel parameters, and sediments) of the site under investigation. The limits of use, assumptions, and inadequacies of the formulae should also be established before the formulae are applied. Examples of application of the methodology of Figure 1 are given in Coleman and Melville (2000), Coleman et al. (2000), and Melville and Coleman (2000).

GENERAL EQUATIONS

General equations are:

$A = Wy$ for a rectangular channel (2)

$R = Wy/[W+2y]$ for a rectangular channel (3)

$V = Q/A$ (4)

$q = Q/W$ (5)

$u_{*c} = [\theta_c(S_s-1)gd_{50}]^{0.5}$ where θ_c can be obtained from Shields diagram (6)

$V_c = 5.75u_{*c}\log\left[5.53\frac{y}{d_{50}}\right]$ for fully turbulent flow and a bed roughness of $k = 2d_{50}$ (7)

The variable y in the above equations is appropriate to the situation being considered, that is (Figure 1), for calculation of y_{ms} adopt $y \equiv y_u$; for $(y_{ms})_c$ adopt $y \equiv y_{ms}$; for y_{ts} or y_{bs} adopt $y \equiv (y_{ms})_c$; for y_{cs} adopt $y \equiv y_{ms}$; and for d_s adopt $y \equiv y_s$.

GENERAL DEGRADATION

Use of a range of the following four methods, combined with field and subsurface observations, together with engineering judgement, typically provides the best approach to initial quantitative evaluation of mean scoured flow depth y_{ms} resulting from degradation at a site.

Lacey (1930)

$$y_{ms} = 0.47\left(\frac{Q}{f}\right)^{1/3} \text{ where } f = 1.76d_m^{0.5} \quad (8)$$

This approach is indicated to be too conservative for large sediment. The relation for f applies for $d_m < 1.3$ mm.

Blench (1969)

$$y_{ms} = 1.20\left[\frac{q^{2/3}}{d_{50}^{\ 1/6}}\right] \text{ for sands of } 0.06 < d_{50}\ (\text{mm}) \le 2.0 \tag{9}$$

$$y_{ms} = 1.23\left[\frac{q^{2/3}}{d_{50}^{\ 1/12}}\right] \text{ for gravels of } S_s \approx 2.65 \text{ and } d_{50} > 2.0 \text{ mm} \tag{10}$$

Maza Alvarez and Echavarria Alfaro (1973)

$$y_{ms} = 0.365\left(\frac{Q^{0.784}}{W^{0.784} d_{50}^{0.157}}\right) \tag{11}$$

This method is valid only for sediments of d_{75} < 6 mm, principally sands and gravels, with predictions being noted to differ to observations for finer materials. For a narrow river, the channel hydraulic mean radius is adopted in lieu of channel width W. Watson (1990) reports extensive use of this method for gravel-bed rivers in New Zealand.

Holmes (1974)
The author indicates total scour to be the sum of y_s and local scour, where

$$y_s \text{ is the greater of } \quad y_s = y_u \quad \text{or} \quad y_s = \frac{y_r V_1 K}{\sqrt{(A/W)}} \tag{12}$$

with $K = \sqrt{\dfrac{W}{4.83Q^{0.5}}} \le 1$, $V_1 = C\left(\dfrac{Q}{A}\right)\left(\dfrac{y_u}{A/W}\right)^{2/3}$ and C = 1.2 where converging flows are encountered, such as in braided streams, and 1.0 in other cases.

This method, where y_s incorporates degradation and contraction scour effects (and also possibly thalweg, bend scour, confluence scour and bed-form effects), is based on field data covering a wide range of sediment sizes collected in New Zealand for scour failures at a number of railway bridges. The method incorporates no safety factor owing to the use of conservative design flows in analyses. Watson (1990) reports on conservative predictions of scour for deep incised channels in gravel-bed rivers, especially when additionally incorporating a safety factor within the analyses.

AVERAGE CONTRACTION SCOUR

For live-bed conditions ($V/V_c \ge 1$) in the (degraded) approach channel of y_{ms}, the average scoured flow depth for a contracted section $(y_{ms})_c$ can be estimated based on Richardson and Davis (1995) (modified from Laursen, 1960), namely

$$\frac{(y_{ms})_c}{y_{ms}} = \left(\frac{Q_2}{Q_{1m}}\right)^{6/7}\left(\frac{W_1}{W_2}\right)^{k_1} \tag{13}$$

The long rectangular contraction basis of this approach may result in conservative predictions. Values of the exponent k_1 are given in Table 1.

Table 1. Values of Contraction Scour Coefficient k_1

u_*/ω	k_1	**Mode of bed material transport**
<0.50	0.59	Mostly contact bed material
0.50-2.0	0.64	Some suspended bed material discharge
>2.0	0.69	Mostly suspended bed material discharge

For clear-water conditions ($V/V_c < 1$) in the approach channel, $(y_{ms})_c$ can be estimated based on competent velocity being achieved through the bridge site, namely

$$(y_{ms})_c = Q/(VW) \quad \text{where } V = V_c = 5.75u_{*c}\log[5.53(y_{ms})_c/d_{50}] \tag{14}$$

Each of (13) and (14) assumes a rectangular channel section. Analyses for thalweg and bend effects can be subsequently adopted to incorporate allowances for variations in flow depths across the bridge section.

BEND SCOUR

The maximum scoured flow depth in a bend y_{bs} can be evaluated using (Maynord, 1996)

$$y_{bs} = F_s(y_{ms})_c\{1.8 - 0.051(r_c/W) + 0.0084[W/(y_{ms})_c]\} \tag{15}$$

where a conservative safety factor of $F_s = 1.19$ is adopted herein. This method is valid for $W/(y_{ms})_c < 125$ and $r_c/W < 10$, $r_c/W = 1.5$ being adopted for $r_c/W < 1.5$, and $W/(y_{ms})_c = 20$ being adopted for $W/(y_{ms})_c < 20$. The expression of Thorne (1988) can also be adopted, namely

$$y_{bs} = (y_{ms})_c\{2.07 - 0.19\ln[(r_c/W) - 2]\} \tag{16}$$

where this method is valid for $r_c/W > 2$. Equations (15) and (16) are recommended to be limited to flows of overbank depths upstream of the bend of less than 20% of the main channel depth. In lieu of adopting (15) or (16), it can be assumed that the scoured area below the flood level, of average depth $(y_{ms})_c$, can be redistributed in a simple triangular form (Neill, 1973) to give a peak flow depth in the bend of

$$y_{bs} = 2(y_{ms})_c \tag{17}$$

Alternatively, the scoured area below the original (upstream, unscoured) bed level, of average depth $[(y_{ms})_c - y_u]$, can be similarly redistributed to give

$$y_{bs} = y_u + 2[(y_{ms})_c - y_u] \tag{18}$$

It is recommended that the above methods for assessment of bend scour that are appropriate to a given bridge site be used together to determine an appropriate value of y_{bs} for the site.

THALWEG EFFECTS

The flow depth in the thalweg y_{ts} can be estimated for a straight channel as the maximum of

$$y_{ts} = 1.27(y_{ms})_c \quad \text{(Lacey, 1930)} \qquad \text{or} \qquad y_{ts} = (y_{ms})_c + (h/2) \tag{19}$$

where amplitude h is the maximum of the thalweg amplitude or the height of alternate-bars in the channel. Expressions enabling calculation of thalweg amplitude and alternate-bar height are given in Melville and Coleman (2000). Alternative graphical methodologies for redistributing average scour across a cross-section to allow for thalweg effects are as used for bend scour estimation, namely (17) and (18) above. In addition, y_{ts} can be estimated by scaling the calculated average scoured flow depth $(y_{ms})_c$ by the ratio of maximum to mean flow depths for the unscoured channel (Maza Alvarez and Echavarria Alfaro, 1973).

CONFLUENCE SCOUR

The maximum flow depth in a confluence y_{cs} can be calculated for different sediment classes using the expressions (Ashmore and Parker, 1983; and Klaassen and Vermeer, 1988)

$$\frac{y_{cs}}{\bar{y}_{ms}} = 2.24 + 0.031\alpha \quad \text{for noncohesive sands and gravels and } \alpha = 30° \text{ to } 90° \tag{20}$$

$$\frac{y_{cs}}{\bar{y}_{ms}} = 1.01 + 0.030\alpha \quad \text{for cohesive material} \tag{21}$$

$$\frac{y_{cs}}{\bar{y}_{ms}} = 1.29 + 0.037\alpha \quad \text{for } 0.6 < Q_s/Q_l < 1 \text{ and uniform sand of } 0.15 < d_{50}\text{(mm)} < 0.25 \tag{22}$$

where $\bar{y}_{ms}$ is the average flow depth in the degraded anabranches approaching the confluence. In regard to (20), poorly-sorted bed material is noted to have lesser confluence scour depths than well-sorted material of the same mean size.

BED-FORM EFFECTS

The peak scoured flow depth owing to the migration of bed forms through the bridge site can be estimated as

$$y_s = y_{ts} + (h/2) \qquad \text{or} \qquad y_s = y_{bs} + (h/2) \tag{23}$$

where h is the maximum bed-form height for the expected types of bed forms over the range of flows occurring at the bridge site. This approach is more applicable to the migration of dunes, bars or antidunes, ripples being typically sufficiently small as to be insignificant in affecting scour magnitudes. Means of determining the types of bed forms occurring for a range of flows in a river, and means of evaluating the heights of these bed forms, are discussed in Melville and Coleman (2000).

LOCAL ABUTMENT SCOUR

Local abutment-scour depth d_s below the surrounding bed level is calculated based on the analyses of Melville (1997) and Melville and Coleman (2000), namely

$$d_s = K_{yL} K_I K_d K_S^* K_\theta^* K_G K_t \tag{24}$$

where the factors of (24) are defined in Table 2 and Figure 2. For the calculations of Table 2, $d_{50a} \equiv d_{50}$ and $V_a \equiv V_c$ for uniform sediments.

Table 2. Factors Influencing Local Abutment-scour Depth

Factor	K	Method of estimation	
Flow depth-abutment size	K_{yL}	$K_{yL} = 2L$	$\frac{L}{y_s} < 1$
		$K_{yL} = 2\sqrt{y_s L}$	$1 < \frac{L}{y_s} < 25$
		$K_{yL} = 10 y_s$	$\frac{L}{y_s} > 25$
Flow intensity	K_I	For uniform sediments: $d_{50a} \equiv d_{50}$ and $V_a \equiv V_c$ For nonuniform sediments: $d_{50a} = d_{max}/1.8 \approx d_{84}/1.8 = \sigma_g d_{50}/1.8$; and $V_a = 0.8V_{ca}$, where V_{ca} is calculated for d_{50a} using (7) and (6)	
		$K_I = \frac{V-(V_a-V_c)}{V_c}$	for $[V-(V_a-V_c)]/V_c < 1$
		$K_I = 1.0$	for $[V-(V_a-V_c)]/V_c \geq 1$

Table 2. Factors Influencing Local Abutment-scour Depth (cont.)

<table>
<tr><th>Factor</th><th>K</th><th colspan="7">Method of estimation</th></tr>
<tr><td rowspan="2">Sediment size</td><td rowspan="2">K_d</td><td colspan="4">$K_d = 0.57\log\left(2.24\dfrac{L}{d_{50a}}\right)$</td><td colspan="3">$\dfrac{L}{d_{50a}} \le 25$</td></tr>
<tr><td colspan="4">$K_d = 1.0$</td><td colspan="3">$\dfrac{L}{d_{50a}} > 25$</td></tr>
<tr><td rowspan="9">Foundation shape</td><td rowspan="6">K_S</td><td colspan="4">Shape</td><td colspan="3">K_S</td></tr>
<tr><td colspan="4">Vertical-wall</td><td colspan="3">1.0</td></tr>
<tr><td colspan="4">Wing-wall</td><td colspan="3">0.75</td></tr>
<tr><td colspan="4">Spill-through 0.5:1 (H:V)</td><td colspan="3">0.6</td></tr>
<tr><td colspan="4">Spill-through 1:1</td><td colspan="3">0.5</td></tr>
<tr><td colspan="4">Spill-through 1.5:1</td><td colspan="3">0.45</td></tr>
<tr><td rowspan="3">$K_S{}^*$</td><td colspan="4">$K_s^* = K_s$</td><td colspan="3">$\dfrac{L}{y_s} \le 10$</td></tr>
<tr><td colspan="4">$K_s^* = K_s + 0.667(1 - K_s)\left(0.1\dfrac{L}{y_s} - 1\right)$</td><td colspan="3">$10 < \dfrac{L}{y_s} < 25$</td></tr>
<tr><td colspan="4">$K_s^* = 1.0$</td><td colspan="3">$\dfrac{L}{y_s} \ge 25$</td></tr>
<tr><td rowspan="5">Foundation alignment</td><td rowspan="2">K_θ</td><td>θ (°)</td><td>30</td><td>45</td><td>60</td><td>90</td><td>120</td><td>135</td><td>150</td></tr>
<tr><td>K_θ</td><td>0.90</td><td>0.95</td><td>0.98</td><td>1.0</td><td>1.05</td><td>1.07</td><td>1.08</td></tr>
<tr><td rowspan="3">$K_\theta{}^*$</td><td colspan="4">$K_\theta^* = K_\theta$</td><td colspan="3">$\dfrac{L}{y_s} \ge 3$</td></tr>
<tr><td colspan="4">$K_\theta^* = K_\theta + (1 - K_\theta)\left(1.5 - 0.5\dfrac{L}{y_s}\right)$</td><td colspan="3">$1 < \dfrac{L}{y_s} < 3$</td></tr>
<tr><td colspan="4">$K_\theta^* = 1.0$</td><td colspan="3">$\dfrac{L}{y_s} \le 1$</td></tr>
<tr><td rowspan="4">Approach-channel geometry</td><td rowspan="4">K_G</td><td colspan="7">Case A (Figure 2): [Simple rectangular river channel] $K_G \equiv 1.0$</td></tr>
<tr><td colspan="7">Case C (Figure 2): [Abutment well back from the flood-channel edge]
Consider only the flood channel flows of y^* and set $K_G = 1.0$</td></tr>
<tr><td colspan="7">Case B (Figure 2): [Abutment in the main channel]
$K_G = \sqrt{1 - \left(\dfrac{L^*}{L}\right)\left[1 - \left(\dfrac{y^*}{y}\right)^{5/3}\left(\dfrac{n}{n^*}\right)\right]}$</td></tr>
<tr><td colspan="7">Case D (Figure 2): [Abutment near the flood channel edge]
Abutment at about the flood-channel edge: Case B with L^*/L=1.0.
Abutment near the flood channel edge but not extending into the main channel: Estimate K_G by interpolating conservatively between estimates for longer (Case B) and shorter (Case C) abutments in the same channel.</td></tr>
<tr><td>Time</td><td>K_t</td><td colspan="7">$K_t = 1.0$ (conservative as time factor relation not presently defined)</td></tr>
</table>

REFERENCES

1. Ashmore, P., and Parker, G. (1983). "Confluence scour in coarse braided streams." Water Resources Research, 19(2), pp. 392-402.
2. Blench, T. (1969). "Mobile-bed fluviology." University of Alberta Press, Edmonton, Canada.
3. Coleman, S. E., and Melville, B. W. (2000). "New Zealand case studies of bridge scour." J. Hyd. Engrg., ASCE, in press.
4. Coleman, S. E., Melville, B. W., and Lauchlan, C. S. (2000). "Bealey Bridge scour failure." Proc., Int. Symp. on Scour of Foundations, Melbourne, Australia, November, 2000.
5. Holmes, P. S. (1974). "Analysis and prediction of scour at railway bridges in New Zealand." New Zealand Engineering, November, pp. 313-320.
6. Klaassen, G. J., and Vermeer, K. (1988). "Confluence scour in large braided rivers with fine bed material." Proc., Int. Conf. on Fluvial Hydraulics, Budapest, Hungary, pp. 395-408.
7. Lacey, G. (1930). "Stable channels in alluvium." Paper 4736, Minutes of the Proceedings of the Institution of Civil Engineers, Vol. 229, William Clowes and Sons Ltd., London, Great Britain, pp. 259-292.
8. Laursen, E. M. (1960). "Scour at bridge crossings." J. Hyd. Div., ASCE, 86(HY2), pp. 39-54.
9. Maynord, S. T. (1996). "Toe-scour estimation in stabilised bendways." J. Hyd. Engrg., ASCE, 122(8), pp. 460-464.
10. Maza Alvarez, J. A., and Echavarria Alfaro, F. J. (1973). "Contribution to the study of general scour." Proc., Int. Symp. on River Mechanics, IAHR, Bangkok, Thailand, pp. 795-803.
11. Melville, B.W. (1997). "Pier and abutment scour - an integrated approach." J. Hyd. Engrg., ASCE, 123(2), pp. 125-136.
12. Melville, B. W., and Coleman, S. E. (2000). "Bridge scour." Water Resources Publications, Colorado, USA, 550 pp.
13. Neill, C. R. (1973). "Guide to bridge hydraulics." Roads and Transportation Assoc. of Canada, University of Toronto Press, Toronto, Canada.
14. Richardson, E. V., and Davis, S. R. (1995). "Evaluating scour at bridges." Federal Highway Administration Report No. FHWA-IP-90-017, Hydraulic Engineering Circular No. 18, Third Edition, Office of Technology Applications, HTA-22, Washington, D. C., November.
15. Thorne, C. R. (1988). "Bank processes on the Red River between Index, Arkansas, and Shreveport, Louisiana." Final Rep. to the U. S. Army Eur. Res. Ofc., Contract number DAJA45-88-C-0018, Dept. of Geography, Queen Mary College, London, England.
16. Watson, A. W. (1990). "A case study of scour assessment at a proposed bridge crossing." RRU Bulletin 84, Vol. 5 'Summary papers and other technical papers presented at the Bridge Design and Research Seminar, Christchurch, 1990', Road Research Unit, Transit New Zealand, Wellington, New Zealand, pp 147-152.

NOTATION

A	=	flow area;
A_c	=	critical flow area for sediment entrainment;
C	=	convergence coefficient for Holmes (1974);
d_m	=	effective mean diameter of bed material;
d_{max}	=	maximum particle size;
d_n	=	sediment size for which n% of the sediment is finer;
d_s	=	local scour depth below the surrounding bed level;
d_{50}	=	median size of bed material (by weight);
d_{50a}	=	median particle size of armour layer;
F_s	=	safety factor;
Fr	=	Froude Number;
f	=	Lacey silt factor;
g	=	acceleration of gravity;
h	=	amplitude (crest to trough), bed-form height;
K	=	coefficient, factor;
K_d	=	sediment-size factor;
K_G	=	approach-channel-geometry factor;
K_I	=	flow-intensity factor;
K_s, K_s*	=	foundation-shape factor;
K_t	=	time factor;
K_{yL}	=	flow depth-abutment size factor;
$K\theta$, $K\theta$*	=	foundation-alignment factor;
k	=	bed roughness;
k_1	=	contraction-scour coefficient;
L	=	abutment length (including bridge approach) measured perpendicular to the channel centreline (Figure 2);
L*	=	width of flood plain (Figure 2);
n	=	Manning roughness coefficient for the main channel of a compound channel;
n*	=	Manning roughness coefficient for the flood plain of a compound channel;
Q	=	flow rate, mean discharge, design discharge;
Q_l	=	larger anabranch flow rate;
Q_s	=	sediment transport rate, smaller anabranch flow;
Q_{1m}	=	flow rate in the approach main channel (not flood plains) transporting sediment;
Q_2	=	total flow rate through the bridge (contracted) section;
q	=	flow rate per unit channel width, $q = Q/W$;
R	=	channel hydraulic radius;
r_c	=	centreline radius of bend curvature;
S_e	=	energy slope, stream slope;
S_0	=	channel slope;
S_s	=	specific gravity of sediment particles, $S_s = \rho_s/\rho$;
t	=	flood peak duration;
$u*$	=	bed shear velocity;

u_{*c}	=	critical shear velocity for particle entrainment;
u_{*ca}	=	critical shear velocity (for particle entrainment) of armour layer;
V	=	mean flow velocity;
V_a	=	(for nonuniform sediments) mean velocity of flow at the "armour peak" ($\equiv V_c$ for uniform sediments);
V_c	=	(critical) mean velocity of flow at the threshold condition for sediment movement;
V_{ca}	=	(for nonuniform sediments) limiting mean velocity of flow for bed sediment armouring;
V_1	=	approach channel velocity;
W	=	channel width;
W_1	=	bottom width of the (degraded) approach main channel (not flood plains);
W_2	=	bottom width of the main channel in the bridge (contracted) section;
y	=	flow depth appropriate to equation, average flow depth, average flow depth in the main channel of a compound channel (Figure 2);
y^*	=	average flow depth in the flood plain of a compound channel (Figure 2);
y_{bs}	=	maximum scoured flow depth in a bend;
y_{cs}	=	maximum flow depth in a confluence scour hole;
y_{ms}	=	flow depth from water surface to mean scoured (degraded) depth;
$(y_{ms})_c$	=	flow depth from water surface to mean scoured depth in a contracted section;
y_r	=	water level rise from low water to flood stage;
y_s	=	flow depth for the combination of general scour and contraction scour;
$y_{s)total}$	=	total scoured flow depth;
y_{ts}	=	flow depth in the channel thalweg;
y_u	=	upstream unscoured flow depth;
$\bar{y}_{ms}$	=	average flow depth for the degraded anabranches approaching a confluence;
α	=	angle of channel confluence (degrees);
θ	=	foundation alignment with respect to flow direction ($\theta = 0°$ being parallel to the river bank in the downstream direction);
θ_c	=	Shields entrainment function, dimensionless critical shear stress;
ρ	=	density of water;
ρ_s	=	density of sediment;
σ_g	=	geometric standard deviation of particle size distribution, $\sigma_g = (d_{84}/d_{16})^{0.5} = (d_{84}/d_{50})$; and
ω	=	fall velocity of sediment particles.

THE EFA, EROSION FUNCTION APPARATUS: AN OVERVIEW

By

Jean-Louis Briaud[1], H.-C. Chen[2], Francis Ting[3]

ABSTRACT

A new apparatus is described to measure the erosion function of a soil. The apparatus is called the EFA (patent pending) or Erosion Function Apparatus (http://tti.tamu.edu/geotech/scour). The erosion function is the relationship between the hydraulic shear stress applied at the soil-water interface by the water flowing over the soil and the erosion rate of the soil. This erosion function can then be used to predict scour of soil by water.

[1] Spencer J. Buchanan Professor, Dept. of Civil Engineering, Texas A&M University, College Station, Texas 77843-3136, USA, (briaud@tamu.edu)
[2] Associate Professor, Dept. of Civil Engineering, Texas A&M University, College Station, Texas 77843-3136, USA.
[3] Associate Professor, Dept. of Civil & Environmental Engineering, South Dakota State University, Brookings, South Dakota 57007, USA.

INTRODUCTION

The erosion rate of clean sands is very high and may be measured in meters per hour. For example a 5 meter deep hole can be created by a single flood around a bridge pier. On the other hand the erosion rate of rock is very slow and may be measured in millimeters per year. For example the Grand Canyon in the USA is about 1.6 km deep and took approximately 20 million years to develop; this leads to an average erosion rate of 0.08mm/yr. For a bridge pier built on clean sand, one needs only to consider the worst flood and calculate the scour depth for that flood because the erosion rate is so high that time is not a factor. For a bridge pier built in rock it is not economical to use the same calculations as for sand because the rate is so slow that even after say 100 years the scour depth in rock may be a very small fraction of the scour depth in sand.

The erosion rate of fine grained soils is intermediate between that of sand and that of rock. There is a need to predict that rate to estimate how large the scour depth will be at the end of the bridge design life. This prediction process starts by a measurement of the erosion function, which links the hydraulic shear stress τ applied at the water-soil interface to the erosion rate of the soil $\dot{z}$. The EFA (Erosion Function Apparatus) was developed to measure the $\dot{z}$ vs τ curve for a given soil.

THE EROSION FUNCTION APPARATUS

The EFA (Figs. 1 and 2) (Briaud et al. 1999 (a) and (b)) was conceived in 1991, designed in 1992, and built in 1993. The sample of soil, fine-grained or not, is taken in the field by pushing an ASTM standard Shelby tube with a 76.2 mm outside diameter(ASTM-D1587). One end of the Shelby tube full of soil is placed through a circular opening in the bottom of a rectangular cross section pipe. A snug fit and an O-ring establish a leakproof connection. The cross section of the rectangular pipe is 101.6 mm by 50.8 mm. The pipe is 1.22 m long and has a flow straightener at one end. The water is driven through the pipe by a pump. A valve regulates the flow and a flow meter is used to measure the flow rate. The range of mean flow velocities is 0.1 m/s to 6 m/s. The end of the Shelby tube is held flush with the bottom of the rectangular pipe. A piston at the bottom end of the sampling tube pushes the soil until it protrudes 1 mm into the rectangular pipe at the other end. This 1 mm protrusion of soil is eroded by the water flowing over it.

EFA TEST PROCEDURE

The procedure for the EFA test consists of:

1. Place the sample in the EFA, fill the pipe with water, and wait one hour.
2. Set the velocity to 0.3 m/s.
3. Push the soil 1mm into the flow.
4. Record how much time it takes for the 1 mm soil to erode (visual inspection through plexiglas window)
5. When the 1 mm of soil is eroded or after 1 hour of flow whichever comes first, increase the velocity to 0.6 m/s and bring the soil back to a 1 mm protrusion.
6. Repeat step 4.

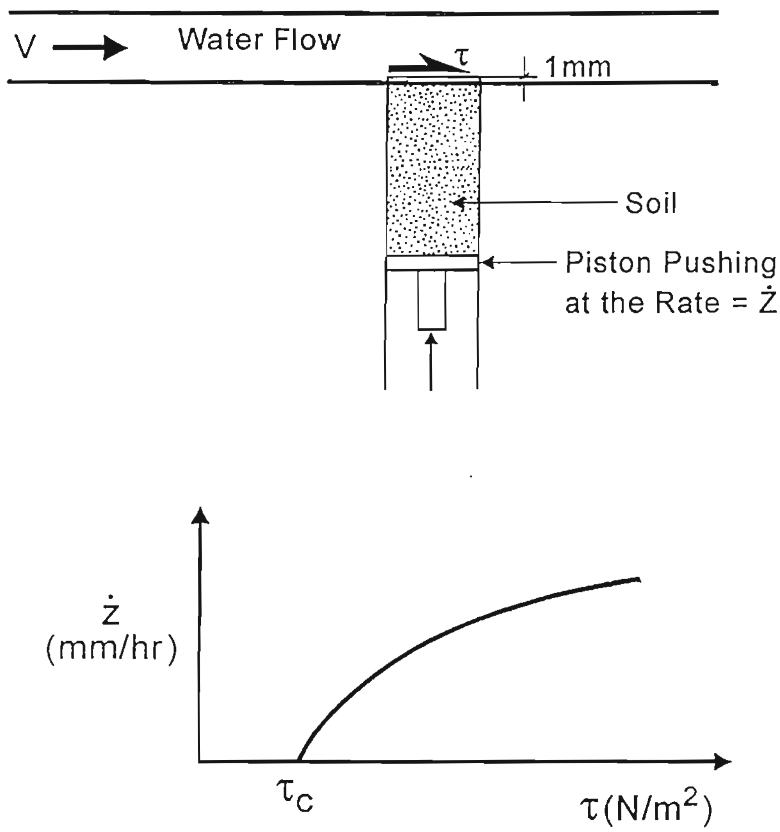

Fig. 1 - Schematic Diagram and Result of the EFA (Erosion Function Apparatus)

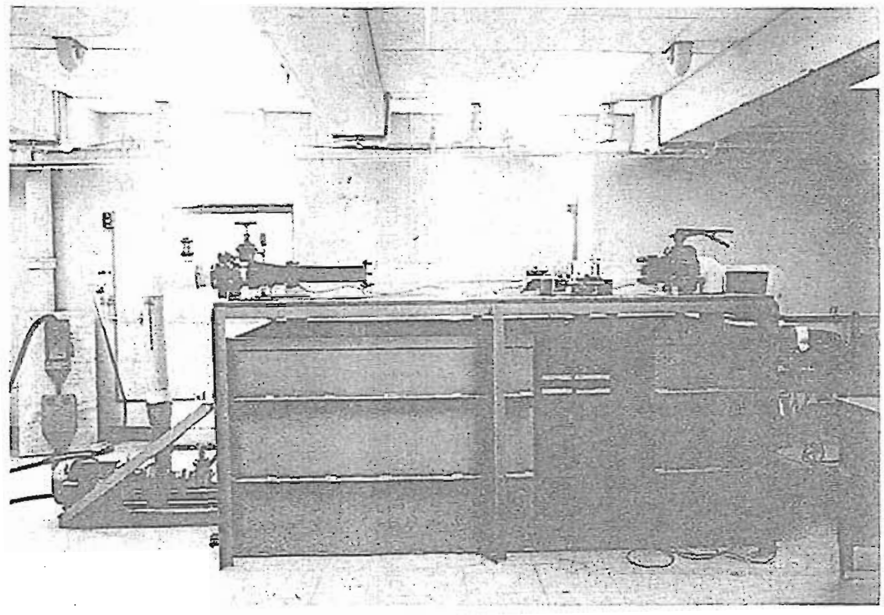

(a)

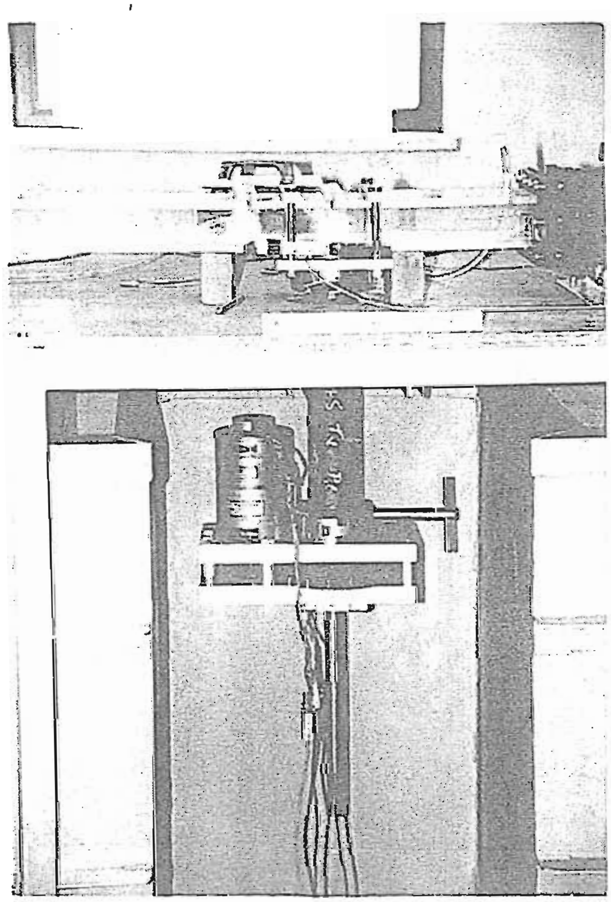

(b)

Fig. 2 - Photographs of the Erosion Function Apparatus (a) General View (b) Close-up of the Test Section

7. Then repeat steps 5 and 6 for velocities equal to 1 m/s, 1.5 m/s, 2 m/s , 3 m/s, 4.5 m/s, and 6 m/s.

EFA TEST RESULTS

The test result consists of the erosion rate $\dot{z}$ versus shear stress τ curve (Fig. 3). For each flow velocity, the erosion rate $\dot{z}$ (mm/hr) is simply obtained by dividing the length of sample eroded by the time required to do so. After several attempts at measuring the shear stress τ in the apparatus it was found that the best way to obtain τ was by using the Moody Chart (Moody, 1944) for pipe flows.

$$\tau = \frac{1}{8} f \rho \upsilon^2$$

Where τ is the shear stress on the wall of the pipe, f is the friction factor obtained from Moody Chart (Fig. 4), ρ is the mass density of water (1000 kg/m^3) and υ is the mean flow velocity in the pipe.

CONCLUSION

An apparatus called EFA (patent pending) (http://tti.tamu.edu/geotech/scour) is described to measure the erosion function ($\dot{z}$ vs τ curve) for a soil. It can be used for any soil or soft rock which can be cored or sampled in a 76.2 mm outside diameter tube. The EFA results can then be used to predict scour of soil by water.

ACKNOWLEDGEMENTS

The EFA was originally developed under sponsorship from the Texas Department of Transportation. The Texas Transportation Institute also contributed to its development.

REFERENCES

1. Briaud, J.-L., Ting, F.C.K., Chen, H.C., Gudavalli, R., Perugu, S., Wei, G., 1999 (a), "SRICOS: Prediction of Scour Rate in Cohesive Soils at Bridge Piers", Journal of Geotechnical and Geoenvironmental Engineering, Vol. 125, No. 4, April 1999, pp. 237-246, American Society of Civil Engineers, Reston, Virginia, USA.
2. Briaud, J.-L., Ting, F.C.K., Chen, H.C., Gudavalli, R., Kwak, K., Philogene, B., Han, S.W., Perugu, S., Wei, G.,Nurtjahyo, P., Cao, Y., Li, Y., 1999(b), "SRICOS: Prediction of Scour Rate at Bridge Piers", Report 2937-F to the Texas Department of Transportation, Texas A&M University, Civil Engineering, College Station, TX 77843-3136, USA.
3. Moody L.F., 1994 "Friction Factors for Pipe Flow", Transaction of the American Society of Civil Engineers, Vol. 66, Reston, Virginia, USA.
4. Munson B.R., Young D.F., Okiishi T.H., 1990, "Fundamentals of Fluid Mechanics", John Wiley & Sons, New York, New York, USA, pp 843.

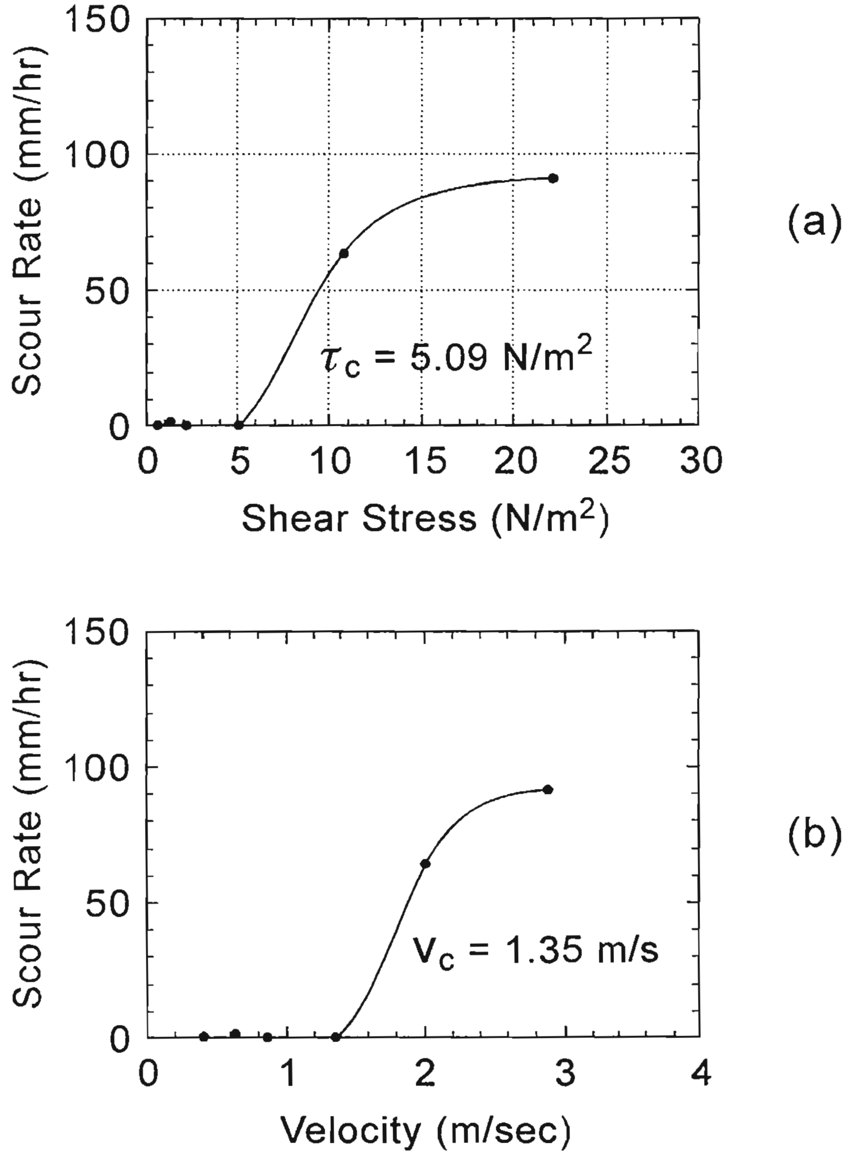

Fig. 3 - Erosion Function for a soil sample taken near Pier 27E of the Existing Woodrow Wilson Bridge (2.6 – 3.2 meters depth) : a) Scour Rate vs. Shear Stress, b) Scour Rate vs. Velocity

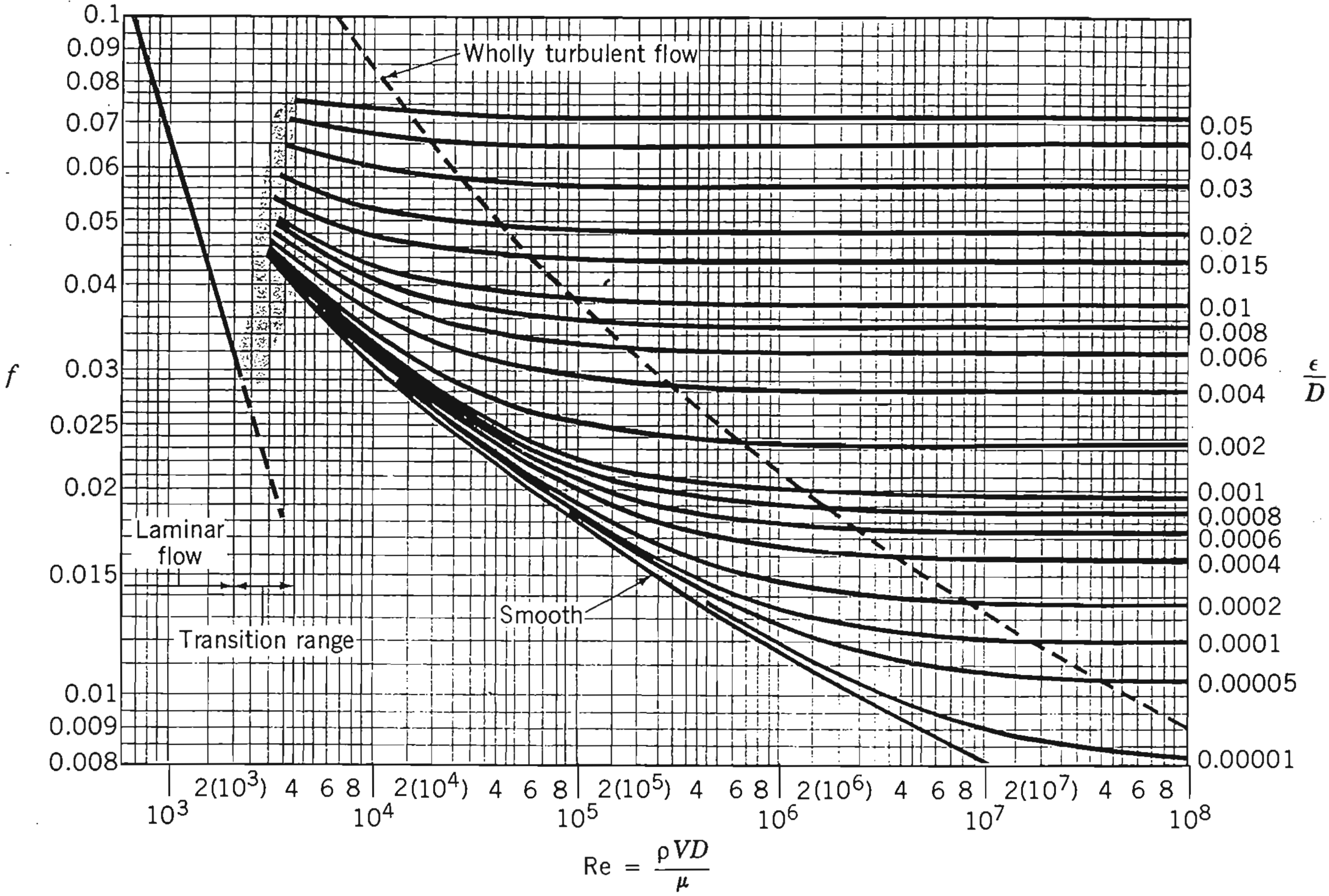

Fig. 4 - Moody Chart (reprinted with permission from Munson et al. 1990)

A LABORATORY METHOD TO EVALUATE THE RATE OF WATER EROSION OF NATURAL ROCK MATERIAL

By

Matthew R. Henderson[1], D. Max Sheppard[2], David Bloomquist[3]

ABSTRACT

Early bridge scour research has focused on scour of cohesionless sediments around piers. Only recently have researchers started to consider other types of sediments. As a result of an expanding data base for cohesionless sediments (and better understanding of the mechanisms governing scour) engineers in the United States have treated erodible materials as cohesionless sediments for the purpose of scour depth calculations. The equations and techniques presented in the U.S. Federal Highway Administration Bridge Scour Document [FHWA Hydraulic Engineering Circular Number 18 (HEC-18)] for estimating scour depths is based on laboratory studies that were conducted with beds consisting of cohesionless sediments (sand). These equations are known to be conservative for cohesionless sediments and are believed to be overly conservative for erodible rock and cohesive materials. The current approach used in calculating scour depths around structures located in bed materials other than sand is to assume that the bed materials will erode to the same depth as sand given sufficient time. However, bed materials at many bridge sites in the State of Florida are composed of materials other than sand, such as limestone and coquina. These materials can offer a greater resistance to erosion than cohesionless sediments. Hence, a laboratory-based testing device was designed and constructed to evaluate the rates of water erosion of these materials. This device – a rotating cylinder erosion testing apparatus – previously used for testing the erosion of cohesive soils was modified and improved to accept intact rock samples. The new apparatus allows a hydraulic shear stress to be applied to a sample, which simulates the action of water flowing over a bed. The average shear stress can be accurately measured as well as the loss of material due to erosion. Laboratory testing procedures and methods have been developed for conducting the erosion experiments using this apparatus on rock samples. Preliminary experiments were conducted on samples of rock materials collected from bridge sites in Florida

INTRODUCTION

The current approach used in calculating the scour depths around structures located in bed materials other than sand is to apply the equations provided in HEC-18 with the assumption that the bed materials will erode to the same depths, given sufficient time, as cohesionless sediments (Annandale et al., 1996, p. 59). The limitation of this approach is that it ignores the ability of materials such as rock to offer more resistance to scour than sand (Annandale et al., 1996, p. 59).

[1] Former Graduate Student - Coastal and Hydraulics Engineer, OEA, Inc., Gainesville, Florida, USA
[2] Professor of Civil and Coastal Engineering, University of Florida, Gainesville, Florida, USA
[3] Associate Professor of Civil and Coastal Engineering, University of Florida, Gainesville, Florida, USA

The sea or riverbeds at a number of bridge sites in the State of Florida are composed of materials other than cohesionless sediments (i.e., other than sand or loose shells). This includes harder materials such as limestone and coquina. The erosion characteristics of these materials are quite different from those of cohesionless sediments. However, due to the current lack of understanding of their erosion characteristics, these rock materials are treated as cohesionless sediments in the current HEC-18 design scour procedures. Since the erosion of rock materials can vary greatly compared to cohesionless sediments, the present approach may be overly conservative in the prediction of scour depths. The Florida Department of Transportation (FDOT) estimates that over designs using these methods have resulted in millions of dollars being wasted on the construction of excessive bridge foundations. Hence, there is a definite need to improve the ability to predict design local and contraction scour depths in erodible rock materials.

CURRENT METHODS TO EVALUATE ROCK EROSION

The FHWA developed an interim guidance to assess rock scourability using empirical methods and testing procedures (Gordon, 1991). These procedures were provided until the results of ongoing research would permit more accurate evaluation procedures.

The guidance recommends the following seven methods to assess the scourability of rock:

- Subsurface Investigation;
- Geologic Formation/Discontinuities;
- Rock Quality Designation (RQD);
- Unconfined Compressive Strength;
- Slake Durability Index;
- Soundness; and
- Abrasion.

The FHWA rock scourability guidance memorandum recommends that design engineers perform several geotechnical tests to evaluate the susceptibility of rock to scour. This memorandum does not provide estimates of the erosion or scour rates of these materials, but provides guidance as to whether the rock materials should be considered a scourable material. The FDOT and University of Florida have conducted some of the recommended tests on rock core samples from bridge sites in Florida to assess their values in relation to the values presented in the guidance document.

Limestone samples collected from the US 441 Bridge site over the Santa Fe River were tested for Unconfined Compressive Strength, Los Angeles Abrasion Test, and Magnesium Sulfate Soundness Test. Statistical analysis of the unconfined compressive strength (q_u) test results indicate that the minimum q_u expected is 1430 kPa or 207 psi (PSI, 1996, p. 5). The Los Angeles Abrasion Test yielded a loss of 72.3% (PSI, 1996, p. 9). The Magnesium Sulfate Soundness Test indicated a loss of 80.0% (PSI, 1996, p. 10).

Tests on limestone samples from a second site produced the following results. The Unconfined Compressive Strength test indicated strengths ranging from 1372 kPa to 1475 kPa (199 psi to 214 psi). Magnesium Sulfate Soundness tests indicated losses from 58.7% to 91.1%.

The guidance memorandum suggests that samples with q_u values below 1725 kPa (250 psi) are not considered to behave as rock (Gordon, 1991). Also, loss rates of 18% from the Magnesium Sulfate Soundness Test can be used as an indirect measure of scour (Gordon, 1991). Rock with loss rates greater than 40% from the Los Angeles Abrasion Test should be considered susceptible to scour (Gordon, 1991). In summary, based on these geotechnical tests, the rock materials in Florida may be susceptible to scour and must be considered in the design and scour protection for bridge sites.

PROPOSED ROCK EROSION PROCESS

A simple but useful definition of rock has been presented in Jumikis (1983):

> Rock is a granular material composed of "grains and glue." There is nothing else involved. The "glue" may be ferroginous, calcareous, argillaceous, or siliceous material, which cements the grains. (Jumikis, 1983, p. 38).

The process of rock erosion by the action of a moving fluid is complex and may be influenced by several factors. The energy imparted by the moving fluid breaks the grains from the glue and subsequently transports the grains downstream. This fundamental description leads to the idea that there is a certain amount of energy required to initiate the erosion of rock. In cohesionless sediments, this concept is known as a critical bed-shear stress. This is the shear stress required to initiate motion of the sediment grains.

Van Rijn (1993) describes the forces acting on a sediment particle resting on a horizontal bed. The fluid forces consist of skin friction forces and pressure forces. The skin friction force acts on the surface of the particles by viscous shear. The pressure force, consisting of a drag and lift force, is generated by pressure differences along the surface of the particle. Particle movement will occur when the moments of the instantaneous fluid forces with respect to the point of contact are just larger than the stabilizing moment of the submerged particle weight (van Rijn, 1993, p. 4.1). In rock materials, there are additional forces that act between the particles tending to maintain the rock as a solid body.

The erosion process in rock can be more complex than just the shear stress acting on a particle. Experimental work performed at the National Research Council of Canada Institute for Marine Dynamics found that weak sedimentary rock tended to erode by breaking into pieces along fractures, bedding planes, and other internal weaknesses. Cornett et al. (1994) presents a simple model for the hydraulic fracturing of rock. The erosion of the rock at the fracture planes was not directly related to the shear stress. The results of the study suggest that the erosion may be driven by hydrodynamic pressures within fractures (Cornett et al., 1994, p. 26).

Annandale (1995) has developed a method for estimating rock erosion. He suggests the following procedure with regards to hydraulic erosion. This approach is based on a rational correlation between the rate of energy dissipation of flowing water and an erodibility classification of the materials (Annandale, 1995, p. 471). The removal of rock material is perceived as occurring in three stages: jacking, dislodgment, and displacement. Flowing water is subject to turbulence, which, in turn, is associated with a loss in energy. Annandale suggests that turbulence causes pressure fluctuations that result in an action that progressively raises or jacks portions of material from its position. Once removed, the material is then dislodged and displaced (Annandale, 1995, p. 472).

ALTERNATIVE ROCK EROSION PREDICITVE METHODS

One method developed for use in estimating the erosion of a wide range of materials including rock, and cohesionless and cohesive soils is known as the Erodibility Index method. This method, developed by Annandale (1995), compares a material's ability to resist erosion, which has been designated as the Erodibility Index, with the erosive power of flowing water. The erosive power of water has been defined in terms of the stream power, which is based on the rate of energy dissipation. The primary geotechnical parameters that are used in the calculation of the Erodibility Index are earth mass strength, block or particle size, discontinuity/inter-particle bond shear strength, and the shape of material units and their orientation relative to the flow (Annandale, 1995, p. 481). The comparison of the stream power with the Erodibility Index determines if a material will or will not erode. This method has been further developed for use in estimating the scour at piles for bridges. A description of this method is given in the Interim Report by the Colorado Department of Transportation titled "Preliminary Procedure to Predict Bridge Scour in Bedrock" (Smith, 1994).

SELECTION OF ROCK EROSION TESTING DEVICE

Even though methods have been proposed for predicting water scour of rock materials, much work is still needed. To evaluate the scour of specific types of rock, it is important to examine several factors. First, it is important to understand a material's reaction to fluid flow. A laboratory study is most suited for this type of investigation since it allows better control of important variables and, in general, more accurate measurements. The work performed for this study consisted of the development of a methodology for the evaluation of a rock's erosion rate as a function of the flow of water over its surface. A laboratory-testing device was required to produce the water flow and to measure both the shear stress applied to the surface of the rock sample and the rate of erosion of the sample surface.

Any laboratory method for testing the erosion rates of rock materials, must take the following into consideration:

- There are difficulties in working with rock as a matrix. First, drilling rigs are required to extract samples of rock (termed cores). This is the most common method of collecting rock samples for analysis. Secondly, rock has the propensity to fracture along weak planes, leaving broken pieces. Therefore, the testing device must be able to work with a limited but to take into consideration natural flaws & faults

amount of sample material and be able to utilize rock cores that are routinely collected as part of bridge pier design and construction.

- The laboratory-testing device must be able to create flowing water over the rock sample. Specifically, the device must be able to apply a hydraulic shear stress to the rock sample surface.

- Along the same lines as described above, the laboratory-testing device must be able to measure the shear stress that is applied to the sample being tested.

- The testing device must be able to generate shear stresses at levels expected in design storm flow conditions. Therefore, the laboratory-testing device must be able to operate at shear stresses that range from ambient to beyond design conditions.

- Based on information obtained from the literature review, rock can be highly resistant to erosion. Since the erosion rates are very small as compared with cohesionless and cohesive sediments, the laboratory-testing device must be able to accurately measure small amounts of lost material while continuously operating for days.

Based on the above-described criteria, the rotating cylinder erosion testing apparatus was selected. This type of device has been used by several researchers to determine critical stresses and rates of erosion of cohesive sediments. A description of this device, which is similar to the Couette viscometer, is given below.

PREVIOUS USE OF ROTATING CYLINDER APPARATUS

Moore and Masch (1962) applied the rotating cylinder principle used in viscometers to measure the scour resistance of cohesive soils. The device was called the rotating cylinder erosion test apparatus. A cylindrical sample of cohesive sediment was suspended inside a larger circular cylinder. The outer cylinder is free to rotate about its axis. The annular gap between the cylinder and sample was filled with fluid. As the outer cylinder is rotated, momentum is imparted to the fluid and the fluid moves, imparting a shear stress to the face of the sample. The cohesive soil sample is stationary but mounted on flexure pivots so that the shear stress transmitted to the sample surface resulted in a slight rotation of the supporting tube. The resulting rotation was calibrated to measure the torque on the sample from which the shear stress could be computed (Moore and Masch, 1962, p. 1444).

As a shear stress was applied to the sample, material was eroded from the face of the sample. The amount of material eroded was measured and the duration that the shear stress was applied was also recorded. From this information, the average rate of erosion could be computed for a given applied shear stress.

Several researchers including Rektorik et al. (1964), Arulanandan et al. (1973), Sargunam et al. (1973), Alizadeh (1974) and Chapius and Gatien (1986) have used similar devices with improvements and enhancements. Akky and Shen (1973) used the rotating cylinder apparatus developed by Arulanandan to evaluate the erosion of cement-stabilized soil. In fact, Chapius and Gatien improved the testing apparatus to accept either intact or remolded cohesive soils, with improved rotation guidance, better alignment, a lower internal friction, and a reduction of the influence of end conditions on the fluid annular flow (Chapius and Gatien, 1986, p. 86). These researchers evaluated the rate of erosion of cohesive sediments with the rotating cylinder device.

THEORETICAL ASPECTS OF THE ROTATING CYLINDER APPARATUS

Essentially, the rotating cylinder works along the same principle as a rotational viscometer. Rotational viscometers operate on the principle that when a cylinder is suspended and immersed in a liquid contained in a vessel which rotates at a constant speed, a balancing couple will be required to keep the cylinder at rest. This couple may be produced by the torsion of a wire from which it is suspended (Merrington, 1949, p. 30).

For a Newtonian fluid, the velocity increases almost linearly from zero at the stationary inner cylinder (no-slip condition) to the velocity of the outer rotating cylinder at the wall of the outer cylinder. For low rotational speeds this approximates laminar flow between two infinite parallel plates. The near linear velocity profile between the two concentric cylinders only occurs during low velocity, laminar flow conditions. As the speed of the outer cylinder is increased, there are changes in the flow regime. The flow begins as a laminar flow but becomes unstable as the velocity increases. The instability grows until a secondary flow is achieved. The secondary flows, described by G.I. Taylor, are a succession of stable toroids or vortices, which have been termed Taylor's rotational vortices. These vortices are well-defined counter-rotating circulation cells. As the outer cylinder speed is increased even further, the Taylor vortices become unstable and ultimately the flow is uniformly turbulent.

Rohan and Lefebvre (1991) investigated certain hydrodynamic aspects of the rotating cylinder erosion tests. The critical Reynolds number between laminar flow and the formation of the above-mentioned Taylor vortices can be calculated. (Rohan and Lefebvre, 1991, p. 167). In fact, there are three regimes of flow that can be distinguished based upon the calculation of the Taylor number (Rohan and Lefebvre, 1991, p. 169):

1. $Ta < 41.3$ = laminar Couette flow;
2. $41.3 < Ta < 400$ = laminar flow with Taylor vortices, and
3. $Ta > 400$ = turbulent flow.

In cases where the flow consists of secondary flows (vortices) or turbulent flow, the velocity profile is no longer a linear relationship from the wall of the stationary inner cylinder to the rotating outer cylinder.

ADVANTAGES AND LIMITATIONS OF TESTING DEVICE

The rotating cylinder test apparatus met several of the design criteria presented above. Specifically:

- a small sample of rock can be used in this type of device as the outer cylinder can be sized to accommodate the size of standard rock cores,
- a flowing water generated shear stress can be applied to the sample,
- the average shear stress on the sample can be measured by measuring the torque that is being applied to the sample,
- small quantities of material being eroded can be measured using precision balances, and
- the apparatus can be operated for long periods of time as the outer cylinder can be driven by a continuous duty motor.

It is also important, however, to discuss the limitations of this type of testing device to understand where uncertainty and bias may be present in the results. The shear stress is computed by measuring the torque on the sample. However, the torque being measured is the torque being applied to the entire sample. Therefore, the calculation of the shear stress results in the average shear stress over the entire sample surface. The results from the experiments assume that the shear stress is uniform across the entire surface of the sample. In actuality, the surface of rock samples can be pitted and uneven. Therefore, there may be variations in the shear stress distribution over the face and thus local shear stresses are likely to be greater that the averaged value computed from the moment on the sample.

In summary the shear stress computed from the measured torque may be biased in the direction of underestimating the shear stress acting on the sample. In addition to the variations in the shear stress over the sample surface there may also be components of the flow acting in directions other than the direction in which the torque is being measured. Thus, there may be a component of shear stress that is eroding the surface of the sample that is not being accounted for in the measurements. In the application of these results, the underestimation of shear stress would provide conservative estimates of the rates of erosion versus shear stress. That is, the results would show greater erosion rates for a given shear stress. The conservative nature of these results would be appropriate for design applications.

ROTATING CYLINDER APPARATUS

The rotating cylinder testing apparatus used in this study was similar to the devices previously used; however, some modifications have been made. Figures 1 and 2 are schematic drawings of the rotating device and Figure 3 is a photograph of the actual device. English units are shown for equipment dimensions as they were used by manufacturers to specify equipment sizes. The metric equivalents were also provided. The major components of the apparatus consist of the following:

- Bodine 1/8-hp Frame 42A motor (2500 RPM at 50 in-oz [353 mm-N] of torque) with controller,

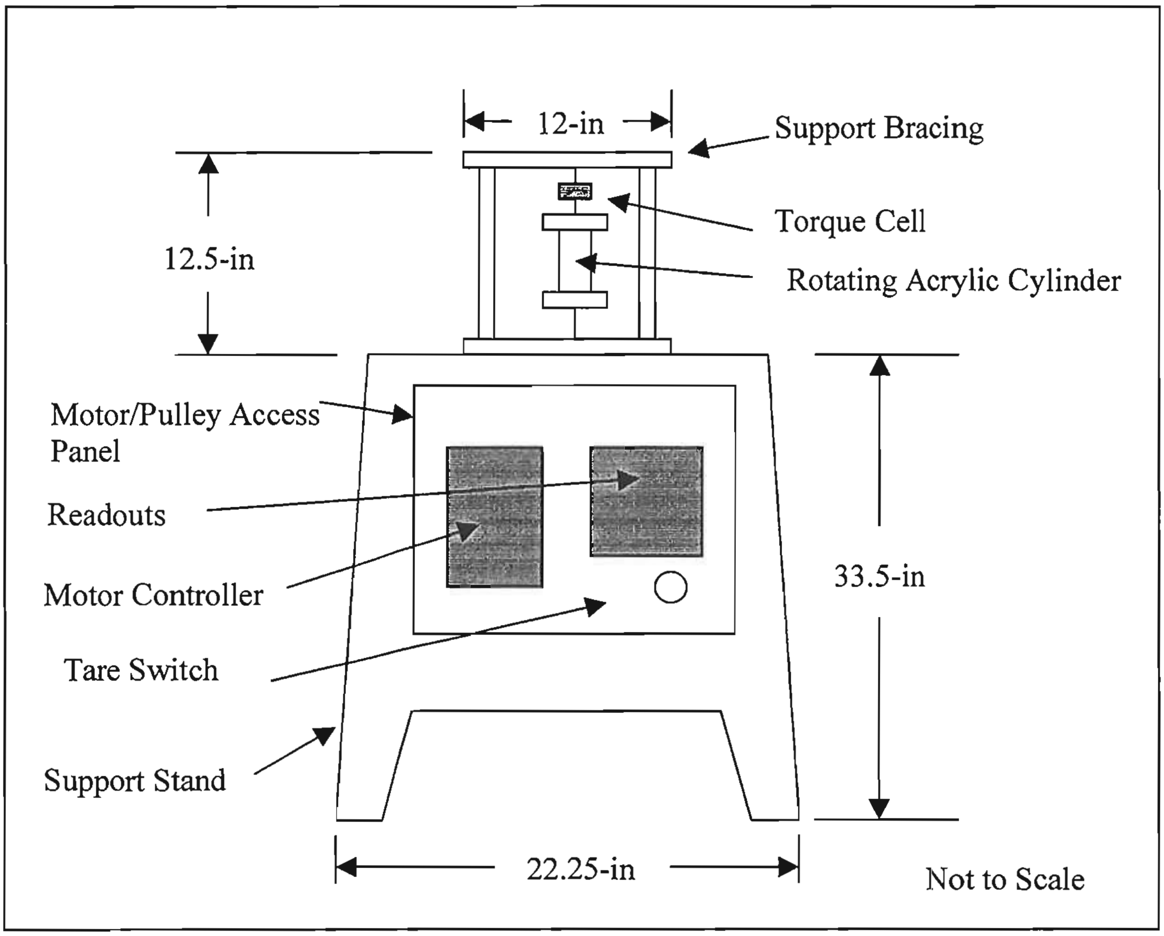

Fig. 1 Rotating Cylinder Test Apparatus Schematic

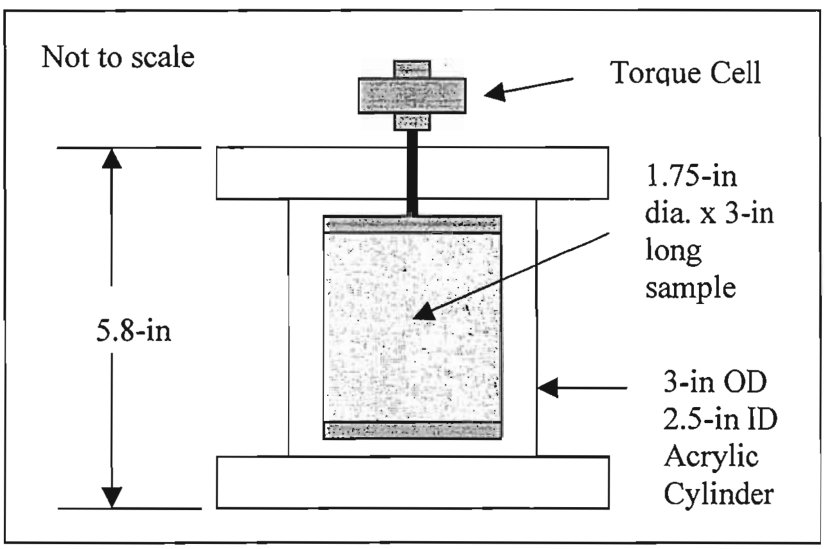

Fig. 2 Schematic of Acrylic Cylinder and Torque Cell

- 3-in (7.62-cm) outside diameter (2.5-in [6.35-cm] inside diameter) acrylic cylinder,
- Omega digital readout, and
- Sensotec Model QWFK-8M Miniature Reaction Torque Transducer (torque cell) with a range from 0 to 25 in-oz (0 to 176.5 mm-N).

The testing apparatus consists of a prefabricated metal stand with a motor access panel placed on the front of the stand. The prefabricated metal stand has adjustable feet, which is used to level the apparatus, and handles mounted to the sides that can be used to transport the device. The motor is mounted beneath the top of the prefabricated metal stand. The acrylic cylinder is mounted to a ½-in (1.27-cm) diameter steel shaft that extends beneath the top of the metal stand. Two pulleys and a belt connect the motor and shaft. The motor controller is mounted on the outside of the access panel.

The rock sample to be tested is fixed between 2 thin plates and is secured by a 3/16-in (0.48-cm) threaded rod placed through the center of the sample. The rock sample/rod system is connected to the torque cell, which is held stationary by the support bracing fixed directly to the apparatus. The output from the torque cell is displayed by the Omega digital readout, which was programmed (following the manufacturers' recommended procedures) to provide the torque output in N-mm. The readout is mounted on the outside of the access panel next to the motor controller. A tare switch is connected to the readout. This allows the readout to be set to zero before a test to facilitate the torque reading. The tare switch is also mounted on the face of the access panel just below the readout.

The addition of the torque cell is an improvement over the previous methods for measuring torque. The torque cell allows for the elimination of bearings or flexure pivots to support the sample and for the measurement of the torque contributions due to end effects. In the previous devices, the cohesive soil sample was mounted on pivots or bearings so that the shear stress transmitted to the sample surface resulted in a slight rotation of the supporting tube. The resulting rotation was calibrated to measure the torque on the sample by using either torsion wires or by a pulley and weight system. In this type of set-up, the friction within the bearings must be accounted for.

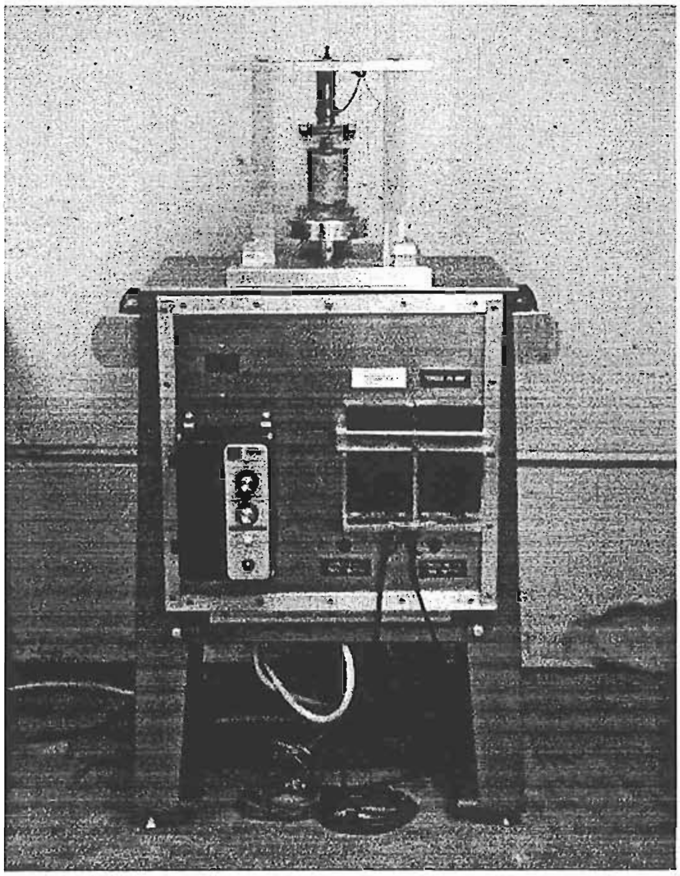

Fig. 3 Rotating Cylinder Test Apparatus

The addition of the torque cell allows for the direct measurement of torque with minimal rotation of the sample. Thus the need for bearings is eliminated. One end of the torque cell is mounted to the fixed support bracing and the sample is mounted to the other end.

To calibrate the torque cell, a moment arm was attached to the shaft where the sample would normally be located. A wire was run from the moment arm, over a pulley, to a pan where brass weights were placed. This allowed a known torque to be placed on the torque cell. The torque reading was plotted versus the expected value.

DETERMINATION OF END EFFECTS

In this type of erosion testing device, the torque measurements of interest are for the net torque exerted on the sample. Water flow over the top and bottom ends of the sample also produces a torque that is measured by the torque cell. Since the ends are protected from being eroded by thin metal plates, the torque being produced on the end of the sample must be taken into consideration. A method to evaluate the end effects with the torque cell was developed.

Experiments were performed to measure the torque exerted on the bottom plate. The experiments consisted of placing the threaded rod with the bottom plate only within the acrylic cylinder. Enough water is added in the rotating cylinder at each RPM tested to cover the underside of the bottom plate only. The torque at each RPM tested was recorded and a plot was developed. As will be discussed in the experimental procedures section, the torque on the bottom plate for a given RPM can be obtained from the plot. This torque is subtracted from the total torque reading. It should be noted that during a particular erosion test, only enough water is added to the cylinder annulus to wet the sides and not the end plate on the top of the sample. Therefore, only the end effects from the bottom plate needed to be considered.

EXPERIMENTAL SAMPLE PREPARATION

Samples that were tested in the apparatus were collected from rock cores obtained by the FDOT. The sample was formed by drilling a horizontal solid cylinder through a vertical core. The rationale for collecting a sample from the side of a core was based on the results of a preliminary experiment performed at the University of Florida. A sample of limestone was collected from a FDOT core and then cut into a cube. To obtain qualitative information about the anisotropy of these samples, a pressure washer was directed at each face of the sample. While this does not simulate field conditions (tangential flow over a bed), it did provide some insight into the erosion properties of the sample. It was discovered that there were differences in the rates at which various faces eroded. These differences in erosion can be attributed to the non-homogeneity and anisotropy of rock samples. It was concluded that in order to most accurately simulate the field condition, the sample face being eroded should be in the same orientation as in the field. By cutting a horizontal solid cylinder from the core, the eroding surface will be closer to the field situation.

The samples for erosion testing were taken from 4-in (10.16-cm) nominal diameter cores collected by the FDOT. The samples were cored from the sides using a concrete wet corer with a 2-in (5.08-cm) diameter core bit. This produced a sample of 1.75-in (4.45-cm) in diameter. The ends of the sample were leveled with a concrete wet saw. This left a sample with a length of approximately 3-in (7.62-cm).

A hole must be drilled in the center of the rock material to connect the end plates as well as to allow the sample to be connected to the torque cell. In preparing the samples, it was discovered that during coring, the samples could easily fracture. To minimize the fracturing, a 3/16-in (0.48-cm) diameter hole was drilled through the center. This minimized the disturbance to the sample and kept the sample intact.

EXPERIMENTAL PROCEDURE

The following is the procedure used to conduct a typical erosion test.

Sample Preparation

1. Prepare the sample for erosion testing as described in above by using a concrete wet corer and masonry drill bit.
2. Record the mass of the sample with the mass balance.

3. Place the sample in the drying oven for at least 16 hours to dry. After that time, record the mass of the sample. The sample is considered dry when the mass change is less than 0.1% in a period greater than 1 hour. Record the sample dry mass.
4. Measure the diameter of the sample with a Pi Tape at a minimum of three locations with the calipers and record the average diameter of the sample.
5. Measure the length of the sample with the calipers.
6. Measure the volume of the sample by gently submerging the sample in a graduated cylinder and measure the volume of water displaced.
7. Compute the sample dry density from the above measurements in g/cm^3.
8. Collect the water and loose material in a drying dish. Place the drying dish in the drying oven to remove the water. Record the mass of remaining material.
9. Completely immerse the sample in water for at least 16 hours to hydrate. The sample is hydrated to simulate a saturated rock formation as may be found in a waterway bed. After that time, record the mass of the sample. The sample is considered hydrated when the mass change is less than 0.1% in a period greater than 1 hour.

Testing Procedure

1. Secure sample on the threaded rod with the platens and place the sample in the rotating cylinder erosion-testing device.
2. Fill the rotating cylinder annulus with water to the proper level. It is important to note that water from the actual field site where the sample was collected should be used.
3. Place the rubber stopper on the acrylic cylinder and then attach sample to torque cell.
4. Set the offset of the torque cell with the tare switch to 0.000 mm-N.
5. Turn on the motor and increase the RPM (as measured by the tachometer) until the desired torque is achieved.
6. Allow the test to run for a minimum of 72 hours. Record the duration of the experiment in min with the stopwatch. Periodically adjust the motor speed to keep a constant torque on the sample. Record the torque in mm-N applied to the sample.
7. Turn off the motor and allow the water within the annulus to cease motion.
8. Remove the sample from the torque cell and cylinder.
9. Empty the water out of the cylinder and clean out the eroded particles in the cylinder.
10. Place the sample in the drying oven for at least 16 hours to dry. After that time, record the mass of the sample. The sample is considered dry when the mass change is less than 0.1% in a period greater than 1 hour. Record the sample dry mass.

There are a few important items to note with regards to the experimental procedures. First, prior to beginning the actual erosion experiments, a preparation run is required. The preparation run is required to remove loose material from the surface of the rock sample prior to measuring the erosion. The coring process disturbs the surface of the sample and this may cause an excessive amount of material to erode that may not have eroded otherwise. The preparation run was conducted after the sample dimensions were recorded but prior to the first experiment.

Also, at times, a slight amount of material would be removed from the sample during the saturation process. This material was collected and weighed (dry weight). This value was then subtracted from mass lost prior to the experiment so the change in mass would reflect the amount of material lost during the experimental run.

EXPERIMENTAL RESULTS

The first experiment was conducted on a rock sample from the site of the 17th Street Temporary Bridge crossing of the Intracoastal Waterway in Fort Lauderdale, Florida. The boring log that accompanied the sample described the rock as a "Loose Cemented Sand". The sample was collected from a proposed bridge pier location at a depth interval of 27.92 m and 30.97 m (91.58 ft and 101.58 ft) below the mudline. The second experiment was conducted on a rock sample from the same bridge site but at a different pier location. The boring log that accompanied this sample described the rock as a "Dark tan sandstone with small voids and no shells." The sample was collected from a depth interval of 29.93 m and 30.54 m (98.18 ft and 100.18 ft) below the mudline. This sample was collected at the same bridge location as the Cemented Sand sample but at a different pier location. At the time of this paper submission two tests were performed with the Sandstone and four with the Cemented Sand.

Figure 4 is a plot of both the Loose Cemented Sand and Dark Tan Sandstone erosion data. A trend line was fitted through the Cemented Sand data using Microsoft Excel. The Cemented Sand and Sandstone samples were similar in appearance and texture. This linear relationship is based on only four data points for the Cemented Sand. Research conducted by Chapius and Gatien in the area of cohesive soil erosion found that between six and ten samples were required to be tested to achieve a good evaluation of the erodibility of a clayey material. This number of samples allows for a statistical determination of the critical shear stress and the mean erosion rate as a function of shear stress (Chapius and Gatien, 1986, p. 86).

Rock is a non-homogenous and anisotropic material. It is anticipated that, similar to the findings Chapius and Gatien, that several samples from a given site must be tested before a meaningful erosion rate versus bed shear stress relationship can be developed. Therefore, the results presented here are preliminary, as only one sample was tested. The test results have the anticipated trend but a number of additional tests are needed before the variability of the samples and the locus of highest values can be established.

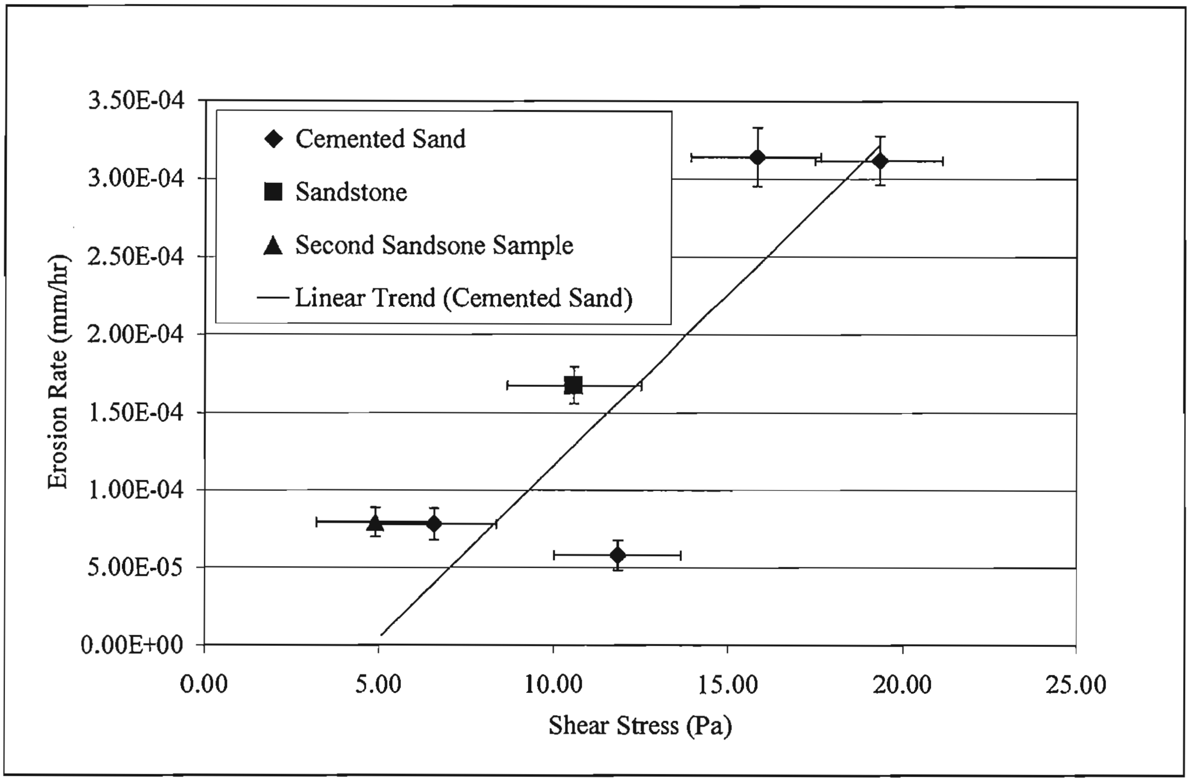

Fig. 4 Cemented Sand and Sandstone Erosion Rate Data

CURRENT RESEARCH

Currently, an improved multiple rotating cylinder device is being constructed to allow for several samples to be tested at varying shear stresses simultaneously. The improved device incorporates recommended design changes identified during the prototype construction and testing process. Also, another flume for the purpose of measuring erosion rates in rock materials is being constructed. In this device, water is circulated through a closed rectangular duct over the face of a rock sample. The face of the sample is advanced upward so as to maintain it flush with the bottom of the flume. This is an attempt to better simulate the *in-situ* conditions with water flowing over a natural bed. The results from this device will be used to compare and contrast with the data from the rotating cylinder apparatus.

ACKNOWLEDGEMENTS

This work was funded by the Research Office of the Florida Department of Transportation. Technical coordination was provided by the State Drainage Engineer, Mr. Shawn McLemore. We appreciate his support and technical input to the research. We also wish to thank Dr. Dave Horhota and Mr. Rick Renna of the Florida Department of Transportation for providing rock samples. Thanks go to Dr. Rob Nairn, of Baird & Associates, and Dr. Andrew Cornett, of the

Canadian Hydraulics Center, for providing information on their rock erosion experiments. Judy Mitrani and Ken Kerr assisted with the experimental work and sample collection.

REFERENCES

1. Akky, M.R., and Shen, C.K., 1973. "Erodibility of a Cement-Stabilized Sandy Soil." Soil Erosion: Causes and Mechanisms; Prevention and Control, Conference Workshop on Soil Erosion, Highway Research Board Special Report 135, Washington, DC, pp. 30-41.

2. Alizadeh, A., 1974. "Amount and Type of Clay and Pore Fluid Influences on the Critical Shear Stress and Swelling of Cohesive Soils." Ph.D. dissertation, University of California, Davis.

3. Annandale, G.W., 1995. "Erodibility." Journal of Hydraulic Research, Vol. 33, No. 4, pp. 471-493.

4. Annandale, G.W., Smith, S.P., Nairn, R., and Jones, J.S., 1996. "Scour Power." Civil Engineering, American Society of Engineers, July, pp. 58-60.

5. Arulanandan,K., Sargunam, A., Loganathan, P., and Krone, R.B., 1973. "Application of Chemical and Electrical Parameters to Prediction of Erodibility." Soil Erosion: Causes and Mechanisms; Prevention and Control, Conference Workshop on Soil Erosion, Highway Research Board Special Report 135, Washington, DC.

6. Chapius, R., and Gatien, T., 1986. "An Improved Rotating Cylinder Technique for Quantitative Measurements of the Scour Resistance of Clays." Canadian Journal of Geotechnical Engineering, Vol. 23, pp. 83-87.

7. Cornett, A., Sigouin, N., and Davies, M., 1994. "Erosive Response of Northumberland Strait Till and Sedimentary Rock to Fluid Flow." National Research Council of Canada, Institute for Marine Dynamics, TR-1994-22, September, Ottawa, Canada, pp. 1-15, 26-27.

8. Gordon, S., 1991. "Scourability of Rock Formations." Federal Highway Administration Memorandum, July 19, Washington, DC.

9. Jumikis, A.R., 1983. Rock Mechanics. 2nd ed., TRANS TECH Publications, Clausthal-Zellerfeld, Federal Republic of Germany, pp. 37-45, 51-53.

10. Merrington, A.C., 1949. Viscometry. Edward Arnold, London, England, p 30.

11. Moore, W.L. and Masch. F.D., 1962. "Experiments on the Scour Resistance of Cohesive Sediments." Journal of Geophysical Research, Vol. 67, No. 4, April, pp. 1437-1446.

12. PSI – Professional Services Industries Inc., 1996. Preliminary Geotechnical Engineering Study, U.S. 441 Bridge Over Santa Fe River, WPI No. 2110486, October 10, pp. 2-10.

13. Rektorik, R.J., and Smerdon, E.T., 1964. "Critical Shear Stress in Cohesive Soils from a Rotating Shear Stress Apparatus." Paper No. 64-216, American Society of Agricultural Engineers, June.

14. Richardson, E.V. and Davis, S.R., 1995. "Evaluating Scour at Bridges." 3rd ed., Hydraulic Engineering Circular No. 18, Publication No. FHWA-IP-90-017, Office of Technology Applications, HTA-22, Washington DC.

15. Rohan, K. and Lefebvre, G., 1991. "Hydrodynamic Aspects in the Rotating Cylinder Erosivity Test." Geotechnical Testing Journal, Vol. 14, No. 2, June, pp. 166-170.

16. Sargunam, A., Riley, P., Arulanandan, K., and Krone, R.B., 1973. "Effect of Physicochemical Factors on the Erosion of Cohesive Soils." Journal of the Hydraulic Divisions, Proceedings of the American Society of Civil Engineers, Vol. 99, No. HY3, March, pp. 555-558.

17. Smith, S.P., 1994. "Preliminary Procedure to Predict Bridge Scour in Bedrock." Colorado Department of Transportation, Report No. CDOT-R-SD-94-14, Denver, CO, December.

18. Van Rijn, L.C., 1993. Principles of Sediment Transport in Rivers, Estuaries, and Coastal Seas. Aqua Publications, Amsterdam, The Netherlands, p. 4.1.

TOWARDS PREDICTING TIME DEVELOPMENT OF LOCAL SCOUR AROUND OFFSHORE PIPELINES

By

Fangjun Li[1] and Liang Cheng[2]

ABSTRACT

Based on an intensive review on the development of numerical models of local scour below offshore pipelines over the last two decades, a numerical model is developed for predicting the time development of scour hole below a pipeline. The present numerical model solves the flow field using a Large Eddy Simulation (LES) model. The morphological change of the seabed is calculated via the continuity equation. The sediment deposition and entrainment rates are linked with the concentration of the sediment. The application of the present model to some laboratory tests demonstrates the robustness of the present model.

INTRODUCTION

Offshore pipelines laid on an erodible seabed are subject to local scour due to the disturbance to the local flow conditions. Local scour can leave the pipeline unsupported over sections that may extend significant distances. The pipeline may then subject to fatigue damage due to the oscillatory loads induced by waves or vortex shedding, or to mechanical damages such as by fishing trawls. An important aspect of pipeline design is the assessment of the likelihood for significant scour to occur and, if necessary, either how the design can be modified to reduce the risk of damage arising from scour or, alternatively, what preventive measures can be taken to reduce the occurrence of scour (Whitehouse, 1998).

Considerable research effort has been devoted to local scour adjacent to offshore pipelines and significant insights to the mechanisms of local scour have been achieved over the last two decades (see Whitehouse 1998; Sumer and Fredsøe 1999). Most of the investigations on local scour around pipelines are experimental and mainly on two-dimensional scour processes. There is no doubt that physical modeling is a fundamental and effective method to understand the mechanisms of scouring process. However, small-scale laboratory tests do suffer from scale effects because most of the scale-down models can not satisfy the similarity laws exactly. There are several scale effects such as the pipe Reynolds number, pipe roughness, in-coming flow turbulence, etc. (Sumer and Fredsøe, 1999). The scale effects need to be considered when the experimental

[1] PhD student, Department of Civil & Resource Engineering, The University of Western Australia, WA6907, Australia.
[2] Senior Lecturer, Department of Civil Engineering, The University of Western Australia, WA 6907, Australia.

results are interpreted to prototype situations. Unfortunately little is known about these scale effects and none of these effects have been studied in a systematic manner (Sumer and Fredsøe, 1999).

In contrast to the scaled-down laboratory tests, numerical models of local scour around pipelines do not suffer from scale effects. Once the numerical model is developed, it can be applied to different operational conditions including those can not be achieved under laboratory conditions. Many issues that could not be investigated thoroughly by model tests can be examined numerically. A typical example of this is the scale effects. Since it is very difficult to carry out experiments with large model pipes under laboratory conditions, the understanding to the scale effects is still limited. However the scale effects can be easily investigated using a proper numerical model. Numerical tests on the same scour process can be run under both model and prototype conditions. The individual factors that may affect the scour process can be isolated and controlled easily by numerical model. In that sense, a good numerical model can certainly be complementary to model tests and can assist design engineers to identify the most crucial cases for which model tests may be run. The ultimate goal of numerical models will be replacing (at least partially) the costly model tests and to be used directly in the design of pipelines.

Development of numerical models for local scour around pipelines has been slow, despite of their relative significance. There mainly two kinds of numerical models on local scour below a pipeline have been developed: simple mathematical models and integrated mathematical models (Sumer and Fredsøe, 1999). The simple model concerns the scour around a fixed pipe while the integrated model considers dynamic interactions between a flexible pipeline and the resulting scour process. Most of the models reported in literature so far are simple models. The idea of the integrated model however is to predict the entire scour process such as the occurrence and disappearance of scour along a pipeline, scouring and backfilling below the pipeline due to the sagging of pipeline. It is obvious that such a model is much more complex than the simple scour model and needs to be based on the development of the simple model. Due to the complexity of the problem and the limited computer resources that were available, current knowledge on the simple models prevents a comprehensive integrated model from being developed. Therefore the focus will be given to the simple mathematical model in this paper.

Over the last two decades, mainly two kinds of numerical model for scour prediction have been developed. One is based on the potential flow theory, such as Hansen et al. (1986) and Li and Cheng (1999a), and the other is based on the k-ε models, such as Leeuwenstein and Wind (1984), Brors (1999) and van Beek and Wind (1990). It has been demonstrated that the potential flow models are able to predict the maximum depth and the upstream part of scour hole correctly. However, none of the potential flow models can explain the gentle slope of the scour hole formed downstream the pipe (Li and Cheng, 1999a). This is mainly due to the fact that the potential flow model can not simulate the vortex shedding process associate with the flow around the pipeline. It has beenn understood (Sumer et al., 1988) that the gentle slope of the scour hole formed downstream the pipeline is mainly due to the vortex shedding around the pipeline.

Early numerical models based on k-ε turbulence models seemed to have difficulties to predict the shape of scour hole. Leeuwestein et al. (1985) developed a numerical model based upon k-ε turbulence model and a sediment transport equation. A numerical package named ODYSSEE was used to calculate the turbulent flow field. As for the computation of the sediment transport and the variation in seabed topography they reported a failure in obtaining a real scour hole shape by using an empirical bed-load formula. This was ascribed to the ignorance of the suspended-load contribution in the model. In the numerical part of the investigation by Sumer et al. (1988), the so-called Cloud in Cell (CIC) method was employed to simulate the flow. It was reported that the CIC method generally gives good prediction on the gross characteristics of the organized wake behind the pipeline. However, there was no evidence in the paper showing that a numerical model was employed to calculate the seabed deformation. Instead, by comparing the effective Shields parameter with its time average value, an important conclusion was drawn by Sumer et al. (1988) that the organised wake behind the pipeline has strong effects on the profile of scour hole downstream of the pipeline. The time-averaged bed shear stress is not a suitable parameter to use in predicting the lee-wake scouring behind a pipeline.

Some improvements on the k-ε based models have been achieved recently. Van Beek and Wind (1990) developed a numerical model based on k-ε turbulence model and a transport equation for suspended sediment. The application of the model to scour prediction below a pipeline with and without an attached spoiler showed fairly agreements with the measured equilibrium scour holes, although a certain degree of underestimation of downstream scour hole was quite evident in the report. The predicted rate of erosion was about three times as fast as in the physical model. Brørs (1999) presented a model that includes the description of fluid flow by the standard k-ε turbulence and the suspended and bed-load sediment transports. Density effects were considered in the vertical momentum equation and in the turbulence equations. Flow around a surface mounted cylinder was predicted in good agreement with the experiments. However, in the scour calculation the model did not predict periodic vortex shedding, even during the later stages of scour development. The author suggested that a fine mesh (5000 nodes) is needed to predict the phenomena of vortex shedding. For the scour calculations, the prediction of a clear water scour hole ($\theta = 0.048$, where θ is the Shields parameter) agreed well with Mao's (1986) experimental measurements. No attempts were made for cases of live bed scour.

Recently, Li and Cheng (1999b) developed a numerical model for local scour around pipelines employing a slightly different approach. The flow around the pipeline is solved using a Large Eddy Simulation (LES) model that results in more accurate prediction of seabed shear stress than traditional k-ε turbulence models. The equilibrium scour hole is determined by iterations, based on the assumption that the shear stress on the seabed is equal or less than the far field shear stress for live bed scour (or the critical shear stress for clear-water scour) every where when the equilibrium scour hole is established. The predicted equilibrium scour hole compared very well with the experimental results by Mao (1986) for both clear water and live-bed conditions (Li and Cheng, 1999b; 2000a). The advantage of the model is that it does not employ any empirical sediment transport formula. However, the disadvantage of the model is that it can not describe the time development of the scour hole due to use of the equilibrium assumption in the model.

In summary, it seems that none of the current models are able to simulate the time development of two-dimensional scour hole accurately even under steady current conditions. The key elements in developing a comprehensive model of time-dependent scour lie in two folds: 1) an accurate flow model that can result in accurate prediction of vortex shedding behind the pipeline and, 2) a proper sediment transport model.

The objective of the present paper is to develop a numerical model that is capable of predicting the time development of local scour below a pipeline. The model will employ the LES flow model developed by Li and Cheng (2000a). The morphological change of the seabed will be calculated in the same fashion as that used by BrØrs (1999). The rate of bed-level change will be determined from the deposition rate D and the erosion rate E. The deposition rate D will be set equal to the difference of setting velocity and upward turbulent velocity times the near-bed concentration. The erosion rate E will be determined from the near-bed turbulence intensity and the concentration gradients. The concentration of the suspended-load will be calculated by solving the scalar transport equation of suspended-load concentration. The boundary condition for the near-bed concentration of suspended-load will be specified using an empirical formula derived from experimental measurements (Zyserman and FredsØe, 1990). Details of the model implementation will be given in the following two sections.

MATHEMATICAL MODEL

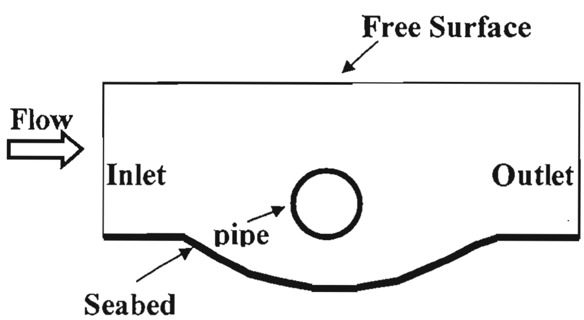

Fig. 1Definition Sketch: calculation domain

Flow model

It has been demonstrated both experimentally (Sumer et al., 1988) and numerically (Li and Cheng, 1999b) that the local scour below a pipeline depends strongly on the vortex shedding flow around the pipeline. Li and Cheng (1999b) demonstrated that the fluctuating seabed shear stress plays an important role in the so-called lee-wake scour process. Therefore accurate prediction of the fluctuating seabed shear stress is very crucial to the prediction of local scour below a pipeline. Past experiences of authors' and some others (Li and Cheng, 1999b; Beaudan and Moin, 1994) indicated that the Large Eddy Simulation (LES) model is suitable for the vortex

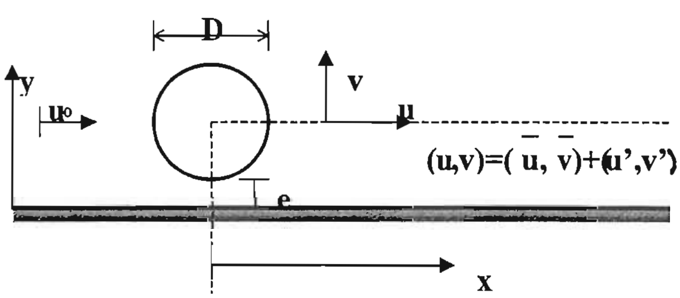

Fig. 2 Definition Sketch: a pipe near a wall

shedding flow around a circular cylinder.

To simulate the flow around the pipeline, the Large Eddy Simulation model employed by Li and Cheng (2000a) is used in the present paper. The spatially-filtered Navier Stokes equations together with the governing equation for centration of suspended sediment can be written in the following dimensionless form:

$$\frac{\partial u}{\partial x} + \frac{\partial v}{\partial y} = 0 \tag{1}$$

$$\frac{\partial u}{\partial t} + u\frac{\partial u}{\partial x} + v\frac{\partial u}{\partial y} + \frac{\partial p}{\partial x} = \frac{1}{Re}\left(\frac{\partial^2 u}{\partial x^2} + \frac{\partial^2 u}{\partial y^2}\right) + \frac{\partial \tau_{11}}{\partial x} + \frac{\partial \tau_{12}}{\partial y} \tag{2}$$

$$\frac{\partial v}{\partial t} + u\frac{\partial v}{\partial x} + v\frac{\partial v}{\partial y} + \frac{\partial p}{\partial y} = \frac{1}{Re}\left(\frac{\partial^2 v}{\partial x^2} + \frac{\partial^2 v}{\partial y^2}\right) + \frac{\partial \tau_{12}}{\partial x} + \frac{\partial \tau_{22}}{\partial y} \tag{3}$$

$$\frac{\partial c}{\partial t} + u\frac{\partial c}{\partial x} + (v - \omega_s)\frac{\partial c}{\partial y} = \frac{\partial\left(\overline{-c'u'}\right)}{\partial x} + \frac{\partial\left(\overline{-c'v'}\right)}{\partial y} \tag{4}$$

In the above equations, c is the concentration of suspended sediment, τ_{ij} is the subgrid scale shear stress, and Re is the Reynolds number based the incoming flow velocity u_o and the diameter of the pipeline D. All quantities in the above equations are normalized by the density of the fluid ρ, incoming flow velocity u_o and the diameter of the pipeline D. Smagorinsky's (1963) subgrid scale (SGS) turbulence model is adopted to close the equations, which relates the turbulence stress to the mean flow using an eddy-viscosity as,

$$\tau_{ij} = \nu_t\left(\frac{\partial u_i}{\partial x_j} + \frac{\partial u_j}{\partial x_i}\right) \tag{5}$$

$$\overline{-c'u'} = \frac{\nu_t}{\sigma_c}\frac{\partial c}{\partial x} \qquad \overline{-c'v'} = \frac{\nu_t}{\sigma_c}\frac{\partial c}{\partial y} \tag{6}$$

where ν_t is the eddy viscosity with $\nu_t = (C_s\Delta)^2\sqrt{2S_{ij}S_{ij}}$, S_{ij} is the strain-rate tensor ($S_{ij} = \frac{1}{2}\left(\frac{\partial u_i}{\partial x_j} + \frac{\partial u_j}{\partial x_i}\right)$), C_s is a coefficient and is taken as 0.1 in this study, σ_c is the turbulent Prandtl-Schmidt number (a value of σ_c =0.5 was suggested by Celik (1988)) and Δ is the filter width related to the grid size as $\Delta=(\Delta x\ \Delta y)^{1/2}$.

Boundary conditions

To solve the above equations, proper boundary conditions have to be specified. At the inlet boundary (see Fig. 1), the transverse velocity component is set to zero, and a uniform profile for the longitudinal velocity component is specified based. A vanishing-gradient of velocity componets is applied at the outlet boundary, and a symmetry boundary condition is prescribed on the top free surface boundary. At the non-slip wall boundary and the cylinder surface, zero velocity components are specified. On the inlet, outlet and wall boundaries, the pressure is obtained by applying the momentum equations in the direction normal to the boundaries.

In addition to the flow boundary conditions, boundary conditions on the concentration of suspended sediment have to be specified. At water and pipeline surfaces, the net sediment flux normal to the surfaces is zero. This results in

$$\overline{c'v_n'} - w_s c \cos\gamma = 0 \qquad (7)$$

where $\omega_s c$ is the downward flux of sediment due to gravity, and $\overline{c'v_n'}$ is the flux of sediment due to turbulence motion (usually upward); γ is the angle between the surface and horizontal plane.

The free falling velocity normally decreases as the concentration of sediment increases. The reduction of ω_s due to high particle concentration is considered using an empirical formula (Richardson and Zaki, 1954):

$$\frac{\omega_s}{\omega_o} = (1-c)^m \qquad (8)$$

where ω_o is the settling velocity of single particle in quiescent water; m is a grain size related constant, m=2.65~5.0.

At the erodible seabed, either the net flux of sediment or sediment concentration need to be specified. Since the residual flux is not readily calculable, alternatively, the near bed suspended load concentration is specified using an empirical formula (Zyserman & FredsØe,1990)

$$c_b = \alpha \frac{0.331(\theta' - 0.045)^{1.75}}{1 + 0.72(\theta' - 0.045)^{1.75}} \qquad (9)$$

where c_b is sediment concentration at an elevation b=2d, d is grain size, α is a coefficient, θ' is Shields parameter related to skin friction; the 0.045 is considered as critical value of Shields parameter for initiation of motion.

Equation (9) is based on the extensive experimental tests for sediment diameter ranged from 0.19 mm to 0.95 mm.

The sloping bed effect on sediment entrainment is considered by the modification of critical Shields parameter.

$$\frac{\theta'}{\theta_o'} = \cos\delta \pm \frac{\sin\delta}{\tan(\phi_S)} \qquad (10)$$

where θ_o' is the Shields parameter related to skin friction on flat bed; δ is the angle between the seabed and the horizontal plane; ϕ_S is the angle of repose. The positive sign on the right hand side in Eq. (10) is for an up slope flow and negative sign is for a down slope flow.

At inlet boundary, a power-law is used to specify the concentration profile (Rouse, 1939).

$$c(y) = c_b \left[\frac{y}{y_b} \frac{h - y_b}{h - y} \right]^{-B} \qquad (11)$$

where h is water depth, b is Rouse number, for d_{50} = 0.36mm sediment B = 2.8, and c_b is reference concentration at the level of y_b above seabed given by Eq. (9).

Numerical method

The governing equations (1) to (4) together with the boundary conditions are solved using finite difference method in a curvilinear coordinate system. The convection terms in equations (2) to (4) are discretized using a third-order upwind scheme and the other terms are discretized using central difference. A second-order scheme is used for all the time dependent terms. For details of numerical implementation, readers are refered to Lei et al. (1999).

Morphological model

The presence of pipeline breaks the local sediment balance and causes the variations in flow field. The location at which deposition or erosion takes place depends on whether the amount of sediment settling, D, is larger or less than the amount of sediment entrainment, E. The net cross boundary flux of sediment is zero only under equilibrium conditions. In general, there is a residual flux, which is normally the cause of morphological change of seabed.

For two-dimensional suspended-load dominant applications, the general sediment continuity equation can be written as

$$(1 - n)\frac{\partial y_s}{\partial t} = (\omega_s - v)c_b + \frac{v_t}{\sigma_c}\frac{\partial c}{\partial y} \qquad (12)$$

where n is the porosity of bed; y_s is bed level.

The first term on the right hand of equation (12) is the rate of deposition of entrained material, expressed as volume of sediment grains settling from suspension onto unit area of bed per unit time. The second term is the actual rate of entrainment of sediment mass from the bed, expressed as volume of sediment grains eroded into suspension from unit area of bed per unit time. Equation (12) indicates that the bed morphological change y_s is not only a result of upward diffusive flux and downward settlement but also the contribution of convective transport vc_b. It should be noted that the bedload sediment transport is not included in the morphological model given in Eq. (12). This implies the use of the assumption that the gradient of bedload transport in the flow direction is negligible. This is mainly based on the experimental findings that the bedload sediment transport is only confined within a very thin layer of a thickness of a few sediment diameters (Zyserman and Fredsøe, 1990).

Solution process

The solution process of local scour below a pipeline will start by solving the flow field and suspended-load concentration field around the pipeline with a specified seabed profile. Once the flow and suspended-load concentration fields are obtained, the morphological change of the seabed can be calculated by solving the continuity equation of sediment transport (Eq. (12)). The flow and suspended-load concentration fields will be calculated again with the updated seabed profile and the seabed is adjusted again with the new flow and concentration fields. This process will be repeated until the desired time of solution is reached. Since the morphological change of the seabed normally has a much larger time scale than the flow field, the solution of the flow field and update of the seabed profile use different time-steps to reduce the computation time. In the present study, the dimensionless time-step used to calculate the flow field is 0.001 while the time step used for morphological calculation is about 2. Given that a typical vortex shedding period is about 0.2, the seabed is updated once in about 10 shedding periods. This can save considerable calculation time.

RESULTS AND DISCUSSION

Validation of the LES model

In order to evaluate the performance of the present LES flow model, calculations are carried out for a case where experimental measurements are available (Jensen, 1987). In Jensen's experiments, the pipe was placed at 0.37D above a plane bed with a water depth 265 mm, the pipe diameter D= 30 mm and a Reynolds number Re= 7000 (based on free-stream velocity and cylinder diameter). A comparable set up is simulated numerically in a domain of 3000×350 mm with a pipe of diameter of 100 mm being placed at the position of 37 mm above the flat bed and 1000 mm from the inlet of the domain. A 153×63 mesh with grid points being concentrated towards the pipe surface and the seabed is employed for all the cases after a careful mesh-dependence study.

Fig. 3 and Fig. 4 give the horizontal and vertical velocity components at a number of sections downstream the pipeline together with the experimental results of Jensen (1987), respectively. It can be seen that the numerical model simulates the gross behaviour of the flow quite accurately. Fig. 5 and Fig. 6 show the comparison of the distributions of r.m.s horizontal and vertical components of velocity with the experimental results of Jesen (1987) at the same cross sections. It is seen again that the numerical results are in a fair agreement with the experimental results. This

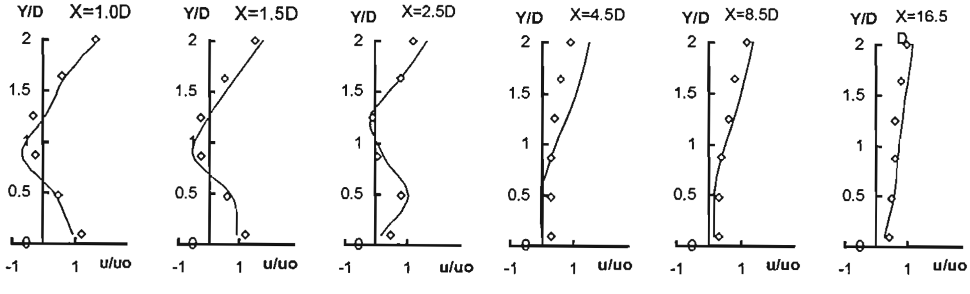

Fig. 3 Time-averaged horizontal velocity component $\bar{u}/u_0$ ° Experiment by *Jensen, --Model prediction*

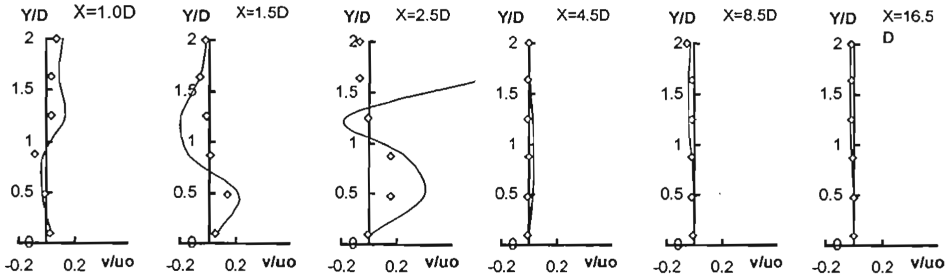

Fig. 4 Time-averaged vertical velocity component $\bar{v}/u_0$. ° Experiment by Jensen, --Model prediction

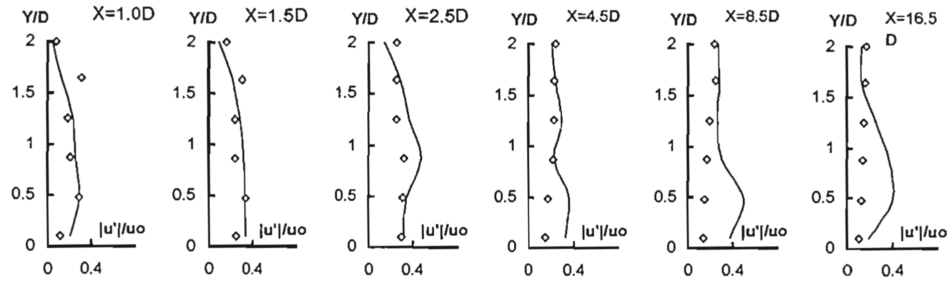

Fig. 5 r.m.s. values of horizontal fluctuations component u'/u_0 . ° Experiment by Jensen, --Model prediction

demonstrates that the present flow model (LES) is able to predict the gross behaviour of the vortex shedding flow investigated here.

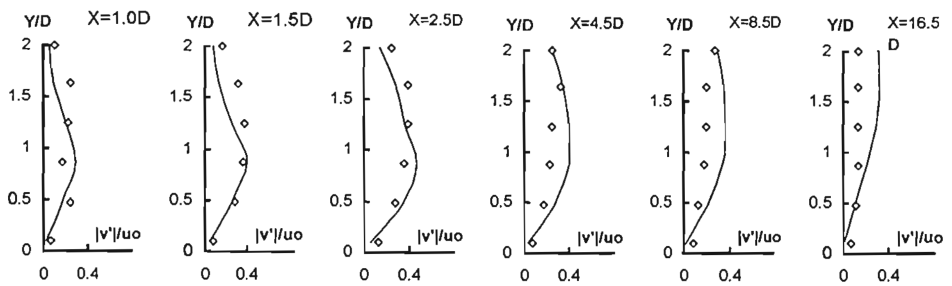

Fig. 6 -- r.m.s. values of vertical fluctuations component v'/u_0. ° Experiment by Jensen, --Model prediction

Local scour below a pipe on the seabed

To validate the numerical model developed in the present paper, some of the model tests conducted by Mao (1986) are chosen here as the test cases of the numerical model. Table 1 gives a summary of the cases for which the numerical tests have been run. The flow conditions, pipe diameters and particle diameter in the experiments are kept the same in the numerical tests. For all the numerical tests, a rectangular domain of 3000×350 mm with a pipe of diameter of 100 mm being placed at 1000 mm from the inlet of the domain. A 153×63 mesh with grid points being concentrated towards the pipe surface and the seabed is employed for all the cases after a careful mesh-dependence study. The numerical results on the time development of the scour hole as well as the maximum scour depth are compared with the experimental results of Mao (1986).

Table 1 Flow and sediment conditions for the numerical tests

Case	Pipe diameter (mm)	Sand size d_{50} (mm)	Flow velocity U_0 (cm/s)	Initial gap ratio e/D	Shields parameter θ
1	100	0.36	35.0	0	0.048
2	100	0.36	50.0	0	0.098
3	100	0.36	50.0	0.5	0.098

Fig. 7 and Fig. 8 show the scour development below the pipeline in time for case 1 and case 2, respectively. In those two cases, the pipe was originally placed on the seabed. The case1 is a case of clear water scour and the case 2 is a case of live bed scour. Measurements of scour profiles are available even at very early stage of the scour development. This is extremely valuable to validate the present numerical model.

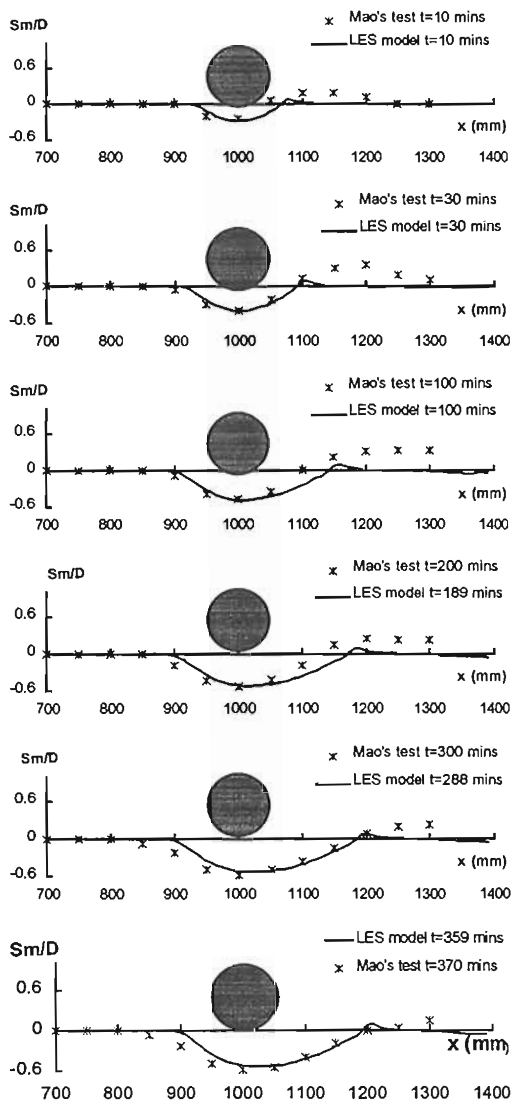

Fig. 7 Comparison of scour hole shapes, D=100 mm , e=0, θ=0.048

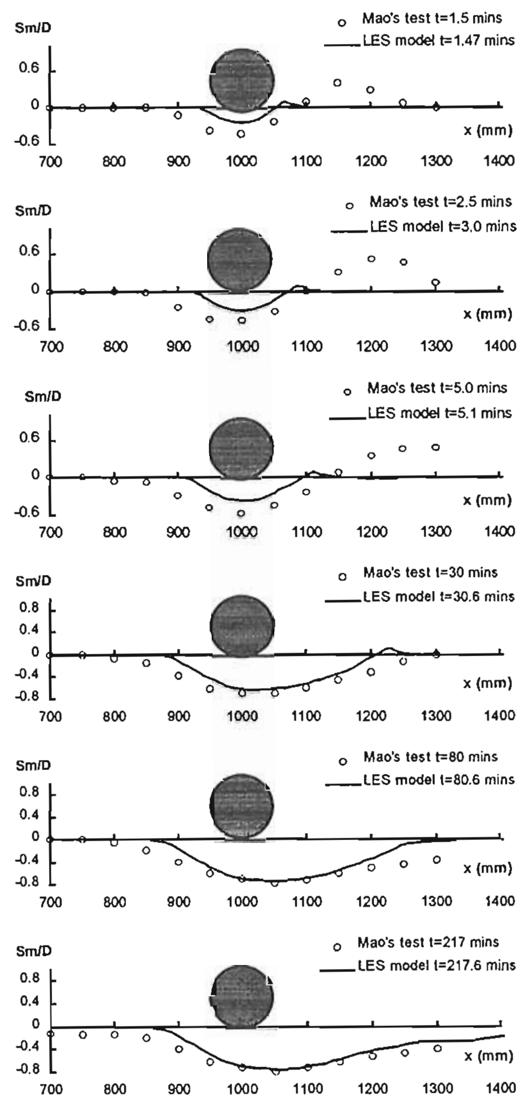

Fig. 8 Comparison of scour hole shapes, D=100 mm , e=0, θ=0.098

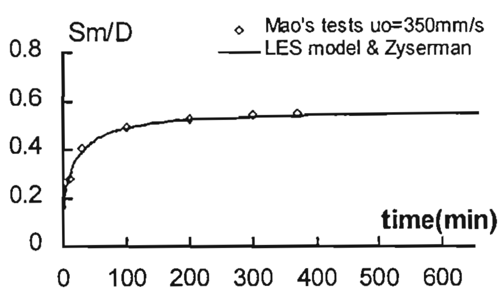

Fig. 9 Time development of scour depth (D=100 mm , θ=0.048)

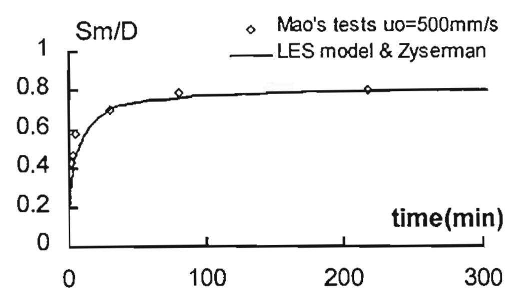

Fig. 10 Time development of scour depth (D=100 mm , θ=0.098)

It can be seen that the predicted time dependent scour profiles generally agree with the experiments very well. Descripancies however exist at relatively early stage of the scour development for both cases. Accumulations of the sediments were observed between 1D and 3D downstream of the pipe in the experiments of Mao (1986). This is not predicted by the numerical model. The main reason for the difference could be that non-uniform sands were used in the experiment while the numerical model can only deal with uniform sands. The accumulation part of the seabed observed in the experiments might be comprised of sands of larger diameters than the diameter used in simulation, d_{50}. The accumulations did disappear when the scour holes approached to equilibrium. The predicted equilibrium scour profiles agree very well with those measured in experiments in deed.

Fig. 9 and 10 gives the time development of maximum scour depth for case 1 and case 2 respectively. It can be seen that the agreement of the numerical results with experimental results are extremely well. The different scour rates at different stages of scour development are well captured. It can be seen that at the early stage of the scour development, the scour rate is very high. This is mainly due to the strong tunnel scouring underneath the pipeline. As the scour develops, the scour rates decrease significantly. This suggests that the scour mechanism has changed from tunnel scour satge to lee wake stage. It is obvious that the lee wave scour has a larger time scale than the tunnel scour. This is consistent with the experimental findings.

Fig. 11 shows the comparison of the numerical results with the experimental results of Mao (1986) for case 3 where

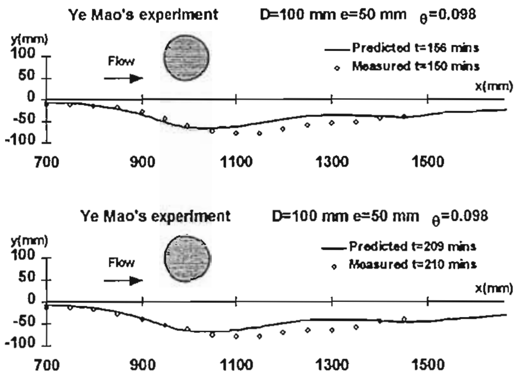

Fig. 11 Comparison of scour hole shapes, D=100 mm , e=0.5, θ=0.098

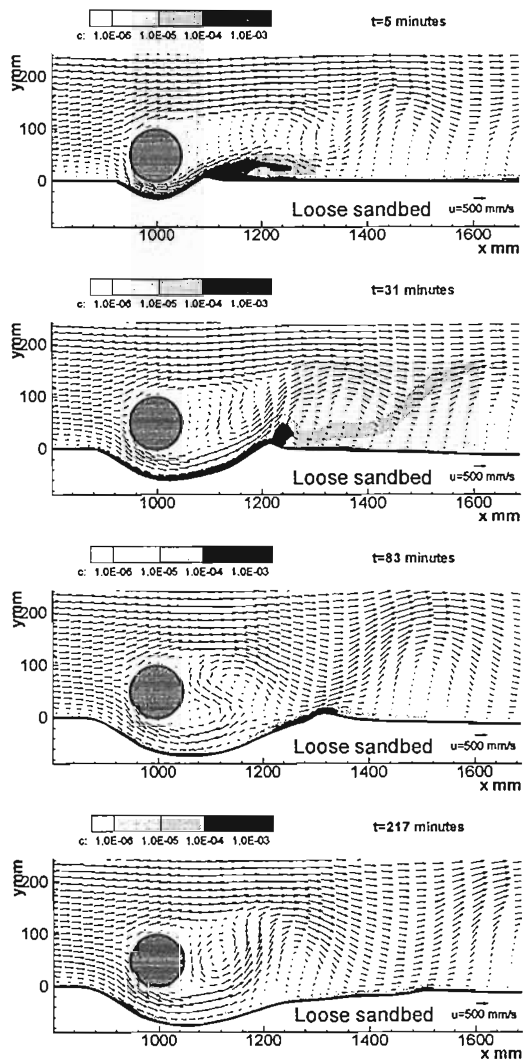

Fig. 12 Flow and sediment concentration fields at different time D=100 mm, e=0, θ=0.098

the pipe was initially placed half a diameter above the original seabed. The lee wake scour is normally the dominant scour mechanism under such a situation. Since the vortex shedding is the major cause of the lee wake scour, it is generally more difficult for the numerical model to predict the scour accurately for such a case. Nevertheless, the present numerical model handles such a situation very well, as shown in Fig. 11. This again demonstrates the rubustness of the present numerical model.

Fig. 12 shows the flow fields around the pipe at different stages of scour development. It can be seen that at early stage of the scour development (t = 5 min), a strong flow jet passes through the gap between the pipe and the seabed. It is believed that this strong flow jet is the major cause of the tunnel scouring. As the scour hole develops, this flow jet becomes weaker and the vortex shedding become more pronouced. The dark colour near the scoured seabed represents the high concentration of the sediment. Initially there is a large concentration area right behind the cylinder and this dark moves downstream gradually as the scour hole develops. When the scour hole almost reaches equilibrium (t = 500 min), the sediment concentration becomes very small even in the neigbourhood of the seabed. This suggests that the seabed shear stress is very close to the shear stress of incoming flow. It can also seen from Fig. 12 that the vortex shedding exists even in the early stage of the scour (t = 5 min). This is consistent with the experimental observation of Mao (1986).

CONCLUSION

A numerical model for local scour below a pipeline has been developed in this paper. The numerical model employs a LES model to simulate the flow field and a sediment concentration for sediment transport. The validation of the flow model and the application of the present model to some of the test cases of Mao (1986) allow the following conclusions being made:

1. The Large Eddy Model predicts the gross features of a flow around a pipeline near a plane boundary quite well;
2. The present numerical model predicts the time development of local scour very well for both clear water scour and live bed scour situations;
3. The model gives good prediction on the local scour below a pipeline that was initally above the seabed. This suggests the model predicts the lee wake scour quite well.
4. The model predicts the time development of the maximum scour depth very well. This suggests that model captures the scour mechanisms (tunnel scouring, lee wake scouring and even the transiotion between the two) very well.
5. The model can be further extended to local scour below pipelines under waves.

REFERENCES

1. BEAUDAN, P. AND MOIN, P. (1994) "Numerical experiments on the flow past a circular cylinder at sub-critical Reynolds number," Report No. TF-62, Stanford University.

2. BRØRS, B. (1999). "Numerical modeling of flow and scour at pipelines" J. Hydr. Engrg., ASCE,125(5), 511-523

3. CELIK, I. AND RODI,W. (1988). "modelling suspended sediment transport in nonequilibrium situations" J. Hydr. Engrg., ASCE, 114(10), 1157-1191.

4. HANSEN, E. A., FREDSOE, J. AND MAO, Y. (1986). "Two-dimensional scour below pipelines," Proc. Fifth Int. Symp. on Offshore Mech. and Arctic Engrg., American Society of Mechanical Engineers, 3, 670--678.

5. JENSEN B.L. (1987). "Large-scale vortices in the wake of a cylinder placed near a wall." Proc. 2nd international conference on Laser anemometry-advances and applications, Strathclyde, UK, 153-163.

6. LEI, C., CHENG, L. AND KAVANAGH, K. (1999) "A finite difference solution of the shear flow over a circular cylinder," Ocean Engineering, Vol. 27, No. 3, pp. 271-290.

7. LEEUWESTEIN, W., BIJKER, E. A., PEERBOLTE, E. B. AND WIND, H. G. (1985). "The natural selfburial of submarine pipelines," Proc 4th Int. Conf. on Behaviour of Offshore Structure (BOSS), Eleevier Science Publishers, 717-728.

8. LEEUWESTEIN, W., AND WIND, H. G. (1984). "The computation of bed shear in a numerical model," Proc 19th Int. Conf. on coastal Engineering, Houston, TX, Vol. 2, 1685-1702.

9. LI, F AND CHENG, L. (1999a). "A numerical model for local scour under offshore pipelines" J. Hydr. Engrg., ASCE, 125(4), 400-406.

10. LI, F. AND CHENG, L. (1999b). "Numerical simulation of pipeline local scour with Lee-wake effects," The 9th International Conference on Offshore and Polar Engineering, ISOPE 99, Brest, Vol,II, 212-216.

11. LI, F. AND CHENG, L. (2000a). 'Prediction of lee-wake scouring of pipelines in currents" J. of Waterway, Port, Coastal, and Ocean Engineering (submitted).

12. MAO, Y. (1986). "The interaction between a pipeline and an erodible bed," Series Paper 39, Tech. University of Denmark.

13. RICHARDSON, J. F. AND ZAKI, W. N. (1954) "Sedimentation and Fluidisation, Part I," Trans. Inst. Chem. Engrs, Vol. 32, No.1, pp 35-53.

14. ROUSE, H. (1939) "Experiments on the mechanics of sediment suspension," Proc. 5th Int. Congr. Appl. Mech., Cambridge, Mass., 550-554.

15. SMAGORINSKY, J. (1963). "Gereral circulation experiments with the primitive equations, I. The basic experiment", Monthly. Weather Review, Vol. 91(3), 99-164.

16. SUMER, B. M., JENSEN, H. R. AND FREDSØE, J. (1988). "Effect of lee-wake on scour below pipelines in current," J. of Waterway, Port, Coastal, and Ocean Engineering, Vol. 114, No. 5, 599--614.

17. SUMER, B. M. AND FREDSØE, J. (1999). "Wave scour around structures," Advances in Coastal and Ocean Engineering, Edited by Philip L.-F. Liu, Vol. 4, 191--249.

18. VAN BEEK., F. A AND WIND., H. G. (1990). "Numerical modelling of erosion and sedimentation around pipelines. Coastal Engineering, 14 107-128.

19. VAN RIJN, L. C. (1984). "Sediment transport, Part II: suspended load transport," J. Hydr. Engrg., ASCE, 110(10), 1613--1641.

20. WHITEHOUSE, R. (1998). "Scour at marine structures," Thomas Telford Publications.

21. ZYSERMAN, J. A. AND FREDSØE, J. (1990). "Data analysis of bed concentration of suspended sediment," J. Hydraulic Engineering, Vol. 120, No. 9, 1021-1042.

EXPERIMENTAL STUDY OF THE SCOUR ON THE SEABED UNDER A PIPELINE IN OSCILLATING FLOW*

By

Pu Qun[1], Li Kun[2]

ABSTRACT

An experimental study of the scour of the seabed under a marine pipeline is presented in this paper. The tests are carried out in a U-shaped oscillatory water tunnel with a box imbedded in the bottom of the test section. By use of the standard sand, clay and plastic grain as the seabed material the influence of the bed material on the scour is studied. The relationship between the critical initial gap-to-diameter ratio above which no scour occurs and the parameters of the oscillating flow is obtained. The self-burial phenomenon occurred for the pipeline not fixed on two sidewalls of the test section and is not observed for fixed pipeline. The effect of the pipe on the sand wave formation is discussed. The maximum equilibrium scour depths for different initial gap-to-diameter ratio, different *Kc* number and different bed sand are obtained.

INTRODUCTION

The sour around a pipeline may influence the in-place stability of the marine pipeline, so it is important for the safety and economy of submarine pipeline design [1,2]. The scour phenomenon around a pipeline is very complex because the scour can be influenced by many environmental elements such as the flow, the topography and the soil. This phenomenon is substantially a result of coupling actions between fluid, solid and seabed. The scour below a pipeline exposed to wave is related to oscillating separated vortex flow. Because of the seabed erosion and that the seabed boundary is in a dynamic condition, the boundary will change and the seabed material will enter the water, which will cause the difference between the separated vortex flow around a pipeline above a erodible bed and that above a plane bed [3]. On the other hand, start and transportation of the sediment in a unsteady flow is a frontier problem in sediment research [4]. In addition, there is complicated interaction between multiple separated vortices during the process of the

* The project is supported by the NNSF of China (19772065) and the Key Project (KZ951-A1-405) of "Ninth Five-year Plan" of CAS.

[1] Prof., Institute of Mechanics, Chinese Academy of Sciences, Beijing 100080, P.R. China
[2] Senior Engineer, Institute of Mechanics, Chinese Academy of Sciences, Beijing 100080, P.R. China

oscillating flow. Furthermore, if it is taken into account that the vortex-induced oscillation of the pipeline may affect the flow field and the transportation of sediment, the problem will be even more complex. Due to the above reason, it is almost impossible to completely simulate the actual situation. Therefore it is necessary to conduct studies on correlation of parameters that influence the scour and scour mechanism. Many studies on scour in wave have been conducted and some engineering formulas have been proposed [1, 5, 6, 7], although they are not as much as in currents. Most of these studies focus on sand bed. In fact seabed is composed of various soil materials. There is clay bed in many continental shelves and coastal water areas. So the study of the effect of different soil material on pipeline scour is important both in engineering design and in academic investigation. Because the oscillating flow is a simplified form of the wave, the tests in present paper are carried out in a U-shaped oscillatory water tunnel with a soil box imbedded in the bottom of the test section. The influence of the bed material on the scour and the self-burial phenomenon are studied. The relationship between the critical initial gap-to-diameter ratio above which no scour occurs and the *Kc* number is obtained. The maximum equilibrium scour depths for different initial gap-to-diameter ratio, different *Kc* number and different sand bed are obtained.

EXPERIMENTAL SETUP AND PROCEDURE

1. Experimental setup

A schematic drawing of the U-shaped oscillating water tunnel is shown in Fig.1. By using an air blower with a butterfly-valve which periodically opens and closes the top of a limb of the water tunnel, the water in the tunnel accomplishes a simple harmonic oscillation:

$$A_0 = A_m \sin \omega t \tag{1}$$

where A_m is the amplitude of the oscillating flow, ω is the cycle frequency $\omega=2\pi/T$, T is the natural period of the oscillating water and equals 2.59s. The amplitude can be varied up to 0.2m. The size of the test section is $0.2\times0.2\times0.8m^3$. A bed box of $0.035\times0.2\times0.6m^3$ is embedded in the bottom of the test section. The undisturbed bed top surface is in the same level with the bottom of the test section. By use of the contour elbow the flow velocities at the inlet and outlet parts of the test section are uniform.

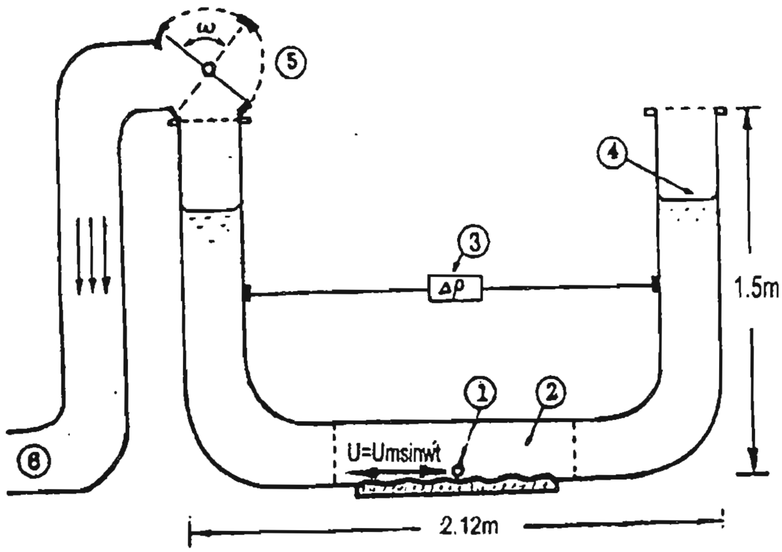

Fig.1 Schematic drawing of the U-shaped water tunnel
1. Test cylinder 2. Working section 3. A differential pressure transducer
4. Water level 5. A butterfly valve 6. Wind tunnel connected with an air blower

2. Pipeline model

The pipe models of diameters D=28.9 and 19.1mm are made of plexiglass and are fixed on two sidewalls of the test section. For the pipelines directly installed on the seabed, the pipe models of outer diameter D=14mm and inner diameter D_i=12mm are made of aluminium with length of 190mm. Different model pipes with different submerged weight are in different initial burial depth.

3. The preparation of the soil sample

Four soil samples are used in the tests for fixed pipeline models: the standard sand, the clay and two kinds of plastic grain with different mean diameter. The standard sand is with characteristics of d_{50}=0.20mm, specific gravity γ=2.59 and saturated unit weight γ_{sat}=10.24kN/m^3. The clay is with characteristics of d_{50}=0.0047mm, $\eta = \sqrt{d_{75}/d_{25}} = 2.86$ and with percent fine grains 72%. The plastic grain is with d_{50}=0.47, 0.68mm and specific gravity γ=1.42. The clay was excavated at 5-7m depth of port area Dongying of China. The clay sample in the bed box used in the present tests is obtained from the clay with the same initial unit weight and after four days of sedimentation in a tank. Then its unit weight is measured. For observation of the scour phenomenon around a pipeline in oscillating flow and investigation of the effect of the sand diameter on bed scour the plastic grain is used as the soil sample.

The standard sand with d_{50}=0.38mm, D_r=0.37, γ_{sat}=19.0kN/m^3 is used as bed material in the tests of unfixed pipe model.

The grain size distribution curves of the standard sand and the plastic sand are given in Fig.2. To ensure that the soil sample is sufficiently saturated, the sand is filled in bed box under the water in a sedimentary tank.

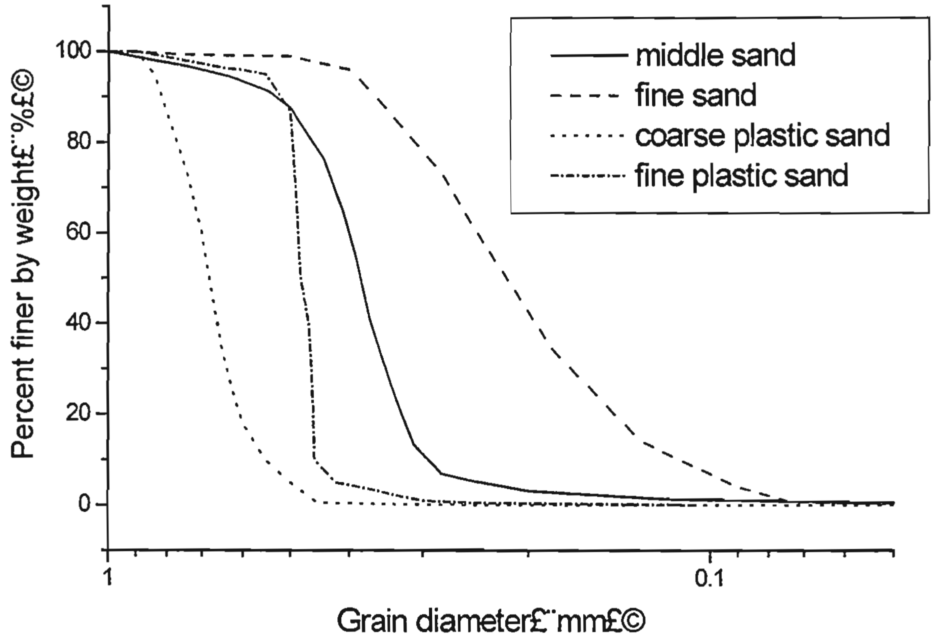

Fig.2 The grain size distribution curves

4. Test procedure

The development of the scour in every test is monitored by a CCD video camera located in front of sidewall of the test section. The oscillating amplitude is gradually increased. When the start of the bed sand is observed, the critical state of the scour is obtained. At certain oscillating amplitude the test is continued until the movable bed is in dynamic equilibrium. Then the maximum equilibrium scour depth and the wavelength of the sand wave are measured. For clay bed the sediment start is determined by sudden change of greyness in the water above the bed. Because the water became not transparent when scour occurred the CCD camera only can record the initial scour process. After two hours experiment the bed box is take out and the bed surface pattern is obtained.

Kc is the Keulegan-Carpenter number defined by

$$K_C = \frac{U_m T}{D} \tag{2}$$

Where $U_m = \omega A_m$ is velocity amplitude of the incoming flow, D is the pipe diameter. Reynolds number is defined by

$$\mathrm{Re} = \frac{U_m D}{\nu} \tag{3}$$

Where ν is kinematic viscosity coefficient of water. The Shields number corresponding to the incoming oscillating flow is defined by

$$\theta = \frac{f \cdot U_m^2}{(\gamma - 1) \cdot g \cdot d_{50}} \tag{4}$$

Where g is gravity acceleration, f is the friction coefficient for the wave-boundary layer, see ref.[8].

EXPEREMENTAL RESULT AND ANALYSIS

1. Scour process around the pipeline

The scour phenomenon for gap-to-diameter ratio e/D=0 is dissimilar to that for e/D not equal to zero. As Kc increase the flow separation and the vortex shedding occur. For e/D=0, the flow around a pipe is the forward separated flow at the corner between the lower pipe surface and the bed surface and is the separated and reattached flow behind the pipe. This flow undergoes an accelerated and decelerated process. Whatever the bed material is, the tests show that the scour occurs at the forward corner of the pipe at first. The sediment moves backwards away from the pipe and reaches the vicinity of the separated point B as shown in Fig 3(a). For standard sand bed the reattached flow behind the pipe is observed. The sediment moves towards two opposite directions away from the reattached point C, as shown in Fig 3(a). The location of C from the pipe is farther than B. With the scour development the sediment stacks up near the point B. The gap between the pipe and the bed occurs after a scour process, the flow pattern changes. For e/D not equal to zero the flow pattern is different from that for e/D=0. When e/D is small, the sediment reciprocates near the point A and then stacks up a little (see Fig 3(b)), whatever the bed is made of standard or plastic sand. When e/D is larger than a certain value, for example e/D=0.45~1.0 for standard sand bed, the reciprocations of sediments are observed at point A, D and E, shown in Fig.3(b). The larger the e/D, the larger the distance between A and D or E. This is dependent on the acting of the shedding vortex of the wake on the sand bed. With the velocity increased the transfiguration development of the bed surface is observed for standard and plastic sand bed. When the velocity is a little larger than the critical value, there is only one main sand valley formed underneath the pipe. As the velocity increases, the second and third sand waves occur successively on both side of the main sand valley. The larger the distance of the sand wave from pipe, the lower the peak of the sand wave is. The sand bed far from the pipe is undisturbed. It looks like there is a propagation and consumption of the wave energy in the liquefied sand bed. The scour holes of the standard sand bed are steeper than that of plastic sand bed. It may be interpreted by their different rest angle.

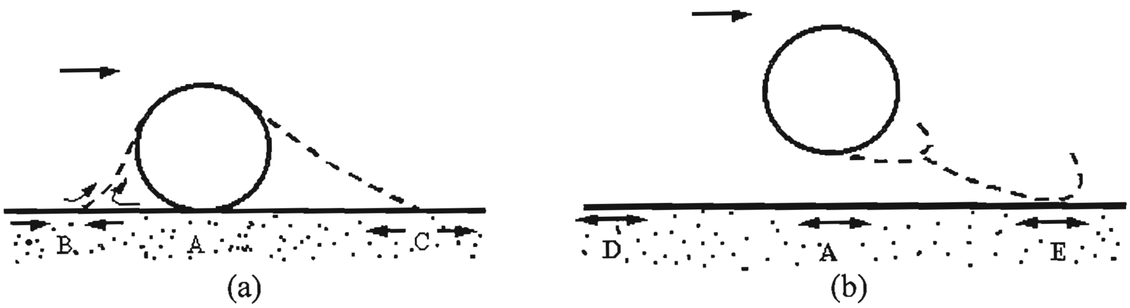

Fig.3 Schematic drawing of sand start for different gap-to-diameter ratio

2. Critical scour parameters

For onset of scour there is a minimum velocity for given *e/D* and one kind of bed soil. It is called the critical state for onset of scour. The test results at critical state for different *e/D*, different Kc and different bed soil are given in Fig.4. It is discovered that the experimental results for different bed soil are located on a series of oblique lines with the same slope in logarithm coordinates shown in Fig.4, although the characteristics of the different sand bed and clay bed are very different and the start mechanisms for them are also different. On the base of investigation in ref.[9] the correlative expression is given by

$$(e/D)_{cr} = 2.2\lg K_C - B \tag{5}$$

Where B is a constant related to the bed material characteristics. This conclusion is convenient in practice to determinate whether the scour of the bed takes place for different bed soil. It shows also that the *Kc* number is a main similar parameter among many similar parameters of the flow that influence the onset of scour. In Fig.4 the experimental results for fine plastic sand bed fall near the fitted straight line for coarse plastic sand bed given in ref.[9]. It is shown that the grain size has no obvious effect on critical scour at the present experimental conditions.

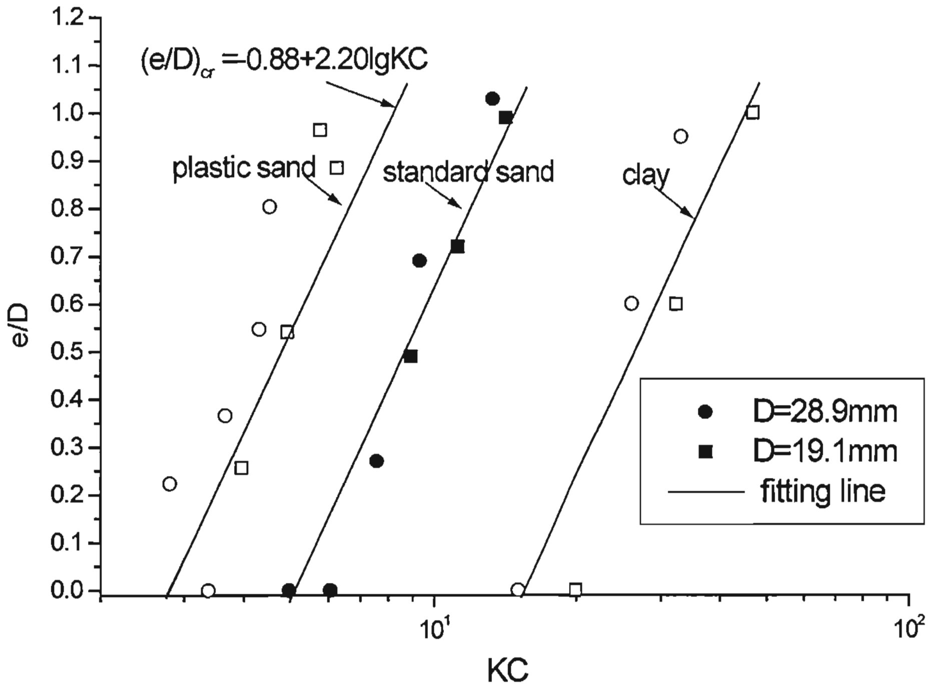

Fig.4 Critical gap-to-diameter ratio vs. *Kc* number

3. Sand wave formation

When there is no pipe on the bed, the start and scour of the sand bed also takes place as the oscillating velocity increase. The scour process for plastic and standard sand bed develops as follows: at first, part of the sand grains on the surface of the bed rocks at the original location with the oscillating frequency, but they do not jump from the bed; then they jump a little distance from the bed and move forth and back with the oscillating flow and the sand grains nearby begin oscillatory motion; in succession some streaming grooves distribute randomly on the surface of the bed. When the velocity is large enough, the regular sand waves form on the bed surface as mentioned in ref.[9]. With the velocity increasing the length and the height of the sand wave increases. At a certain range of velocity, for example at U_m=10.3~14cm/s for fine plastic sand, the length-to-height ratio does not vary and equals approximately to 10, the ratio A_{mcr}/k for coarse and fine plastic sand is nearly the same, where A_{mcr} is the minimum oscillating amplitude at which the sand waves occur and k is the roughness of the bed. A_{mcr}/k for standard sand is larger than that for plastic sand. After the sand wave takes place on standard sand bed, the oscillatory amplitude decreases obviously. It means that as a result of the sand wave formation the drag of the sand bed increase.

When the pipe is present on the sand bed, the scour of the bed takes place as mentioned above. When the oscillating amplitude is larger than a critical value, the regular sand waves also take place on the bed surface far from the pipe. The A_{mcr}/k for the sand bed with a pipe is a little smaller than that without a pipe. It is the same for standard or plastic sand bed. In present experiment it is shown that the critical oscillating amplitude for the same bed soil and different e/D and D is almost the same and the length of the sand wave is also the same. Despite of whether the pipe is present or not, a series of streamwise thin groove distributed along the pipe axis direction is seen on the sand wave valley surface.

4. Self-burial phenomenon

The pipe model used in self-burial test is not fixed on both side of the test section. The submerged weight of the pipe model is 0.68, 0.94 and 1.19N/m and the initial burial depth is 0, 3.6% and 7.1% respectively. The light pipe model rolls away from the original position at U_m=0.09m/s. There is not any trace on the bed surface. But for the heaviest pipe model as the velocity increase gradually, the scour of the bed at both sides of the pipe takes place at certain velocity and the sediment stacks up near the separated point B. It is similar to that for the fixed pipe. But it is different from the fixed pipe that due to the sag of the pipe into the scour valley the gap between pipe and bed cannot form. When the amplitude increases slowly, a scour hole forms gradually near point P that is outside the separated region. The bed sand grains move along the dash line as shown in Fig.5. Following the flow, the sand grains sedimentated at the top of the pipe shake left and right. As a result of the above process the pipe is self-buried gradually. The stability of the self-burial pipe increases. The middle weight pipe model shakes a little in scour hole at a certain velocity, but does not go out of the original place. When the flow amplitude increases drastically at this state, the pipe would roll up. It is seen in experiment that the formation of the self-burial phenomenon of the pipe is related to the accelerating process of the flow. A slow acceleration of flow leads to the self-burial, while a sudden acceleration of flow would bring about the instability of the pipe, especially after a little shaking of the pipe. The self-burial phenomenon is also related to the pipe weight or the initial burial depth. For the same accelerating process the heavier of the pipe weight or the deeper of the burial depth the more easy the self-burial takes place. It is also observed in the experiment that the characteristics of the sediment transportation near the separated point are major factors for the self-burial formation. The self-burial phenomenon does not occur in the tests for fixed pipe model.

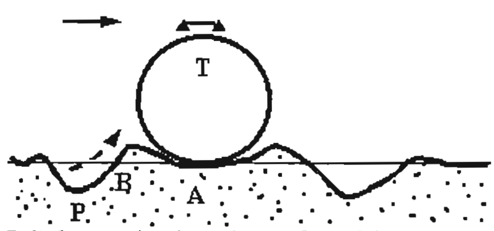

Fig.5 Schematic drawing of self-burial process

5. Maximum equilibrium scour depth

The experimental results of the maximum equilibrium scour depth are obtained at e/D=0~1.0 for the fixed pipe with D=2 and 3cm in the present paper. The ranges of the experimental parameters are listed in Tab.1.

Table 1-Ranges of Experimental Parameters for Different Bed Materials

Bed material	$K_C = \frac{U_m T}{D}$	$\mathrm{Re} = \frac{U_m D}{\nu}$	$\theta = \frac{f \cdot U_m^2}{(\gamma-1)\cdot g \cdot d_{50}}$
Fine plastic grain	4.30~22.20	0.9×10^3~4.0×10^3	0.052~0.273
Coarse plastic grain	3.91~31.90	1.3×10^3~6.5×10^3	0.049~0.395
Standard sand	6.07~32.57	1.3×10^3~4.9×10^3	0.030~0.245

For every bed material the test results can be related by a series of oblique lines in the logarithm coordinates of *S/D* and *Kc*, where *S* is the maximum equilibrium scour depth. For different *e/D* the intercepts of the oblique lines are different, but their slopes only differ a little. Taking the average of these slopes the normalized test results are given in Fig.6, Fig.7, and Fig.8 in logarithm coordinates of *S/(DA)* and *Kc*, for fine, coarse plastic sand and for standard sand bed respectively. Here A represents the intercepts of the oblique lines with average slope and is a function of e/D and D, as seen in Fig.6(b), Fig.7(b) and Fig.8(b). It must be pointed that most results for plastic sand are obtained at live-bed case, but most results for standard sand are taken from the case, where sediment far from the pipe does not move. A changes with *e/D* not very much in Fig.6(b) and Fig.7(b) but it changes obviously in Fig.8(b). From Fig.6, Fig.7, and Fig.8 the following relationship between *S/D* and *Kc* is given by

$$S / D = A \cdot K_C{}^m \tag{6}$$

Where m is a constant of the bed material.

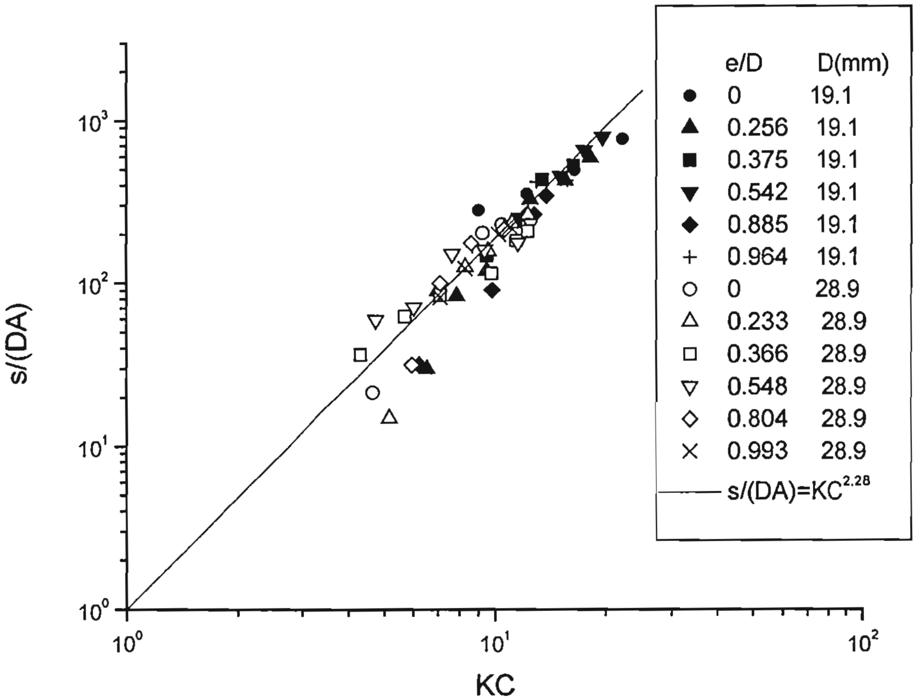

(a)

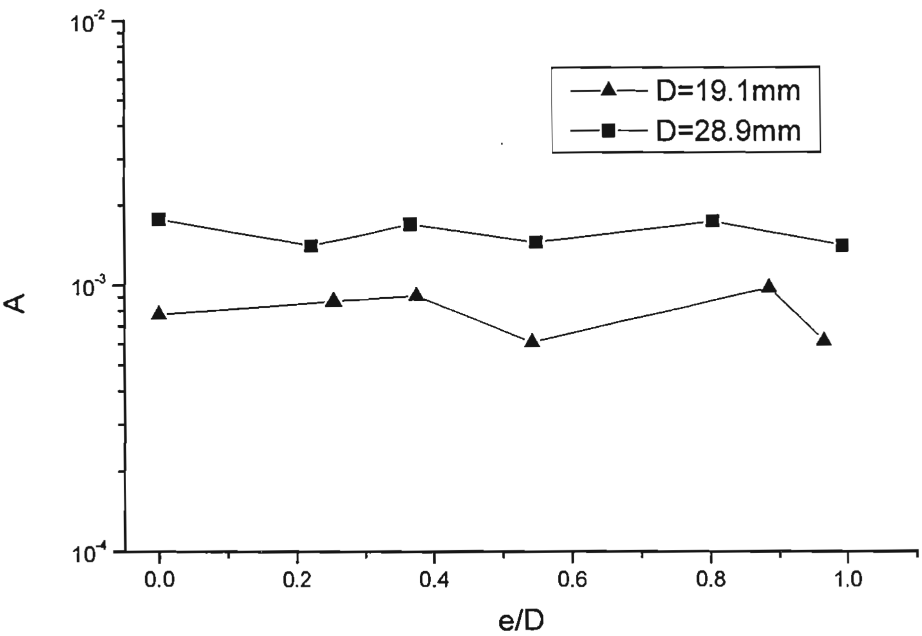

(b)

Fig.6 Dimensionless scour depth vs. *Kc* for fine plastic sand bed

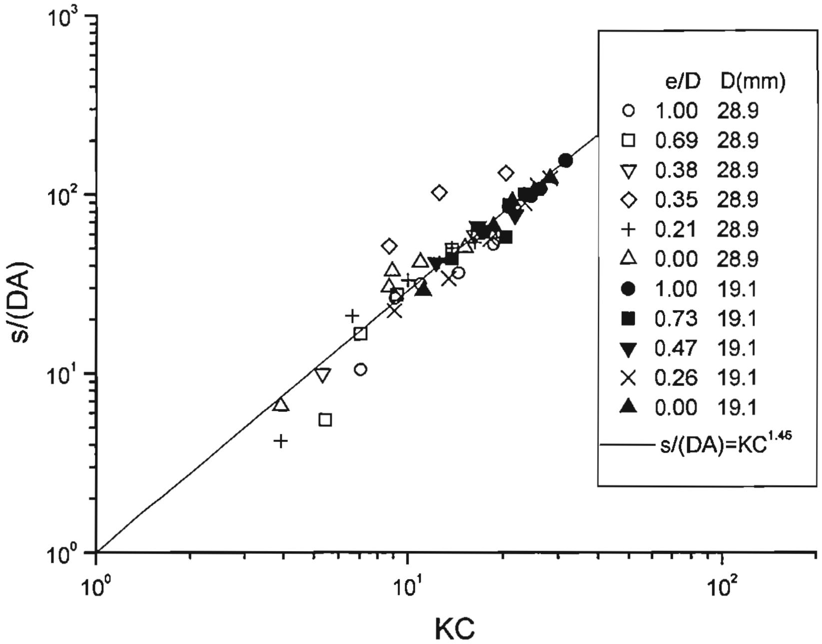

(a)

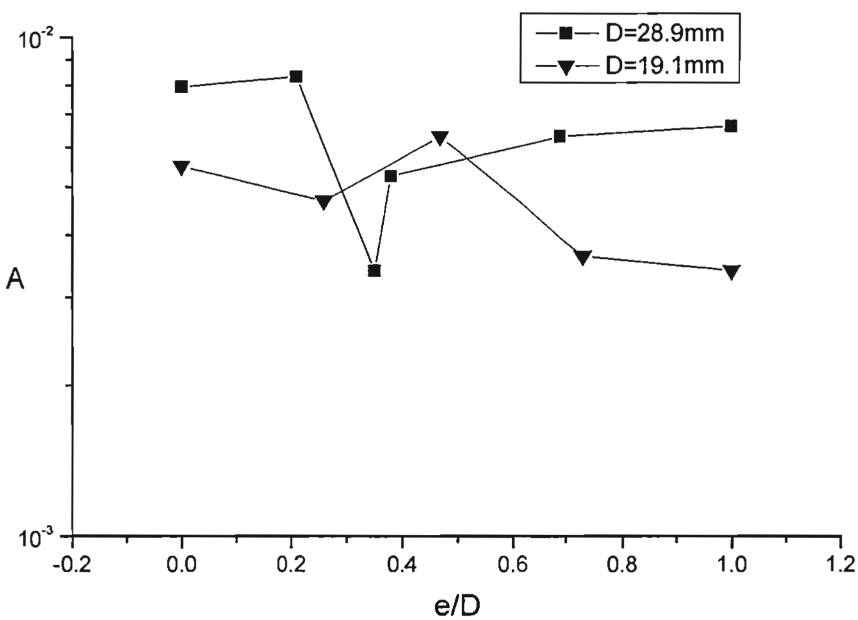

Fig.7 Dimensionless scour depth vs. *Kc* for coarse plastic sand bed
(b)

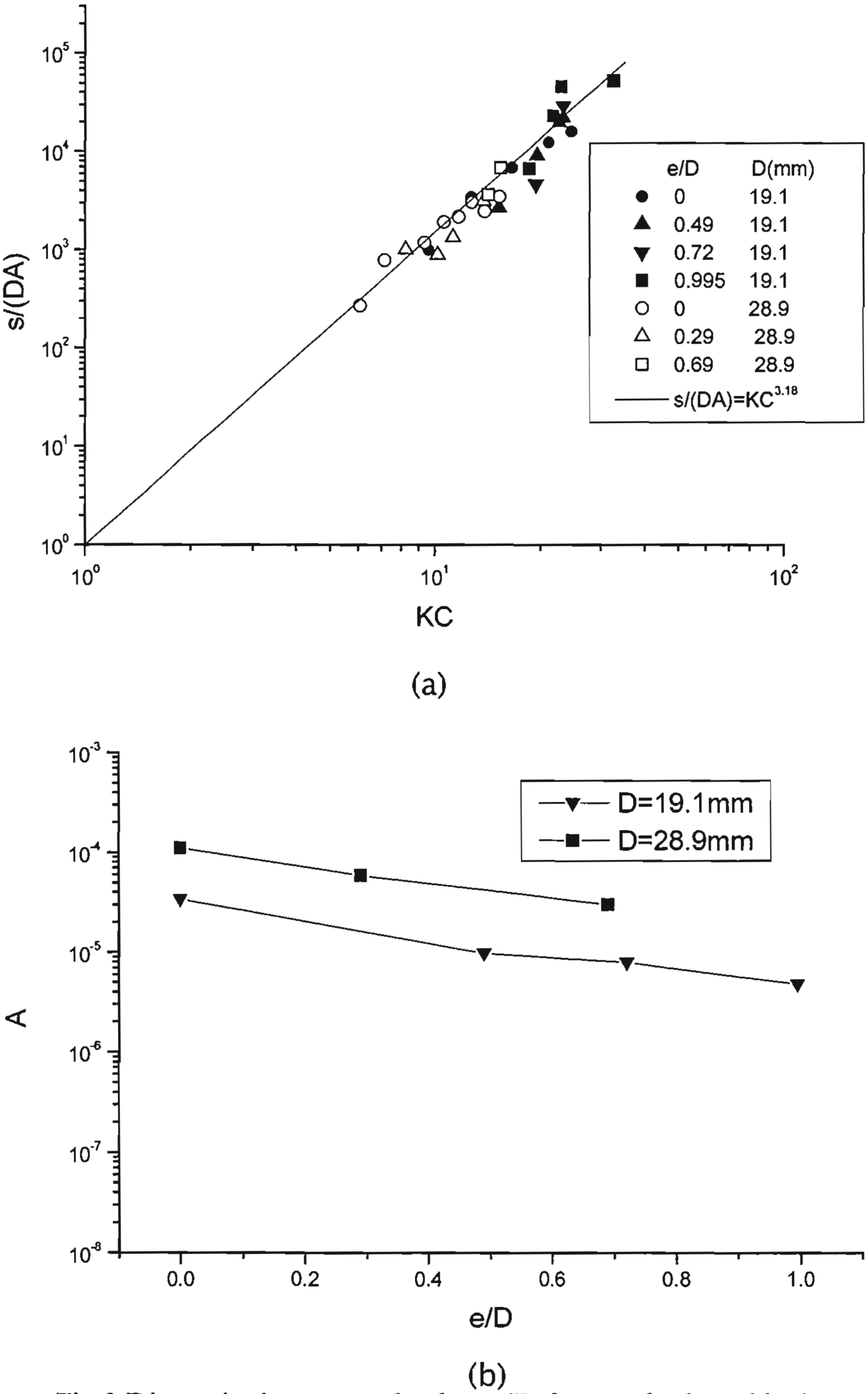

Fig.8 Dimensionless scour depth vs. *Kc* for standard sand bed

CONCLUSIONS

The following conclusions are obtained from the present experiments.

The onset of scour is mainly influenced by Kc number. The relationship between the critical initial gap-to-diameter ratio $(e/D)_{cr}$ above which no scour occurs and the Kc number can given by $(e/D)_{cr} = 2.2\log K_C - B$, where B is a constant of the bed material.

The presence of a pipe can result in a reduction of the dimensionless critical amplitude A_{mcr}/k, above which the sand wave forms on the surface of the bed.

The self-burial phenomenon is observed for pipe that is directly installed on the bed and does not occurs for fixed pipe. The self-burial phenomenon is related to the flow accelerating process and the pipe weight or the initial burial depth.

The relationship between dimensionless maximum equilibrium scour depth S/D and Kc number can given by the expression $S/D = A \cdot K_C{}^m$, where m is a constant of the bed material.

REFERENCES

1. Herbich John B., 1981, "Offshore pipeline design elements", MARCEL DEKKER, INC.
2. Bruschi R., Vitali L., 1994, "Recent advances in offshore pipeline technology", Proceeding of the 4th Int. Offshore and Polar Engineering Conf. Osaka, Japan
3. Sumer B.M., Jensen B.L., Fredsoe J., 1991, "Effect of a plane boundary on oscillatory flow around a circular cylinder", J. Fluid Mech., 225:271-300
4. Plate E J., 1994, "The need to consider non-stationary sediment transport", International Journal of Sediment Research, IRTCES, 9(3): 117-123
5. Sumer B.M., Fredsoe J., 1990, "Scour below pipelines in waves", J. Wtrway., Port, Cost. And Oc. Engrg., ASCE, 116(3): 307-323
6. GoKce K.T., Gunbak A.R., 1991, "Self burial and stimulated self burial of pipelines by waves", 1st Int. Conf. On Offshore and Polar Eng., ISCOPE, Edinburgh, 308-314
7. Cevik E., Yüksel Y., 1999, "Scour under submarine pipelines in waves in shoaling conditions", J. Wtrway., Port, Cost. and Oc. Engrg., ASCE, 125(1): 9-19
8. Fredsoe J., 1984, "Turbulent boundary layer in wave-current motion", J. Hyud. Eng. ASCE, 110(8): 1103-1120
9. Pu Qun, Li Kun, 1999, "Scour of the sand bed below the pipeline in oscillating flow", ACTA Mechanica Sinica, 31(6): 677-681

SCOUR POTENTIAL EVALUATED IN TERMS OF EXCESS PORE PRESSURE INDUCED BY OCEAN WAVES

By

Kouki ZEN[1] and Kiyonobu KASAMA[2]

ABSTRACT

The driving forces causing the scour are classified into two types of external forces; one is the shear force on the surface of soil layer created by the water flow. A typical example is the scour around the pier of bridge across the river. The other is the wave force generated by ocean waves. A large scale of scour in the coastal zone may be mainly attributed to the excess pore pressure fluctuation produced by wave action on the seabed. This paper presents the mechanism of the scour caused by the latter force in the ocean environment.

When ocean waves propagate, the oscillatory pore water pressure is created in the permeable seabed. Due to the spatial difference of oscillatory water pressure, the excess pore pressure, namely the excess hydraulic pressure, is generated and the distribution of excess pore pressure produces the seepage flow in the seabed. When the upward seepage force toward the seabed surface becomes larger than the effective overburden pressure in the seabed, the liquefaction or quick sand occurs. Once the liquefaction occurs at the seabed surface, the sand particles are easily transported by water flow, because the shear resistance of seabed surface becomes nearly equal to zero.

The wave-induced oscillatory pore water pressure in the seabed can be calculated on the basis of the consolidation theory by applying the appropriate initial and boundary conditions and input data. Then, the excess pore pressure is evaluated as the difference between the wave-associated water pressure on the seabed

[1]Professor, Department of Civil Engineering, Kyushu University, 6-10-1 Hakozaki, Higashiku, Fukuoka, 812-8581, JAPAN

[2]Research Associate, Department of Civil Engineering, Kyushu University, 6-10-1 Hakozaki, Higashiku, Fukuoka, 812-8581, JAPAN

surface and the oscillatory pore pressure in the seabed. The seepage force is calculated as the inclination of oscillatory water pressure distribution to the depth.

The upward seepage force in permeable seabed was analyzed using field data to evaluate whether or not the liquefaction occurred. The result of analysis showed that the liquefaction evidently happened. In that sense, the scour potential can be evaluated by estimating the excess pore pressure in the seabed. The excess pore pressure in the seabed is of significance in predicting the scour potential of the permeable seabed in the coastal zone.

INTRODUCTION

The west beach in the city of Niigata was a rich beach and athletic meetings used to be held there. Nowadays, the beach line approaches the private houses behind it due to the remarkable erosion by waves and/or current. The detached breakwaters using a large number of the wave dissipating concrete blocks have been constructed to prevent the erosion. It was found recently, however, that the wave dissipating concrete blocks have sunk into the seabed during the winter season as shown in **Fig.1** (Nishida, et. al, 1985). Many wave

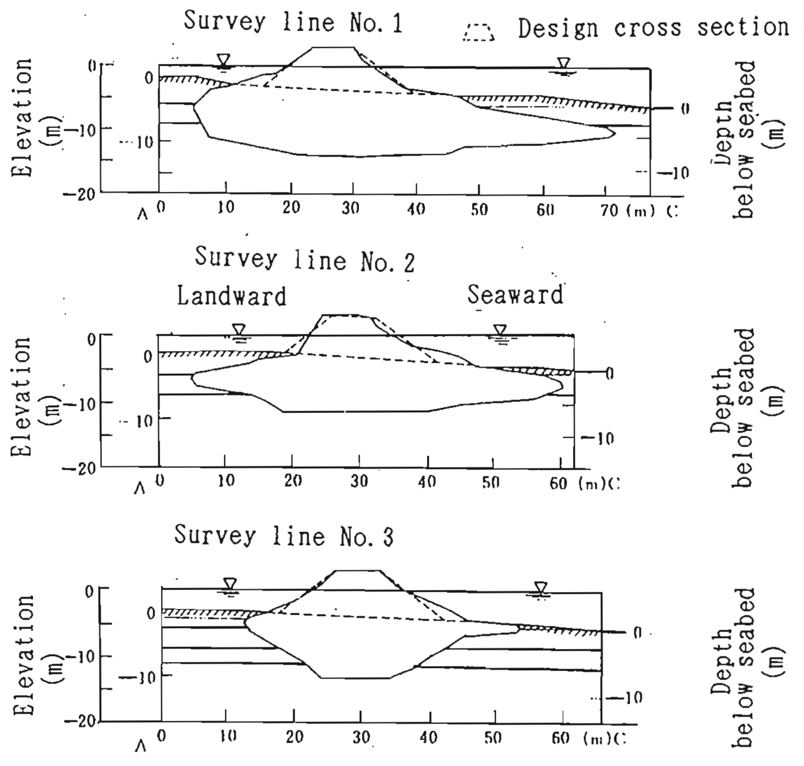

Fig.1 Cross sections of submerged wave dissipating concrete blocks

dissipating concrete blocks have been added in order to maintain the breakwater and protect the erosion of coastline with high potential of erodibility. The similar problem occurs in many other places in Japan such as the Iburi coast in Hokkaido. A large amount of investment has been made every year to prevent the beach from the erosion. Why on earth does the block sink? The problem is that the mechanism of subsidence of the detached breakwater has not been clarified yet. Lots of hydraulic approaches have been made to solve the question. It has come to a conclusion that the cause is attributed to the scour and/or sucking due to waves and/or current. However, it is not clear how do the scour and sucking phenomena occur. Not only the approach from the hydraulics but also one from the geotechnical viewpoint are considered indispensable to clarify the mechanism.

This paper discusses the relation between the scour and wave-induced liquefaction and describes the significance of excess pore pressure evaluation in considering the scour potential in seabed.

WAVE INDUCED EXCESS PORE PRESSURE AND LIQUEFACTION

The amplitude of water pressure exerted on the seabed due to a wave reaches about 16kPa when it propagates the sea surface, 10m above the sea bottom, with 5m of wave height and 7 seconds of wave period. This pressure is not always smaller when compared with the overburden pressure of 10kPa～20kPa used in the design of an apron of port facilities. The sand deposit may comparatively easily liquefy when such water pressure is applied to the sand deposit. If the liquefaction is generated, the sand particles become isolated and they become very easy to move. In addition, it is anticipated that some damage of structures on the liquefied seabed will happen, as no bearing capacity is expected. There seems to be some close relationship between the subsidence of the wave dissipating concrete blocks and the liquefaction of seabed.

The mechanism of the liquefaction due to ocean waves may be considered as follows: The fluctuating water pressure acting on the seabed surface is transferred deep into the seabed with phase lag and attenuation to some extent. Under the situation of the wave trough, the oscillatory water pressure created in the seabed becomes larger than that on the seabed surface. As the result, an upward seepage flow is generated between seabed surface and deeper seabed. When the upward seepage pressure induced by the seepage flow increases further than the effective overburden pressure, the interlocking of sand particles is destroyed and sand particles blow up to the seabed surface. In the meantime, a downward seepage flow from the seabed surface is produced under the wave crest producing the downward seepage force to densify the sand deposit. In such a manner, the liquefaction is repeatedly generated in response to every one wave. This is a remarkable difference in phenomenon from the earthquake-induced liquefaction.

The schematic drawings of the pore pressure and effective vertical stress distributions are illustrated in **Fig.2** from the geotechnical point of view. The solid curves in **Fig.2(a)** indicate the pore pressure beneath a wave trough and a wave crest. The excess pore pressure expressed by **Eq. (1)** is transient in nature, because the $p(0, t)$ and $p(z, t)$ are both oscillatory and periodical in real ocean environment;

$$u_e(z, t) = -\{p(0, t) - p(z, t)\} = -\Delta\sigma'_v(z, t) \qquad (1)$$

Consequently, the effective vertical stress expressed by **Eq. (2)** varies periodically in accordance with the change of the $\{p(0, t) - p(z, t)\}$;

$$\sigma'_v(z, t) = \sigma'_v(z, 0) + \{p(0, t) - p(z, t)\} \qquad (2)$$

If the $\sigma'_v(z, t)$ attains zero or less at certain depths, the soil skeleton will become a liquefied state. Thus, the criterion for the wave-induced liquefaction can be derived from **Eq. (2)** by setting the vertical effective stress, $\sigma'_v(z, t)$, equal to zero or less;

$$\sigma'_v(z, 0) \leqq - \{p(0, t) - p(z, t)\} = u_e(z, t) \qquad (3)$$

where, $p(0, t)$ *and* $p(z, t)$: the wave-induced oscillatory water pressure on the seabed surface and in the seabed respectively, $\sigma'_v(z, 0)$: the initial vertical effective stress at arbitrary depth, z, of the deposit, $\sigma'_v(z, t)$: the vertical effective stress at arbitrary depth, z, of the deposit and time, t, $\Delta\sigma'_v(z, t)$: the wave-associated effective stress change, $u_e(z, t)$: the excess pore pressure at arbitrary depth, z, of the deposit and time, t.

The solid curves in **Fig.2(b)** show the vertical effective stress distribution drawn by replacing the $\sigma'_v(z, 0)$, with $\gamma' z$, where γ' is the submerged unit weight of deposit. The lines numbered ①and ② in **Fig.2(b)** correspond to ones numbered ①and ②in **Fig.2(a)**, respectively. In **Fig.2(b)**, the liquefied zone shown by the slant lines where the vertical stress becomes zero or less appears near the seabed surface, under the wave trough. As the excess pore pressure is positive in this situation, the transient upward seepage flow is generated toward the seabed surface.

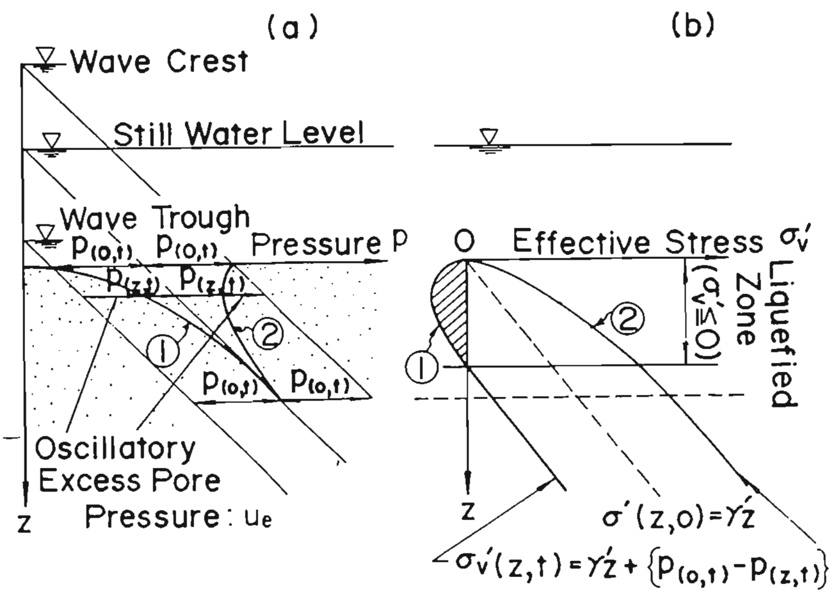

Fig.2 Concept of wave-induced liquefaction and densification: (a) oscillatory excess pore pressure, (b) effective vertical stress

If the $\sigma'_v(z, 0)$, $p(0, t)$ and $p(z, t)$ are given, the liquefaction potential can be evaluated by using **Eq.(3)**. As the $\sigma'_v(z, 0)$ is calculated from the submerged unit weight of deposit and the $p(0, t)$ is conveniently estimated by the linear wave theory, the only factor to be known is the wave-associated pore pressure, $p(z, t)$, the evaluation of which is presented elsewhere (Zen and Yamazak, 1990a, 1990b).

Whereas, if the vertical effective stress change, $\Delta\sigma'_v(z, t)$, reaches positive values, say it exceeds the initial vertical effective stress, $\sigma'_v(z, 0)$, as shown by the line numbered ② in **Fig.2(b)**, the wave-induced stress exerts a force on the soil skeleton to possibly densify the seabed.

The spatial differences of the oscillatory excess pore pressure in the seabed will exert seepage forces on the soil skeleton. As the increment of the vertical effective stress is represented by;

$$\frac{\partial \sigma'_v(z, t)}{\partial z} = j + \gamma' \qquad (4)$$

The vertical effective stress is derived by integrating **Eq.(4)**;

$$\sigma'_v(z, t) = \int j dz + \gamma' z \qquad (5)$$

where, j; the seepage force and γ'; the submerged unit weight of deposit. **Eq.(5)** is equivalent to **Eq.(2)** when the $\sigma'_v(z, 0)$ is identical with $\gamma' z$. The seepage force, j, is derived from **Eq.(2)** by taking $\partial \sigma'_v(z, 0)/\partial z = \gamma'$ and $\partial p(o, t)/\partial z = 0$ into account;

$$j = -\frac{\partial p(z, t)}{\partial z} \qquad (6)$$

The hydraulic gradient, i, and the flow velocity, v, are respectively given by the following equations;

$$i = -\frac{j}{\gamma_w} \qquad (7)$$

$$v = -\frac{kj}{\gamma_w} \qquad (8)$$

Where, γ_w is unit weight of water, k is the coefficient of permeability.

Fig.3 shows the seepage force, j, calculated by using the field data on the wave-induced oscillatory water

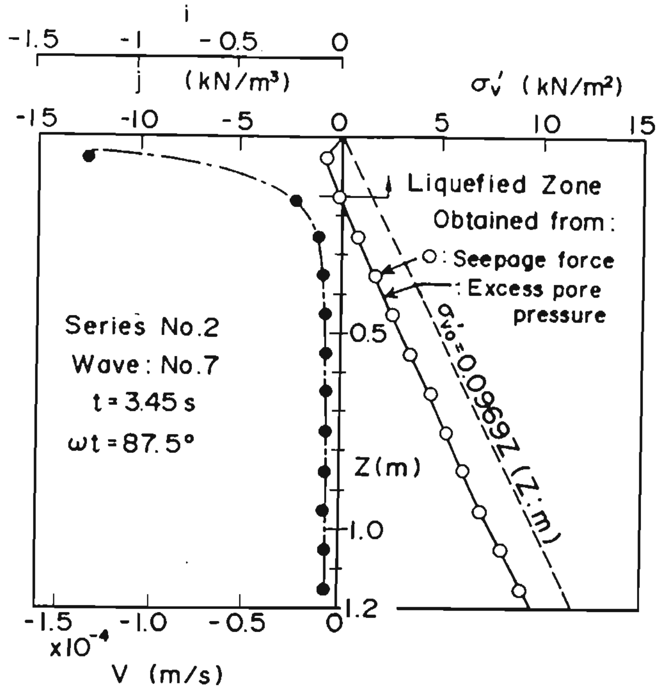

Fig.3 Liquefaction due to seepage flow

pressure, $p(z, t)$ (Zen and Yamazaki, 1991, Zen et al., 1998). The j is approximately calculated using the equation, $j = \Delta p(z, t)/\Delta z$. Then, the i and v are calculated using **Eqs.(7)** and **(8)**, respectively. In **Fig.3**, the seepage force and hydraulic gradient indicated by solid circles become remarkably larger near the seabed surface than those at deeper seabed. Especially, the hydraulic gradient attains more than 1.0 at the seabed surface. This difference is considered to generate the upward seepage flow directing to the seabed surface. The open circles and solid line are the vertical effective stress obtained from **Eq.(2)** and **Eq.(5)**, respectively. According to the liquefaction criterion represented by **Eq.(3)**, the liquefaction is sure to occur at the surface of seabed. The liquefaction creates a large potential for the transportation of suspended sand particles. This is a reason that the scour may be closely related to the wave-induced liquefaction.

RELATIONSHIP BETWEEN SCOUR AND LIQUEFACTION

The phenomena called scour and sucking are understood that the sand particles consisting of seabed are carried away by waves and/or current without sufficient supply of sand in the trace. Then, the magnitude of triggering potential for the scour is noticed to begin with. Generally speaking, the characteristics of sand such as density and strength are different by the sedimentation conditions. Also, in the field of geotechnology, it is the common sense that the characteristics remarkably change due to the action of external forces. When the sand deposit becomes suspended due to some reason, the floated particles may be easily transported even by small intensity of external forces such as bottom flow or vortex. In this meaning, the above-mentioned liquefaction in the seabed may be considered to be closely related to the scour and sucking potential.

A case study is carried out to clarify where the liquefaction of seabed is mostly occurs. The evaluation of the liquefaction potential in sand deposit underneath the detached breakwater shown in **Fig.4** has made. **Fig.5** and **Fig.6** present respectively the effective stress variation to evaluate the liquefaction and the liquefied zone

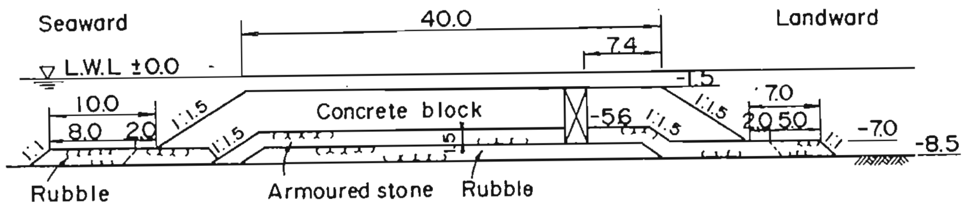

Fig.4 Cross section of detached breakwater (unit; m)

calculated by using the following input data: Namely, the maximum wave height H_{max} ; 7.2m, the wave period, T;11.8s, water depth, d;8.5m, the thickness of permeable sand deposit, l;20.5m, the coefficient of propagation, α;2.0, the coefficient of drainage, C;0.02 and the submerged unit weight of deposit, γ';0.9tf/m^2. The maximum liquefied depth of 1.25m is obtained at the toe of rubble mound under the situation of wave trough. In such situation of seabed, the sand particles will be easily transported. It is the phenomena called the scour or sucking. Though the actual scour and sucking phenomena are very complicated, the liquefaction potential can be an

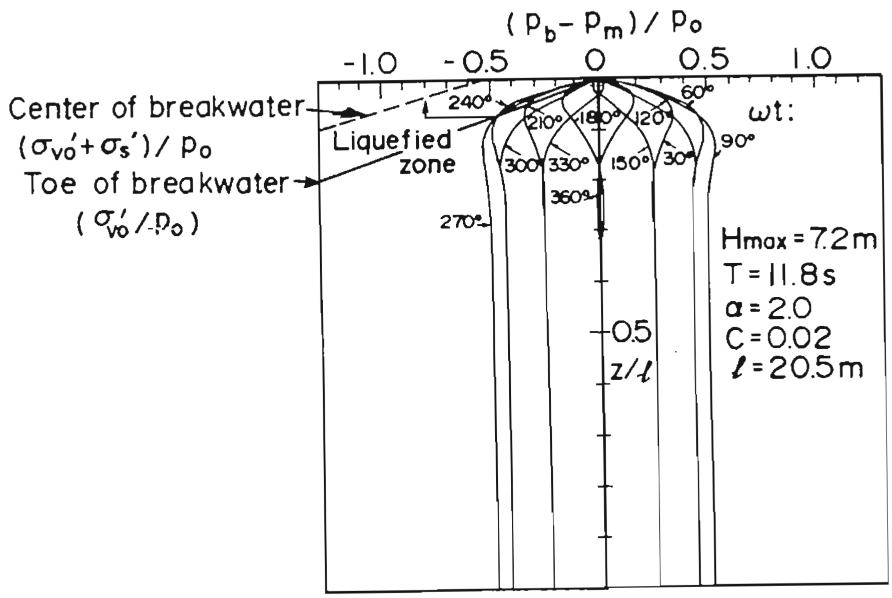

Fig.5 Effective stress variation and liquefaction (in which, p_o; the amplitude of wave-associated water pressure, p_b;$=p(0, t)$, p_m=$p(z, t)$, $\sigma'_{vo}= \sigma'_v(z, 0)$, σ'_s ; the overburden pressure due to rubble mound)

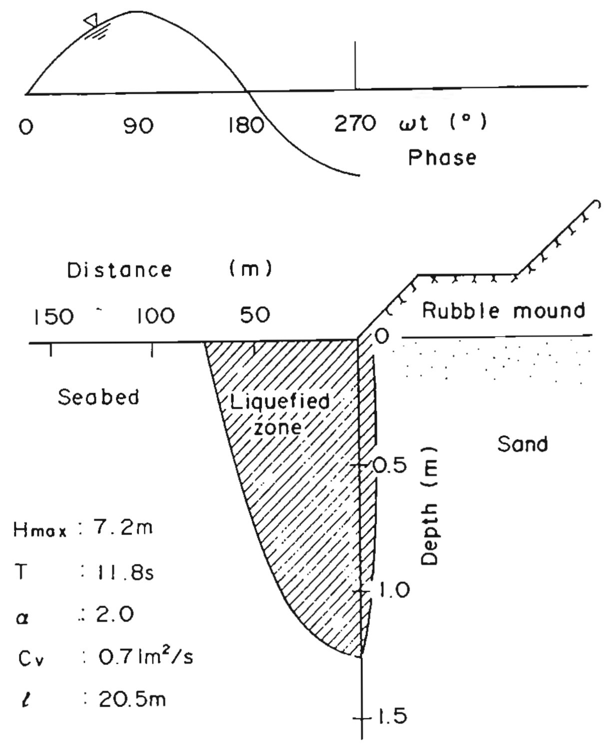

Fig.6 Liquefied zone

index that indicates the potential of scour and sucking.

The comparisons between the liquefied zone shown in **Fig.6** and the scour zone observed in the past field survey are presented in **Fig.7**. It is interesting to note that the observed scouring depths, say the family of solid

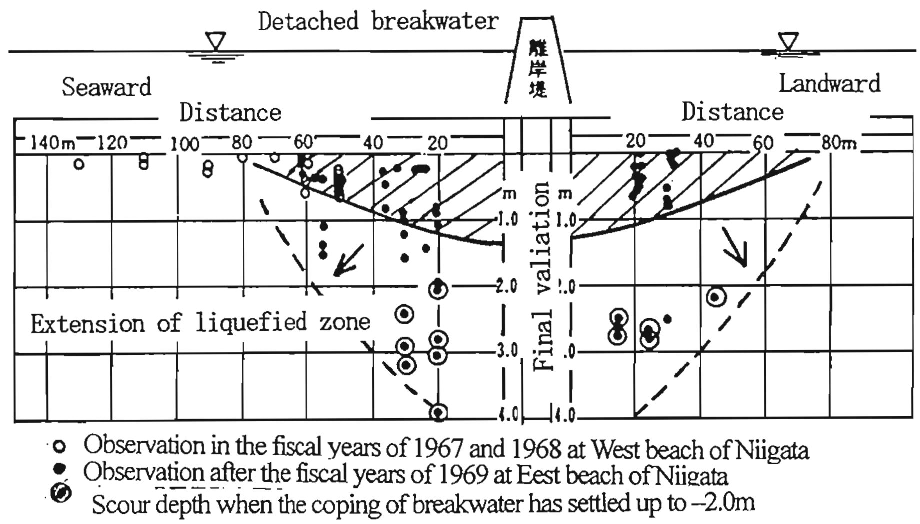

Fig.7 Comparisons of liquefied and scoured zones

and open circles, approximately consists with the liquefied zone illustrated with the slant line. The liquefied zone spreads more and more deep side according to both the duration of storm waves and degree of scouring when wave action is repeated. However, the critical water depth, where the liquefaction hardly happens, exists because the effect of waves at the sea bottom decreases as the water depth increases.

SUBSIDENCE DUE OF BLOCKS TO LIQUEFACTION

The liquefaction is generated around the seabed where the wave dissipating concrete blocks are installed. Then, the bearing capacity of seabed drastically decreases or it is completely lost. **Fig. 8** shows the safety factor calculated assuming the shear strength in the liquefied zone is zero (Zen and Yamazaki, 1995). In this case, the

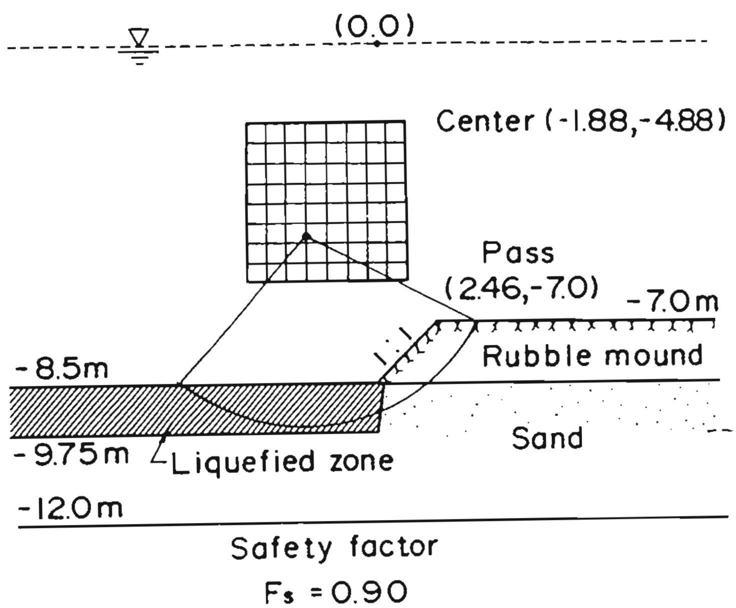

Fig.8 Circular failure

safety factor becomes 0.9, while the value without considering the liquefaction gives over 1.3. It is found that the safety factor of circular failure considering the liquefaction notably decreases, when compared with the safety factor obtained without taking the liquefaction into account. Thus, once the liquefaction happens, the wave dissipating concrete blocks move along with the sliding surface. When such phenomenon has been repeated for long duration, the wave dissipating concrete blocks seem to gradually sink and spread in the seabed as shown in **Fig.1** and **Fig.7**. In addition, the liquefaction will be accelerated due to the loss of overburden pressure caused by the gradual dispersion and sinking of the concrete blocks. The blocks sink gradually into the seabed in proportion to the number of waves acting on them as both the liquefaction and the densification are periodically caused. Namely, under the downward seepage flow, the sand deposit is densified and recovers its strength.

APPROACH TO COUNTERMEASURES

At present, the design procedure and practical method for preventing completely the scour do not exist. As the simplest way, the method separating the shear stress from water flow is applied. From geotechnical point of view, however, it is not always sufficient in ocean environment. In order to prevent the seabed from scour, it is recommended to adapt a method at least taking account of the wave-induced liquefaction. This is achieved, for example, by installing the wave dissipating concrete blocks not directly onto the seabed but onto the rubble mound. Large rubble is not suitable so that the overburden pressure may not be equally transferred to the seabed. It is desirable to increase as much as possible the contact pressure between the wave dissipating concrete blocks and seabed. The problem of liquefaction, however, still remains at the toe of rubble mound, because only quite small overburden pressure is expected there. How to deal with this toe problem is the key for the scour protection. Furthermore, though the conventional countermeasures such as wire-cylinder, cloth, asphalt mat and gravel mat expect the effect to separate the seabed from the wave action and/or current. They have a weak point against the liquefaction since the propagation of fluctuating pressure into sand deposit can not be fully restrained. Is there any countermeasure resistant to the liquefaction? The scour protection in ocean environment may be found out by taking the liquefaction mechanism into account.

CONCLUDING REMARKS

The wave-induced excess pore water pressure in the seabed was analyzed on the basis of the consolidation theory by applying the appropriate initial and boundary conditions and input data. Then, the excess pore pressure was evaluated as the difference between the wave-associated water pressure on the seabed surface and the oscillatory pore pressure in the seabed. The seepage force was calculated as the inclination of oscillatory water pressure distribution to the depth.

The upward seepage force in the permeable seabed was analyzed using the field data to evaluate whether or not the liquefaction occurred. The result of analysis showed that the liquefaction evidently happened. Once the liquefaction occurs in the seabed surface, the sand particles are easily transported by the water flow, as the shear resistance of seabed surface becomes nearly equal to zero. In that sense, the excess pore pressure and wave-induced liquefaction in the seabed are very important in predicting the scour potential of permeable seabed in the coastal zone.

The post-liquefaction phenomenon is one of the further significant topics in making clear of the scour potential in the ocean environment.

REFERENCES

1. Nishida, H. et al., 1985, "Subsidence of detached breakwaters surveyed by using cross-hole method", Proceedings of the 32nd Conference on Coastal Engineering in Japan, JSCE, pp.365-369 (in Japanese).
2. Zen, K. and Yamazaki, H., 1990a,"Mechanism of wave-induced liquefaction and densification in seabed", Soils and Foundations, Vol.30, No.4, pp.90-104.
3. Zen, K. and Yamazaki, H., 1990b,"Oscillatory pore pressure and liquefaction in seabed induced by ocean waves", Soils and Foundations, Vol.30, No.4, pp.147-161.
4. Zen, K. and Yamazaki, H., 1991,"Field observation and analysis of wave-induced liquefaction", Soils and Foundations, Vol.31, No.4, pp.161-179.
5. Zen, K. and Yamazaki, H., 1995," Slope instability due to wave-induced liquefaction in the seabed", River, Coastal and Shoreline Protection: Erosion Control Using Riprap and Armourstone, Edited by C.R.Thorne et al., John Wiley & Sons, pp.381-393.
6. Zen, K., Jeng, D.S.., Hsu, J.R.C. and Ohyama, T.., 1998, "Wave-induced seabed instability: difference between liquefaction and shear failure", Soils and Foundation, Vol.38, No.2, pp.37-47.

SCOUR DOWNSTREAM OF DAMS

By

George W. Annandale[1], Rodney Wittler[2] and Greg A. Scott[3]

ABSTRACT

The paper summarizes methods that are used to predict scour downstream of overtopping dams in the United States of America. These methods can be subdivided into physical hydraulic model studies, rigorous constitutive computer modeling and empirical methods. Conventional procedures are used to conduct physical hydraulic model studies. Rigorous constitutive modeling is based on Keyblock Theory (Goodman & Shi 1985 and Goodman and Hatzor 1991), whereas conventional empirical methods that are used include the Veronese (1937), Yildiz and Uzucek (1994) and the Mason and Arumugam (1985) equations. Keyblock theory is directed at solving scour problems in hard rock blocks, whereas the conventional empirical methods are intended to predict scour in cohesionless granular material.

The essence of the Erodibility Index Method (Annandale 1995) that is used to predict scour in any earth material, including rock, and cohesive and non-cohesive granular earth is also presented in this paper. The presented case studies illustrate the application of this empirical method to predict scour of rock and granular material. Comparison of observed and calculated scour in rock and granular material for field and near-prototype experimental studies indicates satisfactory correlation.

INTRODUCTION

Scour downstream of dams, induced by either large spillway flows or overtopping, influences the safety of dams. This is a matter of interest to United States Federal and State Agencies that own or regulate dams. There are currently more than 75,000 dams in the United States National Inventory of Dams (P.L. 99-662, P.L. 104-303). The U.S. Army Corps of Engineers (USACE) maintains and periodically updates the inventory. Many of these dams could potentially be subject to dam foundation erosion resulting from high flows. The issue is regularly considered during dam safety reviews and re-licensing of projects. Some of the legal requirements pertaining to the safety of dams are contained in the National Dam Inspection Act, P.L. 92-367.

There are two general approaches to the hydrologic and hydraulic safety of dams in the United States. Some agencies prefer to use the PMF or a proportion thereof to assess the impact of hydrologic loading on a project. Other agencies use risk based approaches. The emphasis of

[1] Associate and Director Water Resource Engineering, Golder Associates Inc., 44 Union Blvd., Suite 300, Lakewood, Colorado.
[2] Research Hydraulic Engineer, Water Resources Research Laboratory, US Bureau of Reclamation, Department of Interior, Denver, Colorado.
[3] Senior Technical Specialist, Structural Analysis Group, US Bureau of Reclamation, Department of Interior, Denver, Colorado.

this paper is on methods used in the United States to predict and assess dam foundation erosion, part of either approach towards dam safety.

Dam foundation erosion assessment methods used in the United States include physical hydraulic model studies, rigorous constitutive computer modeling, and empirical procedures. The results from physical model studies are qualitative, although they provide valuable design and dam safety information. Rigorous constitutive modeling, based on Keyblock Theory (Goodman & Shi 1985, Goodman & Hatzor 1991) is complex, although analyses to evaluate specific components of scour problems have been completed. Current analysis procedures using this approach do not fully account for the fluctuating pressures caused by the hydraulic loading that often dominates the scour process.

Empirical equations for predicting scour depth include the Veronese equation (updated by Yildiz 1994) and the Mason & Arumugam (Mason & Arumugam 1985) equation. The principle concern with these equations is their inability to comprehensively account for material properties. The Veronese / Yildiz equation does not contain any allowance for material properties. Although the Mason & Arumugam equation contains an allowance for particle diameter, a large number of dam foundation erosion problems deals with scour of rock. Selection of an appropriate particle diameter to represent rock properties presents a practical problem.

Research by the United States Bureau of Reclamation, Golder Associates Inc. and Colorado State University into an empirical method known as the Erodibility Index Method (Annandale 1995) shows good agreement between observed and calculated scour of earth materials that include rock, and cohesive and non-cohesive granular material. This method uses a geo-mechanical index to quantify the relative ability of earth material to resist erosion. An empirical relationship between the geo-mechanical index and the erosive power of water that defines an erosion threshold for any earth material makes it possible to estimate erosion potential and calculate scour depth.

This paper summarizes the different approaches to assess dam safety issues pertaining to hydrologic loading on dams, and presents methods that are used in the United States to assess dam foundation erosion. Keyblock Theory, conventional empirical equations and the Erodibility Index Method are briefly discussed. The paper concludes with case studies that illustrate application of the Erodibility Index Method.

PMF AND RISK BASED APPROACHES

Current policy by US Agencies to assess the hydrologic safety of dams includes Probable Maximum Flood (PMF) and Risk Based approaches. Traditional standards-based approaches to evaluate the potential for overtopping rely on routing the PMF or some percentage thereof through a reservoir system, to determine the potential depth and duration of dam overtopping, or the potential for damaging spillway flows. Spillways and outlet works are assumed to function in accordance with operating criteria during the routings. The dam must be shown to be stable for this maximum loading in order to pass the standard. Such an analysis includes assessment of the impact of foundation scour on dam stability. The magnitudes of PMF's are based on Hydro-meteorological Reports from the National Weather Service that define the Probable Maximum Precipitation (PMP). Allowances are made for antecedent conditions, storm centering and other factors when calculating the runoff into the reservoir.

An approach being used by some agencies evaluates the risk posed by overtopping of a dam. Instead of only using the magnitude of the maximum hydrologic loading conditions, the likelihood of overtopping flows is also evaluated. The probability of hydrologic inflows of various magnitudes is determined by using regional historical flow records, and geologic "paleoflood" data. The likelihood of a loading that would result in dam overtopping or damaging spillway flows can thus be estimated. The risk associated with these events is:

$$(PL)(PF)(C) \tag{1}$$

PL is the probability of the load
PF is the probability of failure given the load
C are the consequences resulting from failure

The consequences can take the form of loss of life, economic damages, or other types of consequences. Decisions are based on the level of risk posed by a structure.

In either approach, it is necessary to evaluate the potential for failure (including foundation failure due to scour) as the result of overtopping, or potentially damaging spillway flows. For the PMF approach, it must be demonstrated that the dam is safe for the maximum levels of loading. For the risk-based approach, the likelihood of failure for given levels of hydrologic loading must be estimated. The approaches to predict the potential and extent of scour of dam foundations due to high flow, as presented in this paper, are used in both approaches.

SCOUR ANALYSIS APPROACHES

Hydraulic erosion entails an interaction between loads imposed by the erosive power of water and resistance offered by the inherent strength of earth material. A conceptual model of scour, viewed as a process of progressive dislodgment, can be characterized by three stages:

- Jacking (Figure 1(a))
- Dislodgement (Figure (1b)), and
- Displacement (Figure (1c))

Figure 1 illustrates the postulated three stages of scour in a stratum of jointed rock with a dip against the direction of flow. Dip is the angle between the horizontal plane and the plane of the discontinuities within the rock. Water that flows over the earth material will also penetrate the discontinuities within it, causing the water pressure in the discontinuities to equal the hydrostatic head above it. Flowing water, for most practical problems associated with scour, contains turbulence because incorporating excess pwp $\overset{V}{p}$

throughout the whole body of water, noticeably at the bed. Turbulence at the bed causes pressure fluctuations that play an important role in determining the net forces acting on the earth material. The net pressures acting on blocks of rock is the algebraic sum of the hydrostatic pressure within the earth material and the fluctuating pressures at the surface of the bed. The net fluctuating pressures progressively jack material units out of their positions of rest. Once jacked out, they are dislodged by the power of the flowing water, and finally displaced. If the forces exerted by the fluctuating pressures exceed the relative ability of the earth material to resist erosion it will scour. Methods to predict whether erosion will occur or not require quantification of the relative magnitude of fluctuating pressures in flowing water and the relative ability of earth material to resist erosion. Models representing the erosion process for other earth materials can be portrayed in a similar manner as that shown in Figure 1 and explained above. The degree to which the different current scour prediction methods represent this conceptual model differs.

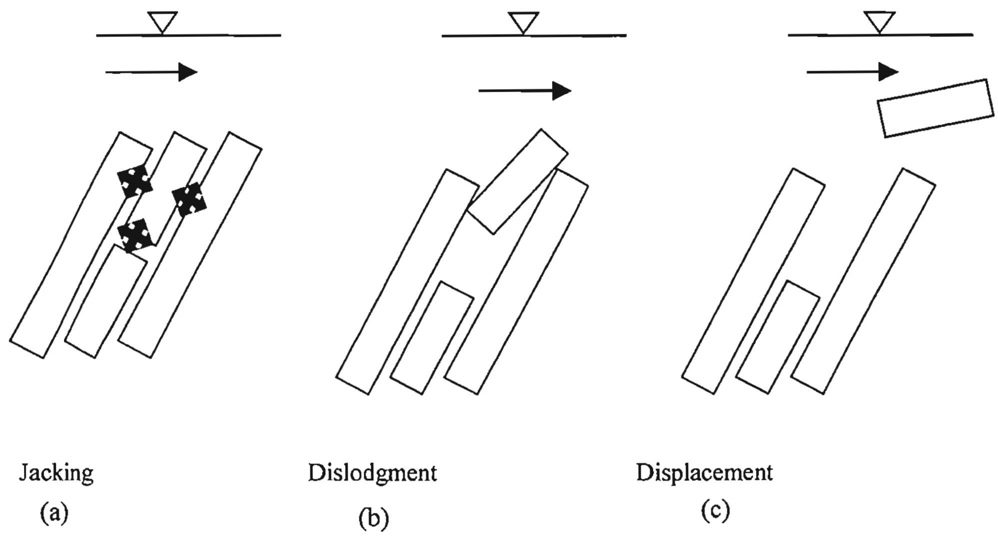

Fig. 1 Conceptual model explaining erosion process in rock. The same model explains erosion of other earth materials.

Current practice pertaining to dam foundation scour prediction in the United States of America includes application of physical hydraulic model studies, rigorous constitutive modeling and empirical methods. Although physical hydraulic model studies emulate the pressure fluctuations of prototypes, representative scaling of material properties is often a problem. Application of Key Block Theory (Goodman & Shi 1985) in rigorous constitutive modeling entails detailed consideration of all forces impacting on rock to predict the potential failure of rock formations. Although current application of this method takes account of material properties, it does not consider the role of fluctuating forces imposed by the hydraulic loading. The Erodibility Index Method (Annandale 1995) is a semi-empirical approach that defines a scour threshold for any earth material, including rock, cohesive and non-cohesive granular material. This method quantifies the relative magnitude of fluctuating pressures acting on the earth material, and empirically accounts for relevant material properties that determine its relative ability to resist erosion. Conventional empirical equations used in the United States (Veronese 1937; Yildiz & Uzucek 1994 and Mason & Arumugam 1985) account for hydraulic loading, while only one marginally accounts for the resistance offered by the earth material.

The execution of physical hydraulic model studies is a mature technology used globally and will not be summarized in this paper. The following text deals with Keyblock Theory, conventional empirical methods and the Erodibility Index Method.

Keyblock Theory

The stability of hard rock blocks against plucking by hydraulic forces is dependent on the three-dimensional geometry of the geological discontinuities. Block Theory (Goodman and Shi 1985) provides a rigorous solution for the removability of a block from a rock mass when exposed by a free surface. The solution is general for any number of joints and free faces. The joint sets and free faces are described as three-dimensional planes by their dip (angle from horizontal) and dip direction (angle from north). A hard rock mass structure usually contains a number of joint sets, and consequently a large number of possible joint combinations must be examined. Block Theory identifies the combinations of joints that form blocks which may be removed from the rock surface. If strength of the joint planes and the forces acting on such blocks are known or can be estimated, the stability of the blocks can be calculated using three-dimensional limit equilibrium techniques.

Goodman and Hatzor (Goodman & Hatzor 1991) extended Block Theory to examine the removability of blocks on the abutment of an arch dam when subjected to overtopping flows. The procedure basically uses the following steps:

1. Joints are mapped, plotted on stereographic projection, and divided into joint sets. A representative attitude, spacing, and friction angle is assigned to each joint set.
2. Each sub-combination of three joint sets is examined using Block Theory to determine the removable combinations.
3. For each removable sub-combination, the relative failure likelihood is estimated by examining the frequencies of the bounding joints, the angles between the joints, and the friction angles of the potential sliding faces. The removable blocks of the most likely combinations are designated as "critical keyblocks".
4. The traces of the bounding joints of the critical keyblocks are drawn as they would appear on the free surface of interest (i.e. abutment surface). These traces are compared to trace maps or photo overlays of joints on the actual surface and actual critical keyblock faces are identified.
5. A limit equilibrium analysis is performed for the identified critical keyblocks under their own weight, and the faces that would tend to open upon movement of the block in its probable mode of sliding are identified.

6. A water pressure is assigned to the potential open faces of the critical keyblocks and the limit equilibrium analysis is repeated. Instability (factor of safety less than 1.0) for this case indicates the block would likely be removed by the flowing water.

Although some modest research examines the effects of hydrodynamic forces acting on the potentially open joint planes, to date the analyses of abutment erosion have only considered hydrostatic forces acting on these joints. The hydrodynamic forces produced by impinging water penetrating the joint planes may be much larger than the hydrostatic forces acting on a joint full of water. Hence, this is an important consideration with regard to abutment erosion, requiring further research.

Conventional Empirical Methods

Equations used in the past to calculate plunge pool scour are the Veronese, Mason and Arumugam, and Yildiz and Uzucek equations. Of these equations only the Mason and Arumugam equation acknowledges that material resistance plays a role in scour. Equation (2) is the Veronese (1937) equation. The equation yields an estimate of erosion measured from the tailwater surface to the bottom of the scour hole.

$$\mathrm{Y_s} = 1.90H^{0.225}q^{0.54} \tag{2}$$

Y_s = depth of erosion below tailwater (meters)
H = elevation difference between reservoir and tailwater (meters)
q = unit discharge (m^3/s/m)

Yildiz and Uzucek (1994) presents a modified version of the Veronese equation, including the angle, α, of incidence from the vertical, of the jet.

$$\mathrm{Y_s} = 1.90H^{0.225}q^{0.54}\cos\alpha \tag{3}$$

Equation 4 is the Mason & Arumugam (1985) prototype equation.

$$Y_s = K\frac{q^x H^y h^w}{g^v d^z} \tag{4}$$

h = tailwater depth above original ground surface (meters)
d = median grain size of foundation material, d_{50} (meters)
g = acceleration of gravity (m/s^2)

$$K = 6.42 - 3.1 \cdot H^{0.10}$$

$$x = 0.6 - \frac{H}{300} \quad v = 0.3$$

$$y = 0.15 + \frac{H}{200} \qquad w = 0.15$$
$$z = 0.10 \qquad d = 0.25m$$

Unlike the Veronese and the Yildiz and Uzucek equations, the Mason and Arumugam equation includes a material factor, *d*. Although it is an attempt to acknowledge the role that material properties play in resisting scour, it is unlikely that this factor adequately represents the variety of material properties found in foundation materials.

Erodibility Index Method

Annandale (1995) developed the Erodibility Index Method by analyzing scour events from approximately 150 field observations and by analyzing published laboratory data pertaining to the initiation of motion of sediment particles subject to flowing water. An erosion threshold was established by plotting the Erodibility Index for different rock types and cohesive and non-cohesive granular soils against stream power, and noting whether scour occurred or not for each event under consideration. The Erodibility Index that was used to quantify the relative ability of the earth material to resist erosion is identical to Kirsten's Excavatability Index (Kirsten 1982). Kirsten's Excavatability Index is used to characterize rock for determining the power requirements of earth moving equipment that can rip the subject material. The index, as formulated in the Erodibility Index Method, is expressed as the product of four parameters,

$$K = M_s K_b K_d J_s \tag{5}$$

K = Erodibility Index
M_s = intact rock strength parameter
K_b = block size parameter
K_d = shear strength parameter
J_s = relative orientation parameter.

The values of the parameters are determined by making use of tables and equations that are published in Annandale (1995) and Kirsten (1982). The intact earth material strength parameter is equated to its unconfined compressive strength in MPa for strengths greater than 10 MPa. The block size parameter is a function of RQD and a joint set number in the case of rock, and a function of median particle diameter in the case of cohesionless granular earth material. The shear strength parameter is a function of a joint roughness number and a joint alteration number, or the tangent of the residual internal angle of friction in the case of granular soils. Relative orientation, in the case of rock, is a function of the relative shape of the rock and its dip and dip direction relative to the direction of flow. The material characteristics are generally obtained from borehole data, field testing (such as vane shear testing) and laboratory testing (to obtain the unconfined compressive strength). It is also possible to obtain parameter values by making use of geologic descriptions of the material.

The relative magnitude of the erosive power of the water is quantified by stream power, also known as rate of energy dissipation. This parameter is used because of its close relation to turbulence intensity and pressure fluctuations (Annandale 1995), the hypothesized principal cause of scour. Stream power, P, is:

$$P = \gamma \cdot q \cdot \Delta E \tag{6}$$

P = stream power (KW/m^2)
γ = unit weight of water (= $9.82 KN/m^3$)
q = unit discharge ($m^3/s/m$)
ΔE = energy loss expressed in terms of head per unit length of flow (m/m)

Annandale (1995) used equation 6 to derive a number of other equations that can be used to calculate stream power for a variety of flow conditions, including headcuts, knickpoint flow, hydraulic jumps, etc. Sets of graphs that can be used to calculate stream power at the base of bridge piers (Smith et al. 1997) have also been developed.

Application of the method requires expertise in engineering geology, and geotechnical and hydraulic engineering. Approaching scour analysis from an interdisciplinary point of view, especially on large important projects, is advisable.

The erosion threshold that relates the Erodibility Index to stream power is presented in Figure 2. The solid markers represent events where scour was observed, whereas the open markers represent events where scour did not occur. The dotted line represents the approximate location of the erosion threshold.

The extent (depth) of scour is determined by comparing the stream power that is available to cause scour to the stream power that is required to scour the earth material under consideration.

Figure 3 shows how the available and required stream power, both plotted as a function of elevation beneath the riverbed, are compared to determine the extent of scour. Scour will occur when the available stream power exceeds the required stream power. Once the maximum scour elevation is reached the available stream power is less than the required stream power, and scour ceases.

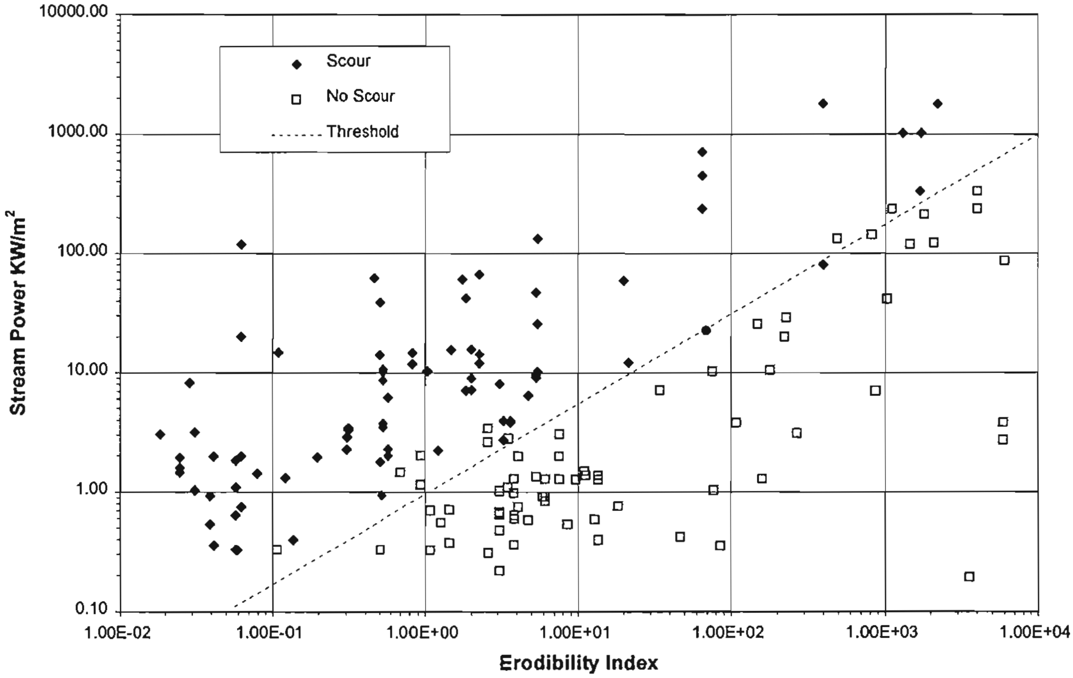

Fig. 2 Erosion Threshold as defined by the Erodibility Index Method (Annandale 1995).

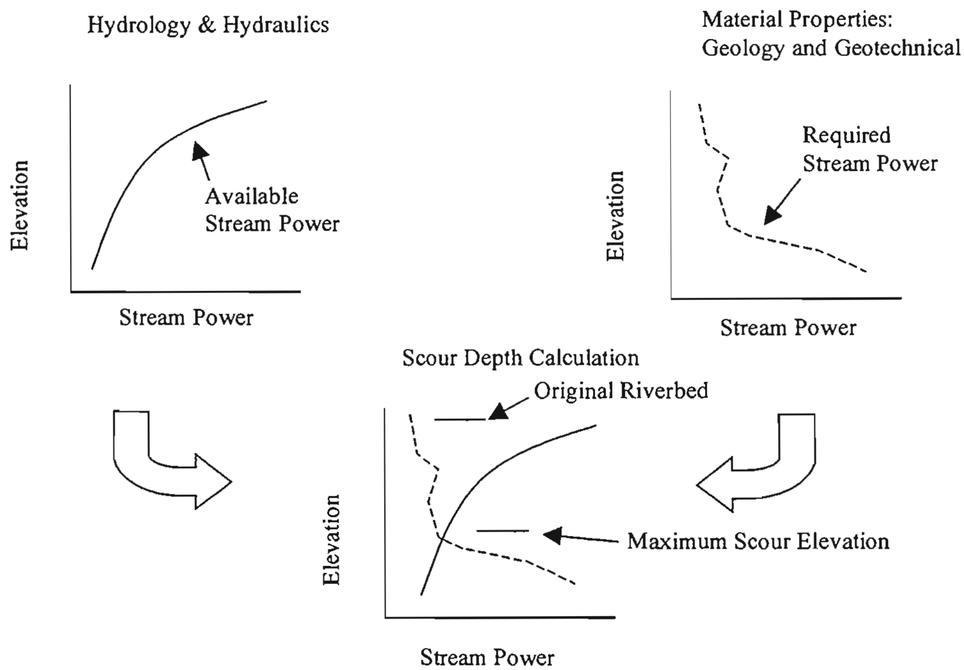

Fig. 3 Determination of the extent of scour by comparing available and required stream power.

The required stream power is determined by first indexing a geologic core or borehole data. The values of the Erodibility Index thus determined will vary as a function of elevation, dependent on the variation in material properties. Once the index values at various elevations are known, the required stream power is determined from Figure 2, as conceptually shown in Figure 4.

Figure 4 indicates that the stream power required to scour a particular earth material is determined by entering the erosion threshold graph on the abscissa, with the Erodibility Index known, moving vertically to the erosion threshold line, and reading the required stream power from the ordinate.

Figure 5 illustrates that the process is repeated as a function of elevation below the riverbed. The values of the required stream power is then plotted as a function of elevation. A method to calculate the change in available stream power as a function of scour hole depth in plunge pools is presented in the section dealing with Case Studies.

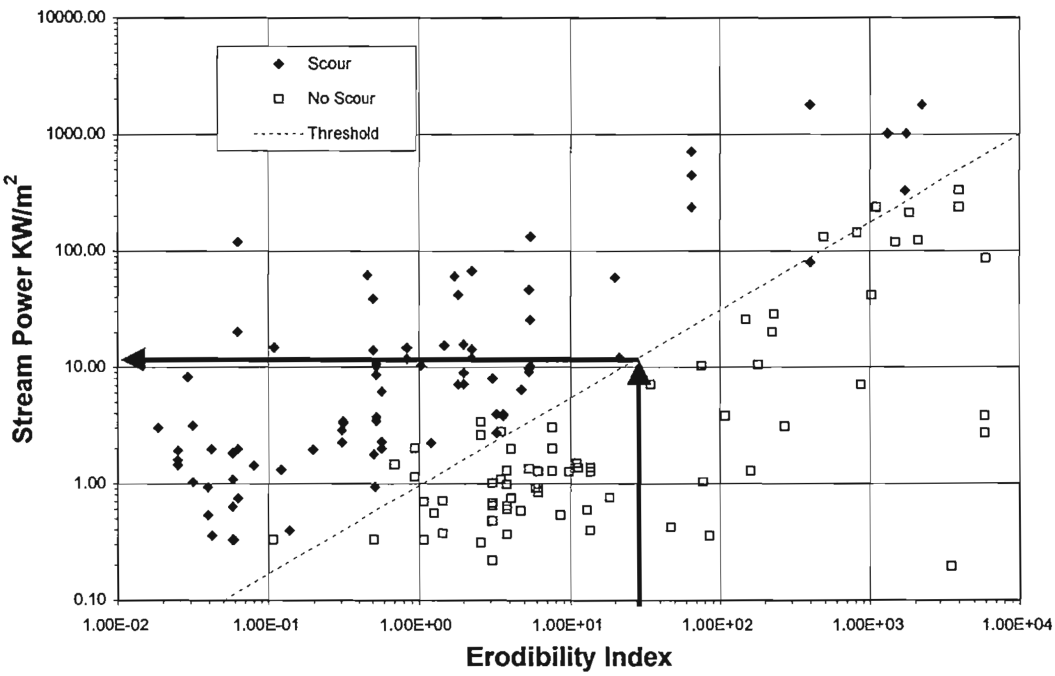

Fig. 4 Determination of stream power that is required to scour earth material once the value of the Erodibility Index is known.

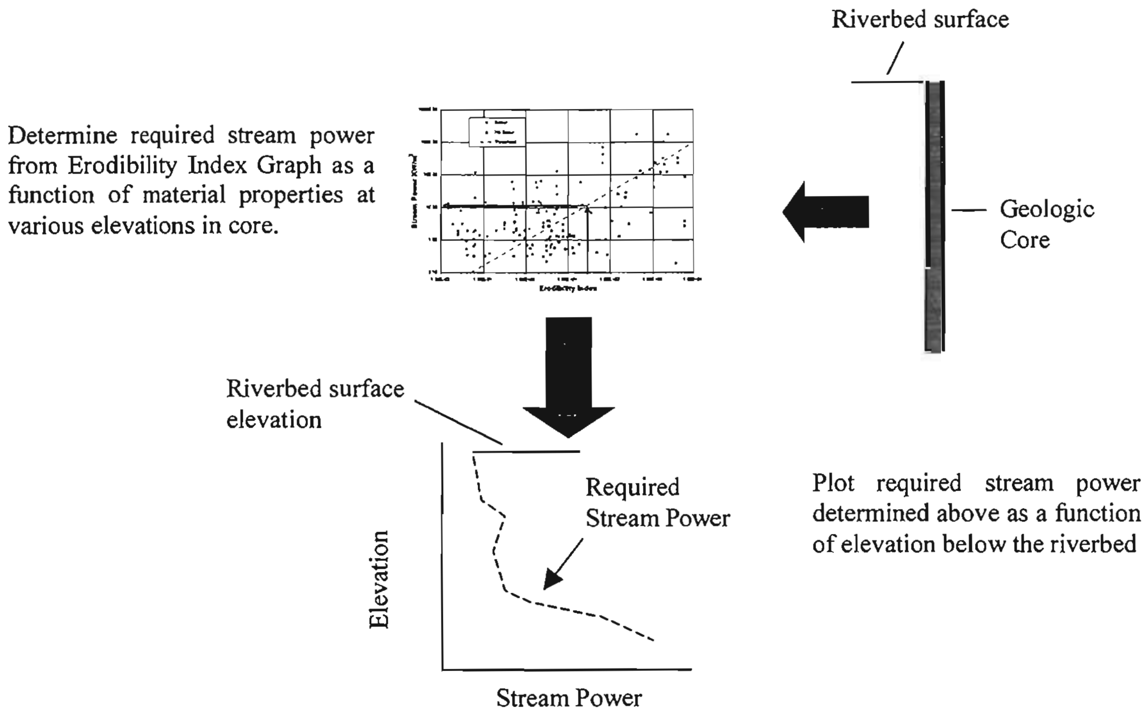

Fig. 5 Development of a relationship between the stream power that is required to scour earth material and elevation below a riverbed by determining the Erodibility Index at various elevations in a geologic core (or from geotechnical borehole data).

CASE STUDIES

Three case studies that illustrate the application of the Erodibility Index Method are presented in this section. The Gibson Dam case study relates the predictions of the Erodibility Index Method to observed scour. The case study dealing with scour of alluvial material illustrates that the method can be used to predict scour extent in granular material, and the section dealing with ongoing research presents a verification of the scour threshold determined by near-prototype scale model studies with simulated rock.

Gibson Dam

Description of site, structure and materials: Gibson Dam is a 199 foot (60.6 m) high concrete thick arch dam with a crest length of 960 feet (292.6 m) (Figure 6). The dam is located on the North Fork of the Sun River in central Montana. It was completed in 1929 with spillway modifications performed in 1938, and overtopping protection added in 1980. The dam crest width is 15 feet (4.6 m) and the maximum base width is 117 feet (35.7 m). The spillway is a drop-inlet, discharging into a shaft and 29.5 foot (9.0 m) diameter tunnel in the left abutment, controlled by six 34 by 12 foot (10.4 m by 3.7 m) radial gates. The foundation is crystalline (Madison Group) limestone in regular beds which have a strike normal to the river and an upstream dip of approximately 75 degrees. The only access to the dam is on a road along the North Fork of the Sun River, downstream of the dam.

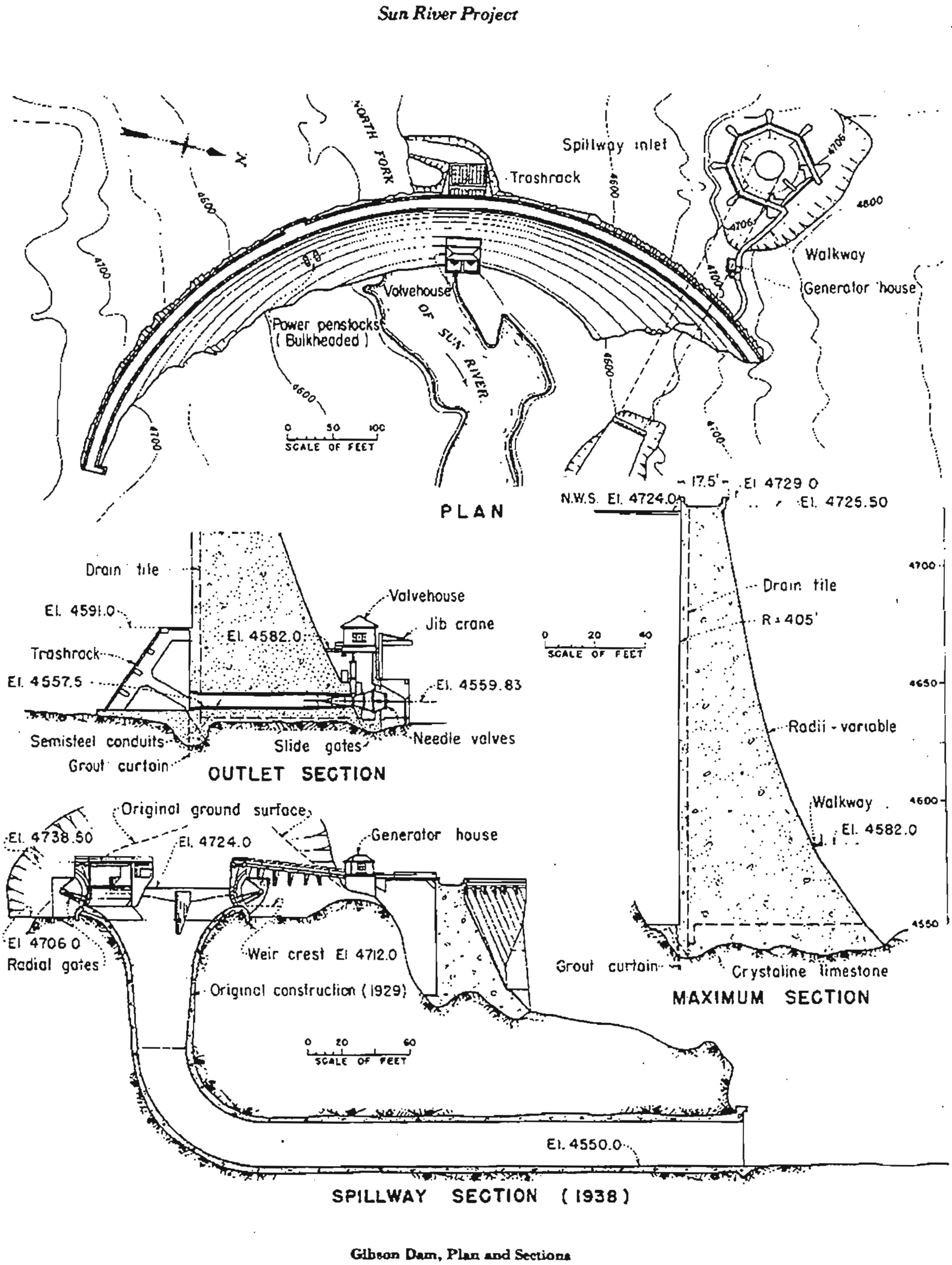

Fig. 6 Plan and sections for Gibson Dam, Montana.

The reservoir has a capacity of 99,100 acre-feet (122×10^6 m^3) with the water surface at El. 4724 feet (1439.9 m). The service spillway capacity at that elevation is 30,000 ft^3/s (850 m^3/s) with the outlet works providing an additional 3,050 ft^3/s (86 m^3/s). The drainage area for the reservoir is 575 square miles (1489 km^2) and in 1970 a new inflow design flood was derived which has a peak discharge of 155,000 ft^3/s (4390 m^3/s) and a five day volume of 365,000 acre-feet (450x106 m^3). The dam is the primary storage feature of the Sun River Project that supplies water for irrigation of more than 90,000 acres (364×10^6 m^2) of land downstream.

Loading: Reservoir inflows reached "unimaginable" levels due to a combination of sustained up slope winds and unusually heavy moisture from the Gulf of Mexico in June of 1964. These conditions caused a rainstorm over a reach 100 miles (161 km) long on the eastern slope of the continental divide and produced 30 hour rainfall amounts of from 8 to 16 inches (203 to 406 mm). The shallow soils along the Rocky Mountains and foothills area were already saturated with spring snowmelt and there was very little capacity for retaining the flows. By 2 P.M. Monday, June 8, overtopping of the dam began as inflows reached an estimated maximum of 60,000 ft^3/s (1700 m^3/s) and remained at this rate for 3 hours. A high water mark inside the spillway control house indicated the dam was overtopped by 3.23 feet (0.98 m). By 8 A.M. Tuesday inflows had dropped to 30,000 ft^3/s (850 m^3/s) and by 10 A.M. water stopped flowing over the parapet. The overtopping event lasted 20 hours.

Behavior under loading: Huge volumes of water fell over the dam and washed down the entire extent of the dam abutments. As the overtopping began at 2:00 P.M., water was flowing over the upstream parapet and was conducted to the right, along the crest roadway, to an area approximately 300 feet (91.4 m) downstream of the dam where the substantial stream of water flowed down the right side canyon wall. The water continued to rise rapidly and by 3:00 P.M. the downstream end of the entire dam crest became a huge waterfall (see Figure 7). Maximum discharge over the parapet was estimated to be 18,500 ft^3/s (524 m^3/s) with reservoir storage at an unprecedented 116,400 acre feet (144×10^6 m^3).

Consequences: Remarkably little damage was caused at Gibson Dam by the overtopping. No structural damage could be found and only three 1 ½ -inch (38 mm) diameter pipes leading to the Valve No.1 hand controls were broken and leaking water. Water had broken the entry door to the valve house and the windows were broken out. The pipe hand railing along the walkway to the valve house was about 50% destroyed. Routine clean-up and typical O&M activities restored the dam to its normal operating condition. A combination of the dam outflows and the additional heavy flow entering the river from Beaver Creek just downstream of the dam destroyed an access road bridge, a large storage building, and much of the access road downstream of the dam.

It should be noted that operating personnel were unable to get to the dam during the event because of the loss of the access road early in the flood. On May 28th, the day before water started over the spillway crest, the operators had left the river outlet discharging 1,800 ft^3/s (51 m^3/s), spillway gates No.2 and 5 fully open, No.3 and 4 completely closed, No.1 open 9 feet, and No.6 open 11 feet (3.4 m). With this gate configuration, outflow could reach 32,200 ft^3/s (911 m^3/s) at a water surface elevation of 4729 feet (1441.4 m). This would have passed the greatest previous flow of record, the flood of June 1916, without overtopping the

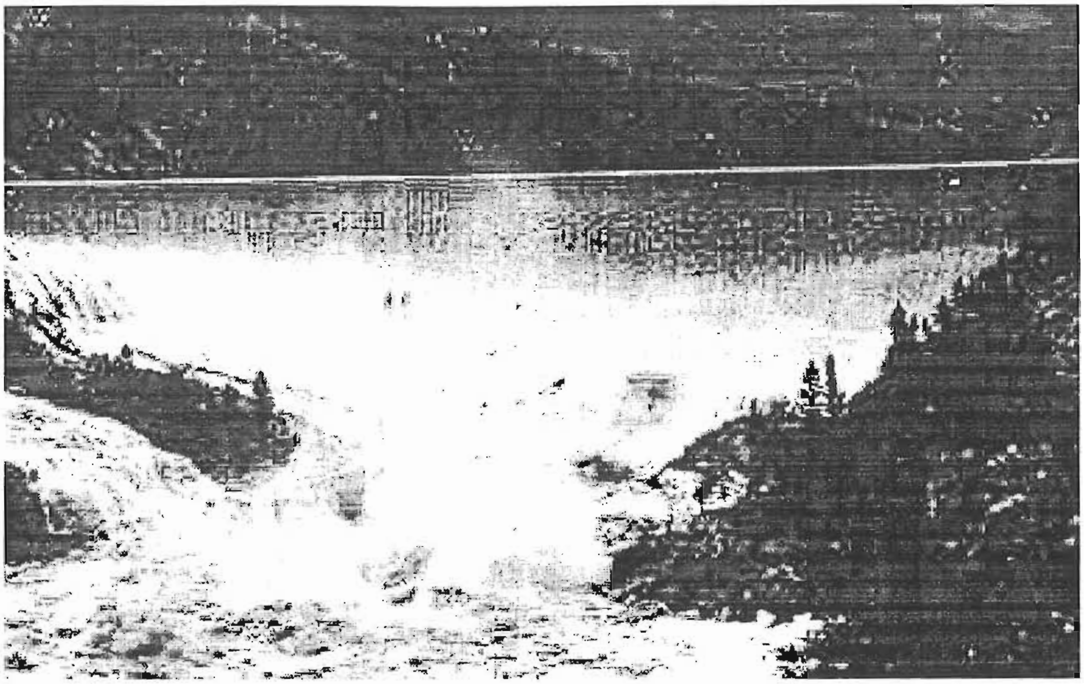

Figure 7 - Gibson Dam, Montana during the flood event of June 1964.

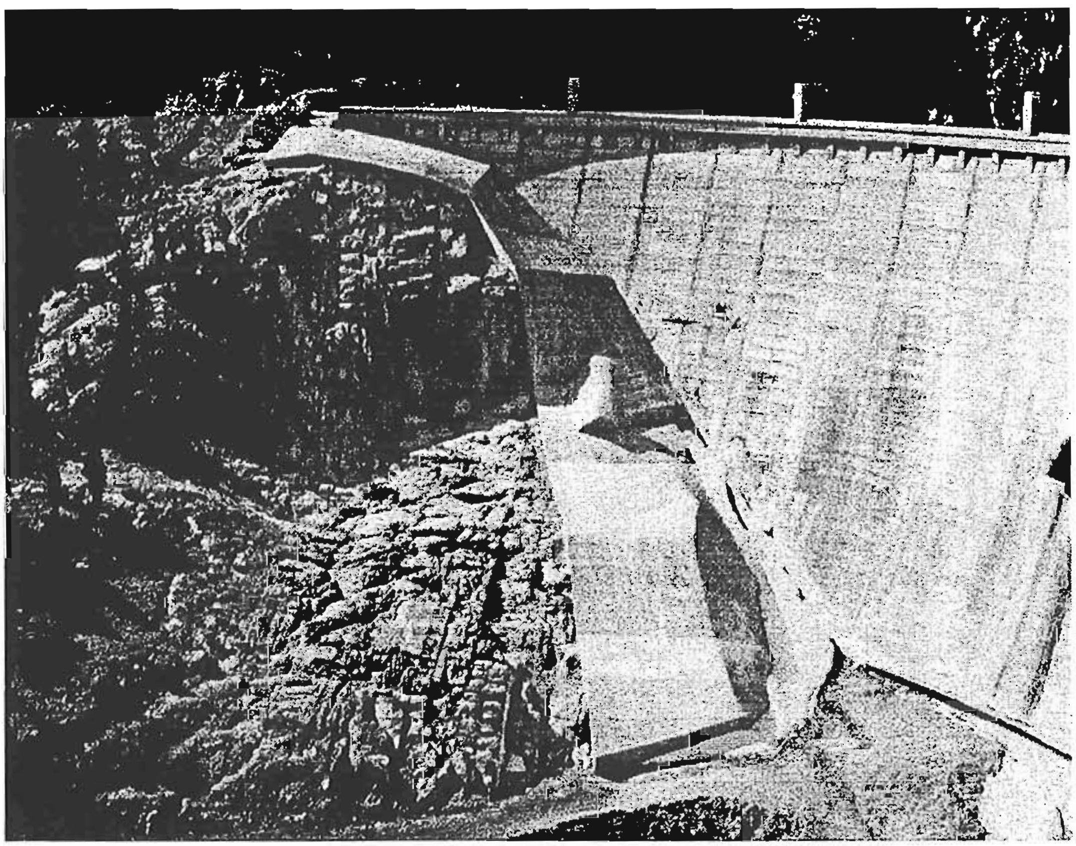

Figure 8 - Concrete on right abutment of Gibson Dam.

dam. Later analysis indicated that the dam would have been overtopped by the 1964 flood even if all gates were fully opened as early as June 1st.

Although the rock strength and jointing appeared to be quite resistant to erosion during this event, a 3 to 5 foot (0.9 to 1.5 m) thick concrete overlay with anchor bolts was placed where the overtopping flow impinged on the right abutment and foundation (Figure 8) to protect against even larger floods up to the probable maximum flood (PMF). The steeper left abutment was treated with rock bolts and a concrete cap in major surface fracture zones (Figure 9). This modification was deemed prudent given the large degree of uncertainty associated with determining erodibility at the time when modifications were designed.

Back calculations: The empirical approach to determining erodibility presented in this paper was subsequently used to determine if it would accurately predict the observed response. This approach is based on the stream power of the impinging jet, and the erodibility index of the material being hit. Annandale's (1995) graph suggests that erosion of rock is possible if the available stream power is greater than the erodibility index raised to the 0.75 power ($Pr >= K^{0.75}$).

The Erodibility Index is computed as $K=(M_s)(K_b)(K_d)(J_s)$. The value of each of the parameters making up the Erodibility Index is obtained from tables in Annandale (1995). M_s is an evaluation of the mass (intact) strength of the foundation. This varies depending on whether the foundation is a granular soil, a cohesive soil, or rock. The majority of the foundation rock at Gibson Dam is limestone and dolomite (referred to as limestone in much of the documentation). For the evaluation at Gibson, the value of M_s is equal to the unconfined compressive strength in MPa. The average value from laboratory tests was 22,900 lb/in^2 (158 MPa). Some weaker intensely fractured beds (about 6 to 10 feet (1.8 to 3.0 m) thick) are present, particularly on the left abutment. The rock in these beds would have a lower strength, perhaps by a factor of 2 to 4 (40-80 MPa). Laboratory testing performed on the concrete during original construction of the dam resulted in an average unconfined compressive strength of about 2940 lb/in^2 (20 MPa).

K_b is an index related to the mean block size. It can be estimated as the rock quality designation (RQD) divided by the joint set number (J_n). The dam foundation limestone varies from thin beds a few inches thick to massive beds, 8 to 10 feet (2.4 to 3.0 m) thick. The rocks were found to be broken by several fissures, which followed the bedding surfaces very closely. Another prominent joint set was mapped on each abutment, and there were other minor joints. This corresponds to a joint set number of 2.24. The RQD was not logged for holes drilled on the downstream right abutment, but in general the rock was recovered in long sticks with a few fractured zones. Based on core recovery numbers and field observations, the average RQD is probably about 90-95%, with isolated areas ranging down to about 80%. This results in K_b values between about 35.7 and 42.4. The intensely fractured beds would have an RQD of about 17% based on field measurements. This corresponds to a K_b value of about 7.6. The concrete was placed in 4-foot (1.2m) lifts using large blocks generally encompassing the entire thickness of the dam. The contraction joints are widely spaced (35 to 60 feet (10.7 to 18.3 m)) and keyed. Although some lift lines exhibit minor seepage at high reservoir elevations, the lifts were cleaned well and also keyed. The value of K_b for the concrete should be high, say about 80 or higher.

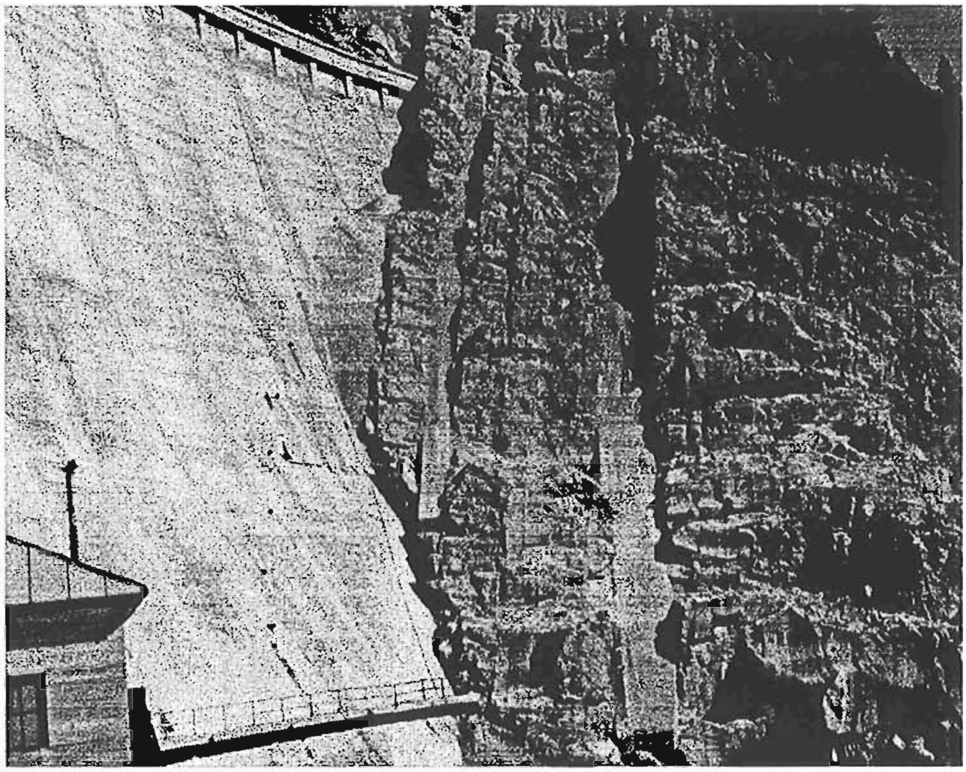

Figure 9 - Dental concrete on left abutment of Gibson Dam.

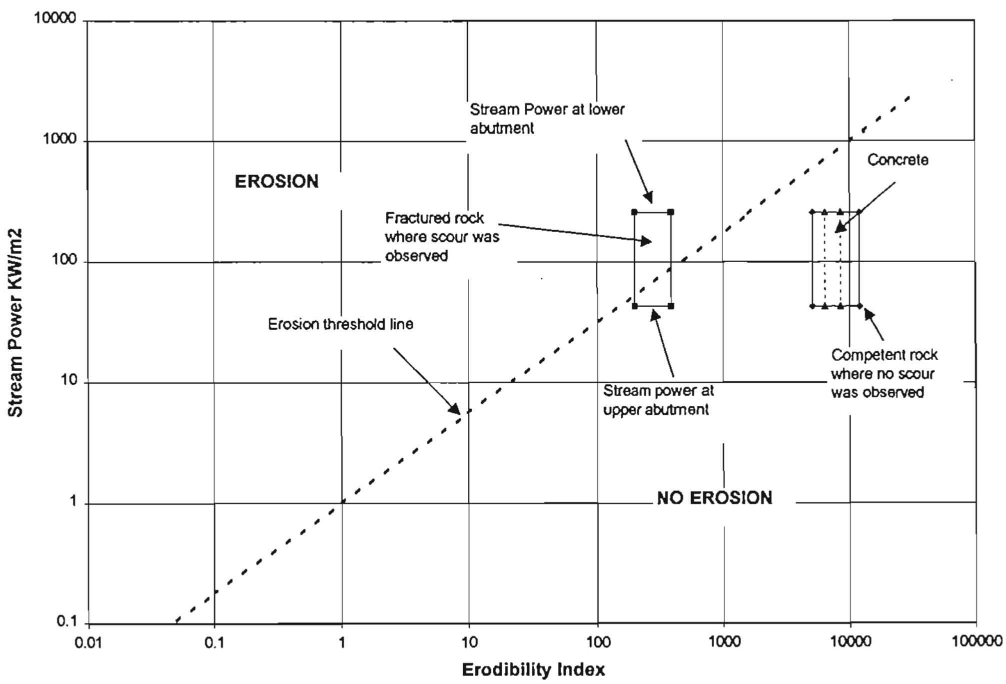

Figure 10 - Rock erosion analysis results for the 1964 flood at Gibson Dam.

K_d represents the inter-block frictional resistance. It can be estimated as the ratio of the joint roughness number over the joint alteration number (J_r/J_a), which is roughly equivalent to the tangent of the friction angle. Based on field observations, the limestone bedding planes are rough and planar, while the joints are very rough and irregular. The bedding strength would likely control the removability. Therefore, the joint roughness was assumed to be rough/planar ($J_r = 1.5$). The J_r for concrete would be described as "stepped" since all the joints are keyed, resulting in a value of about 4.0. The majority of foundation joints were reported as calcite healed or clean and tight, increasing in tightness with depth from the surface (although one joint open up to 3 inches (76 mm) wide at the surface was observed on the right abutment). This results in a J_a of about 0.75 to 1.5. Thus, K_d would range from about 1 to 2. For the intensely fractured beds, the joint roughness number would tend toward the value for rough/planar (1.5), and the joint alteration number could be as high as 2.0, resulting in a K_d value of about 0.75. For the concrete, the joints would be considered to be healed (lift lines) or tight and clean (contraction joints), resulting in J_a between 0.75 and 1.0, and K_d between 4.0 and 5.3.

The relative ground structure number (J_s) represents the orientation of the discontinuities relative to the impinging water, and takes into account the block shapes (long and narrow or roughly cubic). The orientation of the beds is extremely regular, striking 5 to 8 degrees west of north (about cross-canyon) and dipping to the east at angles ranging from 70 to 86 degrees west. The abutments give the appearance that the open bedding planes are spaced roughly twice as close as the open joints. Although the apparent dip of the bedding changes with respect to the plunging jet in relation to the curvature of the dam, an angle of 70 degrees against the flow (beds dip upstream) was assumed on the average. This results in J_s of about 0.9. This value would also apply to the intensely fractured zones. For the concrete, a J_s value of 1.0 would be appropriate.

In summary, the following values of erodibility index (K) are estimated:

- Foundation Rock: 5100 - 12,000
- Intensely Fractured Beds: 200-400
- Concrete: 6400 - 8500

The stream power (defined as the rate of energy dissipation) is low as flow just comes over the top and impinges directly onto the upper abutments, and becomes larger as the fall height increases toward the channel when the reservoir reaches its peak (reflected in the energy available). At maximum overtopping, the depth over the crest (3.2 feet (1.0 m)) corresponded to roughly 19.2 cfs/ft (1.78 $m^3/s/m$) of dam crest. Calculation of stream power for this case follows the procedure outlined in the last case study presented in this paper. These computations indicated the stream power ranged from a low value of 43 kW/m^2 at the upper abutments (fall height of 9 feet (2.7 m)) up to 258 kW/m^2 near the central part of the dam (fall height of 180 feet (54.9 m)).

The results are plotted in Figure 10. The exposed foundation rock and newly placed concrete are not expected to erode based on these results. In general it was felt that the rock and concrete performed extremely well, indicating they should fall well below the threshold for erosion. This is particularly true when it is recognized that the parameters used to estimate erodibility index are based largely on the conditions remaining after the 1964 overtopping event. The intensely fractured zones would be expected to erode, except perhaps near the crest. Although the observed amount of erosion in these zones was not excessive, this is believed to be consistent with the observed behavior.

The results of this study support the conclusion that there probably was some erosion of weak rock (intensely fractured beds) or damaged concrete in areas where there was little dissipation of energy from the tailwater. There was some surficial erosion and scouring of loose material during the experienced overtopping, but not much, as judged from the condition of the foundation after the overtopping. The concrete should not be vulnerable to erosion provided that the concrete remains intact and there isn't degradation of the concrete by cracking, freeze-thaw action, or vandalism. The decision to protect the intensely fractured beds appears to be sound under any scenario. The areas of abutment rock most susceptible to erosion for higher overtopping flows have been protected.

Scour in Alluvial Material

This sub-section summarizes twelve experiments simulating the erosion of a granular material by an impinging jet. A locally available road-base granular material was used in a near-prototype study to simulate alluvial material found near a prototype dam, and an impinging jet set at angles of fifteen, twenty-five, and thirty-five degrees from the vertical was used to simulate flow overtopping the dam. The study results were compared with scour depths calculated with the Erodibility Index Method. The calculation procedure that was used to calculate scour depth in the granular material follows the procedure outlined earlier in this paper. In essence, the maximum scour depth occurs at the elevation where the available stream power is just less than the stream power that is required to scour the earth material. This series of experiments presented here demonstrates the capability of the Erodibility Index to estimate scour downstream of hydraulic structures.

Experiment Facility: The facility includes a basin, 10 m (30.5 ft) wide by 16.75 m (55 ft) long and 4.5 m (15 ft) deep, and an 8.7 cm (3.4375 in) by 3.05 m (10 ft) wide nozzle discharging up to 3.4 m^3/s (120 ft^3/s) at angles ranging from zero to forty-five degrees from vertical.

Figure 11 shows the facility, nozzle, jet, granular material, and the overall configuration of the experiment.

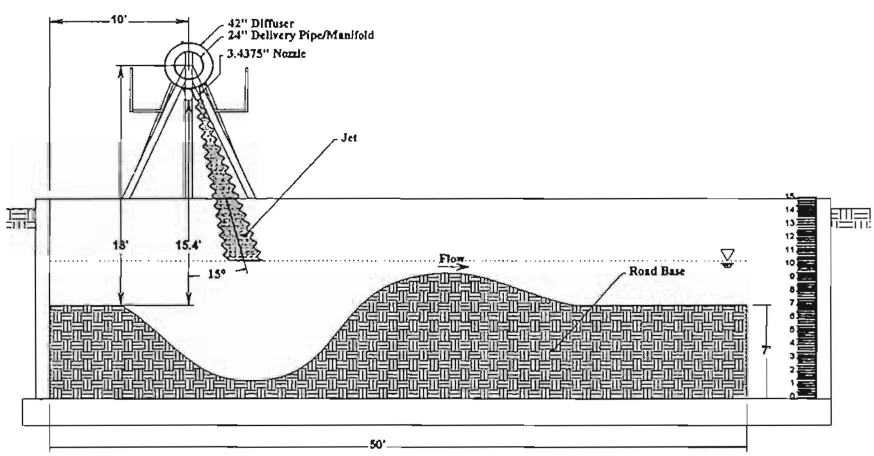

Fig. 11 Profile of experimental facility at Colorado State University.

Experimental Parameters: The series of experiments varied the angle of issuance, and the tailwater and material elevations. Tailwater elevation less material elevation, defined as the hydraulic cushion, varied between 0.30 and 1.82 meters, in three steps. The jet was issued at three angles of 15, 25, and 35 degrees. Combinations of four cushions and three angles resulted in a matrix of twelve experiments (Table 1). The elevation datum of the experimental facility is the floor of the basin. Equation 7 expresses the jet impact angle (α) as a function of the nozzle velocity (v_0), the angle of issuance (ϕ) and the distance between the nozzle and tailwater (Δz). Other experimental parameters include the discharge (Q), the velocity at impact (v_i), the air concentration of the jet at impact (A_i), the nozzle elevation, the water surface elevation, and the median diameter of the road-base material (D_{50}) in meters.

Table 1 - Experimental parameters.

Experiment	ϕ	α	Q	v_o	v_i	A_i	*Noz. El.*	*WS El.*	Δz	D_{50}
1	15°	11.9°	2.74	10.82	5.75	64.7%	6.84	3.35	3.49	1.00E-02
2	15°	12.1°	2.74	10.82	5.80	63.1%	6.84	3.66	3.18	1.00E-02
3	15°	11.7°	2.74	10.82	5.72	66.0%	6.84	3.08	3.76	1.00E-02
4	15°	12.3°	2.74	10.82	5.86	61.5%	6.84	3.93	2.91	1.00E-02
5	25°	20.2°	2.74	10.82	5.85	61.7%	6.89	3.94	2.95	1.00E-02
6	25°	19.5°	2.74	10.82	5.75	65.0%	6.89	3.34	3.55	1.00E-02
7	25°	18.8°	2.74	10.82	5.65	68.3%	6.89	2.56	4.33	1.00E-02
8	25°	19.1°	2.74	10.82	5.69	67.0%	6.89	2.90	3.99	1.00E-02
9	35°	26.9°	2.74	10.82	5.74	65.3%	6.96	3.35	3.61	1.00E-02
10	35°	27.9°	2.74	10.82	5.84	61.9%	6.96	3.97	2.98	1.00E-02
11	35°	26.5°	2.74	10.82	5.70	66.7%	6.96	3.03	3.93	1.00E-02
12	35°	25.8°	2.74	10.82	5.65	68.4%	6.96	2.59	4.37	1.00E-02

$$\alpha = \arctan\left[\frac{v_0 \sin\phi}{\sqrt{(v_0 \cos\phi)^2 + 2g\Delta z}}\right] \tag{7}$$

Erodibility Index (*K*): The Erodibility Index, K, is used to quantify the granular material's relative ability to resist erosion. It is the product of the Mass Strength Number, M_s, the Block Size Number, K_b, the Shear Strength Number, K_d, and Relative Ground Structure Number, J_s.

$$K = M_s \cdot K_b \cdot K_d \cdot J_s \tag{8}$$

Mass Strength Number (M_s)

From Table 1 of Annandale (1995) the Mass Strength Number, M_s, for granular soil between loose and medium density is equal to 0.07.

Block Size Number (K_b)

The particle Block Size Number, K_b, for cohesionless granular materials can be determined directly by (Annandale 1995):

$$K_b = 1000 D_{50}^3 \tag{9}$$

A median grain size, D_{50}, of 10 mm yields a block size number equal to 1.00E-03.

Shear Strength Number (K_d)

For granular materials, the Shear Strength Number, K_d, approximates tan(φ), where φ is the equivalent residual (minimum) friction angle. This angle for the experimental material is approximately 40°, yielding a shear strength number equal to 0.84.

Relative Ground Structure Number (J_s)

The Relative Ground Structure Number, J_s, is equal to 1.0 for granular materials.

Erodibility Index Calculation

The product of the four numbers yields an erodibility index roughly equal to 5.87E-05.

$$K_h = (0.07)(1.00E-03)(0.84)(1.0) \cong 5.87E-05 \tag{10}$$

Required Power: From Annandale (1995), the power (kW/m^2) required, p_R, to erode earth material in the lower range of Erodibility Index numbers is a function of K:

$$p_R = \frac{480}{1000} K^{0.44} \tag{11}$$

Rate of Energy Dissipation

Available Power: The power (kW/m^2) available from the plunging jet to erode the earth material within the plunge pool is a function of jet hydraulics. From Bohrer and Abt (Bohrer 1996) the velocity along the centerline of a jet in a plunge pool is a function of the jet velocity at impact, the angle of impact, the air concentration of the jet at impact (represented by the ratio of air and water densities) and gravitational acceleration. Equation (12) describes this functional relationship, followed by the limits of application. Equation (13) expresses the distance along the centerline.

$$-\ln\left(\frac{v}{V_i}\right) = -0.5812\ln\left[\left(\frac{\rho_i}{\rho_w}\right)\left(\frac{V_i^2}{gL}\right)\right] + 2.107 \tag{12}$$

$$-0.29 \le \ln\left[\left(\frac{\rho_i}{\rho_w}\right)\left(\frac{V_i^2}{gL}\right)\right] \le 2.6$$

$$L = \frac{z_1 - z_2}{\cos\alpha} \tag{13}$$

The rate of energy dissipation, or available power, is a discretized function of the total head at various elevations along the centerline of the submerged jet. Equation (14) shows a discrete expression for the change in head between points j and j+1. As the velocity decays, with decreasing elevation, or increasing displacement along the jet centerline, the total head decreases. Equation (15) yields the corresponding available power.

$$\Delta E_j = \frac{v_j^2}{2g} - \frac{v_{j+1}^2}{2g} + \frac{P_j}{\gamma} - \frac{P_{j+1}}{\gamma} + z_j - z_{j+1} \tag{14}$$

$$p_{Aj} = \frac{\gamma v_j \Delta E_j}{1000} \tag{15}$$

Figure 12 compares the required power, p_R, and the available power, p_A, for experiment 1. The calculated elevation of the maximum scour is located at the point where the available power is just less than the required power.

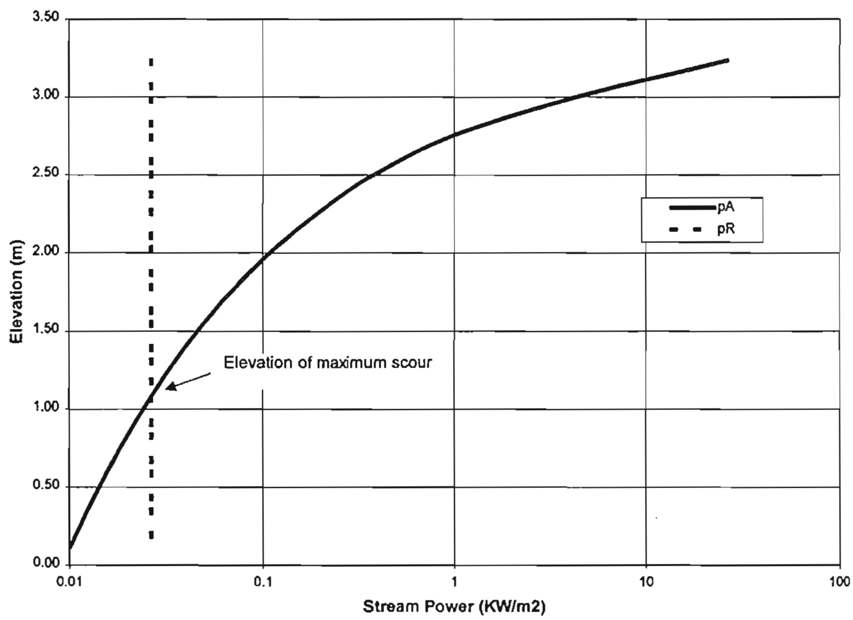

Fig. 12 Comparison of available and required stream power for experiment 1. The elevation of maximum scour is located where the available stream power is just less than the required stream power.

The comparison between observed and calculated scour elevations for all twelve experiments shown in Figure 13 indicates that the method has been used successfully to predict scour depth of granular earth material. The procedure for estimating the depth of scour in a plunge pool accounts for angle of impact, aeration of the jet, hydraulic cushion, and material properties.

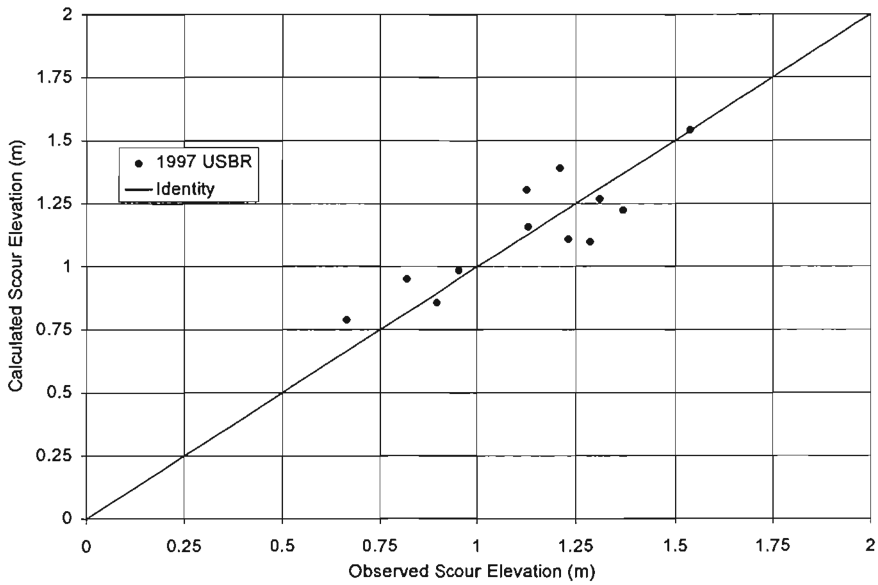

Fig. 13 Comparison of calculated and observed scour elevations for granular material.

Ongoing Research – Erosion of Simulated Rock

This sub-section summarizes an experiment pertaining to the erosion of a simulated rock mass by a impinging jet. Lightweight concrete blocks, placed in two layers and dipped 45 degrees in the downstream direction, simulate a fractured rock mass. The Erodibility Index is used to quantify the relative ability of the simulated rock to resist erosion. The rate of energy dissipation describes the relative magnitude of the erosive power of the water jet.

Experiment Facility: The facility simulates overtopping and erosion in the foundation areas of a dam or spillway. It is the same facility that was used for the experiments pertaining to scour of granular material and includes the following:

A basin, 10 m (30.5 ft) wide by 16.75 m (55 ft) long and 4.5 m (15 ft) deep, with a 8.7 cm (3.4375 in) by 3.05 m (10 ft) wide nozzle that can discharge up to 3.4 m^3/s (120 ft^3/s) at an angle of fifteen degrees from vertical.

Figure 14 shows the facility including diffuser and nozzle, jet, layers of blocks, and the overall configuration of the experiment.

Dimensions of Block: The nominal dimensions of each fluted lightweight concrete block is 3x8x16 inches.

Figure 15 details the commercially available concrete blocks. The flutes are roughly one-half inch wide by one inch deep transverse grooves in the face of the block.

Length, $L = 15.5in$; $J_x = 0.394m$

Width, $W = 7.63in$; $J_y = 0.194m$

Thickness, $T = 2.5in$; $J_z = 0.064m$

Erodibility Index (*K*): The Erodibility Index, *K*, is the product of the Mass Strength Number, M_s, the Block Size Number, K_b, the Shear Strength Number, K_d, and Relative Ground Structure Number, J_s.

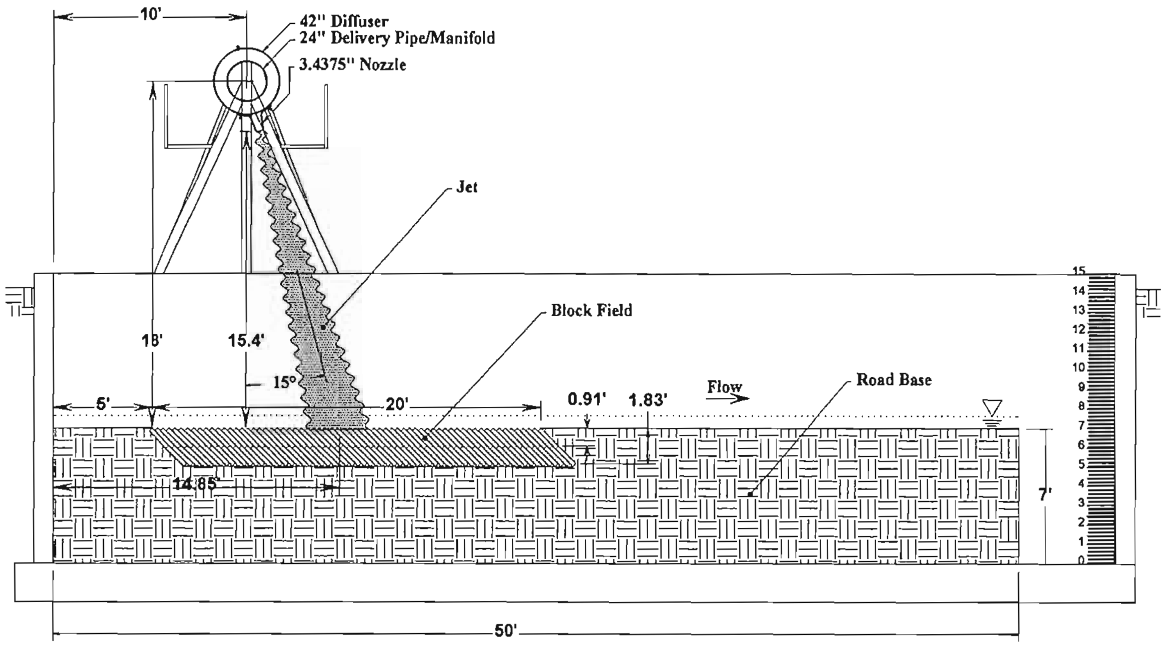

Fig. 14 Profile of prototype facility showing location of simulated rock.

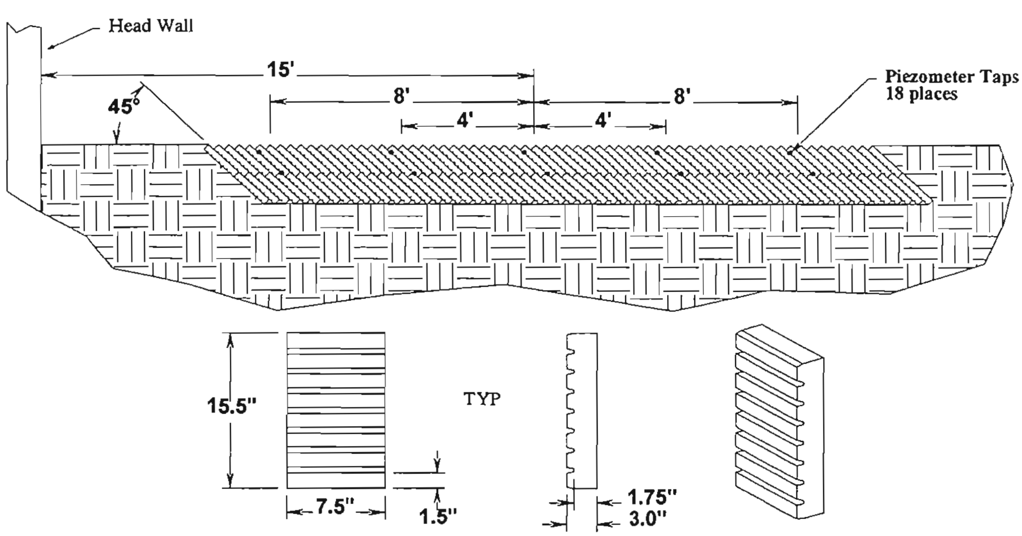

Fig. 15 Concrete block details including locations of piezometer taps.

$$K = M_s \cdot K_b \cdot K_d \cdot J_s \tag{16}$$

Mass Strength Number (M_s)

The Mass Strength Number, M_s, is equal to the product of the Unconfined Compressive Strength, UCS, of the material and the coefficient of relative density (Annandale, 1995). The coefficient of relativity density is the ratio of the material's unit weight to the unit weight of good quality rock (γ_s), roughly equal to 27 kN/m^3. The UCS and unit weight (γ_b) of the concrete blocks was reported by the manufacturer.

$$UCS = 21\text{MPa}(3046psi)$$
$$\gamma_b = 15.73\text{kN/m}^3\left(100\text{Lb/ft}^3\right)$$

$$M_s = \frac{\gamma_b}{\gamma_s}21 = \frac{15.73}{27.00}21 \approx 12 \tag{17}$$

Block Size Number (K_b)

The Block Size Number, K_b, is a function of the Rock Quality Designation (RQD) and the Joint Set Number, J_n.

$$K_b = RQD/J_n \tag{18}$$

The RQD is a function of the orthogonal dimensions of the particle, J_x, J_y, and J_z.

$$RQD = \left[105 - 10/\left(J_x J_y J_z\right)^{0.33}\right] = 47 \tag{19}$$

The joint set number, J_n, for three joint sets, per Table 6 in Annandale (1995) is 2.73.

$$K_b = RQD/J_n = 17 \tag{20}$$

Shear Strength Number (K_d)

The Shear Strength Number, K_d, is the ratio of the joint roughness number, J_r, and the joint alteration number, J_a.

$$K_d = J_r/J_a \tag{21}$$

For rough, irregular planar surfaces, the joint roughness number, J_r, per Tables 8 and 9 in Annandale (1995) is 1.5 and the value of J_a for a joint separation of approximately 5mm is 2.0.

$$K_d = J_r/J_a = 1.5/2.0 = 0.75 \tag{22}$$

(The inter-particle friction angle corresponds to the arctangent value of K_d, i.e. arctangent (0.75) = 36.9°).

Relative Ground Structure Number (J_s)

From Table 7 in Annandale (1995) the value of J_s for a 45 degree dip angle in the direction of flow, and a relative shape of 15.5/2.5 = 6 (i.e., a ratio of 1:6), is 0.44.

Erodibility Index Calculation

The product of the four numbers is an estimate of the erodibility index roughly equal to 69.

$$K_h = (12)(17)(0.75)(0.44) \cong 69 \tag{23}$$

Rate of Energy Dissipation

It is assumed that all the energy is dissipated at the location where the jet impinges on the simulated rock. The total rate of energy dissipation is equal to the product of the unit weight of water (γ), the discharge (Q), and the change in energy, ΔE.

$$P = \gamma \cdot Q \cdot \Delta E \tag{24}$$

The rate of energy dissipation per unit area (p) is equal to the rate of energy dissipation divided by the horizontal projection of the area of the jet at impact, A_i.

$$p = \frac{\gamma \cdot Q \cdot \Delta E}{A_i} \quad \text{(= H)} \qquad \frac{9{,}82 \cdot 1{,}133 \cdot \text{[illegible]}}{3{,}05 \times 0{,}914} = 22{,}6 \tag{25}$$

In this application, the change of energy, ΔE, is equal to the total available energy between the nozzle and the tail water surface. This supposes that 100% of the total available energy is dissipated in the erosion process. The water cushion in the experiment was kept to a minimum in order to simplify the estimate of the rate of energy dissipation.

Table 2 contains the calculations and parameters used to determine the rate of energy dissipation. The total head, H, is the sum of the nozzle elevation and the velocity head minus the tailwater elevation. The calculations assume that the total available head is converted into kinetic energy and dissipates at the point of contact with the foundation. For this experiment with a jet width at impact of 3.0 ft (approximately 1m) a rate of energy dissipation of $p = 22.6$ kW/m^2 is indicated.

Table 2 - Hydraulic and Rate of Energy Dissipation calculations.

Q	40	ft^3/s	1.133	m^3/s
Nozzle Elev.	22.44	ft	6.840	m
Velocity Head	3.74	ft	1.139	m
Tailwater Elevation	7.63	ft	2.326	m
Total H	18.55	ft	5.653	m
Jet Width	10.0	ft	3.048	m
Jet Thickness	3.0	ft	0.914	m
Density of Fluid	9.82	kN/m^3		
$p_{3.0}$	22.6	kW/m^2		

Hydraulic Cushion

Depth gages upstream and downstream of the jet impact zone reported a depth of roughly 0.192 m (0.63 ft) or elevation 7.63 feet at 1.133 m^3/s total discharge. The tailwater depth, or hydraulic cushion, h, directly influences the scour potential of the jet and the rate of energy dissipation calculations. The cushion effect is minor in this experiment because the jet possesses momentum that displaces the tailwater and impacts directly upon the blocks.

Figure 16 shows the experimental data in relation to the original field data and the threshold relationship proposed by Annandale (1995). The proximity of the experimental data to the threshold confirms the erosion threshold for the Erodibility Index Method for the simulated rock.

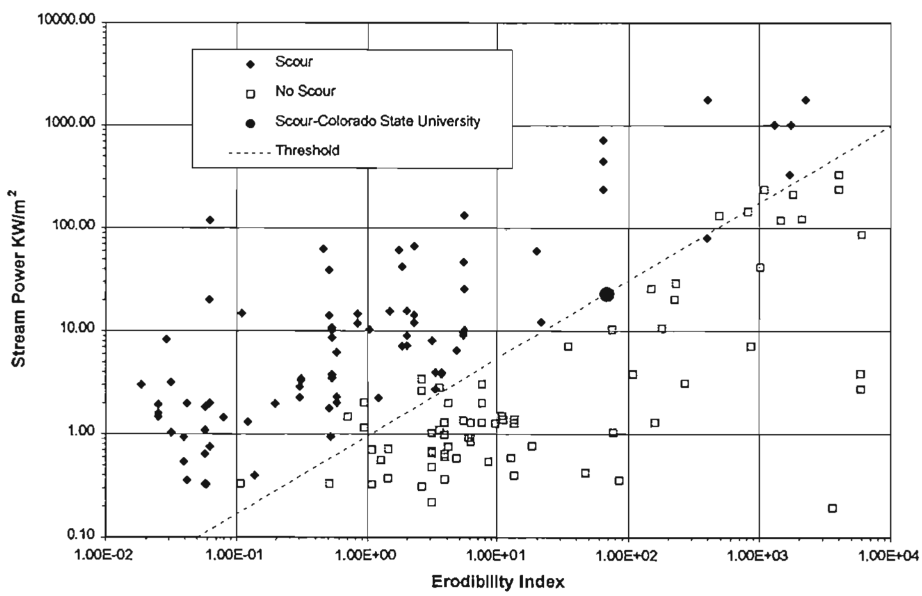

Fig. 16 Experimental data in relation to the original field data and the threshold relationship proposed by Annandale (1995).

SUMMARY

The paper summarizes approaches that are used in the United States of America to simulate scour of dam foundations. These methods include physical hydraulic model studies, rigorous constitutive computer modeling and empirical approaches. Physical model studies provide qualitative information pertaining to scour that is used in making design decisions.

Keyblock Theory (Goodman & Shi 1985) currently forms the basis for constitutive modeling approaches. Although this theory comprehensively takes account of forces acting on hard rock blocks, its application currently lacks appropriate incorporation of the fluctuating water pressures that are considered to be the principal driving forces causing erosion of rock. Additional development to incorporate the driving forces that cause scour of rock is required to ensure representative results.

The empirical methods by Veronese (1937), Yildiz and Uzucek (1994) and Mason & Arumugam (1985) do not adequately incorporate the role of material properties, particularly when considering rock formations, in resisting scour. These methods are considered to have limited application for a large number of dam safety concerns where potential scour of rock requires consideration.

The Erodibility Index Method (Annandale 1995), defines an erosion threshold that can be used to predict the erodibility of any earth material, including rock, and cohesive and non-cohesive granular soils. A procedure to calculate scour depth that is used concurrently with this erosion threshold has been shown to provide reasonable estimates of scour depth when compared to observations. A case study that compares observed scour to calculated scour for granular earth material shows very good agreement. Field and experimental observations pertaining to scour of natural and simulated rock, presented in this paper, furthermore imply that the erosion threshold defined by the Erodibility Index Method reasonably represents the erosion threshold for rock.

REFERENCES

1. Annandale, G.W., 1995, "Erodibility." Journal of Hydraulic Research, Vol. 33, No. 4, pp. 471-494.

2. Bohrer, J.G., Abt, S.R., 1996, "Plunge Pool Velocity Prediction of Rectangular, Free Falling Jets. Dam Foundation Erosion Study", submitted to United States Department of the Interior, Bureau of Reclamation, November.

3. Goodman, R.E. and Hatzor, Y., 1991, "Safety of Dam Deficiencies due to Overtopping: Results of Preliminary Analysis of Abutment Stability based on Block Theory and the Critical Key Block Concept", Submitted to United States Department of the Interior, Bureau of Reclamation, November.

4. Goodman, R. E. and Gen-hua Shi, 1985, "Block Theory and its Application to Rock Engineering". Prentice-Hall, Englewood, Cliffs, NJ.

5. Kirsten, H. A. D., 1982, "A Classification System for Excavation in Natural Materials", The Civil Engineer in South Africa. pp. 292 – 308, July.

6. Mason, P.J., Arumugam, K., 1985, "Free Jet Scour below Dams and Flip Buckets." ASCE Journal of Hydraulic Engineering, Vol. 111, No. 2.

7. Smith, S. P., Annandale, G. W., Johnson, P. A., Jones, J. S. and Umbrell, E. R., 1997, "Pier Scour in Resistant Material: Current Research on Erosive Power", Proceedings of Managing Water: Coping with Scarcity and Abundance, 27th Congress of the International Association of Hydraulic Research, San Francisco, California, pp. 160-165.

8. Veronese, A., 1937, "Erosioni de Fondo a Valle di uno Scarico." Annali dei Lavori Publicci, Vol. 75, No. 9, pp. 717-726, Italy.

9. Yildiz, D., Üzücek, E., 1994, "Prediction of Scour Depth From Free Falling Flip Bucket Jets", Intl. Water Power and Dam Construction, November.

EVALUATION OF GENERAL SCOUR

by

José Antonio Maza-Álvarez[1]

ABSTRACT

General scour or flood erosion is defined as the subsidence of the river bed induced by the water flow during floods. This phenomenon results mostly from the larger capacity of flow, in those events, to carry suspended particles scoured from the bottom which in turn is due to the larger velocities and turbulence of the current. It is assumed that in general terms failures are not induced by local scour considered as an isolated phenomenon, but mostly by general scour and by constriction erosion. The first component is not due to human factors and it always occurs whenever a flood takes place. On the other hand, the constriction erosion is induced by human factors as a result of the narrowing of the river width due to the presence of access ramps and abutments.

A method is proposed in this paper for calculating the general scour. It consists in assuming the initial condition prior to particle suspension and applying the equations of flow resistance from Cruickshank and Maza-Álvarez (1973), or from Karim and Kennedy (1981, 1990) which are almost identical, or otherwise, Manning's equation. Any equation of flow resistance can be used as the starting point to develop the equation for determining the general scour. However, some of them lead to the definition of more complex equations that for the time being can be dispensed with because there are no data available on scouring produced by a wide variety of D_{84} particle sizes. The paper also includes formulas derived in terms of unit flow discharges, following the ideas of Schreider *et al.* (1999). When unit flow discharges are applied, the result may be closer to reality because flow concentration is taken into account as a function of the flow regime of bends and upstream stretches. Evaluation of the general scour is useful for the design of bridges and for projects of river crossings of pipelines when buried under the river bed.

INTRODUCTION

General scour is defined as the overall subsidence of the river bed when large floods occur. It comes as a result of the large capacity of the current to carry bed load particles in suspension. Typically, when the flow discharge decreases particles become suspended therefore rebuilding the initial river bed elevations; in this case, if this elevation is recorded before and after the flood there is no evidence that such scouring ever took place. Other authors include as part of general scour any extensive subsidence of the river bed and not only that produced

[1] Professor, Graduate Division, School of Engineering, Universidad Nacional Autónoma de México; and Manager of Civil Engineering Studies, Comisión Federal de Electricidad, México

during floods. (See for example Breusers and Raudkivi, 1991 and Predwojski, Blazejewski and Pilarczyk, 1995.)

When a certain flow discharge moves through a section of the river and the bed subsides as a result of the general scour, the hydraulic area increases and the average flow velocities decrease. The river bed subsidence continues until an equilibrium is reached between the scouring velocities of the river and the velocities required by the bed load particles to become scoured; or otherwise until a balance is achieved between the flow capacity necessary to suspend the bed particles and the fall velocities of such particles. The general scour is likely to uncover subsoil layers constituted by other materials. This process will be governed not only by the soil stratigraphy but also by the maximum flood discharge. If the flow discharge is associated to a short return period, i.e., from 10 to 50 years, it is quite frequent to encounter a single type of material forming the river bed deposits; on the other hand, when the return period is long –200 years or more- strata with materials different from the bottom are generally uncovered and scoured.

Depending on the distribution of materials found at the subsoil, two different conditions can be present: homogeneous and heterogeneous. The homogeneous distribution condition exists when the scour takes place in one and only material, whereas the heterogeneous condition occurs when the scouring process uncovers two or more layers with different materials. The subsoil materials could be either cohesive, or cohesionless (granular); the dry unit weight is the main physical characteristic of the former, and the particle diameter and specific weight of the latter. The free fall velocity can also be associated to granular particles and both materials properties can be taken into account. In this work mention is only made of scouring occurring in cohesionless or granular materials.

It is important to define the subsidence of the river bed produced by general scour when designing works such as bridge piers or Ranney wells, or when it is intended to span a river with an aqueduct or to cross it with a pipeline buried under the river bed.

The river bed subsidence resulting from general scour has been dealt with by autors such as Leopold, Wolman and Miller (1964) (see figure 1). On the other hand, Lischtvan and Levediev (as mention by Maza-Álvarez, 1959, 1970) proposed a method to quantify the general scour by comparing the mean flow velocity with the mean scouring velocity of the bed material. Field observations have been also performed by Maza-Álvarez and Rico-Rodríguez (1970) and by Schreider, Scachi, Reynares and Franco (1999).

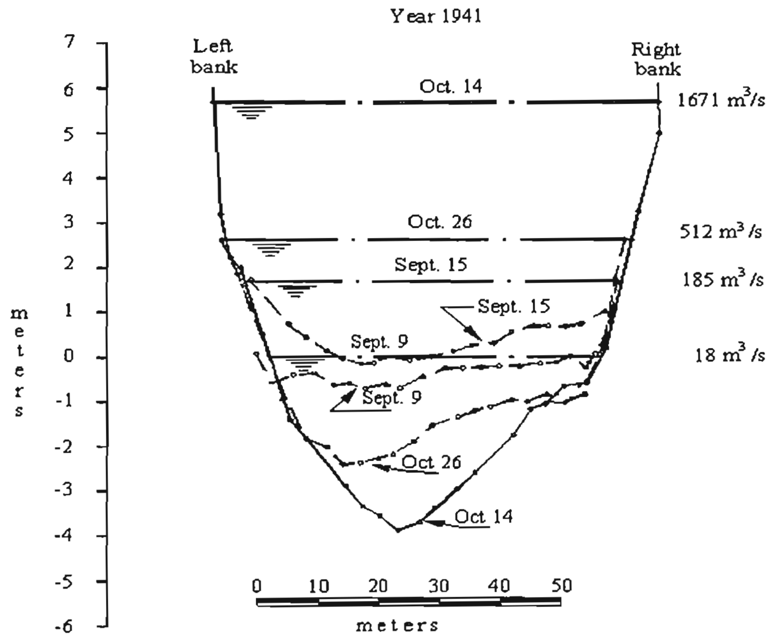

Fig. 1 - General scour and sedimentation recorded at San Juan River, near Bluff, Utah, USA, on Sept.-Oct. 1941

METHOD PROPOSED

The initial movement of bed load particles and their lifting to put them in suspension are random processes governed by the instantaneous shear stress developed in the vicinity of each particle. A stochastic or probabilistic approach to quantify the bottom scour seems to be an adequate solution. However, in this work a different criterion will be applied because of the following reasons: the lack of sufficient reliable data on the conditions under which a particle becomes suspended and remains in suspension; the relative accuracy of the friction-related formulas that are used to obtain the depth of scour; and the complexity of the potential resulting equations of no practical use to designers.

Hypotheses

1.- The first hypothesis establishes that the bed load material is lifted and suspended when the vertical component υ' of the turbulence is larger than the free fall velocity ω of the particles. Since the peak value of υ' is related to the shear velocity U_*, an expression can be written as

$$U_* = a\omega \tag{1}$$

where a is a coefficient and ω is the particle free fall velocity, expressed in m/s the latter is obtained from Rubey's equation that can be established as follows:

$$\omega = F_1 \left[g \, \Delta \, D\right]^{0.5} \tag{2}$$

where:

$$F_1 = \left(\frac{2}{3} + \frac{36\nu^2}{g \, \Delta \, D^3}\right)^{0.5} - \left(\frac{36\nu^2}{g \, \Delta \, D^3}\right)^{0.5} \tag{3}$$

In the two previous equations: g, acceleration due to gravity, in m/s^2; Δ, relative density of submerged particles, $\Delta = (S_s - 1)$; S_s, relative density of particles, $S_s = \rho_s / \rho$; ν, kinematics viscosity of water, in m^2/s; D, particle diameter, in m; and ρ_s and ρ, density of particles and of water, respectively.

The coefficient a, i.e. the ratio U_*/w, expresses the mixing action of the turbulence, and may provide and indicative value of the separation of different modes of transport. Graf (1999) proposes the following values:

Beginning of bed load transport: $a > 0.10$

Beginning of suspended load transport: $a > 0.40$

To establish the beginning of the scouring process, coefficient a reaches higher values as derived from equations 16, 25 and 29 that were obtained with data referred to in this paper. For illustrative purposes, when $D_{84} \leq 0.0002\, m$, the value of a is greater than $2\ (a \geq 2)$.

General scour is produced when the number of particles that become suspended is larger than the number of those that are settled, i.e. when the flow capacity for carrying suspended particles increases with time, a situation occurring at the upwards part of a hydrograph. When the hydrograph shows a downward trend and the flow capacity to maintain the particles in suspension decreases, a larger number of them become settled and the bed elevation increases. As a result, in many rivers, after the transit of a large flood, particularly at the end of the flood season, the river bottom retains the same average elevation as at the beginning of the flood season. .

2.-The second hypothesis establishes that the representative diameter of the bed material under the condition of maximum general scour corresponds to D_{84}.

At the beginning it was deemed convenient to comply with the diameters indicated in each of the formulas of flow resistance presented below, but assuming that the maximum armoring has been already developed; therefore, the formulas were studied and analyzed in terms of the corresponding particle diameter associated to the maximum armoring. The equations developed by Maza-Álvarez and García-Flores (1986) were used to obtain those diameters. However, there was some uncertainty about the degree of armoring that could be reached at the scoured bed as a result of a high sediment transport rate. It is quite probable that the mean bed diameter at the time of the occurrence of the peak scour becomes higher than the value corresponding to the original sample. Therefore, D_{84} of the original sample of the bed material was selected as the representative diameter to obtain the free fall velocity; equation (1) can be then written as follows:

$$U_{*} = a\ \omega_{84} \tag{4}$$

In this last equation the coefficient a can take into account, at least on a partial basis, the fact of considering D_{84} instead of the actual diameter likely to be found at the partly armored river bed. When field measurements are made, if they are taken from the scoured bed, the values of D_x and ω_x proposed by each of the authors of the flow resistance equations referred to in subsequent paragraphs should be taken into account.

3.- The third hypothesis establishes that during the transit of the flood, and therefore during the scouring process, the width of the river bed remains constant. Furthermore, it is considered that during the calculations the flow discharge along a unit width remains theoretically constant when the bed elevation subsides.

PROPOSED EQUATIONS

In order to quantify the general scour it is required to use as starting equation, one related to flow resistance. It is possible in these equations to differentiate the friction induced by the particles from bed undulations, as occurs in those proposed by Engelund, Paris, and Alam, Lovera and Kennedy. Other equations take into account the combined effect of particles and undulations, such as those developed by Garde and Ranga-Raju, Brownlie, Cruickshank and Maza, and Karim and Kennedy. This paper presents the deduction of the equations to evaluate the general scour based on the equation of flow resistance proposed by Cruickshank and Maza; subsequently, only the final equations of general scour obtain from the equations of Karim and Kennedy, and from Manning´s are presented.

FROM THE EQUATION OF CRUICHSHANK AND MAZA (1973)

These authors suggested two equations to obtain the mean velocity U. One of them corresponds to flow under lower regime and the other to upper regime; both are applicable to river beds with particle sizes within the range of sands to gravel $(0.00007 \leq D_{50} \leq 0.008\ m)$. The general depth of scour of the river bed will be then determined when a flood occurs, based on the formula for lower regime and indicating all stages necessary to deduct it.

The equation proposed to evaluate the mean velocity U, for lower regime conditions is:

$$U = 7.58\,\omega_{50}\left(\frac{h}{D_{84}}\right)^{0.634}\left(\frac{S}{\Delta}\right)^{0.456} \tag{5}$$

which is valid if:

$$\frac{1}{S} \geq 83.5\left(\frac{h}{D_{84}\;\Delta}\right)^{0.35} \tag{6}$$

The variables not yet defined are: h, flow depth, in m; D_{84}, particle diameter of bed material in which 84% are smaller than that size, in m; ω_{50}, free fall velocity in clear water for particles with diameter D_{50}, in m/s; and S is the hydraulic gradient.

The general scour is calculated for a flow discharge associated to a certain return period. To perform the calculation of scour it is assumed, at least theoretically, that the design flow discharge moves through the area formed between the maximum elevation of the water surface and the original cross section area surveyed prior to the occurrence of the flood or before the flood season. This condition does not happen in nature because when the maximum water elevation occurs, the maximum scour of the river bed also takes place. In other words, from the very first moment of the flood, and when the flow is already capable of suspending more particles than those being sedimented, the scouring process actually takes place. Therefore, the bed subsidence continues whereas the flow discharge keeps on increasing at the cross section under study.

The assumption referred to before is applied with the purpose of defining the distribution of the unit flow discharges existing across the cross section during the transit of the peak flow discharge. The unit flow discharge along any vertical of a river cross section can be obtained with two different procedures. The first of them is as a function of the initial theoretical flow depth h_0, measured between the maximum water elevation upon passage of the design flow discharge Q_d and the bed elevation given by the original cross section surveyed when flow discharges are small (dry season) (see figure 2). In this case the higher h_0 the higher the unit flow discharges. The second approach to find out the unit flow discharges implies their direct measurement during the transit of the flow discharge Q_d, as suggested by Schreider *et al.* (1999).

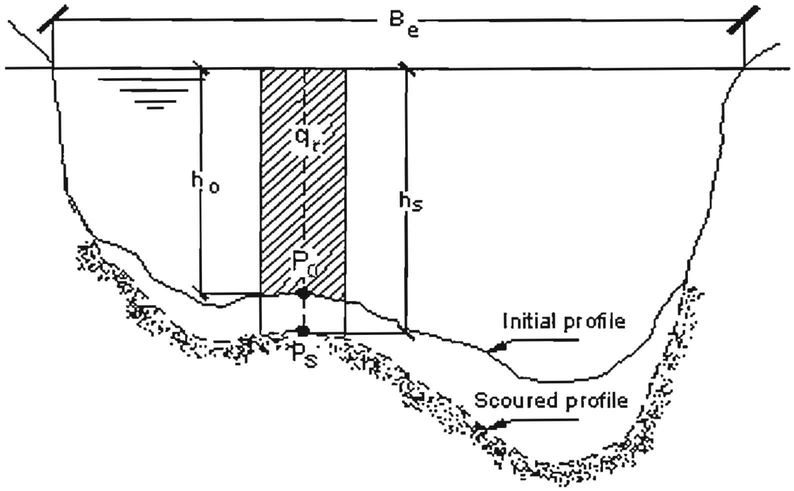

Fig. 2 - General scour at a vertical and scoured cross section

Taking into account the above assumptions and using equation (5), the flow discharge passing through the theoretical cross section already described can be expressed as follows:

$$Q_d = \frac{7.58\, \omega_{50}\, B_e\, h_m^{1.634}}{D_{84}^{0.634}} \left(\frac{S}{\Delta} \right)^{0.456} \tag{7}$$

where B_e is the effective width of the free water surface, in m; and Q_d is the design flow discharge, i.e. the peak flow of the flood for which the general scour is going to be calculated, in m^3/s. Q_d is associated to a certain return period T, to be selected beforehand in terms of the problem to be solved. For example, for calculating the total scour in bridge design, the value of T ranges from 50 to 100 years. On the other hand, h_m is the mean depth of the cross section, in m, defined by the water elevation upon passing of the peak flow discharge of the flood and by the initial profile of such cross section, and given by the relationship $h_m = A/B_e$, where A is the hydraulic area, in m^2.

When passing the flow discharge Q_d, the unit flow q_r that moves through any vertical (unit width) with a depth h_0 is equal to:

$$q_r = \frac{7.58\, \omega_{50}\, h_0^{1.634}}{D_{84}^{0.634}} \left(\frac{S}{\Delta} \right)^{0.456} \tag{8}$$

After dividing equation (7) by equation (8), i.e. Q_d / q_r, and solving for q_r, the following expression is obtained:

$$q_r = \frac{Q_d}{B_e}\left(\frac{h_0}{h_m}\right)^{1.634} \tag{9}$$

This equation defines the distribution of the unit flow discharges through the cross section, as a function of the initial depth h_0.

Mention has been made that such unit flow discharge has to pass during the whole river bed scouring process that will stop upon reaching a certain depth h_s in which the equilibrium is achieved among lifted and settled particles. Therefore, for the equilibrium condition, i.e. for the peak scour, equation (8) can be written as:

$$q_e = \frac{7.58\,\omega_{50}\,h_s^{1.634}\,S^{0.456}}{D_{84}^{0.634}\,\Delta^{0.456}} \tag{10}$$

In order to express the unit flow discharge in terms of the shear velocity U_*, the following transformation can be made:

$$q_e = \frac{7.58\,\omega_{50}\,h_s^{1.178}\,h_s^{0.456}\,S^{0.456}\,g^{0.456}}{D_{84}^{0.634}\,g^{0.456}\,\Delta^{0.456}} \tag{11}$$

where q_e is the unit flow discharge under which particles that become suspended and those already settled are in equilibrium when the flow depth becomes equal to h_s.

If it is taken into account that $U_* = (g\,h\,S)^{0.5}$, equation (11) is transformed as follows:

$$q_e = \frac{7.58\,\omega_{50}\,h_s^{1.178}\,U_*^{0.912}}{D_{84}^{0.634}\,\Delta^{0.456}\,g^{0.456}} \tag{12}$$

As established before, during the full scouring process the unit flow discharge at each unit width remains constant; therefore:

$$q_r = q_e \tag{13}$$

If equations (9) and (12) are matched, then:

$$\frac{Q_d}{B_e}\left(\frac{h_0}{h_m}\right)^{1.634} = \frac{7.58\,\omega_{50}\,h_s^{1.178}\,U_*^{0.912}}{D_{84}^{0.634}\,(g\,\Delta)^{0.456}} \tag{14}$$

The shear velocity U_* at the moment of peak scour is considered to be associated to the free fall velocity of D_{84} diameter particles because a certain degree of armoring should be available.

In what refers to the value of ω_{50}, it can be inferred that D_{50} during the scouring and armoring process (either partial or maximum armoring) is larger than the equivalent diameter of the original sample; it was therefore decided to work with ω_{84}. Furthermore, in the case of coefficient a the difference of assuming ω_{84} instead of ω_{50} included in the formula of flow resistance of Cruickshank and Maza-Álvarez, can be taken into account. Coefficient a of equation (4) will be labeled a_c to tell it apart from those to be used at a later stage. Therefore, the equation to obtain the depth of scour h_s, at a vertical with an initial depth h_0 when a flow discharge equal to Q_d moves through the cross section of a river, can be written as follows:

$$h_s = \left[\frac{Q_d}{B_e} \left(\frac{h_0}{h_m} \right)^{1.634} \frac{D_{84}^{0.634} \left[g\ \Delta \right]^{0.456}}{7.58\ a_c^{0.912}\ \omega_{84}^{1.912}} \right]^{\frac{1}{1.178}} \tag{15a}$$

If it is expressed in terms of the unit flow discharge, then:

$$h_s = \left[\frac{q_r\ D_{84}^{0.634} \left[g\ \Delta \right]^{0.456}}{7.58\ a_c^{0.912}\ \omega_{84}^{1.912}} \right]^{\frac{1}{1.178}} \tag{15b}$$

where q_r is the unit flow discharge at the vertical where it is desired to determine the value of h_s, which in turn can be either measured during the transit of the flood or quantified according to equation (9).

The coefficient a_c of equations (15*a*) and (15*b*) was obtained from the results of Lischtvan and Levediev method and it was verified with data obtained from the Paraná and Leyes rivers, within the range of fine to medium sand, provided by Schreider and Scachi through a personal communication. Therefore, the coefficient a_c will be equal to:

$$a_c = \exp\left[Ln\left(\frac{q_r^{0.19}}{D_{84}^{0.153}} \right) + \frac{3 \times 10^{-8}\ Ln\ D_{84} + 3.04 \times 10^{-7}}{D_{84}^2} - 2.33 \right] \tag{16}$$

Subsequently, equations (15*b*) and (16) were applied with data from the Mississippi and Magdalena rivers; the results are shown in figure 3.

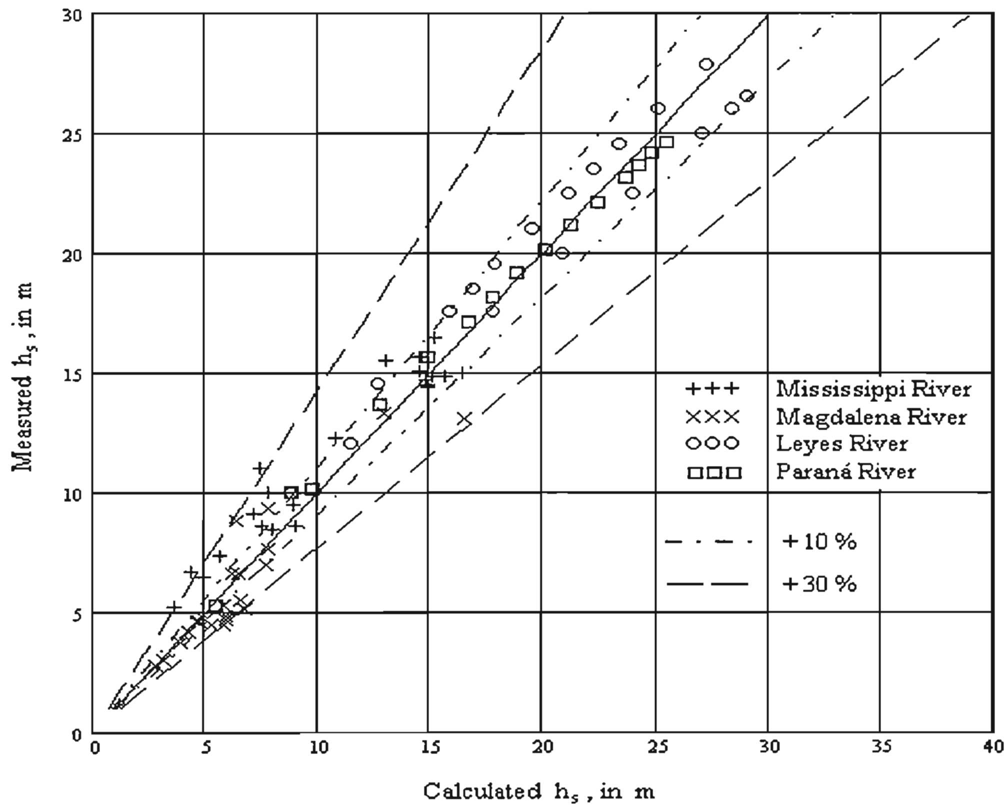

Fig 3 - General scour depth, measured and calculated

To obtain the profile of the scoured cross section equations (15*a*) or (15*b*) will have to be applied at each vertical where it is intended to determine the depth of scouring. The points thus obtained will be linked together.

There is not general scour when $h_s \leq h_0$

Limits of applicability

If it is assumed that the results obtained with the method of Lischtvan and Levediev are correct, a fact that has not been proved by the author outside the range of sand particles, and if the data of the Paraná and Leyes rivers are taken into account, then equations (15) and (16) are applicable within the following boundaries:

$$0.0001 \leq D_{84} \leq 0.50\, m \tag{17}$$

$$5 \leq q_r \leq 70\; m^2/s \tag{18}$$

Equations (15) and (16) were only verified with the real data available (Mississippi, Magdalena, Leyes and Parana rivers) for

$$0.00014 \leq D_{84} \leq 0.0069\ m \tag{19}$$

$$5 \leq q_r \leq 55\ m^2/s \tag{20}$$

FROM THE EQUATION OF KARIM AND KENNEDY (1981, 1990), GROUP I

Karim and Kennedy presented as equation of Group I the following one:

$$\frac{U}{(g\ \Delta\ D_{50})^{0.5}} = 2.822 \left[\frac{q}{(g\ \Delta\ D_{50}^3)^{0.5}} \right]^{0.376} S^{0.31} \tag{21}$$

where q is the unit flow discharge, in m^2/s; and U is the mean velocity associated to q, in m/s.

When U is solved to obtain an explicit relationship of the mean value, the following expression is derived:

$$U = 5.273\ (g\ \Delta\ D_{50})^{0.5} \left(\frac{h}{D_{50}} \right)^{0.6026} S^{0.4968} \tag{22}$$

The following results were obtained from the previous procedure:

a) Distribution of the unit flow discharges through the width of the cross section

$$q_r = \frac{Q_d}{B_e} \left(\frac{h_0}{h_m} \right)^{1.6026} \tag{23}$$

b) The depth of the general scour h_s, in terms of the initial depth h_0, when the flow discharge Q_d passes through the cross section, i.e.

$$h_s = \left[\frac{Q_d}{B_e} \left(\frac{h_0}{h_m} \right)^{1.6026} \frac{D_{84}^{0.1026}}{5.273\ g^{0.032}\ \Delta^{0.5}\ (a_k\ \omega_{84})^{0.9936}} \right]^{\frac{1}{1.1058}} \tag{24}$$

c) Coefficient a of equation (4), known as a_k in this application, was obtained and tested with a procedure similar to that used for determining a_c. Its value is given by the following relationship:

$$a_k = \exp\left[Ln\left(\frac{q_r}{D_{84}}\right)^{0.222} + \frac{1.4 \times 10^{-8}\ Ln\ D_{84} + 1.41 \times 10^{-7}}{D_{84}^2} - 2.247 \right] \tag{25}$$

FROM MANNING'S EQUATION

Manning's formula has the advantage of taking into account other additional hydraulic losses as part of its roughness coefficient n, and not only the losses associated to the bed load friction. However, it has to be obtained with accuracy because it directly affects the evaluation of the velocity. As it is well known, Manning's equation establishes the following relationship:

$$U = \frac{1}{n} h^{2/3} S^{1/2} \tag{26}$$

When proceeding as explained for the equation of Cruickshank and Maza, the following results were obtained:

d) Distribution of the unit flow discharges through the width of the cross section:

$$q_r = \frac{Q_d}{B_e}\left(\frac{h_0}{h_m}\right)^{5/3} \tag{27}$$

e) The depth of the general scour in terms of the initial depth h_0, when a flow discharge Q_d moves through the cross sectional area:

$$d_s = \left[\frac{Q_d}{B_e}\left(\frac{h_0}{h_m}\right)^{5/3} \frac{n\, g^{0.5}}{a_m\, \omega_{84}} \right]^{6/7} \tag{28}$$

f) Coefficient a of equation (4), known as a_m in this application, was obtained and tested with a procedure similar to that used for determining a_c. Its value is given by the following relationship:

$$a_m = \exp\left[0.87 + Ln\left(\frac{n\, q_r^{0.18}}{D_{84}^{0.315}}\right) + \frac{1.4 \times 10^{-8}\ Ln\ D_{84} + 1.42 \times 10^{-7}}{D_{84}^2} \right] \tag{29}$$

Limits of applicability

Since coefficients a_k and a_m corresponding to the friction equations developed by Karim and Kennedy, and by Manning, respectively, were obtained by using the same data for determining the coefficient a_c given by equation (16), the limits of applicability of equations (24) and (28) are exactly the same as those corresponding to expression (15*a*) as indicated in equations (17) to (20).

It is necessary to take into account that there is not general scour when $h_s \le h_0$.

AVAILABLE DATA

In the first place the results obtained from the method of Lischtvan and Levediev were used although the original data from which it was developed are not known; however, such data have been accepted as valid for this work. Data derived from cross sections determined when different flow discharges passing through the rivers Mississippi, USA; Magdalena, Colombia; and Paraná and Leyes in Argentina, were made available. Since they were not specifically obtained to study the phenomenon of general scour, values of some parameters are still missing. As an example, at the Mississippi and Magdalena rivers the initial depth h_0 is not known but the mean water height of the scoured cross section, h_{ms}, was indeed available. For this reason, an assumption was made in this work, that could be valid, in the sense that $h_0 = h_m$ at the vertical where the mean scour depth is h_{ms}. Therefore in equations (15*a*), (24) and (28) it was accepted that $h_0 / h_m = 1$. It was not possible at the Paraná and Leyes rivers to find out an accurate grain size distribution curve representative of the bed load material where the maximum depth had been reached.

COMMENTS

The main comments can be summarized as follows:

1) When using equations (15*a*), (24) and (28) to obtain the depth of the general scour h_s at each vertical of the cross section it can be found that such parameter is a function of the initial depth h_0 $[h_s = f\,(h_0)]$; therefore, the scoured cross section is "*parallel*" to the initial cross section. This statement is not necessarily true because during a flood the flow might not be distributed as a function of h_0 and it may become concentrated at a certain zone of the cross section, or otherwise, zones with very low velocities are likely to exist. If this occurs, the distribution of the unit flow q_r given by equations (9), (23) and (27) is not necessarily complied with. This situation can be particularly evident at the exit of a curve when it has been subjected to lateral erosion during the flood passage.

2) The effective width B_e, when it is desired to evaluate the general scour at the riverbed section of a bridge crossing, is obtained by subtracting from the width of the free water surface the projections of the piers at a plane perpendicular to the flow direction.

3) When designing a bridge or the crossing of a pipeline under the river bed it is not required to obtain a profile of the scoured cross section but only the maximum depth of scour h_s that occurs where h_0, has its greater value. Because of the mobility of the rivers, such maximum scour is likely to occur at any zone of the cross section during the service life of the structure. It is recommended to survey several cross sections, upstream and downstream from the site where the work will be located, to obtain the maximum scour at each of them, and considering that each one is located at the site under study. The maximum scour thus obtained should be considered for the design of the structure. Only at rivers with bank protection there is an assurance that the maximum scour occurs close to the concave edge of the curves.

4) Equations (15*a*) and (24) provide nearly the same results as opposed to equation (28) that relies on the accuracy with which Manning's friction coefficient has been determined.

5) It can be observed in figure 3 that most of the depths calculated from equation (15*a*) show a difference of $\pm 10\%$ with respect to the observed values. Almost all values fall within a range of $\pm 30\%$.

6) To calculate the scouring around bridge piers and abutments, the values of h_s and of $U = q_r / h_s$ should be first calculated in order to substitute them subsequently is some equation applicable to scouring of piers or abutments.

7) When unit flow discharge is desirable to be taken into account, its application is however subordinated to the availability of such value because it is not possible to be obtained in many rivers, particularly during the passage of short-lived floods.

CONCLUSIONS

Equations (15*a*), (24) and (28) have been developed to be able to determine the general scour depth h_s, as a function of the initial water height h_0, or otherwise in terms of the unit flow discharges, provided they could be measured taking into account equations (9), (23) and (27). The equations are applicable to any cross section of the river and can be also used to calculate the scour when a constriction, either natural or artificial, exists because the actual width of the stream is taken into account in the equations. They are also used to determine the general scour occurring close to the concave edge of the curves.

The coefficient a of equations (16), (25) and (29) is bound to be corrected when sufficient data are available, particularly in the case of rivers with no sandy bed materials, because equations (15*a*), (24) and (28) were only validated for a particle size range of $0.00014 \leq D_{84} \leq 0.0069\ m$. For larger particle diameters the values obtained with the method of Lischtvan and Levediev were assumed to hold valid.

REFERENCES

1. Breusers, H.N.C., Raudkivi, A.J., 1991, "Scouring", A.A. Balkema, Rotterdam, Netherlands, pp. 37-41.
2. Brownlie, W.R., 1981, "Compilation of Alluvial Channel Data: Laboratory and Field", W.M. Keck Laboratory of Hydraulics and Water Resources, Division of Engineering and Applied Science, California Institute of Technology, Pasadena, Cal., USA, pp. 183-191.
3. Cruickshank, V., Maza-Álvarez, J.A., 1973, "Flow Resistance in Sandy Bed Channels", Proc. International Symposium on River Mechanics, IAHR, Vol. 1, pp. 337-345, Bangkok, Thailand.
4. Graf, W.H., 1993, "Fluvial Hydraulics", John Wiley and Sons, New York, USA, pp. 356.
5. Hamill, L., 1999, "Bridge Hydraulics", E and FN Spon, London, pp. 259-260.
6. Hoffmans, G.J.C.M., Verheij, H.J., 1997, "Scour Manual", A.A. Balkema, Rotterdam, Netherlands, pp. 26-29.
7. Karim, M. F., Kennedy, J.F., 1981, "Computer-Based Predictors for Sediment Discharge and Friction Factor of Alluvial Stream", Iowa Institute of Hydraulic Research, Report No. 242, University of Iowa City, Iowa, USA.
8. Karim, M. F. , Kennedy, J.F., 1990, "Menu of Couple Velocity and Sediment-Discharge Relations for Rivers", Journal of Hydraulic Engineering, ASCE, Vol. 104, No. HY7, pp 1045-1059.
9. Leopold, L.B., Wolman, M. G., Miller, J. P., 1964, "Fluvial Processes in Geomorphology", W.H. Freeman and Co., San Francisco, USA, pp. 227-241.
10. Maza-Álvarez, J.A., 1966, "Total Scour in Bridge Piers", Thesis to obtain the Master Degree in Hydraulics, National University of Mexico, pp. 4-41. Mexico City. In Spanish.
11. Maza-Álvarez, J.A., Rico-Rodríguez, A., 1970, "Contribution to the Evaluation of General Scour in Natural Channels", Proc. IV Latin American Congress of Hydraulics, IAHR, Vol. 2, pp. 214-224. Oaxtepec, Mor, Mexico. In Spanish
12. Maza-Álvarez, J.A., García-Flores, M., 1986, "Distribution of Bed Sediments in National Channels", Proc. XII Latin American Congress of Hydraulics, Vol. 3, pp. 104-109, Sao Paulo, Brasil. In Spanish.
13. Przedwojski, B., Blazejewski, R., Pilarczyk, K.W., 1995, "River Training Techniques", A.A. Balkema, Rotterdam, Netherlands, pp. 379-383.
14. Schreider, M., Scachi, G., Reynares, M., Franco, F., 1999, "Aplication of the Lischtvan-Levediev Method to Calculate the General Scour in Sandy Beds". Proc. International Congress on Hydraulic Engineering (in print), Havana, Cuba. In Spanish

FLOW ANGLE OF ATTACK AT PERPENDICULAR BRIDGE CROSSINGS

By

Marco Falcón [1] and Mauro Nalesso [2]

ABSTRACT

In this paper the formation of alternate bars, central bars, or multiple transverse bars, for flow in a straight river reach of constant width, is studied as an instability problem of the mobile bed. Once a specific, doubly periodic perturbation of the mean bed level is selected, and the governing principles, laws, and empirical friction and sediment transport relations are imposed, expressions are obtained for the bed wave celerity, rate of growth of the bed amplitude, and additionally, it is possible to estimate the longitudinal wavelength to which the maximum rate of growth corresponds, and also to determine the dominant type of bars: alternate, central or multiple.

Instead of working with a totally vertically-integrated version of the governing equations, care has been taken to solve for a three-dimensional solution of the transverse velocity component, thus avoiding the error of having to relate the transverse bed-shear with the mean transverse velocity component.

Assuming that the linearized perturbation solutions are acceptable, up to values of the ratio of bed amplitude to depth equal to one tenth, it is found that significant deviation angles of the local velocity vector (angles of attack) from the longitudinal direction exist, at certain specific locations, depending upon the type of bed deformations present. Thus it is shown that bridge piles and abutments adequately aligned with straight parallel banks, still can be subjected to locally approaching flows at significant angles of attack owing to the development of various types of sediment bars.

INTRODUCTION

Scour of rectangular-shaped bridge piles is significantly sensitive to the angle of attack of the approaching flow: a pile is generally set such that its major length is parallel to the approach-flow velocity vector (in a straight, constant-width reach, the major length would be parallel to the banks), and thus the magnitude of scour will depend upon the smaller rectangular length (width of the pile), as Laursen and Toch (1956) and Melville (1999) have reported (see figure 1). However these authors show that if for various possible reasons, the angle of the approach-flow with respect to the pile major axis deviates from

[1] Professor, Institute of Fluid Mechanics, Faculty of Engineering, Central University of Venezuela, Caracas, Venezuela.

[2] Graduate Student, Institute of Fluid Mechanics, Faculty of Engineering, Central University of Venezuela, Caracas, Venezuela.

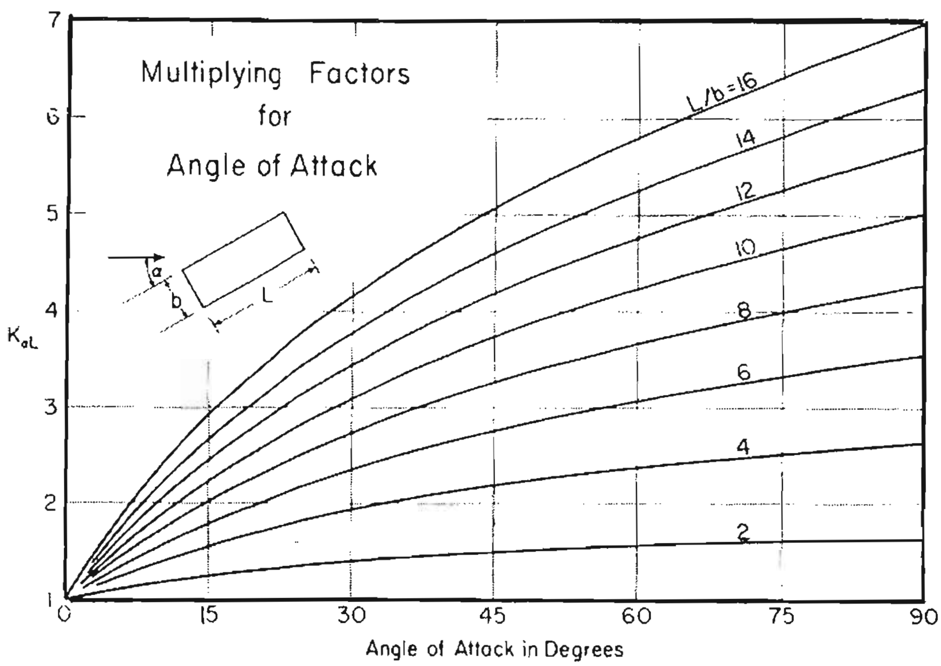

Fig. 1 Design factors for piers not aligned with flow (Laursen and Toch, 1956)

zero, the magnitude of scour can increase by a factor of up to about three times the scour calculated for zero angle of attack.

During the past two years the authors of the present paper have been studying the development of alternate, central and multiple bars, as an instability of the movable, cohesionless bed of straight channels of constant width (see figure 2). A review of the literature indicates that the vertical variation of the transverse velocity component has been simply represented by its mean, vertically-integrated value, and thus, an empirical relation between the transverse bed-shear stress and the above mean velocity, similar to an analogous relation in the longitudinal direction, is used. In the latter case the friction relation (Darcy's Law) is adequate, but not so in the transverse direction, for which incorrect magnitudes and directions of the transverse bed shear stress may be implied.

ANALYSIS

A summarized version of the analytical solution for the propagation of transverse sediment bars on the bed of an initially unperturbed, uniform, free-surface flow in a channel of constant depth d_0, constant width B, and constant longitudinal slope S_0, is presented herein.

The unperturbed forward velocity distribution is given as

$$U(Z) = U_0\left(\frac{n+1}{n}\right)\eta^{1/n}, \tag{1}$$

where U_0 is the vertical mean of U(z), $n = 1/\sqrt{f}$ is Nunner's coefficient, described by Odgaard and Kennedy (1983), f is the Darcy-Weisbach friction factor of the flow, and $\eta = z/d_o$ is a dimensionless vertical coordinate which takes the value zero at the bed and increases up to unity at the free surface.

A doubly periodic perturbation of the bed is given by

$$b(x, y, t) = b_0(t)\,\mathrm{sen}\left(\frac{2\pi}{\lambda x}(x - U_b t)\right)\cos\left(\frac{2\pi}{\lambda y}(y - \delta_{by})\right), \tag{2}$$

where $b_0(t)$ is the slowly-varying amplitude of the perturbed bed; λx and λy are the longitudinal and transverse wavelengths of the perturbation, respectively, the latter being directly determined by the width of the channel and the type of bars (for alternate bars λy=2B, for central bars λy=B and so forth); Ub is the longitudinal celerity of the perturbation and δb_y is a transverse space lag which also is determined by the type of bars selected.

At this point it is worthwhile mentioning that Ub has generally been found to be positive, so that the wave bed patterns move slowly downstream, and the positions at which the angular deviation of the velocity vector is greatest, also move downstream such that bridge piles will always be subjected, sooner or later, to the deviatory approach flow.

The free-surface of the flow is given as

$$H(x, y, t) = d_0 + a_0(t)\,\mathrm{sen}\left(\frac{2\pi}{\lambda x}(x - U_b t - \delta_{ax})\right)\cos\left(\frac{2\pi}{\lambda y}(y - \delta_{ay})\right), \tag{3}$$

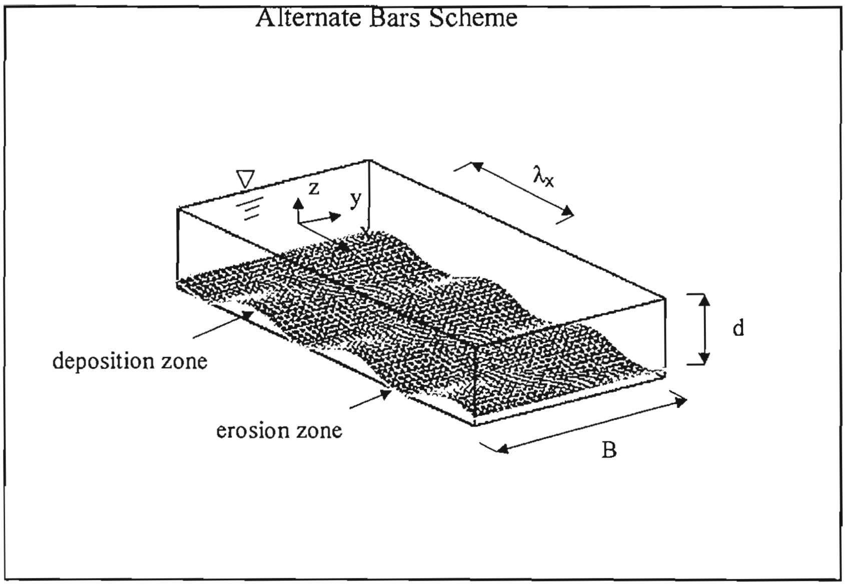

M

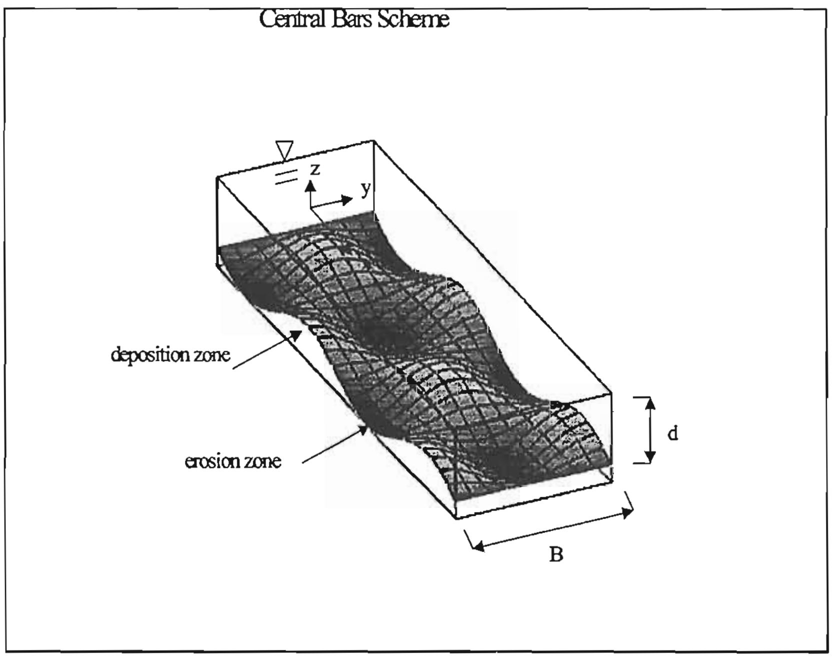

M

Fig. 2 - Bed Instabilities For a Straight Channel With Constant Depth

where $a_0(t)$ is the slowly varying amplitude of the free-surface perturbation, and δa_x and δa_y are phase lags to be determined. Note that an expression for the transverse free-surface slope, H_y', can be obtained by differentiating (3) with respect to y.

The three-dimensional mathematical structure for the transverse velocity component is

$$V(x,y,z,t) = V_0 \operatorname{sen}\left(\frac{2\pi}{\lambda x}(x - U_b t - \delta_{vx})\right)\cos\left(\frac{2\pi}{\lambda y}(y - \delta_{vy})\right) + \mu(x,y,z,t), \tag{4}$$

where V_0 is the amplitude of the mean, vertically-integrated, transverse velocity component, δv_x and δv_y are phase lags to be determined, and μ is the rotational component of V(x, y, z, t) given by (4). This means that only μ will generate transverse shear stress on horizontal planes, according to Boussinesq's turbulence model

$$\tau_{zy} \approx \rho\varepsilon\,\partial\mu/\partial z, \tag{5}$$

and in addition the boundary conditions

$$V(x,y,\eta = 0,t) = 0 \quad ; \quad \int_0^1 \mu(x,y,t,\eta)\,d\eta = 0 \tag{6}$$

are imposed (the second b.c. on μ follows from the definition of V_0), and ε is the turbulent eddy diffusion coefficient.

The transverse bed-shear stress is assumed given as

$$\tau_{0y} = \tau_{0y0} \operatorname{sen}\left(\frac{2\pi}{\lambda x}(x - U_b t - \delta_{\tau x})\right)\cos\left(\frac{2\pi}{\lambda y}(y - \delta_{\tau y})\right), \tag{7}$$

where τ_{oyo} is the amplitude of the transverse bed-shear stress, $\delta\tau_x$ and $\delta\tau_y$ are phase lags to be determined.

The eddy diffusion coefficient can be deduced from Boussinesq's model applied in the longitudinal direction, however it was found that use of an approximate model given by

$$\varepsilon(\eta) = M'U_0 d_0 \eta^{\frac{1}{4}}, \tag{8}$$

is adequate.

The complete flow and sediment bed geometry system must satisfy the following laws and principles:

1) Transverse, vertically-integrated dynamic equation:

$$H_y' + \frac{\tau_{oy}}{\gamma d_o} + \frac{1}{g}\frac{\partial}{\partial x}\left[\int_0^1 UV\,\eta\,d\eta\right] = 0, \tag{9}$$

where g is the acceleration of gravity and γ is the fluid specific weight.

2) Transverse, local dynamic equation:

$$\frac{1}{\gamma}\frac{\partial\tau_{zy}}{\partial z} = H'_y + \frac{U}{g}\frac{\partial V}{\partial x}, \tag{10}$$

3) Continuity equation for the fluid:

$$\frac{\partial}{\partial y}(Vd) = -\frac{\partial}{\partial x'}(Ud), \tag{11}$$

4) Longitudinal, vertically integrated dynamic equation:

$$\frac{\partial d}{\partial x'}\int_0^1 U^2 d\eta + d\frac{\partial}{\partial x'}\int_0^1 U^2 d\eta = -g\frac{\partial H}{\partial x'}d - \frac{\tau_{0x}}{\rho}, \tag{12}$$

5) Sediment conservation equation:

$$\frac{\partial q_{sx}}{\partial x'} + \frac{\partial q_{sy}}{\partial y} + (1-N)\frac{\partial b}{\partial t} = 0, \tag{13}$$

where x′=x-Ubt, N is the sediment deposit porosity, and qs_x and qs_y are unit, volumetric, sediment transport, bed load rates in the x and y directions, respectively, and where qs_x is given by the power law

$$q_{sx} = m\left[U(x',y) - U_{cr}\right]^P, \tag{14}$$

where m and p are empirical constants (determined for the unperturbed flow) and Ucr is the critical velocity for incipient motion of D_{50} of the bed sediment.

6) Closure condition on the sediment transport vector:

It is assumed that the direction of motion of the sediment transport is aligned with the resultant force vector, parallel to the bed, on a representative bed particle, D_{50}, and thus

$$\frac{q_{sy}}{q_{sx}} = \frac{\left[-\frac{4\pi}{3}\left(\frac{D}{2}\right)^3(\gamma_s - \gamma)\frac{\partial b}{\partial y} + \tau_{0y}\pi\left(\frac{D}{2}\right)^2\right]}{\gamma d_0 S_0 \pi\left(\frac{D}{2}\right)^2}, \tag{15}$$

where γ_s is the sediment specific weight.

The solution to the problem is obtained by inserting the variables involved and their assumed sinusoidal structures into the equations which must be satisfied.

The resulting linear system is solved by computer and thus, for any set of input variables, compute values of the vertical distribution of the transverse velocity component are given at various positions on the alternate bar or central bar systems; The downstream celerity of the bed wave system and the initial rate of growth of the bed wave amplitude is given for any previously selected value of λx. This allows determination of λx to which corresponds the maximum bed amplitude amplification, which is considered the dominant wavelength and thus an approximation to the physical result.

VERIFICATION

The theoretical results were tested with the experiments of Garcia and Niño (1993), performed in a channel 0.4m wide. A Comparison with experimental results is shown in Table I. It can be seen that the bed wave celerities are of correct order of magnitude and that the theoretical wavelengths underpredict the experimental values. It should be mentioned that the experimental bars had very large amplitudes, of the same order of the depth of flow.

Also it is noteworthy that the predicted wavelengths are very close to a well-established value (Yalin, 1991) of 6 widths, equal to 2.40m. Therefore it is possible that the

Table 1. Comparison of λx and Ub theoretical vs. García y Niño λx y Ub (1993).

		λx (m)		Ub ($x10^{-3}$) dimensionless	
Run	**So**	**García y Niño**	**Theoretical**	**García y Niño**	**Theoretical**
1	0,0056	3,60	2,25	0,66	1,71
2	0,0056	3,70	2,35	1,02	2,84
3	0,0032	3,66	2,45	0,7	0,0405

Boussinesq's Turbulent Model with variable ε

obvious non-linearity present in the cited experiments explains the discrepancy between predicted and observed wavelengths.

CALCULATIONS OF THE ANGLE OF ATTACK

The angular deviation of the flow velocity vector, (in a plane parallel to the mean free surface, at any point within the flow) with respect to the longitudinal direction is the angle of attack, α, in bridge-pile scour terminology.

It is should be emphasized in this paper that a three-dimensional calculation of the transverse velocity component was obtained from the local form of the transverse dynamic equation, together with Boussinesq's model. The results show that sometimes the transverse shear stress on the bed, and the mean transverse velocity component, Vm, are in the same direction, but, at other positions on the bed wave pattern, these quantities occur in opposite directions. Therefore it does not seem convenient, as is practically done in all vertically integrated models of bar formation, to assume a quadratic law for

$$\tau_{oy} = C_f \rho Vm^2$$

where C_f is constant (taken from an analogous law for the longitudinal bed shear stress) because it assumes that τ_{oy} and Vm are always in the same direction.

By assuming that the linearized theory is valid for values of b_0/d_0 up to 1/10, the vertical distribution of $\alpha(\eta)$ for a typical case is presented in Tables 2 and 3 for alternate bars, and Tables 4 and 5 for central bars. The indicated values of λx are those to which correspond maximum rates of growth of the amplitude. For alternate bars the vertical distribution of the deviatory angle, α (i.e. the angle of attack) is calculated at x′= 0 (null transverse bed slope) and x′= lx/4 (maximum transverse bed slope), along the central longitudinal axis (y = 0). It can be seen that within 30% of the depth, from the bottom, significant values of the angle of attack are achieved. A similar conclusion is reached for the case of central bars at locations that are B/4 away from the banks. It should be noticed that the worst possible cases (x′= $\lambda x/4$) will always reach the piles because of the downstream motion of the bars.

B(m)	d(m)	λx (m)	So (m/m)	D50 (mm)
40	2	220	0.001	0.53

x= 0 ;   y= 0

η	V(η) (m/s)	U(η) (m/s)	α(η)
0	0.00	0.00	0.00
0.1	-0.37	2.27	9.16
0.2	-0.72	2.51	16.00
0.3	-1.04	2.66	21.37
0.4	-1.32	2.78	25.43
0.5	-1.55	2.87	28.35
0.6	-1.72	2.94	30.27
0.7	-1.84	3.01	31.37
0.8	-1.90	3.07	31.80
0.9	-1.93	3.12	31.35
1.0	-1.94	3.17	31.43

x= λx/4 ;   y= 0

η	V(η) (m/s)	U(η) (m/s)	α(η)
0	0.00	0.00	0.00
0.1	-0.45	2.30	11.17
0.2	-1.01	2.55	21.60
0.3	-1.57	2.70	30.18
0.4	-2.07	2.81	36.32
0.5	-2.45	2.90	40.16
0.6	-2.69	2.98	42.10
0.7	-2.80	3.05	42.45
0.8	-2.79	3.11	41.93
0.9	-2.73	3.16	40.86
1.0	-2.72	3.21	40.23

Table 2- Attack Angle for Alternate Bars (case 1)

B(m)	d(m)	λx (m)	So (m/m)	D50 (mm)
40	2	235	0.0001	0.53

x= 0 ; y= 0

η	V(η) (m/s)	U(η) (m/s)	α(η)
0	0.00	0.00	0.00
0.1	-0.27	0.72	20.50
0.2	-0.34	0.80	23.20
0.3	-0.41	0.84	25.73
0.4	-0.46	0.88	27.77
0.5	-0.51	0.91	29.27
0.6	-0.54	0.93	30.24
0.7	-0.57	0.95	30.74
0.8	-0.58	0.97	30.83
0.9	-0.58	0.99	30.63
1.0	-0.59	1.00	30.29

x= λx/4 ; y= 0

η	V(η) (m/s)	U(η) (m/s)	α(η)
0	0.00	0.00	0.00
0.1	0.17	0.72	13.39
0.2	0.00	0.80	0.10
0.3	-0.16	0.84	10.77
0.4	-0.30	0.88	18.75
0.5	-0.41	0.91	24.35
0.6	-0.50	0.93	27.98
0.7	-0.55	0.95	30.06
0.8	-0.58	0.97	30.98
0.9	-0.60	0.99	31.10
1.0	-0.60	1.00	30.85

Table 3- Attack Angle for Alternate Bars (case 2)

B(m)	d(m)	λx (m)	So (m/m)	D50 (mm)
40	2	240	0.001	0.53

x=0; y= 10

η	$V(\eta)$ (m/s)	$U(\eta)$ (m/s)	$\alpha(\eta)$
0	0.00	0.00	0.00
0.1	0.09	2.03	2.42
0.2	0.17	2.24	4.26
0.3	0.24	2.37	5.80
0.4	0.30	2.47	7.03
0.5	0.36	2.55	7.96
0.6	0.40	2.62	8.60
0.7	0.42	2.68	8.97
0.8	0.44	2.73	9.12
0.9	0.45	2.78	9.10
1.0	0.45	2.82	8.99

x= $\lambda x/4$; y= 10

η	$V(\eta)$ (m/s)	$U(\eta)$ (m/s)	$\alpha(\eta)$
0	0.00	0.00	0.00
0.1	0.22	2.03	6.20
0.2	0.42	2.24	10.71
0.3	0.61	2.37	14.39
0.4	0.77	2.47	17.26
0.5	0.90	2.55	19.39
0.6	1.00	2.62	20.82
0.7	1.06	2.68	21.65
0.8	1.10	2.73	21.98
0.9	1.12	2.78	21.94
1.0	1.12	2.82	21.69

Table 4- Attack Angle for Central Bars (case 1)

B(m)	d(m)	λx (m)	So (m/m)	D50 (mm)
40	2	255	0.0001	0.53

x=0 ; y=10

η	V(η) (m/s)	U(η) (m/s)	α(η)
0	0.00	0.00	0.00
0.1	0.11	0.71	9.08
0.2	0.21	0.79	15.17
0.3	0.30	0.83	20.02
0.4	0.38	0.87	23.74
0.5	0.45	0.90	26.41
0.6	0.49	0.92	28.17
0.7	0.52	0.94	29.16
0.8	0.54	0.96	29.52
0.9	0.55	0.98	29.43
1.0	0.55	0.99	29.12

x= λx/4 ; y= 10

η	V(η) (m/s)	U(η) (m/s)	α(η)
0	0.00	0.00	0.00
0.1	0.11	0.71	8.72
0.2	0.22	0.79	15.64
0.3	0.32	0.83	21.13
0.4	0.83	0.87	43.76
0.5	-0.48	0.90	28.28
0.6	-0.54	0.92	30.23
0.7	-0.57	0.94	31.33
0.8	-0.59	0.96	31.73
0.9	-0.60	0.98	31.66
1.0	-0.60	0.99	31.36

Table 5- Attack Angle for Central Bars (case 2)

The present model can be used to test which type of bars will be dominant for given flows conditions. As the width/depth ratio increases it correctly predicts a tendency from alternate bars towards central and multiple bars. The results indicate that if alternate bars are present, angles of attack at mid width (at the channel center) will be greatest; if central bars are dominant, then the largest angles of attack would occur at B/4 from the banks.

In some torrential flows alternate and central bars occur simultaneously (Furbish, 1998). Field research regarding the superposition characteristic should be considered.

In conclusion, straight-approach flows towards bridge structures are scarce and it would appear to be worthwhile to take field data upstream of the bridge site in order to check natural deviation angles of the velocity vector for design purposes.

REFERENCES

1. Laursen E. M., Toch A., 1956, "Scour Around Bridge Piers And Abutments," Iowa Highway Research Board, Bulletin N°4, Iowa Institute of Hydraulic Research, State University of Iowa, Iowa, USA.
2. Furbish D. J., 1998, "Irregular Bed Forms In Steep, Rough Channels," *Water Resources Research*, Vol. 34, No. 12, December, 1998, pp 3635-3648.
3. Melville B. W., 1995, "Pier And Abutment Scour: Integrated Approach," *Journal of Hydraulic Engineering,* Vol. 123, No. 2, February, 1997, pp 125-136, ASCE, New York, N.Y., USA.
4. Yalin M. S., Silva A. M. F., 1991, "On The Formation Of Alternate Bars," Euromech 262, Balkema, Rotterdam, 1991.
5. González, N., Nalesso, M., 1998, "Análisis de la Formación de Islas Fluviales Centrales," Degree Dissertation, Universidad Metropolitana, Caracas, Venezuela.
6. Garcia, M., Niño, Y., 1994, "Dynamics of Sediment Bars In Straight And Meandering Channels: Experiments On The Resonance Phenomenon," *Journal of Hydraulic Research*, Vol. 31, No. 6, 1993.

PREDICTING THE MAGNITUDE AND POSITION OF MAXIMUM SCOUR DEPTH DOWNSTREAM OF CULVERT OUTLETS USING ARTIFICIAL NEURAL NETWORKS

By

S. L. Liriano[1] and R. A. Day[2]

ABSTRACT

Prolonged scouring downstream of culvert outlets can eventually lead to collapse of the outlet and damage to the infrastructure above, typically a highway or railway. Knowledge of the position and extent of scouring during the design stage can enable engineers to reduce the potential scouring capacity at the outlet or design effective bed and bank protective measures to mitigate erosion. The depth of scour at the outlet is currently predicted using empirical equations with different equations being appropriate to different culvert shapes, sediment properties and hydraulic conditions. A small number of research programmes have also led to equations for predicting the location of maximum scour depth, however these are often dependant on a prior knowledge of the total scour length or depth. Engineers need a model that is applicable to all conditions. This paper reports the results of a preliminary study looking at the use of artificial neural networks (ANN) to predict the maximum depth of scour and the location of this maximum scour depth downstream of culvert outlets. The results obtained from the ANN are compared with empirical equations and show that a prediction of better or at the very least equal reliability to the empirical equations can easily be obtained for maximum scour depth. For the position of maximum scour depth the results from the ANN also fall within +/-15% of the measured results however it is not possible to compare the ANN with previous formulae for predicting the location of maximum scour depth.

INTRODUCTION

Hydraulic structures, such as culverts are necessary features of all waterways in urban, semi-urban and rural areas. They are often provided for drainage and water level control, allowing the land above to be developed, however most have an adverse impact on the river level itself through local scouring. In particular excessive scouring downstream of culverts can lead to the culvert being undermined and the infrastructure that it protects collapsing, causing both environmental and economical problems.

Engineers, utility and infrastructure managers, planners and environmentalists need models to assist in quantifying the effects that these structures have on the morphology of river

[1] Post-Doctoral Research Assistant, Water Engineering Research Group, University of Hertfordshire, Hatfield, Herts, UK, AL10 9AB.
[2] Senior Lecturer, Water Engineering Research Group, University of Hertfordshire, Hatfield, Herts, UK, AL10 9AB.

channels. In particular models need to be quick and robust to ensure that rapid decision-making can take place and offer the opportunity for real-time predictions. Mathematical algorithms for modelling precisely the size and extent of scouring are still some way off and current practise is to use empirical models to make these judgements. The empirical models are frequently improperly used with field conditions falling outside the scope of the particular empirical model since there are many of these, each with different ranges of applicability.

This paper describes the development of a basic feed forward artificial neural network trained by back-propagation to model scour downstream of culvert outlets. This model has been developed using data collected by the authors on a recent EPSRC research project grant number GR/L15296. Using ANN's to predict scouring downstream of outlets is an extension of the original experimental work and some success has been achieved to date.

BACKGROUND

Scouring downstream of culvert outlets has been the subject of a number of experimental research programmes. Studies such as those by Abida and Townsend (1991), Blaisdell and Anderson (1988), Lim (1995), Lim and Chiew (1996), Opie (1967), Rajaratnam (1981), Rajaratnam et al. (1977, 1983), Ruff et al. (1982) and others have resulted in a selection of empirical equations for predicting scour depth, and in some cases length, for particular hydraulic conditions. The design engineer is therefore presented with a range of equations and has the responsibility to select the appropriate equation for the particular hydraulic and sedimentary conditions. This presents a particular problem since in general culverts operate under a range of conditions and are most likely to fail when operating under abnormal conditions that may not have been represented by the original scour equations. Therefore a generic model is required that allows for more flexible conditions to be considered and can give a real-time estimate of the scour depth that may be expected when adverse weather conditions prevail.

Abida and Townsend (1991), Chatterjee et al. (1994) and Lim et al. (1995) all give expressions for the location of the maximum scour depth. In each case this location is found to be a function of the scour hole dimensions, either maximum length of scour or maximum volume of scour, and therefore the design engineer first requires some estimation of these parameters.

ARTIFICIAL NEURAL NETWORKS

Interest in Artificial Neural Networks has grown rapidly over the past decade and ANNs are being applied to an extraordinary range of problems in areas as diverse as finance, medicine, engineering and physics. ANN techniques were inspired by a desire to understand the method by which the human brain learns and the development of Artificial Intelligence. The paper Artificial Neural Networks in Hydrology, I:Preliminary Concepts by the ASCE Task Committee on Application of Artificial Neural Networks in Hydrology (Rao, 2000) gives a good introduction of the subject without exploring too deeply the mathematical algorithms and computing terminology.

Artificial neural networks offer significant advantages over existing mathematical models for such problems. Since the ANN learns from the training set it is able to take into account the hidden effects and trends in the data without requiring a complete understanding of the science of the problem. This can also be considered a disadvantage of such techniques, however in areas such as sediment transport and turbulent flow, such as downstream of a culvert outlet, where solutions to the governing equations are not well defined a technique that is not reliant on understanding can be advantageous.

Some use has been made of artificial neural networks in the more general area of sediment transport, Trent et al. (1993). ANN have been applied to scouring at bridge piers by Trent et al. (1993) and it was found using 515 field measurements of scouring split into training and testing data, that ANN's improved upon the predictions of empirical equations.

THE MODEL

A feed-forward artificial neural network trained by back-propagation is used in this study, this is illustrated in figure 1. The nodes are arranged in layers with an input layer where the casual variables are fed into the ANN and a single output layer with a number of hidden layers in-between. For predicting maximum scour depth 12 hidden layers have been used, for the position of maximum scour depth there are 9 hidden layers, the number of hidden layers for the optimum result has been determined by trial and error. The hidden layers each consist of 7 nodes, equal to the number of input nodes determined from dimensionless analysis. The output layer consists of the values predicted by the ANN for either the maximum scour depth or the location of the maximum scour depth and represents the model output. Each node in the hidden layer and the output layer uses the sigmoid transfer function.

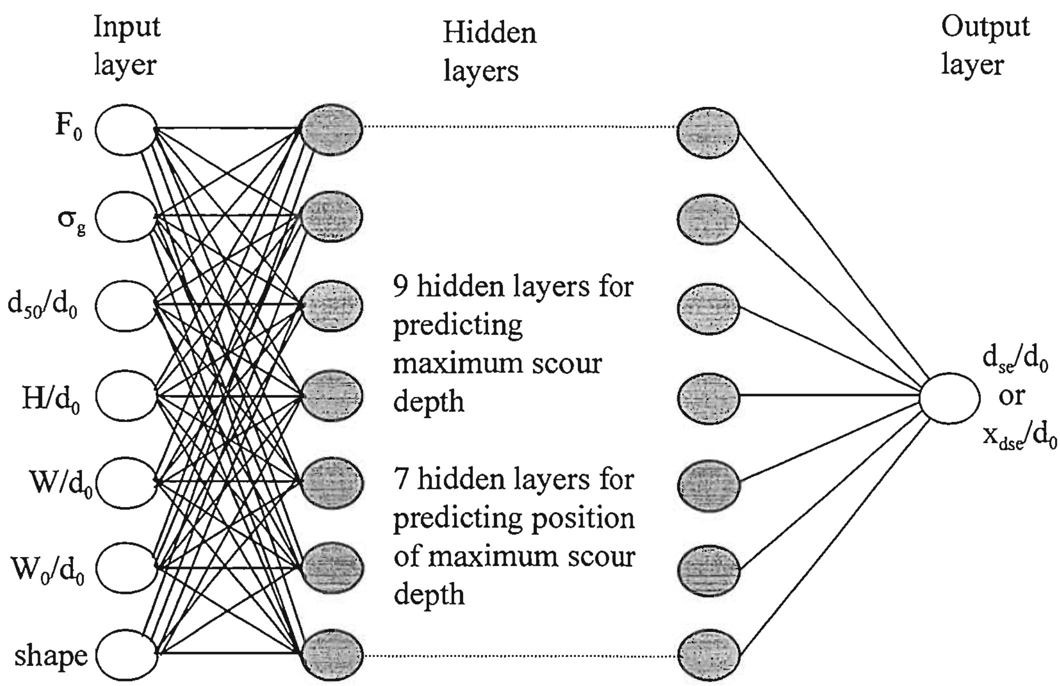

Fig. 1 Artificial Neural Network Model, symbols defined in the next section.

The network requires the data set to be divided into 3 categories; a training set, a testing set and a validating set. Both the training and the testing sets are used in training the network. The validation set consists of 'unseen' data that has not been used in the training of the network.

Using back propagation the network learns through an iterative procedure involving two steps performed many times. First the network is shown examples of the data which pass forward to the output layer then the error in the output is computed and the second step starts backward through the network. The errors at the output layer are propagated backward through the network and the weights adjusted to minimise the error in the output data. Using this technique it is possible for the network to become trapped in a local minima and for this reason a supervised training is used. After the training data has been presented to the network a pre-determined number of times a test data set is presented and the performance of the network with the training and test data sets is compared. The result from the previous presentation of the test data is compared and if there has been an improvement the network continues training. If there is no improvement the cycle of presenting training and testing data continues until no improvement has been seen with the test data in 30 consecutive attempts. At this point training is terminated and the weights set to those from which the best result was obtained with the tests data. This prevents the network over-learning the training data by checking the performance with the test data and reduces the likelihood of the network reaching a local minimum as opposed to the global minima by continuing training for 30 cycles after a minimum error has been achieved.

Once the network has been trained a further validating set of data not used previously is presented to the network and the output from the ANN compared with the known output in order to assess the predictive capabilities of the network.

VARIABLES FOR DETERMINING SCOUR PARAMETERS

Scour depth is dependant on many variables that can be grouped in general to describe the physical properties of the outlet and receiving channel, the bed material and the flow characteristics. These can be listed as

$$d_{se} \text{ or } x_{dse} = f(\rho, \mu, u_0, d_0, H, W, W_0, g, \rho_s, d_{50}, \sigma_g, \text{shape}) \qquad (1)$$

where d_{se} is the maximum depth of scour, x_{dse} is the location of the maximum scour depth, ρ is the density of water, μ is the dynamic viscosity of water, u_0 is the mean velocity at the outlet, d_0 is the pipe diameter for circular outlets and outlet height for non-circular outlets, H is the depth of water in the downstream receiving channel (tailwater depth), W is the width of the receiving channel, W_0 is the width of the outlet, g is the acceleration due to gravity, ρ_s is the density of the sediment bed material, d_{50} is the median sediment size σ_g is the geometric standard deviation of the sediment bed material and describes how graded the material is, shape is the shape of the outlet.

Given that the flow is turbulent in each case and assuming that the viscous effect is not important a dimensional analysis of (1) gives

$$\frac{d_{se}}{d_0} \text{ or } \frac{x_{dse}}{d_0} = f\left(F_0, \frac{H}{d_0}, \frac{W}{d_0}, \frac{W_0}{d_0}, \frac{d_{50}}{d_0}, \sigma_g, \text{shape} \right) \tag{2}$$

where $F_0=u_0/[(S-1)gd_{50}]^{0.5}$ is the densimetric Froude number and $S=\rho_s/\rho$ is the specific gravity of the sediment. Physically F_0 represents the ratio of the tractive force acting on the individual sediment grain to the submerged weight retaining the grain in place. Empirical equations are typically a function of densimetric Froude number only and are applicable over a limited range of parameters only. The ratio of the outlet width to outlet depth and the channel width to outlet depth are both included, as the former is a function of the outlet shape whilst the amount of jet expansion at the outlet is related to the later.

The data for the ANN consists of all the variables in (2) above. The epoch size has been set to 6 and training terminates either after 30 consecutive failures to improve the prediction from the test data or after 65000 epochs. The test data is presented to the network at 200 epoch intervals.

DATASET

The data-set used in this study consists of the authors original data in addition to data kindly made available by Dr S.Y. Lim (Assoc. Prof. Nangyang Technical University, Singapore), Mr. F. Ade (formerly the University of Alberta, Canada) and Dr T.R. Opie (formerly Colorado State University, USA). Further data has been added from published data sets from Abida and Townsend (1991), Ali and Lim (1986), Rajaratnam (1981), Rajaratnam and Berry (1977), Rajaratnam and MacDougall (1983) and Ruff et al. (1982). Table 1 shows the data sets used, the number of results included and the hydraulic conditions and sediments used in the respective experiments. It can be noted from the table below that the distribution of the data is not uniform across all variables. In particular there is less data on rectangular and square outlets than on round outlets and very little data on graded sediments. The distribution of submergence ratio (tailwater depth to outlet diameter or height) data is uneven with a cluster of data in the range 0 – 3.0 and then additional data at much greater submergence ratios, up to 107.

Table 1. Experimental data used in ANN.

Researchers	Culvert shape	Vertical dimension of jet	Sediment uniformity	F_0	Submergence ratio	No. of results
Abida and Townsend	Rectangular	76mm	Uniform and graded	0.44 - 11.44	0.14 – 1.55	20
Ade and Rajaratnam	Circular	5mm, 19mm, 25.4mm	Uniform	6.29 – 88.2	0.75, 25, 124	12
Aderibigbe and Rajaratnam	Circular	5mm, 14mm, 25.4mm	Uniform and graded	2.79 – 29.46	12, 21, 60	31
Ali and Lim	Square	51mm	Uniform	4.17	0.49	4
Lim	Circular	15mm, 26mm	Uniform	1.91 – 24.6	0.47	16
Liriano	Circular	20mm, 52mm, 146mm, 311mm	Uniform	2.2 – 9.0	0.5 – 3.0	50
Opie	Circular	309mm, 442mm, 914mm	Uniform	0.38 – 3.8	0.29 – 1.1	21
Rajaratnam	Circular	3.6mm, 6.6mm, 24.9mm	Uniform	4.4 – 14.1	15, 58, 107	14
Rajaratnam and Berry	Circular	25.4mm	Uniform	8.6 – 12.4	24	4
Rajaratnam and MacDougall	Rectangular	6.4mm, 12.7mm, 23.3mm, 33.3mm	Uniform	4.3 – 18.3	1.0	12
Ruff et al.	Circular and Square	102mm	Uniform and graded	5.5 – 33.7	0, 0.25, 0.45	55

In total 239 results were available for predicting maximum scour depth and 175 for predicting the location of the maximum scour depth. The data from Ruff et al. (1985) did not include information on the location of the maximum scour depth and this information was also not available for 8 results from Abida and Townsend (1991) and 1 result from Aderibigbe and Rajaratnam (1998). Table 2 below shows the division of the data into training, testing and validating sets.

Table 2. Division of data into training, testing and validating sets.

	Training data	Testing data	Validating data
Scour depth	186	26	27
Location of scour depth	130	18	27

RESULT OF TRAINING FOR SCOUR DEPTH

From the trained network the densimetric Froude number is considered to be the most significant variable for predicting scour depth. This is also the conclusion of several experimental studies (Rajaratnam and Berry, 1977, Blaisdell and Anderson, 1988, Lim, 1995). The effect of removing densimetric Froude number from the set of variables had a 4 times larger effect than that of removing the next most significant variable. Outlet shape was found to be the next most significant closely followed by width of the receiving channel and width of the culvert outlet. The sediment size, sediment gradation and tailwater depth were found make only a slight difference to the overall prediction of scour depth when they were removed from the input variables.

Studies that have explored outlet shape have reported that shape is a significant factor and that the scour depth can vary by up to 40% depending on the shape of the outlet (Abt et al. 1984). The effect of tailwater depth has received some attention experimentally however the effect of tailwater depth is still a point of debate. For low tailwater depths it is considered that there is an effect on the depth of scour. The tailwater depths in the dataset cover a large range and therefore the overall result shows the tailwater depth to be insignificant. A different result may be obtained if the input data was restricted to a smaller range of tailwater depths.

VALIDATION OF ANN

Figure 2 below shows a comparison of the measured scour depth and that predicted by the trained network using previously unseen data and shows good agreement. The test data set in this case includes some of the authors' experimental data and data from 3 previously published studies by other researchers.

It can be clearly seen that the artificial neural network is successfully predicting the scour depth to with +/- 15% in most cases.

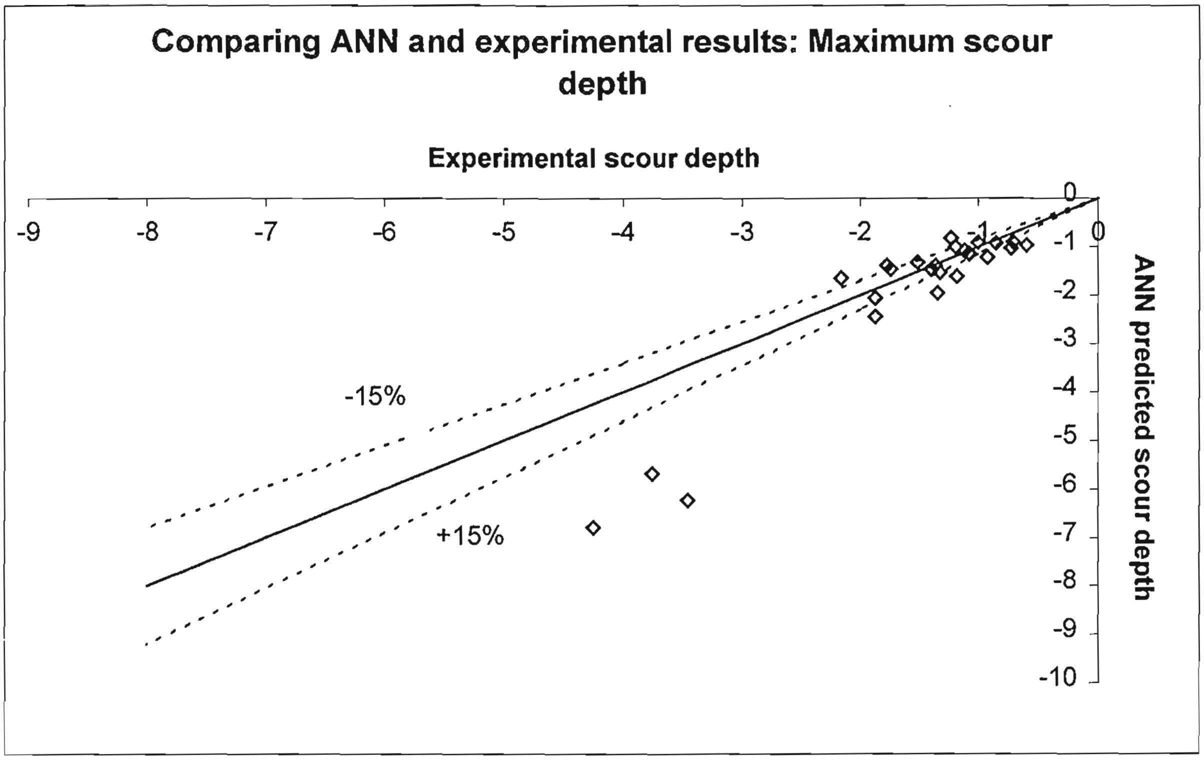

Fig. 2 Comparison of the ANN results and the experimental results for data not seen during network training.

COMPARISON OF ANN AND EXISTING EMPERICAL MODELS

Figure 3 shows a comparison of the predicted and experimental results obtained by applying the models of Lim (1995), Chiew and Lim (1996), Abt et al. (1994) and Liriano (1999). Each model is only applied to the selection of the validation data which is included in the range over which the equation is applicable, as shown below. This immediately illustrates the difficulty engineers may have in comparing different flow conditions or outlet shapes where different equations may need to be applied. The ANN is applicable to all the cases. In general the empirical equations show a poorer fit to the experimental data than the ANN with data being both under and over-predicted.

The equations used were:

Lim (1995)	$d_{se}/d_0=0.45F_0$ $d_{se}/d_0=0.45$	$1<F_0<10$, $H<1.0d_0$, $\sigma_g<2.0$, $F_0>10$, $H<1.0d_0$, $\sigma_g<2.0$,
Liriano (1999)	$d_{se}/d_0=a\ln(F_0)+b$ where: $a=0.877(H/d_0)^{-0.37}$ and $b=0.20\ln(H/d_0)-0.24$	$3<F_0<9$, $0.5d_0<H<2.0d_0$, $\sigma_g<2.0$, circular outlets
Chiew & Lim (1996)	$d_{se}/d_0=0.21F_0$	$H>>1$, $4.8<F_0<85.3$, $H>>1.0d_0$, circular outlets
Abt et al. (1984)	$d_{se}/d_0=-3.67(F_0^{0.57}d_{50}^{0.4}\sigma_g^{-0.4})$	circular outlets

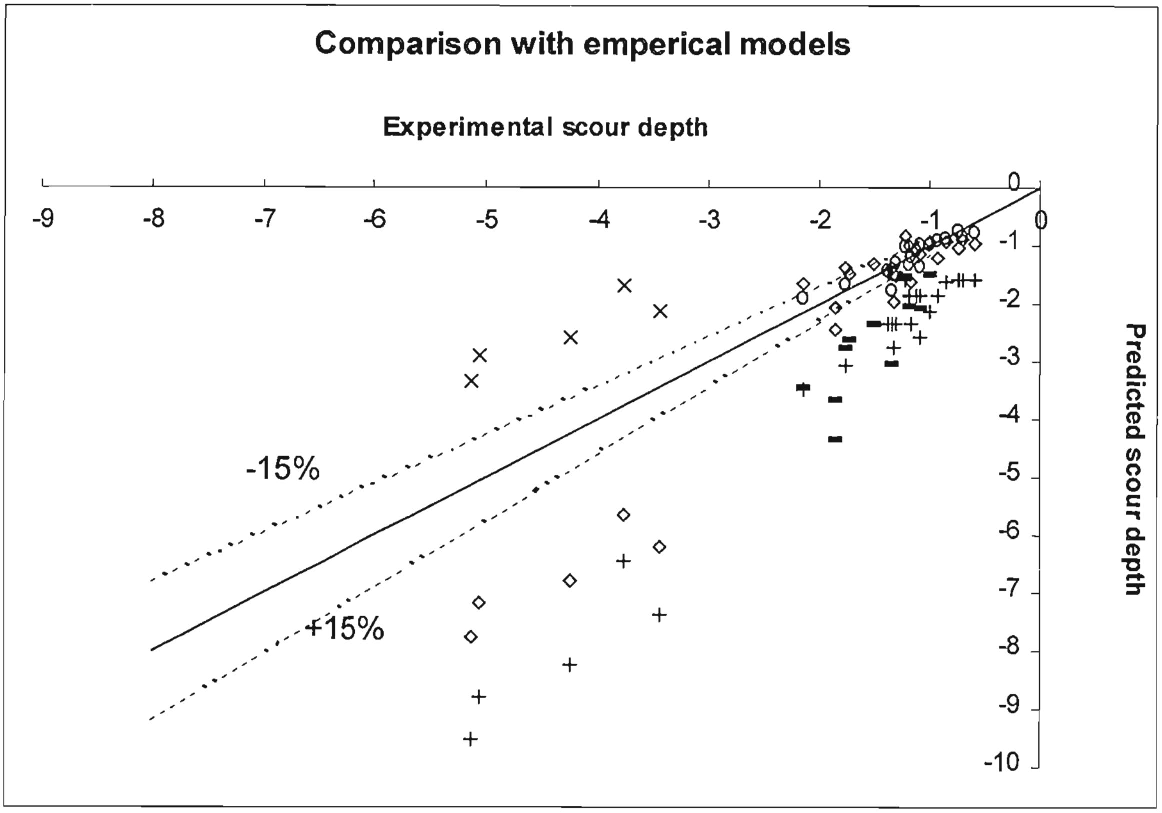

Fig. 3 Comparison with empirical models from previous research. ↓= ANN, - = Lim, o = Liriano, x = Chiew and Lim and + = Abt et al.

RESULTS OF TRAINING FOR PREDICTING LOCATION OF SCOUR DEPTH

For predicting the location of the maximum scour depth 9 hidden layers were used. This was found to give the best prediction of the location of maximum scour depth by trial and error. When less than 6 hidden layers were used the ANN failed to accurately predict the location of the maximum scour depth for the rectangular shaped outlets used in validation. The most significant variable for predicting the location of the maximum scour depth was the ratio of the culvert width to the culvert depth. For circular and square outlets this ratio is 1 but for rectangular outlets this ratio is more important varying up to the channel width. The next most significant variable was the densimetric Froude number followed by the ratio of the channel width to the culvert width. The ANN therefore finds the downstream channel dimensions and spread across the width of the outlet more significant for predicting the location of the scour depth than the magnitude of the scour depth. Ruff et al. (1985) noted that the flow from square outlets dispersed more than that from round areas and impacted over a wider area than the more concentrated jet from the circular outlet which may reinforce the findings from the ANN analysis.

VALIDATION OF ANN FOR PREDICTING THE LOCATION OF MAXIMUM SCOUR DEPTH

Figure 4 below shows a comparison of the measured location of maximum scour depth and the location predicted by the ANN. The same data set is used as for the prediction of maximum scour depth and again it can be seen that most of the results fall within +/- 15%.

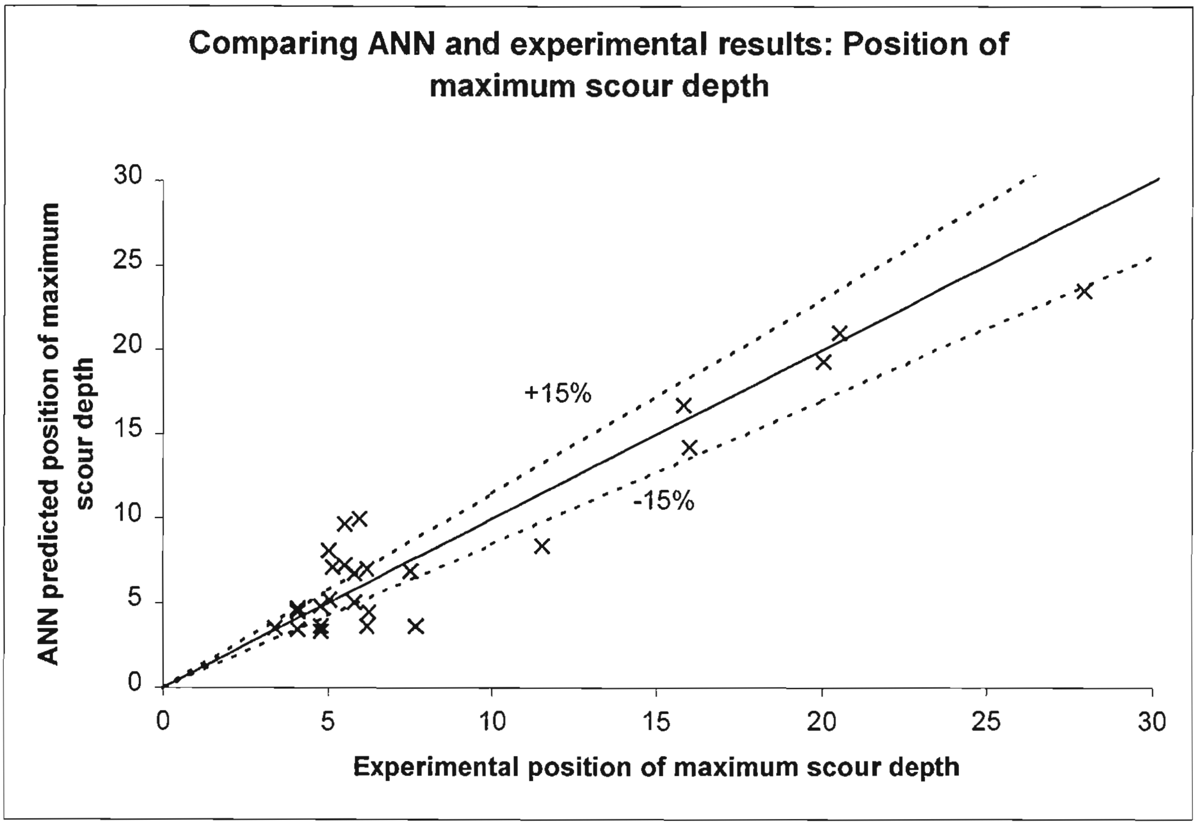

Fig. 4 Comparison of predicted and experimental results for data not seen during training of the ANN for position of maximum scour depth.

It is not possible to compare this result with previous work because the equations that have been published relate to scour length normalised by maximum scour length, which has not included in this work so far.

CONCLUSIONS

The aim of this research was to determine whether maximum scour depth and the location of maximum scour depth could be reliably determined using Artificial Neural Networks. A database of 239 scour depth readings and 175 location of scour depth readings has been compiled and two neural networks constructed. The results of the trained network compare well with the experimental results for unseen data and the following conclusions can be drawn:

1. Scour depth and the location of maximum scour depth can be predicted using ANNs
2. In many cases scour depth and the location of maximum scour depth are predicted to +/-15% of the experimental results
3. Prediction of maximum scour depth using an ANN is of equal or better reliability than using current empirical equations
4. Further experimental work is required to provide a full set of results for neural network analysis, particularly work on graded sediments and culvert outlet shapes other than circular. Further work on the effect of tailwater depth may also be beneficial.

The application of artificial neural networks to scouring shows the potential to lead to a flexible tool for engineers however the lack of experimental data available at the present time limits the model. Artificial neural networks have the advantage of being applicable to a wider range of hydraulic conditions than traditional empirical models removing the requirement of the designer to choose the appropriate equation for the anticipated hydraulic conditions. Further work is required to provide a complete data set to train the network and validate it usefulness.

REFERENCES

1. Abida H. and Townsend R.D. (1991). "Local scour downstream of box-culvert outlets." *J. of Irrigation and Drainage Eng.* ASCE. Vol 117. May/June 1991 pp425-440.
2. Abt S.R., Kloberdanz R.L. and Mendoza C. (1984). "Unified culvert scour determination." *J. of Hydr Eng.* ASCE. Vol 110. Oct 1984 pp1475-1479.
3. Ade F. and Rajaratnam N. (1998). "Generalised study of erosion by circular horizontal turbulent jets." *J. of Hydr Res.* IAHR. Vol 36 pt 4. April 1995 pp613-635.
4. Aderibigbe O. and Rajaratnam N. (1998). "Effect of sediment gradation on erosion by plane turbulent wall jets." *J. of Hydr Eng.* Vol 124 pt10 Oct 1998 pp1034-1042.
5. Ali K.H.M. and Lim S.Y. (1986). "Local scour caused by submerged wall jets." *Proc. Inst of Civ Engrs.* Vol 81 pt 2 Dec 1986 pp607-645.
6. Blaisdell F.W. and Anderson C.L. (1988). "A comprehensive generalised study of scour at cantilevered pipe outlets." *J. of Hydr Res.* Vol 26 pt4 April 1988 pp357-376.
7. Chatterjee S.S., Ghosh S.N. and Chatterjee M. (1994). "Local scour due to submerged horizontal jet". *J. of Hydr Eng.* Vol 120 pt8 Aug 1994 pp973-992.
8. Chiew Y.M. and Lim S.Y. (1996). "Local scour by a deeply submerged horizontal circular jet." *J. of Hydr Eng.* ASCE. Vol 122 Sept 1996 pp529-532.
9. Lim S.Y. (1995). "Scour below unsubmerged full flowing culvert outlets." *Proc. Inst of Civil Engrs Water, Maritime and Energy.* Vol 112 pt2. June 1995 pp136-149.
10. Liriano S.L. (1999) "The influence of near-bed turbulent bursting structures on scour downstream of pipe culvert outlets". PhD Thesis, University of Hertfordshire, Hatfield, UK.
11. Opie T.R. (1967). "Scour at culvert outlets." MSc Thesis, Colorado State Univ., Fort Collins, Colorado, extract only.
12. Rajaratnam N. (1981). "Erosion by plane turbulent wall jets." *J. of Hydr Res.* IAHR Vol 19 pt4 April 1981 pp339-358.
13. Rajaratnam N. and Berry B. (1977). "Erosion by circular turbulent wall jets." *J. of Hydr Res.* IAHR Vol.15 pt3 Mar 1983. pp277-289.
14. Rajaratnam N. and MacDougall R.K. (1983). "Erosion by plane wall jets with minimum tailwater." *J. of Hydr Eng.* ASCE. Vol. 109 no.7 July 1983 pp1061-1064.
15. Rao S.G. (2000). "Artificial Neural Networks in Hydrology I: Preliminary Concepts." *J. of Hydrologic Eng.* ASCE. Vol 5 No. 2 April 2000 pp115-123.
16. Ruff J.R., Abt S.R., Mendoza C, Shaikh A. and Kloberdanz R. (1982) "Scour at culvert outlets in mixed bed materials." Colorado State Univ. Engineering Research Centre Report no. FHWA/RD – 82/011. Fort Collins, Colorado. Sept 1982.
17. Trent R., Gagarin N. and Rhodes J. (1993). "Estimating pier scour with artificial neural networks." *Hydraulic Engineering '93*, San Francisco, California 25-30 July 1993. pp1043-1049.

18. Trent R., Molinas A. and Gagarin N. (1993). "An artificial neural network for computing sediment transport." *Hydraulic Engineering '93*, San Francisco, California 25-30 July 1993 1049-1054.

SOME ASPECTS OF THE ARGENTINE EXPERIENCE ON LOCAL SCOUR

By

Raúl Antonio Lopardo[1]

ABSTRACT

This paper deals on three different subjects, as examples of the contribution of Argentine research on local scour: local scour at bridge piers, local scour downstream ski jump structures and local scour downstream hydraulic jump energy dissipators.

Firtly, the proposal of Cotta and Jensen to avoid the local scour at bridge piers, developed at the sixties in La Plata National University. The practical results were published in the Latin American Congress of the IAHR in Spanish. It has good diffusion in South America, as it was included in the Bridge Design Manual of Venezuela.

Secondly, the INCYTH equation for local scour downstream flip buckets, intentionally oversimplified in order to be of use as an initial estimate of scour. It requires only the knowledge of the unit discharge and the fall height from the reservoir level to tailwater level. It should be noted that during the design stage many parameters are usually unknown, such as the size of blocks formed by fracture of the rock at different depths near the jet impact. For preliminary calculations, this equation demonstrates acceptable performance for the data of other authors, even with data published later than its formulation.

Finally, the phenomenon of local erosion downstream of hydraulic jump energy dissipators in large flatland dams, when rocks submitted to severe pressure fluctuations compose the riverbed, which is well different of the case customarily studied in alluvial bed rivers. This problem was analyzed by means of results of fluctuating pressures (statistic values of amplitudes and frequencies) in the base of a hydraulic jump stilling basin, downstream a continuous end sill, taking into account the amplification of the process and the trend to induce important depressions. When granular materials compose the bed, the presence of the end sill collaborates with a controlled scour downstream near the structure. If large rocks compose the bed, prototype experimental data demonstrates that the end sill has not a beneficial action. It increases flow fluctuations and concentrates the turbulent energy around a dominant frequency, removing bigger blocks and favoring local scour. A methodology is proposed for the calculation of the weight of eventual protecting blocks or the anchorage bars to avoid the removal, taking into account the incident Froude Number of the jump and the relationship among broad and length of the block.

INTRODUCTION

As it is usual in other countries, more than 50% of the bridge failures in Argentina were caused by hydraulic problems, more specifically because underestimated scour. It is true

[1] Scientific Manager, National Institute of Water and Environment (INA), C.C. 46, (1082) Aeropuerto Ezeiza, Argentina

that most of them had not good hydrologic estimation of floods but scour estimation was also discussed.

The change of statistical aspects of floods (the annual volume of la Plata River basin increased in the last twenty years) requires a new evaluation of bridge design and scour recalculation. When big floods are present in the downstream region of the Paraná River, the flood valley has more than forty kilometres wide during large periods (more than one month). In this conditions the scour in bridges cannot be calculated by usual hydraulics conditions. When scour is developing the section is increasing, but the upstream water level remains practically constant. For this type of processes, there are some local experiences.

In 1949 Dr. Schoklitsch was appointed "Extraordinary Professor" at the Hydraulics Institute of the Exact Sciences and Technology School at the University of Tucumán. In 1953 Dr. Schoklitsch began his academic and scientific activities at the National University of Cuyo, in San Juan, at the foot of the Andes Mountains. It should be pointed out that Dr. Schoklitsch's research dealt basically with the movement of water-transported solids. Based on his works to verify Sternberg's theories and revise Du Boys's, he formulated new equations on the movement of uniform grain-size sands, specific friction, and critical drag force. On the other hand, his known equation to allow the maximum depth calculation of local scour downstream energy dissipators was published previously, when the author was professor in Europe. Nevertheless, the influence of Schoklitsch equations on the argentine design of structures under scour conditions was detected in a wide range of engineers.

Three different subjects can expose the contribution of Argentine research on local scour: local scour at bridge piers, local scour downstream ski jump structures and local scour downstream hydraulic jump energy dissipators.

1- The proposal of Cotta and Jensen to avoid the local scour at bridge piers

The protection against local scour around bridge piers in alluvial rivers, is an local system developed by Cotta and Jensen (2), after a long experimental research from laboratory tests at the "Guillermo Céspedes" Hydraulic Laboratory of the La Plata National University.

The construction system consists in a corbel slab emerging from the pier section just at the bed level. The slab avoids the horseshoe vortex action on the movable bed.

The comprehensive design of the protection structure can be observed in the Figure 1,

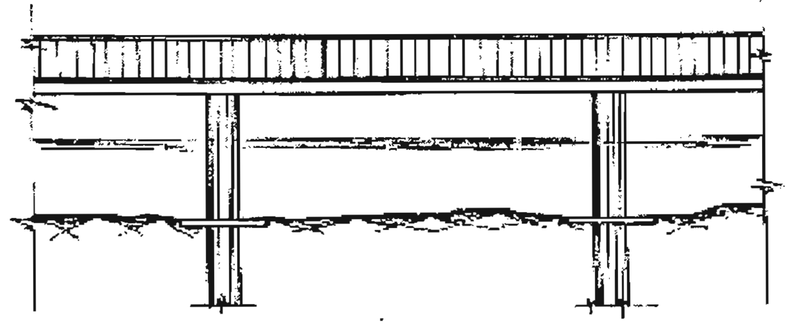

Fig. 1 General design of the protection structure

where the general dimensions and relationships of the system can be obtained.

The protection system can be applied to circular or rectangular cylindrical piers, with sections as there are presented in the Figure 2.

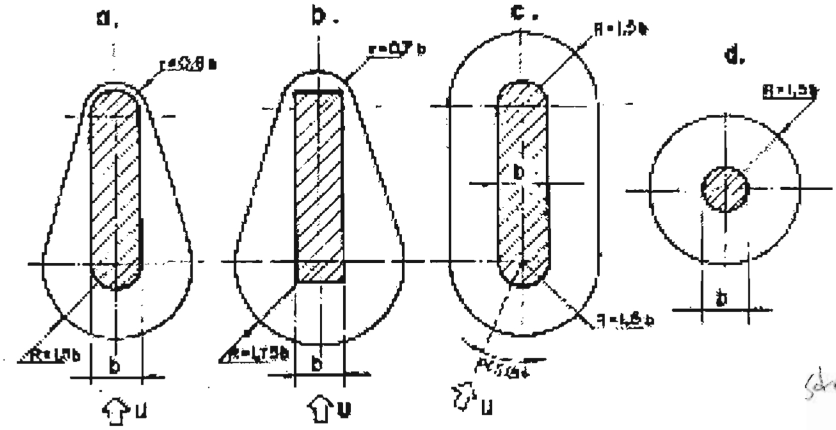

starre Konstruktion - abzulehnen!

Figure 2: Bridge sections ant velocity direction

When the stream direction is not the same than the pier longitudinal direction, but the angle between them is lower than 15°, the alternative "c" presented in the Figure 2 is recommended by the authors.

For angles up to 15° the authors suggest the use of circular piers, with circular added structure, as it is presented in the Figure 2 "d".

The authors design is only valid if the added structure is located at the bed level, or preferentially down the river bed level. If the added structure will emerge up the bed level, the system will be not effective.

The slab thickness must be lower than 0,08 b (where "b" is the pier representative dimension, wide or diameter) because an eventual emerging situation which will be negative (Figure 3). wieso?

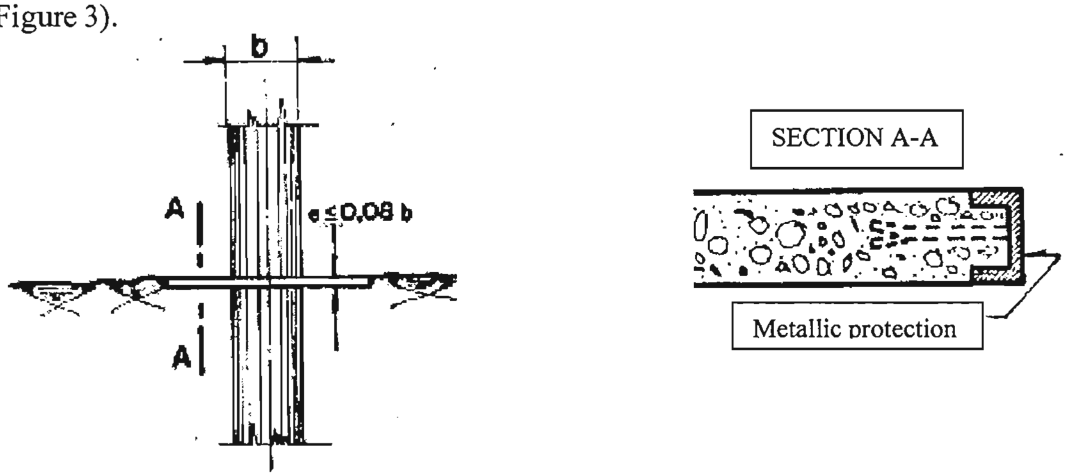

Fig. 3 Details of the protection structure

The concrete of the slab must be protected against stone's abrasion in all the perimeter by means a metallic piece with "u" section, as it is presented in the figure 3.

If river bed can descend by general or transversal erosion, the slab must be located at the minimum level calculated for the bed.

The practical results of this protection system were published in the Latin American Congress of the IAHR in Spanish (2). It has good diffusion in South America, as it was included in the Bridge Design Manual of Venezuela (11).

2- The INCYTH equation for local scour downstream flip buckets

An intentionally oversimplified formula for the estimation of the maximum depth of scour downstream ski-jump spillways was presented by Chividini et al (3) in order to be of use as an initial estimation.

This equation can be expressed as:

$$y/\Delta H = K\, Z^{*0.5}, \tag{1}$$

where y is the maximum depth of scour (Figure 4), ΔH is the fall distance between the reservoir level to the tailwater level, and Z^* is called the "fall number":

und was ist K ?
Schwerkraft ?

$$Z^* = q/(g\, \Delta H^3)^{0.5}, \tag{2}$$

where q is the unit discharge and g is the acceleration due to gravity.

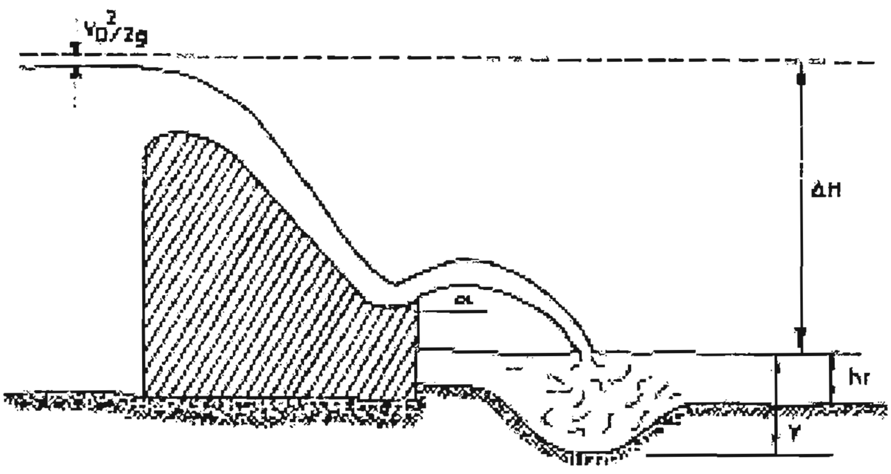

Figure 4: Ski-jump erosion notation

The equation was developed by means of laboratory tests carried out by the authors and sixty six laboratory experimental results of other authors (with standard deviation of 18%) and seventeen prototype results (with standard deviation of 26%). The validity field for this estimate expression covers the scour of no cohesive bed materials and energy losses coefficient in the spillway chute (ratio between the theoretical and actual velocity in the ski-jump section) over 0.75.

The INCYTH equation requires only the knowledge of the unit discharge and the fall height from the reservoir level to tailwater level. It should be noted that during the design stage many parameters are usually unknown, such as the size of blocks formed by fracture of the rock at different depths near the jet impact. For prototype preliminary calculations, this equation demonstrates acceptable performance, as it was demonstrated by Mason and Arumugam (8).

The best advantage of the INCYTH equation is that allows a simple preliminary calculation with an excellent mean performance, without the rock size knowledge (it is very difficult to estimate this parameter in advance of the dam construction).

But the more interest of this equation was demonstrated by Lopardo and Sly (7) with its validation, by means of scour registered in prototype for other authors and published after the INCYTH equation publication.

These results were published by Balloffet (1) for Tarbela Dam in Pakistan, by Riedel (10) for Colbún Dam in Chile, by Oliveira Lemos and Matias Ramos (9) for Cahora Bassa Dam in Africa, and by Keming et Al (4) for more than twenty prototype scour data from Chinese dams.

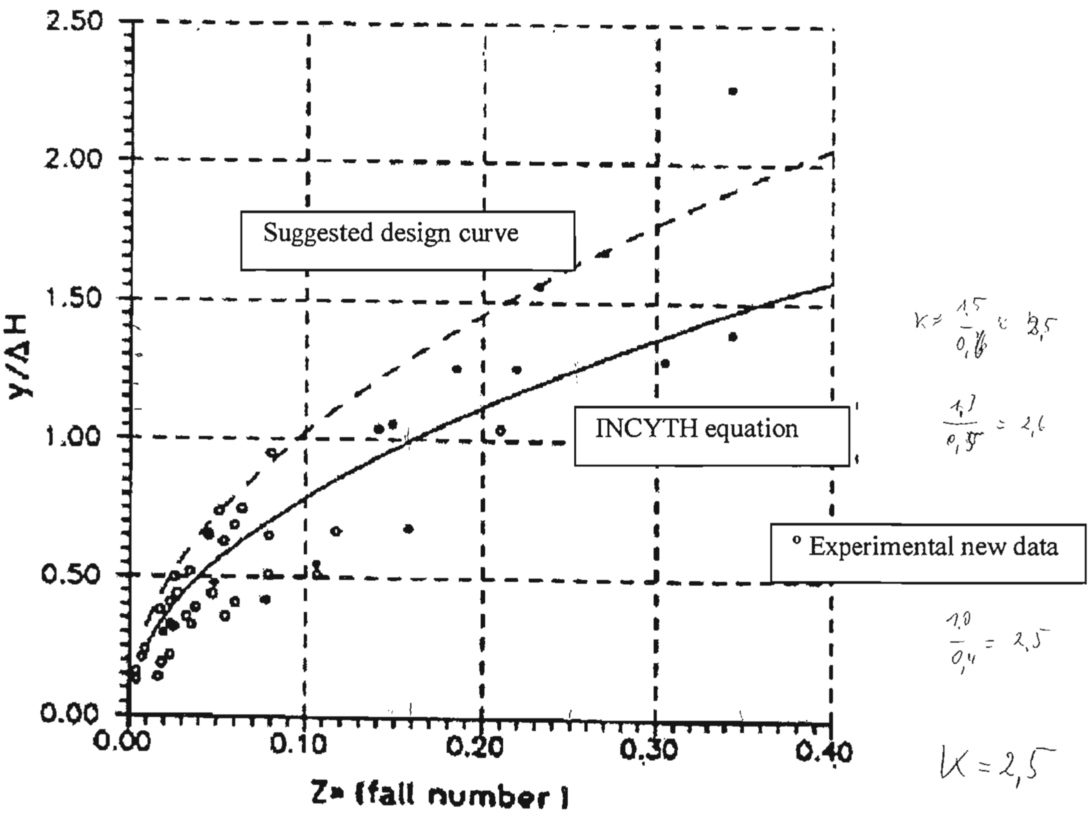

Figure 5: Comparison of INCYTH equation and new prototype data

As it is observed in the Figure 5, the INCYTH equation is always a good mean solution for these new prototype data coming for authors. Nevertheless, due to the safety conditions needed by engineering design, it is better to include a safety coefficient to cover the 99% of existing prototype data. It is demonstrated that this coefficient must be approximately 1.3. The INCYTH equation with this safety coefficient is also presented in the Figure 5 as a "suggested design curve".

3- Local scour on rocky beds downstream stilling basins

Energy dissipators of large flatlands dams usually consist of hydraulic jump stilling basins. Internal flow of a hydraulic jump is essentially macroturbulent showing severe random pressure and speed fluctuations. Incident kinetic energy has a transformation along the jump converting to potential energy. It also generates fluctuation energy which is transported by different scales vortex. This energy is gradually dissipated downstream the jump.

Rapidly variable pressure fields in space and time trends to enlarge existing bed discontinuities or create them when it is composed by erodable rock. Fluctuating pressures propagation inside the rocky structure causes it to break into minor pieces. Alternatives forces induced by pressure fluctuations pull some blocks out of the bed. Drainage established among the blocks reduces fluctuations amplitude. The cavity created previously enlarges by ascending streams generated in the zone when the jet hits against the bed.

Water pressure is highly variable along the interface rock-water being greater than average in certain zones and lesser in the others. When rocky blocks dimensions increase, space-time correlation of fluctuating pressures trends to reduce. A strong ascendant instantaneous force will be generated if there is an important simultaneity of actions. Blocks should have reduced dimensions, turbulence should be of a large scale or both causes should present together for this to happen. There are clear evidence that macroturbulence largely exceeds conventional stilling basins length. He presented some practical examples where turbulence intensity decay begun at twice the basin length (basins designed using classical jump length)

Macroturbulent nature of flow inside a hydraulic jump stilling basin is responsible for the existence of strong pressure fluctuations. Many papers has been written giving a warnings about its highly destructive nature (5). Presence of structural discontinuities helps to severely amplify pressure fluctuations amplitude. Also spectrums show a tendency of energy concentration around a dominant frequency. Forced hydraulic jumps can be produced inserting a chute element in the laboratory canal. Consider that this element consist of a despicable thickness situated at a distance x_0 from jump start, of height h_b and Reynolds number is high enough to admit viscous forces influence is negligible. The expression to calculate a non dimensional coefficient that ground upon root mean square fluctuating pressure amplitudes ($\sqrt{p'^2}$) is:

$$C'_p = \sqrt{\frac{p'^2}{\rho V_1^2 / 2}} \qquad (3)$$

$$C'p = C'p\,(x/h_1,\, x_0/h_1,\, h_b/h_1,\, F_1) \qquad (4)$$

where Section 1 is the upstream section of the jump (where it begins) and ρ = fluid specific mass, h_1 = vertical depth at Section 1, V_1 = velocity at Section 1, and F_1 = Froude Number at Section 1. This expression has been obtained through dimensional analysis.

There are several specific cases of stilling basins shorter than jump's length with end sills. Results of fluctuating pressures has been obtained for the most critical situations. Experiments conditions covered a wide set of flows among $3 < F_1 < 7$. Pressure transducers where located on the end sill and downstream, on the rocky simulated bed (Figure 6). Physical model simulated Yacyreta's main spillway stilling basin. This dam is located on Paraná River (Argentina - Paraguay). The end sill was not vertical and of low height.

It can be stated that fluctuating pressures coefficient presents a strong decreasing trend related to Froude number at Section 1. It goes from $C'p = 0.09$ for $F_1 = 3$ to $C'p = 0.015$ for $F_1 = 7$. Strouhal Number (S_p) versus Froude Number at Section 1 has a decreasing tendency too, similar for all transducers.

A later work developed for the same Yacyreta's stilling basin (6) registered a large quantity of fluctuating pressures amplitudes and frequency data on the basin's floor. Among the numerous values reported for the intakes located downstream the end sill the more interesting are: $C'p$ = fluctuating pressures coefficient, $p'_{0.1\%}$ = negative values of instantaneous pressures with 0.1% probability of being trespassed, f_p = dominating frequency and f_z = zero crossing frequency.

Stilling basins with an end sill designed using the conventional criteria on adequate rocky river beds have a dimension of 60% of hydraulic jump's length. It is interesting to notice that these cases can be interpreted through this elementary analysis developed using a two-dimensional barrier. In that way can be concluded that end sills are not useful structures if river bed downstream the basin is not formed by granular materials. Some totally negative aspects about rock blocks removed by the flow are also present. Blocks that are removed generates an irreversible situation favouring further erosion.

An experimental work was carried out to determine maximum uplift forces on large dimensions bed blocks downstream of a two-dimensional barrier. Instantaneous values of actions are obtained performing a discrete integration of "n" pressure values measured simultaneously using pressures gauges and a computational storage system. The force is define as:

$$F'_{ij} = \Sigma_i \, p'_{ij} \, d\Omega_i \,, \tag{5}$$

where p'_{ij}= fluctuating pressure registered by sensor "i" at time step "j", i = number of sensor varying among 1 and n, n = total number of sensor, j = number of data being registered varying among 1 and N, N = total number of measures (time steps), and $d\Omega_i$ = area assigned to sensor "i".

Parameter j works as time but in a discrete manner because sampling frequency is constant for all the acquisition time. A maximum of 16384 forces data are obtained throughout all sampling period. Working over the recorded data file statistical indicators can be obtained expressing mean and extreme fluctuating forces values. Similar to the concept of C'p the following non dimensional coefficient is defined.

$$C'_F = \frac{F'_{(rms)}}{1/2\rho U_1^{\,2} ab} \tag{6}$$

where "a" and "b" are the dimensions of the calculation slab. Those experiences where developed using depths at Section 1 higher than 3 cm and Reynolds number over 100,000.

Only results obtained for $F_1 = 4$ and $x/h_1 = 26$ will be used for further calculations in this paper.

$$\begin{array}{ll} a/h_1 = 3 & C'_F = 0.021 \\ a/h_1 = 4 & C'_F = 0.026 \\ a/h_1 = 5 & C'_F = 0.017 \end{array} \tag{7}$$

Estimations about the dimensions of basaltic rock blocks that could be removed by the flow downstream Salto Grande dam's stilling basin have been made. This dam is located on Uruguay river (between Argentina and Uruguay). An exigent condition that really occurred was taken a base of comparison: $q = 70.87\ m^2/s$, $F_1 = 4.17$, $l = 64$ m (basin's length), $h_1 = 3.09$ m, $L_r = 82$ m (jump's length), $U_1 = 22.96$ m/s, $x/h_1 = 26.5$ (non dimensional position).

Results obtained are enough to calculate C'_F coefficient through root mean square force $F_{(rms)}$. C'_F is not a good indicator of extreme instantaneous forces values. Using data registered for Froude number equal to 4 with fix barrier experiments, a relationship between uplift extreme 0.1% and mean values has been found. Extreme values are 3.07 to 3.20 times higher than root mean square values. The idea of all this calculations is to obtain an estimation of minimum rock blocks thickness to assure stability its own weight. For this working conditions flow can lift even a block of 1.70 m of thickness and linear dimensions of several meters. This number is in good concordance with visual measures realised during a restoration of the stilling basin.

Localised erosion of importance should not be admitted downstream a spillway with a hydraulic jump stilling basin which dimensions have been designed using classical criteria. Though, this is never accomplished. In general, erosion downstream a stilling basin which length is equal to the theoretical jump's length is never zero. The problem is that jump's lengths given by macroscopically conditions being the last section the one where the downstream depth corresponding to free jump is reached and average speed is easily determined using continuity and momentum equations.

Velocity profile is usually assumed as uniform in that section (as channel turbulent flow profile). In fact this is not true being it more and more different while Froude Number at Section 1 decreases. This disturbance implies very low surface speeds and high speeds near the bottom, with an erosive capacity highly superior to the one calculated using average speed. It has happened that some kind of basalt classified as non erodable have been found in places where large flatlands dams have been built. Using standard criteria stilling basins have been designed with a length of 60% of the theoretical. End sills of those basins generates conditions of forced hydraulic jump if they are of enough height, favouring macroturbulence and local erosion of the river bed. A warning against considering that a rocky bed submitted to severe pressure fluctuations behave as an alluvial bed is given. Equilibrium is dynamical in this last case, reaching a final condition after scouring. On the contrary, when the bed is composed of meteorized rock of several dimensions blocks, the remotion of one of this blocks is irreversible. Erosion process on rocky beds is then completely different than the analysed for granular material in laboratory.

The presence of an end sill is beneficial when river bed is alluvial, separating that controlled but inevitable erosion from the structure. When river bed is composed by rock end sills does not help but favour erosion generating an increase of speed fluctuations, concentrating energy around a dominant frequency that trends to remove large blocks.

REFERENCES

(1) Balloffet, A. (1987): "Erosión y sedimentación: revista de métodos de análisis" (Scour and sedimentation: revue of methods for analysis), First Argentine Seminar on Large Dams, Ituzaingó, Corrientes, Vol. 2, pp. 151-189.

(2) Cotta, R.D. and Jensen, P.D. (1966): "Dispositivo para anular la erosión en lechos móviles provocada por pilares interpuestos" (Dispositive to avoid the scour on movable beds due to pier´s interference), II Latin American IAHR Congress, Caracas, Venezuela, Vol. 1, pp 14-26.

(3) Chividini, M.F. et Al (1983): "Evaluación de la socavación máxima aguas debajo de aliviaderos en salto de esquí" (Evaluation of maximum scour downstram ski-jump spillways), Proceedings of the XI Water National Congress, Córdoba, Argentina, Vol. 6, pp. 187-210.

(4) Keming, A. et Al (1987): "Free jet scour to rock riverbed", XXII IAHR Congress, Energy dissipation Seminar, Lausanne, Switzerland.

(5) Lopardo, R.A., De Lío, J.C. and Vernet, G.F. (1987): "The role of pressure fluctuations in the design of hydraulic structures" in Design of Hydraulic Structures, pressed by R. Kia and M.L. Albertson, Colorado State University, Fort Collins, pp. 161-175.

(6) Lopardo, R.A. and Lapetina, M. (1997): "Local scour on rocky beds downstream stilling basins, in Management of Landscapes Disturbed by Channel Incision, edited by S.S.Y. Wang, E.J. Langendoen and F.D. Shields, The University of Mississippi, Oxford, USA, pp. 288-295.

(7) Lopardo, R. And Sly, E. (1992): "Constatación de la profundidad máxima de erosión aguas debajo de aliviaderos en salto de esquí" (Validation of the maximum depth of scour downstream ski-jump spillways), Revista Latinoamericana de Hidráulica IAHR, Sao Paulo, Brasil, N° 4, pp. 7-23.

(8) Mason, P.J. and Arumugam, K. (1985): "Free jet scour below dams and flip buckets", ASCE, Journal of Hydraulic Engineering, Vol. 11, N° 2, pp. 220-235.

(9) Oliveira Lemos, F. And Matías Ramos, C. (1984): "Hydraulic modelling of free jet energy dissipation", Symposium on Scale Effects in Modelling of Hydraulic Structures, Esslingen am Neckar, Germany, pp. 7.6/1-7.6/5.

(10) Riedel, R. (1989): "Socavación aguas abajo del salto de esquí del vertedero de la presa de Colbún" (Scour downstream the ski-jump spillway of Colbún Dam), IX National Congress of Chilean Hydraulic Engineering Society, Santiago, Chile.

(11) Sardi Socorro, V.A. and Martínbez de la Plaza, C. (1972): "Manual de procedimientos para el cálculo hidráulico fluvial de puentes" (Procedure manual for the fluvial hydraulic bridge design), Ministerio de Obras Públicas, Caracas, Venezuela, Vol. 2.

BRIDGE SCOUR PROBLEMS IN KOREA

By

Tae Hoon Yoon[1], Soo Sam Kim[2], Gye Woon Choi[3], Sangseom Jeong[4]

ABSTRACT

Bridge scour problems have recently become important issues for civil engineers in Korea. The reasons are: first, the catastrophic collapse of the Sung-su Grand bridge has led to a reconsideration of safety measures and inspection methods for all bridges, including underwater structural integrity inspections and sediment scour measurements. Second, relatively older small and medium sized bridges were designed and built without considerations of scour effects. A recent evaluation of 100 bridges in Korea for scour sensitivity showed that about 85% are scour critical and thus, they would fail if subjected to the design flood. In these respects, this paper presents the brief summary of scour practices, the techniques of scour monitoring systems and scour protection techniques available for bridge foundations in Korea.

INTRODUCTION

In South Korea, many bridge constructions are in progress in river and costal areas. Bridge scour problems have recently become important issues within the Korean geotechnical and water resources engineering community. The reasons are numerous but the most important factors can be summarized as follows. First, the catastrophic collapse of the Sung-Su Grand Bridge crossing the Han river has led to a reconsideration of safety measures and inspection methods for all bridges. These safety concerns have pushed local governments to include underwater structural integrity inspections and sediment scour measurements. Second, relatively older small and medium sized bridges were designed and built without considering scour effects, and measurements show that these bridges do suffer from severe scour problems.

In addition to bridge transversing rivers, active development of the coastal areas has brought increased pressure to build coastal bridges such as the Seohae, the Youngjong and the Kwangan Grand Bridges. Interestingly among them, the site of the Seohae Grand Bridge was not a favorable site on which to build a bridge due to the relatively large tidal motion. It is true that much work has been done in the field of river bridge scouring (Breusers and Raudkivi, 1991) and there seems too many empirical formulas to apply. It is

[1] Professor, Dept. of Civil Engineering, Hanyang University, Seoul, Korea.
[2] Professor, Dept. of Civil and Environmental Engineering, Chung Ang University, Seoul, Korea.
[3] Associate Professor, Dept. of Civil Engineering, University of Inchon, Inchon, Korea.
[4] Associate Professor, Dept. of Civil Engineering, Yonsei University, Seoul, Korea.

however very hard to find studies in the field of coastal bridge scouring (Escarameia, 1998).

Scour at bridge pier is a complicated three-dimensional problem involving interaction of fluid forces on movable and nonuniformly distributed bed grains. Although several analytical solution, experimental research and field investigations for bridge scour have been conducted, no comprehensive and universally accepted solution is so far available. Even though many methods and equations are available for predicting bridge scour, hydraulic and/or bridge design engineers are often at a loss over which method or equation is applicable for the specific bridge sites.

To provide better understanding on the types of scour problems and practice for bridge piers, the authors gather the general information through comprehensive literature review, which covers over 20 publications reported in Korea. Before 1990, most of the research related to scour was conducted based on experiments. Since 1990, much work has been done in many fields: the estimation of scour depth by numerical modeling, study on the scour in coastal zones, and the evaluation of the safety of hydraulic facilities. This paper describes the state-of-the-art of bridge scour problems in Korea based on the techniques of scour monitoring systems and scour protection techniques.

SCOUR PROBLEMS IN KOREA

Of the total amount of precipitation in a year in Korea, two-thirds of that amount falls during the summer mostly in the type of typhoons and heavy rainfall. Table 1 shows a record of the damages that have been reported during the last ten years. It can be seen that of the total number of natural disasters that have been reported, over 90% of them were related to heavy rain and typhoon. Table 2 is a record of the damages of pavements, rivers, railroads, and hydraulic facilities that were due to scouring during the last 15 years. It is found that the damage caused by scouring occupies more than 75% of the total damage cost in a year.

Focusing our attention to damaged bridges, Table 3 lists the number of damaged bridges due to scouring. As can be seen in 1987 there were 255 bridges reported to be damaged. Every year about 100 bridges are reported damaged due to scouring. A thorough investigation into the matter concludes that over 85% of the damaged bridges have piers under poor conditions due to scouring.

There are many reasons for piers to experience scouring. Some are unavoidable. It is therefore essential that there be more care taken when designing piers of bridges. It is needless to say that they be designed considering the natural environment surrounding the bridges. Unfortunately it is a pity that the bridges in Korea have not taken these factors into account.

Table 1. Damage conditions by Natural disaster (1985 – 1994)

(unit: %)

Year	**85**	**86**	**87**	**88**	**89**	**90**	**91**	**92**	**93**	**94**	**Average**
Typhoon	27.8	72.4	47.4	0.0	21.7	0.2	63.2	21.8	44.6	13.3	31.2
Heavy rain	69.3	20.3	50.5	91.5	63.4	91.5	32.7	62.5	40.0	58.9	58.1
Storm	2.5	2.4	2.0	6.0	9.8	4.4	1.6	14.0	12.1	3.1	5.8
Others	0.4	4.9	0.1	2.5	5.1	3.9	2.5	1.7	3.3	24.7	4.9

Table 2. Damage situations due to Scour Unit: $) means %

Year	Pavement	River	Hydraulic facilities	Rail road
1981	4,572,849 (6.9)	14,637,483 (22.1)	16,549,909 (24.9)	172,998 (0.3)
1982	3,831,937 (11.5)	9,751,582 (29.2)	6,538,955 (19.6)	46,606 (0.1)
1983	131,348 (3.7)	204,939 (5.8)	271,954 (7.7)	- (0.0)
1984	15,278,930 (15.2)	31,071,099 (31.0)	24,259,601 (24.2)	254, 725 (0.3)
1985	3,258,714 (8.9)	7,303,228 (19.9)	8,148,796 (22.3)	10,106 (0.0)
1986	2,711,103 (8.6)	4,835,894 (14.9)	5,187,558 (16.0)	437 (0.0)
1987	41,720,680 (9.3)	105,140,420 (23.4)	87,978,508 (19.6)	882,164 (0.2)
1988	9,087,858 (13.2)	19,744,90544 (28.6)	9,242,678 (13.4)	233,332 (0.3)
1989	15,054,673 (8.8)	44,133,509 (25.9)	48,052,752 (28.2)	1,031,981 (0.6)
1990	28,240,968 (12.3)	49,686,425 (21.6)	30,589,363 (13.3)	2,446,328 (1.1)
1991	24,632,219 (9.9)	61,201,390 (24.7)	46,831,811 (18.9)	113 (0.4)
1992	28,240,968 (16.5)	49,686,425 (16.1)	30,589,363 (21.9)	44,606 (0.4)
1993	21,722,368 (17.0)	26,210,772 (20.5)	23,432,113 (18.3)	773,248 (0.6)
1994	15,266,966 (10.9)	11,520,953 (21.8)	9,234,417 (19.1)	243,177 (0.3)
1995	62,143,474 (17.5)	57,457,443 (16.2)	54,021,278 (15.2)	1,417,115 (0.4)

Table 3. Number of Damaged Bridges due to scouring

Year	81	82	83	84	85	86	87	88	89	90	91	92	93	94	95	Avg
No of bridges	141	47	4	177	53	37	255	51	112	89	162	89	90	28	140	98.3

In Korea, Before 1990 just a few researches related to the scour were conducted based on experiments. Lee(1984) conducted the research on the local scour at bridge piers and concluded the pier Reynolds number and turbulent strength are the main parameters for forecasting the maximum scour depth. Kim(1985a) conducted the experiments about the maximum scour depth including the vortex mechanism at circular pier. Kim(1985b) compared the maximum scour depths calculated using the existing scour equations with his experiment data which were obtained from the model tests using the diatomite as the channel bed material. Since 1990, much work has been done in many fields: the estimation of scour depth utilizing numerical models, the detailed characteristics of local scour at bridge piers in cohesive soil (Choi, 1998), sack gabion as scour countermeasures (Yoon, 1998), and automatic real-time scour measurements (Lee and Yeo, 1998).

SCOUR MONITORING SYSTEMS

There are some monitoring devices available for bridge scour measurements in Korea. They are GPR(Ground Penetrating Radar), Magnetic Collar, Fathometer and buried rod. Here, an automatic real time bridge Scour Monitoring System(SMS), designed by Lee and Yeo (1998) and then used to detect the scouring process of Seohae Grand Bridge, is introduced.

Seohae Grand Bridge is a coastal highway bridge crossing Asan Bay Channel. Fig. 1 shows the bridge location map enclosed by Korean peninsula. The construction started in 1994 and will be completed in 2001. The most significant problem from the perspectives of costal engineers of the construction site is the world's famous and largest tidal motion measuring up to a tidal level difference of 9.3m bringing tidal current speed up to 0.8m/s. Also, concurrent development plans in that area resulted in the current speed adding up to 2.65m/s. Field bridge engineers reported excessive bridge scour depth more than 8m from the design bed level.

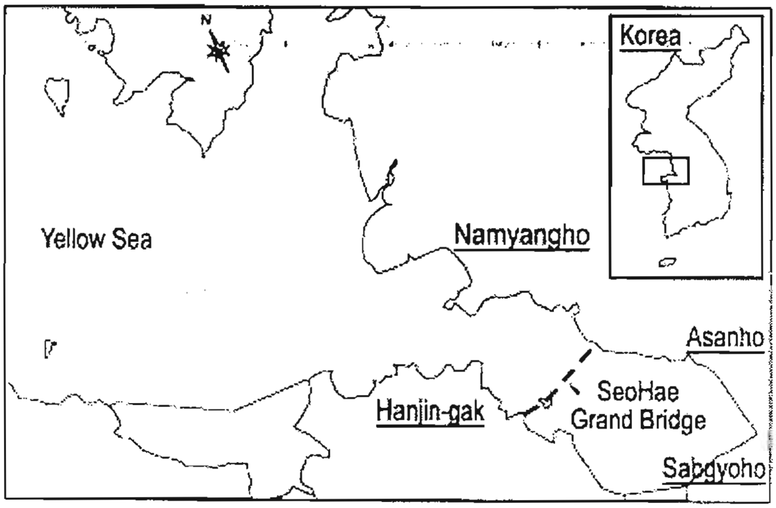

Fig. 1 – Map of Seohae Grand Bridge Construction Site

During the construction of bridge piers in the Asan Bay Channel with high tidal currents, field engineers reported unexpected increase in the scour depths due to vast developments of Harbor in Bay region, resulting in flow contraction at some sections of the channel. An advisory meeting in the Korea Highway Cooperation recommended to investigate scour problems around piers and urgently find out the proper protection method against such a dangerous scouring near the Seohae Grand Bridge.

However, the most common methods are to adapt empirical formula which have been based on measurements from all over the world for various conditions and bridge design in different water systems. Interestingly, there has been no single field experiment which continuously monitors bridge scour process under high flow or flood conditions. The reason is that inexpensive and adequate devices do not exist to monitor bridge scour process for long enough time periods and to obtain spatially and temporally dense enough data sets. Without the proper data obtained under site-specific conditions, rational design methods cannot be developed. Therefore, it was asked to develop the device able to measure the scour depth with credibility. Furthermore, it must work in the salty water of tidal basin. According to this requirement, an automatic real time bridge Scour Monitoring System(SMS) was applied for this project. Scour Monitoring System developed did a good job to figure out the general scour trends in short and long time scales. The measured data revealed that current scour progress shows to be in equilibrium state governed by the semi-diurnal tidal cycle in this region. Fig. 2 shows the block diagram of the SMS.

The project is comprised of three components: real-time monitoring of bridge scour processes, numerical simulation of proposed developments in Asan Bay to determine their effects in flow conditions and bridge scour; and physical model testing to study local bridge scour causes, as well as a preliminary study of bridge scour protection schemes. The schematic diagram with contents in each component is drawn in Fig. 3.

x Hat's was gebracht?
Verifikation von Formeln?

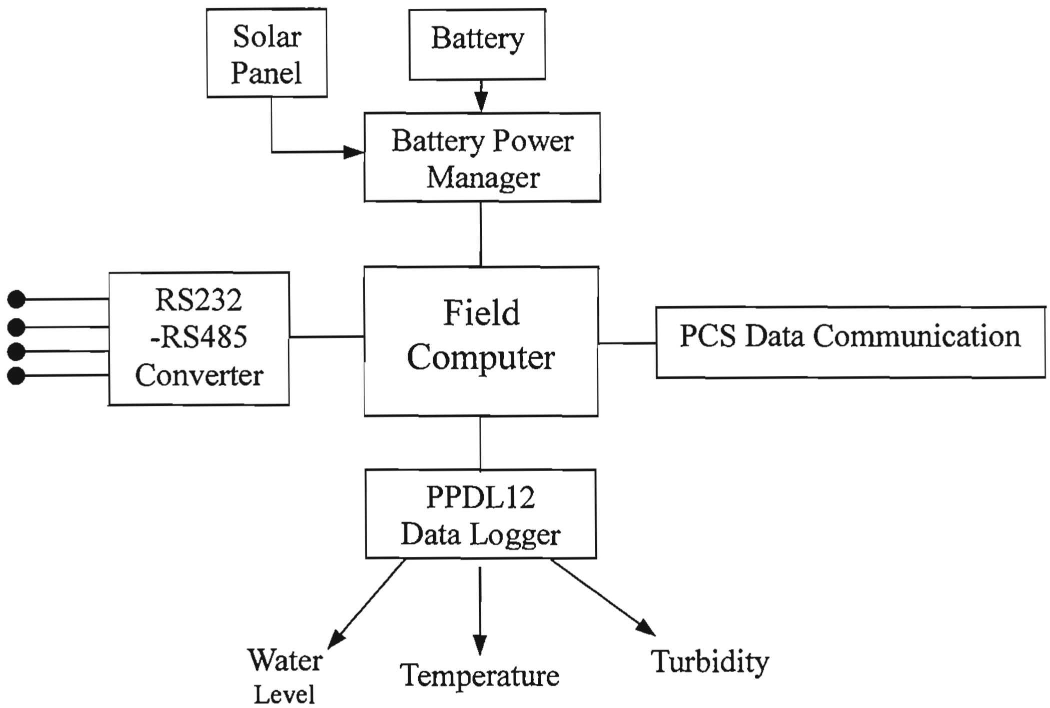

Fig. 2 – Block Diagram of SMS Configuration

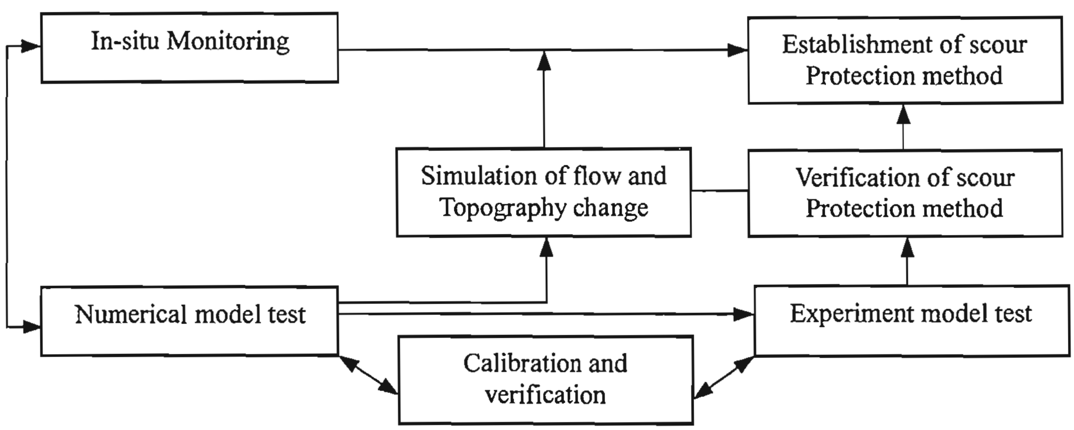

Fig. 3 – Schematic Diagram

SCOUR PROTECTION METHODS

There are several methods available for bridge scour protection in Korea (Fig. 4). One of these methods is riprap, which has been used for a long time for its easier installation and lower cost than other protection methods. Because of those reasons, ripraps have been used and studied also in Korea.

For riprap scour countermeasures for uniform pier, Yoon (1998) has noted that the pier width is a significant factor in determining the riprap size. As in the local scour for nonuniform pier, ripraps placed around nonuniform piers should be influenced by the pier nonuniformity in size.

Significant factors on the magnitude of ripraps for uniform piers were found to be approach velocity and flow depth, width of pier and riprap cover. Such factors for nonuniform piers were found to behave in a similar way to uniform piers. It has been seen that the critical velocity increases with increasing riprap size as noted by Richardson et al(1993), Parola(1993), and Chiew(1995). The effects of flow depth on the stability of riprap stones are two-fold. When the water depth is deep, the critical velocity increases with decreasing water depth. However, the critical velocity become decreasing with further decreasing of water depth. The reasoning of the existence of two flow regimes is given by Yoon(1998).

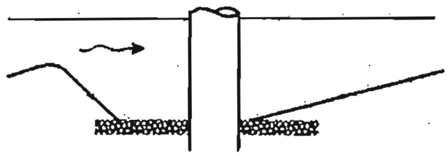

(a) Rip-rap protection

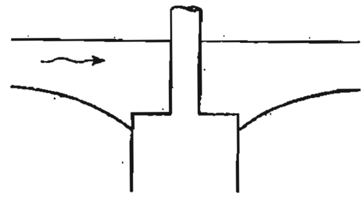

(b) Circular pier with caisson

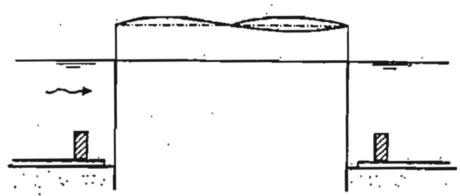

(c) Separated vertical deflector

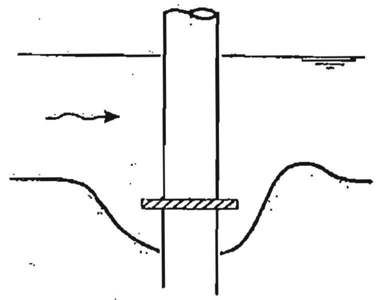

(d) Horizontal deflector

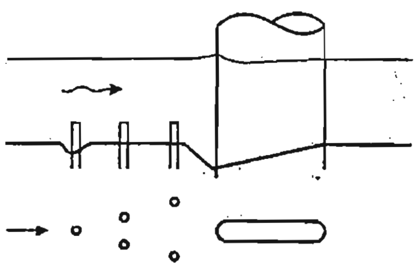

(e) Piles in front of a pier

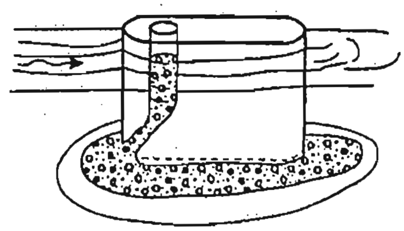

(f) Grouting

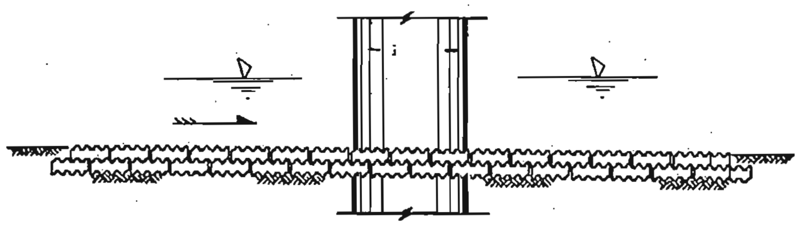

(g) Concrete block around pier

Fig. 4 – Local Scour Protection Method

For nonuniform piers two additional factors such as the width and the height of footing are involved. Those factors are examined for their effects on the size of riprap. The critical velocities are very much dependent upon the height of footing implying that critical velocity decreases with increasing height of footing.

The stability of riprap stones around piers is sensitive to changes in elevation of the top of the foundation. When the top elevation is the same as the streambed or slightly above streambed, it acts as a scour protective layer by intercepting the downflow and protecting the streambed. It implied that for the identical conditions smaller stones can be used to attain the same level of protection if there is a footing whose top elevation is at streambed or slightly above it. If the height of footing rises further, critical velocity decreases resulting in reduced protection.

There are some other methods used to protect bridge-pier scour in Korea; Mattress protection and deflectors. Mattress protection has been proposed as a new concept using artificial protection for local protection around a big, circular pier in a bed of fine sand. This protection consists of numerous bundles of polyester filaments which can be suspended under a frame cantilevered from the pier. The first prototype test showed promising results (Carstens 1976). In general, special attention has to be given to providing a tight connection between the mattress and the pier, because even though a small gap, the downflow can induce severe erosion that extends under the mattress. Deflector has been used for reducing the intensity of the downflow near the pier (Carstens 1976; Dargahi 1987). But, this method has not been used widely and frequently, because there are no design rules are available for the determination of the width and the height of the deflector, which is fixed to the pier, and it did not noticeably reduce the erosion depth.

CONCLUSIONS

The main objective of this study was to gather the general information on the scour problem, scour practice, and scour solutions in Korea. Before 1990, most of the research done on bridge scour was based on experiments. The test results from such experiments were not applicable to multiple situations because most of the experiments were carried out at localized conditions. Thus hydraulic and/or bridge design engineers are often at a loss over which method or equation is applicable for the specific bridge sites.

Since 1990, much work has been done in many fields in Korea: the estimation of scour depth utilizing numerical models, the detailed characteristics of local scour at bridge piers in cohesive soil, sack gabion as scour countermeasures, and scour monitoring systems in coastal zones. Lately there have also been advanced research focusing on the evaluation of safety of hydraulic facilities and research concerning with environmental matters.

ACKNOWLEDGEMENTS

The authors wish to thank Dr. Lee and Prof. Yeo, Hydraulic lab. at Myongji University for their contribution to this study.

REFERENCES

1. Breusers, H., Raudkivi, A. 1991. "Scouring Hydraulic Structures Design Manual 2," IAHR, Balkema, Rotterdam.

2. Carstens, T., 1976, "Seabed Scour by Currents near Platforms," *3rd Conference on port and ocean engineering under arctic conditions*, University of Alaska: 991-1006.
3. Chiew, Y. M., 1995, "Mechanics of Riprap Failure at Bridge Piers," *Journal of Hydraulic Engineering*, ASCE, 121(9), pp. 635-645.
4. Choi, G.W., Ahn, S.J., Kim, J.S., Ahn, C.J., 1995, "Piers Scour Prediction in Pressure Flow," *Korean Journal of Hydroscience*, Vol. 6, June, Seoul, Korea.
5. Choi, G.W., Ahn, S.J., Kang, K.W., 1991"State-of-the-art of Pier Scour Prediction of Design Application," *Korean Journal of Hydroscience*, Vol. 2, June, Seoul, Korea.
6. Choi, G.W., Kim, G.H., Ahn, K.S., Seoh, B.H., 1998 "Local Scour at Bridge Piers in the Cohesive Soil in the Yellow Sea," *Water Resource Engineering,* Vol. 2, pp1894-1899, Seoul, Korea.
7. Dargahi, B., 1987, "Flow Field and Local Scouring around a Cylinder," Bulletin TITRA-VBI-137, Department of Hydraulics Engineering, Royal Institute of Technology, Stockholm, Sweden.
8. Escarameia, M., 1998. "Laboratory Investigation of Scour around Large Structures in Tidal Waters," *Proceedings of ICHE '98*, Hamburg, Germany.
9. Jarrett, R. D., Boyle. J. M., 1986, "Pilot Study for Collection of Bridge-scour Data," U. S. Geological Survey, Water-Resources Investigations Report 86-4030.
10. Jung, D.W., 1991, "Experimental Study on Characteristics of Protection against Local Scour around Bridge Piers," *M.S. thesis*, Han Yang University, Seoul, Korea.
11. Kim, J.H., 1985, "The Experimental Study for the Maximum Scour Depth around Bridge Piers," *M.S. thesis*, Seoul National University, Seoul, Korea.
12. Kim, H.S., 1985, "Study on the Scour around Bridge Piers," *M.S. thesis*, Seoul National University. Seoul, Korea.
13. Lee, J., Yeo, W.K., 1998, "Development of a Field Monitoring System for Real-Time Coastal Data Acquisition," Technical Report of Observation Network Enhancement Workshop, Korea Ocean Research and Development Institute, 105-115.
14. Parola, A C., 1993, "Stability of Riprap at Bridge Piers," *Journal of Hydraulic Engineering*, ASCE, 119(10), pp. 1080-1093.
15. Richardson, E. V., Harrison, L. J., Richardson, J. R., and Davis, S. R., 1993, "Evaluating Scour at Bridges, Hydraulic Engineering Circular No. 18," FHWA-IP-90-017, FHWA, February, pp. 41-44.
16. Yoon, T.H., Park, K.D., Kim, C.H., 1998 "Effects of Foundation Geometry on Riprap Scour Countermeasures around Bridge Piers "Proceedings of 3rf Korea-Japan Bilateral Symposium pp240-242 Water Resources and Environmental Research, Seoul.
17. Yoon, T.H., Namgung, D., 1998 " Effect of Nonuniformity of Pier Dimensions on the Bridge Pier Scour," Journal of the Hydraulic Division, Proceeding of Korean Society of Civil Engineers, Vol 18, No.2-6, pp 553-562, Seoul, Korea.
18. Yoon, T.H., Yoon, S.B., Oh, C.S., 1998, "Sack Gabion as Scour Countermeasures," Journal of the Hydraulic Division, Proceeding of Korean Society of Civil Engineers, Vol 18, No.2-1, pp 13-22, Seoul, Korea.

BRIDGE SCOUR EVALUATION IN THE UNITED STATES

by

E.V. Richardson[1], J.R. Richardson[2], and P.F. Lagasse[3]

ABSTRACT

In September 1988 The U.S. Federal Highway Administration (FHWA) issued Technical Advisory T514023 entitled "Scour at Bridges" to State Highway Departments or Departments of Transportation which recommended that each State evaluate every bridge over a stream as to its vulnerability to scour of its foundations. Accompanying the advisory was a document entitled "Interim Procedures for Evaluating Scour at Bridges." This was the first U.S. publication which gave specific recommendations and equations for evaluating scour. Subsequently, FHWA issued Hydraulic Engineering Circulars (HEC's) 18, 20, and 23 which gave state-of-practice for evaluating bridge scour for bridges over riverine and tidal waterways, stream stability at highway structures and bridge scour and stream instability countermeasures. This paper presents the FHWA's recommendations for bridge scour and stream instability evaluation.

INTRODUCTION

In September 1988, the U.S. Federal Highway Administration (FHWA) issued Technical Advisory T514023 entitled "Scour at Bridges" to State Highway Departments or Departments of Transportation which recommended that each State evaluate every bridge over a stream as to its vulnerability to scour of its foundations. The Advisory stated: "Most waterways can be expected to experience scour over a bridge's service life (which is now approaching 100 years). Exceptions might include waterways in massive, competent rock formations where scour and erosion occur on a scale that is measured in centuries..... The added cost of making a bridge less vulnerable to scour is small when compared to the total cost of a failure which can easily be two or three times the original cost of the bridge itself. Moreover, the need to ensure public safety and to minimize the adverse effects stemming from bridge closures requires our best effort to improve the state-of-practice of designing and maintaining bridge foundations to resist the effects of scour."

Accompanying the advisory was a document entitled "Interim Procedures for Evaluating Scour at Bridges". This was the first U.S. publication which gave specific recommendations and equations for evaluating scour. Subsequently, in 1991, this document was revised and issued as Hydraulic Engineering Circular 18 (HEC-18) entitled "Evaluating Scour at Bridges." Also, in 1991 a companion document (HEC-20) entitled "Stream Stability at Highway Structures was issued."

[1]Senior Associate, Ayres Associates and Emeritus Professor of Civil Engineering, Colorado State University, Fort Collins, CO
[2]Assistant Professor, Department of Civil Engineering, University of Missouri, Kansas City, MO
[3]Senior Vice President, Ayres Associates, P.O. Box 270460, Fort Collins, CO 80527

As new knowledge was obtained the two documents were revised. HEC-18 in 1993 and 1995 (Richardson and Davis, 1995) and HEC-20 in 1995 (Lagasse et al., 1995). Also in 1997 HEC-23 entitled "Bridge Scour and Stream Instability Countermeasures-Experience, Selection and Design Guidance" was issued (Lagasse et al., 1997). These three documents, which have been endorsed by the American Association of State Highway and Transportation Officials (AASHTO, 1992), represent the present state of practice in the United States for evaluating and design for stream stability and scour at highway bridges. Presently (2000) all three documents are being revised.

HEC-18 presents methods and equations for evaluating and inspecting scour at bridges over riverine and tidal waterways. HEC-20 presents methods for evaluating stream stability and HEC-23 provides methods and equations for the design of countermeasures for stream instability and scour at highway bridges.

BACKGROUND

Bridge failures cost millions of dollars each year as a result of both direct cost necessary to replace and restore bridges, and indirect costs related to disruption of transportation facilities. However, of even greater consequence is loss of life from bridge failures. In the United States there are over 575,000 bridges in the National Bridge Inventory. These numbers include federal highway system, state, county and city bridges. Approximately 84 percent of these bridges are over water. Erosion of the foundations of the bridges resulting from stream instability, long-term degradation, contraction scour and local scour cause 60 percent of bridge failures. There has been 25 fatalities from bridge failures in the United States since 1987 (Richardson and Lagasse, 1999).

Rhodes and Trent (1993, Richardson and Lagasse, 1999, p. 1013) document that $1.2 billion was expended in the U.S. for restoration of flood damaged highway facilities during the 1980s. They state that this amount is conservative because they (1) only include the amount funded by the U.S. Government which ranges from 75 to 100 percent of the total restoration costs, and (2) the funds were only for disaster that are very large and do not include the hundreds of smaller events that occur every year. These costs do not include the additional indirect costs to highway users for fuel and operating costs resulting from temporary closure and detours and to the public for costs associated with higher tariffs, freight rates, additional labor costs and time. Rhodes and Trent also demonstrate that the indirect cost (operating a vehicle over a detour and time lost traveling when a bridge failed) can exceed by several times the direct cost of bridge replacement or repair.

Bridge scour research in the U.S. started in the early 1950s through Carl Izzard's efforts to have the U.S. Bureau of Public Roads (predecessor agency to the Federal Highway Administration) and Iowa State Highway Department fund Laursen's research on bridge scour (Laursen and Toch, 1956; Laursen, 1958, 1960, and 1963). However, only recently has extensive data of field measurements of scour at bridges become available (Landers and Mueller, 1996 and Richardson and Lagasse,1999, p. 585). Also, many analytical techniques are recommended for use simply because they are the best currently available and are overly conservative. For example, many equations for determining local sour depths at bridge abutments use abutment and roadway approach length as a variable instead of the flow they intercept (Richardson and Richardson, 1992, 1993 and Richardson and Davis, 1995). In the field case, this is a spurious correlation.

All material on the stream bed and banks at a bridge crossing will erode. It is just a matter of time. Some material, such as granite may take hundred's of years. Whereas, sand bed streams will erode to the maximum depth of scour in hours. Sandstones, shales, and other sedimentary bed rock material, do not erode in hours or days but will over time erode to the extent that a bridge will be in danger unless the substructure are founded deep enough. Cohesive bed and bank material such as clays, silty clays, silts and silty sand or material such as glacial tills, which are cemented by chemical action or compression, will erode. The erosion of these materials is slower than sand bed material but their ultimate scour will be as deep as the scour depth in a non-cohesive sand bed material (Jackson et al., 1991, Richardson and Lagasse, 1999, p. 578, and Briaud et al., 1999). Briaud et al. (1999) describes a procedure for determining the scour rate in cohesive soils. The procedure uses a special laboratory flume named the Erosion Function Apparatus (EFA). Shelby tube samples of the subsurface cohesive soils are extruded into the EFA and subjected to flows of varying velocity to determine a plot of erosion rate vs velocity. From the flood history and hydraulic characteristics of the river at the bridge site and the results from the EFA tests, a time-dependent scour rate can be developed. If the assumption is made that the future flow conditions of the river will be similar to the historic conditions, a time rate of scour can be projected into the future for a period equal to the anticipated service life of the bridge to determine a depth of scour. The method assumes that the depth of scour is a function of time and that scour will continue to occur until the scour depth is equal to the ultimate scour depth similar to what would occur in a sand bed. The depth obtained from the EFT tests can be compared to the ultimate scour depth from an existing equation to aid in the analysis.

Scour at bridge crossings is a sediment transport process. Long term degradation, contraction scour and local scour at piers and abutments result from the fact that more sediment is removed from these areas than is transported into them. If there is no transport of bed material into the bridge crossing, **clear-water** scour exists. Transport of appreciable bed material into the crossing results in **live-bed** scour. In this latter case the transport of the bed material may limit scour depth. Whereas, with clear-water scour the scour depths are limited by the critical velocity or critical shear stress of a dominant size in the bed material at the crossing.

Typical clear-water scour situations include (1) coarse bed material streams, (2) flat gradient streams during low flow, (3) local deposits of larger bed materials that are larger than the biggest fraction being transported by the flow (rock riprap is a special case of this situation), (4) armored stream beds where the only locations that tractive forces are adequate to penetrate the armor layer are at piers and/or abutments, and (5) vegetated channels where, again, the only locations that the cover is penetrated is at piers and/or abutments. During a flood event, bridges over streams with coarse bed material are often subjected to clear-water scour at low discharges, live-bed scour at the higher discharges and then clear-water scour on the falling stages. Clear-water scour reaches its maximum over a longer period of time than live-bed scour (See Figure 1). In fact, local clear-water scour may not reach a maximum until after several floods.

Floods tend to scour the material at a bridge crossing during the rising limb of the flood and refill these scour holes during the recession limb. Often, the redeposited material in the scour hole is more easily eroded by subsequent floods. Post-flood inspection of the bridge crossing may indicate the material around the foundations are adequate, when in fact, the bridge is in jeopardy of failing during the next flood. This infilling also, makes it difficult to obtain field measurement of scour depths because the measurements have to be made during a flood.

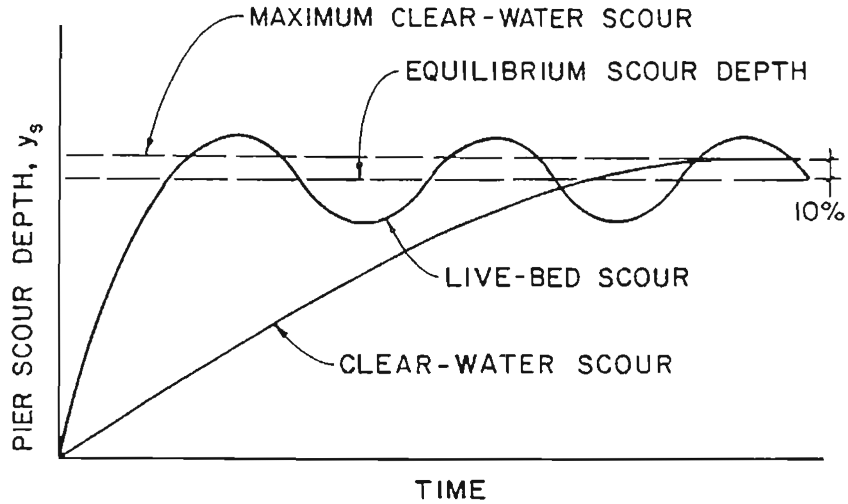

Figure 1. Pier Scour Depth in a Sand-Bed Stream as a Function of Time (not to scale) (Richardson and Davis, 1995).

The magnitude of the scour depth depends on the flow variables of the stream (discharge, flow velocity and depth, angle of the flow to the bridge, etc.), bed and bank material characteristics (bed rock, alluvial or non-alluvial, cohesive or non-cohesive, size distribution, etc.) and bridge characteristics (size and shape of the pier and abutments, width of opening, elevation of the deck, etc).

Design Discharge

The magnitude of the flow variable depends on the selection of a design discharge. The selected design discharge for a bridge is based on the design life of the bridge, bridge importance, consequence of failure, etc. The design discharge for a divided highway with large average daily traffic (ADT) (interstate highway, autobahns, etc.) would be larger than for a farm to market or logging road. Some engineers advocate a maximum possible flood for important bridges (Laursen, 1998) others recommend risk analysis. Important bridges are those with large ADT, Interstate highways, school bus and ambulance routs, and etc.

The Federal Highway Administration (FHWA) in HEC-18 (Richardson and Davis, 1995) recommends that bridges should be designed to resist the flood event(s) that are expected to produce the most severe scour conditions. HEC-18 recommends the 100-year flood or the overtopping flood when it is less than the 100-year flood. Overtopping refers to flow over the approach embankment(s), the bridge itself or both. Also, investigate other flood events if there is evidence that such events would create deeper scour than the 100-year or overtopping floods. In addition HEC-18 states, "Bridges should be designed to withstand the effects of scour from a super-flood (a flood exceeding the 100-year flood) with little risk of failing. This requires careful evaluation of the hydraulic, structural, and geotechnical aspects of bridge foundation design. It is recommended that this super-flood or check flood be on the order of a 500-year event."The bridge design for the 100 year or overtopping flood should be designed with the normal safety factors but checking the design for the super flood is made with safety factors of 1.0. Also, "The foundation should be designed by an interdisciplinary team of engineers with expertise in hydraulic, geotechnical, and structural design."

TOTAL SCOUR

Total scour at a highway crossing is composed of long-term degradation, general scour (contraction and other general scour), and local scour. The components are assumed additive. In addition, lateral shifting of a stream can cause or increase the scour of bridge foundations. Each of the three types of scour and stream instability are introduced separately below.

Long-Term Aggradation and Degradation

Aggradation is the deposition of sediment in the bridge reach of a stream. Whereas, degradation is the erosion of the sediment in the bridge reach. The former causes the bed elevation to increase and the later causes the bed elevation to decrease. These riverbed elevation changes are over long lengths and time due to natural or man made changes. Long term degradation is defined as long-term scour and is added to the other scour components to obtain total scour but long term aggradation is not usually considered because over time it could stop or change to degradation.

Long-term bed elevation changes (aggradation or degradation) may be the natural trend of the stream or may be the result of some modification to the stream of watershed condition. The streambed may be aggrading, degrading, or not changing in the bridge crossing reach. When the bed of the stream is neither aggrading or degrading, it is considered to be in equilibrium with the sediment discharge supplied to the bridge reach. It is the long-term trends, not the cutting and filling of the bed of the stream that might occur with contraction scour, that must be determined. The engineer must assess the present state of the stream and watershed and determine future changes in the river system, and from this, determine the long-term stream bed elevation changes.

Factors that affect long-term bed elevation changes are dams and reservoirs upstream and downstream of the bridge, changes in watershed land use (urbanization, deforestation, etc.), channelization, cutoff of meander bends (natural or man-made), changes in the downstream base level (control) of the bridge reach, gravel mining from the streambed, diversion of water into or out of the stream, natural lowering of the total system, movement of a bend, bridge location in reference to stream planform and stream movement in relation to the crossing (Keefer et al., 1980). Richardson et al. (1990) provide examples of long-term bed elevation changes.

Analysis of long-term stream bed elevation changes must be made using the principles of river mechanics in the context of a fluvial system analysis. Such analysis of a fluvial system requires the consideration of all influences upon the bridge crossing, i.e., runoff from the watershed to the channel (hydrology), the sediment delivery to the channel (erosion), the sediment transport capacity of the channel (hydraulics), and the response of the channel to these factors (geomorphology and river mechanics). Many of the largest impacts are from man's activities, either in the past, present, or future. Analysis requires a study of the past history of the river and man's activities on it; a study of present water and land use and stream control activities; and finally contacting all agencies involved with the river to determine future changes to the river system.

A method to organize such an analysis is to use a three-level fluvial system approach. This method provides three levels of detail in an analysis (1) a qualitative determination based on general geomorphic and river mechanics relationships, (2) engineering geomorphic analysis using established qualitative and quantitative relationships to establish the probable behavior of the stream system to various scenarios of future conditions, and (3) quantifying the changes in bed elevation using available physical process mathematical models such as BRI-STARS (Molinas, 1993) or HEC-6 (U.S. Army Corps of Engineers, 1993). The approach is extrapolation of present trends, and using engineering judgment to assess the result of the changes in the stream and watershed. Recent FHWA reports, such as "Stream Channel Degradation and Aggradation: Analysis of Impacts to Highway Crossings" (Brown et al., 1980), "Stream Stability at Highway Structures" (Lagasse et al., 1995) and "Highways in the River Environment" (Richardson et al., 1990) discuss methodologies to determine long tem elevation trends. The discussion of degradation, aggradation and sediment transport in Vanoni (1975) is very useful in understanding and determining long term degradation.

General Scour

General scour is a uniform or non-uniform lowering of the waterway bed as the result of the passage of high flow. It may result from contraction of the flow (contraction scour) or the flow around a bend (other general scour). General scour is different from long term degradation in that it may be cyclic and /or related to the passage of a flood.

Contraction Scour Contraction scour occurs when the flow area of a stream at flood stage is reduced, either by a natural contraction or by a bridge and/or its approach embankments. From continuity, a decrease in flow area results in an increase in average velocity and bed shear stress through the contraction. Hence, there is an increase in erosive forces in the contraction and more bed material is removed from the contracted reach than is transported into the reach. This increase in transport of bed material from the reach lowers the bed elevation. As the bed elevation is lowered, the flow area increases and, in the riverine situation, the velocity and shear stress decrease until relative equilibrium is reached. That is, either the quantity of bed material that is transported into the contraction is equal to that removed from the reach, **live-bed scour** or the mean velocity (V) or average shear stress (τ_0) in the contraction is less than the critical velocity (V_c) or critical (τ_c) of the median diameter (D_{50}) of the bed material, **clear-water scour**. Clear-water contraction scour occurs when (1) there is no significant bed material transport in the upstream reach into the downstream bridge reach or (2) the material being transported in the upstream reach is transported through the downstream bridge reach mostly in suspension.

In coastal streams which are affected by tides, as the cross-section area increases the discharge from the ocean may increase and thus the velocity and shear stress may not decrease. Consequently, equilibrium may not be reached. Thus, at tidal inlets which experience clear-water or live-bed scour, contraction scour may result in a continual lowering of the bed (long-term degradation) (Richardson et al., 1993, 1995 and Richardson and Davis, 1995).

Live-bed contraction scour is typically cyclic. That is, the bed scours during the rising stage of a runoff event, and fills on the falling stage. The contraction of flow due to a bridge can be caused by either a natural decrease in flow area of the stream channel or by abutments projecting into the channel and/or the piers blocking a large portion of the flow area. Contraction can also be caused by the approaches to a bridge cutting off floodplain flow. This can cause clear water scour on a setback portion of a bridge section and/or a relief bridge because the floodplain flow does not normally transport significant concentrations of bed material sediments. Other factors that can cause contraction scour are (1) ice formation or jams, (2) natural berms along the banks due to sediment deposits, (3) island or bar formations upstream or downstream of the bridge opening, (4) debris, (5) the growth of vegetation in the channel or floodplain, and (6) pressure flow.

Other General Scour In a natural channel, the depth of flow and velocity are always greater on the outside of a bend. In fact there may well be deposition on the inner portion of the bend at the point bar. Other General Scour at a bridge located on or close to a bend will be concentrated on the outer part of the bend. Also, in bends the thalweg (the part of the stream where the flow is deepest and, typically, the velocity is the greatest) may shift toward the center of the stream as the flow increases. This can increase scour and the nonuniform distribution of the scour in the bridge opening (chute channel).

Local Scour

Erosion of the stream bed around a pier or abutment as the result of the pier or abutment obstructing the flow is *local scour.* These obstructions accelerate the flow and create vortexes that remove bed material around them.

Lateral Shifting of the Stream

In addition to the above, lateral shifting of a stream (stream instability) may erode the approach roadway and abutments of a bridge and/or change the angle of the flow to the piers and abutments (angle of attack). This later can increase local scour at the piers or abutments.

CONTRACTION SCOUR EQUATIONS

Contraction scour equations are based on the principle of conservation of sediment transport. In the case of live-bed scour, this simply means that the fully developed scour in the bridge cross-section reaches equilibrium when sediment transported into the contracted section equals sediment transported out and the conditions for sediment continuity are in balance. For clear-water scour, the transport into the contracted section is essentially zero and maximum scour occurs when the shear stress reduces to the critical shear stress of the bed material.

To determine if the contraction scour at a bridge is **clear-water** or **live-bed** determine if the critical velocity (V_c) or critical shear stress (τ_c) of the median diameter (D_{50}) of the bed material in the channel upstream from the bridge opening is larger than the average velocity or shear stress (clear-water scour) or smaller (live-bed scour). **Or calculate the contraction scour depths using both equations and take the smaller scour depth (Richardson and Davis, 1995).**

Live-Bed Contraction Scour Equation

Richardson and Davis (1995) in HEC-18 recommend a modified Laursen (1960) equation for live-bed contraction scour. It is based on a simplified transport function (Laursen, 1956) to obtain equilibrium sediment transport in a long contraction. In short contractions such as at a bridge it over estimates the scour depth (Richardson and Davis, 1995). The equation is:

$$\frac{y_2}{y_1} = \left(\frac{Q_2}{Q_1}\right)^{\frac{6}{7}} \left(\frac{W_1}{W_2}\right)^{K_1} \tag{1}$$

$y_s = y_2 - y_0 =$ (Average scour depth, m)

where:

y_1	=	average depth in the upstream main channel, m
y_2	=	average depth in the contracted section, m
y_0	=	average depth in the contracted section before contraction scour, m
W_1	=	bottom width of the upstream main channel, m
W_2	=	bottom width of main channel in the contracted section, m
Q_1	=	flow in the upstream channel transporting sediment, m^3/s, cms
Q_2	=	flow in the contracted channel, cms. Often this is equal to the total discharge unless the total flood flow is reduced by relief bridges or water overtopping the approach roadway
k_1	=	exponents determined below depending on the mode of bed material transport
V_*	=	$(gy_1S_1)^{1/2}$ shear velocity in the upstream section, m/s
w	=	median fall velocity of the bed material based on the D_{50} (see Figure 2)
g	=	acceleration of gravity (9.81 m/s^2)

S_1 = slope of energy grade line of main channel, m/m
D_{50} = median diameter of the bed material, m

Any set of consistent units (English or Metric) can be used.

The value of y_0 may be difficult to determine because of residual contraction scour from previous floods or other factors. Never-the-less, y_0 must be determined. A reasonable value can be determined by a study of the channel using cross-sections and longitudinal profiles from upstream, through the bridge, and downstream.

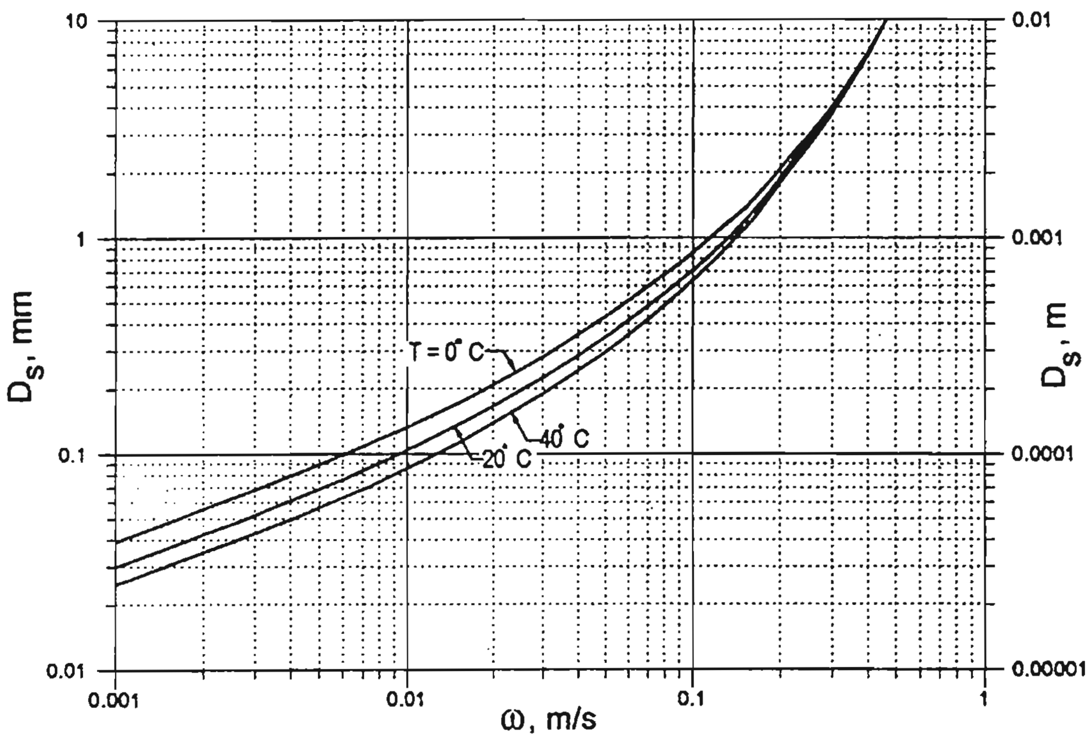

Figure 2. Fall Velocity of Sand-Sized Particles.

Clear-Water Contraction Scour Equations

Following a development given by Laursen (1963) Richardson and Davis (1995) developed the following equations for determining the clear-water contraction scour in a long contraction:

$$\tau_0 = \tau_c \tag{2}$$

where:

τ_0	=	average bed shear stress, contracted section, N/m_2
τ_c	=	critical bed shear stress at incipient motion, N/m^2

The average bed shear stress using y for the hydraulic radius (R) and the Manning equation to determine the slope (S_f) can be expressed as:

$$\tau_0 = \gamma y S_f = \frac{\rho g V^2 n^2}{y^{\frac{1}{3}}} \tag{3}$$

For noncohesive bed materials and for fully developed clear-water contraction scour the critical shear stress can be determined using Shields (Vanoni, 1975) relation.

$$\tau_c = K_s (\rho_s - \rho) g D \tag{4}$$

The bed in a long contraction scours until $\tau_0 = \tau_c$ resulting in the following:

$$\frac{\rho g n^2 V^2}{y^{1/3}} = K_s \ (\rho_s - \rho) g D \tag{5}$$

Solving for the depth (y) in the contracted section gives:

$$y = \left[\frac{n^2 V^2}{K_s (S_s - 1) D}\right]^3 \tag{6}$$

In terms of discharge (Q) the depth (y) is

$$y = [\frac{n^2 Q^2}{K_s \ (S_s - 1) \ D \ W^2}]^{3/7} \tag{7}$$

where:

V	=	average velocity in the contracted section, m/s
Q	=	discharge, m^3/s or cms
D	=	diameter of smallest non transportable bed material particle, m

γ	=	the unit weight of water (9,800 N/m^3)
n	=	Manning roughness coefficient
K_s	=	Shield's coefficient
S_s	=	specific gravity (2.65 for quartz)
ρ	=	density of water (999 kg/m^3)
ρ_s	=	density of sediment (quartz 2,647 Kg/m^3)
g	=	acceleration of gravity (9.81 m/s^2)

Equation 7 is the basic equation for the clear-water scoured depth (y) in a long contraction. Shield's coefficient for initiate of motion ranges from 0.03 to 0.1 (Vanoni, 1975). Strickler's equation for n given by Laursen, in metric units, is $n = 0.041\ D^{1/6}$. Research discussed in Richardson et al. (1990) recommends the use of the effective mean bed material size (D_m) in place of the D_{50} size. The use of D_m would also be in accordance with the work of Froehlich (1995). D_m is approximately 1.25 $D_{50.}$ Using K_s of 0.039, $n = 0.041\ D_m^{\ 1/6}$ and $S_s = 2.65$ in Equation 7 results in:

$$y = [\frac{0.025\ Q^2}{D_m^{\ 2/3}\ W^2}]^{3/7} \tag{8}$$

$$y_s = y - y_0 \qquad \text{(Average scour depth)} \tag{9}$$

where:

D_m	=	diameter of the bed material (1.25 D_{50}) in the contracted section, m
y_s	=	depth of scour in the contracted section, m
y_0	=	original depth in the contracted section before scour, m

Other variables as previously defined.

Clear-water contraction scour equations assume homogeneous bed materials. However, in stratified materials, the clear-water contraction scour equation could be used sequentially.

Both the live-bed and clear-water contraction scour equations are the best that are available and should be regarded as a first level of analysis. If a more detailed analysis is warranted, a sediment transport model such as BRI-STARS (Molinas, 1993) or HEC-6 (U.S. Army Corps of Engineers, 1993) could be used.

CRITICAL VELOCITY FOR MOVEMENT OF BED MATERIAL

The velocity and depth given in Equations 6 are associated with initiation of motion of the indicated size (D). Rearranging Equation 6 to give the critical velocity for beginning of motion of bed material of size D result in:.

$$V_c = \frac{K_s^{1/2}\,(S_s - 1)^{1/2}\,D^{1/2}\,y^{1/6}}{n} \tag{10}$$

Using $K_s = 0.039$, $S_s = 1.65$, and $n = 0.041\,D^{1/6}$

$$V_c = 6.19\,y^{1/6}\,D^{1/3} \tag{11}$$

where:

V_c = Critical velocity above which bed material of size D and smaller will be transported, m/s

Other variables as previously defined.

Additional discussion of beginning of motion is given in Vanoni 1975, pages 91 to 107 for non-cohesive sediments and 107 to 114 for cohesive sediments.

LOCAL SCOUR

The basic mechanism causing local scour at piers or abutments is the formation of vortices at their base (known as the horseshoe and wake vortexes at a pier, Figure 3, and horizontal and vertical vortexes at an abutment, Figure 4). The horseshoe and horizontal vortexes results from the pileup of water on the upstream surface of the obstruction and subsequent acceleration of the flow around the nose of the pier or abutment. The action of the vortex removes bed material from around the base of the obstruction. The transport rate of sediment away from the base region is greater than the transport rate into the region, and, consequently, a scour hole develops. As the depth of scour increases, the strength of the vortex is reduced, thereby reducing the transport rate from the base region. Eventually, for live-bed local scour, equilibrium is reestablished and scouring ceases. For clear-water scour, scouring ceases when the shear stress caused by the horseshoe vortex equals the critical shear stress of the sediment particles at the bottom of the scour hole.

In addition to the horseshoe vortex around the base of a pier, there are vertical vortices downstream of the pier called the wake vortex (Figure 3). Both the horseshoe and wake vortices remove material from the pier base region. However, the intensity of wake vortices diminishes rapidly as the distance downstream of the pier increases. Therefore, immediately downstream of a long pier there is often deposition of material.

Factors which affect the magnitude of local scour at piers are (1) width of the pier; (2) length of the pier if skewed to flow; (3) depth; (4) velocity of the approach flow upstream of the pier; (5) size and gradation of bed material; (6) angle of attack of the approach flow; (7) shape; (8) bed configuration; (9) ice formation or jams; and (10) debris. The scour results from free surface flow unless the bridge is submerged or overtopped. Then the scour results from pressure flow. The shape of many piers is complex. The piers may rest on footings or pile caps on piles. The footings or pile caps may be at the bed, in the flow or at the mean water elevation by design or erosion.

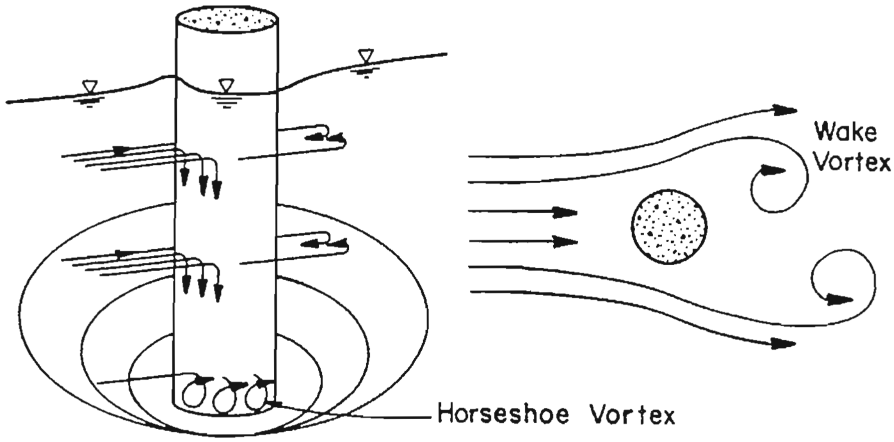

Figure 3. Schematic of scour at a cylindrical pier (Richardson and Davis, 1995).

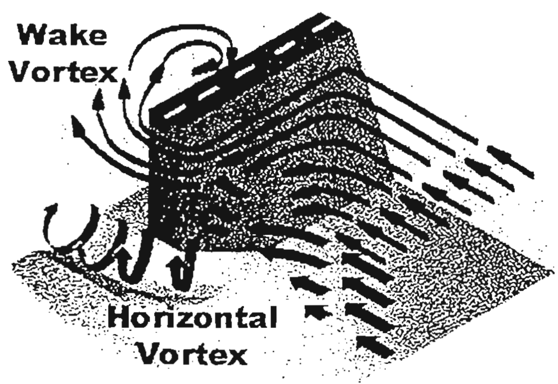

Figure 4. Schematic representation of scour at an abutment (Richardson, 2000).

In Figure 5, from flume studies in sand bed material, the ratio of scour depth to pier width (y_s/a) as a function of the ratio of approach velocity to critical velocity (V/V_c) for different size bed material is given. Non-dimensional scour (y_s/a) starts when the mean approach velocity is approximately 0.5 V_c (the critical velocity for the beginning of motion of the bed material) (V/V_c = 0.5) and reaches a maximum when the ratio equals 1.0. This maximum value of the non-dimensional scour depth decreases with a decrease in the bed material size. The scour that takes place from $V/V_c = 0.5$ to 1.0 is clear water scour. For values of $V/V_c > 1.0$ the scour is live bed. As can be seen from Figure 5 after $V/V_c = 1.0$ The non-dimensional scour depth decrease and then increases. The bed configuration after $V/V_c = 1.0$ in the flumes is either ripples or dunes. When the live-bed scour non-dimensional depth starts to increase with an increase in V/V_c the bed configuration is changing to plain bed and antidunes. The increase in non-dimensional scour depth results because with plain bed and antidune flow conditions some of the sediment in transport washes through the scour hole. At large values of V/V_c the scour condition is similar to clear-water scour. That is, the bed material that is being transported upstream of the pier is swept through the scour hole and takes no part in the scouring process.

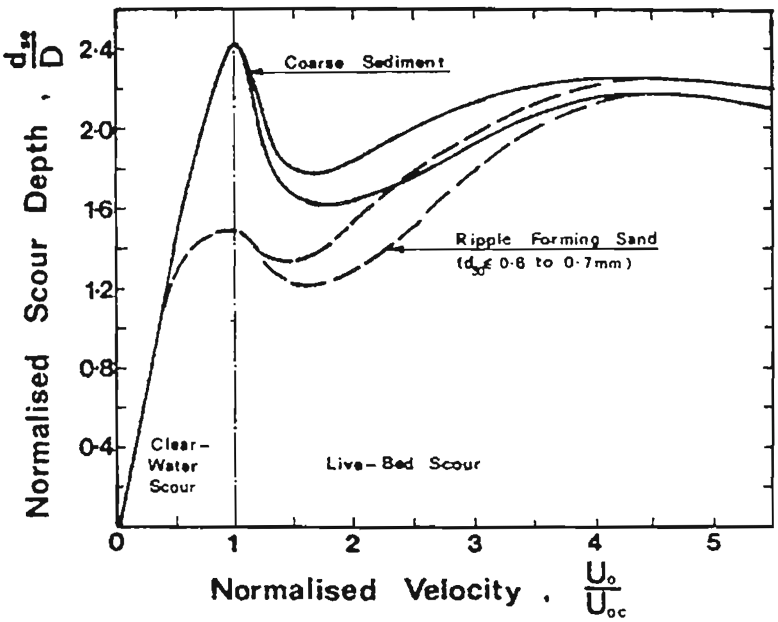

Figure 5. Non-dimensional local scour depth as a function of non- dimensional velocity and bed material size (Melville, 1984).

At abutments in addition to the horizontal vortex that forms around and erodes its base there is a vertical vortex that results from flow separation at the downstream side of the abutment (Figure 4). This vortex erodes the approach embankment and the abutment foundations on the downstream corner and side. Thus, there are two scour problems at abutments, (1) a scour hole at the abutment base resulting from the horizontal vortex and (2) erosion of the downstream approach embankment and abutment foundation by the vertical vortex caused by the flow separation.

Factors which affect the magnitude of local scour at abutments are (1) discharge intercepted by the abutment and returned to the main channel at the abutment (in laboratory flumes this discharge is a function of projected length of an abutment and approach roadway into the flow); (2) depth of flow, (3) velocity of the flow at the upstream and downstream end of the abutment; (3) size and gradation of bed material; (4) angle of attack of the approach flow; (5) shape; (6) bed configuration; (7) ice formation or jams; and (8) debris. The scour results from free surface flow unless the bridge is submerged or overtopped. Then the scour results from pressure flow. As with piers abutments may have complex shape.

EQUATION FOR LOCAL SCOUR DEPTH AT PIERS

Local scour at piers has been studied extensively since the late 1940s (Laursen, 1958, 1960, 1963, and Laursen and Toch, 1956) (Richardson and Lagasse, 1999, p. 13). As a result of the many studies there are many equations. In general the equations are for ultimate (maximum scour) in sand beds. In preparation of the Interim Procedures and the subsequent HEC-18's, a study was made of the more common pier scour equations. The study utilized Jones (1983) report but included additional equations such as Melville and Sutherland's (1988). The study determined that the Colorado State University (CSU) (Richardson et al., 1990) equation enveloped all the scour data, but gave lower values of scour than the other equations such as Jain and Fischer's (1979), Laursen's (1960), Melville and Sutherland's (1988), and Neill's (Blench, 1969) equations.

A recent study of 22 scour equation using field data presented by Landers and Mueller (1996) and Richardson and Lagasse, (1999, p. 585) indicated the HEC-18 equation was good for design because it rarely under predicted measured scour depth, but frequently grossly over predicted the observed scour (Mueller, 1996). The data contained 384 measurements of scour at 56 bridges. The HEC-18 equation slightly under predicted 6 of the 384 scour measurements. The maximum deviation was 3 ft when the scour depth was 25 ft. The HEC-18 equation over estimated scour in course bed streams because of restriction placed on a correction factor K_4 for coarse bed material. A K_4 factor for coarse bed material developed by Mueller (1996) decreased the over prediction without changing the under prediction.

HEC-18 PIER SCOUR EQUATION (RICHARDSON AND DAVIS, 1995)

The HEC-18 for both live-bed and clear-water pier scour equation is:

$$\frac{y_s}{y_1} = 2.0\, K_1\, K_2\, K_3\, K_4 \left(\frac{a}{y_1}\right)^{0.65} Fr_1^{0.43} \tag{12}$$

In terms of y_s/a, Equation 12 is:

$$\frac{y_s}{a} = 2.0\, K_1\, K_2\, K_3\, K_4 \left(\frac{y_1}{a}\right)^{0.35} Fr_1^{0.43} \tag{13}$$

$$y_s \le 2.4\, a \qquad Fr < 0.8 \tag{14}$$
$$y_s \le 3.0\, a \qquad Fr > 0.8$$

where:

y_s	=	scour depth, m
y_1	=	flow depth directly upstream of the pier, m
K_1	=	correction factor for pier nose shape from Figure 6 and Table 1
K_2	=	correction factor for angle of attack of flow from Equation 15 or Table 2
K_3	=	correction factor for bed condition from Table 3
K_4	=	correction factor for size of bed material
a	=	pier width, m
L	=	length of pier, m
Fr_1	=	Froude Number = $V_1/(gy_1)^{½}$
V_1	=	Mean velocity of flow directly upstream of the pier, m/s

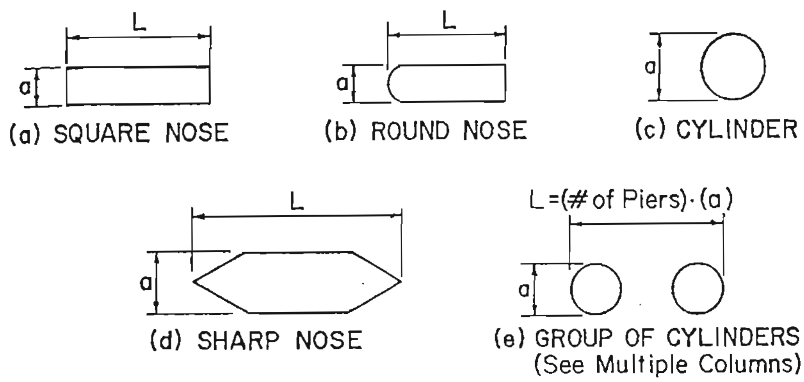

Figure 6. Common Pier Shapes.

Table 1. Correction Factor K_1 for Pier Nose Shape.	
Shape of Pier Nose	K_1
(a) Square nose	1.1
(b) Round nose	1.0
© Circular cylinder	1.0
(d) Sharp nose	0.9
(e) Group of cylinders	1.0

Table 2. Correction for Angle of Attack θ of the Flow.			
Angle	L/a=4	L/a=8	L/a=12
0	1.0	1.0	1.0
15	1.5	2.0	2.5
30	2.0	2.75	3.5
45	2.3	3.3	4.3
90	2.5	3.9	5.0
Angle = skew angle of flow L = length of pier, m			

Table 3. Increase in Equilibrium Pier Scour Depths (K_3) for Bed Condition.		
Bed Condition	Dune Height m	K_3
Clear-Water Scour	N/A	1.1
Plane bed and Antidune flow	N/A	1.1
Small Dunes	3> H < 0.6	1.1
Medium Dunes	9> H >3	1.1 to 1.2
Large Dunes	H >9	1.3

Note: 1. The correction factor K_1 for pier nose shape should be determined using Table1 for angles of attack up to 5 degrees. For greater angles, K_2 dominates and K_1 should be considered as 1.0. If L/a is larger than 12, use the values for L/a = 12 as a maximum.

Note: 2. The correction factor for angle of attack of the flow K_2 given in Table 2 can be calculated using the following equation:

$$K_2 = (\text{Cos } \theta + L / a \text{ Sin } \theta)^{0.65} \tag{15}$$

If L/a is larger than 12, use L/a = 12 as a maximum in Equation 15.

Note: 3. The correction factor K_3 results from the fact that for plane-bed conditions, which is typical of most bridge sites for the flood frequencies employed in scour design, the maximum scour may be 10 percent greater than computed with the CSU equation (Richardson et al., 1990). In the unusual situation where a dune bed configuration with large dunes exists at a site during flood flow, the maximum pier scour may be 30 percent greater than the predicted value. This may occur on very large rivers, such as the Mississippi. For smaller streams that have a dune bed configuration at flood flow, the dunes will be smaller and the maximum scour may be only 10 to 20 percent larger than equilibrium scour. For antidune bed configuration the maximum scour depth may be 10 percent greater than the computed equilibrium pier scour depth.

Note: 4. Equation 14 results from observations by Chang, (Richardson and Davis, 1995) and Melville and Sutherland (1988) that there was an upper limit of the ratio of scour depth to pier width (y_s/a) for cylindrical piers for Froude Number was less than 1.0. Research by Jain and Fischer (1979) obtained values of the ratio of 3 for Froude Numbers larger than 1.0. These upper limits were derived for circular piers and were uncorrected for pier shape and for skew. Also, pressure flow or debris can increase the ratio.

Mueller (1996) K_4 Correction Coefficient

Mueller (1996) developed a K_4 correction coefficient from a study of 384 field measurements of scour at 56 bridges. It is as follows:

$$K_4 = 1 \text{ if } D_{50} < 2 \text{ mm or } D_{95} < 20 \text{ mm} \tag{16}$$

if D_{50} >=2 mm and D_{95} >= 20 mm

then

$$K_4 = 0.4\,(K_5)^{0.15}$$

where

$$K_5 = \frac{V_1 - V_{icD_{50}}}{V_{cD_{50}} - V_{icD_{95}}} > 0 \tag{17}$$

V_{icDx} = the approach velocity corresponding to critical velocity for incipient scour in the accelerated flow region at the pier for the grain size D_x, m/s

$$V_{icD_x} = 0.645\left(\frac{D_x}{a}\right)^{0.053} V_{cD_x} \tag{18}$$

V_{cDx} = critical velocity for incipient motion for the grain size D_x ,m/s.

Mueller (1996) used a variable Shield's parameter to define the critical velocity for incipient motion. However, for the coarser size of bed material for which K_4 is applicable it can be determined using Equation 11.

Although this K_4 provides a good fit with the field data the velocity ratio terms so formed that if D_{50} is held constant and D_{95} increases the value of K_4 increases rather than decrease (Mueller and Jones, 2000). For field data an increase in D_{95} was always accompanied with an increase in D_{50}.

Pier Scour for Exposed Footings

Pier footings and/or pile caps may become exposed to the flow by long-term degradation, contraction scour, or lateral shifting of the stream. Computations of local pier scour depths for footings or pile caps exposed to the flow based on footing or pile cap width appear to be too conservative. Calculations of scour depths for the Schoharie Creek bridge failure were closer to the measured model and prototype scour depths when pier width was used rather than footing width (Richardson et al., 1987). A model study of scour at the Acosta Bridge at Jacksonville, Florida, by Jones (1989) found that when the top of the footing was flush with the streambed, local scour was 20 percent less than for other conditions tested. In a generalized study, it was found that a footing extending upstream of the pier reduced pier scour when the top of the footing was located flush or below the bed, but scour holes became deeper and larger in proportion to the extent that the footing projected into the flow field. Based on this study, the following recommendation was made for calculating pier scour if the footing is or may be exposed to the flow in HEC-18 (Richardson and Davis, 1995).

> "It is recommended that the pier width be used for the value of 'a' in the pier scour equations if the top of the footing (or pile cap) is at or below the streambed (after taking into account long-term degradation and contraction scour). If the pier footing extends above the streambed, make a second computation using the width of the footing for the value of "a" and the depth and average velocity in the flow zone obstructed by the footing for the 'y' and 'V' respectively in the scour equation. Use the larger of the two scour computations."

The average velocity in the flow zone obstructed by the footing (V_f) is determined using the following equation:

$$\frac{V_f}{V_1} = \frac{\ln\left(10.93\frac{y_f}{k_s}+1\right)}{\ln\left(10.93\frac{y_1}{k_2}+1\right)} \tag{19}$$

where:

V_f	=	average velocity in the flow zone below the top of the footing, m/s
y_f	=	distance from the bed to the top of the footing, m
k_s	=	grain roughness of the bed, normally taken as the D_{84} of the bed material, m
y_1	=	depth of flow upstream of the pier, m

The values of V_f and y_f would be used in Equation 12 to compute the depth of scour for the footing to be compared to the depth of scour for the pier width.

Pier Scour for Exposed Pile Groups

Experiments were conducted by Jones (1989) to determine guidelines for specifying the characteristic width of a simple pile group (Figure 7) that are or may be exposed to the flow (as the result of long-term degradation and/or contraction scour) when the piles are uniformly spaced laterally as well as longitudinally in the stream flow. The following was concluded:

> "Pile groups that project above the streambed [as the result of long-term degradation and/or contraction scour] can be analyzed conservatively by representing them as a single width equal to the projected area of the piles ignoring the clear space between piles. Good judgment needs to be used in accounting for debris because pile groups tend to collect debris that could effectively clog the clear spaces between pile and cause the pile group to act as a much larger mass."

For example, five 0.41-meter cylindrical piles spaced at 1.8 meters (Figure7) would have an 'a' value of 2.05 meters. This composite pier width would be used in Equation 12 to determine depth of pier scour. The correction factor K_1 in Equation 12 for the multiple piles would be 1.0 regardless of shape. If the pile group is a square as in Figure7 then K_2 would be 1.0. However, if the pile group is a rectangle use the dimensions as if they were a single pier and the appropriate L/a value for determining K

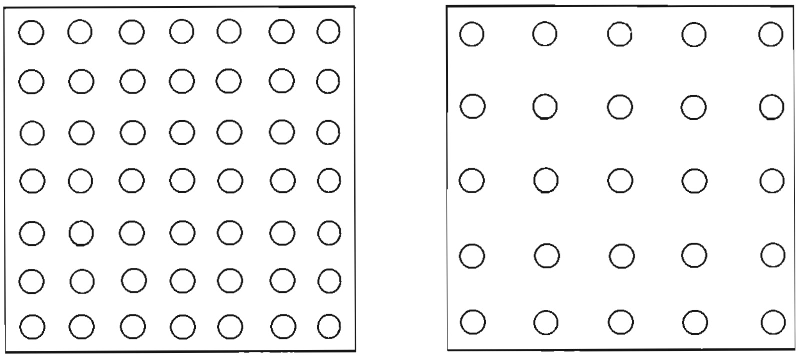

Figure 7. Simple Pile Groups.

The depth of scour for exposed pile groups will be analyzed in this manner except when addressing the effect of debris lodged between piles. If debris is evaluated, it would be logical to consider the multiple columns and debris as a solid elongated pier. The appropriate L/a value and flow angle of attack would then be used to determine K_2. If the pile group is exposed to the flow as the result of local scour then it is unnecessary to consider the piles in calculating pier scour.

An alternate procedure for pile groups was given by M. Salim and J.S. Jones (1996, Richardson and Lagasse, 1999, p. 335) from research at the Turner-Fairbank Highway Research Center. The scour depth is computed using Equation 12 assuming an equivalent solid pile group with piles touching each other set at the same skew angle to the flow direction. This scour depth is corrected using the following factors.

$$y_{s\ \text{pile group}} = K_s K\alpha\, y_s \tag{20}$$

$$K_s = 0.57\left(1 - e^{(1-S/a)}\right) + e^{0.5(1-S/a)} \tag{21}$$

where:

S	=	spacing between centers of the piles
a	=	diameter of the piles
K_s	=	correction factor for spacing
$K\alpha$	=	correction factor for angle of attack on simple pile groups, Figure 8
y_s	=	scour depth of an equivalent solid pier set at the same skew angle to the flow

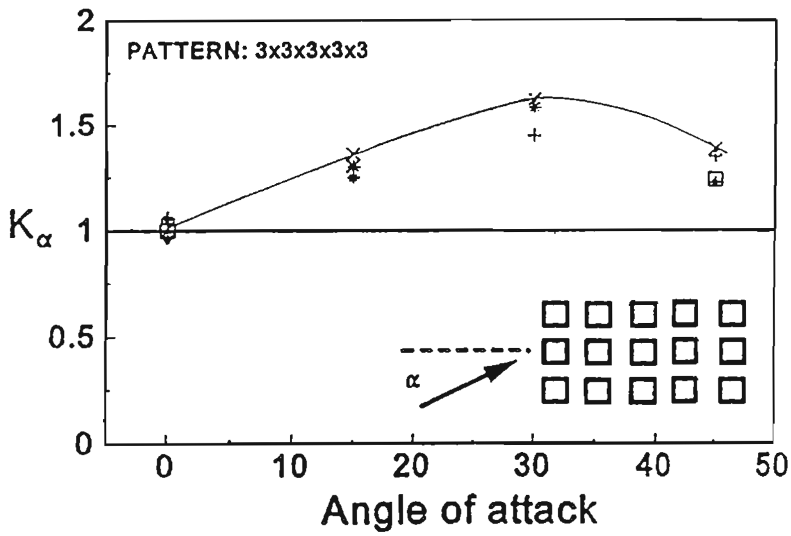

Figure 8. K_α as a function of angle of attack (after Salim and Jones, 1996).

Scour depths for complex pile groups (not uniformly spaced laterally and longitudinally in the stream flow) can not be determined by these methods. Scour for complex pile groups would require a physical model study.

Pile Caps Placed at the Water Surface or in the Flow

For pile caps placed at or near the water surface or in the flow, HEC-18 (Richardson and Davis, 1995) recommended that the scour analysis include computation of scour caused by the exposed pile group, computation of the pier scour caused by the pile cap and pier scour caused by the pier if the pier is partially submerged in the flow. A conservative estimate of local scour will be the largest pier scour computed from these three scenarios

When computing the pier scour caused by the pile cap, a conservative estimate is to assume that the pile cap is resting on the bed and determine V_f and y_f from Equation 19. Use Equation 12 for pile cap, pier shaft and exposed pile groups as recommended in the previous discussions. Research is underway to develop a less conservative and more realistic equation (Salam and Jones, 1996 and Jones, 1998)

Multiple Columns Skewed to the Flow

Scour depth for multiple columns (as illustrated as a group of cylinders in Figure 6) skewed to the flow, depends on the spacing between the columns. The correction factor for angle of attack would be smaller than for a solid pier. How much smaller is not known. Raudkivi (1986) in discussing effects of alignment states "..the use of cylindrical columns would produce a shallower scour; for example, with five-diameter spacing between columns the local scour can be limited to about 1.2 times the local scour at a single cylinder." Thus for multiple columns spaced 5 diameters or more apart and at an angle Richardson and Davis (1995) recommend that the local scour depth can be taken as 1.2 times the local scour depth at a single column.

For multiple columns spaced less than 5 pier diameters apart, the pier width 'a' is the total projected width of all the columns in a single bent, normal to the flow angle of attack. This composite pier width would be used in Equation 12 to determine depth of pier scour. The correction factor K_1 would be 1.0 regardless of column shape. The coefficient K_2 would also be equal to 1.0 since the effect of skew would be accounted for by the projected area of the piers normal to the flow (Richardson and Davis, 1995).

The depth of scour for a multiple column bent will be analyzed in this manner except when addressing the effect of debris lodged between columns. If debris is evaluated, it would be logical to consider the multiple columns and debris as a solid elongated pier.

Pressure Flow Scour

Pressure flow, which is also denoted as orifice flow, occurs when the water surface at the upstream face of the bridge is greater than or equal to the low chord of the bridge superstructure and the water is in significant contact with the bridge deck. At higher approach flow depths, the bridge can be entirely submerged with the resulting flow being a complex combination of the plunging flow under the bridge (orifice flow) and flow over the bridge (weir flow). In many cases, when a bridge is submerged, flow will also overtop adjacent approach embankments. Hence, for any overtopping situation, the total weir flow can be subdivided into weir flow over the bridge and weir flow over the approach.

Abed (Abed, 1991, and Abed et al., 1991), from a limited clear-water flume study at Colorado State University, stated that pressure flow could increase pier scour depths by 2.3 to 10 times. These results were obtained by comparison of scour depths for free surface and pressure flow simulations with similar hydraulic characteristics. However, sometimes when a bridge becomes submerged, the average velocity under the bridge is reduced due to a combination of additional backwater caused by the bridge superstructure impeding the flow, and a reduction of the discharge which passes under the bridge due to weir flow over the bridge and approach embankments. As a consequence scour depths are reduced.

Jones (Jones et al., 1993, 1996 and Richardson and Lagasse, 1999, p. 288) in clear-water pressure flow studies at FHWA's Turner-Fairbank Research Center, found that (1) local pier scour with pressure flow has two components; (2) one component is vertical contraction scour caused by the bridge superstructure and the other is local pier scour caused by the pier obstructing the flow; (3) the magnitude of the local pier scour with pressure flow is approximately the same as for free surface flow; and (4) that the two components are additive.

Arneson (1997, Arneson and Abt, 1998), in a comprehensive live-bed flume study of pressure flow scour sponsored by the FHWA verified Jones findings. Equation 12 is used to determine the local pier scour component caused by the pier obstructing the flow. For the vertical contraction pier scour component he developed the following equation.

$$\frac{y_{cps}}{y_1} = -5.08 + 1.27\left(\frac{y_1}{H_b}\right) + 4.44\left(\frac{H_b}{y_1}\right) + 0.19\left(\frac{V_b}{V_c}\right) \tag{22}$$

where:

y_{cps}	=	depth of vertical contraction deck scour, m
y_1	=	flow depth upstream of bridge deck, m
H_b	=	distance from bridge deck to channel bed, m
V_b	=	average velocity of flow through bridge opening, m/s
V_c	=	critical velocity of the bed material, m/s

Scour Depths With Debris

Debris lodged on a pier usually increases local scour at a pier. The debris may increase pier width, local velocity and deflect the flow downward. This increases the transport of sediment out of the scour hole. When floating debris is lodged on the pier, the scour depth is estimated by assuming that the pier width is larger than the actual width. The problem is in determining the increase in pier width to use in the pier scour equation. Furthermore, at large depths, the effect of the debris on the scour depths should diminish. Also, debris lodged on piers and abutments can deflect the flow against another pier of abutment resulting in very large angles of attack, and larger velocities. This may be worse than the scour at the pier or abutment with the debris.

As with estimating local scour depths with pressure flow, only limited research has been done on local scour with debris. Melville and Dongol (1992) have conducted a limited quantitative study of the effect of debris on local pier scour and have made some recommendations. However, additional laboratory studies will be necessary to better define the influence of debris on local scour.

TOPWIDTH OF PIER SCOUR HOLES

The topwidth of a scour hole in cohesionless bed material from one side of a pier or footing can be estimated from the following equation (Richardson and Abed, 1993), Richardson and Davis, 1995), and Richardson and Lagasse, 1999, p. 311):

$$W = y_s\,(K + \cot\theta) \tag{22}$$

where:

W	=	topwidth of the scour hole from each side of the pier or footing, m
y_s	=	scour depth, m
K	=	bottom width of the scour hole as a fraction of scour depth
θ	=	Angle of repose of the bed material and ranges from about 30° to 44°

If the bottom width of the scour hole is equal to the depth of scour y_s (K = 1) the topwidth in cohesionless sand would vary from 2.07 to 2.80 y_s. At the other extreme if K = 0, the topwidth would vary from 1.07 to 1.8 y_s. Thus, the topwidth could range from 1.0 to 2.8 y_s and will depend on the bottom width of the scour hole and composition of the bed material. In general, the deeper the scour hole, the smaller the bottom width. A topwidth of 2.0 y_s is suggested for practical application.

LOCAL SCOUR AT ABUTMENTS

Local scour at abutments has two components (see earlier discussion and Figure 4). This vertical vortex There are no equations to determine the erosion caused by the downstream vertical vortex which erodes the downstream corner of the abutment and approach roadway. The abutment is protected from erosion caused by this vertical vortex by riprap or a short guidebank (Lagasse et al., 1995). Available equations are for the scour caused by the horizontal vortex.

Equations for predicting local scour depths caused by the horizontal vortex are almost all based on laboratory data. For example the equations by Liu et al. (1961), Laursen and Toch (1956), Laursen (1980), Froehlich (1989), and Melville (1992, 1997). The problem is that little field data on abutment scour exist.

All equations in the literature, prior to 1993, were developed using the abutment and roadway approach length (L) as one of the variables and result in excessively conservative estimates of scour depth. As Richardson and Richardson (1992 and 1998) point out in a discussion of Melville's (1992 and 1997) papers and in a 1993 paper the reason the equations in the literature predict excessively conservative abutment scour depths for the field situation is that, in the laboratory flume, the discharge intercepted by the abutment is directly related to the abutment length; whereas, in the field, this is rarely the case. Thus, using the abutment length in the equations instead of the discharge returning to the main channel at the abutment results in a spurious correlation between abutment lengths and scour depth. Therefore, engineering judgment is required in designing foundations for abutments. In most cases, foundations can be designed with shallower depths than predicted by the equations when the foundations are protected with rock riprap and/or a guide bank (Richardson and Davis, 1995). The design of guide banks is given Lagasse et al., (1995).

Abutment Site Conditions

Abutments can be at the channel bank, set back from the natural stream bank or project into the channel. They can have various shapes and can be set at varying angles to the flow. Scour at abutments can be live-bed or clear-water scour. Finally, there can be varying amounts of overbank flow intercepted by the approaches to the bridge and returned to the stream at the abutment. More severe abutment scour will occur when the majority of overbank flow returns to the bridge opening directly upstream of the bridge crossing. Less severe abutment scour will occur when overbank flows gradually return to the main channel upstream of the bridge crossing.

Abutment Shape

There are three general shapes for abutments: (1) spill-through abutments, (2) vertical-wall abutments with wing walls, and (3) vertical walls without wing walls. Depth of scour is approximately double for vertical-wall abutments as compared with spill-through abutments. In Table 4 coefficients for correcting scour equations for abutment shape (Froehlich, 1989) is given.

Table 4. Abutment Shape Coefficients (Froehlich, 19989)

Description	K_1
Vertical-wall abutment	1.00
Vertical-wall abutment with wing walls	0.82
Spill-through abutment	0.55

Skew Adjustment of Abutment Scour Depths

Figure 9 shows the effect of flow angle of attack on abutment scour (Ahmed, 1953). As shown an abutment or spur angled downstream decreases scour depth. Whereas an abutment angled upstream into the flow increases the scour depth.

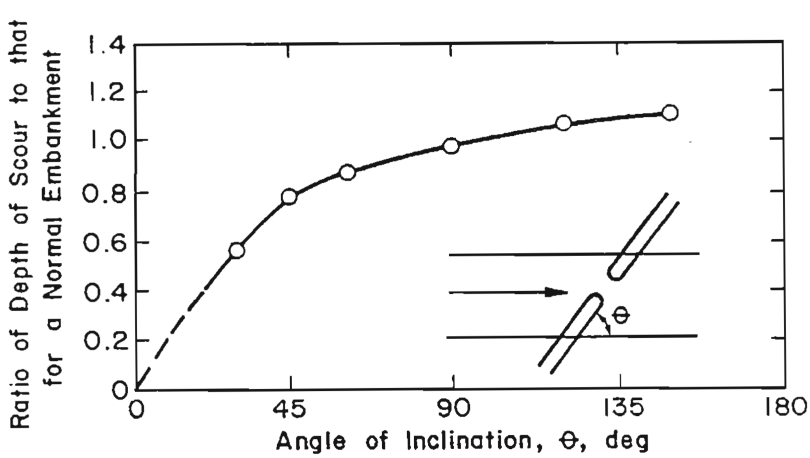

Figure 9. Adjustment of Abutment Scour Estimate for Skew (After Ahmad, 1953).

Design for Scour at Abutments

The lack of adequate abutment scour equations (fundamentally wrong and over conservative) lead the Federal Highway Administration to recommend that foundation depths for abutments be set at least 1.8 meters below the streambed, including long-term degradation and contraction scour and protect the foundations with rock riprap and/or guide banks (Richardson and Davis, 1995). To aid in design of the foundations Froehlich's's (1989) live-bed scour equation for L/y < 25 and a modification of HIRE's (Richardson et al., 1990) equation for L/y > 25 were given. The HIRE equation was based on field data of scour at the end of spurs in the Mississippi River (obtained by the US Corps of Engineers.

Froehlich's Abutment Scour Equation for L/y < 25

$$\frac{y_s}{y_a} = 2.27\, K_1\, K_2 \left(\frac{L'}{y_a}\right)^{0.43} Fr^{0.61} + 1 \tag{24}$$

where:

K_1	=	Coefficient for abutment shape (see table 4)
K_2	=	Coefficient for angle of embankment to flow
K_2	=	$(\theta/90)$ (see figure 9 for definition of θ) $\theta<90^0$ if embankment points downstream $\theta>90^0$ if embankment points upstream
L'	=	Length of abutment (embankment) projected normal to flow, m
A_e	=	Flow area of the approach cross section obstructed by the embankment, m^2
Fr	=	Froude Number of approach flow upstream of the abutment, $V_e/(gy_a)^{1/2}$
V_e	=	Q_e/A_e, m/s
Q_e	=	Flow obstructed by the abutment and approach embankment, m^3/s
y_a	=	Average depth of flow on the floodplain, m
y_s	=	Scour depth, m

The 1 added to the equation caused it to envelope 98 percent of the data in the development of the equation by statistical methods.

HEC-18 Equation for L/y > 25

$$\frac{y_s}{y_1} = 4\ Fr^{0.33}\ \frac{K_1}{0.55} \tag{25}$$

where:

y_s	=	Scour depth, m
y_1	=	Depth of flow at the abutment on the overbank or in the main channel, m

Fr	=	Froude Number based on the velocity and depth adjacent to and upstream of the abutment
K_1	=	Abutment shape coefficient (from table 4)

To correct equation 25 for abutments skewed to the stream, use Figure 9.

Recent Abutment Scour Depth Equations

Recent abutment scour equations have appeared in the literature that are not based on the abutment length but on the flow intercepted by the abutment and approach embankment. These are:

1. Chang and Davis equation (Richardson and Lagasse, 1999, p. 401) which is based on Laursen, live bed contraction scour equation.

2. Strum (1999) equation for abutments in compound with variable set backs from the main channel.

3. Richardson and Trivino (1999) equation based on momentum exchange

4. Kouchakzadeh and Townsend (Richardson and Lagasse, 1999, p. 417) equation based on momentum exchange.

These equations have not been tested in the field so the 1995 HEC-18 recommendations are still valid in the U.S.

COMPUTER MODELS

The hydraulic bridge routines of either the computer models WSPRO (Shearman, J.O., 1987) or HEC-RAS (U.S. Corps of Engineers, 1997, Richardson and Lagasse, 1999, p. 669) can determine the one-dimensions flow variable for use in the determination of scour depths at a bridge. These models determine average flow depths and velocities over the roadway and bridge, as well as average velocities and depths approaching and under the bridge.

STREAM INSTABILITY

Streams are dynamic. Areas of flow concentration continually shift bank lines. In meandering streams having an "S-shaped" planform, the channel moves both laterally and downstream. A braided stream has numerous channels which are continually changing. In a braided stream, the deepest natural scour occurs when two channels come together or when the flow comes together downstream of an island or bar. This scour depth has been observed to be 1 to 2 times the average flow depth (Northwest Hydraulic Consultants Ltd., 1973) (Richardson and Davis, 1995).

A bridge is static. It fixes the stream at one place in time and space. A meandering stream whose channel moves laterally and downstream into the bridge reach can erode the approach embankment and affects contraction and local scour because of changes in flow direction. A braided stream can shift under a bridge and have two channels come together at a pier or abutment, increasing scour. Descriptions of stream morphology are given by Richardson et al., (1990), (Lagasse et al., 1995) and Schumm (1977) among others.

Factors that affect lateral shifting of a stream and the stability of a bridge are the geology and geomorphology of the stream, location of the crossing on the stream, flood characteristics, the characteristics of the bed and bank material and wash load.

It is difficult to anticipate when a change in planform may occur. It may be gradual with time or the result of a major flood event. Also, the direction and magnitude of the movement of the stream are not easily determined. It is difficult to properly evaluate the vulnerability of a bridge due to changes in planform. It is important to incorporate potential planform changes into the design of new bridges and design of countermeasures for existing bridges.

Countermeasures for lateral shifting and instability of the stream may include changes in the bridge design, construction of river control works, protection of the foundations with riprap, or careful monitoring of the river in a bridge inspection program. HEC-18 (Richardson and Davis, 1995) recommends that foundations of piers and abutments located on floodplains be placed at elevations approximating those for piers located in the main channel.

To control lateral shifting requires river training works, bank stabilizing by riprap and/or guide banks. Design methods are given in publications of the Federal Highway Administration, U.S. Army Corps of Engineers and American Association of State Highway and Transportation Officials (AASHTO). Of particular importance are "Hydraulic Analysis for the Location and Design of Bridges," Volume VII-Highway Drainage Guidelines, (AASHTO, 1992), "Highways in the River Environment" [Richardson et al., 1990]; "Spurs and Guide Banks" (Richardson and Simons, 1974); "The Design of Spurs for River Training," (Richardson et al., 1975); "Use of Spurs and Guidebanks for Highway Crossings" [Richardson and Simons, 1984], "Stream Stability at Highway Structures" [Lagasse et al., 1995], "Streambank Stabilization Measures for Highway Stream Crossings," (Brown, S.A., 1985); "The Streambank Erosion Control Evaluation and Demonstration Act of 1974," (U.S. Army Corps of Engineers, 1981); "Streambank Protection Guidelines For Landowners and Local Governments," (U.S. Corps of Engineers, 1983); and Bridge Scour and Stream Instability Countermeasures (Lagasse, et al., 1999)

SCOUR IN TIDAL AFFECTED WATERWAYS

Scour (erosion) of the foundations of bridges over tidal waterways in the coastal region, that are subjected to the effects of astronomical tides and storm surges is a combination of long-term degradation, contraction scour, local scour, and waterway instability (Richardson et al., 1993 and 1995) (Richardson and Lagasse, 1999, pp 689 - 815). These are the same scour mechanisms that affect nontidal (riverine) streams. Although many of the flow conditions are different in tidal waterways, the equations used to determine riverine scour are applicable if the hydraulic forces are carefully evaluated.

Bridge scour in the coastal region results from the unsteady diurnal and semi-diurnal flows resulting from astronomical tides, large flows that can result from storm surges (hurricanes, nor'easters, and tsunamis), and the combination of riverine and tidal flows. Also, the small size of the bed material (normally fine sand) as well as silts and clays with cohesion and littoral drift (transport of beach sand along the coast resulting from wave action) affect the magnitude of bridge scour. In addition, tidal flow are subjected to mass density stratification and water salinity but these have only a minor effect on bridge scour. The hydraulic variables (discharge, velocity, and depths) and bridge scour in the coastal region can be determined with as much precision as riverine flows. These determinations are conservative and research is needed for both cases to improve scour determinations. Determining the magnitude of the combined flows can be accomplished by simply adding riverine flood flow to the maximum tidal flow or routing the design riverine flows to the crossing and adding them to the storm surge flows.

Some of the similarities and differences between tidal and riverine flows are:

- Tidal flows are unsteady with short duration peak flows. Riverine flows are also unsteady and many have short duration peak flows. Existing scour equations predict scour depths for these short duration peak riverine flows. Also, waterways in the coastal zone are composed of fine sand which erode easily. Therefore, riverine scour equations will predict scour depths in short duration tidal flows.

- Astronomical tides, with their daily or twice daily in and outflows, can and do cause long-term degradation if there is no source of sediment except at the crossing. This has resulted in long-term degradation of several feet per year with no indication of stopping (Butler and Lillycrop, 1993) (Vincent et al., 1993). Existing scour equations can predict the magnitude of this scour, but not the time history (Richardson et al., 1993, Richardson and Davis, 1995).

- Mass density stratification (saltwater wedges), which can result when the denser more saline ocean water enters an estuary or tidal inlet with significant freshwater inflow, can result in larger velocities near the bottom than the average velocity in the vertical (Sheppard, 1993). However with careful evaluation, the correct velocity can be determined for use in the scour equations. With storm surges, mass density stratification will not normally occur. The density difference between salt and freshwater, except as it causes saltwater wedges, is not significant enough to affect scour equations. Density and viscosity differences between fresh and sediment-laden water can be much larger in riverine flows than the differences between salt and freshwater. Salinity can affect the transport of silts and clays by causing them to flocculate and possibly deposit, which may affect stream stability and must be evaluated. Salinity may affect the erodibility of cohesive sediments, but this will only affect the rate of scour, not ultimate scour.

- Littoral drift is a source of sediment to a tidal waterway (Sheppard, 1993) and its availability can decrease contraction and possible local scour and may result in a stable or aggrading waterway. The lack of sediment from littoral drift can increase long-term degradation, contraction scour, and local scour. Evaluating the effect of littoral drift is a sediment transport problem involving historical information, future plans (dredging, jetties, etc.) for the waterway and/or the coast, sources of sediment, and other factors.

- **There is one major difference between riverine scour at highway structures and scour resulting from tidal forces**. In determining scour depths for riverine conditions, a design discharge is used (discharge associated with a 50-, 100-, and 500-year return period). For tidal conditions, a design storm surge elevation is used (elevation for the 50-, 100-, and 500-year storm surge return period), and from the storm surge elevation, the discharge is determined. That is, for the riverine case, the discharge is fixed; whereas, for the tidal case, the discharge may not be. In the riverine case, as the area of the stream increases, the velocity and shear stress on the bed decrease because of the fixed discharge. In the tidal case as the area of the waterway increases, the discharge may also increase and the velocity and shear stress on the bed may not decrease appreciably. Thus, long-term degradation and contraction scour can continue until sediment inflow equals sediment outflow or the discharge driving force (difference in elevation across a highway crossing an inlet, estuary, or channel between islands or islands and the mainland) reduces to a value that the discharge no longer increases(Richardson et al., 1993, Richardson and Davis, 1995).

  The reason the design discharge for the same return periods for tidal waterways may increase is the discharge is dependent on the design storm surge elevation, volume of water in the tidal prism upstream of the bridge, and the area of the waterway under the bridge at mean tide. If there is erosion of the waterway from the constant daily flow from the astronomical tides or from the storm surge, the discharge which may increase as the waterway area increase.

SCOUR CALCULATIONS

Long-term degradation, contraction scour, and local scour can be determined in tidal affected waterways using methods and equations given previously for riverine flows (Richardson and Davis, 1995).

PRELIMINARY ANALYSIS OF TIDAL SCOUR

As a preliminary analysis determine (1) classification of the tidal crossing, (2) tidal characteristics, (3) lateral, vertical, and overall stability of the waterway and bridge foundations, and (4) characteristics of the riverine and tidal flows. In this design plans, boring logs, inspection and maintenance reports, fluvial geomorphology, historical flood, scour and tidal information, 100- and 500-year return period storm surge elevations, riverine flows, etc. are collected and analyzed. In addition, field reconnaissance and contact with relevant agencies such as the Federal Emergency

Management Agency, National Oceanic and Atmospheric Administration, U.S. Geological Survey, U.S. Coast Guard, U.S. Corps of Engineers, state agencies, etc. are used.

The crossing is classified as an inlet, bay, estuary or passage between islands or islands and the mainland. The crossing may be tidally affected or tidally controlled. Tidally affected crossings do not have flow reversal, but the tides act as a downstream control. Tidally controlled crossings have flow reversal. The limiting case for a tidal-affected crossing is when the magnitude of the tide is large enough to reduce the discharge through the bridge to zero.

The objectives of the preliminary analysis are to determine the magnitude of the tidal effects on the crossing, the overall long-term vertical and lateral stability of the waterway and bridge crossing, and the potential for waterway and crossing to change.

DETERMINATION OF HYDRAULIC VARIABLES

The general procedure is to determine (1) design flows (100- and 500-year storm tides and riverine floods), (2) hydraulic variables of discharge, velocity, and depths. These variables are then used to determine the scour components (depths of degradation, contraction scour, pier scour, and abutment scour) using the equations and methods given previously., and (3) evaluation of the results. HEC-18 gives method and equations for determining the hydraulic variables for unconstricted tidal affected waterway and constricted waterways. Also, describes 1- and 2-dimensional computer programs for determining storm surge hydrographs and resulting hydraulic variables. These 1- and 2-dimensional models are also described by Ayres Associates, 1994; Bingham Young University, 1997; Burkau, 1993; Froehlich, 1996; U.S. Corps of Engineers, 1996; and Zevenbergen et al., 1997a,b.

REFERENCES

1. Abed, L.M., 1991, "Local Scour Around Bridge Piers in Pressure Flow," Ph.D. Dissertation, Colorado State University, Fort Collins, CO.
2. Abed, L.M., Richardson, E.V., and Richardson, J.R., 1991, "Bridges and Structures," Transportation Research Record 1290, Vol. 2, Third Bridge Engineering Conference, Transportation Research Board, Washington, D.C.
3. Ahmad, M.,1953, "Experiments On Design And Behavior Of Spur Dikes," Proceedings IAHR, ASCE Joint Meeting, Univ. of Minn.
4. AASHTO, 1992, "Hydraulic Analysis for the Location and Design of Bridges," Vol. VII, Highway Drainage Guidelines, American Association of State Highway and Transportation Officials, Washington, D.C.
5. Arneson, L.A., 1997 "The Effects of Pressure Flow on Local Scour in Bridge Openings," Ph.D. Dissertation, Colorado State Univ., Fort Collins, CO.
6. Arneson, L.A. and Abt, S.R., 1998, "Vertical Contraction Scour at Bridges with Water Flowing Under Pressure Conditions," presented at TRB Annual Meeting, Washington, D.C., 30p.

7. Ayres Associates, 1994, "Development of Hydraulic Computer Models to Analyze Tidal and Coastal Stream Hydraulic Conditions at Highway Structures," Final Report, Phase I, South Carolina Department of Transportation, Columbia, SC.
8. Blench, T., 1969, "Mobile Bed Fluviology," University of Alberta Press, Edmonton, Alberta Canada..
9. Briaud, J.L., Ting, F.C., Chen, H.C., Gudavalli, R., Perugu, S., and Wei, G., 1999, "SRICOS: Prediction of Scour Rate in Cohesive Soils at Bridge Piers," ASCE Jour. Of Geotechnical and Geoenvironmental Engineering, Reston VA, April.
10. Brigham Young University, 1997, "SMS Surface Water Modeling System," Reference Manual, Version 5.0, *Engineering Computer Graphics Laboratory*, Provo, UT.
11. Brown, S.A., McQuivey, R.S., and Keefer, T.N., 1980, "Stream Channel Degradation and Aggradation: Analysis of Impacts to Highway Crossings," Report FHWA/RD-80/159, Federal Highway Administration, Washington, D.C., p. 202.
13. Brown, S.A., 1985, "Stream Bank Stabilization Measures for Highway Engineers," FHWA/RD-84.100, Federal Highway Administration, Washington, D.C.
14. Burkau, R.L., 1993, "UNET - One Dimensional Unsteady Flow Through a Full Network of Open Channels," Report CPD-66, U.S. Army Corps of Engineers, Hydrologic Engineering Center, Davis, CA.
15. Butler, H.L., and Lillycrop, J, 1993, "Indian River Inlet: Is there a Solution?" Hydraulic Engineering, Proc., 1993 National Conference, ASCE, Vol. 2, pp. 1218-1224.
16. Chang, F.F.M., 1973, "A Statistical Summary of the Cause and Cost of Bridge Failures," Federal Highway Administration, U.S. Department of Transportation, Washington, D.C.
17. Froehlich, D.C., 1989, "Abutment Scour Prediction," Paper presented at 68th TRB Annual Meeting, Washington, D.C.
18. Froehlich, D.C., 1995, "Contracted Scour at Bridges: Clear-water conditions with Armoring." Hydraulic Engineering, ASCE, Reston, VA.
19. Froehlich, D.C., 1996, "Finite Element Surface-Water Modeling System: Two-Dimensional Flow in a Horizontal Plane," FESWMS-2DH, Version 2, User's Manual, Federal Highway Administration, McLean, VA..
20. Jackson, L.E., Thompson, P.D., Richardson, E.V., 1991, "Hatchie River and Schoharie Creek Bridge Failures," ASCE Hydraulic Engineering Proc., 1991 National Conf. Nashville, TN.
21. Jain, S.C. and E.E. Fisher, 1979, "Scour Around Circular Bridge Piers At High Froude Numbers," Report FHWA-RD-79-104, NTIS, Springfield, VA.
22. Jones, J.S., 1983, "Comparison of Prediction Equations for Bridge Pier and Abutment Scour, Transportation Research Record 950, TRB, National Research Council, Washington, D.C., pp. 202-209.
23. Jones, J.S., 1989, "Laboratory Studies of the Effects of Footings and Pile Groups on Bridge Pier Scour," U.S. Interagency Sedimentation Committee Bridge Scour Symposium, U.S. Department of Transportation, Washington, D.C.
24. Jones, J.S., Bertoldi, D.A., and Umbrell, E.R., 1993, "Preliminary Studies of Pressure Flow Scour," ASCE Hydraulic Engineering, Reston, VA, pp 916-921.
25. Jones, J.S., Bertoldi, D.A., and Umbrell, E.R., 1996, "Interim Procedures for Pressure Flow Scour," ASCE North American Water and Environment Congress, Reston, VA.

26. Jones, J.S., 1998, Personal Communication.
27. Keefer, T.N., McQuivey, R.S., and Simons, D.B., 1980, "Stream Channel Degradation and Aggradation: Causes and Consequences to Highways," FHWA Report FHWA/RD-80/038, Washington, D.C. , 86 p.
28. Lagasse, P.F., Schall, J.D., Johnson, F., Richardson, E.V., and Chang, F., 1995, "Stream Stability at Highway Structure," Second Edition, HEC-20, FHWA Report FHWA-IP-90-014, U.S. Department of Transportation, 144 p.
29. Lagasse, P.F., Byars, M.S., Zevenbergen, L.W., and Clopper, P., 1999, "Bridge Scour and Stream Instability Countermeasures," HEC-23, FHWA Report HI-97-030, U.S. Department of Transportation.
30. Landers , M.N. and Mueller, D.S., 1996, "Channel Scour at Bridges in the United States," FHWA Report FHWA-RD-95-184, U.S. Depart. of Transportation, McLean, VA, 128 p.
31. Laursen, E.M., 1958, "Scour at Bridge Crossings," Bulletin No. 8, Iowa Highway Research Board, Ames, IA, 52 p.
32. Laursen, E.M., 1960, "Scour at Bridge Crossings," Journal of the Hydraulics Division, ASCE, Vol. 89, HY3.
33. Laursen, E.M., 1963, "An Analysis of Relief Bridge Scour," Journal of the Hydraulics Division, ASCE, Vol. 92, HY3.
34. Laursen, E.M. and Toch, A., 1956, "Scour Around Bridge Piers and Abutments," Bulletin No. 4, Iowa Highway Research Board, Ames, IA, 60 p.
35. Liu, M.K., Chang, F.M., and Skinner, M.M., 1961, "Effect Of Bridge Construction On Scour And Backwater," Dept. of Civil Engineering, Colorado State University, Report No. CER60-HKL22.
36. Melville, B.W., 1983, "Live-Bed Scour at Bridge Piers," ASCE Jour. of Hydraulic Engineering, Hydraulic Division, Vol. 110, No. 9.
37. Melville, B.W., 1992, "Local Scour at Bridge Abutments," ASCE Jour. of Hydraulic Engineering, Hydraulic Division, Vol. 118, No. 4.
38. Melville, B.W., 1997 "Pier and Abutment Scour: Integrated Approach," ASCE, Journal Hydraulic Division, Vol. 123, No. 2.
39. Melville, B.W. and Sutherland, A.J., 1988, "Design Method for Local Scour at Bridge Piers," American Society of Civil Engineers, Jour. Hydr. Division, Vol.114, No 10.
40. Melville, B.W. and Dongol, D.M., 1992, "Bridge Pier Scour with Debris Accumulation," American Society of Civil Engineers, Jour. Hydr. Division, Vol.118, No 9.
41. Molinas, A., 1993, "Bri-stars Model for Alluvial River Simulation." Hydraulic Engineering, ASCE, Vol. 2, pp. 1726-1731.
42. Mueller, D.S., 1996, "Local Scour at Bridge Piers in Nonuniform Sediment Under Dynamic Conditions," Ph.D. Dissertation, Colorado State University, Fort Collins, CO.
43. Mueller, D.S. and Jones, J.S., 2000, Personal Communication.
44. Northwest Hydraulic Consultants, Ltd, 1973, Personal Communication.
45. Raudkivi, A.J., 1986, "Functional Trends of Scour at Bridge Piers," ASCE Jour. of Hydraulic Division, Vol. 112, No. 1, Reston, VA.
46. Rhodes, J. and Trent, R., 1993, "Economics of Floods, Scour, and Bridge Failures," Hydraulic Engineering, ASCE, Vol. 1, 1993, pp. 928-933, 1993.

47. Richardson, E.V. and Simons, D.B., 1974, "Spurs And Guide Banks," Open File Report, Colorado State University Engineering Research Center, Fort Collins, CO.
48. Richardson, E.V., Stevens, M.A., and Simons, D.B., 1975, "The Design of Spurs for River Training," Proc. XVIth IAHR Congress, Sao Paulo, Brazil.
49. Richardson, E.V., and Simons, D.B., 1984, "Use of Spurs and Guidebanks for Highway Crossings," Proc. Second Bridge Eng. Conf., Tran. Research Board Report 950, Washington, D.C.
50. Richardson, E.V., Lagasse, P.F., Schall, J.D., Ruff, J.F., Brisbane, T.E., and Frick, D.M., 1987, "Hydraulic, Erosion and Channel Stability Analysis of the Schoharie Creek Bridge Failure, New York," Resources Consultants, Inc. and Colorado State University, Fort Collins, CO.
51. Richardson, E.V., Simons, D.B., and Julien, P., 1990, "Highways in the River Environment," Revision of Richardson, E.V., Simons, D.B., Karaki, S., Mahmood K., and Stevens, M.A., 1975 "Highways in the River Environment, Hydraulic and Environmental Design Considerations Training and Design Manual," FHWA-HI-90-016, Federal Highway Administration, U.S. Department of Transportation, Washington, D.C.
52. Richardson, E.V., Richardson, J.R., and Edge, B.E., 1993, "Scour at Highway Structures in Tidal Waters," Hydraulic Engineering, ASCE, Vol. 2, pp. 1206-1212.
53. Richardson, E.V. and Abed, L., 1993, "The Top Width of Pier scour Holes in Free and Pressure Flow," Hydraulic Engineering, ASCE, Vol. 2.
54. Richardson, E.V. and Davis S.R., 1995, "Evaluating Scour at Bridges, Third Edition," HEC-18, Report FHWA-IP-90-017, FHWA, U.S. Department of Transportation, Washington, D.C., 204 p.
55. Richardson, E.V. and Lagasse, P.F., Editors, 1999, "Stream Stability and Scour at Highway Bridges, Compendium of Papers ASCE Water Resources Engineering Conferences, 1991 to 1998," ASCE, Reston, VA.
56. Richardson, E.V. and Richardson, J.R., 1998, "Discussion of B.W. Melville, 1997 paper Pier and Abutment Scour: Integrated Approach," ASCE Jour. of the Hydraulics Division, Vol, 124, HY7, pp. 771-772.
57. Richardson, E.V., 1998, Personal Communication.
58. Richardson, J.R. and Richardson, E.V., 1992, Discussion of B.W. Melville, 1992 paper Local Scour at Bridge Abutments, Journal of the Hydraulics Division, ASCE, Vol. 119, HY9, 1993, pp. 1069-1071.
59. Richardson, J.R. and Richardson, E.V., 1993, "The Fallacy of Local Abutment Scour Equations," Hydraulic Engineering, ASCE, Vol. 1, pp. 749-755.
60. Richardson, J.R., Richardson, E.V., and Edge, B.L., 1995, "Bridge Scour in the Coastal Region," Proc. of the Fourth International Bridge Engineering Conference, TRB, National Research Council, Washington, D.C.
61. Richardson, J.R. and Trivino, 1999, Personal Communication.
62. Salim, M. and Jones, J.S., 1996, "Scour Around Exposed Pile Foundations," ASCE North American Water and Environment Congress, Anaheim, CA, 10 p.
63. Schumm, S.A., 1977, "The Fluvial System," Wiley and Sons, 338 p.

64. Shearman, J.O., 1987, "Bridge Waterways Analysis Model for Mainframe and Microcomputers," WSPRO/HY-7, Federal Highway Administration, U.S. Department of Transportation, Washington, D.C.
65. Sheppard, D.M., 1993, "Bridge Scour in Tidal Waters," Transportation Research Record 1420, Washington, D.C., pp. 1-6.
66. Strum, T.W., 1999, "Abutment Scour Studies for Compound Channels," FHWA Report FHWA-RD-99-156, U.S. Dept. of Transportation, McLean, VA, 132 p.
67. U.S. Army Corps of Engineers, 1981, "The Streambank Erosion Control Evaluation and Demonstration Act of 1974," Final Report to Congress, Executive Summary and Conclusions, Washington, D.C.
68. U.S. Corps of Engineers, 1983, "Streambank Protection Guidelines For Landowners and Local Governments," Waterways Experiment Station, Vicksburg, MS, 60 p.
69. U.S. Army Corps of Engineers, 1993, "Scour and Deposition In Rivers And Reservoirs, Computer Program HEC-6," Hydrologic Engineering Center, Davis, CA.
70. U.S. Army Corps of Engineers, 1997 "HEC-RAS River Analysis," Hydrologic Engineering Center, Davis, CA.
71. Vanoni, V.A., Editor, 1975, "Sedimentation Engineering." ASCE Manual 54, New York, NY.
72. Vincent, M.S., Ross, M.A., and Ross, B.E., 1993, "Tidal Inlet Bridge Scour Assessment Model," Transport Research Record 1420, Washington, D.C., pp 7-13.
73. Zevenbergen, L.W., Richardson, E.V., Edge, B.L., Lagasse, P.F., and Fisher, J.S., 1997, "Development of Hydraulic Computer Models to Analyze Tidal and Coastal Stream Hydraulic Conditions at Highway Structures," Final Report, Phase II. South Carolina Department of Transportation, Columbia, SC.
74. Zevenbergen, L.W., Hunt, J.H., Byars, M.S., Edge, B.L., Richardson, E.V., and Lagasse, P.F., 1997, "Tidal Hydraulic Modeling for Bridges; Users Manual," Pooled Fund Study SPR-3(22), Ayres Associates, Fort Collins, CO.

SCOUR IN SUDAN: PRACTICE AND PROBLEMS

By

Yahia E-A. Mohamedzein[1] and Assim El Sanosi[2]

ABSTRACT

The Republic of Sudan occupies about 1 million square miles and is the largest country in Africa. The River Nile and its 10 tributaries are the main rivers, plus hundreds of seasonal streams. Highway and railroad bridges were built across these waterways and more bridges are to be built for modern transportation systems. Current design practice in Sudan assumes scour depth of 4m to 6m for bridges. Bridges crossing the Nile and its main tributaries are usually supported on deep foundation bearing on rock, well below the scour depth and thus no scour-induced failures were reported for these main bridges. However failures due to scour occurred in highway bridges crossing seasonal streams. Three cases where foundation failure occurred due to scour were presented in this paper. Plausible causes of scour were related to inadequate hydraulic design, poor compaction of fill beneath the foundations and backfill around the bridge piers and abutments, placement of foundation within the scour zone, and obstruction of bridge openings. The three bridges were repaired and remedial measures for scour protection included well compacted fill and backfill overlain by stone pitching and cement mortar cover.

INTRODUCTION

The Republic of Sudan occupies about 1 million square miles and is the largest country in Africa. The River Nile and its 10 tributaries are the main rivers (See Figure 1). In addition hundreds of seasonal streams are also exist. About 11 major bridges were built across the Nile and its tributaries dating back to early 1900's. Hundreds of highway bridges crossing seasonal streams were also constructed. Rivers and seasonal waterways in Sudan differ substantially in terms of hydraulic characteristics such as flow speed. Rivers such as White Nile and its tributaries are characterized by large catchement areas, low flow head, low speed, and large width of stream and flat banks. In contrast the Blue Nile, the Nile and Atbara River originate from hilly areas and flow with high speed in very narrow streams. The seasonal streams are generally characterized by flash floods during a short period of time and with very high flow speed that can destruct trees and stream banks. According to these facts scour depth differs substantially in Sudan.

The geotechnical aspects of design of bridges in Sudan depend on whether the bridge crosses permanent rivers or seasonal streams. The difference between the design approaches for each case is considered in the followings.

---

[1]Assistant Professor, Building and Road Research Institute, University of Khartoum, Khartoum, Sudan.

[2]Graduate Student, Faculty of Engineering and Architecture, University of Khartoum, Khartoum, Sudan.

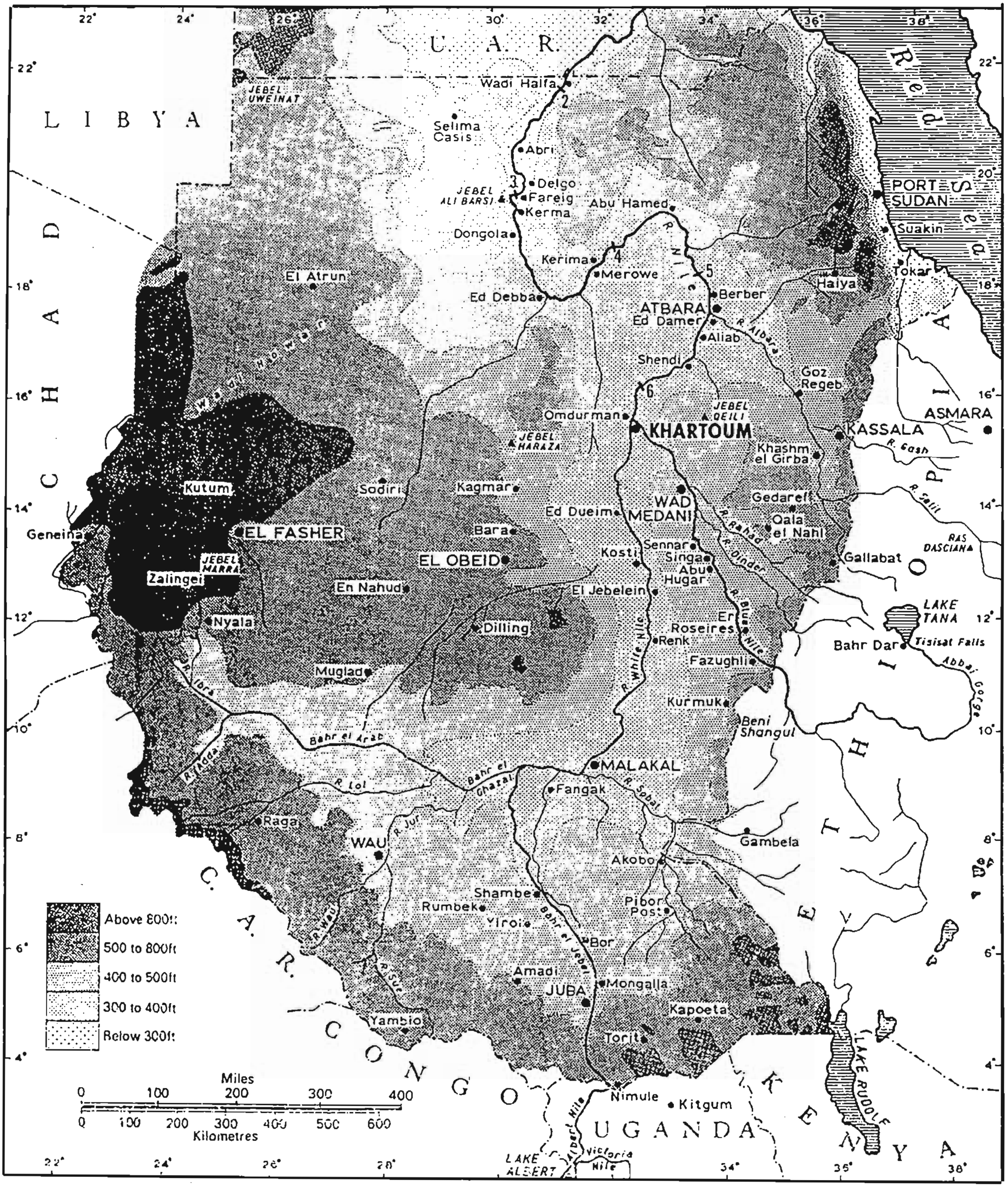

Fig. 1 – Rivers and Seasonal Streams in Soudan

BRIDGES CROSSING PERMANENT RIVERS

The soils in permanent rivers in Sudan (Nile, White Nile, Blue Nile and Atbara rivers) generally consist of loose sand or soft silt or clay (see Table 1). Depth of bedrock below riverbed generally varies from few meters to 20m. About 11 bridges were built across these rivers. The bridges are multi span and multi-lane steel or concrete structures. The bridges connect major highways and are subjected to heavy traffic loads. The type and depth of foundation are usually governed by the settlement and bearing capacity considerations rather than by scour depth. This is because of the presence of soft or loose formation to depths much greater than the scour depth. Also the heavy loads from the superstructure require a competent formation (usually bedrock) to carry the imposed loads. All bridges constructed across rivers in Sudan were supported on drilled piers or caissons socketed within the bedrock. No cases of scour were reported in these bridges. Since most of these bridges were built more than 50 years scour failure may not occur in these structures. It worth mentioning, however; that the design of these bridges is very conservative.

BRIDGES CROSSING SEASONAL STREAMS

Construction of bridges across seasonal streams is associated with the construction of the new highway systems in Sudan during the last 25 years. Structures for water drain in seasonal streams generally consist of concrete or steel bridges and concrete box culverts and less frequently steel or metal culverts. Since the seasonal streams are located in rural uninhabitant areas, very limited data is available on their hydraulic and hydrologic characteristics, the hydraulic design of most bridges and culverts crossing seasonal streams is unsafe in most cases. Frequent failures due to inadequate hydraulic design were reported (NHA, 2000).

Soil conditions in seasonal streams are variable but generally include fine silty sand. Bedrock is deep except at few locations in Northeastern, Southwestern and Southern Sudan. Table 2 shows typical soil conditions at some streams and design scour depth. Typical practice assumes scour depth of 4m and in rare cases 5 to 6m. The scour depth is usually assumed and no tests are performed. Empirical correlations using worldwide formula are not properly used due to inadequate hydraulic data.

Table 2 also lists 3 cases where bridges and culverts were failed due to scour failure. Both geotechnical and hydraulic factors contributed to failure. These cases will be considered below.

ELAWATIB BRIDGE

ElAwatib Bridge was constructed on Khartoum-Shendi Road. The bridge is a 4 span precast concrete girder with cast-in-situ deck slab. The total length of the bridge is 60m. The girders are simply supported on 3-wall piers and 2 abutment walls which transfer structural loads to strip footings. Footings were placed at a depth of about 2.5m on a 1m compacted fill layer.

The geotechnical investigation (BRRI 1994) for this bridge indicated a general soil profile consisting of loose to medium dense silty sand extending to about a depth of 3 below ground level. Very dense clayey sand prevails below this depth to the

Table 1- Soil Conditions at Major Bridges Crossing Rivers in Sudan.

Bridge	River	Construction Date	Soil Description	Foundation	Performance
Blue Nile Bridge	Blue Nile	1908	Grey sand of varying degree of fineness with clay and gravel. Sandstone below a depth of 15m.	Spread footing at the north abutment bearing at a depth of 1o ft (3m) on hard clay. 12-inch (0.3m) diameter pine piles at the south abutment. Piers of diameters of 11ft (3.35m) and 16ft (4.88m) bearing on sandstone about 60ft (18.3m) below riverbed.	No scour
Old White Nile Bridge	White Nile	1928	3 to 8m of Soft clay and silt underlain by grey Nubian Sandstone	Caisson of diameters 16ft(4.88m) socketted an average of 5ft (1.524m) into the Nubian Sandstone	No Scour
Shambat Bridge	The Nile	1968	About 4m of silty clay at banks. Sand below the silty clay at the banks and from riverbed at the main stream. Sand is loose to medium dense and about 4 to 15m in thickness . Sandstone with inclusions of mudstone prevails below the sand.	Caissons socketted into the sandstone.	No scour
New White Nile Bridge	White Nile	Jan. 2000	Soft highly plastic silt about 5 to 7m deep underlain by a 2m layer of medium dense clayey sand overlying Nubian Formation. The Nubian Formation consists of alternating layers of weathered sandstone and mudstone up to 25m. Sandstone prevails below that depth.	Large diameter bored piers (dia. 1.2m) at a depth of 15m.	-----
Atbara Bridge	Atbara River	Jan. 2000	About 7.5m to 11m of medium stiff silty/clay on the banks. Loose to medium dense sand below the silty clay at the banks and from the riverbed at the main stream. Basement complex of chist below a depth of 15m.	Drilled piers bearing at least 2m into the fresh bedrock.	---
Tuti Bridge	Blue Nile	To be constructed	Medium stiff, medium to highly plastic silt on the river banks. The silt is compressible. Loose to medium dense fine-grained silty sand underlies the silt at riverbanks and from the riverbed at the main flow section. Weathered Nubian sandstone below a depth of 12 to 15m.	Drilled piers bearing on slightly weathered Nubian sandstone below a depth of 15 to 20m below the riverbed. Pier diameter 1 to 1.2m	----

Table 2- Soil Conditions at Highway Bridges Crossing Seasonal Streams in Sudan.

Bridge or Stream Name	Highway	Construction Date	Soil Description	Foundation Type	Performance
Gadamballia	Medani-Gadarif	1976	Highly plastic clay to a depth of 7 to 8m. The top 2.5m are soft. The clay is stiff to very stiff below that depth. Weathered bedrock underlies the clay.	Box culvert with 2m apron under the riverbed.	Scour failure in 1998.
Umdilka	Medani – Sennar	1979	Highly plastic clay to a depth of 15	Box culvert bearing on the highly plastic clay	Scour failure 3 times
Awatib	Khartoum-Shendi	1995	3m of loose to medium sense sand overlies very dense clayey gravelly sand.	Spread footing on a depth of 2.5m over a 1m compacted fill layer.	Scour failure in 1996.
Elkrbkan	Khartoum-Shendi	1995	About 2 to9m of dense to very dense clayey sand followed by very dense silty sand.	Spread footings on very dense clayey sand at a depth of 4m.	No scour
Kaboushia	Shendi-Atbara	1997	Medium dense to dense clayey sand, silty sand and sandy gravel up to a depth of 2.5m followed by stiff highly plastic clay. Mudstone below a depth of 7.5m	Spread footings on 2m of compacted fill layer. Bottom of foundation at 4m.	No scour.
Eldan	Shendi - Atbara	1997	Very stiff to hard sandy silty clay to a depth of 17m. The clay contains substantial amounts of gravel and stone fragments in the top 2 to 3m. The clay is highly plastic below a depth of 3 to 4m. Natural moisture content of the highly plastic clay is less than plastic limit.	Spread footing bearings at 4m.	No scour.
Kaja	Zalingi-Elgenina	1998	Loose to medium fine-grained silty sand underlain by a layer of stiff clayey sand and dense sandy clay followed by weathered sand stone .	Driven steel H-piles (HP14 and HP12) about 6 to 20m in length driven to refusal on weathered sandstone.	No scour.
Haram and Abu Khedra	Rabak-Renk	To be constructed	Very stiff highly plastic clay (about 1 to 3m) in thickness underlain by very dense clayey sand (more than 15m deep).	Spread footings below the highly plastic clay (below a depth of 3m).Scour is <2m due to flat topography and low flow speed.	-----
Kiai	Nyala-El Riheed El Biridi	To be constructed	Loose silty sand (thickness about 6 to 9m) with thin inclusions of clay and silt. Medium dense clayey sand below the loose silty sand up to a depth of 12 to 15m. Very dense clayey sand prevails below that depth.	Pile foundations bearing on the very dense clayey sand below a depth of 12 to 15m.	---
Azoom	Zalingi-Elgenina	Under Construc Tion	Very loose to loose poorly graded fine grained sand (variable thickness of 2.5 to 18.5m) followed by medium dense poorly graded fine grained sand grading into a thin layer (2to4m) of very dense clayey sand and silty sand. Bedrock below a depth of 3.5-40.0m .	Steel H pile driven to the bedrock.	-----

.naximum depth explored (about 15m). The average d_{50} is about 0.5mm in the top 3 to 4m layers. The geotechnical consultant recommended the foundation to be constructed on the very dense clayey sand at least 4m below the streambed. In contrast to as built footings no fill materials were recommended.

The bridge was completed and opened for traffic in 1995. During the fall of 1996 (August 1996) the bridge failed after a heavy rain upstream which produced continuous flow for 3 days with the peak flow during the first 6 hours. The failure was in a form of large settlement and tilting of the northern pier due to scour. Total settlement was about 35cm. The simply supported beams slided on the top of the wall pier causing caving in of the girder.

The past failure investigation (NHA, 1997) attributed the causes of failure to: -

(i) Foundations were supported on loose fill within the sour zone. In this respect the recommendations of the geotechnical consultant were not implemented and the excavation for foundation and placement of fill material were not inspected by a geotechnical engineer.

(ii) The hydraulic design underestimates the amount and velocity of flow.

(iii) There was an increase in flow caused by presence of debris, soil piles and trapped tree branches.

Remedial measures consisted of removal of the failed pier. The foundation was placed on the competent soil formations below a depth of 4m. Selected well-compacted backfill was placed above the foundation around the pier. At the locations of other piers the loose fill material was removed to the top level of the foundation. The loose compacted fill below the foundation was stabilized by cement grout. Selected well-compacted backfill was placed above the foundation and around the piers. The loose soil between piers and abutments was replaced by well-compacted fill and overlain by 0.5m stone pitching with cement-sand mortar. The zone of stone pitching extended up to 7.5m upstream and down stream. Additional remedial measures included construction of relief box culvert on one side of the bridge. The stream is meandering and recommendations were outlined for further training of the stream. Other recommendations included periodical inspection of the bridge and cleaning of the bridge openings.

All these remedial measures were implemented in the summer of 1997 and the bridge performed very well during the falls of 1998 and 1999.

GADAMBALIA BRIDGE

The bridge consists of 8-cell concrete box culvert that was constructed in 1976 (NHA, 2000). Each cell is 5.5m wide and 1.75m high. The culvert was functioning well until scour appeared down stream. In 1993 an apron was constructed along the down stream face of the culvert. The apron is about 0.5m in the thickness and extends to a depth of 2m below the bottom of culvert. During the fall of 1998 the culvert was washed out.

Post failure investigation revealed that the scour depth is 4.5m (compared to 1.75m assumed in design of culvert). Geotechnical investigation after failure (BRRI 1998) indicated a subsoil profile that consists of highly plastic clay that extends to 7 to 8m below the ground surface. The highly plastic clay is soft up to 2.5m depth and becomes stiff to very stiff below that depth. The highly plastic clay is underlain by weathered bedrock. The average d_{50} of the soils in the top 4m is about 0.006mm.

Remedial measures consisted of replacement of the culvert by a 5 span deck girder concrete bridge. The bridge was supported on driven precast concrete piles that were driven to the weathered bedrock. Suspended pile cap was constructed about 0.3m above the streambed. The option of piles and suspended caps was considered because of the expansive nature of the highly plastic clay. The bridge was constructed in the summer of 1999 and performed well during the fall 1999.

UM DILKA BRIDGE

This 2-cell box culvert was constructed in 1979 on Sennar-Medani Road (NHA,2000). The actual width of the stream is 26m, however; the width of the culvert was only 3m. The culvert washed out 3 times since its construction.

Post failure investigation in 1999 revealed that the scour depth ranged from 1 to 3m. The geotechnical investigation after failure (BRRI 2000) revealed a subsoil condition that consists of highly plastic clay extending to a depth of 15m. The highly plastic clay is underlain by clayey sand extending to the maximum depth explored (about 20m).

Based on geotechnical and hydraulic investigations it was decided to replace the culvert with a one span bridge. The proposed new bridge will be supported on piles bearing below a depth 8m. The bridge will be constructed this summer.

SUMMARY AND CONCLUSIONS

A review of the geotechnical aspects of scour as related to design of bridges in Sudan is presented. Two distinguished trends of foundation design for bridges are identified: - One design practice for major bridges crossing permanent rivers and another for highway bridges crossing seasonal streams. The former bridges are supported on piles or piers bearing on bedrock well below the scour depth. Settlement and bearing capacity considerations rather than scour depth control the design of these bridges. No failure cases were recorded for these bridges although some of them were constructed more than 80 years ago.

Highway bridges crossing seasonal streams are susceptible to scour problems because of inadequate hydraulic data and incompetent geotechnical practice. Case histories have shown that scour caused failure of bridges. The following factors contributed to scour-induced failure of bridges in Sudan:

1) Construction of foundations within the scour zone.
2) Placement of inadequate compacted fill beneath the foundation.
3) Lack of geotechnical investigation or improper implementation of recommendations given by the geotechnical consultant.
4) Excavation for foundation and placement and compaction of fill and backfill is not supervised by a geotechnical engineer.
5) Practical methods are not used to predict the scour depth.
6) Hydraulic and hydrologic data is not sufficient which results in inadequate hydraulic design.
7) Obstruction of bridge openings by soil heaps, construction debris and tree branches.
8) Most of the seasonal streams in Sudan are meandering and require training.
9) Stone pitching is not used to protect the streambed in the vicinity of the bridge and the stream banks.

REFERENCES

(1) BRRI, 2000, " Geotechnical Investigation for Umdilka Bridge, Medani-Sennar Road" Building and Road Research Institute, University of Khartoum, Sudan.

(2) BRRI, 1998, " Geotechnical Investigation for Gadamblia Bridge, Medani-Gadarif Road" Building and Road Research Institute, University of Khartoum, Khartoum, Sudan.

(3) BRRI, 1994, " Geotechnical Investigation for Awatib Bridge, Khartoum-Shendi Road" Building and Road Research Institute, University of Khartoum, Sudan.

(4) The Engineer, 1915, "The Development of the Sudan" London, UK.
The Engineer, 1929, " The Khartoum-Omdurman Bridge" London, UK.

(5) NHA, 2000, "Failure of Gadamblia and Umdilka Bridges" The National Highway Authority, Khartoum, Sudan

(6) NHA, 1997, "Investigation of Awatib Bridge Failure and Remedial Measurements" The National Highway Authority, Khartoum, Sudan.

SETTING TRAIN SUSPENSION RULES ON THE BRIDGES PRONE TO SCOUR IN CONSIDERATION WITH RIVER-BED CHARACTERISTICS

by

Junichi Tanaka[1],Masanori Mikami[2]

ABSTRACT

East Japan Railway Company (JR East) has over three thousand river bridges. These bridges are occasionally damaged by scour around the piers due to heavy rainfalls or typhoons. Among those events there have been the cases of tilting or collapse of bridge piers, which might put railway transport in unsafe. Operational rules for train suspension in case of bridge scour hazard have been established and renovated on the basis of those cases. This paper presents some important bridge scour cases and outlines the current train suspension rules in JR East which represent the empirical knowledge learnt from those cases.

RIVERS IN JAPAN

Terrain Characteristics in Japan are that more than 80 percent areas are mountainous. Therefor, The characteristics of river in Japan are short river length and steep riverbed slope compared with the Mainland Rivers (Fig.1). Water of 100km length river fallen within 6 to 8 hours. In addition, Climate of Japan has many precipitation. For example, Average precipitation in Tokyo was 1460mm one year (1951 to 1980). For this purpose, rivers in Japan has a bigger coefficient of river regime. That is to say, river flow of inundation, and conveyance of gravel are large, because of much precipitation. A prominent Dutch civil engineer who gave many suggestion about harness river of Japan in the late 19th Century said "River of Japan that is not a river, that is a torrent".

RAILWAY BRIDGES OF JR EAST

Six passenger railway companies and a traffic Railway Company formed on division, and privatization of Japan national Railway since 1987. East Japan Railway Company (JR East) is the largest railway company in Japan. JR East has a network of 7,538km of tracks in Tokyo area, and carry sixteen million and eighteen thousand passengers a year.

Almost lines of JR East maintains over three thousand river bridges. These bridges were usually built before the Second World War. Bridges at this time were built at the point of

1 Assistant Manager, Equipment Maintenance Dept., East Japan Railway Company
2 Manager, Takasaki Office, East Japan Railway Company

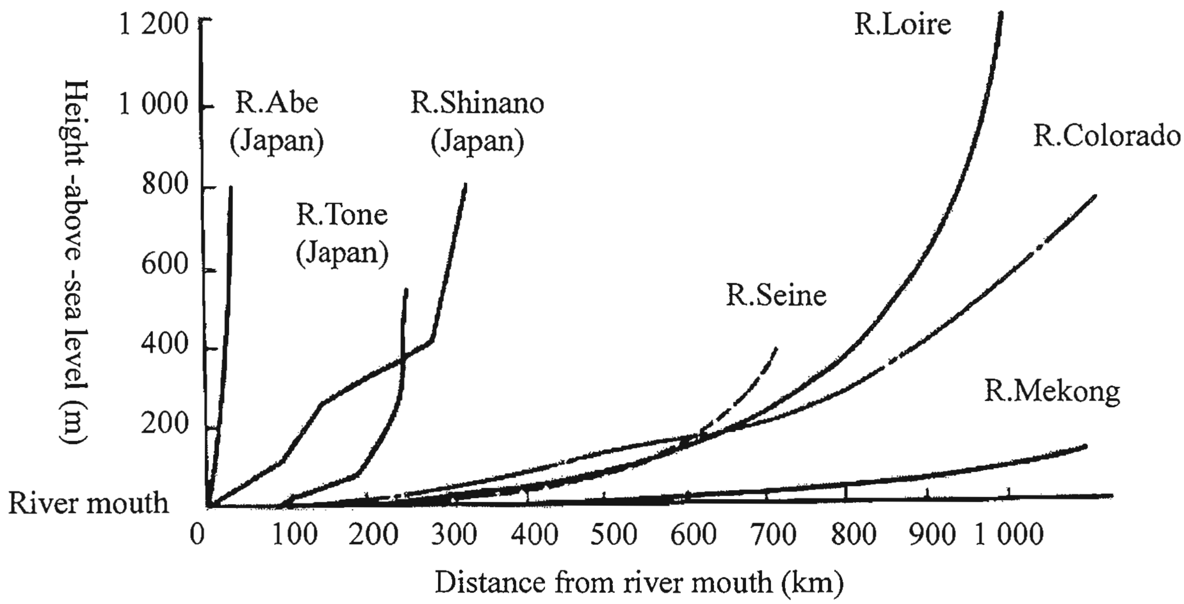

Fig.1-Japanese Rivers Contrasts With Continental Rivers

narrower river width with short span, and most of bridge piers have shallow spread footings or wooden pile foundation.

After The Second War, Japan hold a highly development period. River sand was excavated largely on using concrete, and affections of dams building, riverbed declined tendentious notably. As a result, shallow spread footing that was located at torrent affected by riverbed declined either, scour disasters affected easily.

IMPORTANT SCOUR DAMAGE SASES IN JAPANESE RAILWAY BRIDGES

1. Fuji River bridge of Toukaido line

   This disaster took place in 1982. Toukaido line is one of the most important lines in Japan which links up Tokyo city and Osaka city. Fuji River bridge was had disaster by typhoon. In this case, two bridge piers collapsed because of scour, and four beams washed away. (Fig.2)

2. Rokumaizawa bridge of Tazawako line

   This damage case occurred in 1995. Tazawako line parallels canyon transverse mountain chain, link up Morioka city and Akita city, join express trains from Shinkansen. In this case, foundation of the bridge pier sloped for score because of heavy rain as it turned out the track alignment was distorted by approximately 10mm. The bridge was built on a river that with 1/10 gradient steep riverbed.(Fig.3). In order to restitute task, train was stopped one month approximately.

3. Nagakigawa bridge in Hanawa line

   This disaster took place in September, 1997. Hanawa line is a mountain line, link up Morioka city and Odate city. In this case, Riverbed decline advanced on this bridge. In order to protect bridge feet from riverbed decline, Sheet piles foundation were located in downstream region. As a result, a head of 3m height arised because piles. Bridge pier topple downed, because the sides of piles were scoured (Fig.4, Fig.5). Just that time train passed through here, train derailed. In order to restitute task, train operation was suspended for approximately one month.

ESTABLISHMENT OF TRAIN SUSPENSION RULES

On the safe operate train, it is important for prevent bridge pier topple down from scour. In Japan, Scour phenomenon happen to raising of water on account of typhoon and heavy rain. On the safe operation, JR-EAST hold control methods of operation on rising period. This method was on use of Tarapore equation, and presumes scour depth from water depth and bridge pier width. It is beginning with Fuji river disaster. As figure 6 shows, bygone disasters were included in this equation.

In addition, a new meteorological observation and information transmission system has been introduced for protection of train operation against natural disasters in general for all

Fig.2- The Fujigawa bridge with it's lost beams and piers

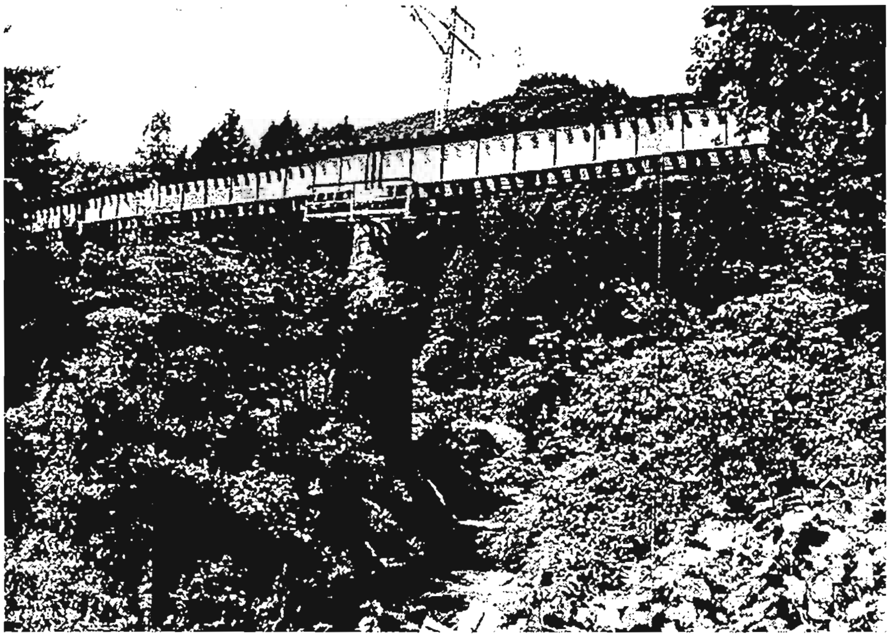

Fig.3-An Inclined Pier of Rokumaizawa bridge

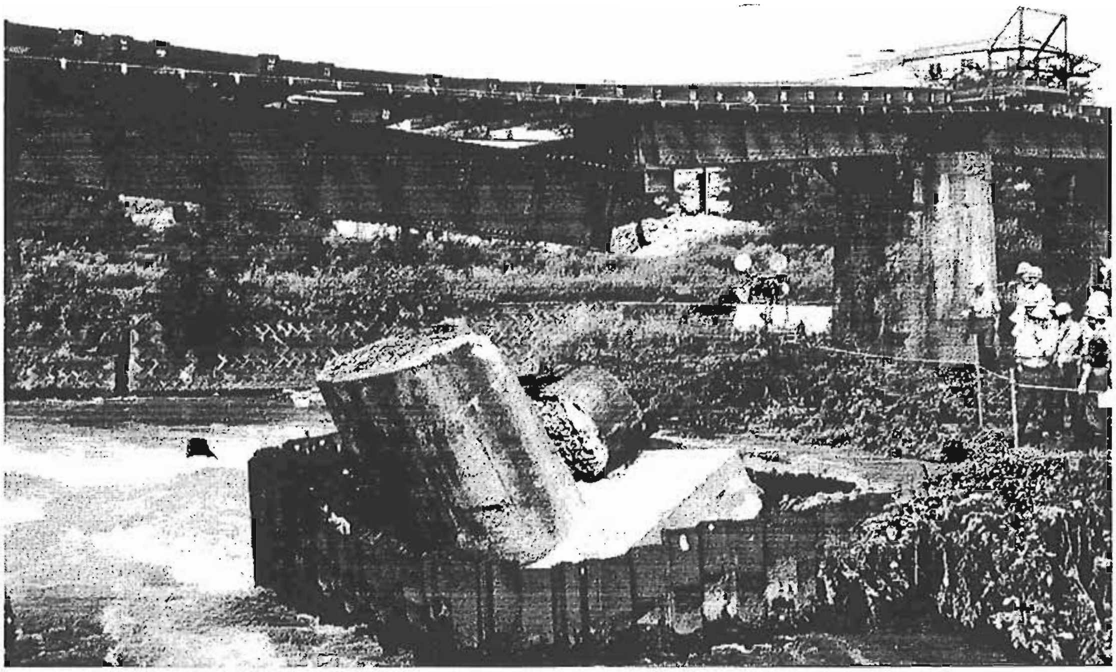

Fig.4-A Collapsed Pier of Nagakigawa bridge

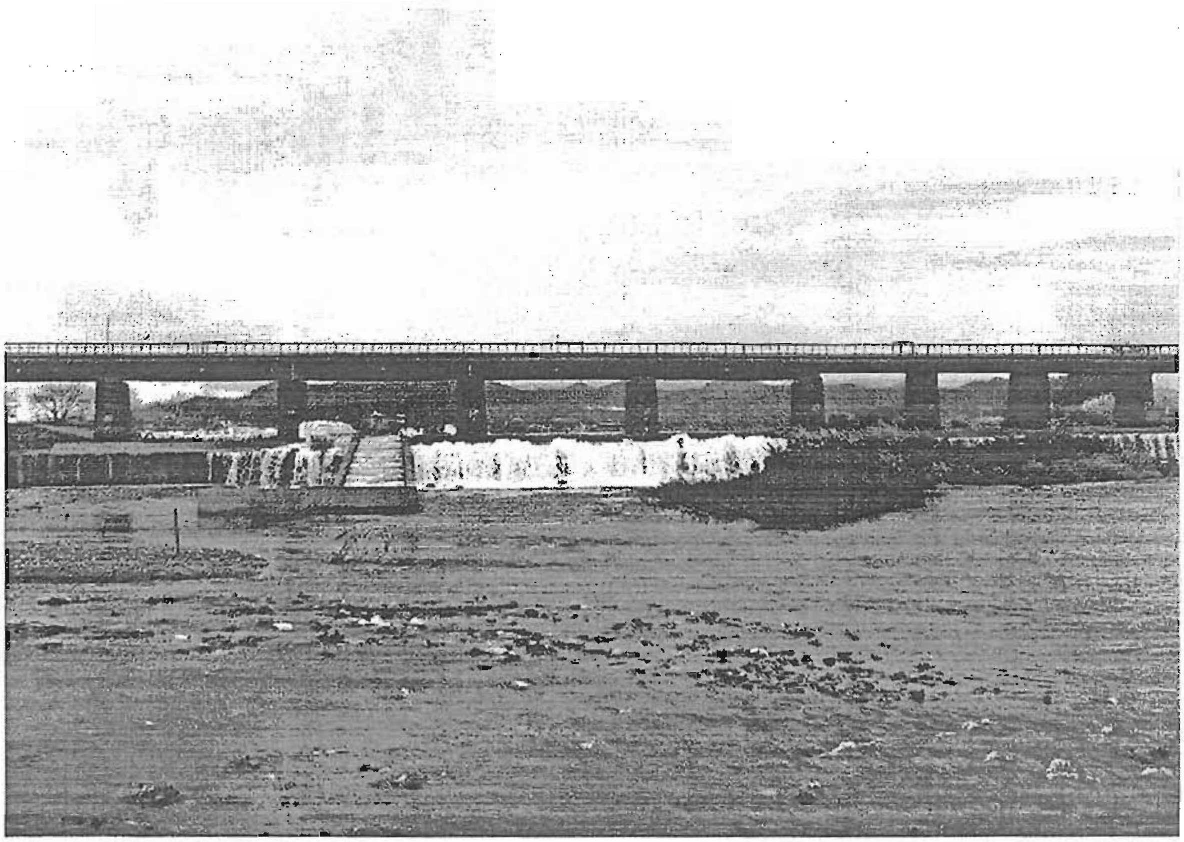

Fig.5- The head on the downstream of Nagakigawa bridge

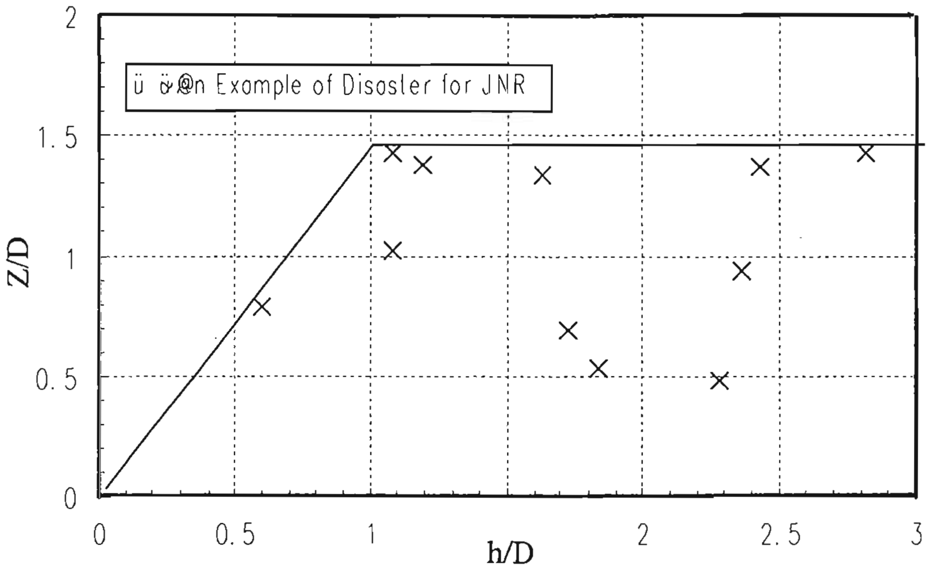

Z: The Depth of Bridge Pier Scouring
D: The Width of Bridge Pier Fall at Right Angles with Water Flow
h: The Depth of River

Fig.6-The current estimation method to estimate bridge pier scour depth

JR East lines. This system includes water gages under bridge piers and data transmission devices between sites and each regional train operation control center (TOC). At the moment when scour depth that presumed from water level approach to the end of bridge pier, Orders to stop train will be issued from TOC. Therefore, Train will not pass through the bridge that is in unsafe status according to this rule. (Fig.7)

However, disasters of 1995 and 1997 mentioned below proved that there are several types of score cases that cannot be foreseen by this rule. To analyze disasters both in 1995 and 1997, Follow things were studied.

1) Cause 1

Gradient of riverbed in disaster of 1995 was steep, which is the rivulet than be called river. Thus, water level almost does not increase with river flows increase, reversely, erosion force increased with increment of flow rate. Such as these rivers, it is impossible to presume scour depth on the basis of water level.

(An example for a calculation)

Generally water level approximately 10cm

Basis 100 years probable rain fall approximately 60cm

2) Cause 2

Both disasters of 1995 and 1997, head arisen in downstream region. This is become with cumulation of riverbed decline age long.

RIVER CHARACTEEERISTICS OF SCOUR CASES

Analysis of twelve bridge piers scours cases in JR-EAST that there are some causes of scour which are inherent to their river characteristics. As figure 8 shows, causes of scour are related to particularities which riverbed decline, large affection of downstream head, curvature of river course and others. However, the inference of scour depth so far has been made solely from the water level value of a bridge location; variation in river characteristics are not been taken into account for scours depth estimation.

We investigated riverbed decline that had intensely affection for scour in 19 rivers system, and 112 localities of JR-EAST area. Investigated results, we looked out swift tendency of riverbed decline under 1960 to 1970. The period of gathers river sand and built dams just in time is consistent with on highly development period of Japan.

Fluctuate rate of river bed shows in figure 9. We compared the mean riverbed level values per water system, and found a decline tendency in all of 19 water systems. On the other hand, riverbed decline rate show a convergent tendency in the last 10 years. Presumably, it can be considered to the effect of so called “the river sand gathering restriction law”, which was enacted in and around 1970’s.

However, heads were formed in downstream of bridges because of accumulation of riverbed decline until now.

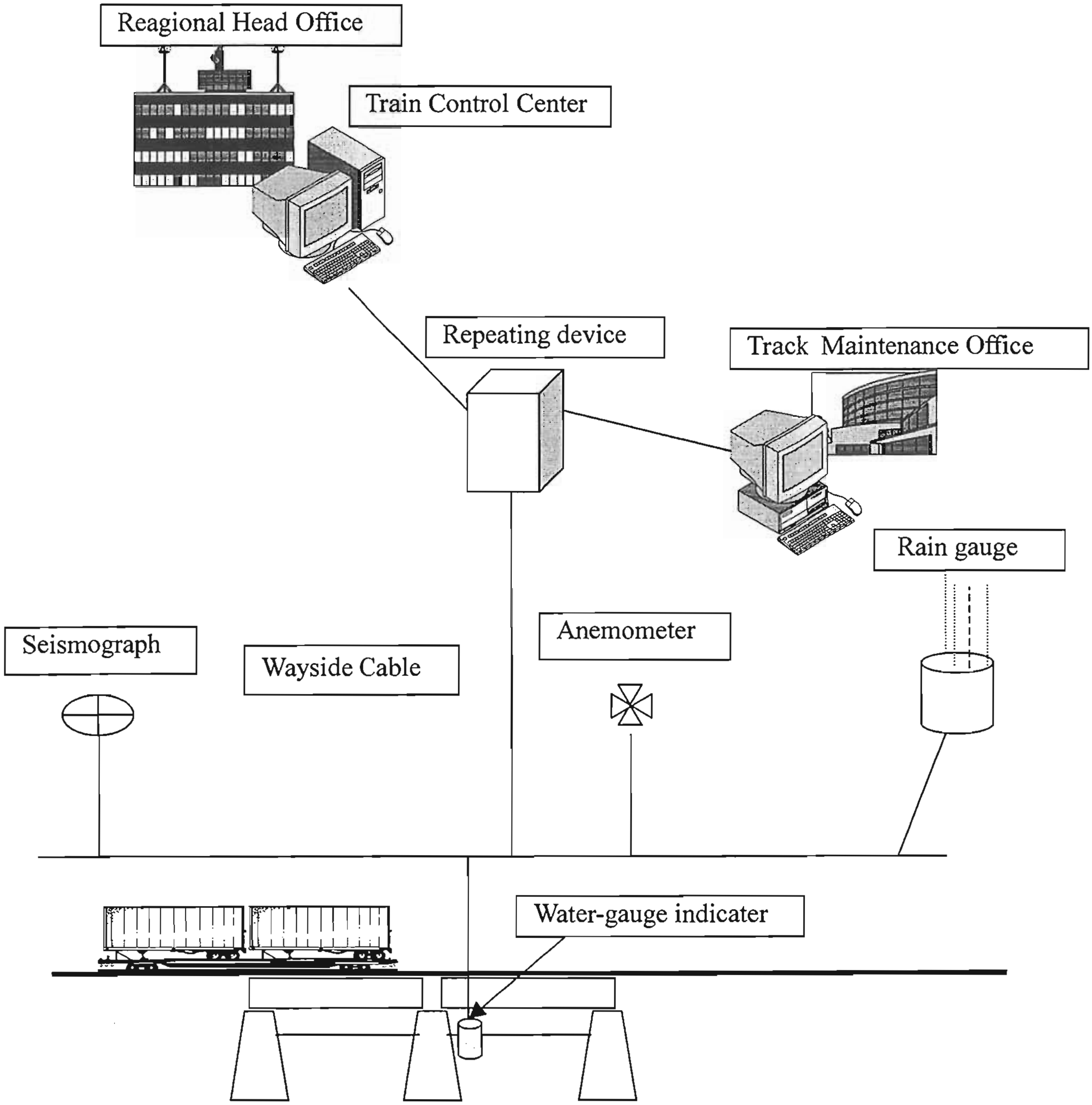

Fig.7- JR-EAST's meteorological observation and data transmission system

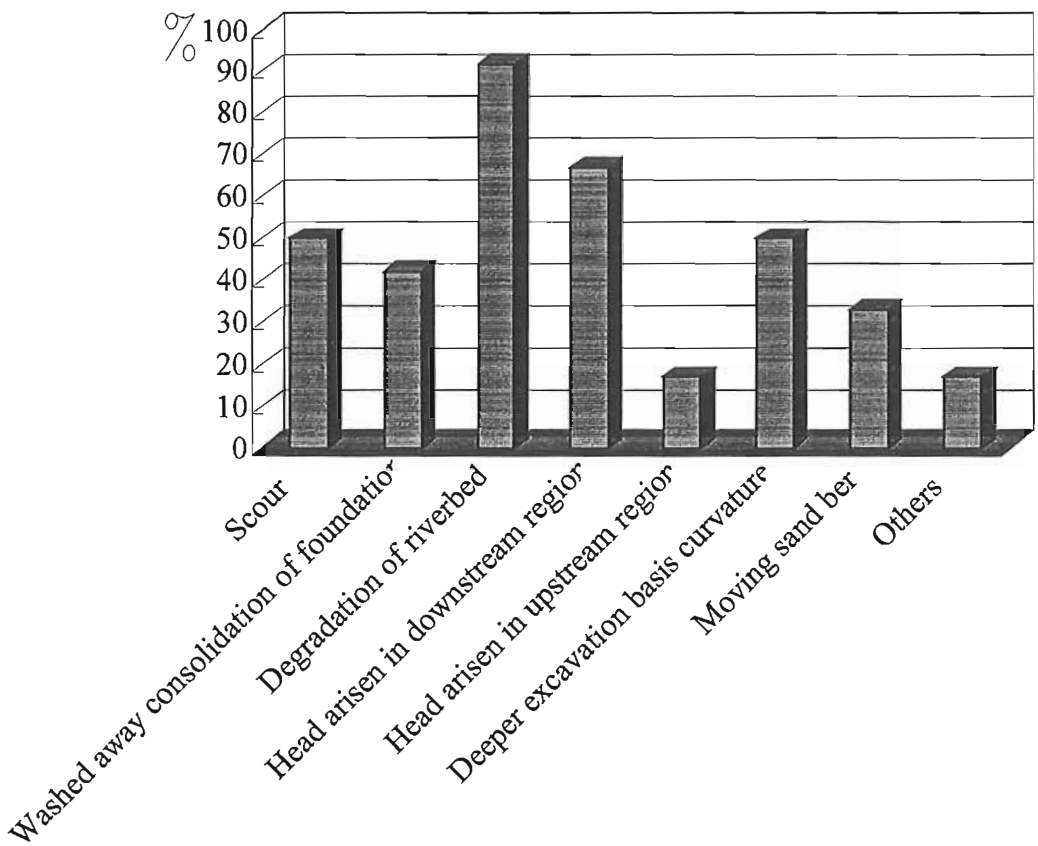

Fig.8 Estimated causes of scour in the 12 investigated cases

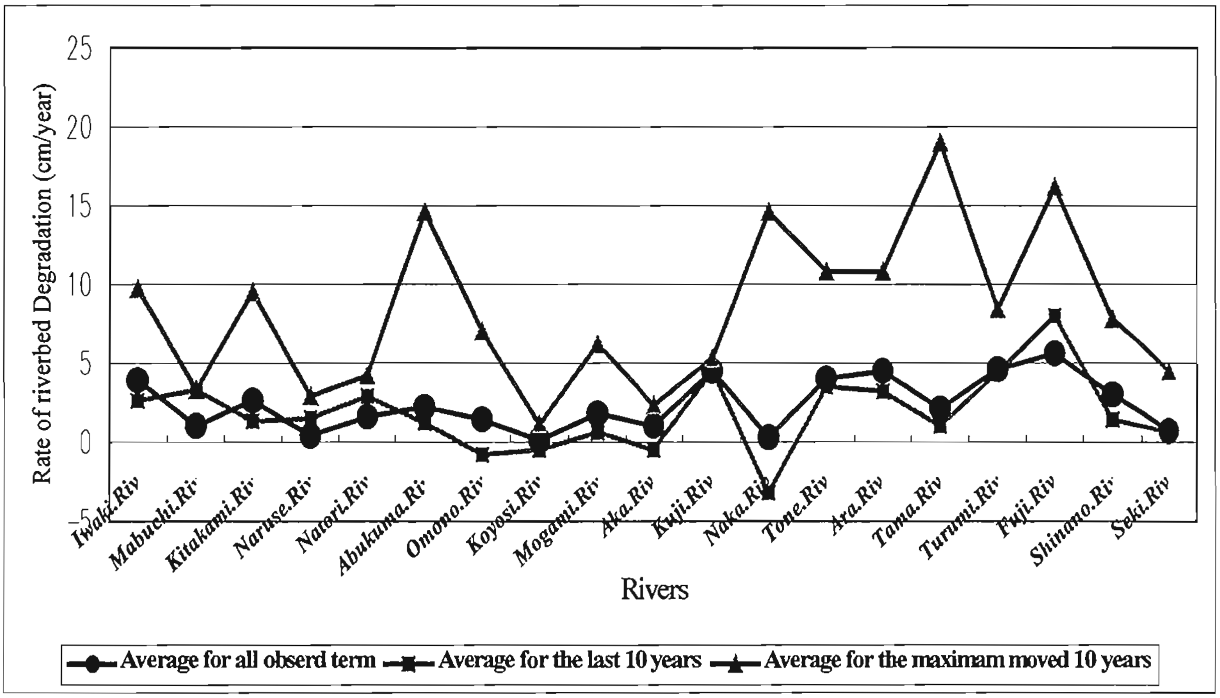

Fig.9 - Riverbed degradation in various rivers

RECENT REVISION IN TRAIN SUSPENSION RULES

As the result of investigation on sour cases of 1995 and 1997, we revised our train suspension rules as below.

1) An independent rule of scour monitoring was set for mountain streams whose flow velocity is large. This is because the above investigation proved the use of Tarapore equation to estimate scour depth is not appropriate for those fast flows as the hydraulic regions of Froude number 1 or larger. In addition, we made a picture diagram usable with river width coefficient and gradient for classification of any water cannel into either the "river" class, for which Tarapore equation is applicable, or the "mountain stream" class above mentioned. On the bridge that located on selected mountain tall streams, we plan to install scour monitoring devices that we have recently developed.

2) A new method was introduced to take river characteristics into account in estimating scour depth around individual bridge piers. In this method, the rule to locate the "origin of scour" was standardized in accordance with the river characteristics as below:

- Effect of a head that formed in downstream of the bridge
- Deeper excavation due to the location of the bridge in a steep curvature
- Deeper excavation due to the location of the bridge in a narrower river channel.

CONCLUDING REMARKS

In this paper, some important bridge scour cases and the outlines of the current train suspension rules against bridge scour hazard in JR East were described. The significant advantage of the new rules is are accuracy of scour depth estimation and versatility of application in accordance of various river characteristics. The new rules are planed to be applied from April 2000.

REFERENCES

1. Noboru, Sukegawa., et al., *"Kasen Kogaku"(Engineering of River). 3 nd ed*(in Japanese). Tokyo: Kajimashuppankai,1995

NEW ZEALAND REFLECTIONS ON BRIDGE SCOUR

By

Stephen E. Coleman[1], Bruce W. Melville[2], Christine S. Lauchlan[3]

ABSTRACT

New Zealand is a country with numerous rivers and streams and a high density of bridged river crossings. On average, at least one serious bridge failure each year in New Zealand can be attributed to scour of the bridge foundations, bridge scour having been a high-priority issue for transportation authorities in New Zealand over many years. Selected cases of bridge-scour damage that have occurred within New Zealand are presented herein to provide an overview of the range of scour processes occurring within the country. Owing to New Zealand's remarkably diverse terrain, the cases presented cover ranges of bed materials, flood magnitudes, bridge foundation configurations, and river morphologies. The presented case studies highlight important bridge-scour design considerations: including relevant aspects of river morphology to be considered (including variability in river course); that bridges can suffer potentially significant scour damage in floods smaller than the design floods traditionally used in scour analyses; that the effects of human intervention into a river (in the form of mining and river training works for example) in the vicinity of a bridge site can significantly impact bridge stability; and that the expected scour depth at a given bridge foundation can be severely underestimated if the combination of the full range of possible scour components is not considered for the foundation.

TYPES OF SCOUR

The types of scour that can occur at a bridge crossing can be classified as follows (Figure 1):

- ***Total scour*** is the combination of individual scour components at a bridge crossing.
- ***General scour*** occurs irrespective of the existence of the bridge and can occur as either long-term or short-term scour.
- Long-term general scour develops over a time scale normally of the order of several years or longer, and includes progressive degradation or aggradation and lateral bank erosion due to ***channel widening*** or ***meander migration***.

[1] Senior Lecturer, Department of Civil and Resource Engineering, The University of Auckland, Auckland, New Zealand.
[2] Associate Professor, Department of Civil and Resource Engineering, The University of Auckland, Auckland, New Zealand.
[3] Postdoctoral Fellow, Delft University of Technology, Faculty of Civil Engineering and Earth Sciences, Delft, the Netherlands.

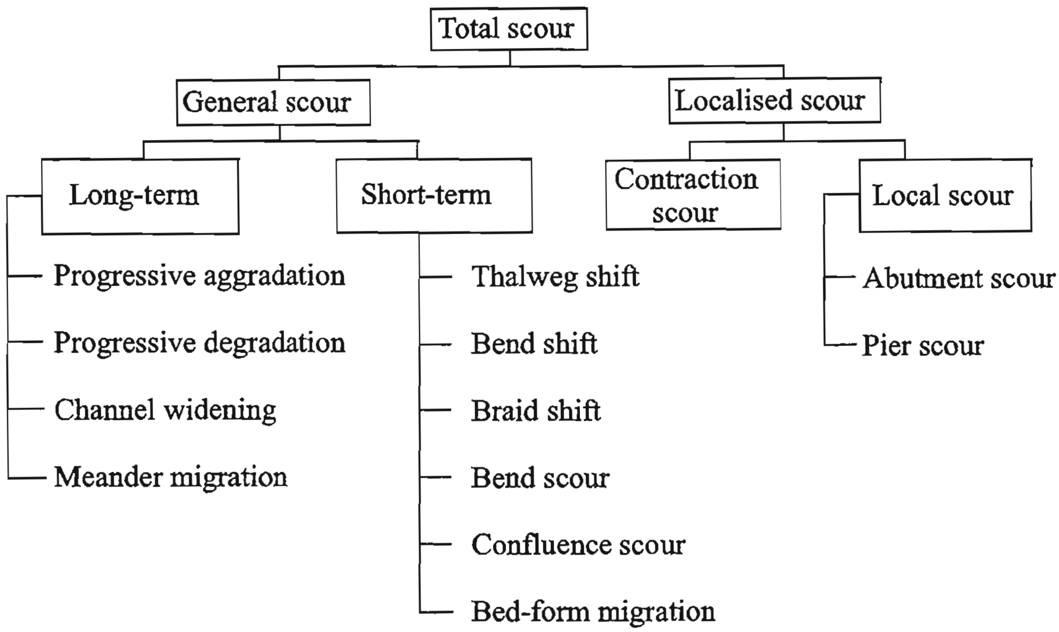

Fig. 1 Types of Scour at a Bridge Crossing.

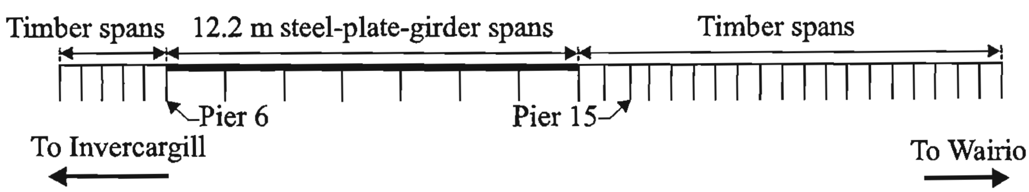

Fig. 2 Front Elevation of the Branxholme Rail Bridge in 1994, Looking Downstream (after Melville and Coleman, 2000).

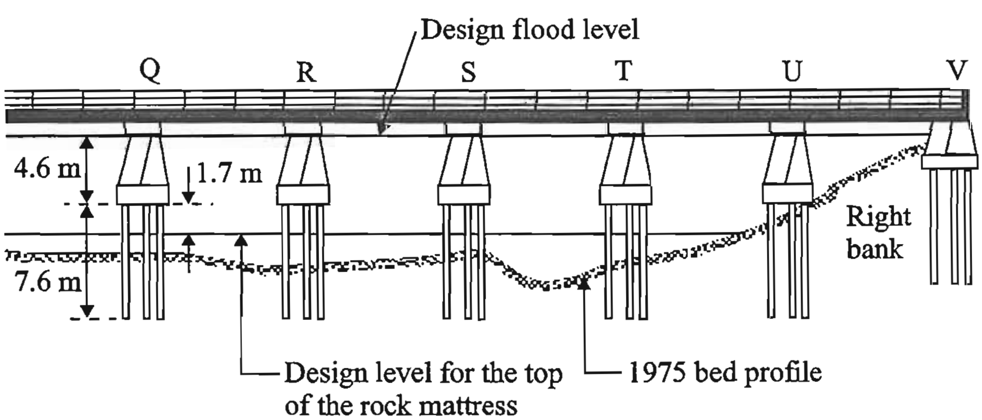

Fig. 3 Front Elevation of the Oreti River Road Bridge in 1975, Looking Downstream (after Melville and Coleman, 2000).

- ***Progressive degradation (aggradation)*** is the general lowering (raising) of the riverbed at the bridge site.
- Short-term general scour develops during a single or several closely-spaced floods. This type of scour includes scour arising from a ***lateral shift of a channel bend, a channel braid or the channel thalweg***; ***vertical scour in a bend***; ***scour at a confluence***; and ***scour arising from bed-form migration***.
- ***Localised scour*** is directly attributable to the existence of the bridge, and includes contraction scour and local scour.
- ***Contraction scour*** occurs where the bridge foundations (including approaches) constrict the flow.
- ***Local scour*** results from the direct interference of the bridge foundations with the flow, and includes ***abutment scour*** and ***pier scour***.

The effects of ***debris rafting*** at a bridge site further magnify any erosion around the foundations and also any lateral and vertical forces on the bridge due to debris and sediment loads.

Cases of bridge-scour damage are presented in the remainder of this paper in order to illustrate the range of these scour processes occurring for New Zealand conditions.

NEW ZEALAND CASES OF BRIDGE-SCOUR DAMAGE

Aggradation: Bullock Creek Road Bridge

The 49-m-long four-span single-lane Bullock Creek Road Bridge on State Highway 6 was built in 1938. In 1972, a major flood set off several slips in the catchment, which is on the line of the Alpine fault. The landslip-deposited material has subsequently been moved downstream by freshes and floods, this material repeatedly causing bed aggradation and bridge closure at the Bullock Creek bridge site. The sediment at the bridge site is predominantly gravels and cobbles, with a representative size of 30-150 mm, and with larger fractions up to the order of 1 m in size. The braided channel upstream of the bridge flows between large terraces formed by deposited landslip material that has been pushed to the edges of the channel.

A flood in January 1983 caused aggradation to a level more than 1 m above the deck level of the original bridge. Subsequent to this flood, the existing bridge was removed and the main channel was excavated. A replacement bridge was constructed about 100 m downstream of the original bridge, with the soffit level of the new bridge 2-3 m higher than that of the previous bridge.

Since the bridge replacement, the river has aggraded and cut down quite regularly. With the aggradation, the river has outflanked the bridge at each end, although the new bridge has not been buried. Bulldozers have occasionally been used to push aggraded bed material across to the riverbanks, the river then cutting down again in the central channel. It is expected that once the slips in the catchment stabilise, possible future degradation at the bridge site may require the construction of a rock weir to protect the bridge foundations.

Degradation: Little Man River Road Bridge
The two-way four-span Little Man River (Dry Creek) Road Bridge on State Highway 6, built in 1927, is 48.8 m long. The abutments and piers were founded on three and four respectively 7.6-m-long driven ironbark timber piles. The piles were of the order of 0.3-0.4 m in diameter. In 1985, timber planks were used to connect the piles to form solid piers to bed level. Except for the outer piles of the piers, which were raked at 1 in 9, all piles were vertical. The maximum pier height recorded in 1982 was 3 m.

The channel is braided with the bridge located at a channel contraction. The channel at the bridge site is relatively level across the floodway. Within 1 km downstream of the bridge, the river flows into the Whataroa River, which then flows about 20 km to the coast. The bed consists of cobbles and gravels with lesser amounts of sands and silts.

In the 1980s, the bridge suffered general scour arising from the Whataroa River, the downstream hydraulic control for the bridge site, either migrating or suffering a drop in bed level, which then resulted in a drop in the bed level at the bridge site. Undermining of the piers would have occurred had remedial action not been taken post-1985. The principal action consisted of the installation of a substantial rock weir extending downstream of the bridge. The weir constructed was of the order of 2 m high. Over time, the weir has been repeatedly topped up as the riverbed has continued to degrade.

Degradation: Oreti River Road Bridge and Branxholme Rail Bridge
Rock weirs were also used to remedy degradation at the two-lane 20-span 244-m-long Oreti River Road Bridge (built in 1955) on State Highway 99, and the 31-span 198-m-long Branxholme Rail Bridge (built in the 1890s) located 4 km upstream on the same river. In contrast to the Little Man River Road Bridge, degradation at these bridges has arisen due to human activities, principally in-channel gravel mining operations.

The slab piers of the Oreti River Road Bridge are supported on eight 0.4 m square reinforced-concrete piles driven no further than 7.6 m below the underside of the pile cap. Each pier pile cap measures 7.3 m x 1.0 m x 1.8 m (wide). The piers are oriented at approximately 80^{o} to the bridge centreline in order to be more aligned with river flows. The section of the Branxholme Rail Bridge relevant to the scour history incorporates Piers 6 to 15 (Figure 2), these piers consisting of 5 timber piles (3 plumb and 2 raked at 1 in 5). The piles for a given pier are of 0.3-0.4 m diameter and are numbered from downstream (Pile 1) to upstream (Pile 5). The pile caps measure approximately 0.3-0.4 m x 0.3 m x 4 m. 1916 piling records indicate that the piles for Piers 6 to 15 were sunk to approximately 12 m to 14 m below rail level.

Surface gravels at these bridge sites are of a median size of d_{50} = 11 mm and overlie blue-grey papa (mudstone/ siltstone) strata (at 13-14m below rail level for the Branxholme Rail Bridge). The river channel between and upstream of these two bridges has been mined for aggregates since the 1930s, gravel plants removing practically the entire available bed load. The significant gravel extraction has resulted in the larger sediment sizes in the river decreasing in size with time; the bed lowering generally by up to about 6 m; and exposure, softening, and erosion of the papa strata upstream of the bridges. For the 60 km reach upstream of these two bridges, the river presently grades from a braided channel to a point-bar and side-bar dominated channel with occasional mid-channel bars.

Over this reach, the river is free to meander within the floodway. Riverbanks within the floodway are low and usually grassed, and the floodplain is low. Spillovers into the extensive low floodplain are minimised by extensive stopbanks and willow protection. Debris accumulation can be a problem for the piers central in the river. At the road bridge, the river incorporates a flood plain of approximately 150 m width, with flow approaching the bridge at approximately 70° to the bridge centreline. Meandering has resulted in the river approaching the Branxholme Rail Bridge at an angle of about 20° to the bridge centreline.

Gravel-mining-accelerated degradation has occurred over the lives of both of these bridges on the Oreti River. Degradation at the Branxholme Rail Bridge has been further exacerbated by the upstream interception of bed-load sediments by a weir used to facilitate water withdrawal. Flooding in February 1994 resulted in several piles of Pier 7 of the Branxholme Rail Bridge being undermined. This flood constitutes the third largest annual maximum over the period 1977-1996.

In 1975, a weir composed of vertical timber piles was noted to be across the entire main channel 66 m downstream of the centreline of the Oreti River Road Bridge. Between 1977 and 1978, a rock weir was constructed with the existing timber weir as its upstream face and defining the weir crest level. A rock mattress was also constructed beneath the bridge (Figure 3). The mattress extends across the width of the main channel, with the 16-m-wide crest at a level of 1.7 m below the level of the underside of the pile caps and centred along the bridge centreline. Despite continued degradation of the river upstream, the rock weir and mattress have prevented further significant degradation of the streambed at the bridge site. Although some rock has been replaced due to fretting, the structures haven't needed to be topped up to compensate for general scour resulting from the mining.

As a result of the 1994 scour damage of the Branxholme Rail Bridge, Piers 7 and 11 were underpinned using steel H-piles driven to 18-21 m below rail level, and a rock weir was constructed downstream of the bridge. The weir centreline varies from 6 m to 12 m downstream of the bridge centreline. The crest of the weir is 2.5 m wide and is generally 9 m below rail level, with elevated sections towards the banks to facilitate fish passage along the river. The rock weir was expected to require maintenance by topping up, as a result of flood damage for example. Flood-level warnings have been set to enable the railway line to be closed in extreme events.

Degradation: Ashburton River Road Bridge

This road bridge (on State Highway 1) over the Ashburton River is a 340-m-long, two-lane, reinforced-concrete structure that was built in 1931. The bridge comprises 31 slab-type piers (Figure 4), about 25 of which lie within the active river channel. Each pier is founded on seven 400 mm reinforced-concrete octagonal piles. These piles were driven to a relatively uniform depth of between 6.5 m and 6.7 m below the underside of the pile caps.

The Ashburton River in the vicinity of the bridge site is about 280 m wide, is straight, uniform in slope and width, and is bounded by trees and straight stopbanks. The channel is braided and there is evidence of active bed movement. The bed material is well-graded gravel. Over the life of the bridge, various stopbanking, river-clearing works and gravel-extraction works have taken place over extensive lengths of the river, upstream and downstream of the bridge. The extraction of gravel from the river has been, and continues to be, controlled.

General scour exacerbated by gravel extraction from the river has resulted in a gradual lowering of the bed level at the bridge site (Figure 4). Concern for the vulnerability of the bridge to scour damage was accentuated by the shallowness of the foundation piles, and also debris rafts forming at the site increasing the potential for local scour pier undermining and bridge damage or failure in significant floods.

Rock aprons were constructed in 1979 around each of the piers within the active channel (Figure 4). Each apron measures 5 m wide, 15 m long and 1.6 m thick. Rock riprap of a median size d_{50} of 0.5 m was used to construct the aprons, with the upper surface of each apron located beneath the riverbed surface and approximately 2 m below the base of the pile cap. Aprons act to reduce the scour potential at piers both by armouring the bed against local scour due to local hydraulic vortices, and also by protecting against general scour by dropping at the apron extremities as this scour develops. Aprons nevertheless cannot provide total assurance against scouring, particularly for ongoing general degradation. Inspection in 1994 indicated the rock apron to be exposed at one pier only. Bed levels in the river channel continue to be regularly monitored.

Degradation and Channel Widening (also Bend and Local Scours): Blackmount Road Bridge
The 82-m-long single-lane Blackmount Road Bridge (Figure 5) crossing the Mararoa River forms part of Weir Road from Clifden to Manapouri in the South Island of New Zealand. Pier B (C) was supported by two staggered rows of four (three) driven vertical 0.4 m x 0.4 m concrete piles.

About 1.5 km downstream of the bridge site, the river flows into the Waiau River. Owing to water levels being lower than anticipated, the waterway area at the bridge site is in excess of that required to pass the 100-year flood. The bridge is located in a mild right-hand bend of the river (radius of curvature ≈ 500 m), the river approaching the bridge at about 60° to the bridge centre-line. The wall-type piers were aligned perpendicular to the bridge centre-line, with Pier B towards the outside of the bend (Figure 5). Below the underside of the pile cap for Pier B were about 2 m of gravels (large) and boulders underlain by about 11 m of tight gravels with some sands and sand lenses. Debris accumulation, principally parts of trees, can occur at the bridge piers.

During the failure event in August 1980, the channel scoured across the width of the flood flows. The flood that caused failure peaked at about 900 m^3/s, the largest recorded flood peak over the period 1963-1996, with a peak flow duration of about 6 hours. The flows at an angle to the wall-type pier resulted in undermining and removal of Pier B. With the loss of the foundation, the bridge superstructure buckled but remained in place. The deflected bridge deck profile had a maximum deflection at the position of the removed pier of approximately 3 m. A maximum scour depth of about 2.9 m was subsequently measured at the position of the failed Pier B, scour depths decreasing with distance away from this pier. Slipping of the undermined embankment around Pier C (degradation-associated channel widening) exposed the piles for this pier.

Remedial work consisted of restoring the riverbed to the original level using natural riverbed material, replacing Pier B (about 3.5 m closer to Pier C), reinstating the slipped material around Pier C, protecting the piers and the embankments using rock riprap, and replacing the superstructure with similar steel trusses. The new Pier B consists of a 1.5-m-diameter concrete cylinder down to the restored bed level, then a 1.9-m-diameter concrete cylinder encased in a steel shell extending

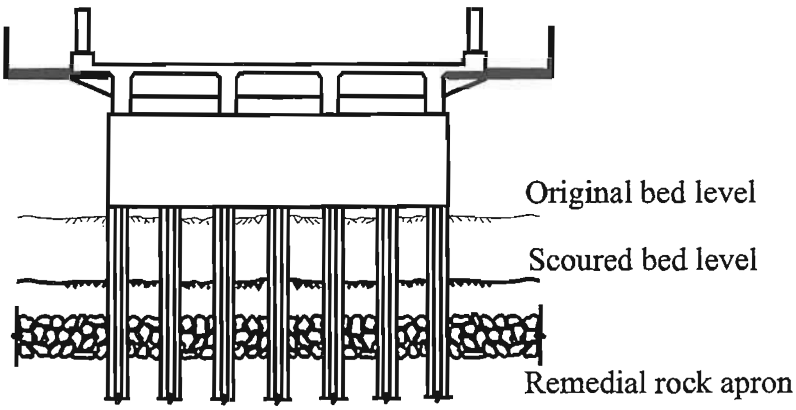

Fig. 4 Typical Side Elevation of a Foundation and Remedial Works for the Ashburton River Road Bridge (after Coleman and Melville, 1999).

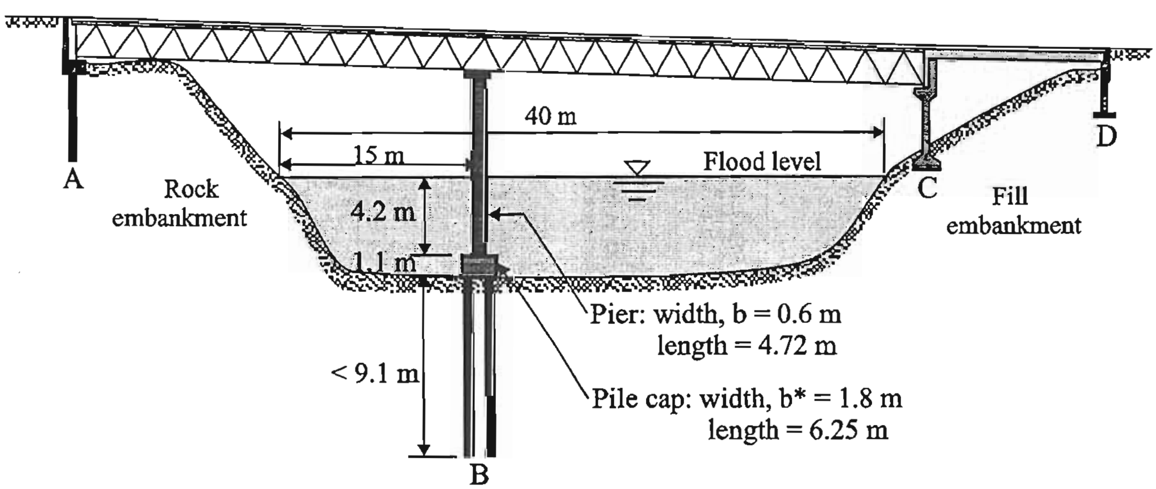

Fig. 5 Schematic Elevation of Blackmount Road Bridge, Looking Downstream.

down to 12 m below bed level. This pier was protected by a circular rock mattress extending 3 m out from the face of the pier and extending from the restored bed surface to a depth of 3 m.

Bend Scour and Shift (and Local Scour): Waipaoa River Rail Bridge
The Waipaoa River Rail Bridge crosses the Waipaoa River on the Palmerston North to Gisborne rail line in the North Island of New Zealand. The bridge was initially constructed about 1938 as a 220 m long railway bridge.

As a consequence of flooding in 1948-1951, the bridge was lifted by 0.6-0.7 m and lengthened to about 330 m at the Palmerston North (southern) end of the bridge. Each of the four new foundations was a barbell-style concrete pier supported by two cylinders of 2.44 m diameter extending down to 16-22.5 m below the local mean sea level (MSL) datum. River training works upstream of the bridge were subsequently used to bring the deep part of the channel under the bridge extension, which was supported by the new deeper cylinders.

The bridge is located approximately 1.5 km from the mouth of the Waipaoa River. As a consequence of the May 1948 flood, a flood control scheme was completed in essence in 1961, a major engineered cut-off located immediately upstream of the bridge essentially making the 1 km reach upstream of the bridge into a significant sharp left-hand bend of about 90° (Figure 6). The river bend on which the bridge is located has since been migrating, changing both the river alignment and also where the flow is focused with respect to the bridge, with repeated overflows and erosion to the south (Figure 6).

The river bed has been and is continually degrading. A 1973 soil profile at the bridge site shows 0.5 m of clay/ silt below MSL, underlain by 3.5 m of clay/ sand, 8.5 m of sand, and then 17.5 m of sand with some thin layers of clay.

Cyclone Bola passed over the East Cape region of New Zealand over the period 6-9 March 1988, the cyclone imposing considerable damage to the region. On March 7-8 1988, flooding at the bridge site broke the stopbank to the south and outflanked the true right-hand-side abutment by a distance of 120-130 m (Figure 6), the river bend attempting to continue migration patterns apparent from earlier records of the river profile (Figure 6). The bridge failure event was estimated to be of a peak flow rate of 5300 m^3/s, some 20 % above the original 100-year design flow rate.

Damage to the bridge arose from a combination of general scour (degradation and bend scour) observed over a significant width of the channel, local pier scour and lateral bend migration. The southern abutment and the three adjacent piers were significantly affected by a combination of local scour and general scour, the abutment being undermined whilst acting as a pier (having been outflanked), rotating, and moving 130 mm in the upstream direction.

Remedial work consisted of underpinning the southern abutment as a pier, imposing passage limitations on traffic using the bridge, a programme of scour monitoring, extending the bridge, and revised stopbanking and groyne and riprap protection of the outside of the bend upstream of the bridge site. The abutment was underpinned using 3 shell piles of 0.75 m diameter at each end of an extended pile cap, the piles extending to about 23 m below the local MSL. In order to limit loads on the existing piers adjacent to the abutment, a low-speed limit was imposed for traffic on the bridge.

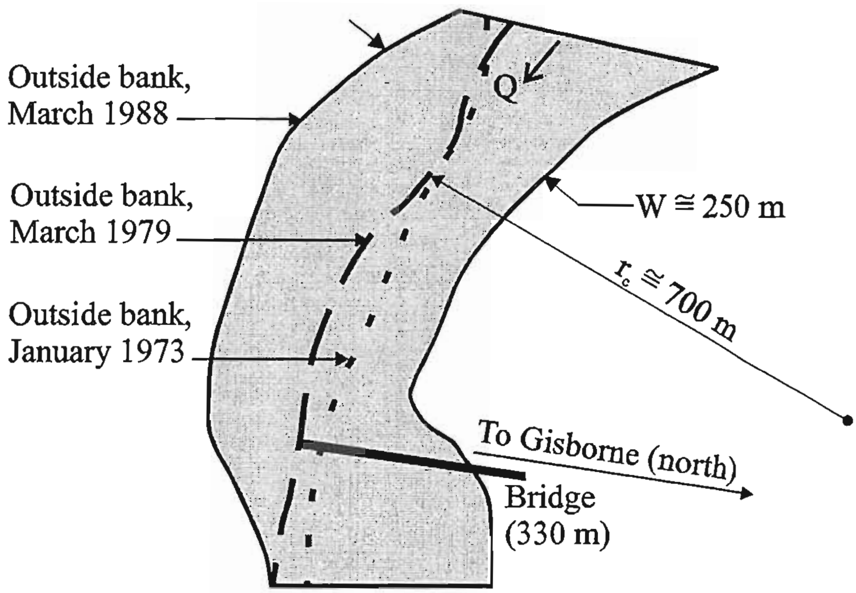

Fig. 6 Schematic Plan View of the Near-field for the Waipaoa River Rail Bridge.

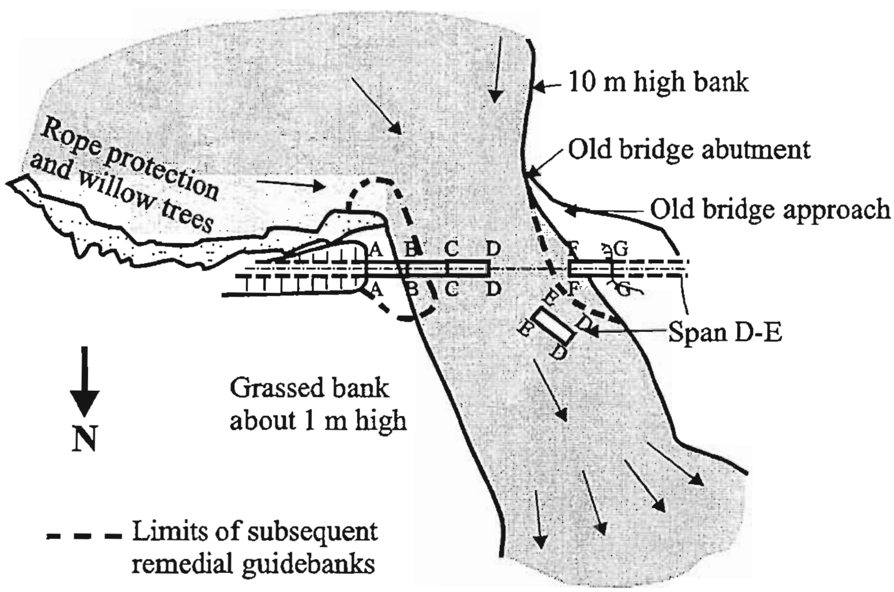

Fig. 7 Schematic Site Plan of the Waitangitaona River Road Bridge Failure (after Coleman and Melville, 1999).

Traffic was also to be stopped from crossing the bridge at predetermined wind intensities and flood magnitudes. This latter remedial measure was adopted based on the low volume of traffic using this line. The bridge was extended to the south by twelve steel-plate-girder spans of 12.2 m length. The new piers consist of a reinforced-concrete cap supported by two reinforced-concrete piles of 0.75 m diameter raked at 1:6 (H:V) along the line of the pier, the piles extending down to about 20 m below the local MSL datum.

Braid Shift and Confluence Scour (and Local Scour): Bealey Bridge

The influence of braid shift on bridge vulnerability to scour, including evidence of the relative significance of confluence scour, is highlighted in the accompanying bridge-scour case study of Bealey Bridge given in the proceedings of this symposium (Coleman et al., 2000). This case study also highlights that bridges can suffer potentially significant scour damage in floods much smaller than the design flood.

Contraction Scour (and Local Scour): Waitangitaona River Road Bridge

This six-span two-lane bridge across the Waitangitaona River (State Highway 6) is 149 m long and was built in 1968 to replace a bridge that needed to be raised owing to channel aggradation (resulting from a major slip upstream in the 1920s). The new bridge was supported by reinforced-concrete abutments and slab piers, each pier being supported by a row of nine 380 mm square blunt-ended prestressed concrete piles. All but the central pile were raked at 1:8 (H:V) along the line of the pier. The piles for the piers were driven to 9.3 m below minimum bed level. The channel bed is composed of surface gravels and cobbles with relatively minor amounts of sands and silts, and a substrata of medium to dense gravels.

The bridge spans a sudden contraction section of a wide channel containing a braided river at low flows (Figure 7). A shift and shortening in the river course downstream of the bridge resulted in rapid bed degradation at the bridge site during construction of the bridge in 1967. This degradation and later flooding resulted in piles extending to only 6.8 m below the minimum bed level. The angle of flow attack on the slab piers also increased at this time. The channel was relatively flat between the five central piers.

On 12 March, 1982, a flood occurred for which the peak flow was estimated to be 700 m^3/s (AEP = 2%), the bridge design flood flow being 850 m^3/s. Debris, including trees up to 20 m long and 1.2 m in diameter, were noted in the flow and adjacent to the piers as the flood receded. The skewed approach flows held the debris against the sides of the exposed piles of the piers during the flood event.

For the 1982 flood, it appears that the two approach embankments concentrated flow between Piers D and F at an angle of about 30° to the face of Pier E (Figure 7). The flood flows at a skewed angle to the pier, exacerbated by debris accumulation effects, resulted in increased lateral loading and increased scour depths for Pier E. Pier E was consequently scoured out, with the associated loss of the two adjoining deck spans (Figure 7). The remaining sections of the bridge were undamaged. Scour holes at the piers were noted to be infilled as the flood receded.

New guidebanks extending into the channel were subsequently established through the bridge site (Figure 7). A 1.5-m-thick riprap layer at a slope of 2:1 (H:V), extended by a horizontal riprap toe apron 2 m thick with its upper surface at the existing bed level, was used to protect existing piers located within the new guidebanks. For these piers, the existing piles were also supplemented with three steel H-piles at each end of the pile cap. These additional piles extend to 13 m below the design bed level. Each remaining pier in the revised stream channel was underpinned with two cylinders of 1.5 m diameter at 11 m centres, each cylinder connected to the existing pier via a 1.0 m octagonal column above the design bed level. The cylinder foundations were driven to 13 m below the bed. In order to allow some clearance to minimise any debris accumulations at the piers, the existing piled foundations and mass concrete skirt for each of the piers in the revised stream channel were removed along with the base of the slab pier to 2m above the design flood levels.

Thalweg Shift Effects

While not as visually apparent as channel shift for braided streams, a shift in the thalweg will alter local bed elevations and can change the point and/or angle of attack for a flow. This can lead to markedly increased scour at a pier or abutment, or the possibility of increased scour around piers not originally designed to be in the main channel. Yeo (1991) attributes 1985 damage to the approach of a bridge in Thames, New Zealand, to a shift in the thalweg towards the true-right bank, this shift concentrating flow at the approach.

Bed-form Migration Effects

The magnitudes of sediment waves influence bridge scour because wave troughs momentarily and locally lower bed elevations as waves propagate through a site (sand dunes growing to heights of up to the depth of the overlying water body). In addition, gravel-bar migration can reduce channel waterways and redirect flows at bridge sites, possibly resulting in increased scour owing to flows concentrating at bridge foundations or in channel confluences. For most flows inducing general sediment motion at a bridge site, sediment waves will be migrating through the bridge site and influencing scour at the bridge foundations.

REFERENCES

1. Coleman, S. E., and Melville, B. W. (1999). "New Zealand case studies of scour at bridge foundations." Proc., International Association for Bridge and Structural Engineering Colloquium on 'Foundation for major bridges: design and construction', New Delhi, India, 22-24 February, 1999, 335-340.
2. Coleman, S. E., Melville, B. W., and Lauchlan, C. S. (2000). "Bealey Bridge scour failure." Proc., International Symposium on Scour of Foundations, Melbourne, Australia, November, 2000.
3. Melville, B. W., and Coleman, S. E. (2000). "Bridge scour." Water Resources Publications, Colorado, USA, 550 pp.
4. Yeo, E. H. (1991). "General scour at bridge sites." Report No. 501, School of Engineering, The University of Auckland, Auckland, New Zealand, 312pp.

LOCAL SCOURING AND SCOUR COUNTERMEASURE IN MALAYSIA

By

Yee-Meng Chiew[1], See-King Ng[2], Siow-Yong Lim[3]

ABSTRACT

The paper presents information pertaining to the design and maintenance of bridges in Malaysia. It also outlines the procedure on how bridges are inspected, and eventually how remedial actions are taken in the event that failure is detected. Three bridge sites, that is Pukin River Bridge, Keratong River Bridge and Plentong River Bridge are cited as recent case history on how local scouring affected the integrity of the bridge, and how the local authority tackled the problem. The data also reveal that a certain scour countermeasure appears to be successful when applied to a particular site, but fails miserably when used in a different location.

INTRODUCTION

Bridges are normally built to span either a valley or a stretch of water. In the latter case, it forms a link between two land masses across a river, a bay or a strait. The bridge needs to be designed to satisfy not only the structural, but also the hydraulic requirements. The hydraulic design includes considerations of both the capacity of the flood peak through the bridge opening as well as the ability of the bridge foundation to withstand the loading imposed on the bridge. The integrity of the bridge is often jeopardized when scouring occurs at its foundation. Studies reported in the literature (Smith 1976) have shown that most of the bridge failures in the United Kingdom and USA are due to scouring at its foundation. This is reinforced by the experience in Malaysia. Ng and Razak (1998) reported that bridge failure due to structural damage is very rare in the country. The main cause of bridge failure is over-topping of the bridge deck or washout of embankment during major floods.

Despite having so much data that clearly point towards the important correlation between bridge failures and hydraulic requirements, practicing engineers often overlook its importance in their design. This is especially so with the lack of proper considerations of the fluid-sediment-structure interaction, which is the main cause of foundation failure around the structure. One of the main reasons that the hydraulic aspects are often neglected is because structural engineers, who are tasked to design bridges, are often unsure of the implications.

[1] Associate Professor, School of Civil & Structural Engineering, Nanyang Technological University, Singapore 639798

[2] Senior Assistant Director (Rehabilitation), Bridge Unit, Public Works Department, Malaysia

[3] Associate Professor, School of Civil & Structural Engineering, Nanyang Technological University, Singapore 639798

The main objective of this paper is show how the hydraulic aspect of bridge design is tackled in Malaysia. The effect on foundation scour on the integrity of the bridge is highlighted. Three different bridge sites, that is Pukin River Bridge, Keratong River Bridge and Plentong River Bridge were chosen as examples to illustrate how remedial actions were taken to arrest erosion, although success is not always guaranteed.

HYDRAULIC DESIGN PRACTICES IN THE PUBLIC WORKS DEPARTMENT (PWD) MALAYSIA

Because hydraulic considerations are extremely important to ensure the integrity of a bridges and culverts, the Malaysian authority has placed high emphasis in the hydraulic design of bridges. In the Public Works Department, Malaysia, the design philosophy builds upon the considerations that bridges may fail due to:

(a) inadequate flow capacity leading to over-topping of the bridge deck or the approach embankments;
(b) increased loading on the structure from water, sediment or debris; and
(c) failure of the foundations or supports as a result of bridge scouring.

The solution to the first problem involves the determination of the design discharge and the flow capacity, and to ensure that the former is less than or equal to the latter. The design discharge can be calculated using either the measured stream flow data or rainfall records. In Malaysia, guidelines for the procedures to calculate this value are contained in a series of documents published by the Drainage and Irrigation Department (DID) under the Ministry of Agriculture. Some of these publications are Heiler (1973, 1974), Heiler and Chew (1974), Lewis et al (1975) and Taylor and Toh (1980). The Public Works Department (PWD) in Malaysia utilizes a 100-year storm for bridge design and a 50-year storm for culvert design.

To counteract the second problem, the department proposes the provision of a freeboard, which is the vertical distance between the highest water level and the soffit level of the bridge deck. A value ranging from 0.3 m to 1.0 m is used, with the lower value for channels that are not expected to have debris or floating logs. However, if debris and floating logs are expected in the river, the force exerted by these objects on the piers must also be considered in the design of the pier. The standard practice by the Public Works Department (Public Works Department Malaysia, 1982, 1985) to calculate these forces is as follows:

For debris:

- the force shall be computed based on a minimum depth of 1.22 m (4 feet) of debris; and
- the force shall be computed based on the assumption that the length of the debris is equivalent to half the sum of the adjacent spans.

For floating logs:

- the force shall be computed based on the assumption that the log weighs 2 tonnes, and travels at the normal stream velocity; and

- the log shall be assumed to stop at a distance of 30.5 cm (12 inches) for timber piers, 15.2 cm (6 inches) for column-type concrete piers, and 7.6 cm (3 inches) for solid-type concrete piers.

The third problem involves failure of the structure due to scouring at its foundation. The local authority does not normally estimate the probable depth of scour for short and medium bridges. The common practice is to use only piled foundation. No guideline for scour protection such as riprap is available.

Recently, the Public Works Department in Malaysia, in collaboration with the Japan International Cooperation Agency has undertaken two studies (JICA and PWD 1992, 1996) and identified many "hydraulic defects" in Malaysian bridges. These are summarized as follows:

(a) Inadequate bridge opening;
(b) Inadequate slope protection around abutment;
(c) Unsuitable bridge siting at sharp bends;
(d) Piers skewed to river flow;
(e) Obstacles like old bridge piers remain under bridge;
(f) Floating logs or debris not removed; and
(g) Rivers and mining activities near the bridge sites.

The main causes of the above defects are attributed to both design and maintenance. The level of uncertainty associated with hydraulic designs far exceeds those associated with structural design. For example, the ability to accurately predict flood levels is much more difficult than to predict the effect due to vehicular loads. Furthermore, the design location is normally subjected to changes that occur both upstream and downstream of the bridge site, but the designer is often unaware of future changes or unable to control such changes. With this in mind, a proper design of hydraulic structures involves not only the necessity of an accurate set of hydraulic calculations, but also a good conceptual design of the structure as well as the entire waterway. In this respect, the Public Works Department in Malaysia has adopted the following recommendations from the Drainage and Irrigation Department in the country:

- the bridge structure should cross the river perpendicularly;
- abutments should not protrude into the waterway;
- the number of piers in the river should be minimized;
- the shape of bridge piers should, as far as possible, be oval; and
- the pile caps should be buried by at least 1.2m below the expected scoured depth.

BRIDGE INSPECTION

To ensure the integrity of a bridge, it is necessary that an accurate prediction of the hydraulic parameters and an appropriate measure to prevent any adverse effect on the hydraulic structure are carried out at the design stages. In addition, it is also crucial that a system of surveillance exists to identify hydraulic problems in existing bridges so that immediate remedial actions can be activated. In Malaysia, the traditional approach is that the PWD district offices undertake inspection of bridges and culverts after each flood season.

Generally, Malaysia's rivers flow in abundance, a result of the high rainfall in the country, with an annual average rainfall of 2420 mm in Peninsular Malaysia, and 2630 mm and 3830 mm for Sabah and Sarawak, respectively. The flooding season normally takes place during the North-East Monsoon, which lasts from November to February. During this period, very heavy rainfall occurs, with as much as 600 mm in 24 hours in extreme cases, along the east coast of Peninsular Malaysia, Sabah and Sarawak. Yusof (1996) reported that the inspection exercise has been expanded to include condition survey and this has become mandatory since 1995. The inspection is essentially visual and involves the assignment of a numerical rating to each bridge or culvert to indicate its condition. A rating of "1" represents excellent condition whereas a rating of "5" means critical condition (Public Works Department Malaysia 1995). Table 1 shows an example of the checklist used in the country. Only items related to hydraulic problems are indicated. A description of the damages and proposed maintenance activities is recorded in the checklist accordingly.

Table 1. Partial Inspection Checklist used for Bridges in Malaysia

Bridge Components	**Ratings**		**Damages**	**Maintenance**
	Old	**New**		
Slope Protection				
Pier				
etc.				

With regard to scouring problem, the annual mandatory bridge inspection would only be able to detect erosion problems above the waterline, such as slope protection around the abutment. The present scheme is not able to reveal potential scouring problem at the piers beneath the waterline. To overcome this drawback, the department occasionally engages specialist divers to carry out underwater inspection. The obvious predicament with this tactic is that the divers often do not have adequate knowledge in bridge engineering. Besides, visibility is normally very poor under water. The PWD Malaysia has recently acquired an echo depth-sounding device called Fathometer (from Raytheon, USA). It can be used to measure water depth and determine the extent and severity of scouring.

REMEDIAL ACTIONS

Remedial actions play an essential role in the total management of a bridge against failure. An adequate design and frequent inspection may be futile without appropriate remedial actions to arrest deterioration of the bridge due to adverse hydraulic effects. Ng and Razak (1998) have identified the following remedial actions:

- replacement of the bridge;
- modification of the bridge;
- replacement of the scoured material;
- provision of armor material; and
- provision of flow control.

Replacement or reconstruction of the entire bridge with due considerations of the current hydraulic requirements may be very effective in arresting deterioration of the bridge. However, this involves high cost and disruption to traffic flow. Modification of the bridge is a step towards cost reduction as compared to replacing the entire bridge. This includes altering the foundation, such as adding piles; underpinning and construction of relief culverts.

Replacement of scoured material involves placement of erosive resistance material such as crushed aggregates or riprap stones. In the light of recent investigations by Chiew (1995) and Chiew and Lim (2000) on the failure behavior of riprap layer at bridge piers, this method is likely to require recurrent maintenance, especially under live-bed conditions where bedforms are present. In addition, the replacement of scoured material is often not done in accordance with specifications and the replaced material may protrude into the river and cause obstruction to the flow, aggravating the erosion problem. In the local context, the provision of armor material refers to the construction of a revetment to protect the sub-structure of the river bank. The commonly used material are gabions, riprap, grouted riprap, bagged concrete, sand bags and precast concrete blocks. Finally, the provision of flow control refers to the training of rivers in such a way as to eliminate the undesirable hydraulic effect on the bridge structure. This involves the construction of spur dikes and sheet piles.

All the above methods, except the construction of spur dikes, had been used by the Public Works Department in Malaysia. Table 2 shows a summary of some of the projects undertaken by the department. Ng and Razak (1998) reported that the department tends to favor using a flexible revetment system, such as sand bags, over a rigid system like concrete blocks. In many instances, a change to the main flow direction of the river has been identified as the main cause of the problem at the bridge site. The department is currently contemplating doing some river training works as a longer-term solution.

Table 2 PWD Cases of Scouring at Bridges in Malaysia

River Name	Defects/Problems	Remedial Actions
Pukin River, Pahang	General and local scour	Armor using precast concrete interlocking blocks (flex-slab system)
Keratong River, Pahang	General and local scour	Gabions and sand bags (proprietary products)
Plentong River, Johor	General and local scour; earlier protection work washed out	Armor using gabions, sheetpiles and precast concrete interlocking blocks (flex-slab system)
Trolak River, Perak	Collapse of approach embankment	Reconstruction of approach embankment using RE system with gabions
Buloh River, Selangor	Pier on footing scoured and settled	Replacement with a bridge
Salor River, Kelantan	General and local scour	Armor using sand bags (proprietary products)
Geliga River, Terengganu	General and local scour	Underpinning and replacement with a bridge

The seven bridge sites in Table 2 are some recent examples of scour-related problems that have occurred in Malaysia. In order to illustrate how these problems are tackled, the first three bridge sites, that is, Pukin River Bridge, Keratong River Bridge and Plentong River Bridge are presented in more detail in this paper. A site visit to the three bridges was made between January 3-4, 2000 by the writers. During the site visit, assistance was rendered by PWD Senior Technician, Mr Tan Chee Kean, and personnel from the district office of the Public Works Department in Johor Bahru. The aim of the visit is to ascertain the success or failure of the countermeasure used in each of these bridge sites.

PUKIN RIVER BRIDGE

Pukin River Bridge, which was built around 1983, spans across the river with the same name. It serves as a vital road link between the Kuantan-Segamat Highway and the Selancar Felda Scheme. The overall length of the bridge is approximately 55 m, and it consists of three equal-distance spans. The superstructure of the bridge is in the form of prestressed I-beams, supported on two 910-mm diameter cylindrical piers. Official reports from the Public Works Department Malaysia recorded that severe scouring and erosion of the slope embankment around both the abutments has occurred as early as 1992. The failed slope embankment was reinstated using the flex-slab slope protection system (a type of precast concrete blocks) in 1993.

Approximately two years after actions were taken to remedy the failure of the slope embankment, another flood in June 1995 has further aggravated the slope embankment at one of the bridge abutments. The personnel from the Bridge Unit of the Public Works Department Malaysia and the District Office had carried out a detailed joint inspection after the flood to investigate the defects at the bridge. Observations showed that the slope embankment at the bridge abutment had collapsed partially although the majority of the slabs were intact. They reported that "the flex-slab at the toe of the slope embankment was slightly crumbled". The original manufacturer of the flex-slab system laid in 1993 carried out an independent inspection of the site on June 21, 1995. They reported that the main cause of the failure of the flex-slab system is earth movements due to seepage. It was unfortunate that no detailed information is available on any scouring that may have formed at the toe of the abutment. Hence, one is unable to determine whether there is a correlation between failure of the flex-slab system along the embankment and scouring that could have occurred at the toe of the abutment.

The recommendation by the authority was to reinstate the failed slope embankment to avoid further loss of fill material and disintegration of the flex slab. To that end, the following steps were recommended:

- The existing flex slab at the abutment shall be dismantled and stored at a separate location. The broken slabs shall be removed and disposed;
- The existing ground profile shall be trimmed to a minimum depth of 300 mm and a geotextile filter fabric with a minimum weight of 180 g/m^2 shall be laid;
- The material loss at the slope embankment shall be replaced with crush stones ranging from 50-100 mm;
- The crush stones shall be compacted to build up the slope to the existing profile in preparation for laying the flex slab; and

- The new slope shall be protected using the flex-slab protection system.

Figure 1 shows the sectional view of the abutment and the proposed scour countermeasure at Pukin River Bridge. The new slope embankment was completed at the end of 1996. On the day of the site visit (January 4, 2000), the flex-slab system was still in place, and no defects were apparent.

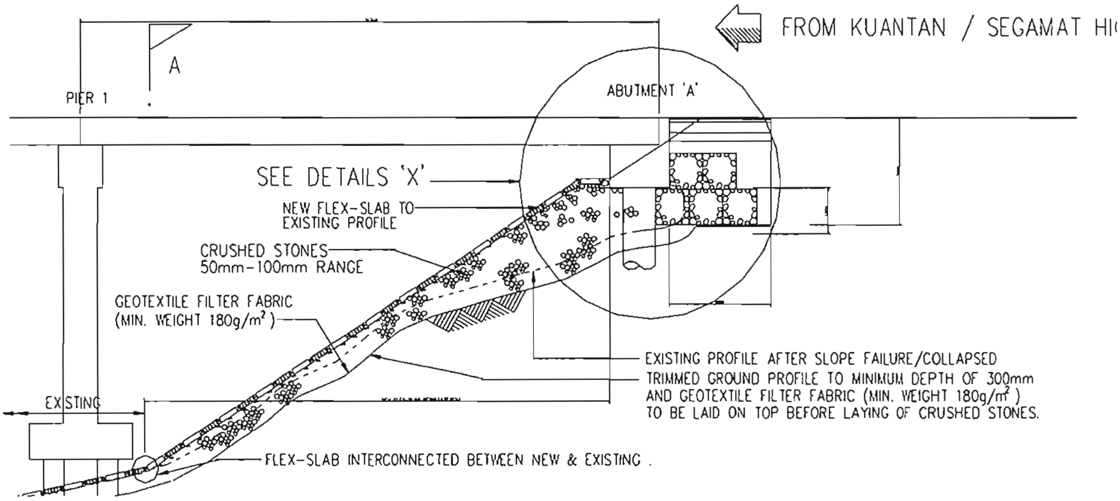

Fig. 1 Sectional View of Bridge Abutment at Pukin River Bridge

KERATONG RIVER BRIDGE

Keratong River Bridge links the towns of Bahau to Keratong in Pahang, Malaysia. The bridge is located at a curved section of the river, and it is supported on six rectangular piers each with a size of 0.914 m x 8.54 m on a pile cap with a size of 4.27m x 9.14m. Figure 2 shows the alignment of the bridge to the river, and the supporting structures. Pier 2 is located on the outer bend of the river, with its pile cap protruded slightly into the waterway. As such the protrusion will cause local scouring at the toe of Pier 2 (Lim, 1997; Lim and Cheng, 1998). In addition, its location at the bend further aggravates the extent of localized scouring at the abutment.

During a recent flood, severe river bank erosion has occurred, causing slope failure along a 50 m stretch on the upstream bank of the abutment. This realignment of the channel geometry

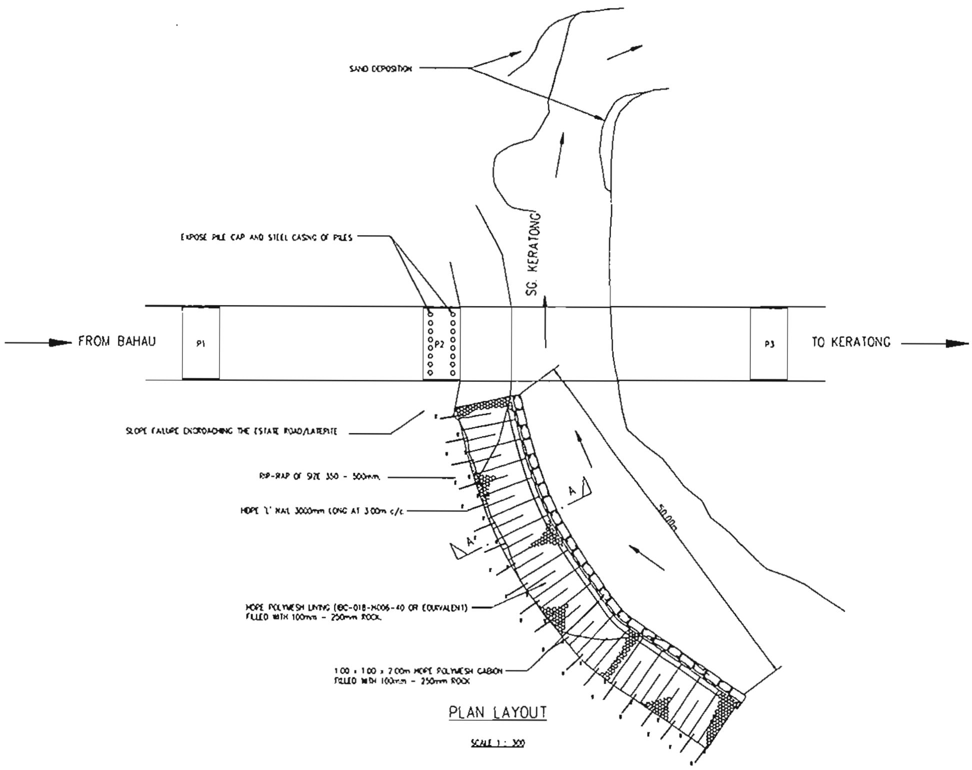

Fig. 2 Plan View of Keratong River Bridge

may have caused the shifting of the thalweg of the channel bed, and thereby directing the main flood flow towards Pier 2. Consequently, the toe of the approach fill slope was eroded, and undermining of the fill material occurred causing slope failure at Pier 2. The result is that the pier pile cap and steel casing of the piles have been exposed, and the flow encroached all the way onto the estate road. The damage can be attributed to the increased velocity of the river flow during the flood and the migration of the channel flow towards Pier 2.

The scour protection measures for this bridge is to use tubular gabions filled with sand to protect the toe of Pier 2 and conventional box gabions for the river banks. The tubular gabions are fabricated using high-density polyethylene (HDPE) mesh. They can be filled mechanically or manually with gravels or sand to form tubular bags. The tubular sand bags used in this case is 0.636m in diameter and of varying length to suit the site condition. They are arranged in a longitudinal and transverse direction, interlocking using HDPE 'T'-nail (see Figure 3). The site visit showed that the scour countermeasure worked well for this bridge and no apparent defects were detected. However, it must be pointed out the HDPE material is flammable, evident from the burnt marks on the material observed during the site visit. Apparently, local residents have used the site as a picnic location, hence the burnt marks on the tubular sand bags.

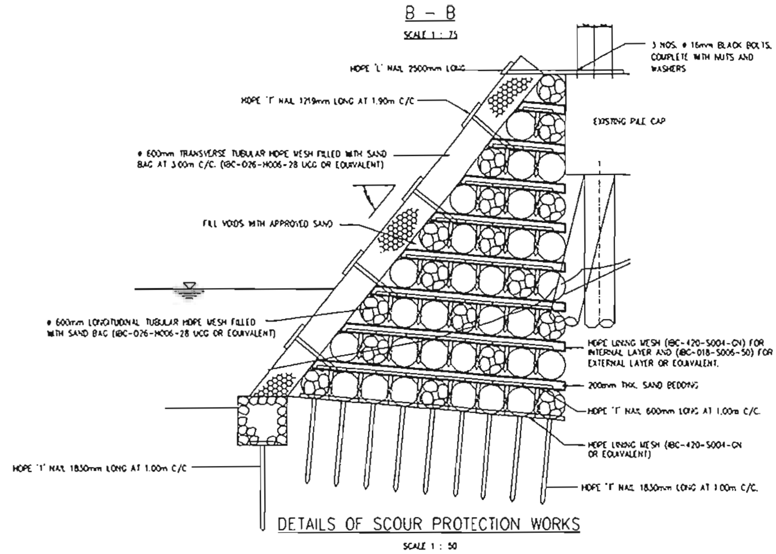

Fig. 3 Details of Scour Protection Works Using Tubular Gabion at Keratong River Bridge

PLENTONG RIVER BRIDGE

Plentong River Bridge is a dual carriage road linking Johor Bahru to Pasir Gudang Port along Federal Trunk Route 17 in the state of Johor, Malaysia. The bridge, which was constructed in 1983, consists of two separate structures each carrying two lanes of traffic in one direction. The structures comprise a three-span bridge of pretension inverted T-girders, and the length of the spans are 11.25m, 15.75m, and 11.25m, respectively. Two cylindrical bridge piers with diameter = 1.32 m support each of the two structures (see Figure 4).

Scour problems at Plentong River Bridge were reported very early in the life of the bridge, and sheet piles were used to protect one of its abutments (see Figure 5). However, this countermeasure did not seem to arrest erosion completely. In 1995, the flex-slab system was used as a more permanent solution after the apparent success of the method for Pukin River Bridge. However, this system did not work as anticipated and failed. To arrest further erosion, the District Office of the Public Works Department used gabions and rubbled pitching type of protection as a temporary measure (see Figure 6). The scouring problem at this bridge is now continuously being monitored to check that it is not detrimental to the overall safety of the superstructure.

On the day of the site visit (January 3, 2000), observations clearly showed that erosion had occurred along the riverbank at the bridge site. Sheet piles and a grade-control structure were apparent on the upstream end of the bridge. The upstream grade-control structure appeared to have re-directed the flow towards the pier and the abutment (see Figure 4). It is envisaged that during flood flows in the preceding monsoon season, scouring at both the pier and abutment

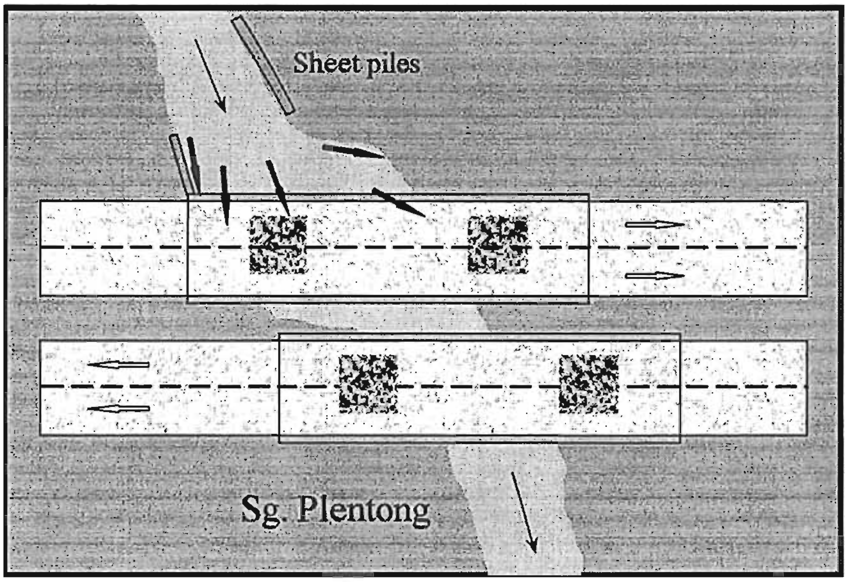

Fig. 4 Plan View of Plentong Bridge

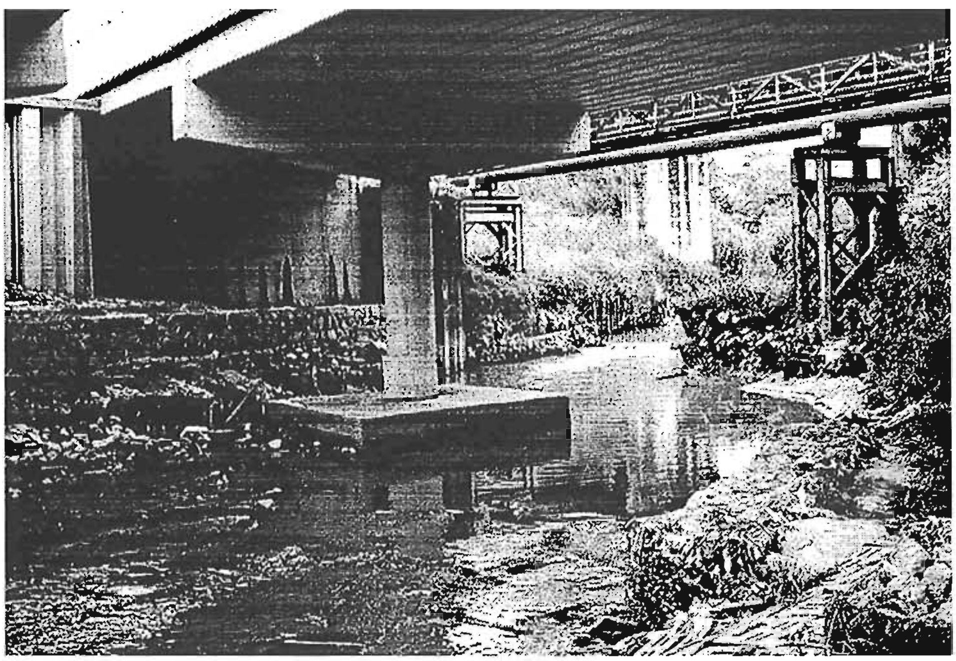

Fig. 5 Plentong River Bridge (flow from top right to bottom left)

Fig. 6 Use of Gabions as a Temporary Scour Countermeasure at Plentong River Bridge (looking downstream)

would have been substantial, contributing to the failure of the flex-slab system. This can be seen in Figure 6, which shows that severe erosion has taken place along the abutment, and the flex-slab system on the abutment has collapsed. The photograph in Figure 5 also shows severe scouring at the pier, damaging the flex-slab system on the approach fill slope. It can be seen that the flex-slabs are lying around the site of the pier.

It is interesting to note that the same scour countermeasure method, vis-à-vis the flex-slab system, which appears to work reasonably well for Pukin River Bridge, fails miserably in the case of Plentong River Bridge. This conflicting performance of a particular scour countermeasure at different bridge sites is not only confined to Malaysia, but is also confirmed by an extensive site visit program of many bridges in the U.S.A. by Parker et al. (1998). The search for a comprehensive method of scour protection, suitable for varying site conditions, is top most in the mind of bridge engineers.

CONCLUSIONS

Despite the many bridge failures due to scouring at their foundation, the search for an all-encompassing scour countermeasure method is still elusive. One of the main reasons for such a poor record on bridge failure is the lack of a systematic research investigation on scour countermeasure at bridges. A cursory search of published literature will immediately reveal that little has been done to examine the performance of scour countermeasure on bridge foundations, even for the most commonly used scour countermeasure, vis-à-vis riprap protection. Many of the previous studies on riprap protection were confined to determining riprap sizing for bridge pier applications. As far as the writers are aware, no specific study has been devoted to bridge abutment. Furthermore, most of these studies were conducted under a clear-water condition, and their validity when applied to a live-bed condition remains unproven. Only recently, the study by Chiew and Lim (2000) has ventured into riprap protection under a live-bed condition. Even so, riprap protection around an abutment continues to remain in uncharted territories.

In addition, the experience gained on the success or failure of a particular scour countermeasure under a given flow condition often remains the "property" of a particular agency or company. This knowledge is often not shared although blame should not be levied so quickly on the practitioners. Generally, there are not many platforms on which such experience and knowledge can be disseminated. It is hoped that the information on how bridge design is conducted in Malaysia, and the three examples cited above will encourage discussion for mutual benefits amongst researchers and practitioners in this area.

ACKNOWLEDGEMENTS

The authors would like to thank Mr. Leow Choon Heng, Assistant Director of Bridge Unit for providing the data relating to the three case studies outlined in the paper. Special thanks also go to Dr. Hiew Kim Loi, Deputy Director of Drainage and Irrigation Department Malaysia for information on Malaysian rivers. The views expressed in this paper may not be that of the Public Works Department of Malaysia.

REFERENCES

1. Chiew, Y. M. (1995). "Mechanics of Riprap Failure at Bridge Piers". Journal of Hydraulic Engineering, ASCE, 121(9), pp. 635-643.
2. Chiew, Y. M. and Lim, F. H. (2000). "Failure Behavior of Riprap Layer at Bridge Piers under Live-Bed Conditions". Journal of Hydraulic Engineering, ASCE, 126(1), pp. 43-55.
3. Heiler, T. D. (1973). "Estimation of the Design Rainstorm", DID Hydrological Procedure No. 1, Ministry of Agriculture and Fisheries Malaysia (Revised and updated by Mohd. Fadhillah b. Hj. Mahmood, Salena bt. Salleh, Leong Tat Meng and Teh Siew Keat in 1982 and reprinted in 1990).
4. Heiler, T. D. (1974). "Rational Method of Flood Estimation for Rural Catchment in Peninsular Malaysia", DID Hydrological Procedure No. 5, Ministry of Agriculture and Fisheries Malaysia (Reprinted in 1995).
5. Heiler, T. D., and Chew, H. H. (1974). "Magnitude and Frequency of Floods in Peninsular Malaysia", DID Hydrological Procedure No. 4, Ministry of Agriculture and Fisheries Malaysia.
6. Japan International Cooperation Agency and Public Works Department Malaysia (1992). "The Study on the Maintenance and Rehabilitation of Bridges in Malaysia", Final Report, Volume II, Main Report, August.
7. Japan International Cooperation Agency and Public Works Department Malaysia (1996). "The Study on the Standardization of bridge Design in Malaysia", Final Report, Volume II, Main Report, August.
8. Lewis, K.V., Cassell P. A., and Fricke T. J. (1975). "Urban Drainage Design Standards and Procedures for Peninsular Malaysia", Ministry of Agriculture and Rural Development Malaysia.

9. Lim, S. Y. (1997). "Equilibrium Clear-Water Scour around an Abutment". Journal of Hydraulic Engineering, ASCE, 123(3), pp. 237-243.
10. Lim, S. Y. and Cheng, N. S. (1998). Prediction of Live-Bed Scour at Bridge Abutments". Journal of Hydraulic Engineering, ASCE, 124(6), pp. 635-638.
11. Ng, S. K. and Razak R. A. (1998). "Bridge Hydraulic Problems in Malaysia". Proceedings of the 4th International Seminar on Bridges and Aqueducts 2000, Feb. 7-9, 1998, Mumbai, India.
12. Parker, G., Toro-Escobar, C., and Voigt, Jr., R. L. (1998). "Countermeasures to Protect Bridge Piers from Scour", Final Report, National Cooperative Highway Research Program, Transportation Research Board, National Research Council, St Anthony Falls Laboratory, University of Minnesota, December, 360 pp.
13. Public Works Department Malaysia (1982). "Bridge Loading" Lecture Notes for Bridge Design Course Organized by Bridge Unit, Design and Research Branch.
14. Public Works Department Malaysia (1985). "Chapter 6: Pier", Bridge Design Guide, Bridge Unit, Public Works Department, Malaysia.
15. Public Works Department Malaysia (1995). "Annual Bridge Inspection Manual". March.
16. Smith, D. W. (1976). "Bridges Failures". Proceedings of the Institution of Civil Engineers, Vol. 60, Part 1, pp. 367-382.
17. Taylor, M. A. W., and Toh Y. K. (1980). "Design Flood Hydrograph Estimation for Rural Catchments in Peninsular Malaysia", DID Hydrological Procedure No. 11, Ministry of Agriculture Malaysia.
18. Yusof, N. M. (1996). "Annual Mandatory Inspection: Results and Findings". International Seminar on Bridge Engineering and Management, Jakarta, Indonesia, September 10-13.

BRIDGE INSPECTION FOR SCOUR VULNERABILITY

By

E. V. Richardson[1], J. R. Richardson[2] and P. F. Lagasse[3]

ABSTRACT

Bridge inspection is an important tool to protect the traveling public from bridge failures caused by either structural failure of the superstructure or scour of the foundations. Over 60 % of bridge failures in the U.S. is scour of the bridge foundations. Inspection to determine if conditions have changed since the bridge was built so that the bridge is scour vulnerable or scour critical is complex and difficult. With 484,856 bridges over water in the United States inspection for scour vulnerability is a major State responsibility. The difficultly of inspection to determine scour vulnerability and the need for inspectors to be well trained in scour, fluvial geomorphology, and stream morphology is illustrated by three bridge failures that resulted in the loss of 25 lives.

INTRODUCTION

The United State established the National Bridge Inspection Standards (NBIS) under the 1968 Federal-aid Highway Act as the result of the Silver Bridge structural failure over the Ohio River at Point Pleasant, West Virginia, on December 15 1967 (Harrison and Densmore, 1991, also, Richardson and Lagasse, 1999, p 215). As a result of the Act all 50 States have a bridge inspection organization responsible for the inspection program. With a few exceptions all 577,000 bridges on the National Bridge Inventory are inspected every two years. If under water foundations can not be inspected visually and by probing an under water inspection is required every 5 years. There are over 100 items in the Federal Highway Administrations (FHWA) publication "Recording and Coding Guide for Structural Inventory and Appraisal of the Nation's Bridges" (FHWA, 1995) that the state highway departments report on for each inspection. For a simple bridge the inspection may take only 3 or 4 hours but a complex bridge may take over a week. There are 4 condition ratings in the inspection that relate to bridge scour. These are Item 60, Substructure, Item 61, Channel and Channel Protection, and Item 71, Waterway Adequacy.

In addition , Items 92 and 93, Critical Feature Inspection denotes special features, such as underwater, that need special inspection. An Item 113, Scour Critical Bridges, was added in 1988 as part of FHWA's issuance of Technical Advisory T5140.20 requiring the States to conduct a scour evaluation program. This item is not coded by inspectors.

---

[1]Senior Associate, Ayres Associates, Inc., and Professor Emeritus, Civil Engineering Dept, Colorado State Univ., Ft. Collins, CO.

[2]Assistant Professor, Civil Engineering, Univ. of Missouri, Kansas City, MO 64100.

[3]Senior Vice President, Ayres Associates, Inc., P.O. Box 270460, Ft. Collins, CO 80527.

Condition rating are used to describe the existing, in-place bridge as compared to the as-built condition. Inspectors are to accurately record the present condition of the bridge foundations and the stream, in addition to the condition of the superstructure, approaches and etc. They are to identify conditions that are indicative of potential problems for further review and evaluation by others.

The scour evaluation program was started in 1988 as the result of Technical Advisory T5140.20 which was superceded by T5140.23 in 1991. The evaluation is to be conducted by an interdisciplinary team of hydraulic, geotechnical and structural engineers who can make the necessary engineering judgments to determine the vulnerability of abridge to scour. This program resulted from the failure of the I-90 bridge over Schoharie Creek in upstate New York which killed 10 people (NTSB, 1988 and Richardson, et al, 1987). There are 471,407 bridges over water in the National bridge inventory. As of November, 1999, 481,155 have been screened as to their scour vulnerability and 353,738 have been evaluated. The statistic from the screening are as follows:

- Low Risk 345,033
- Scour Susceptible 23.492
- Unknown Foundations 87,093
- Tidal 1,055
- Scour Critical 23,582

The evaluation program in the U. S. is on schedule and scour countermeasures have been taken on bridges that have been identified as scour susceptible or scour critical. Replacement bridges are being constructed as rapidly as funds can be provided. An important scour countermeasure is riprap protection, scour monitoring before, during and after a flood and the inspection program (Richardson and Davis, 1995, Lagasse et al, 1995, 1997a and 1997b). Inspection for scour is extremely difficult because of the many factors that impact the scour vulnerability of a bridge. Some of these factors are stream instability, drainage area changes, changes in flood magnitude, potential changes in angle of attack, stream changes upstream and downstream of the bridge, long term degradation, changes in land use, urbanization, gravel mining, and etc.

This paper describes in more detail scour inspection and use three case histories to illustrate the difficulties in inspection for scour vulnerability.

FHWA "RECORDING AND CODING GUIDE" (1995)

During the bridge inspection, the condition of the substructure, bridge waterway opening, channel protection, and scour countermeasures are evaluated, along with the condition of the stream. FHWA's "Recording and Coding Guide" (FHWA, 1995) gives guidance" for rating the present condition of the bridge.

Item 60, Table 1, give the condition Rating of the bridge. It is general, and does not include specific details for scour. Condition ratings are used to describe the existing, in-place bridge as compared to the as-built condition. Evaluation is for the materials related, physical condition of the deck, superstructure, and substructure components of a bridge. The condition evaluation of channels and channel protection and culverts is also included. Condition codes are properly used when they provide an overall characterization of the general condition of the entire component being rated. Conversely, they are improperly used if they attempt to describe localized or nominally occurring instances of deterioration or disrepair. Correct assignment of a condition code must, therefore, consider both the severity of the deterioration or disrepair and the extent to which it is widespread throughout the component being rated. The load-carrying capacity will not be used in evaluating condition items. The fact that a bridge was designed for less than current legal loads and may be posted shall have no influence upon condition ratings. Portions of bridges that are being supported or strengthened by temporary members will -be rated based on their actual condition; that is, the temporary members are not considered in the rating of the item. Completed bridges not yet opened to traffic, if rated, shall be coded as if open to traffic (FHWA, 1995).

Items 61 (Channel and Channel Protection) and 71(Waterway Adequacy) are given in tables 2 and 3 respectiviely. Item 113, table 4, is specific to scour and it impacts Item 60 the condition rating. The following sections present approaches to evaluating the present condition of the bridge foundation for scour and the overall scour potential at the bridge.

INSPECTION PROCEDURES

A well organized bridge inspection procedure is to have 1) an office review, 2) field inspection and 3) notification procedure to follow should problems be identified (Harrison and Densmore, 1991, Richardson and Lagasse, 1999, p215).

Office Review (Richardson and Davies, 1995)

It is desirable to make an office review of bridge plans and previous inspection reports prior to making the bridge inspection. Information obtained from the office review provides a better basis for inspecting the bridge and the stream. Items for consideration in the office review include:

1. Has an engineering scour evaluation study been made? If so, is the bridge scour-critical?

2. If the bridge is scour-critical, has a plan of action been made for monitoring the bridge and/or installing scour countermeasures?

3. What do comparisons of streambed cross sections taken during successive inspections reveal about the streambed? Is it stable? Degrading? Aggrading? Moving laterally? Are there scour holes around piers and abutments?

4. What equipment is needed (rods, poles, sounding lines, sonar, etc.) to obtain streambed cross sections?

5. Are there sketches and aerial photographs to indicate the planform location of the stream and whether the main channel is changing direction at the bridge?

6. What type of bridge foundation was constructed? (Spread footings, piles, drilled shafts, etc.) Are footing and pile tip elevations known? Do the foundations appear to be vulnerable to scour? What are the sub-surface soil conditions? (sand, gravel, silt, clay rock?)

7. Do special conditions exist requiring particular methods and equipment (divers, boats, electronic gear for measuring stream bottom, etc.) for underwater inspections?

8. Are there special items that should be looked at? (Examples might include damaged riprap, stream channel at adverse angle of flow, problems with debris, etc.)

Field Site Visit (Richardson and Davies, 1995)

Safety Considerations. The bridge inspection team should understand and practice prudent safety precautions during the conduct of the bridge inspection. Warning signs should be set up at the approaches to the bridge to alert motorists to the activity on the bridge. This is particularly important if streambed measurements are to be taken from the bridge, since most bridges have minimal clearances between the parapet and the edge of the travel lane. Inspectors should wear brightly colored vests so that they are conspicuous to motorists.

When measurements are made in the stream, the inspector should be secured by a safety line whenever there is deep or fast flowing water. If waders become overtopped, they will fill and may drag the inspector downstream and under water in a matter of a few seconds.

The inspection team should leave word with their office regarding their schedule of work for the day. The team should also carry a cell phone with them so that they can get immediate help in the event of an emergency.

Table 1. Item 60 - Substructure (FHWA, 1995)

This item describes the physical condition of piers, abutments, piles, fenders, footings, or other components. Rate and code the condition in accordance with the previously described general condition ratings. Code N for all culverts.

All substructure elements should be inspected for visible signs of distress including evidence of cracking, section loss, settlement, misalignment, scour, collision damage, and corrosion. The rating given by Item 113 - Scour Critical Bridges, may have a significant effect on Item 60 if scour has substantially affected the overall condition of the substructure.

The substructure condition rating shall be made independent of the deck and superstructure.

Integral-abutment wingwalls to the first construction or expansion joint shall be included in the evaluation. For non-integral superstructure and substructure units, the substructure shall be considered as the portion below the bearings. For structures where the substructure and superstructure are integral, the substructure shall be considered as the portion below the superstructure.

The following general condition ratings shall be used as a guide in evaluating Items 60:

Code	Description
N	NOT APPLICABLE
9	EXCELLENT CONDITION
8	VERY GOOD CONDITION - no problems noted.
7	GOOD CONDITION - some minor problems.
6	SATISFACTORY CONDITION - structural elements show some minor deterioration.
5	FAIR CONDITION - all primary structural elements are sound but may have minor section loss, cracking, spalling or scour.
4	POOR CONDITION - advanced section loss, deterioration, spalling or scour.
3	SERIOUS CONDITION - loss of section, deterioration, spalling or scour have seriously affected primary structural components. Local failures are possible. Fatigue cracks in steel or shear cracks in concrete may be present.
2	CRITICAL CONDITION - advanced deterioration of primary structural elements. Fatigue cracks in steel or shear cracks in concrete may be present or scour may have removed substructure support. Unless closely monitored it may be necessary to close the bridge until corrective action is taken.
1	"IMMINENT" FAILURE CONDITION - major deterioration or section loss present in critical structural components or obvious vertical or horizontal movement affecting structure stability. Bridge is closed to traffic but corrective action may put back in light service.
0	FAILED CONDITION - out of service - beyond corrective action.

Table 2. Item 61 - Channel and Channel Protection (1995)

This item describes the physical conditions associated with the flow of water through the bridge such as stream stability and the condition of the channel, riprap, slope protection, or stream control devices including spur dikes. The inspector should be particularly concerned with visible signs of excessive water velocity which may affect undermining of slope protection, erosion of banks, and realignment of the stream which may result in immediate or potential problems. Accumulation of drift and debris on the superstructure and substructure should be noted on the inspection form but not included in the condition rating.

Rate and code the condition in accordance with the previously described general condition ratings and the following descriptive codes:

Code	Description
N	Not applicable. Use when bridge is not over a waterway (channel).
9	There are no noticeable or noteworthy deficiencies which affect the condition of the channel.
8	Banks are protected or well vegetated. River control devices such as spur dikes and embankment protection are not required or are in a stable condition.
7	Bank protection is in need of minor repairs. River control devices and embankment protection have a little minor damage. Banks and/or channel have minor amounts of drift.
6	Bank is beginning to slump. River control devices and embankment protection have widespread minor damage. There is minor stream bed movement evident. Debris is restricting the channel slightly.
5	Bank protection is being eroded. River control devices and/or embankment have major damage. Trees and brush restrict the channel.
	Bank and embankment protection is severely undermined. River control devices have severe damage. Large deposits of debris are in the channel.
3	Bank protection has failed. River control devices have been destroyed. Stream bed aggradation, degradation or lateral movement has changed the channel to now threaten the bridge and/or approach roadway.
2	The channel has changed to the extent the bridge is near a state of collapse.
1	Bridge closed because of channel failure. Corrective action may put back in light service.
0	Bridge closed because of channel failure. Replacement necessary.

Table 3. Item 71 - Waterway Adequacy (FHWA, 1995)

This item appraises the waterway opening with respect to passage of flow through the bridge. The following codes shall be used in evaluating waterway adequacy (interpolate where appropriate). Site conditions may warrant somewhat higher or lower ratings than indicated by the table (e.g., flooding of an urban area due to a restricted bridge opening).

Where overtopping frequency information is available, the descriptions given in the table for chance of overtopping mean the following:

Remote	- greater than 100 years
Slight	-11 to 100 years
Occasional Frequent	- 3 to 10 years
Frequent	-less than 3 years

Adjectives describing traffic delays mean the following:

Insignificant	- Minor inconvenience. Highway passable in a matter of hours.
Significant-	-Traffic delays of up to several days.
Severe	- Long term delays to traffic with resulting hardship.

Functional Classification

Principal Arterials - Interstates, freeways, or Expressways	Other Principal and Minor Arterials and Major Collectors	Minor Collectors, Locals	
	Code		Description
N	N	N	Bridge not over a waterway
9	9	9	Bridge deck and roadway approaches above flood water elevations (high water). Chance of overtopping is remote.
8	8	9	Bridge deck above roadway approaches. Slight chance of overtopping roadway approaches.
6	6	7	Slight chance of overtopping bridge deck and roadway approaches.
4	5	6	Bridge deck above roadway approaches. Occasional overtopping of roadway approaches with insignificant traffic delays.
3	4	5	Bridge deck above roadway approaches. Occasional overtopping of roadway approaches with significant traffic delays.
2	3	4	Occasional overtopping of bridge deck and roadway approaches with significant traffic delays.
2	2	3	Frequent overtopping of bridge deck and roadway approaches with significant traffic delays.
2	2	2	Occasional or frequent overtopping of bridge deck and roadway approaches with severe traffic delays.
0	0	0	Bridge closed.

Table 4. Item 113 - Scour Critical Bridges (FHWA, 1995)

Use a single-digit code as indicated below to identify the current status of the bridge regarding its vulnerability to scour. Scour analyses shall be made by hydraulic/geotechnical/structural engineers. Details on conducting a scour analysis are included in the FHWA Technical Advisory 5140.23 titled, "Evaluating Scour at Bridges." Whenever a rating factor of 4 or below is determined for this item, the rating factor for Item 60 - Substructure may need to be revised to reflect the severity of actual scour and resultant damage to the bridge. A scour critical bridge is one with abutment or pier foundations which are rated as unstable due to (1) observed scour at the bridge site or (2) a scour potential as determined from a scour evaluation study.

Code	Description
N	Bridge not over waterway.
U	Bridge with "unknown" foundation that has not been evaluated for scour. Since risk cannot be determined, flag for monitoring during flood events and, if appropriate, closure.
T	Bridge over "tidal" waters that has not been evaluated for scour, but considered low risk. Bridge will be monitored with regular inspection cycle and with appropriate underwater inspections. ("Unknown" foundations in "tidal" waters should be coded U).
9	Bridge foundations (including piles) on dry land well above flood water elevations.
8	Bridge foundations determined to be stable for assessed or calculated scour conditions; calculated scour is above top of footing.
7	Countermeasures have been installed to correct a previously existing problem with scour. Bridge is no longer scour critical.
6	Scour calculation/evaluation has not been made. (Use only to describe case where bridge has not yet been evaluated for scour potential.)
5	Bridge foundations determined to be stable for calculated scour conditions; scour within limits of footing or piles.
4	Bridge foundations determined to be stable for calculated scour conditions; field 'review indicates action is required to protect exposed foundations from effects of additional erosion and corrosion.
3	Bridge is scour critical; bridge foundations determined to be unstable for calculated scour conditions: - Scour within limits of footing or piles. - Scour below spread-footing base or pile tips.
2	Bridge is scour critical; field review indicates that extensive scour has occurred at bridge foundations. Immediate action is required to provide scour countermeasures.
1	Bridge is scour critical; field review indicates that failure of piers/abutments is imminent. Bridge is closed to traffic.
0	Bridge is scour critical. traffic. Bridge has failed and is closed to traffic.

General Site Considerations In order to appreciate the relationship between the bridge and the river it is crossing, notice should be given to the conditions of the river up- and downstream of the bridge:

- Is there evidence of general degradation or aggradation of the river channel resulting in unstable bed and banks?

- Is there evidence of on-going development (urbanization) in the watershed and particularly in the adjacent floodplain that could be contributing to channel instability?

- Are there active gravel or sand mining operations in the channel near the bridge?

- Are there confluences with other streams? How will the confluence affect flood flow and sediment transport conditions?

- Is there evidence at the bridge or in the up- and downstream reaches that the stream carries large amounts of debris? Is the bridge superstructure and substructure streamlined to pass debris, or is it likely that debris will hang up on the bridge and create adverse flow patterns with resulting scour?

- The best way of evaluating flow conditions through the bridge is to look at and photograph the bridge from the up- and downstream channel. Is there a significant angle of attack of the flow on a pier or abutment?

Assessing the Substructure Condition Item 60, Substructure, is the key item for rating the bridge foundations for vulnerability to scour damage. When a bridge inspector finds that a scour problem has already occurred, it should be considered in the rating of Item 60. Both existing and potential problems with scour should be reported so that a scour evaluation can be made by an interdisciplinary team. The scour evaluation is reported on Item 113 (Table 4) in the "Recording and Coding Guide." If the bridge is determined to be scour critical, the rating of Item 60 should be evaluated to ensure that existing scour problems have been considered. The following items are recommended for consideration in inspecting the present condition of bridge foundations:

1. Evidence of movement of piers and abutments;

    - Rotational movement (check with plumb line)
    - Settlement (check lines of substructure and superstructure, bridge rail, etc., for discontinuities; check for structural cracking or spalling)
    - Check bridge seats for excessive movement

2. Damage to scour countermeasures protecting the foundations (riprap, guide banks, sheet piling, sills, etc.), Has riprap placed around piers and/or abutments been removed or replaced with river run material. A common cause of damage to abutment riprap protection is runoff from the ends of the bridge which flows down

to the riprap and undermines it. This condition can be corrected by installing bridge end drains.

3. Changes in streambed elevation at foundations (undermining of footings, exposure of piles), and

4. Changes in streambed cross section at the bridge, including location and depth of scour holes.

    - Note and measure any depressions around piers and abutments
    - Note the approach flow conditions. Is there an angle of attack of flood flow on piers or abutments?

In order to evaluate the conditions of the foundations, the inspector should take cross sections of the stream, noting location and condition of streambanks. Careful measurements should be made of scour holes at piers and abutments, probing soft material in scour holes to determine the location of a firm bottom. If equipment or conditions do not permit measurement of the stream bottom, this condition should be noted for further action.

Assessing Scour Potential at Bridges The items listed in Table 5 are provided for bridge inspectors' consideration in assessing the adequacy of the bridge to resist scour. In making this assessment, inspectors need to understand and recognize the interrelationships between Item 60 (Substructure), Item 61 (Channel and Channel Protection), and Item 71 (Waterway Adequacy). As noted earlier, additional follow-up by an interdisciplinary team should be made utilizing Item 113 (Scour Critical Bridges) when the bridge inspection reveals a potential problem with scour.

Cross-Sections and Underwater Inspections Perhaps the single most important aspect of inspecting the bridge for actual or potential damage from scour is the taking and plotting of measurements of stream bottom elevations in relation to the bridge foundations. Where conditions are such that the stream bottom cannot be accurately measured by rods, poles, sounding lines or other means, other arrangements need to be made to determine the condition of the foundations. Other approaches to determining the cross section of the streambed at the bridge include:

1. Use of divers
2. Use of electronic scour detection equipment
3. What are the shapes and depths of scour holes?
4. Is the foundation footing, pile cap, or the piling exposed to the stream flow; and if so, what is the extent and probable consequences of this condition?
5. Has riprap around a pier been moved or removed?

Table 5. Assessing the Scour Potential at Bridges (Richardson and Davis, 1995).

1. UPSTREAM CONDITIONS

a. Banks

STABLE: Natural vegetation, trees, bank stabilization measures such as riprap, paving, gabions; channel stabilization measures such as dikes and jetties.

UNSTABLE: Bank sloughing, undermining, evidence of lateral movement, damage to stream stabilization measures etc.

b. Main Channel

- Clear and open with good approach flow conditions, or meandering or braided with main channel at an angle to the orientation of the bridge.
- Existence of islands, bars, debris, cattle guards, fences that may affect flow.
- Aggrading or degrading streambed.
- Evidence of movement of channel with respect to bridge (make sketches, take pictures).
- Evidence of ponding of flow.

c. Floodplain

- Evidence of significant flow on floodplain.
- Floodplain flow patterns - does flow overtop road and/or return to main channel?
- Existence and hydraulic adequacy of relief bridges (if relief bridges are obstructed, they will affect flow patterns at the main channel bridge).
- Extent of floodplain development and any obstruction to flows approaching the bridge and its approaches.
- Evidence of overtopping approach roads (debris, erosion of embankment slopes, damage to riprap or pavement, etc.).
- Evidence of ponding of flow.

d. Debris

- Extent of debris in upstream channel.

e. Other Features

- Existence of upstream tributaries, bridges, dams, or other features, that may affect flow conditions at bridges.

Table 5. Assessing the Scour Potential at Bridges (continued).

2. CONDITIONS AT BRIDGE

a. Substructure

- Is there evidence of scour at piers?
- Is there evidence of scour at abutments (upstream or downstream sections)?
- Is there evidence of scour at the approach roadway (upstream or downstream)?
- Are piles, pile caps or footings exposed?
- Is there debris on the piers or abutments?
- If riprap has been placed around piers or abutments, is it still in place?

b. Superstructure

- Evidence of overtopping by flood water (Is superstructure tied down to substructure to prevent displacement during floods?)
- Obstruction to flood flows (Does superstructure collect debris or present a large surface to the flow?)
- Design (Is superstructure vulnerable to collapse in the event of foundation movement, e.g., simple spans and nonredundant design for load transfer?)

c. Channel Protection and Scour Countermeasures

- Riprap (Is riprap adequately toed into the streambed or is it being undermined and washed away? Is riprap pier protection intact, or has riprap been removed and replaced by bed-load material? Can displaced riprap be seen in streambed below bridge?)
- Guide banks (Spur dikes) (Are guide banks in place? Have they been damaged by scour and erosion?)
- Stream and streambed (Is main current impinging upon piers and abutments at an angle? Is there evidence of scour and erosion of streambed and banks, especially adjacent to piers and abutments? Has stream cross section changed since last measurement? In what way?)

d. Waterway Area Does waterway area appear small in relation to the stream and floodplain? Is there evidence of scour across a large portion of the streambed at the bridge? Do bars, islands, vegetation, and debris constrict the flow and concentrate it in one section of the bridge or cause it to attack piers and abutments? Do the superstructure, piers, abutments, and fences, etc., collect debris and constrict flow? Are approach roads regularly overtopped? If waterway opening is inadequate, does this increase the scour potential at bridge foundations?

Table continues

Table 5 Assessing the Scour Potential at Bridges (continued).

3. DOWNSTREAM CONDITIONS

a. Banks

STABLE: Natural vegetation, trees, bank stabilization measures such as riprap, paving, gabions, channel stabilization measures such as dikes and jetties.

UNSTABLE: Bank sloughing, undermining, evidence of lateral movement, damage to stream stabilization measures, etc.

b. Main Channel

- Clear and open with good "getaway" conditions, or meandering or braided with bends, islands, bars, cattle guards, debris, and fences that retard and obstruct flow.
- Aggrading or degrading streambed.
- Evidence of movement of channel with respect to the bridge (make sketches and take pictures).
- Evidence of extensive bed erosion.

c. Floodplain

- Clear and open so that contracted flow at bridge will return smoothly to floodplain, or restricted and blocked by dikes, development, trees, debris, or other obstructions.
- Evidence of scour and erosion due to downstream turbulence.

d. Other Features

- Downstream dams or confluence with larger stream which may cause variable tailwater depths. (This may create conditions for high velocity flow through bridge.)

For the purpose of evaluating resistance to scour of the substructure under Item 60 of the "Recording and Coding Guide," the questions remain essentially the same for foundations in deep water as for foundations in shallow water:

1. What is the configuration of the stream cross section at the bridge?

2. Have there been any changes as compared to previous cross section measurements? If so, does this indicate that (1) the stream is aggrading or degrading; or (2) local or contraction scour is occurring around piers and abutments?

Post-Inspection Documentation Following completion of the bridge inspection, the new channel cross section should be compared with the cross sections taken during previous inspections. The results of the comparison should be evaluated and documented. Many bridge inspectors now utilize lap top computers to facilitate the documentation of the inspection findings. Computers will also facilitate plotting of successive channel cross-sections to enable rapid evaluation of the changes. A bridge scour expert system, CAESAR, (TRB, 1999) is available to assist in this process.

Notification Procedures The States have established a positive procedures of promptly communicating inspection findings to proper agency personnel for action. The procedure provides for action for any condition that a bridge inspector considers to be of an emergency or potentially hazardous nature. In some states the inspector can close a bridge which he considers dangerous. Whereas, in other states he notifies a designated authority who takes the necessary action. Conditions which do not pose an immediate hazard, but still warrant further action, are conveyed to those responsible for action. Normally, an independent revue authority is established to be sure that corrections are made to a problem that an inspection has identified.

CASE HISTORIES OF BRIDGE INSPECTION PROBLEMS

Introduction

Since 1987 there have been three bridge failures with loss of life that illustrate the importance of bridge inspections. In two of the failures inspectors failed to observe changed conditions that if corrected may have saved the bridge. In the third case, the inspectors documented the changes, but there was no follow-up action to evaluate the changes and to protect the bridge. In the following sections, the inspection problems associated with these bridge failures are described and issues related to inspection are highlighted.

Schoharie Creek Bridge Failure

On April 5, 1987 the New York State Thruway Authority Bridge (I-90) over Schoharie Creek collapsed killing 10 persons (Richardson et al,1987 and NTSB, 1988). The National Transportation Safety Board investigated the collapse and gave as the probable cause as:

> "............the failure of the New York State Thruway Authority (NYSTA) to maintain adequate rip rap around the bridge piers, which led to severe erosion in the soil beneath the spread footings. Contributing to the accident were ambivalent plans and specifications used for construction of the bridge, an inadequate NYSTA bridge inspection program, and inadequate oversight by the New York State Department of Transportation and the Federal Highway Administration. Contributing to the severity of the accident was the lack of structural redundancy in the bridge."

The bridge was built in 1953 on piers with spread footings and no piles. The footings were 1.5 m (5 ft) deep, 5.5 m (18 ft) wide and 25 m (82 ft) long. The tops of the footings were at the streambed and incised into a substrate consisting of ice contact stratified draft (glacial till). The footings were protected by riprap. In 1955 the bridge survived a larger flood (2084 m^3/s (73,600 cfs)) than the 1987 flood (1759 m^3/s (62,100 cfs)). However, from 1953 to 1987 the bridge was subjected to many floods which progressively removed riprap from the piers, enabling the spread footings to be undermined during the April 1987 flood.

The NYSTA inspected the bridge annually or biennially with the last inspection on April 1, 1986. A 1979 inspection by a consultant hired by NYSTA indicated that most of the riprap around the piers was missing. However, the 1986 inspection failed to detect any problems with the condition of the riprap at the piers. Based on the Safety Board findings, the conclusions from this failure are that inspectors and their supervisors must recognize that riprap is not a permanent countermeasure for scour, and inspectors must be trained to recognize when riprap is missing and the significance of this condition.

Hatchie River Bridge Failure

On April 1, 1989 the northbound U.S. Route 51 bridge over the Hatchie River in Tennessee collapsed killing eight persons (Bryan, 1989 and NTSB, 1990). The National Transportation Safety Board investigated the collapse and gave as the probable cause:

> ".........the northward migration of the main river channel which the Tennessee Department of Transportation failed to evaluate and correct. Contributing to the severity of the accident was the lack of redundancy in the design of the bridge spans."

A 2-lane bridge on Route 51 was opened to traffic in 1936. It was (1,219 m (4,000 ft)) long and spanned the main channel (approximately 91 m (300 ft)) and the majority of the floodplain. In 1974 a second 2-lane (southbound) bridge was added. Its length was 305 m (1,000 ft) and centered approximately on the main channel downstream from the northbound bridge. The earth fill approaches to the new southbound bridge blocked the floodplain flow that had formerly moved through the open bents of the 1936 (northbound) bridge. This concentrated the flow in both bridges and caused the main channel to move northward and into the floodplain bents of the northbound bridge.

Each of the floodplain bents of the 1936 (northbound) bridge was on a pile cap (bottom elevation 237.9 ft) supported by five untreated wooden piles 6 m (20 ft) long. The main channel bridge was on piers with a pile cap (bottom elevation 223.67 ft) supported on 6 m (20 ft) long precast concrete piles. The northward movement of the channel exposed the piles of the bent next to the channel to local pier scour and it collapsed dropping three spans. The channel migration was documented by Tennessee DOT and U.S. Army Corps of Engineers (USACE) data (Bryan, 1989). At the time of the collapse the flow was not large 244 m^3/s (8,620 cfs) but the flow was overbank and of long duration. The maximum flood peak for the 1989 flood season was (813 m^3/s (28,700 cfs)) with a 3-year recurrence interval.

Since 1975, the bridge had been inspected on 24 to 26 month intervals and the last inspection was in September 1987. The NTSB report stated "the 1979, 1985, and 1987 inspection reports accurately identified the channel migration around column bent 70," (the floodplain bent that failed). The report further stated "....on-site inspections of the northbound U.S. 51 Bridge adequately identified the exposure of the column bent footings and piles due to the northward migration of the Hatchie River channel." The report also noted that the inspectors did not have design or as-built plans with then during the inspection. Because of this, the inspectors were mistaken in the thickness of the pile cap and calculated that 0.3 m (1 ft) of the bent piles was exposed. Whereas, the piles were actually exposed .9 m (3 ft) in 1987. The Safety Board noted other (unrelated) bridge collapses where inspectors did not have design or as-built plans, and as a result, deficiencies were overlooked that contributed to bridge failures. Therefore, the Safety Board believes that "it is essential for inspectors to have available bridge design or as-built plans during the on-site bridge inspection."

The NTSB noted that although TDOT inspectors measured the streambed depth at each substructural element and the USACE maintained historical channel profile data at the bridge "a channel profile of the river was not being maintained by TDOT." As a result the TDOT evaluator of the inspection report used only the 1985 and 1987 measurements and would not have been able to determine the extent of channel migration. In other words, if the profiles had been plotted, the evaluator should have easily detected the lateral migration.

The Safety Board also noted that an underwater inspection did not occur in 1987 because the bridge foundation was submerged less than 3 m (10 ft), TDOT criteria at that time. In 1990, TDOT changed the criterial to 1 m (3.5 ft). The Safety Board stated "a diver inspection of the bridge should have been conducted following the 1987 inspection because of the exposure of the untreated timber piles noted in the inspection report."

In conclusion, inspectors should have design or as-built plans on site during an inspection and should measure and plot a profile of the river cross section at the bridge. Submerged bridge elements that can not be examined visually or by feel should have an underwater inspection. Good communication must be established between inspectors, evaluators and decision makers. Changes in the river need to be evaluated through comparisons of successive channel cross sections to determine whether the changes are (1) random and insignificant or (2) represent a significant pattern of change to the channel which may endanger the stability of the bridge.

Arroyo Pasajero Bridge Failure

On March 10, 1995 the two I-5 bridges over Los Gatos Creek (Arroyo Pasajero) in the California Central Valley near Coalinga collapsed killing seven persons and injuring one. CALTRANS retained a team of engineers from FHWA, US Geological Survey, and private consultants to investigate the accident. No report was prepared by CALTRANS but three of the investigators, in the interest of bridge engineering, prepared a paper which was published by ASCE (Richardson et all, 1997 and Richardson and Lagasse, 1999, p631). The probable cause of the failure was:

The minimum scour depth from long-term degradation 3 m (10 ft) from inspection records, contraction scour 2.6 m (8.5 ft) calculated using Laursen's live bed equation, and local pier scour 2 m (6.7 ft) determined from a model study, exposed 2.7 m (8.9 ft) of the cast in place columns below the point where there was steel reinforcement. The force of the flood waters (at an angle of attack of 15 to 26 degrees) on the unreinforced columns, with their area increase by a web wall and debris, caused the bridge to fail.

The bridges, built in 1967, were 37 m (122 ft) long, with vertical wall abutments (with wing walls) and three piers. Each pier consisted of six 406 mm (16 inch) cast in place concrete columns. The columns were spaced 2.3 m (7.5 ft) on centers. They were embedded 12.5 m (41 ft) below original ground surface but only had steel reinforcing for 5.2 m (17 ft) below the original ground surface. The abutments were on pile-supported footings and the piles were 11.3 m (36.7 ft) long. A flood in 1969 lowered the bed 1.83 m (6 ft) and damaged one column. In repairing the damage CALTRANS maintenance constructed a web wall 2.4 or 3.6 m (8 or 12 ft) high, 11.6 m (38 ft) long and 0.6 m (2 ft) wide around the columns to reinforce them. The elevation of the bottom of the web wall was unknown.

Los Gatos Creek is an ephemeral stream (dry most of the time) which drains from the eastern side of the coastal range onto an alluvial fan whose head is approximately 3.2 km (2 mi) upstream of the two bridges. About 548 m (1,800 ft) upstream of the bridges Chino creek (also ephemeral) joins Los Gatos Creek. At the time of construction Chino Creek spread over and infiltrated into its alluvial fan. Some time after construction a channel was constructed connecting the two streams and increasing the drainage area of Los Gatos Creek by about 33 percent.

The Los Gatos Creek channel upstream of the bridge is from 91 to 122 m (300 to 400 ft) wide, but only 46 to 76 m (150 to 250 ft) wide downstream. The 37 m (122 ft) wide bridge severely constricts the channel and the March 10, 1995 flood ponded upstream of the bridge. From 1955 to 1995, differential land subsidence between bench marks approximately 2.4 km (1.5 miles) upstream and 8.5 km (5.3 mi) downstream was measured as 3.5 m (11.5 ft). The bed of the stream is sand and the bedform is plane bed. Discharges are hard to quantify for this stream. For the 1995 flood, the USGS using slope area methods determined that the discharge ranged from 462 to 1141 m^3/s (16,300 to 40,300 cfs) and the most probable discharge was 773 m^3/s (27,300 cfs) with a recurrence interval of 75 years based on historical data.

The factors involved in the I-5 bridge failure were:

- Increase in channel slope by subsidence
- Change in the original design by maintenance adding a web wall between columns to repair damage from an earlier flood. With an angle of attack from 15 to 26 degrees this action potentially increased local pier scour depth by a factor of 3.6 to 4.4
- Increase in drainage area of 33 percent above the bridge by land use change and the construction of a channel to link two streams (Chino Creek to Los Gatos Creek)

- Long-term degradation of 3 m (10 ft) since the bridge was built

- Significant contraction of the flow, i.e., channel width of 91 to 122 m (300 to 400 ft) wide to a bridge width of 37 m (122 ft)

In conclusion, the various factors that contributed to this failure illustrate the complexities of inspection and the need for all elements of a State Highway Agency (inspection, maintenance, design and management) to be involved in the process. Inspectors must continually observe the conditions at the bridge, and the stream channel above and below the bridge, and communicate actions, conditions, and changes in the bridge and stream to the different sections of the organization.

Conclusions

These three cases illustrate the difficulty and necessity for inspection of bridges. They also illustrate the need for good communication between inspection, maintenance, design and management. Inspectors must have design or as-built plans on site; must take, plot, and compare cross sections of the channel at the bridge, and they must observe and carefully document the conditions of the bridge and the channel upstream and downstream. Maintenance must inform inspection, design and others when they make changes to a bridge or channel. A "can do" attitude is great but sometimes the consequences can be bad. Communication is very important. Design needs to inform inspection and maintenance of design assumptions and what to look for. Maintenance, because they are the "eyes" of the highway departments, must look for changes and inform others.

SUMMARY

Inspection is a very important aspect of bridge safety. With an aging infrastructure bridge inspection is a very important tool to assure that bridges are safe for the traveling public. The importance and difficulty of inspection requires a well trained engineering staff and detailed procedures in the Departments of Transportation to carry out the inspection program.

REFERENCES

1. Bryan, B.S., 1989, "Channel Evolution of the Hatchie River near the U.S. Highway 51 Crossing in Lauderdale and Tipton Counties, West Tennessee," USGS Open-File Report 89-598, Nashville, TN.

2. FHWA, 1995, "Recording and Coding Guide for the Structure Inventory and Appraisal of the Nation's Bridges," Federal Highway Administration, U. S. Department of Transportation, Washington, D.C.

3. Harrison, L.J. and Densmore, D.H., 1991, " Bridge Inspection Related to Bridge Scour," Proceedings ASCE Hydraulic Engineering Conference, Nashville, TN, Reston, VA.

4. Lagasse, P.F., J.D. Schall, and E.V. Richardson, 1995, "Stream Stability at Highway Structures," Hydraulic Engineering Circular No. 20, Second Edition, FHWA-IP-90-014, Federal Highway Administration, Washington, D.C.

5. Lagasse, P.F., M.S. Byars, L.W. Zevenbergen, and P.E. Clopper, 1997a, "Bridge Scour and Stream Instability - Countermeasures - Experience, Selection, and Design Guidelines, Hydraulic Engineering Circular No. 23, FHWA HI-97-030, Federal Highway Administration, Washington, D.C.

6. Lagasse, P.F., E.V. Richardson, J.D. Schall, and G.R. Price, 1997b, "Instrumentation for Measuring Scour at Bridge Piers and Abutments," NCHRP Report 396, Transportation Research Board, National Research Council, National Academy Press, Washington,

7. NTSB, 1988, "Collapse of the New York Thruway (I-90) Bridge over the Schoharie Creek, Near Amsterdam, New York, April 5, 1987," NTSB/HAR-88/02, NTSB, Washington, D.C.

8. NTSB, 1990, "Collapse of the Northbound U.S. Route 51 Bridge Spans over the Hatchie River near Covington, Tennessee," April 1, 1989, NTSB/HAR-90/01, National Transportation Safety Board, Washington, D.C.

9. Richardson, E.V., P.F. Lagasse, J.D. Schall, J.F. Ruff, T.E. Brisbane, and D.M. Frick, 1987, "Hydraulic, Erosion and Channel Stability Analysis of the Schoharie Creek Bridge Failure, New York," Resource Consultants, Inc. and Colorado State University, Fort Collins, CO.

10. Richardson, E.V. and Davis, S.R., 1995, "Evaluating Scour at Bridges," Hydraulic Engineering Circular 18, Third Edition, FHWA-HI-96-031, Federal Highway Administration, Washington, D. C.

11. Richardson, E.V., J.S. Jones, and J.C. Blodgett, 1997, "Findings of the I-5 Bridge Failure," ASCE Hydraulic Engineering Proceedings of Theme A, 27th IAHR Congress, San Francisco, CA.

12. Richardson, E.V. and Lagasse, P.F., Editors, 1999, "Stream Stability and Scour at Highway Bridges," Compendium of ASCE Water Resources Papers Engineering Conferences 1991 to 1998, Reston, VA.

13. Transportation Research Board, 1999, "CAESAR: An Expert System for Evaluation of Scour and Stream Stability," NCHRP Report 426, National Research Council, National Academy Press, Washington, D.C.

DEVELOPMENT OF NEW SCOUR MONITORING DEVICESFOR RAILWAY BRIDGES

by

Osamu Suzuki[1], Makoto Shimamura [2]

ABSTRACT

Scour monitoring of railway bridge piers is a crucial procedure for safe train operation. The operation should be suspended whenever the bridges are at risk of scour damages. This has been a difficult and unreliable decision process because bridge pier under flood water is not observable directly by naked eyes. This paper describes the outlines of four new scour monitoring devices developed for the particular purpose of train operation safeguard against scour hazard and discuss their functions and characteristics obtained from experimental results.

THE STATUS QUO

In Japan, approximately 200 railway companies operate 37,188km of tracks and carry 22 billion passengers a year. East Japan Railway Company (JR East) is the largest railway company in Japan and one of seven railway companies that formed on the division and privatization of Japanese National Railways. At present, JR East has a network of 7,538 km of tracks in Tokyo area and eastern Honshu and 6 billion passengers use our network a year. Fig.1 shows the networks of JR East. In JR East area, there are approximately 3,000 bridges over water and approximately 600 bridges of them should be considered of the countermeasure against risk of scour hazard.

[1] Researcher, Safety Research Laboratory, East Japan Railway Company, suzuki@head.jreast.co.jp
[2] Senior Chief Researcher, Safety Research Laboratory, East Japan Railway Company, m-shimamura@head.jreast.co.jp

As the most part of the catchment areas consist of mountainous terrains, one of the characteristics of rivers in Japan is their short and steep riverbed topology. In and around 1960's, as Japanese economy rapidly grew, many dams were constructed in upstream districts of these rivers to suffice greater demand for electricity and water. These dams have disturbed supplies of streambed material from upstream districts to downstream districts. Thus, riverbed elevations have tended to degrade at many rivers in Japan.

Most of the bridges in JR East were built before the Second World War. They have the characteristics because of budget and technology constraints such as

(1) They have short span steel girder and relatively many bridge piers,
(2) Most of the bridge piers have shallow spread footing or wooden pile foundation, and
(3) They were built at the site of relatively narrower river width, because reduction of bridge.

Photo.1 shows the view of an example of such ordinary bridges in JR East.

Higher velocities of river flow at narrower width sites and flow obstruction caused by bridge piers encourage scour of bridge foundation. As a result, these bridges are relatively vulnerable to scour damage compared with the bridges built recently.

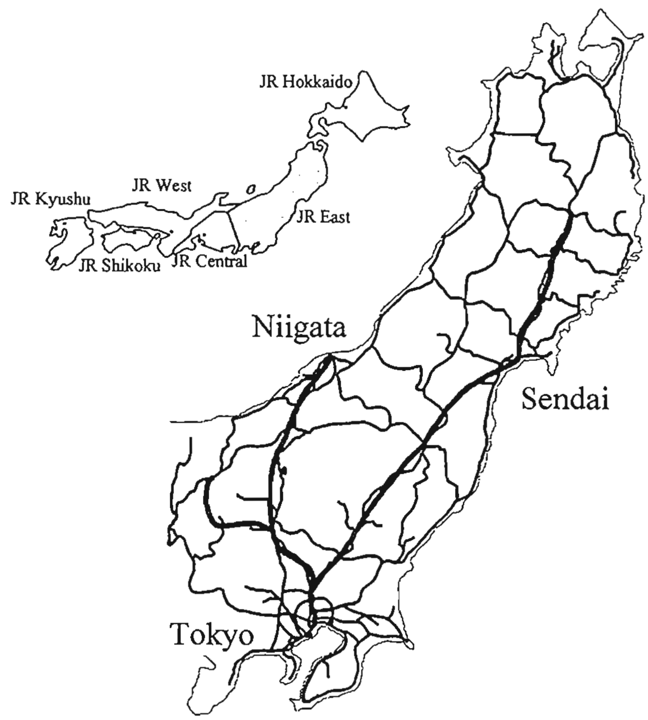

Fig.1 The networks of JR East

Photo.1 The view of example of such ordinary bridges in JR East

THE RULE FOR REGULATION OF TRAIN OPERATION DURING HIGH WATER

In order to avoid fatal train accidents due to bridge damage caused by scouring bridge foundation, it is necessary to set any train suspension rules to be applied for train operations during flood. As the judgment of the magnitude of scour hazard by visual inspection is difficult because of large flow depth, high flow velocities and turbidity of flow, etc., inferential scour depth around a pier foundation based on water level monitoring instead of direct observation of scour has been used to make decisions on train suspensions and resumption during high water.

In this procedure, scour depth is estimated by means of the empirical relationship among scour depth, water level and bridge pier width. When the estimated scour depth at the spread-footing base of the bridge pier of interest reaches to certain threshold value, orders to suspend train operation are to be transmitted to the train operators. Fig.2 shows outline of regulation of train operation during high water.

There are approximately 700 on-line water level gages on bridge piers and water level is measured individually on real time.

PROBLEMS IN THE RULE FOR REGULATION CURRENTLY IN FORCE

The rule currently in force is based on empirical approach. To avoid train accidents caused by scour hazard, this estimation should be determined considering worst-case scenarios and is added unclear safety margin. Thus, for most of bridge piers, the estimated scour depth gives greater values than actual scour depth. This causes many unnecessary train cancellations and most of the scour alarm cases to be "false positive".

On the other hand, the rule currently in force is not reliable enough to issue the order to suspend train operation well before the bridge pier should be at risk in some kind of site-situation. The scour hazard occurred in 1995 and it was difficult to assess the magnitude of scour hazard with the rule currently in force. The site-situation of this scour hazard is showed in photo.2. The reason for this hazard occurrence is incline of the bridge pier caused by the scouring of the bridge foundation. This bridge is constructed over a flume where on average slope of 10(horizontal) to 1(vertical). In this kind of flume with steep slope, stream becomes super-critical flow and water level hardly rises during a flood.

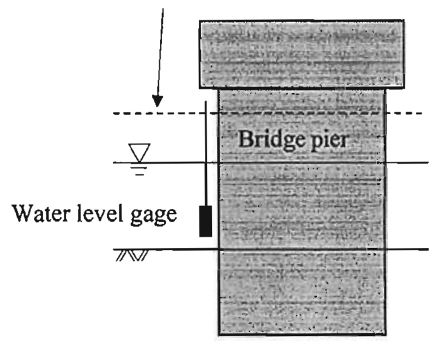

Fig.2 outline of regulation of train operation during high water

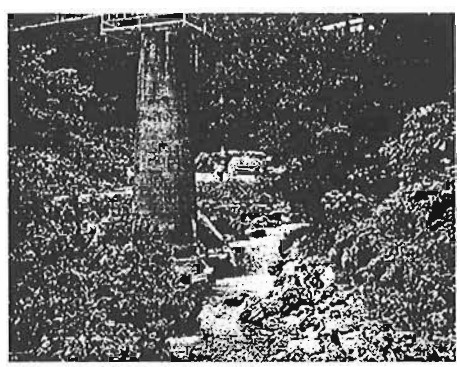

Photo.2 Site-situation of scour hazard

SCOUR MONITORING DEVICES TO MONITOR RIVERBED LEVEL

The Safety Research Laboratory of JR East has worked away at developing several scour monitoring devices to improve reliability of the rule. The following sections introduce the outlines of these scour monitoring devices. (Fig.3)

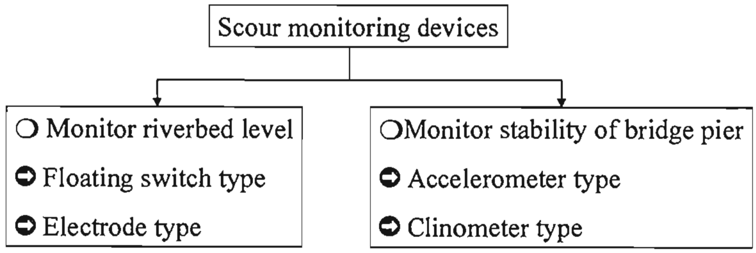

Fig.3 Developed scour monitoring devices

1. Floating switch type

This device is consists of a mechanical sensor with float and a supporting pipe. The principle of this device is shown in Fig.4. This is set to be buried around the bridge pier in advance. When bridge foundation is scoured and riverbed material around the device is washed away, sensor can float up into water and is shacked by stream. On such an occasion, sensor issues a warning. This device can monitor the progress of scour. Photo.3 shows floating switch type scour monitoring device.

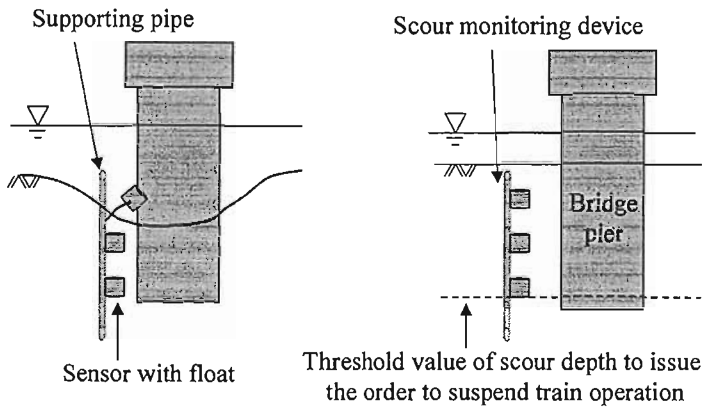

Fig.4 Principle of floating switch type scour monitoring device

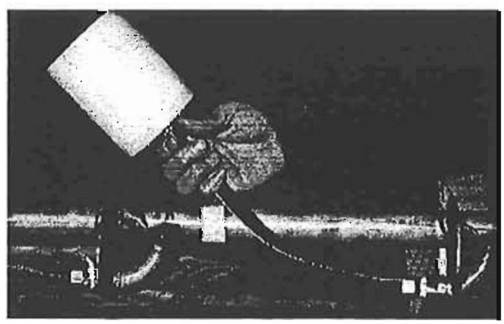

Photo.3 Floating switch type scour monitoring device

2.Electrode type

This device measures electrical resistance and evaluates the riverbed level from the difference of electrical resistance between water and riverbed material. Fig.5 shows the principle of this device. This is also set to be buried around the bridge pier in advance. As scour developed, electrical resistance of the main electrode changes. The riverbed level is evaluated by the following equation:

$$Z = (S_m - S_s) \cdot L_m / (S_w - S_s)$$

where, Z is distance from bottom of main electrode to riverbed level, S_m is conductance of main electrode, L_m is length of main electrode, S_s is conductance of auxiliary electrode in riverbed material per unit length and S_w is conductance of auxiliary electrode in water per unit length. Fig.6 shows the correlation between an evaluated riverbed level and an actual riverbed level. From this figure, the evaluated riverbed level and actual riverbed level are in good accordance. This device can precisely evaluates the riverbed level on real time. Photo.4 shows electrode type scour monitoring device.

Following effects are expected in case to use the above scour measuring devices.

(1) Determination to install countermeasures and to resume the train operation becomes easier, because the riverbed elevation around the bridge pier can be determined precisely.

(2) These devices are also effective for the flume with steep slope that stream becomes super-critical flow and water level hardly rises during a flood.

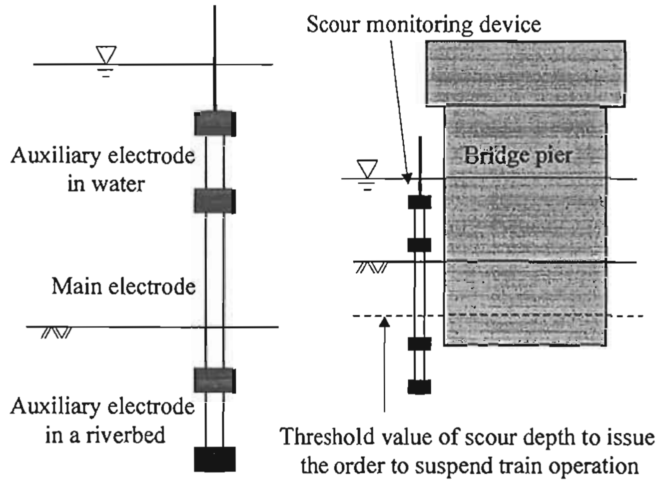

Fig.5 Principle of electrode type scour monitoring device

The rule for regulation of train operation during high water with these devices also has problems as follows:

1. In this rule, unclear safety margins still remain, because the relationship between bridge pier stability and scour depth is not clear.
2. Scour monitoring devices must be set at the most vulnerable points around the bridge pier, because this device can only monitor scour depth at the point where it is set.

In case that monitoring object has closer relationship with bridge pier stability, reliability of the rule is improved. Two scour monitoring devices that monitor natural frequency or inclination of bridge pier has been developed.

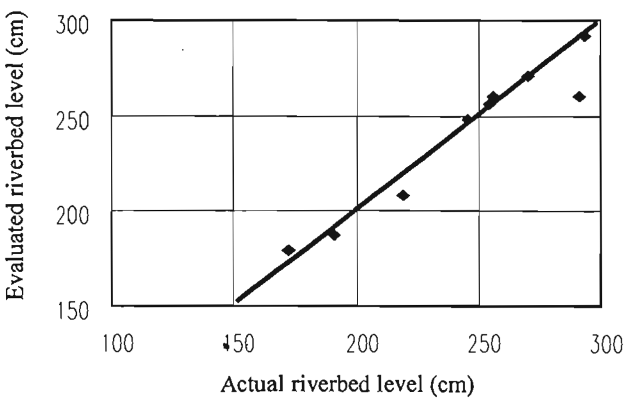

Fig.6 Correlation between an evaluated riverbed level and an actual riverbed level

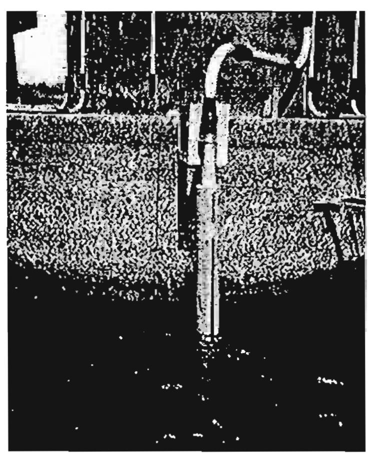
Photo.4 Electrode type scour monitoring device

SCOUR MONITORING DEVICE TO MONITOR STABILITY OF BRIDGE PIER

1. Accelerometer type

(1) Principle

This device evaluates bearing capacity of the bridge pier from the natural frequency of a bridge pier. This technique is popular for evaluation of bridge pier soundness with percussion of heavy weight[1]. To calculate natural frequency, microtremor is measured on the bridge pier. Because microtremor is disturbed with noises, specification of natural frequency of the bridge pier is very difficult in its crude condition. To solve this difficulty, "Weighted Spectrum Area (WSA)" is calculated as indicator to evaluate bearing capacity. WSA is area of spectrum of microtremor that is measured on bridge pier. Spectrum is multiplied by weighted function that emphasizes the shape of spectrum in case bridge pier is sound.

(2) Basic idea of the regulation of train operation

When bearing capacity of the bridge pier decreases, WSA also decreases. However, it is very difficult to specify WSA when the bridge pier does not have enough bearing capacity for train to pass.

WSA is fluctuating within some small limited range, because noises in microtremor influence a shape of spectrum. Threshold value to suspend train operation is determined statistically. Threshold value set to the lower bound value of the WSA that is inferred statistically with the fluctuation data. When the measured value becomes lower than threshold value, immediately, the order to suspend train operation is issued. The basic idea of method to regulate train operation is showed in Fig.7.

(3) Result of examination

The flume experiment is carried out

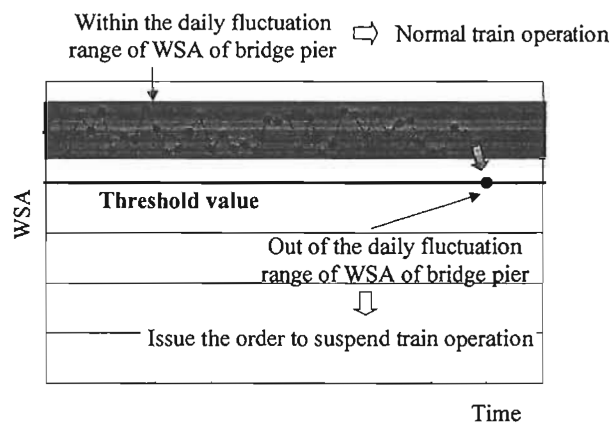

Fig.7 Basic idea of the regulation of train operation

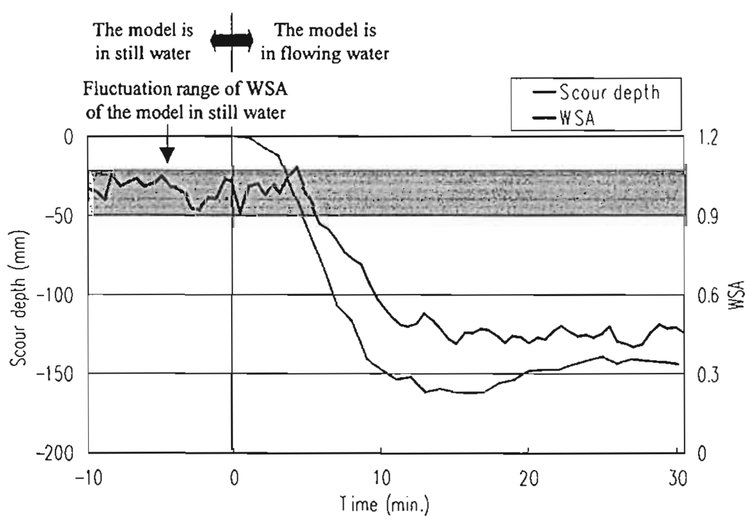

Fig.8 The result of flume experiment

with 1/20 scaled cylindrical pier model and uniform sand (d_m=1mm) to investigate correlation between a scour depth around the model foundation and WSA of the model. The result of the experiment shows in Fig8. The change of WSA before flume experiment is also shown in Fig.8. Although scour does not occur around the model foundation before flume experiment, WSA fluctuated within some small limited range. During the flume experiment, as scour develop, WSA become lower than the fluctuation range of WSA before flume experiment. The result of the experiment shows good correlation between a change of scour depth and a change of WSA.

2. Clinometer type

(1) Principle

This device monitors an inclination of bridge pier caused by scouring the foundation of bridge pier.

(2) Basic idea of the regulation of train operation

An inclination of bridge piers can be influenced by surrounding temperature and is fluctuating within some small limited range. Threshold value to issue the order to suspend train operation is also determined statistically. Threshold value of inclination of bridge pier is determined as the upper bound value of the inclinations that is inferred statistically with the fluctuating data. When the inclination of bridge pier exceed the threshold value, it is considered that bridge pier has some disorder and the immediate inspection is needed. Moreover, in case displacement of track caused by incline of bridge pier is not safe enough for a train to pass, the order to suspend train operation should be immediately issued. The basic idea of method to regulate train operation is shown in Fig.9.

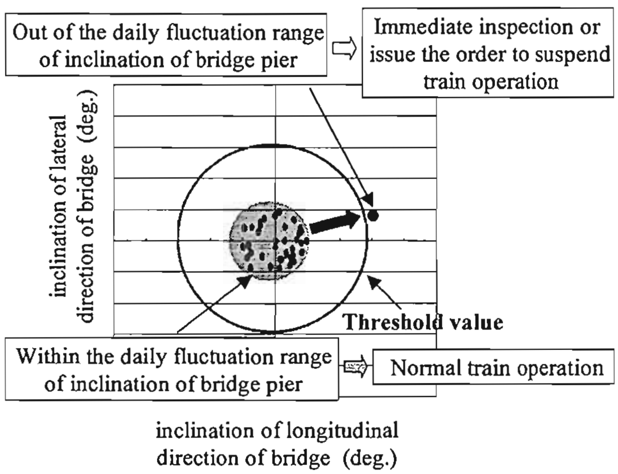

Fig.9 The basic idea of method to regulate train operation

(3) Result of examination

Inclinations of the actual bridge piers are monitored by the clinometer for 6 months. Hysteresis figure of the inclinations of the bridge piers is shown in Fig.10. From this figure, the daily fluctuations of

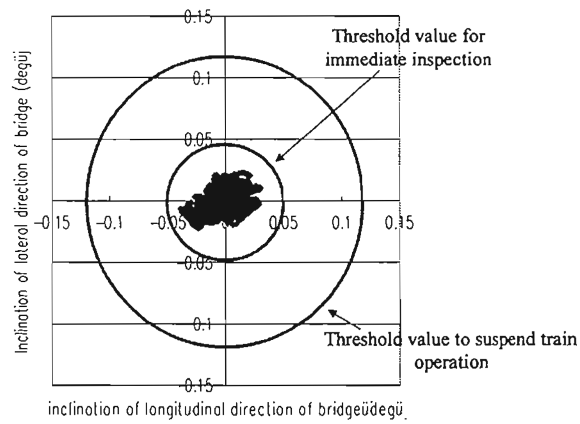

Fig.10 Hysteresis figure of the inclinations of actual bridge pier

inclinations of bridge piers stay inside of the small limited range and much smaller than the inclination that has a bad influence on the track.

Above scour monitoring device is low-cost, because only one scour monitoring device is set on bridge pier in order to evaluate stability of bridge pier. And following effects are expected in case to use above scour monitoring devices.

(1) The rule for regulation of train operation during high water with above scour monitoring devices become more reliable, because monitoring objects of these devices have closer relationship with stability of bridge foundation.
(2) These devices are also effective for the flume with steep slope that stream becomes super-critical flow and water level hardly rises during a flood

CONCLUSIONS

Table 1 shows summary of the four scour monitoring devices developed by JR East. Scour monitoring devices except for accelerometer-type were made for practical use. At present, new regulation of train operation during high water including with installing a scour monitoring is considered by JR East.

Table 1 Summary of Scour Monitoring Devices

Type of scour monitoring	Characteristics	Use for
Floating Switch Type Electrode Type	Those can monitor an elevation of riverbed.	Assessment of the risk of abutment or revetment failure
Accelerometer Type Clinometer Type	Those can monitor stability of bridge pier.	Assessment of the risk of Bridge pier failure

REFFERENCE

1) Nishimura, A., Tanamura, S., 1989 "A Study on Integrity Assessment of Railway Bridge Foundation (in Japanese)", RTRI Report Vol.3, No.8

REAL-TIME BRIDGE SCOUR ASSESSMENT AND WARNING

By

Jeffrey M. Di Stasi[1] and Carlton L. Ho[2]

ABSTRACT

A method to assess bridge scour potential is presented. The purpose of the method development is to provide agencies such as state Departments of Transportation (DOTs), state police, and local police a means of assessing the hazard posed by bridge scour. This method is based upon a spatial decision support system (SDSS). The SDSS is an interoperable code that will allow for flexibility in spatial calculation. The SDSS is a JAVA based program designed with interchangeable modules (data management, algorithm, and graphical user interface). Because the code is JAVA based, the program can run on any platform. It is important to recognize that the SDSS was originally envisioned for use as a means to assess seismically induced landslide hazard, but is flexible enough to be used for all types of spatial analysis (Miles et al, 1999). For this application, the SDSS calculates bridge scour hazard using different types of data sets, analytical algorithms, and spatial analysis.

The data sets are archival (foundation design, geometrics, stream bed contours, location, etc.) and temporal (climatalogical, hydrological, bridge scour monitors, etc.). Archival data can be periodically modified as needed. Analytical algorithms are based upon recommendations from the Federal Highways Administration Hydraulic Engineering Circulars 18 and 20. Other algorithms could be simply implemented using the modular nature of the SDSS.

An important aspect of evaluating the hazard potential is an assessment of types of data that are available and the format in which these data are kept. A survey of the available data is made of the New England region of the United States of America. A survey was made of federal and regional agencies to determine the types of available data. In addition, existing scour programs in each New England state are reviewed to provide an understanding of the each state's program and its direction. Recommendations are made for the development of additional means of data acquisition for better real-time assessment. Ultimately, the SDSS could be used as a web-based monitoring scheme for real-time dissemination of bridge scour hazard warning for safety and maintenance related public agencies.

INTRODUCTION

The collapse of the Schoharie Creek Bridge in New York in 1987 was the first catastrophic event that brought bridge scour into the public spotlight. Since then, the Federal Highway Administration (FHWA) has focused its efforts on identifying and coding all bridges regarding their scour susceptibility through qualitative and quantitative means. In 1989, the FHWA mandated that all states evaluate stream stability and the potential for scour at bridges over water. Technical advisories TA5140.20 "Scour at Bridges" (U.S. Department of

[1] Grad. Asst., Dept. of Civ. and Env. Engineering, Univ. of Mass., Amherst, MA 01003
[2] Assoc. Prof., Dept. of Civ. and Env. Engineering, Univ. of Mass., Amherst, MA 01003

Transportation, 1988) and TA5140.23 "Evaluating Scour at Bridges" (U.S. Department of Transportation, 1991) were issued in 1988 and 1991, respectively, to provide guidance for states as they developed and implemented scour evaluation programs for existing bridges and new bridge designs. In 1991, Hydraulic Engineering Circular 20 (HEC-20) "Stream Stability at Highway Structures" was published by the FHWA to help provide guidelines for identifying stream instability at highway stream crossings (Lagasse et al, 1991). In 1995, Hydraulic Engineer Circular 18 (HEC-18) "Evaluating Scour at Bridges Third Edition" was released by the FHWA, which presented a revised methodology for a full scour analysis, including the design, evaluation, and inspection of bridges for scour (Richardson and Davis, 1995). Of particular concern are scour critical bridges, which are bridges that could experience catastrophic failure or become structurally unstable as a result of excessive scour caused by a destructive flood event. A single digit rating system within the National Bridge Inspection Standards (NBIS) was also developed by the FHWA to help classify the vulnerability of bridges to scour.

Now that most of the bridges have been evaluated, inventoried, and coded with regard to scour, the next logical step is to develop a systematic means of classifying and prioritizing bridges for remediation. The objective of this research is to develop a strategy for the organization of a statewide network of scour monitoring devices to assist in the allocation of resources during potentially destructive flood events, which would include assessing bridge scour in real-time. This would be accomplished using a web-based approach, which consists of a platform independent code that utilizes a SDSS.

Unfortunately, the scour equations found in HEC-18 may not predict accurate scour depths. This may be due, among other things, to the inability to conduct tests on large-scale laboratory models. Therefore, new scour equations should also be researched that could also be used along with the current equations.

BACKGROUND

Through the NBIS, scour critical bridges are addressed in the Item I113 code in the Recording and Coding Guide for the Structure Inventory and Appraisal of the Nation's Bridges National Bridge (Report No. FHWA-PD-96-001). A scour critical bridge is classified as such according to one of the following: (1) observed scour at the bridge site or (2) scour potential as determined by a scour evaluation study. A single digit code is used to describe the stability of the bridge's pier and abutment foundations. Scour critical bridges are identified by a code of 3 or less (U.S. Department of Transportation, 1995).

Over the past ten years, state DOTs in New England have devoted a large amount of time to assigning I113 codes for each bridge. Many bridges were assigned codes after an initial screening was performed, without the need for a full scour analysis. This was done through a review of existing information for the bridges, including, but not limited to, bridge plans, hydrologic files, FEMA flood studies, and USGS stream gage data. For a large number of bridges, however, the initial screening was not sufficient and a full comprehensive scour analysis was required. This usually meant hundreds of bridges for each state. Of those bridges that were put through a scour evaluation study, many still remain either uncoded or were assigned a temporary code until a more thorough analysis could be performed. One reason for this has been that for many of the older bridges, no plans were available and thus the foundations were unknown. In other cases, hydraulic or FEMA studies were not available or complex hydraulic conditions necessitated a more intensive analysis. While many of these states have coded the majority of their bridges, no state has completely finished this task due in large part to unknown foundations, although temporary codes may have been used for the time being. For the most part, all of the bridges with known foundations have received an I113 code.

There have been a few different approaches to addressing bridges with unknown foundations. One is to code the bridge as a 3 (scour critical). This was done to save time and money and was based upon results of other similar bridges that received full scour evaluations. Another approach is to code the bridge as U (unknown foundation) for now until subsurface investigations can be performed based upon prioritization (Nardone, 2000). The investigations can be accomplished through borings or geophysical testing methods, such as ground penetrating radar. Obviously, this approach is more costly, but it permits a full scour evaluation to be conducted and instead of assuming all of these bridges are scour critical, some may be able to be removed from this list. This could also save money in the long term as well, which will be discussed later in the paper.

All states must deal with the same scour problem, yet when it comes to available resources such as money and personnel, no two states are alike. The implementation of a SDSS will help level the field for all states, permitting all parties to evaluate and monitor scour using the same models.

GENERAL SCOUR ANALYSIS

To some extent, all of the states in New England have developed a flowchart that outlines the general procedure followed for a typical bridge scour analysis. Each state's scour program was a result of a collective effort between geotechnical, hydraulic, and structural engineers. In many cases, the services of outside consultants were also needed. In general, all bridges underwent an initial review of existing information, which was mainly qualitative. Bridges that were clearly stable or unstable were coded after this process. A bridge that displayed extensive scour during a field inspection could be coded just as easily as a bridge that was founded on bedrock. For those bridges determined to be scour susceptible (i.e. their vulnerability to scour was not as apparent), they were put through a full Level 2 scour analysis or some abbreviated analysis (Glenn, 2000).

Engineering judgement was also brought into the analysis as flood and bridge history were considered along with existing data, records, and reports. For example, considerations would be made in the instance where a bridge was determined to be scour critical for a 10-year event, but had withstood two separate 50-year events. Analysis of the bridge for a 10-year event may have estimated scour depths that classify the bridge as scour critical, but clearly the structure did not fail. Some states addressed this issue by adding a second character to the single-digit I113 code, which was based upon a modified version of the Maryland State Highway Administration (MSHA) 113 rating system, to supplement the I113 code in order to more realistically describe the scour susceptibility of a bridge. An example of this is described below:

> "...a single-span bridge which has been standing for 50 years may be scour critical, solely due to the calculated abutment scour. For such a bridge, we might select a MSHA rating of '3A' which denotes scour critical, but with a mild scour risk." (Whitman & Howard, Inc., 1996)

This additional character in the code can also be useful in the prioritization of bridges for remediation.

One approach to conducting bridge scour studies is discussed in-depth in the following section.

COMPARATIVE SCOUR ANALYSIS

The Connecticut Department of Transportation (CONNDOT) initially conducted its scour evaluation studies in general accordance with the aforementioned procedures. After a period of time, faced with prohibitive costs and a large number of bridges remaining to be analyzed, CONNDOT, along with the Federal Highway Administration (FHWA) and consultants, developed a new method that would provide an I113 code without requiring a full Level 2 scour analysis. This new method, called the comparative scour analysis, utilized the results of previous Level 2 scour analyses while generating time and cost savings (CHA, 1998).

Prior to the introduction of the comparative scour analysis, approximately 300 bridges received a full Level 2 scour analysis, including an I113 code. At this point, CONNDOT took a step back from their scour studies and decided to take another approach for the remaining bridges, which resulted in the implementation of the comparative scour analysis. It was decided that the 1350 remaining bridges would be placed in one of three categories: (1) Low Risk, (2) Level 2, or (3) "advance to the next phase." Examples of Low Risk bridges included those which were a box culvert or those founded on competent rock. Level 2 bridges included, but were not limited to, those that were not considered low risk, had complex hydraulics, or were considered very important, based upon traffic volume, replacement cost, structure size, etc. The purpose of this categorization was to identify those structures that were clearly stable or unstable. Any bridge not placed in the first two categories fell into the "advance to the next phase" category (CHA, 1998).

The susceptibility to scour was less clear for the bridges placed in the "advance to the next phase" category. These bridges were candidates for either a Phase III or Phase IV evaluation. Upon completion of an office review and site visit, a bridge could either be coded using the comparative analysis, recommended for a full Level 2 analysis, or advance to the next phase to obtain additional information (i.e. structural stability analysis) to determine the recommended rating without needing a full Level 2 study. A structural stability analysis would be performed on bridges for which predicted scour depths were calculated to be within the spread footing or pile foundation that was exposed, but not completely undermined. The analysis would address concerns that the bridge would become unstable due to the calculated scour depths and stability checks would be made to ensure minimum factors of safety still applied for bearing pressure, overturning, and sliding. The difference between Phase III and Phase IV is that Phase III represented the validation process of the comparative analysis and includes bridges which are representative of those found across the state. Once final approval had been given to the comparative process, Phase IV was initiated and the remaining bridges were evaluated following the same procedure (CHA, 1998).

Those bridges that were already rated using the Level 2 analysis served as the group of rated bridges with which the unrated bridges would be compared. The comparative analysis was purely qualitative in nature, but it was still used to provide recommendations for the NBIS Item 113 rating (Antoniak and Levesque, 2000).

In order to justify the comparison of two bridges, one rated and the other unrated, primary and secondary criteria had to be met. Primary criteria were considered to be Single vs. Multiple Span and Stream Character Category. Secondary criteria were listed as Estimated Stream Velocity, Foundation Type (at Abutments and Piers), Ratio of the Upstream Channel Width to the Width of the Channel Beneath the Bridge, and Angle of Attack. A valid comparison mandated that, at the very least, all primary criteria were met. The greater the number of secondary criteria that were met, the closer the similarity of the two bridges (CHA, 1998).

Application of Comparative Analysis

Although the comparative analysis may not be applied exactly the same way should another state adopt it, the concept certainly would still be valid. As previously mentioned, I113 codes have been assigned to most of the bridges with known foundations. The only ones that remain are bridges that are uncoded or received a temporary code due to unknown foundations. The comparative analysis may provide incentive to states that may have been reluctant to determine the foundations of bridges that are currently unknown, whether they do so through borings, geophysical methods, or recovered plans. While it is easy and inexpensive to code a bridge with unknown foundations as scour critical without doing any analysis, initial savings could be lost if that bridge is monitored at a later date. It would be a misuse of resources to place a monitor on or near a bridge that was not scour critical, simply because it was too costly to determine the foundations initially. The resources should only be applied to those bridges that are truly scour critical.

Perhaps even more importantly, the comparative analysis would allow for information to be shared among states. For example, a database or web-based system containing information pertaining to rated bridges (full Level 2 analyses) in Connecticut could be accessed to find a bridge which could be compared with an similar unrated bridge in Vermont, assuming the proper criteria was met. Through the use of queries, several rated bridges could be pulled up for possible comparison of the unrated bridge. Based upon a review of the Level 2 scour reports for the rated bridges, a decision will be made to determine if a rating can be recommended using the comparative process. If a rating cannot be made, then the bridge could be forwarded to a Level 2 or abbreviated analysis. Once the most appropriate bridge is selected for the comparison, using engineering judgment, the report for the Level 2 bridge, and field reports for the unrated bridge, an appropriate Item I113 rating will be recommended. It should be noted that the comparative process only compares unrated bridges with bridges that have been through a full Level 2 scour analysis. A bridge that received a rating through comparative analysis cannot be considered a rated bridge to be compared with another unrated one.

There are some conditions that should be satisfied if this analysis is to be adopted and used by other states. First, a large and representative group of bridges must be available for comparison; otherwise, the analysis would be limited in its scope. States may even wish to develop their own database of bridges that were rated using a Level 2 analysis if they feel that would better represent the bridge types and conditions in their state. In the event that bridge or stream conditions drastically changed, a bridge could be reanalyzed using the comparative analysis. However, if this occurred to a bridge that initially received a Level 2 analysis, there would be two options. It could be placed back into the group of rated bridges used for comparison only if another Level 2 analysis was performed or it could removed altogether from the sample group and be reassigned a code as an unrated bridge through a comparative analysis. Second, it would be more appropriate for states in regions with similar geologic and climatic histories to compare and rate their bridges. Bridges in New England and Florida with similar geologic and hydraulic conditions would likely be rare. Third, a central database or web-based system should be established which contained information and reports for all bridges in a particular region and could be accessed by each DOT. This would eliminate any barriers that would hinder the exchange of information between states.

Before any analysis or procedure is adopted, though, it is highly recommended that interested parties first review the comparative scour analysis in detail that was developed by the CONNDOT Hydraulic & Drainage Unit.

COMPUTATIONAL STRATEGY

After identifying and evaluating the current methods and procedures used to perform scour evaluation studies, a strategy for the research was developed. The proposed research is in response to the problem statement presented by the New England Transportation Consortium, which was comprised of a representative from each New England state, on how to better prepare and organize themselves for scour-related problems at bridges caused by an anticipated flood event. A strategy was developed to accomplish this, which will (1) document sources of information pertaining to stream monitoring, precipitation, storm prediction, and evacuation routing, (2) identify locations where existing monitoring systems do not provide coverage over scour critical bridges, and (3) develop a conceptual model of a monitoring system that incorporates hazard and risk assessment and would assist in the prioritization of bridges jeopardized by scour. The system will be web-based and platform independent for universal accessibility. It will allow each state to monitor scour at critical bridges during a storm event independent of existing monitoring schemes. The data file format must be compatible with all DOT supported software.

The strategy for the model of the monitoring system will emphasize the determination and source of the input parameters and the algorithms to be used in the spatial modeling framework. The first step is to catalog all of the bridges, their attributes, and the existing monitoring systems (e.g. stream gages, rain gages, scour monitors) in a GIS application (e.g. ArcInfo, Arcview). The second step is to determine what data is available that pertains to scour and the format in which the data is stored. This includes establishing which data is archival and which is real-time. Archival data, which refers to information that will, for the most part, be constant (e.g. bridge geometry, channel characteristics, bed material, etc.) can be stored as part of the bridge attributes. The predicted scour depths and the corresponding flow and flow depths for critical storm events as well as the current Item I113 code should also be stored as archival data for reference. If one of the attributes does change, it can easily be changed within the application, as discussed in the next section. The real-time data (e.g. streamflow), which is periodically refreshed or updated (e.g. hourly), can be loaded to the user's computer from a server. Finally, equations that are used to calculate scour depths must be identified. This will include the HEC-18 equations, which are currently the standard equations used for scour analyses, as well as any other equations that have been developed or used for scour. The data that is available will be compared to the parameters for the equations to ensure that all inputs are satisfied. Through the integration of archival and real-time data, and the selection of an applicable scour equation, predicted scour depths will be calculated in real-time and the system can alert the user of a potential bridge failure due to scour during an event.

This approach will also allow scour depths calculated from different equations to be compared and perhaps give interested parties a better understanding of which scour equations work best under certain conditions. If actual scour depths from previous storm events were measured in the field and stored in the bridge attributes as well, then these depths could also be compared with the predicted results.

The SDSS code will be written in Sun Microsystems Java 1.2 for the model. Java is platform independent, which is due to the application of the concept of a virtual machine. The virtual machine allows for low-level operating system implementation to be separated from high-level coding. Java was selected for the approach as a result of its algorithmic flexibility, its ability to be accessed from the web by all parties, and the familiarity of the authors with it (Miles et al, 1999).

GRAPHICAL USER INTERFACE COMPONENTS

The graphical user interface (GUI) components serves the purpose of making the system more user-friendly. It does this by masking the complexity of the user tasks and the differences between the numerous underlying components. Through direct-manipulation, the GUI will include several components for use in managing spatial data requirements (input parameters), model configuration (algorithms), and analysis output (Miles et al, 1999). Direct-manipulation refers to performing computing tasks through physical action instead of syntax. Several advantages of direct-manipulation are cited by Schneiderman (1988), such as control-display compatibility, reduced error rates, faster learning, longer retention, and more user explanation.

The GUI will be based upon a tree model, which will be familiar and comfortable for most users. Its structure will not only aid in the understanding of information such as model configuration and input parameters, but also in the structure of the information in terms of organization and relation. The flexibility of the tree will also permit modification of spatial data parameters, such as in the instance where a model component is added or changed (Miles et al, 1999).

The three components of the GUI include the Spatial Data Manager, the Model Manager, and the Output Manager. The Spatial Data Manager will contain all spatial data requirements, which will be represented by branches of the tree in the GUI. The Model Manager will list all of the models (algorithms) that can be selected for analysis, permit editing of model parameters, and perform the analysis through direct-manipulation. The Output Manager will have the same configuration as the Spatial Data Manager, except that it will organize and present the results of the analysis (Miles et al, 1999). A flowchart is shown in Figure 1 to provide a visual reference of the system components:

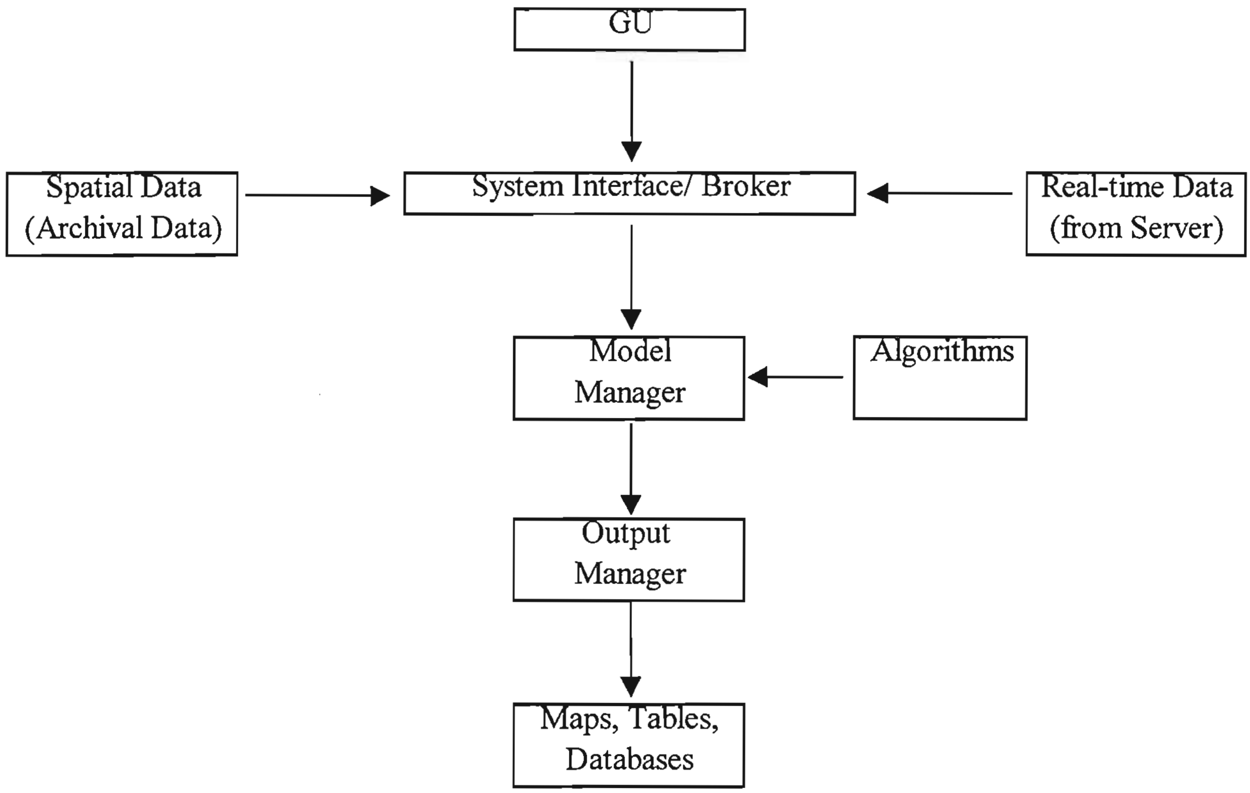

Fig. 1. Proposed system architecture for spatial decision support system (SDSS)

APPLICATIONS OF THE STRATEGY

Engineering Application

Some states have expressed their satisfaction with the scour codes they assigned using the HEC-18 scour equations. They understand that the equations can be overly conservative, but they feel the requirements that were established by the FHWA regarding scour analyses have been met (Nardone, 2000). Other states have indicated their interest in identifying new equations that could more accurately predict measured scour depths in the field. The application of new equations can not only provide better estimates of scour depth, but could also reduce the number of bridges determined to be scour critical (Antoniak and Levesque, 2000). Revising codes for bridges that were initially coded as scour critical could significantly impact the allocation of new monitoring devices, the routing of traffic during an evacuation, and the prioritization of bridges for remediation.

Connecticut has already taken this initiative of adopting new equations by amending the local abutment scour equation by Froehlich, as presented in HEC-18, Third Edition. The current formula is as follows:

$$Y_s / Y_a = 2.27 K_1 K_2 \left(\frac{L^1}{Y_a} \right)^{0.43} Fr^{0.61} + 1 \tag{1}$$

where

K_1 = coefficient for abutment shape (See Table 6, Section 4.3.6 in HEC-18 Third Ed., dated Nov. 95)
K_2 = coefficient for angle of embankment to flow (Refer to Section 4.3.6, Figure 16 in HEC-18, Third Ed., dated Nov. 95)
L^1 = the length of abutment projected normal to flow
Y_a = average depth of flow in the floodplain = A_e / a'
A_e = the flow area of the approach cross section obstructed by the embankment
Fr = the Froude number = $V_e / (g\, y_a)^{0.5}$
$V_e = Q_e / A_e$
Q_e = the flow obstructed by the abutment and approach embankments
Y_s = scour depth

CONNDOT reported that the +1 value was initially intended as a factor of safety, but was not in Froehlich's original paper. This value increases the predicted scour depth by the depth of the overbank flow. Based upon the conservative nature of the equation based upon laboratory data with regard to actual field data, CONNDOT, after consulting with researchers, chose to replace the +1 value with a value of +0.05 and reanalyze their bridges using this revised equation. The predicted scour depth is now referred to as the *amended scour depth* (CONNDOT, 1999). Therefore, the amended local abutment scour equation is:

$$Y_s / Y_a = 2.27 K_1 K_2 \left(\frac{L^1}{Y_a} \right)^{0.43} Fr^{0.61} + 0.05 \qquad (2)$$

In the event that a new equation is developed or modified, such as the one presented above, it could very easily be added as a model. For this equation, no additional spatial data requirements would be necessary, but an additional branch of the tree would be added to the Model Manager. A flowchart representing the system architecture for the engineering application is shown below in Figure 2:

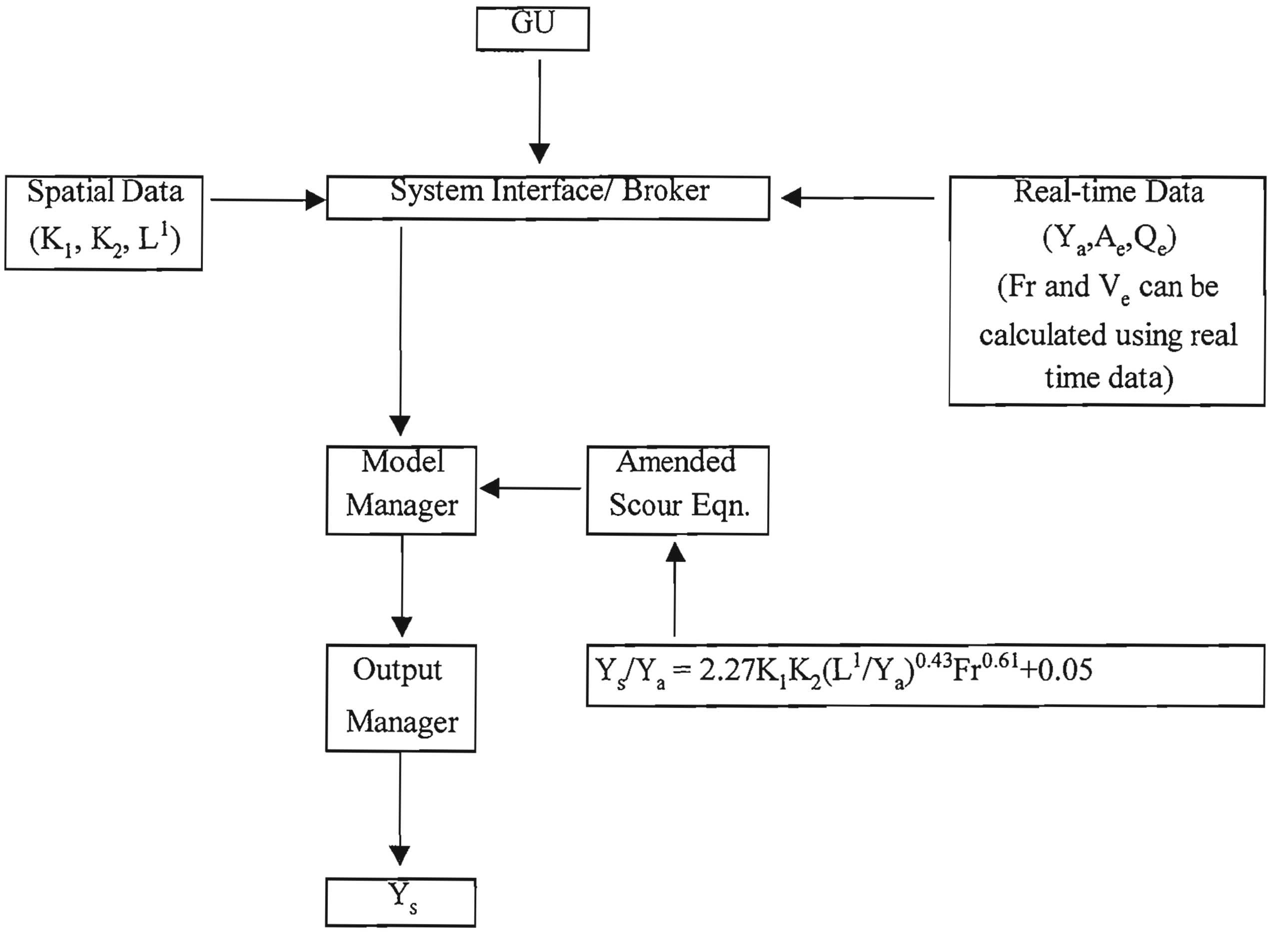

Fig. 2: Flowchart of system architecture for engineering application

The output would contain, among other things, the calculated value of Y_S. Instead of going back through all of the scour critical bridge files in order to recalculate predicted scour depths using the new model, the scour analysis can immediately be conducted through the GUI. The new results can then be compared with scour depth results using existing models. The more models that are available for analysis, the more informed DOT officials will be regarding the scour susceptibility of a bridge.

Comparative Application

Algorithms such as the Comparative Scour Analysis could also be introduced and used in the web-based approach. The spatial data, which contains the bridge attributes, would have to include the primary and secondary criteria established for the rated bridges. Queries could be used to identify rated bridges that are similar to unrated bridges according to matching criteria. From the comparison, approximate scour depth values can be estimated for the unrated bridge from the rated bridge. Therefore, if flows at the structure evaluated by the comparative analysis approach magnitudes similar to critical flows for the rated bridge, the system can warn the user of the potential hazard. A flowchart representing this application is shown in Figure 3:

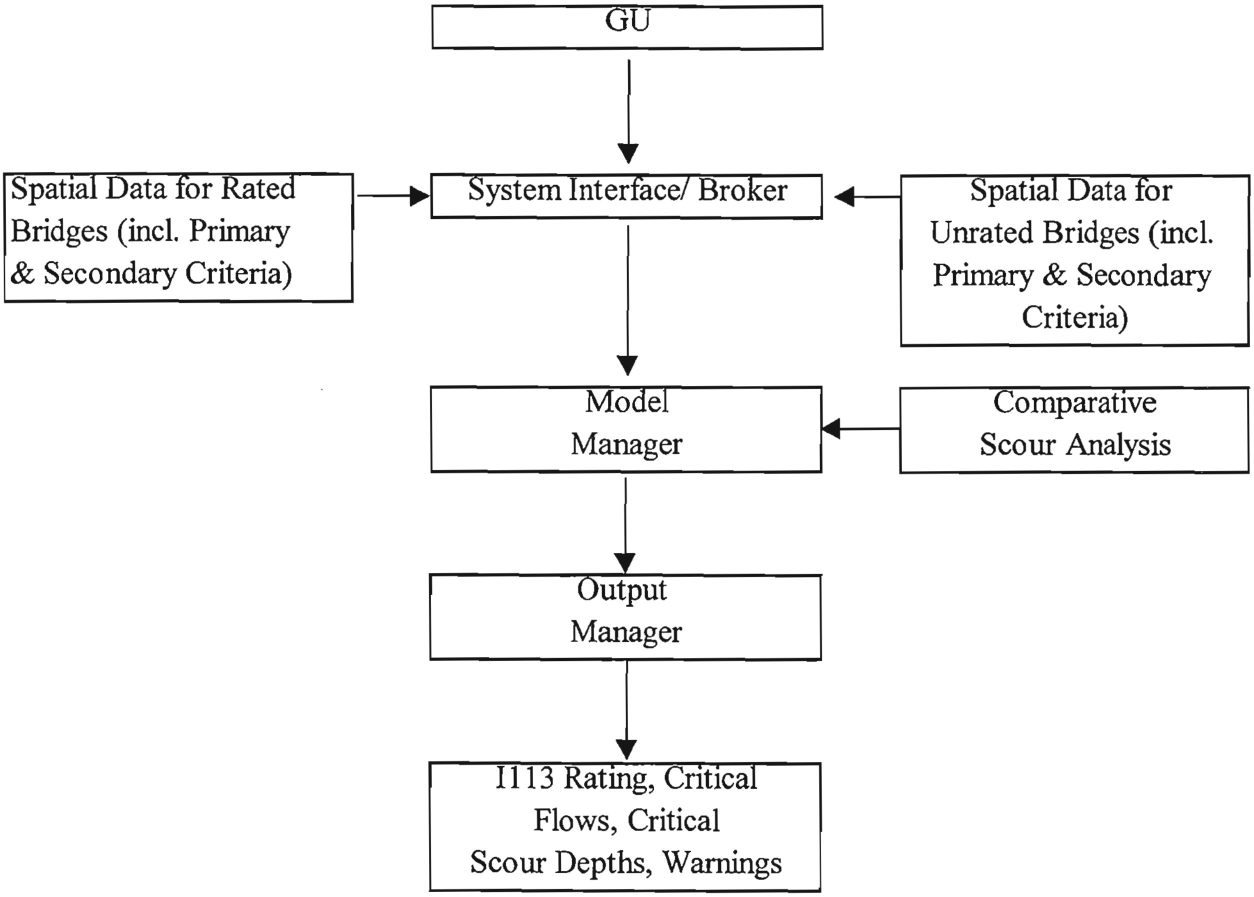

Fig. 3: Flowchart representing system architecture for comparative application

Connecticut plans on using the revised abutment equation to reevaluate the 300 rated (full Level 2 scour analysis) bridges that served as the sample of bridges with which unrated bridges were compared. The state's goal is to reduce the number of scour critical number of bridges and it is hoped that the revised equation can predict more accurate and less conservative scour depths (CONNDOT, 1999). Changes in the results of the Level 2 bridge scour analyses would impact the ratings of those bridges that were rated using the Comparative Analysis. The versatility of the system would allow the user to immediately implement the new equation and begin calculating revised real-time scour depths for the Level 2 bridges. By having critical flows stored within the spatial data, new scour depths could also be computed or even updated for critical floods (e.g. overtopping, 100 year, 500 year). If the results of the analysis of a Level 2 bridge were changed, then the Comparative Analysis could be rerun to ensure that bridges rated using this procedure were still compared with similar rated bridges. It would be easy and quick to make any modifications within the system.

SURVEY OF THE NETC

Despite the discussion of the approach of the real-time monitoring system, there are still many things that can be done to improve the current evaluation of scour. Meetings with DOT officials and NETC members resulted in additional suggestions to deal with scour.

Documentation of Existing Sources

In addition to acquiring data for scour calculations for the real-time monitoring system, part of the preparation process for a storm event is organizing the information already available to the DOTs. It is already known what bridges will be problematic from the I113 codes. The current problem is that people involved with bridge inspections don't have direct lines of communication with people involved in tracking the coming event (Nardone, 2000). If the people who are directly involved with bridge inspections are aware of and have direct access to the information provided by certain agencies or organizations, then they will know how to better allocate their resources in the field. Table 1 lists some examples of agencies or organizations and the information they provide.

Table 1. Sources of Climatic and Hydrologic Data

Agency/ Organization	Information
United States Geological Survey (USGS)	Real-time Flow Data, Historical Flow Data, Precipitation Data
United States Army Corps of Engineers (USACE)	Flood Warnings, Weather Forecasts, Precipitation Data, Real-time Flow Data
National Weather Service (NWS)	Flood Warnings, Weather Forecasts, Precipitation Data, Real-time Flow Data Historical Flow Data
Federal Emergency Management Agency (FEMA)	Flood Studies, Flood Warnings

There certainly is not a lack of people preparing for and tracking a storm. However, if the available information can be shared or centralized between the two groups, then the response to the event will be much more efficient. For an anticipated flood event at any scour critical bridge, information such as the predicted maximum flow, duration of maximum flow, and time and stage when the river crests should be readily available and accessible so that prior to the event, it will have already been determined whether or not the bridge will be in jeopardy. This could simply be done by having a direct hyperlink to the proper website(s) where the flow data is presented. Additional information such as the flow at which the bridge becomes scour critical as determined from the scour equations, high flows that have occurred in the past without causing failure, current foundation elevations, and critical scour elevations should also be included. The more data that can be accumulated and organized before the event, the better prepared the state's Emergency Agency will be to respond.

Creation of Coverages of Existing Monitoring Systems in GIS

Once the sources of hydrologic data are documented, the location of existing monitoring systems will be identified (e.g. DEP rain gages, USGS stream gages, and bridge scour monitors). A geographical information system (GIS) will then be established to catalog the attributes of the monitoring systems. One layer will be created that contains the location and attributes of the existing monitoring systems. This layer will be overlain by another one containing the location of scour critical bridges (those with an I113 code of 3 or less), as reported by the state DOTs. Gaps in the coverage will be identified where existing monitoring systems do not overlap regions in which scour critical bridges are located (Nardone, 2000). Installing monitoring devices on all of the bridges would be preferable, but budget constraints prevent this. Instead, a better understanding of the spatial orientation of our monitoring systems will aid in the allocation of additional devices, whether it may be stream gages, rain gages, or bridge scour monitors. This further reinforces the idea that unknown foundations must be determined. Otherwise, monitoring devices may be installed in places where they are not necessarily needed. Money will have to be spent up front to determine unknown foundations, but some of that money could be recouped through a better distribution of new gages and new monitors.

Creation of Bridge Scour Action Plans

A Bridge Scour Action Plan (BSAP) was originally developed for Massachusetts that would have prioritized the implementation of actions outlined in the plan based upon the cost of a bridge replacement along with the structure's vulnerability to scour. Each bridge was to have had a BSAP that identified those officials responsible for monitoring or closing the bridge as well as information regarding the location and elevation of the foundations and the critical scour elevation. This plan, however, never was put into effect. The state cancelled remediation projects due to a lack of funds and while it has been discussed, the Emergency Management Service (EMS) has no formal emergency procedure for closing bridges during a flood event (Nardone, 2000).

The development of Bridge Scour Action Plans, similar to those originally proposed for Massachusetts, is highly recommended for all scour critical bridges. According to the NBIS program, all bridges in a state must be given an I113 code. The problem exists in that not all of the bridges are owned and maintained by the state DOT. Generally speaking, for bridges owned by local municipalities that were identified as scour critical, a letter is sent out to notify the owner of the bridge as to the condition of the bridge and the scour critical determination. Recommendations for repair or countermeasures may also be included (Nardone, 2000). However, for small towns where there is no engineer or the owner does not have a technical background, the findings in the letter may not receive proper consideration, especially if it is only distributed once. Five or ten years down the road, the initial letter may not be remembered. Another problem that could arise is the repair of the bridge is the responsibility of the owner. Local municipalities, even after receiving the findings of the scour analysis for their bridge, may not decide to implement a remediation program, whether it is due to cost or their contention that the predicted scour depths are extremely conservative. It would be prudent to move all bridges under the jurisdiction of the state DOT. The DOT is the agency responsible for inspecting and monitoring bridges and it seems naïve to have the agency perform all of the analyses, but not allow them to install corrective measures even though the DOT is most familiar with the problem. Regardless of whose jurisdiction the repair of the bridge fell under, by having an action plan in place, an active response is prepared and ready in case of a flood event.

CONCLUSIONS

Difficulties with current scour analyses are time consuming and costly. One problem is that information needed for the analyses is not always centralized or easily accessible. In some cases, several outside consultants were used by state DOTs to conduct Level 2 scour analyses. This makes it difficult to consolidate and organize information. Another problem is that current analyses are unable to respond immediately to changing bridge or stream conditions. In addition, new or revised scour equations that are introduced in the literature would require a great deal of effort for DOTs to rerun the scour analyses. The HEC-18 equations are known for their conservative results in some instances. Some states do not have the resources to perform additional analyses. Others may be content with their current Item I113 codes since the HEC-18 equations are conservative to begin with and there is no incentive for them to do the analyses again.

The development of the strategy of a real-time scour monitoring system would provide state and local officials with an alternative method to evaluating bridge scour. The advantages of this are numerous, with the versatility of the approach being the best advantage. The approach provides a mechanism for estimating bridge scour automatically in real-time. The data is centralized and very accessible and the interface is user-friendly. Analyses can be performed quickly and at the user's discretion. A particular model might not be a very good one, but it is the responsibility of the user(s) to decide which models are suitable for their purposes. Multiple algorithms, whether it be models or analyses like the Comparative Scour Analysis, could be used for analysis, instead of just one or two. There is a great deal of flexibility when adding new models and the results of these models can be compared very easily. DOTs that may have initially shied away from performing additional or new scour analyses would now have the ability to do so at a much smaller cost. The more pro-active DOTs are when dealing with scour, the greater the benefit to themselves and society as a whole. In the meantime, gaps in the existing coverage where scour critical bridges are not overlain by stream gages, rain gages, or bridge monitors should be identified so that resources can be allocated more appropriately. The implementation of this strategy could ultimately aid in the improved identification of and response to scour critical bridges jeopardized by a potentially destructive storm event.

ACKNOWLEDGEMENTS

The authors would like to acknowledge the New England Transportation Consortium for providing funds for the research presented in this paper. They would also like to thank the following people and their organizations for the valuable contributions they have provided:

Paul Nardone, *Massachusetts Highway Department*; Jeff Glenn, *EarthTech, Inc.*; Edward Kent, *EarthTech, Inc.*; Yolanda Antoniak, *Connecticut Department of Transportation*; Dennis Levesque, *Connecticut Department of Transportation*; David E. Powelson, *New Hampshire Department of Transportation*; Erick Boehmler, *United States Geological Survey*; Gene Parker, *United States Geological Survey*; Gary Hoar, *Maine Department of Transportation*; Richard

Tetreault, *Vermont Agency of Transportation*; D. Max Sheppard, *University of Florida*; Joe Boardman, *Rhode Island Department of Transportation*

REFERENCES

1. Antoniak, Yolanda and Levesque, Dennis. 2000. Connecticut Department of Transportation. From conversation on March 17th.

2. Clough, Harbour & Associates LLP. 1998. "Comparison Methodology." *Prepared for the Connecticut Department of Transportation.*

3. Connecticut Department of Transportation. 1999. "CONNDOT Comparative Analysis." *Prepared for EarthTech, Inc.*

4. Glenn, Jeff. 2000. EarthTech, Inc. From conversation on March 16th.

5. Lagasse, P.F., Schall, J.D., Johnson, F., Richardson, E.V., Richardson, J.R., Chang, F. "Stream Stability at Highway Structures," Federal Highway Administration Hydraulic Engineering Circular No. 20, Publication No. FHWA-IP-90-014, Feb. 1991.

6. Miles, S.B., Keefer, D.K., and Ho, C.L. (1999). "Seismic landslide hazard analysis: from hazard map to decision support system," U.S. Conference on Lifeline Earthquake Engineering: Settle, WA (abstract accepted).

7. Nardone, Paul. 2000. Massachusetts Highway Department. From conversation on March 15th.

8. Richardson, E.V. and Davis, S.R. "Evaluating Scour at Bridges Third Edition," Federal Highway Administration Hydraulic Engineering Circular No. 18, Publication No. FHWA-IP-90-017, Nov. 1995.

9. Schneiderman, B., 1998, Designing the user-interface: Strategies for effective human-computer-interaction, Addison-Wesley Longman: Menlo Park, CA, 639 p.

10. U.S. Department of Transportation, FHWA, 1988, Technical Advisory TA5140.20, "Scour at Bridges," Office of Engineering, Bridge Division, Washington, D.C.

11. U.S. Department of Transportation, FHWA, 1991, Technical Advisory TA5140.23, "Evaluating Scour at Bridges," Office of Engineering, Bridge Division, Washington, D.C.

12. U.S. Department of Transportation, FHWA, 1995, "Recording and Coding Guide for the Structure Inventory and Appraisal of the Nation's Bridges," Office of Engineering, Bridge Division, Publication No. FHWA-PD-96-001, Washington, D.C.

13. Whitman and Howard, Inc. 1996. "Final Report Scour at Bridges Management Contract Phase II." *Prepared for the Rhode Island Department of Transportation Division of Maintenance*.

PROTECTION OF THE HUTT ESTUARY BRIDGE AGAINST LOCAL SCOUR

by

Christine S. Lauchlan[1], Bruce W. Melville[2], Stephen E. Coleman[3]

ABSTRACT

Bridge piers can experience severe undermining of their foundations through local scouring and this can result in failure of the structure. In order to protect the bridge piers, countermeasures such as riprap are often employed. The riprap acts as an armouring device, preventing the removal of sediment from around the base of the pier and inhibiting the formation of a local scour depression. Previous studies of the Hutt River, New Zealand, have indicated that a number of bridges on the river have piers that are 'at risk' of undermining by local and general scouring actions under flood conditions. In order to confirm such findings for the Hutt Estuary Bridge, both general and local scour depth predictions were reassessed for the site using a physical model study. The range of general and local scour depths for the site under different flood conditions, as determined by Melville (1997), were used as the benchmark for the physical model results. Two piers of the bridge had been identified by previous studies as being at risk of undermining by scour. The physical model study was used to confirm the predicted local scour depths for the specific pier shape, alignment to the flow and flow conditions for the 'at risk' piers. A range of initial sediment bed levels was tested for the models due to uncertainty in the general scour depth predictions for the site. It was then proposed to install a riprap protection layer around each pier identified as at risk from undermining to prevent scour-hole formation. Two riprap size prediction equations were used to ascertain an appropriate rock size for the site, and then a model study was undertaken to confirm the size and layout requirements for the riprap protection layer. The model was tested under live-bed conditions and the design of the riprap protection was modified to improve its performance. The final design riprap layout was then developed into a prototype design and has since been installed around the endangered piers of the Hutt Estuary Bridge.

INTRODUCTION

The Hutt Estuary Bridge is located 1 km upstream of the mouth of the Hutt River, near Wellington, New Zealand. The bridge has a history of scour problems due to significant bed degradation, the degradation arising from uncontrolled gravel mining at several sites upstream.

Studies such as Robb (1992), Fischer and Watson (1996), and Melville (1997) have attempted to estimate the depths of the expected general and local scour at the bridge site under flood conditions. The studies provide varying estimates of scour depth at the bridge piers and

[1] Postdoctoral Fellow, Delft University of Technology, Faculty of Civil Engineering and Earth Sciences, Delft, the Netherlands
[2] Associate Professor, Dept. of Civil and Resource Engineering, The University of Auckland, Auckland, New Zealand
[3] Senior Lecturer, Dept. of Civil and Resource Engineering, The University of Auckland, Auckland, New Zealand

abutments. However, they all imply that some of the bridge piers are at risk from undermining during a 1% AEP flood event. Melville (1997) showed that Piers 1 and 2 (Figure 1) are most at risk .

The purpose of the present study was to confirm the local scour results of Melville (1997) and to develop an effective riprap protection design; by undertaking a physical model study of the Hutt Estuary Bridge. The depth of local scouring around the affected piers was determined for varying levels of general scour. The results indicated a range of likely local scour depths, all of which are likely to result in undermining of the pier foundations. From this information, an effective scour countermeasure system was developed using riprap stones placed around the base of the pier. The riprap layer was model tested under both aligned and non-aligned flow conditions and for varying layer configurations. The recommended design produced a reduction in scour of 88 % compared to the unprotected case and this configuration has recently been installed at the Hutt Estuary Bridge site.

Background

The 5-span Hutt Estuary Bridge (Figure 1) is 179 m long, each span being 32 m in length. The bridge piers are rectangular (1.1 m wide, 16.4 m long) with slab footings. Each footing has been encased with steel caissons (5.5 m wide, 16.4 m long), Figure 2. The approximately 7.6 m deep caissons were installed to protect the piers against bed degradation. Bed material is a coarse river sand with a median size d_{50} = 2 mm. Flood levels are controlled by the associated sea levels at the river mouth.

For the 1 % AEP design flood, the flood level is 2.4 m above mean sea level (MSL). The general scour depth was estimated using the Blench (1969) equation at approximately 4.1 m below MSL (Figure 2). From this, it is estimated that following general scour the top of the caissons would be about 2.3 m above the scoured bed. For this level of general scour the method of Melville and Raudkivi (1996) for predicting local scour depths, predicts a total scoured depth (general and local scour levels combined) of 13.1 m below flood level (Figure 2). This equates to a depth of approximately 1.5 m below the base of the caisson for Piers 1 and 2, which would seriously endanger the bridge in the design flood (Melville,1997). Recalculation of flood levels by the Hutt City Council has indicated a reduced flow depth for a 1 % AEP event of 1.86 m above MSL (Woodward-Clyde, 1998), which corresponds to a total scour depth from the water surface of 12.56 m.

Piers 1 and 2 are located at 104.6 m and 136.6 m respectively from the western bank of the river, and are angled at between 5° and 10° to the approach flow (Figure 1).

METHODOLOGY

A model of a single pier/caisson was constructed to a model-prototype length scale of (1/20). The model was restricted to a single pier, because for the pier spacing of 32 m the local scour hole around each pier should be unaffected by the presence of the other piers. The model was tested in a 1.52 m wide, sediment-recirculating and flow-recirculating flume. At a scale of (1/20) the flume width is equivalent to a channel width of 30.4 m, i.e. similar to the individual bridge spans (32 m).

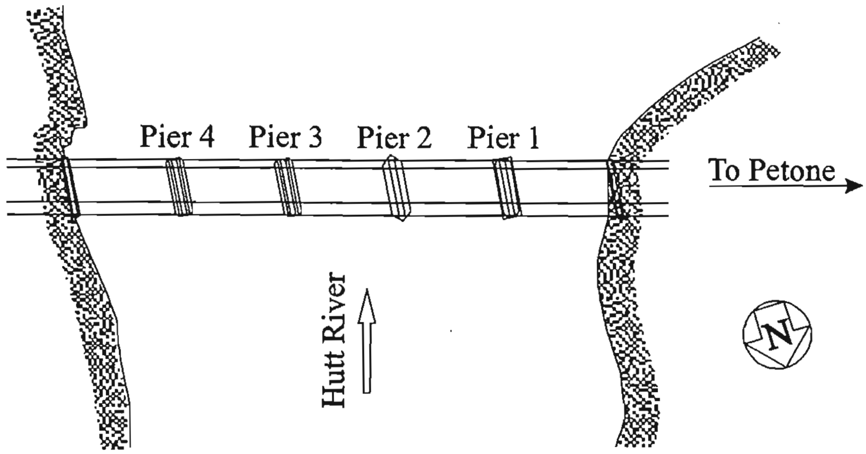

Figure 1 - Plan View of the Hutt River Estuary Bridge

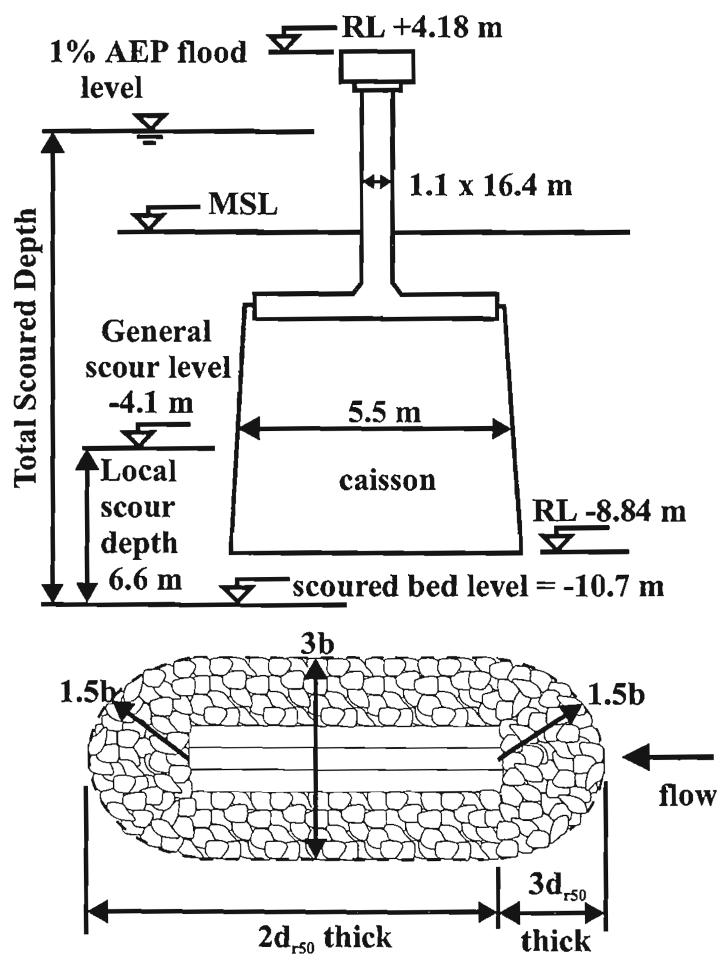

Figure 2 - Hutt Estuary Bridge Pier Dimensions and Recommended Riprap Configuration.

As mentioned, the prototype bed material has a median size d_{50} of 2 mm. Consequently, it was not possible to satisfy the relative length scale for the bed sediment. Instead a uniform sand with d_{50} = 0.95 mm was used in the tests. The riprap material tested was scaled according to the length scale.

All experiments were conducted under live-bed conditions with the flow depth being taken as the average depth of water above the average bed level. Both the unprotected and protected tests were conducted under flow conditions corresponding to the recalculated 1 % AEP flood event, Table 1. In addition, two protected pier tests (Tests 6 and 7) were conducted for the 2 and 5 % AEP events (Table 1). Flow velocities were measured using a laser doppler anemometry system located approximately 5 m from the upstream pier face. Local scour depths were measured using a sonar depth sounder (Coleman, 1997). The scour depth was measured at the upstream pier face where the maximum scour depth is likely to occur (aligned flow conditions). This was confirmed during the experiments. The duration of each experiment was 500 minutes.

Table 1 - Preliminary Design of Riprap Protective Layer Using Lauchlan (1999) and Hydraulic Engineering Circular 18 (HEC-18) (Richardson and Davis, 1995).

Return Period (yr)	Flow Rate (m^3/s)	Froude Number (-)	Bed Level (below MSL)	Flood Level (above MSL)	Flow Depth (m)	Riprap Size (mm) *Lauchlan (1999)*	Riprap Size (mm) *HEC-18*
100	2100	0.47	4.1	1.86	5.96	764	801
50	1900	0.45	3.8	1.79	5.59	674	677
20	1600	0.42	3.4	1.63	5.03	571	549

LOCAL SCOUR DEPTH MEASUREMENTS

The local scour depth is highly dependent on the general scour level. Testing therefore required that the local scour level be measured for general scour levels ± 1 m from the actual predicted general scour level. Table 2 gives the results of the present study along with scour depths predicted using Melville (1997).

Scenario 1 is where the flow rate past the pier for a given flood volume remains the same independent of the bed level. This alters the flow velocities and flow depths and results in different Froude numbers for each of the bed levels tested. Scenario 2 ensures the Froude number, flow velocity and flow depth remain the same, but the flood level is varied. Figure 3 shows the typical scour hole formed around the pier.

The results in Table 2 show the measured scour depths to be in good agreement with predicted local scour depths. This confirmed that Piers 1 and 2 of the Hutt Estuary Bridge were indeed at risk of undermining due to scouring under the 1 % AEP flood conditions.

Table 2 - Predicted and Measured Local Scour Levels at Pier 1 for the 100 Year Return Period Flood.

Bed Level after General Scour (m below MSL)	Predicted Local Scour Depth (m) *Melville (1997)*	Measured Local Scour Depth - Scenario 1 (m)	Measured Local Scour Depth - Scenario 2 (m)
-3.1	5.9	6.9	6.1
-4.1	6.6	6.9	6.9
-5.1	7.2	7.2	7.1

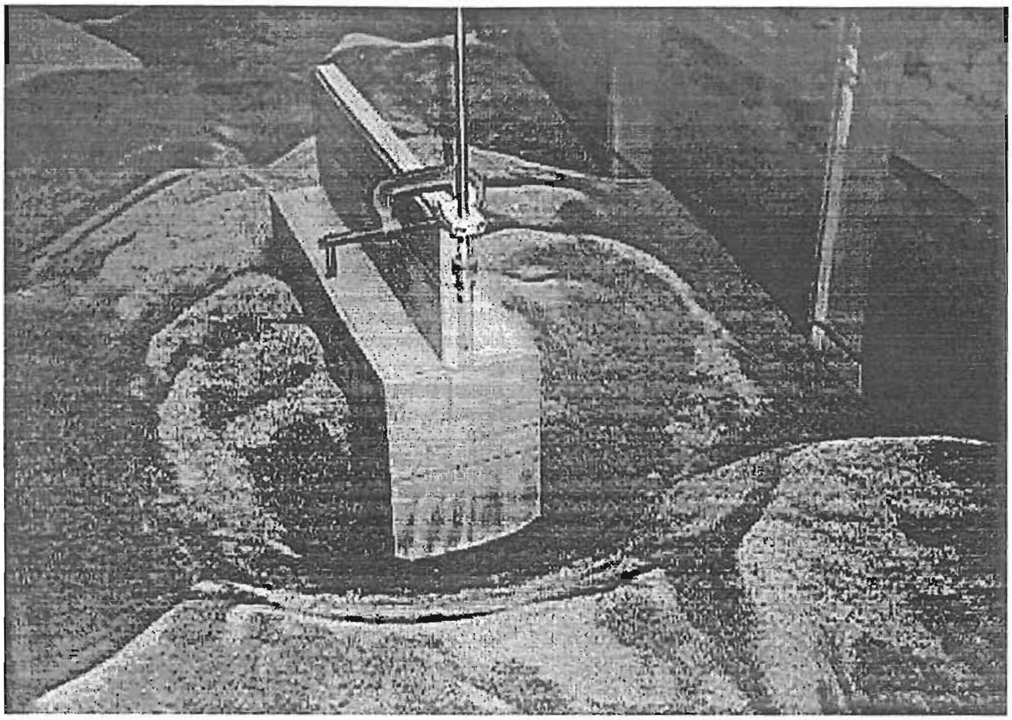

Figure 3 - Typical Local Scour Hole around the Unprotected Pier (for aligned flow and a general scour level of -3.1 m below MSL).

SCOUR COUNTERMEASURES

Once it was confirmed that Piers 1 and 2 would require protection against scouring actions an analysis of the required riprap layer was conducted. A wide range of possible riprap size prediction equations exists. Two riprap size prediction equations were chosen; that given in HEC-18 (Richardson and Davis, 1995), and the equation of Lauchlan (1999). These two methods have been assessed previously (Lauchlan, 1999) as providing realistic estimates of riprap size for bridge scour protection. The predicted riprap sizes are given in Table 1. Based on these results a rock riprap size (d_{r50}) of 700 - 800 mm was suggested. Quarry rock, readily available in close proximity to the Hutt Estuary Bridge, could be obtained with a d_{r50} of 700 mm (model riprap size d_{r50} = 35 mm); hence a model riprap size based on this value was chosen. Additional tests were also performed for a smaller riprap material with d_{r50} = 560 mm (model riprap size d_{r50} = 28 mm). It was decided to test this smaller material as substantial cost savings would be realised by using this riprap. The riprap configuration chosen is shown in Figure 1. In all experiments the riprap was initially placed so that the top surface of the stones was level with the surrounding sediment bed level, i.e. an embedment depth of zero. Both aligned and non-aligned flow conditions were used.

Test results are shown in Table 3. In all the experiments, the only stone movement that occurred was at the upstream pier face and along the edges of the layer at the sides. At the pier face in Tests 1, 3, 4, 5, 6 and 7, a small local scour depression formed. In Test 2 the introduction of a thicker layer in the upstream area virtually eliminated the local scour hole. Measured scour depths of the stones in the riprap layer were compared to the measured scour depths for the unprotected pier computed under the same conditions. The percentage scour reduction is calculated as {[(unprotected d_s - riprap protected d_s)/unprotected d_s] x 100}, where d_s is the scour depth.

Tests 2 and 4 showed that the performance of the riprap layer was improved by the addition of an extra layer of stones to the upstream portion. This increased the scour protection by 26 % for the aligned pier and 11 % for the non-aligned pier.

It was also found that a reduction in stone size (Test 5) resulted in a 12 % reduction in scour protection ability when compared to the equivalent larger stone test (Test 4). Both tests used the same layer configuration, flow velocity and approach flow angle. The smaller stones experienced deeper local scouring and more advanced edge failure but still provided a significant (76 %) reduction in the maximum local scour depth.

Tests 6 and 7 utilised the smaller riprap in the same configuration as Test 5 but under lower flow conditions. These tests were undertaken to confirm the level of protection afforded by this protection layer for the smaller stone size.

All the tests show that installation of a protective riprap layer can substantially reduce the magnitude of local scouring at a bridge pier. The results indicate that a scour reduction of between 70 and 97 % is achievable for the Hutt Estuary Bridge, both when the pier is aligned and non-aligned to the oncoming flow. These results are in agreement with Lauchlan (1999), who bases her riprap size prediction equation on an allowable scour in the riprap layer of up to

20 %. The riprap sizes tested were between 9 % and 24 % less than the size predicted by Lauchlan (1999).

The layer configuration used in Test 4 provided the greatest protection for the at-risk piers. Test 4 uses the same riprap configuration as Test 2 but the pier was orientated at an angle of 10° to the flow, which is the maximum prototype river orientation. This layout consists of a 2 d_{r50}-thick layer thickened to 3 d_{r50} upstream of the pier. This protection was installed around Piers 1 and 2 of the Hutt Estuary Bridge over the summer of 1999. To date, the riprap protection layer has not experienced any flows at or above the design flow conditions.

Attempts have been made to assess the positions of the prototype riprap stones on the sediment bed. However, a layer of silt has formed on the surface of the stones and detection of the riprap beneath this layer is difficult. Further development of monitoring techniques and equipment is necessary so that comparison of laboratory and field data is possible.

Table 3 - Riprap Layer Test Results.

Test	% AEP	d_{r50} (mm)	Layer Thickness, t	Alignment Angle, θ	Percentage Scour Reduction (%)
1	1	35	$2d_{50}$ throughout	0	71
2	1	35	$3d_{50}$ upstream, $2d_{50}$ elsewhere	0	97
3	1	35	$2d_{50}$ throughout	10	77
4	1	35	$3d_{50}$ upstream, $2d_{50}$ elsewhere	10	88
5	1	28	$3d_{50}$ upstream, $2d_{50}$ elsewhere	10	76
6	2	28	$3d_{50}$ upstream, $2d_{50}$ elsewhere	10	78
7	5	28	$3d_{50}$ upstream, $2d_{50}$ elsewhere	10	83

CONCLUSIONS

1. The present hydraulic model study confirmed the local scour depths expected at the Hutt Estuary Bridge, predicted by Melville (1997), for the 1% AEP event. The scour levels were measured at the upstream pier face for various general scour depths and confirmed that Piers 1 and 2 are likely to be at risk from undermining.
2. Test results show that a significant level of scour reduction can be achieved by installing riprap protection layers at the Hutt Estuary Bridge.
3. The protection ability of the riprap layer was significantly enhanced (from 71 to 97 % scour reduction for an aligned pier, and from 77 to 88 % scour reduction for a non-aligned pier) by increasing the thickness of the upstream portion of the layer from 2 d_{50} to 3 d_{50}.
4. The riprap configuration in Tests 2 and 4 was recommended for installation. The protection comprised of an approximately 1400 mm thick layer of 700 mm riprap, thickened to 2100 mm upstream of the pier face. It is predicted that this layout can reduce the local scour depth by as much as 88 % when the flow is skewed 10° to the axis of the pier.

ACKNOWLEDGEMENTS

The authors would like to thank John Wood, consulting engineer, for his input to this project.

REFERENCES

1. Blench, T. (1969). "Mobile-bed Fluviology." University of Alberta Press, Edmonton, Canada.
2. Coleman, S.E. (1997). "Ultrasonic measurement of sediment bed profiles." Proc., 27th Congress of the International Association of Hydraulic Research, San Francisco, California, USA, August, B221-B226
3. Fisher, T. and Watson, A. (1996). "Hutt River Estuary Bridge Scour Assessment." Works Consultancy Services Report.
4. Lauchlan, C.S. (1999). "Pier Scour Countermeasures", PhD, University of Auckland, Auckland.
5. Melville, B.W. (1997). "Review of Scour Predictions for the Hutt Estuary Bridge." Auckland UniServices Report, Auckland
6. Melville, B.W. and Raudkivi, A.J. (1996). "Effects of Foundation Geometry on Bridge Pier Scour." *Journal of Hydraulic Engineering*, ASCE, 122(4), 203-209
7. Richardson, E.V. and Davis, S.R. (1995). "Evaluating Scour at Bridges." Hydraulic Engineering Circular No. 18, FHWA-IP-90-017, Fairbank Turner Highway Research Centre, McLean, Virginia
8. Robb, C. (1992). "Phase 1 - Hutt River Flood Control Scheme Review. Topic 4: River Channel Capacity." Report for the Wellington Regional Council, Wellington
9. Woodward-Clyde. (1998). "Assessment of Environmental Effects - Hutt Estuary Bridge." Woodward-Clyde, Wellington, September

HYDRAULIC PROPERTIES OF CONCRETE BLOCKS FOR BED PROTECTION

By

Sung-Uk Choi[1], Joongcheol Paik[2], and Woncheol Cho[1]

ABSTRACT

Recent laboratory experiments reported that cable-tied blocks perform excellently among many countermeasures for local scour around the bridge piers. G-blocks are concrete blocks being placed around the bridge piers in order to protect the channel bed from local scour. The surface of G-blocks is made uneven with uniform roughness height to increase friction. For G-blocks to perform their role successfully, the roughness should not be significantly different from that of natural channels. Otherwise they will cause serious problems of local erosions. Furthermore, they should be safe against the flow force. If they are moved by the flow, they will not only be invalid for bed protection but also make adverse effects on the channel conveyance. In this paper, hydraulic properties of G-blocks are investigated through laboratory experiments. Flume experiments indicate that both logarithmic and power laws can be applied to intermediate-scale roughness by G-blocks, and that the roughness characteristics of G-blocks are similar to those of natural channels. It is also shown that the resistance by G-blocks changes depending upon the placement angle of the roughness elements to the flow direction. Furthermore, the critical weight of G-blocks required to withstand strong current is estimated in terms of mean velocity for an individual block and mat-type blocks.

INTRODUCTION

Flows tend to accelerate when they have to circumvent a longer path compared to their neighbors. This results in local scour around the bridge piers, piles, and other hydraulic structures constructed in water course. Many countermeasures have been devised for the remedy of local scour. Examples are riprap, gabion, cable-tied blocks, sacrificial pile, and collar. They are either armoring or flow-altering countermeasure. Among these, ripraps have been the most common choice because of the long design experience.

However, supplying ripraps for protection against scour becomes pessimistic in the future. Big stones for guaranteed use are being exhausted and environmental regulations make the use of ripraps more difficult than ever. Furthermore, it is true that ripraps have been the most common choice but not the best choice. Engineers have

[1] Professor, Department of Civil Engineering, Yonsei University, Seoul, 120-749, Korea

[2] Postdoctoral Researcher, Department of Civil Engineering, Yonsei University, Seoul, 120-749, Korea

believed that there should be a more effective countermeasure than ripraps. This encourages engineers to search alternatives to ripraps.

Recent experiments by Parker et al. (1998) showed that cable-tied blocks provide outstanding protection for the bridge piers from local scour among various countermeasures. Their advantages include flexibility, ability to withstand strong current, a pre-attached geotextile, resistance to ice, and cost competitiveness (Parker et al., 1998). Although the use of cable-tied concrete blocks is a relatively advanced technique, few attempts were made regarding hydraulic properties of those blocks.

Experiments by Jones et al. (1995) indicate that there are two failure modes in the blocks paved on the channel bottom. The first is by overturning of blocks located at the leading edge and the second is by uplifting of inner blocks. In the light of their experimental results, the followings can be suggested: First, it is important to maintain the roughness of the block-paved bed similar to that of natural channels in order to prevent severe local erosion at the leading and tailing edges. This will reduce the chance of failure of the first-type mode. Secondly, the block should be heavier enough to withstand the severe flow safely. The only resisting force of the block (either single or mat-type) against the flow forces comes from its (or their) submerged weight.

In the present paper, basic laboratory experiments are introduced to study hydraulic properties of cable-tied blocks. Flow resistance relationships such as logarithmic and power laws are applied to block-paved open-channel flows, and their validity is investigated. Values of Manning's roughness coefficient are estimated, and they are compared with the roughness of natural channel and the roughness by ripraps. Finally, the critical weight of the block is obtained not to make a motion when the block is exposed to strong flows.

FLOW-RESISTANCE RELATIONS

For fully-developed turbulent open-channel flows with intermediate-scale resistance, the logarithmic or power law equation is known to be appropriate for the mean velocity. The logarithmic equation due to Keulegan (1938) has the form of

$$\frac{U}{U_*} = \frac{1}{\kappa}\log\frac{R}{k_s} + \beta \tag{1}$$

where U = mean velocity, U_* = shear velocity, R = hydraulic radius, k_s = roughness height, κ = von Karman constant (= 0.41), and β = constant. In the problem at hand, the characteristic roughness height (k_s) in eq.(1) characterizes not only the height of the roughness elements but also their orientation to the flow, geometric alignment, and spacing. Many relationships for k_s corresponding to various bed materials have been proposed (Griffiths, 1981; Aguirre-Pe And Fuentes, 1990; Maynord, 1991; Ferro and Giordano, 1991). By replacing k_s with the height of roughness elements D and by using Darcy-Weisbach formula, eq.(1) is rewritten in the form of

$$\left(\frac{8}{f}\right)^{1/2} = C_1 \log\left(\frac{R}{D}\right) + C_2 \tag{2}$$

where f = Darcy-Weisbach friction factor, and C_1 and C_2 are constants. In the derivation, the relationship for shear velocity such as $U_* = \sqrt{gRS}$, where S is the channel slope, is used. Note that the left hand side of eq.(2) is simply another expression of the mean velocity normalized by shear velocity and that constants, C_1 and C_2 rather than $1/\kappa$ and β, are preferred by some researchers for fitting's purpose.

An alternate form of mean velocity formula using the power law is given by

$$\frac{U}{U_*} = C_3 \Psi^a \left(\frac{R}{D}\right)^{1/6} \tag{3}$$

where Ψ is a shape factor defined by $(P/B)^{1/2}$, where P and B represent the wetted perimeter and the channel width, respectively. The relationship between roughness coefficient (n) and friction factor (f) can be obtained by equating Manning's and Darcy-Weisbach's equations. This leads to the following expression:

$$\left(\frac{8}{f}\right)^{1/2} = \frac{K_n R^{1/6}}{n g^{1/2}} \tag{4}$$

where K_n is a constant for unit conversion, which has a value of 1 $\mathrm{m}^{1/2}/\mathrm{s}$ and 1.486 $\mathrm{ft}^{1/2}/\mathrm{s}$ for metric and English units, respectively.

The shear stress at the bottom is frequently expressed as

$$\tau_b = \rho C_f U^2 \tag{5}$$

where C_f is the bed resistance coefficient. In general, the shear stress by eq.(5) is decomposed into friction and pressure components. Since $\tau_b = \rho U_*^2$, the bed resistance coefficient is given by

$$C_f = \frac{f}{8} \tag{6}$$

which relates bed resistance coefficient to Darcy-Weibach friction factor.

EXPERIMENT AND RESULTS

Figure 1 shows two blocks, namely, G2 and G3 blocks, used in the experiment. Model blocks were made with undistorted scale of 1/15 and 1/12 for G2 (113×80×43 mm, 2.30 kg) and G3 blocks (142×100×42 mm, 1.15 kg), respectively. The top and bottom faces of the block are corrugated to provide roughness with the channel and to increase tightness with the bottom, respectively. G2 blocks are designed to be tied by U-bolt in one-direction, and to be interlocked by themselves in the other direction. Whereas G3 blocks are tied by U-bolt in both directions. The crest width, bottom width, and the height of the roughness elements of G2 and G3 Blocks are 6.7, 20, and 10 mm,

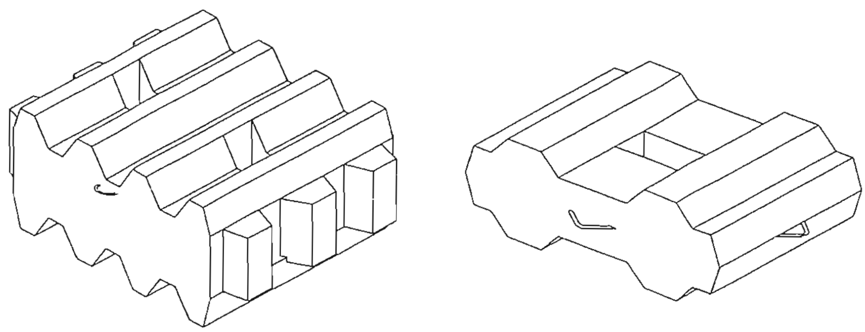

(a) G2 block (b) G3 block

Fig. 1. Configurations of G2 and G3 blocks

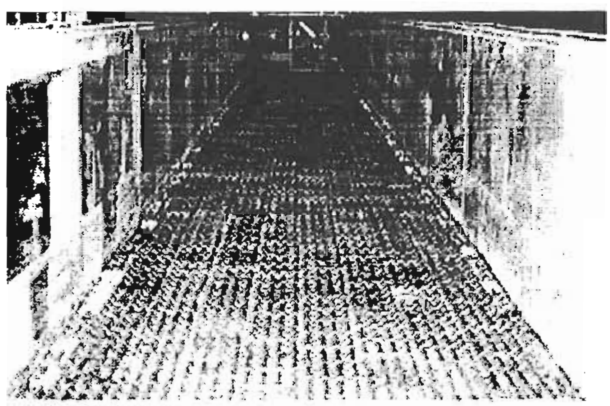

Fig. 2. G2 blocks with roughness elements parallel to the flow direction

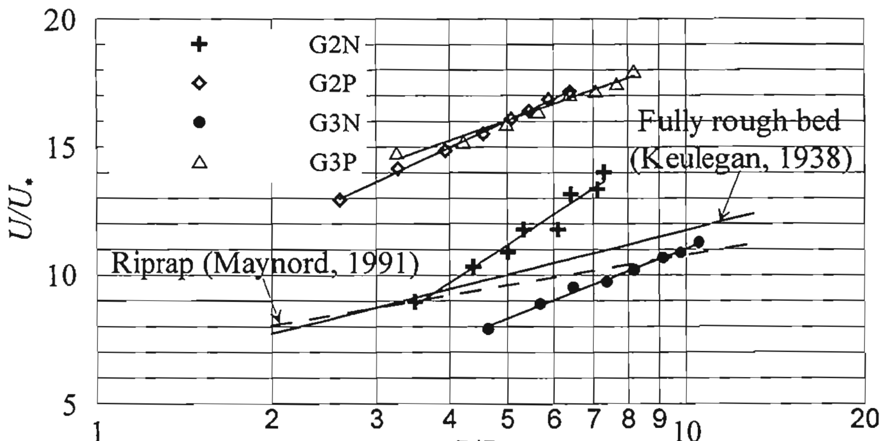

Fig. 3. Normalized mean velocity versus relative depth

and 15.8, 31.7, and 7.8 mm, respectively.

Experiments were conducted in a tilting flume, which is 0.9 m wide, 0.6 m deep, and 12 m long, in Yonsei University, Seoul, Korea. The flume consists of iron bottom and sidewall of acryl plate. The discharge was measured by the sharp-crested weir located at the upstream of the flume. At the bottom of the channel, blocks were placed with roughness elements normal or parallel to the flow direction (Figure 2 shows G2 blocks with roughness elements placed parallel to the flow direction).

The generated discharge and water depth ranged in 0.009-0.057 m^3/s and 2.7–10.3 cm, respectively. Bed slopes were changed between 0.0032-0.0037. This flow condition results in Froude number of 0.44–0.89 and Reynolds number of 8000–49000.

In Figure 3, normalized velocity (U/U_*) versus relative depth (R/D) are plotted to see the validity of logarithmic resistance law, eq.(2). Symbols represent experimental data, and their best fits are given by lines. Also plotted are logarithmic law for open-channel flows on the rough bed by Keulegan (1938) and Maynord's (1991) experimental results with ripraps. In the figure, G2N and G2P denote arrangement of G2 blocks where roughness elements are placed normal and parallel to the flow direction, respectively. Note that all data are in the range of intermediate-scale roughness ($3 \le R/D \le 10$). In the figure, the logarithmic law appears to be valid for open-channel flows on the bed paved by G-blocks. In fact, the experimental data are fitted by lines with negligible deviations. Notice also that the flow resistance by G-blocks is mainly determined by the placement angle of the roughness elements to the flow direction. That is, the roughness elements placed normal to the flow direction yields higher resistance than roughness elements placed parallel. In general, G3N shows highest resistance, and both G2P and G3P are about the same level of resistance. Blocks show greater changes in friction as R/D increases than ripraps (1.7 cm < D_{90} < 13.0 cm) in Maynord (1991).

For logarithmic law and power law, regression analysis with experimental data is performed, and values of coefficients are given in Table 1.

Table 1. Coefficients used in flow resistance equations

Bed material	C_1	C_2	AAD ×100	C_3	a	AAD ×100	$C_3\Psi^a$
G2 (normal)	15.13	0.58	0.03	5.80	6.18	0.04	9.1-13.6
G2 (parallel)	10.71	8.53	0.01	10.39	2.67	0.00	11.3-12.8
G3 (normal)	9.02	2.00	0.03	5.55	3.20	0.07	6.4 - 7.6
G3 (parallel)	8.09	10.38		11.68	0.97		12.0-12.6
Riprap D_{50} (Maynold,1991)	3.88	6.88	0.02	-	-	0.05	6.89
Rough bed (Keulegan, 1983)	5.75	5.99		-	-		8.1

AAD (Absolute Average Deviation) $= \frac{1}{N}\left|\sum\left[(8/f)^{1/2}_{\text{Calc}}/(8/f)^{1/2}_{\text{Expr}} - 1\right]\right|$

In all curve fittings, negligible absolute average deviations are obtained, indicating that both logarithmic and power laws are valid to describe resistance of block-paved open-channel flows.

With the help of eq.(4), values of Manning's roughness coefficient n are converted from f, and they are plotted against discharge per unit width in Figure 4. It appears that G3 blocks produce the highest and the lowest roughness when the roughness elements are placed normal and parallel to the flow direction, respectively. This conforms to the previous figure. In the figure, values of Manning's n range between 0.011-0.022, which corresponds to values of 0.016-0.031 for prototype. This suggests that overall roughness by G-Blocks is less than the roughness by riprap ranging 0.032-0.036 (Maynord, 1991). Also, roughness provided by G-blocks is not significantly different from that of natural channels.

In the design practice of blocks, the concept of permissible shear stress can be used. That is, the shear stress by the design flow should not exceed the permissible shear stress of the blocks. Figure 5 depicts the change of bed shear stress with mean velocity. In the figure, a linear relationship between bed shear stress and mean velocity is observed mainly due to non-constant values of C_f. For G3P, the permissible shear stress is estimated to be 170–240 $\mathrm{kg/m^2}$ by assuming Coulomb friction coefficient of μ = 0.8. However, the permissible shear stress of ripraps with diameter of 15-30 cm ranges between 9.76-19.53 $\mathrm{kg/m^2}$ (ASCE and WEF, 1992). This indicates that G-blocks are much safer from movement by the flow force than ripraps.

In Figure 6, the critical weight of the block versus mean flow velocity is plotted. Here, the critical weight is defined by the weight required to resist flow forces. First, a mat type installation, where blocks are shacked by U-bolt, is considered. The total shear force is calculated by using eq.(5), and a value of Coulomb friction coefficient of μ = 0.8 is assumed. The second case considered is for a single block. Values of drag coefficient of 0.80 and lift coefficient of 0.25 from the hexahedron (Naudascher, 1991) are used in accounting for the mobility of a single block. Resulting critical weights of mat-type and single block are given as a function of mean velocity in Figure 7. In the figure, the last letter S and M in the legend denote single and mat-type, respectively. It is observed that blocks withstand the flow better when they are tied together, and that clear difference between two critical weights is seen.

CONCLUSIONS

Laboratory experiments were carried out to investigate hydraulic properties of G-blocks for bed protection against local scour around bridge piers. It has been shown that both logarithmic and power laws are appropriate for intermediate-scale roughness by G-blocks. Roughness of the channel bed paved by G-block did not show significant difference compared with that of natural channels. The permissible shear stress estimated from the experiments revealed that G-blocks are much safer from the transport by the flow than ripraps. Finally, the critical weight needed to resist flow forces were calculated for a single block and mat-type blocks.

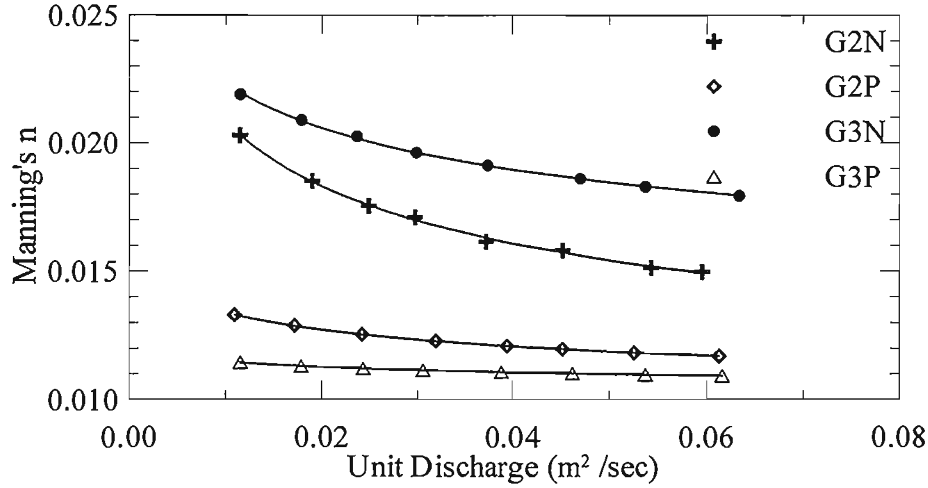

Fig. 4. Manning's n versus unit discharge

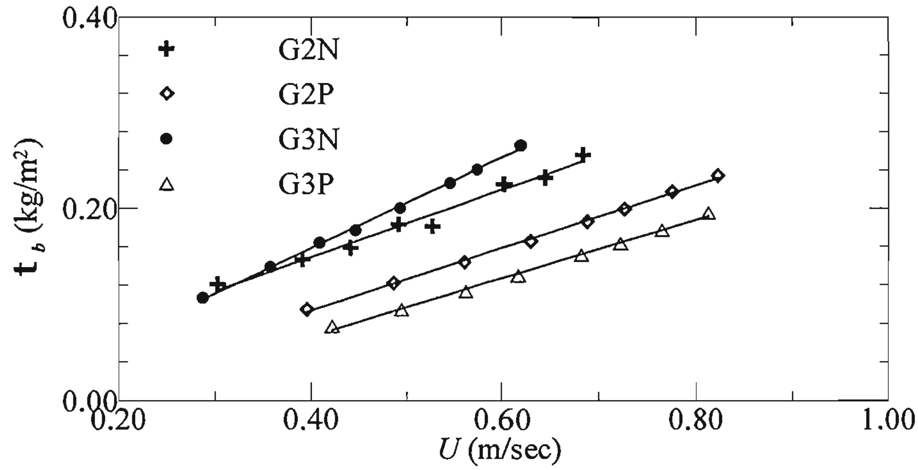

Fig. 5. Bottom shear stress versus mean velocity

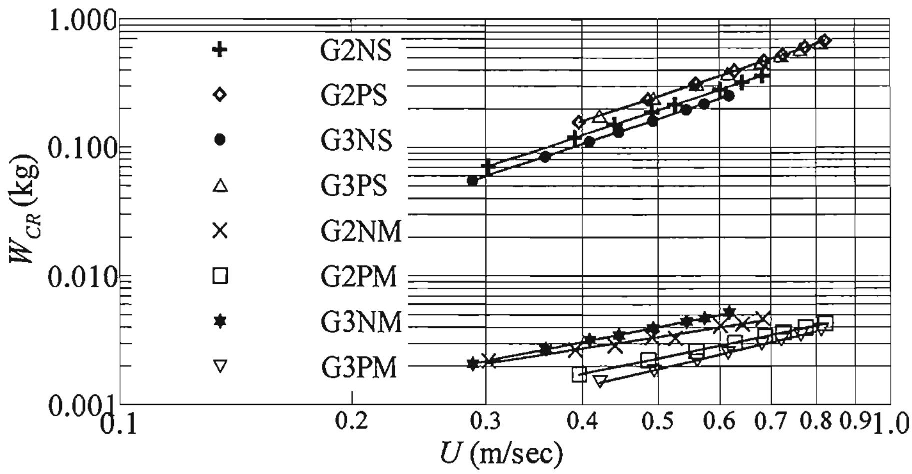

Fig. 6. Critical weight of G-blocks versus mean velocity

REFERENCES

1. Aguirre-Pe, J., and Fuentes, R. (1990). "Resistance to flow in steep rough streams." *J. Hydr. Engrg.*, ASCE, Vol. 116, No. 11, pp. 1374-1387.
2. American Society of Civil Engineers and Water Environment Federation. (1992). *Design and Construction of Urban Stormwater Management Systems.* ASCE Manuals and Reports of Engineering Practice No. 77 and WEF Manual of Practice FD-20, ASCE, New York, NY and WEF, Alexandria, VA.
3. Ferro, V., and Giordano, G. (1991). "Experimental study of flow resistance in gravel-bed rivers." *J. Hydr. Engrg.*, ACSE, Vol. 117, No. 10, pp. 1239-1246.
4. French, R.H. (1987). *Open Channel Hydraulics*. McGraw Hill Book Co., New York, NY.
5. Griffiths, G.A. (1981). "Flow resistance in coarse gravel-bed rivers." *J. Hydr. Div.*, ASCE, Vol. 107, No. 7. pp. 899-918.
6. Jones, J.S., Bertoldi, D., and Stein, S. (1995). "Alternative scour countermeasures." *Proc. First Int. Conf. on Water Res. Engrg.* ASCE, San Antonio, Texas.
7. Keulegen, G.H. (1938). "Laws of turbulent flow in open channels." J. Res. Natl. Bur. Stand., (U.S.), Vol. 21, No. 1, pp. 707-741.
8. Maynord, S.T. (1991). "Flow resistance of riprap." *J. Hydr. Engrg.*, ASCE, Vol. 117, No. 6, pp. 687-696.
9. Naudascher, E. (1991). *Hydrodynamic Force.* IAHR Hydraulic Structures Design Manual 3, A.A. Balkema, Rotterdam, Netherlands.
10. Parker, G., Toro-Escobar, C., and Voigt, R.L.Jr. (1998). "Countermeasures to protect bridge piers from scour." *Nat. Cooperative Highway Res. Program Rep. 24-7*, Univ. of Minnesota, Minneapolis, MN.

THE PROBLEM OF SCOUR AND COUNTERMEASURES

By

Dr. B.R. Phani Kumar[1]

ABSTRACT

The problem of scour has caused many bridge failures and, therefore, needs to be prevented by suitable countermeasures. Several methods have been suggested for the prevention of scour. They are based on model studies for the protection of embankments and piers from undermining by scour. Riprap arrests the progress of the erosive cycle. Walls of river banks are protected, in some cases, by gabions. Similarly, spur dikes and mattresses of bamboo sticks are also successfully used for preventing scour. The paper discusses the problem of scour and different countermeasures in detail.

INTRODUCTION

Scour is a serious problem to combat with in bridge engineering, as it has been the major cause of failure of most of the bridges. Scour is a natural phenomenon in which soil particles are removed from their environment by moving water. Because of this continuous removal of soil, bridge piers and abutments are subjected to undermining (Terzaghi, 1936).

SCOUR CHARACTERISTICS

Three types of scour have been recognized. The first form of scour (Lane et al, 1954) takes place as a result of flooding. This causes suspension of material in the river bed. The velocity of water increases, thereby increasing the erosive capacity. Solid particles will be lifted and moved and suspended when the flow returns to normal. This type of scour, called general scour, is particularly great where the channel is narrow. Bridge piers are generally founded below the depth of general scour.

The second form of scour, called local scour, is caused by the presence of some obstruction to the stream such as a pier. Within the proximity of the pier the flow pattern changes, becomes turbulent and erodes the soil. This localized scour (Laursen et al, 1956) is of greater intensity and acceleration, and is a function of velocity of flow, shape of the pier etc.

The third form of scour is bank scour which occurs due to lateral bending of the channel. Water strikes the outer side of the bend and erodes the material. The inside of the bank is filled with the eroded sands and silts. The foundations of any structure placed adjacent to the outside of a bend must be protected.

---

[1] Dr.B.R.Phani Kumar, Department of Civil Engineering, JNTU College of Engineering, Kakinada-533 003, INDIA

The different characteristics of scour are a function of the relationship between the solid material and the capacity of the river to remove it. The erosive capacity depends on the flow velocity which, in turn, depends on the hydraulic characteristics of the river, the intensity of the flood and the characteristics of the material in the river bed. The resistance of the bed material to erosion may not be often satisfactorily characterized in terms of its properties like dry unit weight in case of cohesive soils and average diameter in case of cohesionless soils. Hence, there is a need to depend on the real observations and, accordingly, resort to preventive measures.

COUNTERMEASURES

Various countermeasures to scour have been suggested and practiced. They have been found to show satisfactory performance in protecting embankments and piers. A discussion of different measures for preventing scour follows:

Riprap or coarse rock fill is one of the most widely used protection measures (Searcy, 1967). Generally, a filter is placed between the riprap and the natural ground in order to prevent the finer soil from clogging the void space of the riprap. By using riprap the progress of the erosive cycle is stopped and the hydraulic area of the channel is not reduced.

In some places where coarse rock for riprap is not available gabions will be used. Gabions are wire baskets filled with gravel or coarse aggregate. They are stacked to form bank protection walls. If coarse aggregate is not available, stacks of cloth bags filled with sand and cement are used for protecting the walls of banks. Gabions are quite effective in controlling scour.

Another preventive measure for scour is the use of mattresses for bank protection. It is the one of the oldest practices. These mattresses consist of woven sticks of wood or bamboo. Sometimes, concrete slabs are also used as mattresses.

The structures employed for diverting the high velocity flow from reaching the bank are called spur dikes which have been found to give excellent results. They are embedded in the river bank and extend into the channel. Their design is a function of river geometry, length of the dikes and spacing between the dikes. If the spur dikes are built with their tops sloping down towards the center of the river, local scour around the end of the dike can be reduced.

CONCLUSION

Many bridges have been investigated to fail due to undermining by scour. Localized scour in the proximity of any obstruction like a pier is of quick progress. Scour can be prevented by different countermeasures. Riprap with a filter reduces the progress of erosive cycle. Gabions and mattresses made of wood or concrete slabs protect walls of river banks. Spur dikes arrest local scour.

REFERENCES

1. Lane, E.W., Borland, W.M., 1954, "River Bed Scour during Floods", Transactions, ASCE, Vol.119, p.1072.
2. Laursen, E.M., Toch, A., 1956, "Scour around Bridge Piers and Abutments", Iowa Highway Research Board, Bulletin 4.
3. Searcy, J.K., 1967, "Use of Riprap for Bank Protection", Hydraulic Engineering Circular No.11, Bureau of Public Roads.
4. Terzaghi, K., 1936, "Failure of Bridge Piers due to Scour", Proceedings, International Conference on Soil Mechanics and Foundation Engineering, Cambridge, Mass, Vol.2, p.26.

SHEAR STRESS CONCEPT IN GRANULAR FILTERS

By

Gijs J.C.M. Hoffmans[1], Henk den Adel[2] and Henk J. Verheij[3]

ABSTRACT

Scour is a natural phenomenon caused by the flow of water in rivers and streams and occurs as a part of the morphological changes caused by rivers or as a result of man-made structures. For the Dutch Delta Works hydraulic structures were often constructed on fines with loose packing. To guarantee the geotechnical stability of these structures the bed in their immediate vicinity had to be protected. Though several types of bed protection can be distinguished, for example concrete blocks, asphalt, and granular filters (with or without geotextiles) the scope of this paper is limited to granular filters. In the Netherlands geometrically sand-tight filters are usually used. The stability of these filters is mainly determined by the geometrical properties of the materials. Consequently, these classical filters with numerous layers are very expensive. In this study a model relation for sizing a geometrically open granular filter is discussed. Our goal is to promote discussion than rather to try to solve the many problems in the complex field of filtration in geotechnical engineering.

INTRODUCTION

Non-geometrical granular filters have a hydraulic mode of operation; i.e. the reduction of the hydraulic shear stresses on the base material is such that erosion is prevented. Available knowledge of the hydrodynamic forces, lift and drag, acting on particles in granular filters is mainly based on experience and laboratory and field measurements which has proven inadequate for the purpose of developing a highly accurate design criterion. This is due to the numerous factors that influence the stability, and to the definite probabilistic nature of the acting forces which may at times be significantly in excess of mean values and consequently cause movement. Verheij and Den Adel (1998) calibrated and validated model relations for granular filters that are based on the Navier Stokes equation for uniform flow, the so-called Forchheimer relation and the hypothesis of Boussinesq.

Figure 1 shows a horizontal one-layer filter with a thickness d above the base material. Considering uniform flow the shear stress distribution in the open flow is linear. Usually the mean flow velocity in the downstream direction can be approximated by a logarithmic function. The velocities and shear stresses in the filter layer will be briefly discussed by applying the three aforementioned equations.

[1] Ministry of Transport, Public Works and Water Management, Hydraulic Engineering Division, Delft (email is g.j.c.m.hoffmans@dww.rws.minvenw.nl)

[2] Geodelft, Delft, The Netherlands

[3] Delft Hydraulics, Delft, The Netherlands

In a granular filter and with uniform flow conditions the balance of forces acting on a control volume can be given by (Shimizu *et al.*, 1990)

$$\frac{\partial \tau}{\partial z} + F + \rho g i = 0 \tag{1}$$

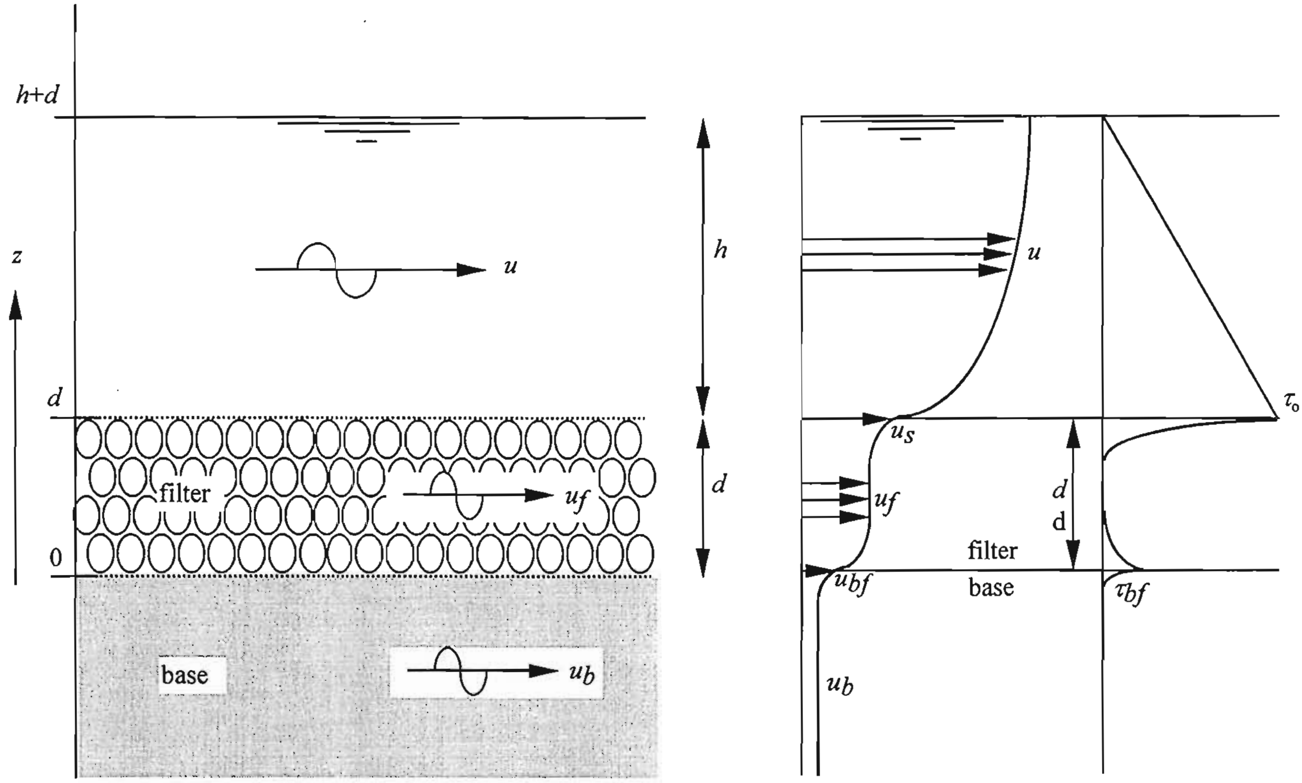

Fig. 1 Overview of definitions for a one-layer filter

in which τ is the shear stress, z is the vertical co-ordinate, F is the seepage resistance, ρ is the fluid density, g is the acceleration of gravity and i is the energy gradient. The first term represents the momentum transfer from the free surface flow to the filter bed. To solve equation (1) the seepage resistance and the shear stress have to be related to parameters that express the loading in granular filters. The Forcheimer relation reads:

$$F = -\rho g\left(au + bu^2\right) \tag{2}$$

where u is the (mean) filter velocity and a and b are constants (with a dimension). The first term in (2) represents the Darcy's law and is applicable in laminar flow conditions, whereas the second term characterises the resistance in turbulent flow conditions. The hypothesis of Boussinesq can be given by:

$$\tau = \mu \frac{\partial u}{\partial z} \quad \text{with} \quad \mu = \rho \nu_t \tag{3}$$

where ν_t is the eddy viscosity. It should be remembered that the shear stress in granular layers is not a shear stress following the definition of the shear stress in open channel flow. The shear stress in this study must be considered as a loading parameter.

Most of the turbulence-model-development and application work was carried out in the area of mechanical and aeronautical engineering. In the early eighties Rodi (1984) assessed the applicability of turbulence models to hydraulic flow problems. However, these models have not been extensively validated for flow in porous mediums such as granular filters. Therefore in this study some assumptions have been made about the eddy viscosity. In general, the eddy viscosity is related to a representative length scale and to a representative flow velocity. The length scale has been determined by the open space or by the magnitude of the particle sizes. Here the eddy viscosity is approximated by:

$$\nu_t = \alpha u D_{f,15} \tag{4}$$

where α ($\cong$ 0,9) is a constant and $D_{f,15}$ is the diameter of the filter material (exceeded by 85% of the weight percentage). Combining equations (1), (2) and (3) and assuming turbulent conditions (a = 0) the distribution of the shear stress in a one-layered filter can be modelled by (Verheij *et al.*, 2000):

$$\tau = \tau_{bf} e^{-\xi z} + \tau_0 e^{\xi(z-d)} \quad \text{with} \quad \xi = \sqrt{\frac{2gb}{\alpha D_{f,15}}} \quad \text{and} \quad b = \frac{2.2}{n^2 g D_{f,15}} \tag{5}$$

where τ_{bf} is the shear stress at the interface of the filter layer and the base layer, τ_0 is the bed shear stress (or shear stress at the interface of the flow and the filter layers), d is the thickness of the filter material and n (= 0.4) is the porosity. For turbulent flow conditions the damping parameter is approximately equal to $\xi = 5.5/D_{f,15}$. Since the damping parameter ξ is smaller than the characteristic length scale in the filter material, the continuum assumption in Forcheimer's equation is violated. Therefore the applicability of equation (5) is limited. Nevertheless the relation between τ and z will hold. Though the relation between ξ and $D_{f,15}$ may be quantitatively invalid, there is experimental evidence that ξ is inversely proportional to $D_{f,15}$. The filter velocity as function of the vertical co-ordinate can be written as:

$$u(z) = \sqrt{C_1 e^{z\xi} + C_2 e^{-z\xi} + i/b} \quad \text{with} \quad C_1 = \frac{2\left(\tau_0 - \tau_{bf} e^{-\xi d}\right)}{\alpha\rho D_{f,15}\xi\left(e^{\xi d} - e^{-\xi d}\right)} \quad C_2 = \frac{2\left(\tau_0 - \tau_{bf} e^{\xi d}\right)}{\alpha\rho D_{f,15}\xi\left(e^{\xi d} - e^{-\xi d}\right)} \tag{6}$$

The parameters C_1 and C_2 can be expressed by the velocities as well: u_{bf} and u_s (with u_{bf} = $u(z = 0)$ and $u_s = u(z = d)$)

$$C_1 = \frac{\left(u_s^2 - i/b\right) - e^{-\xi d}\left(u_{bf}^2 - i/b\right)}{\left(e^{\xi d} - e^{-\xi d}\right)} \qquad C_2 = \frac{e^{\xi d}\left(u_{bf}^2 - i/b\right) - \left(u_s^2 - i/b\right)}{\left(e^{\xi d} - e^{-\xi d}\right)} \tag{7}$$

When the influence of the permeability ratio of the filter and base material is included, the boundary condition for the filter velocities at $z = 0$ and at $z = d$ can respectively be given by:

$$u(z = 0) = \sqrt{u_f u_b} \qquad u(z = d) = \sqrt{\frac{2\tau_0}{\alpha\rho D_{f,15}\xi} + u_f^2} \tag{8}$$

For uniform and laminar flow conditions (b = 0) Verheij *et al.* (2000) derived similar relations for both the filter velocities and shear stresses. The damping parameter for laminar flow is approximately 6 times larger than for turbulent flow ($\xi = 30/D_{f,15}$). For a two-layer filter also an analytical solution can be derived.

CONCEPT OF GRASS

Particle transport occurs when there is no balance between load (shear stress) and strength (inter particle friction). When the load is less than some critical value, the bed material remains motionless. Then the bed can be considered as fully stable. But when the load over the bed attains or exceeds its critical value, particle motion begins. The beginning of motion is difficult to define and this can be ascribed to phenomena that are random in time and space. In 1936, Shields published his experimental results for the initiation of movement of uniform granular material on a flat bed, later known as the Shields-criterion although Rouse proposed the well-known curve.

In the Shields diagram, the influence of fluctuating shear stresses on bed particles is not directly specified. Though the distribution of the instantaneous bed shear stress is unknown, there are indications that this distribution has to be asymmetrical owing to sweeps and ejection (Lu and Willmarth, 1973). When dealing with the concept of Grass, the exact shape of the distribution is irrelevant because a characteristic bed shear stress can be defined, this being a time-averaged value and a fluctuating term that originates from the turbulence near the bed. The characteristic value is a value that is higher or lower than the time-averaged value. Usually characteristic values are expressed as a mean value and a fraction or manifold of the standard deviation. In fact, the problem of bed stability will now be transferred to the magnitude of this fluctuation. In addition to the random nature of the load, another random variable in the process of initial instability is determined by the strength of the particles close to the bed.

To make an adaptation to non-uniform flow it is useful to analyse the influence of the turbulence in the vicinity of the bed for uniform flow. For this exercise the concept of Grass (1970) can be applied, this being based on statistical assumptions for both the loading and strength parameters (Figure 2). The characteristic bed shear stress ($\tau_{0,k}$) and the characteristic strength, which is the critical bed shear stress ($\tau_{c,k}$) can be respectively written as:

$$\tau_{0,k} = \tau_0 + \gamma\sigma_0 \qquad \text{and} \qquad \tau_{c,k} = \tau_G - \gamma\sigma_c \tag{9}$$

where γ is determined by an allowable transport of the bed material, σ_0 is the standard deviation of the instantaneous bed shear stress and τ_0 is the time-averaged bed shear stress, σ_c is the standard deviation of the instantaneous critical bed shear stress and τ_G is the time-averaged critical bed shear stress according to Grass. A specific transport will occur if $\tau_{0,k} = \tau_{c,k}$ which will be elucidated later.

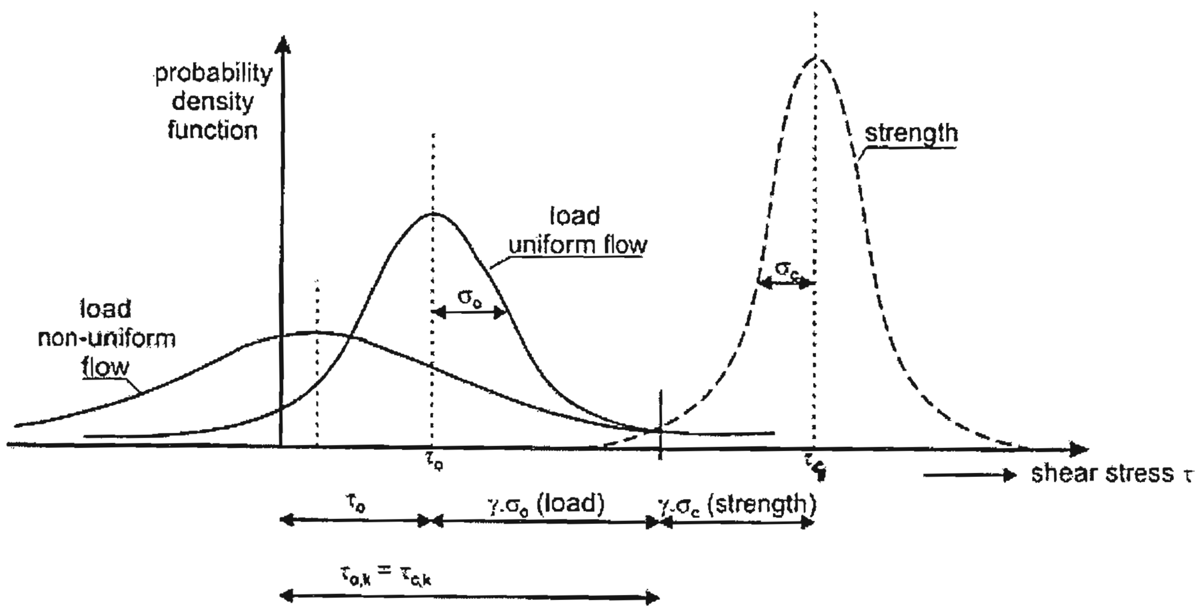

Fig. 2 Probability functions of the loading and strength parameters (Grass, 1970)

If the characteristic loading near the bed is equal to the characteristic strength (thus $\tau_{0,k} = \tau_{c,k}$) and if $\sigma_c = \alpha_{c,f}\tau_G$ with $\tau_G = \Psi_{c,G,f}\Delta_f\rho g D_{f,50}$ (analogous to the Shields concept) and assuming $\gamma_{strength} = \gamma_{load} = \gamma$, a general relation for the filter layer follows:

$$\Delta_f D_{f,50} = \frac{\tau_0 + \gamma\ \sigma_0}{\Psi_{c,G,f}\rho g(1-\alpha_{c,f}\gamma\ )} \tag{10}$$

where $\alpha_{c,f}$ is a coefficient representing the variation of the material characteristics of the filter layer. For uniform flow Grass found that a bed of nearly uniform sand (α_c = 0.3) was completely stable for γ = 1 and for γ = 0 a significant transport of sediment particles was observed. Based on his experiments, he reported that for γ = 0.625 the criterion of Shields was met for the initial movement of sands up to a size of 250 μm. In his opinion the γ = 0.625 criterion was also in agreement with observations of Vanoni and Tison when using the Rouse curve as a basis for the critical shear stress prediction.

The critical bed shear stress τ_G is approximately 1.5 times higher than the time-averaged bed shear stress and thus 1.5 times higher than the mean critical value according to Rouse.

FILTER MODEL RELATIONS

In a similar way model relations can be derived for filters at the interface of the filter and the base layer (Figure 3). Using equation (5) the mean load parameter at the interface is (z = 0):

$$\tau(z=0) = \tau_{bf} + \tau_0 e^{-\xi d} \tag{11}$$

Assuming $\tau_{bf} = \eta\tau_0$ and applying the concept of Grass, the characteristic load can be given by:

$$\tau_k(z=0) = (\tau_0 + \gamma\sigma_0)(\eta + e^{-\xi d}) \tag{12}$$

The characteristic strength of the base material is:

$$\tau_{c,k}(z=0) = \tau_G - \gamma\sigma_{c,b} = \Psi_{c,G,b}\Delta_b\rho g D_{b,50}(1-\gamma\alpha_{c,b}) \tag{13}$$

By combining equations (10), (11) and (13), the following model relation for open granular filters will be obtained:

$$\frac{D_{f,50}}{D_{b,50}} = \frac{1}{\eta + e^{-\xi d}}\frac{1-\gamma\alpha_{c,b}}{1-\gamma\alpha_{c,f}}\frac{\Psi_{c,G,b}}{\Psi_{c,G,f}}\frac{\Delta_b}{\Delta_f} \tag{14}$$

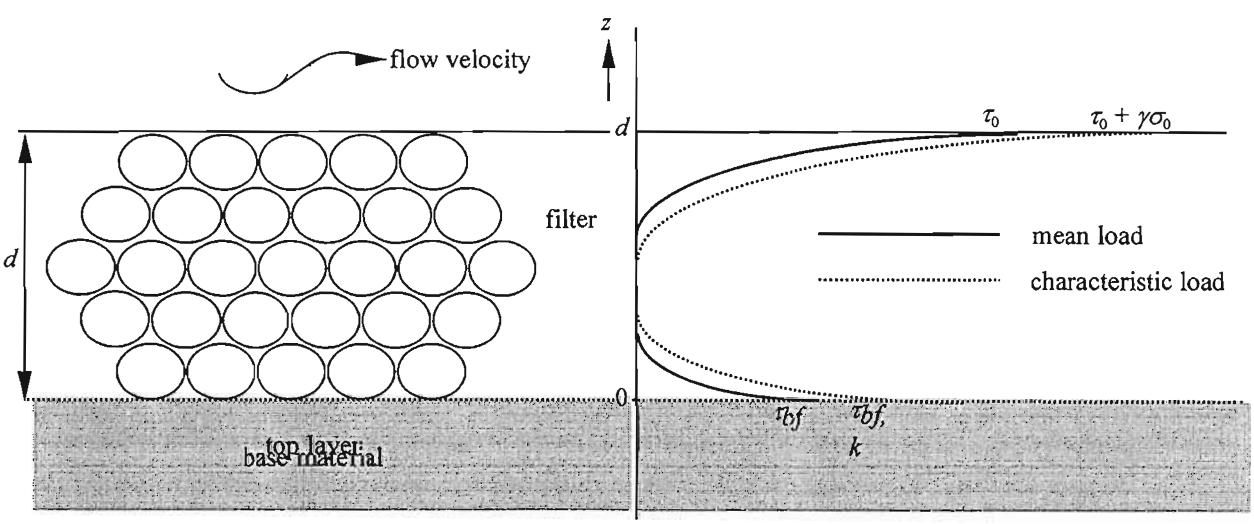

Fig. 3 Distribution of the mean and characteristic load

Although characteristic values for both loading and strength are included, the resulting ratio of D_f/D_b is independent of the fluctuations in the loading. There are two reasons for this rather unexpected result: First it is assumed that both filter and base material will display initial movement under the same loading conditions. Second, fluctuations in the load exert a load on the filter material similar to that on the base material. The effects of non-uniform flow have been taken into account by applying equation (10) and can be represented by the standard deviation of the instantaneous bed shear stress (Hoffmans, 1992,1996).

With equation (14) the influence of particle gradation on the stability of the base material can be explained in a qualitative way. For example, when the base material is more graded than the filter material, $\alpha_{c,b}$ is greater than $\alpha_{c,f}$. Consequently, the required ratio D_f/D_b is less when this value is compared to situations where base and filter materials do have the same gradation. If only the filter material is broadly graded, $\alpha_{c,f}$ is greater than $\alpha_{c,b}$, so the maximum value of D_f/D_b is higher than for similarly graded materials. These predictions correspond with observations in flume experiments. A broadly graded base material has more fines than a more uniform material. The material in the filter layer has to prevent the erosion of the fines. This can only be achieved by reducing the filter velocities or by putting more fines into the filter layers. A broadly graded material in the filter layer has relatively more fines, which reduce the pore velocity in the filter and so also the loading on the base material. Hence, the broadly graded filter material is allowed to have an average grain size that is larger than for uniform material.

Using the assumptions $\alpha_{c,b} = \alpha_{c,f}$ and multiplying both sides by $D_{f,15}/D_{f,50}$, equation (14) reduces for high values of ξd into:

$$\frac{D_{f,15}}{D_{b,50}} = \frac{D_{f,15}}{D_{f,50}} \frac{1}{\eta} \frac{\Psi_{c,G,b}}{\Psi_{c,G,f}} \frac{\Delta_b}{\Delta_f} \tag{15}$$

The value of η has been calibrated by using experimental results obtained by Van Huijstee *et al.* (1991). In these 9 flume experiments the instability of the filter layer and the base layer was simultaneously observed. The mean value of η is about 0.01 with the boundaries $0.005 < \eta < 0.025$. Hoffmans (1996) also found a value of 0.01 on the basis of the Japanese tests of Shimizu *et al.* (1990). Remark that the calibration and validation of η was based on uniform-flow experiments.

The resemblance to traditional relations derived by Terzaghi is surprising. The stability between filter and base layer for geometrically sand-tight filters is:

$$\frac{D_{f,15}}{D_{b,85}} < 5 \quad \vee \quad \frac{D_{f,50}}{D_{b,50}} < 10 \tag{16}$$

which means $\eta \cong 0.1$.

The differences between equations (15) and (16) can be ascribed to a safety factor that varies from 4 to 20. This analysis shows that for uniform flow the relations for geometrical sand-tight materials are strongly oversized. When the turbulence intensities are much higher, for example downstream of sills, the value of η ($\eta \cong 0.01$) might be questionable. Under these conditions the ratio D_f/D_b probably tends to the geometrical value of about $\eta \cong 0.1$. It should be remarked that in this study, equation (15) has not been validated for non-uniform flow conditions.

Bakker *et al.* (1995) and Stephenson (1979) discussed filter model relations, which predict similar ratios between particle sizes of filter and base material. Although the prediction potential of these relations is reasonable for the experiments investigated, they depend on the ratio R/Df, which is not realistic for uniform flow conditions.

DAMPING PARAMETER

The damping parameter (ξ) is related to material properties both for laminar and turbulent flow. For laminar flow ξ is approximately $30/Df_{15}$. Following Ikeya (1991) the damping parameter varies from $14/Df_{50}$ to $30/Df_{50}$. In both cases the length scale of the damping is much smaller than the particle diameter of the grains in the filter layer. Consequently, the influence of the boundary layer is practically negligible in the case of laminar flow.

For turbulent flow conditions Verheij *et al.* (2000) found $\xi \cong 5{,}5/Df_{15}$ whereas Ikeya (1991) arrived at the following: $1/Df_{50} < \xi < 6/Df_{50}$. Ikeya discussed a suggestion made by Stephenson (1979) that the turbulent boundary layer in the filter layer is approximately, $1.5Df_{50}$ which was later independently confirmed by the measurements of Suzuki (1992). Summarising equation (15) is valid for both laminar and turbulent flow.

The difference between results of the Dutch and Japanese researchers can be attributed to a different way of modelling the eddy viscosity and to different values for the coefficients in the so-called Forcheimer relation. The Japanese assumed a constant eddy viscosity in the filter layer. In this study the eddy viscosity is related to the varying filter velocity (see equation 4). Note that the eddy viscosity is not a physical parameter, but a parameter that helps us to relate velocities to shear stresses. Since no measurements of filter velocities in relation to loading parameters are available no conclusions can be drawn at present.

CONCLUSIONS

In this study model relations for both the filter velocity and the shear stress at the interface filter-base material are presented. Although the exact relation between the damping parameter in a filter material and its material properties is disputable, the type of relation between characteristic length scale and particle size will hold, in spite of the fact that the assumptions for a continuum approach are violated.

It should be noted that the term shear stress is somewhat misleading. In fact the distribution of the shear stress in filter layers has to be considered as a distribution of a loading parameter. A model relation has been discussed for geometrically open filters, which can be used for both uniform and non-uniform flow. This relation is based on simultaneous instability of filter and base material. The influence of the grading effects of the filter and base materials has been shown qualitatively. This relation corresponds closely to the traditional stability relation of Terzaghi for geometrical filter design and represents the range of the magnitude of the safety factor.

To increase the accuracy of the model presented here more detailed information is needed, in particular the value of η, which may be found by carrying out experiments with non-uniform flow conditions. It is necessary to use sophisticated equipment to measure filter velocities and loading parameters.

REFERENCES

1. Bakker, K.J., Verheij, H.J., de Groot, M.B., 1995, Design relationship for filters in bed protection, ASCE, Journal of Hydraulic Engineering, Vol. 120, No. 9, p.1083-1088.
2. Grass, A.J., 1970, Initial instability of fine bed sand, Hydraulic Division, Proceedings of the ASCE, Vol. 96, No. HY3, p.619-632.
3. Hoffmans, G.J.C.M., 1992, Two-dimensional mathematical modelling of local-scour holes, Doctoral thesis, (**also** 'Communications on Hydraulic and Geotechnical Engineering' of the Faculty of Civil Engineering, Delft University of Technology, Report No. 92-7).
4. Hoffmans, G.J.C.M., 1996, The influence of turbulence on geometrically open filters (in Dutch), Road and Hydraulic Engineering Division, Delft, The Netherlands.
5. van Huijstee, J.J.A., Verheij, H.J., (1991), Design relations for granular filters in bed protections (in Dutch), Delft Hydraulics, Report on model investigations Q572, Delft, The Netherlands.
6. Ikeya, T, 1991, An analytical estimate of the velocity distribution through protection layers, note prepared during his visit in the Netherlands, Delft Hydraulics, Delft, The Netherlands.
7. Lu, S.S., Willmarth, W.W., 1973, Measurements of the structure of the Reynolds stress in a turbulent boundary layer, Journal of Fluid Mechanics, Vol. 60, Part 3, p.481-511.
8. Rodi, W., 1984, Turbulence models and their application in hydraulics, A state of the art review, IAHR monograph, Balkema, Rotterdam, The Netherlands.
9. Shimizu, Y., Tsujimoto T., Nakawaga, H., (1990), Experiment and macroscopic modelling of flow in highly permeable porous medium under free surface flow, Journal of Hydroscience and Hydraulic Engineering, Vol. 8, No. 1, pp. 69-78.
10. Suzuki, K, 1992, Reduction of local scour depth by armour coat formation downstream of consolidation work, Proceedings 8th Congress, APD-IAHR, Vol. B. pp. 453-458.
11. Stephenson, D., 1979, Rockfill in Hydraulic Engineering, Elsevier Scientific Publishing Company.
12. Verheij, H.J., den Adel, H., 1998, Evaluation of recent desk study results on granular filters, Delft Hydraulics, Desk study Q2416, Delft, The Netherlands.
13. Verheij, H.J., den Adel, H., Petit, H., 2000, Design formulas for granular filters, Delft Hydraulics, Desk study Q2629, Delft, The Netherlands.

INFLUENCE OF RESERVOIR ON RIVER BED SCOUR

By

Narimantas Ždankus[1]

ABSTRACT

Sudden fluctuation of river flow rate, sedimentation of stream load increase scouring capacity of the flow and cause hardly predictable long lasting scour of a river bed going on after the construction a reservoir on the river. Many years are required to restore equilibrium of the stream-bed interaction mechanism. Complexity of a scour phenomenon, seepage influences on the flow structure and soil stability conditions introduce additional difficulties in predicting scour results. The phenomena are analysed on the example of Nemunas river scour downstream from Kaunas hydropower plant reservoir (see Fig. 1), constructed 40 years ago. A scour phenomenon is analysed; suggestions for designing similar structures are formulated.

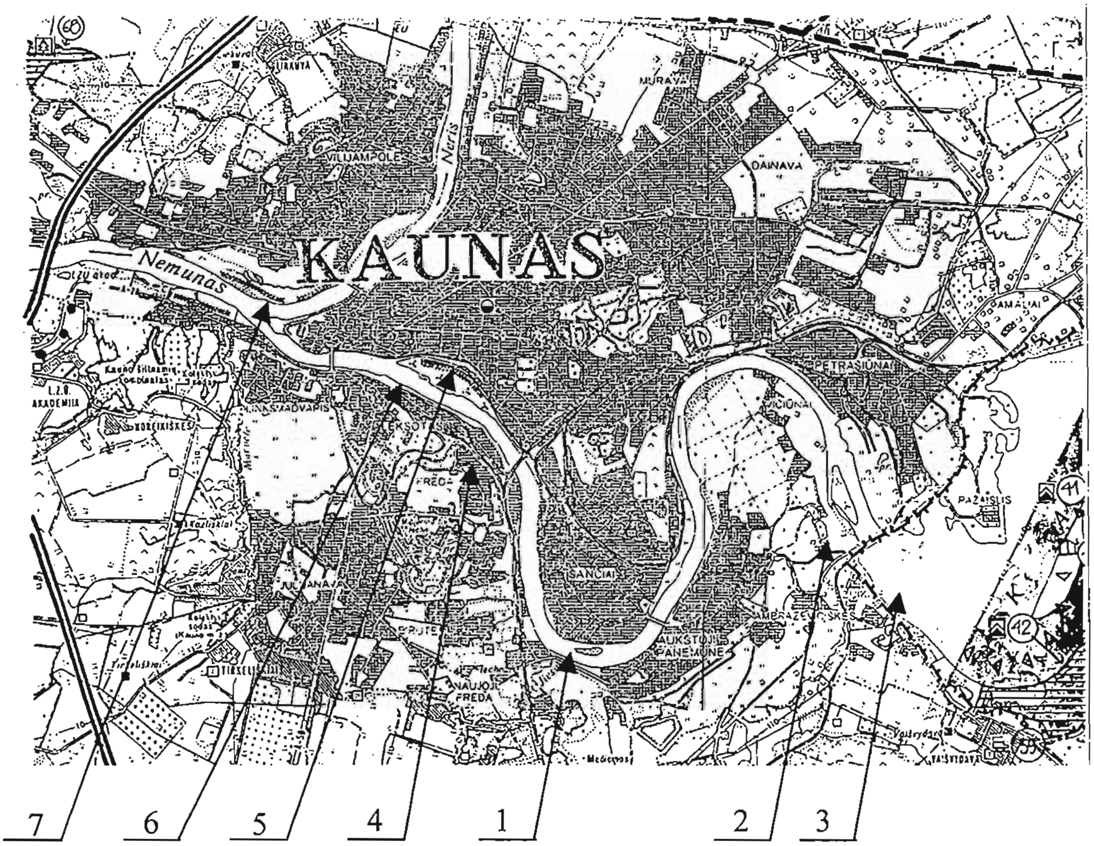

Fig. 1. Zone under investigation: 1-river Nemunas; 2-hydropower plant; 3-reservoir; 4-railway bridge; 5-town centre; 6-island; 7-river Neris

[1] Professor, Geoengineering Chair, Civil Engineering and Architecture Dept., Kaunas Univertity of Technology, LT-3028, Lithuania

INTRODUCTION

Alluvial sediments form bed and banks of river Nemunas, mainly by sand and sandy loam. Lenses and layers of gravel and clay are common in the banks of the river. Bottom of the river is rather flexible. Sand waves and bars, reinforced zones of gravel layer outcrops, tough clay and boulders vary from place to place. Average velocities in talweg vary within the limits from 1.0 to 1.5 m/s. In spring flood period at some zones the velocities may reach magnitude of 1.8 m/s, sometimes in dry time it may drop to 0.8 m/s level. Velocity significantly varies in time depending on the

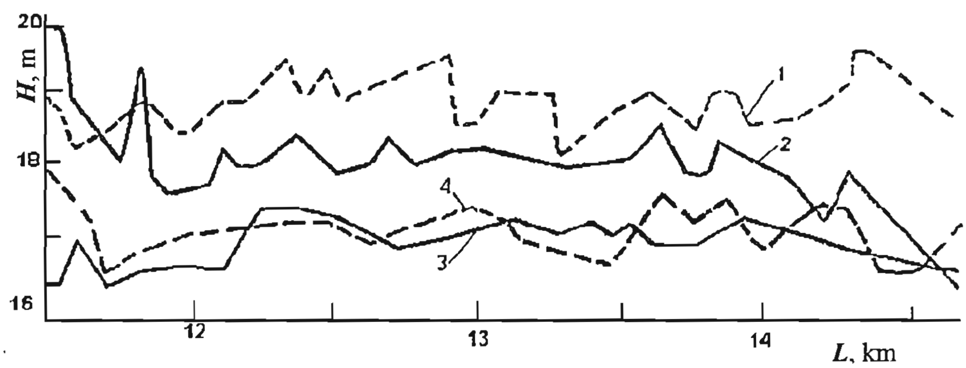

Fig. 2 Longitudinal profiles of river bed downstream railway bridge in: 1-1963; 2-1978; 3-1981; 4-1985.

regime of a hydropower plant, scour and sedimentation may go on at the same spot at different periods of time.

Due to the effect of Kaunas hydropower plant transformations of river bed goes on in the zone of 30 km length at the centre and suburbs of Kaunas town. The bottom level at present is on the average 1.0 m below the previous level of 1959, when the plant was constructed. At some places the bed was lowered up to 2 m (see Fig. 2). Moorings and embankments of the tow, pipelines and cables are under the constant danger of damage due to scour of both structures toe and bottom of the river. Municipality of the town realised possible consequences of the threat. They applied to scientists of Kaunas University of Technology to investigate the phenomenon and to formulate some proposals to stop the deformations of the river bed. Field and laboratory investigations were performed and some suggestions were offered.

SCOUR AND SELFLINING OF NON-COHESIVE HETEROGENEOUS GROUND

Scour strength of non-cohesive soils depends mainly on the diameter of soil particles and degree of heterogeneity. There are many formulas for computation of admissible non-scouring velocity for the type of the soil (Zdankus, 1965). Most of these formulas are designed for computation of maximal admissable non-scouring mean flow velocity. We consider that maximal momentary bottom velocity is a more suitable parameter for estimation of flow scouring power and suggest the following formula

$$u_{\mathrm{mbadm}}=42\sqrt{\boldsymbol{D}}+21+37\boldsymbol{D}\ , \mathrm{cm/s} \qquad (1)$$

where u_{mbadm} is maximal momentary bottom non-scouring velocity at the distance of $\boldsymbol{D}/2$ from the bottom level and $\boldsymbol{D}$ is mean diameter of a soil particle in cm.

According to the results of our investigations relationship between maximal momentary bottom u_{mb} and mean velocity of flow v may be expressed by empirical formula

$$k_b = \frac{u_{mb}}{v} = 1.32 + \frac{1}{D(50 - 1.55D) = 2.33} - 0.272\, lg\left(\frac{h}{D}\right). \qquad (2)$$

Formed by heterogeneous gravel river bottom roughness the character of flow velocity distribution in verticale and soil scour strength depends on heterogeneity of the soil (Sieben, 1999). The dependency may be estimated multiplying admissable non-scouring velocity by a correction coefficient computed by our formula

$$k_h = 1 - 0.32\, lg\left(\frac{D_m}{D_r}\right), \qquad (3)$$

Here D_m and D_r are maximal (corresponding percentage of 95%) and rated diameters of soil particles respectively.

It is evident that smaller than D_r soil particles will be washed out from the surface of the soil until selflining is completed and the surface is reinforced by the layer of soil particles larger or equal to rated diameter D_r (see Fig. 3). Thickness of a reinforcement layer may be determined by our formula

$$h_r = 0.023 P_r D_r^2 / D_m. \qquad (4)$$

Here P_r is percentage of rated diameter taken from a grain-size distribution diagram.

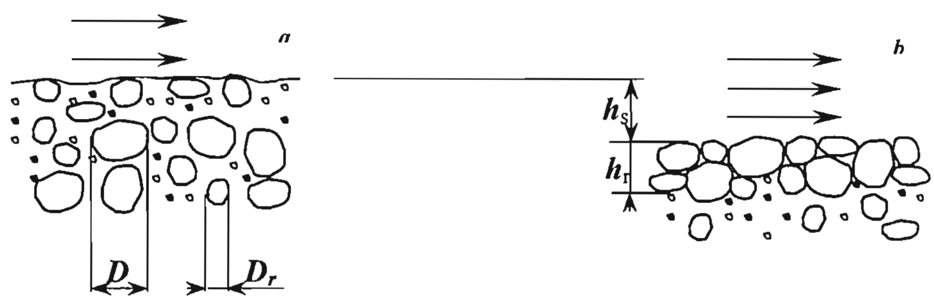

Fig. 3 Surface of heterogeneous ground before (a) and after selflining (b)

Scour depth h_s (see Fig. 3) containing large particles necessary for lining quantity may be computed from our formula

$$h_s = h_r \frac{P_r}{100 - P_r}. \qquad (5)$$

Lining layer may be broken by an occasional flood wave of high velocities. Then the layer of large particles then is being mixed with smaller ones. While new reinforcing layer is being formed scour and lowering of bottom level proceeds once again until new reinforcing layer has been formed.

SCOUR OF COHESIVE SOIL

Clayey soil scour process differs greatly from that of non-cohesive soil. Particles of the last one remain immobile if velocity is less than scouring. Cohesive soil scour goes on at any, even at much less than admissible non-scouring, velocity. At small velocities intensity of cohesive soil scour is small and the process is similar to melting, where the smallest particles gradually loose contact with the mass of a solid body under the process of swelling. Increment of flow velocity leads to gradual increment of scour intensity, therefore, it is rather difficult to determine the velocity which may be considered as non-scouring (Mirtshullavva, 1962).

Our device (Zdankus, 1968) for investigation of cohesive soil scour strength makes it possible to observe the scour process and estimate it in quantitative parameters. Outflowing from a nozzle of the device (see Fig. 4) water jet simulates the river flow bottom layer, therefore jet velocity is considered equal to maximal momentary bottom velocity. It may be applied to calculate mean flow velocity using formula (2).

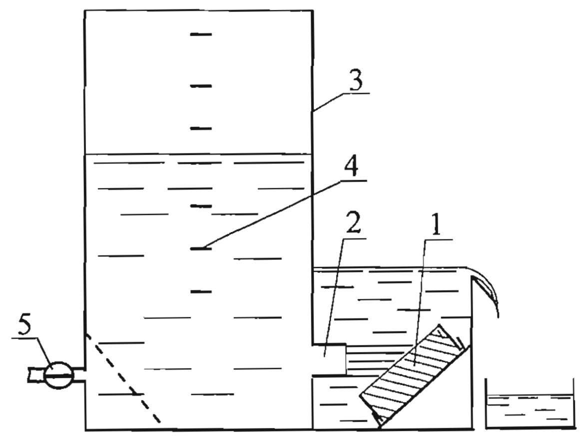

Fig. 4 Device for investigation of cohesive soil scour strength:
1-soil sample; 2-nozzle; 3-tank; 4-scale; 5-water supply line

INFLUENCE OF SEEPAGE AND SLOPE INCLINATION ON SCOUR

Ground water flow may influence the scour process (Zdankus, 1965). It increases stability of soil particles on the surface when water infiltrates into the bed of the river and decreases when water leaves the soil (Nian-Shen Cheng, Yee-Meng Chiew, 1999). The seepage changes both distribution of river flow velocities and magnitude of maximal momentary bottom velocity. The velocity is higher in a case of upward seepage and lower for downward seepage. Entering the ground water presses soil grains to the surface and increases their stability. Leaving the soil water lifts the grains and reduces their stability (see Fig. 5).

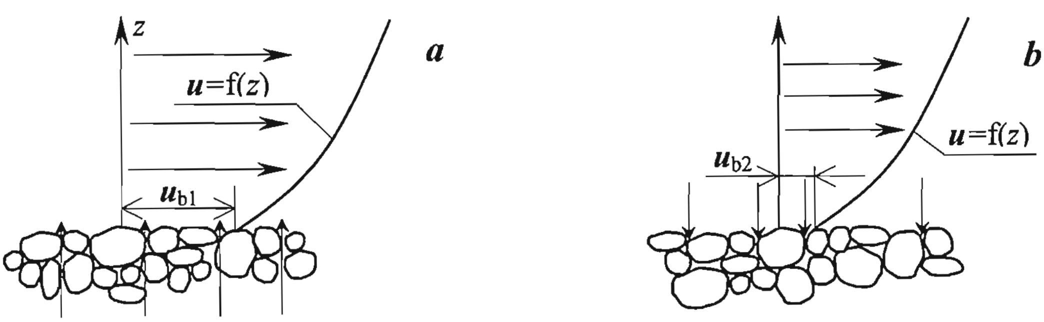

Fig. 5 Scheme of upward (*a*) and downward (*b*) seepage influence
on soil particles and river flow

Conditions of soil particle stability on an inclined slope of a river bank are worse than those on a horizontal bottom of a river bed. Perpendicular gravity force $\boldsymbol{F}_p$, which is equal to the gravity force $\boldsymbol{F}_g$ projected to the slope plane, tends to move soil particle down along the slope (see Fig. 6). Simultaneous influence of seepage and soil surface inclination on stability of soil particles may be examined analysing all forces acting on a single soil particle.

Seepage force may be expressed as

$$F_s=0.785C_s\rho gI_vD^3, \quad (6)$$

where C_s is seepage flow drag coefficient, ρ is water density, I_v is vertical component of a seepage hydraulic gradient.

Gravity force is directed downward. Its magnitude depends on the mass of a particle and may be expressed in the following way

$$F_g=0.524(\rho_s-\rho)gD^3. \quad (7)$$

Here ρ_s is density of a soil particle.

Horizontally directed hydrodynamic drag force is

$$F_h=0.393C_r\rho\ u^2_{mb}. \quad (8)$$

Here C_r is drag coefficient for river flow.

Soil particles on the slope inclined by α angle are acted by perpendicular force

$$F_p=F_g\sin\alpha \quad (9)$$

therefore, they are under less favourable stability conditions than those on horizontal surface (Zdankus, 1973). Thus, inclination of soil surface in the slope reduces soil scour strength.

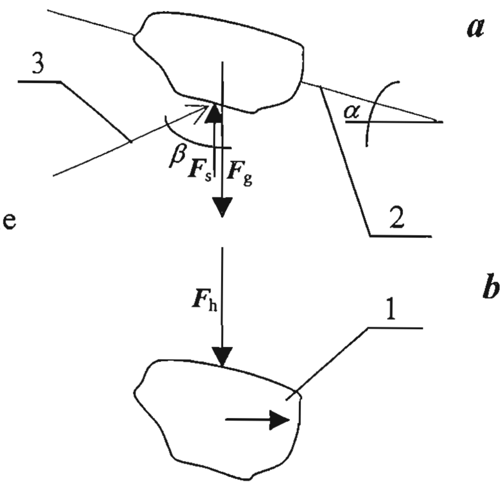

Fig. 6 Scheme of forces acting soil particle on slope: ***a***-vertical cross section; ***b***-plane; 1-soil particle; 2-slope line; 3-direction of ground water flow

Two equations for a critical state of the particle for shift and overturn may be set up and solved with respects to velocity u_{mb}. Maximal momentary bottom non-scouring velocity formula would be obtained. The formula would express dependency of the velocity on diameter D to 1.5 degree. Unfortunately, there are no possibilities to take into account the influence of seepage on the structure of a boundary layer of the flow and maximal momentary bottom velocity. Therefore, solution of the equations has no sense, and only empirical formulas may be suggested. Here is a formula developed by us on the ground of our investigation results

$$k_s=(1-0.1I_v)\cos\alpha\sqrt{1-\frac{tg^2\alpha}{tg\varphi}}. \quad (10)$$

Here k_s is non-scouring velocity correction coefficient; I_v is vertical component of ground water flow hydraulic gradient: positive for upward seepage and negative for downward one; α is slope inclination angle; φ is soil internal friction angle.

Seepage gradient depends on the ground water level at a river bank, permeability of ground and water level rise or drop rate. Drawdown curve for ground water flow must be computed to determine a hydraulic gradient. Hydrogeological conditions and permeability coefficients should be known for computations. Our device to test non-cohesive soils (Zdankus, 1987) suitable for permeability investigations good enough.

It should be mentioned here, that influence of seepage to scour is important merely to non-cohesive soils. Therefore, our attention was paid mainly to this type of soils. Ground water motion in cohesive soils is so slow, that seepage may have no influence on scour of such soils.

RESERVOIR INFLUENCE ON SCOUR PROCESS

Any reservoir significantly changes river hydraulic regime. It causes these changes of the regime:

1) damps caused by floods natural fluctuations of both the river flow rate and the levels;
2) creates artificial fluctuations caused consumption of water accumulated in reservoir;
3) reduces concentration of sediments in river water;
4) increases evaporation of water;
5) influences the ice phenomenon, content and concentration of water flora and fauna.

All enumerated phenomena influence the river scour process significantly. All of the are observed in the river Nemunas after construction of Kaunas water power plant in 1959.

Our investigations allow us to state that the second and the third from the enumerated above changes are the most important for river scour, which goes on rather intensively up to the present time. Stabilisation of the river bed is not reached yet, therefore, river bed deformations are very actual due to the constant threat for underwater structures and communications of Kaunas town.

According to the results of our investigation sudden fluctuations of the flow rate and water level in Nemunas downsteem hydropower plant are the main reason of intensive river bed scour. Fluctuations are regular and happen every day when turbines of the plant are switched on in the morning time and switched off each evening. Investigation of filling and emptying waves (Zdankus, 1985) showed that the front of a filling wave has increased a hydraulic gradient and water velocity is enlarged here. Because of that the bed of the river for the period of 5 – 15 min receives an impact of the increased velocity impulse. At that time within 0.5 – 1.0 h the depth of the river flow increases in 0.5 – 1.5 m and downward seepage proceeds. Seepage in this direction increases soil particles stability, therefore, despite enlarged velocitie scour of the bottom is hardly possible. The opposite picture may be imagined for the period of an emptying wave after turbines are switched of. The front of an emptying wave has reduced hydraulic gradient and velocities, however upward seepage decreases stability of soil particles. Then scour of soil is possible.

Filling and emptying waves impact the bed of a river every day. The waves move up soil particles periodically and make the bed resistant to scour. The impact of the waves brakes the reinforcing layer, as it was noticed by our observations. In many places a firm and compact layer of large particles of soil disappear and there we find flexible sand bars. In spring flood time river bed receive much more impacts. Stronger filling and emptying waves are formed by the operation of spillway gates. In this period turbines work under the basic regime. Nevertheless, after each spring flood the bottom of the river changes significantly as it is seen from bottom profiles 3 and 4 (see Fig. 2).

Scouring power of the river flow depends also on the concentration of the suspended sediment. The majority of sediment load is deposited in the reservoir. Thus, river flow downsream the reservoir has increased scouring capacity and it may also cause additional scour of the river bed.

Suspended sediment concentration in Nemunas river is not large. It does not exceed 70 g/m^3 in spring and is less 50 g/m^3 in summer storm flood time. During the other period of year the concentration of suspended sediments is much smaller. Deposition of sediments in reservoir and increment of flow scouring capacity do not cause impact on the river bed as filling and emptying waves do. Therefore, it is unbelievable, that decrement of sediment concentration is the main reason causing heavy scour of Nemunas river downstream Kaunas hydropower plant.

CONCLUSIONS

Sudden fluctuation of river flow rate and water level are the main reasons of bed scour. Intensity of the scour is as great as sudden and frequent fluctuations are.

Heterogeneity of non-cohesive soils influences scouring strength of the soils. Formulas (3) and (5) are suggested for computing non-scouring velocity and scour depth.

REFERENCES

1. Mirtshullavva T. E., 1962, "Instructions for Determination of Admissable (Non-Scouring) Flow Mean Velocity of Cohesive Grounds". USSR Ministry of Agriculture. Administration of Water Economy. Moscow, USSR. – in Russian.
2. Nian-Shen Cheng and Yee-Meng Chiew, 1999, "Incipient Sediment Motion with Upward Seepage". Journal of Hydraulic Research, Vol. 37, No 5, pp 665-681, IAHR, Delft, The Netherlands.
3. Sieben J., 1999, "A theoretical Analysis on Armouring of River Beds". Journal of Hydraulic Research, Vol. 37, No 3, pp 313-326, IAHR, Delft, The Netherlands.
4. Zdankus N., 1965, "Investigation Through Momentary Bottom Velocities Scour Strength of Non-Cohesive Ground in Prismatic Channels". Doctor thesis. Kaunas Polytechnic Institute, Lithuania. – 145 p. – in Russian.
5. Zdankus N., 1968, "Device for Investigation of Cohesive Ground". Description of invention, cl. 42 o, 15, to certificate No 213433. Moscow, USSR. – in Russian.
6. Zdankus N., 1973,"Scouring Capacity of Flow in Narrow Open Channel", Proceedings of International Symposium on River Mechanics, pp. 831-839, Bangkok, Thailand.
7. Zdankus N. and other, 1985, "Field Investigations of Filling Wave". Proceedings of the 29th Scientific-Technical Conference, V.2, pp 185. Kaunas Polytechnic Institute, Lithuania. – in Russian.
8. Zdankus N., 1987, "Device for Determination of Permeability Coefficient". Description of invention, cl.G 01 N 15/08, to certificate No 1296907. Moscow, USSR. – in Russian.

BEALEY BRIDGE SCOUR FAILURE

By

Stephen E. Coleman[1], Bruce W. Melville[2], Christine S. Lauchlan[3]

ABSTRACT

At 2 am on 20 October 1998, Pier B of the Bealey Bridge over the Waimakariri River in the South Island of New Zealand (State Highway 73) was undermined, the pier settling about 1.7 m as a truck was being driven over the bridge. The failure flood event was estimated to be less than the mean annual flood at the site, with flow in the braided gravel-bed river remaining within channel braids and not extending across the width of the flood channel. The failure can be ascribed to braid migration at the bridge site resulting in a combination of a confluence of channel braids immediately upstream of the failed pier, with flows at a highly skewed angle to the slab-type pier, and a forced bend in the flow channel at the position of the failed pier. Remedial measures included underpinning of Pier B, and, recognising the ongoing movement of the channel braids, management of the braids and monitoring of the remaining piers. This case serves to highlight that where-as the potential for scour is typically assessed based upon large magnitude floods, bridges can suffer potentially significant scour damage in much smaller floods. In addition, this case highlights that combinations of the full range of possible scour components need to be considered when assessing bridge scour.

BRIDGE DETAILS

The narrow, two-way, single-lane, straight, essentially horizontal bridge consists of 20 spans (Figure 1) of a reinforced concrete T-beam (beam and slab) superstructure, the spans being simply supported. The 18 central spans are 13.4 m long, with end spans of 13.0 m and 13.2 m. Owing to space limitations for the true-right approach to the bridge, this end of the bridge deck is splayed to ease traffic entry onto the bridge. A passing bay on the upstream side of the bridge is located between Piers J and M (approximately halfway along the bridge). The bridge carries neither lighting nor utilities. The bridge is of significant commercial, tourist and general importance in forming part of State Highway 73 connecting the East and West Coasts of the South Island of New Zealand via the scenic Arthur's Pass across the Southern Alps.

The foundations consist of abutments and slab-type piers supported by piles. The centrelines of the piers are perpendicular to the bridge centreline, but are not perpendicular to the centrelines of the principal channel braids and are at an angle of about 24° to the flood channel centreline (Figure 1).

[1] Senior Lecturer, Department of Civil and Resource Engineering, The University of Auckland, Auckland, New Zealand
[2] Associate Professor, Department of Civil and Resource Engineering, The University of Auckland, Auckland, New Zealand
[3] Postdoctoral Fellow, Delft University of Technology, Faculty of Civil Engineering and Earth Sciences, Delft, the Neatherlands

The true-left abutment (Abutment V) forms the end of a rock-protected embankment that extends a shingle terrace (covered with scrub and intersected with old flood channels) at the confluence (immediately downstream of the bridge) of the Bealey and Waimakariri Rivers. This terrace forms a constriction of the flood channel (Figures 1 and 2). A significant amount of training works is in place to protect the true-left approach to the bridge and the associated abutment. The true-left embankment further focuses flood channel flows at a general angle of about 40° to the pier centrelines.

The slab-type piers (Figure 3) and abutments are founded on 0.36 m octagonal reinforced-concrete driven displacement piles acting in a combination of bearing and friction. No as-built records exist for the pile depths. Design pile lengths for the piers and abutments were 7.9 m and 10.4 m respectively. Pile heads were to be stripped for a distance of 0.8 m, indicating a design pile depth for the piers of 7.1 m below the base of the pile cap. The piles of Pier B were noted to have experienced problems during driving. Test pile records indicate that two test piles at Pier B, located on the bridge centreline and 1.2 m upstream of this position, were driven to 6.6 m and 5.2 m respectively below the base of the pile cap. An additional octagonal test pile is located 4.9 m downstream of the bridge centreline at Pier B (Figure 3). Pier D has an additional pile tied into the upstream end of the pile cap (Figure 3). No records exist to indicate that this pile forms part of any underpinning remedial measures for the pier. It is conjectured that the extra pile at Pier D may have been a test pile that was subsequently tied into the bridge pier. Piers K and L (supporting the passing bay) are founded on 5 piles at 1.26 m centres. Piers H and O (located at the positions of expansions joints for the bridge) are founded on 4 staggered piles at centres of 0.86 m to 0.89 m. The remaining piers are founded on 3 piles at 1.3 m centres, the pile caps and pier stems for these piers measuring 3.2 m (long) x 0.6 m (wide) x 0.9 m (deep) and 3.0 m (long) x 0.5 m (wide). Abutment V (Figure 1) is supported by 3 piles at 1.3 m centres. The true-right abutment (Abutment A, Figure 1) is founded on rock, with the true-right limit of the flood channel comprising a rock cliff.

RIVER MORPHOLOGY, FLOWS AND SEDIMENTS

Braid movement dominates flood-channel development. At the time of bridge design, braid channels beneath the proposed bridge passed adjacent to the true-right cliff and at about 75% along the proposed bridge length from Abutment A (about Pier Q to Pier R). Two channels also passed true-left of Abutment V. The flow channel adjacent to the cliff and Abutment A (Figures 1 and 2) appears to have been reasonably stable over the history of the bridge. There is no progressive degradation of the riverbed through the bridge site.

Design drawings in the 1930s indicate a flood level across the entire width of the bridge channel section of 1.55 m above the level of the bases of the pile caps. For the 1998 failure event however, flows remained within the channel braids and did not extend across the flood channel.

Over the 1990s, a braid adjacent to the true-left embankment appears to have migrated downstream as a meandering channel (Figure 2). In line with this development, a section of this channel flowing at an angle of about 6° to the bridge centreline (84° to pier centrelines) propagated downstream and approached the bridge (Figure 2). This resulted in flows occurring at a highly-skewed angle to the bridge piers, these flows then negotiating a left-hand channel bend before passing beneath the central region of the bridge (Figure 2). For the 1998 failure flood, it appears that such flows did not pass beneath the central region of the bridge but continued along the upstream side of the bridge (Figure 2). These flows then merged with flows at the true-right side of the flood channel before impacting on the piers at the true-right end of the bridge (Figure 3).

The 1998-failure-event flow beneath the bridge was concentrated within the one braid channel. The velocities for the concentrated flows were noted to be high and in excess of the 2 m/s velocity estimated for flows passing the failed pier four days after the failure event. The surface width of the channel has been estimated at about 12 m to 20 m. At the peak of the failure flood, flow is estimated to have extended approximately from Abutment A to Pier H (94 m), with flow and erosion concentrated at Piers C and (in particular) B on the outside of the left-hand bend in the channel (Figure 3). The fixed nature of the cliff forming the true-right limit of the flood channel may have aided in forcing the flow passing across the upstream face of the bridge to pass beneath the bridge at the position of Pier B.

The flood flow was estimated to be less than the mean annual flood at the site. The writers have not obtained quantitative estimates of flow magnitudes at the bridge site. Within about 15 km downstream of the Bealey Bridge, the mean annual flood at the Mt White Road Bridge across the Waimakariri River has been estimated at 1200 m^3/s (Melville and Coleman, 2000). Recognising the relative magnitudes of flows into the Waimakariri River between the Bealey Bridge and the Mt White Bridge, and that the failure event was less than the mean annual flood, a failure flow of 200 m^3/s is adopted for the risk-assessment scour analyses presented below. The bridge failure is estimated to have occurred at about the time of the flood peak at the site. From photographs taken within hours after the failure event (Figure 3), flood levels at the bridge appear to have peaked at about the level of the top of the 0.9-m-deep pile caps.

The bed material was noted to be of a wide grading with particles ranging from sands to 200-300 mm cobbles. A median bed sediment size of d_{50} = 50-70 mm was estimated. Design drawings indicate a bed material of shingle.

HISTORICAL SCOUR

In 1948, the upstream edge of Pier Q dropped by about 60 mm, with Pier Q rotating in the plane of the pier. For Pier Q, the points of Piles 1, 2 and 3 were found to be driven to 7.6 m, 6.1 m, and 7.6 m respectively below ground level. The pier was underpinned by three piles at each end of an extended pile cap (located beneath the existing one). Each new pile consisted of three rails welded together and was of a design length of 7.0 m. From 1949 to 1958, the bridge was monitored in terms of the levels of the upstream and downstream wheelguards on the superstructure, perhaps in recognition of ongoing bed erosion problems.

OCTOBER 1998 SCOUR EVENT

The failure flows of 19-20 October 1998 eroded the bed around the piles of Pier B leaving the pier basically hanging, supported by the superstructure. At 2 am on 20 October 1998, Pier B settled about 1.7 m as a truck passed over the bridge towards Abutment V. The driver carried on over the remainder of the bridge to complete his journey westward. In failing, Pier B rotated about the junction of the deck with Pier C. Cracking was evident at the tops of Pier C and Abutment A owing to rotation of the adjoining deck sections as Pier B settled.

The cause of failure was ascribed to local scour exacerbated by a combination of flow concentration at a skewed angle to the pier, bend scour and also confluence scour (Figure 3). Consistent with the effects of bend scour on the failure, increasing scour depths were noted (after the failure event) for Piers D, C and B respectively. For braided rivers then, it may be that the maximum flow within a channel braid may constitute a worse scour scenario than a larger flood spread across the width of the flood channel. Confluence scour may have contributed to the failure with two channel braids intersecting immediately upstream of the failed pier for the failure event. The true-left embankment extending into the channel did not appear to have influenced the failure by causing any constriction of the failure flows (of minor magnitude), but it did contribute to concentration of the flows at a skewed angle to the failed pier.

ASSESSMENTS OF SCOUR DEPTHS

Attempts to measure scour depths subsequent to failure were frustrated by high flow velocities. Measurements within four days of failure indicate a peak scour depth of about 2.7 m below the level of the bases of the pile caps. It is recognised however, that scour holes tend to fill in as a flood recedes.

The failure flow can be approximated as a single channel flow approximately parallel to the upstream face of the bridge, with the flow passing around a bend beneath the bridge (at Pier B) and subsequently proceeding in a downstream direction (Figure 3). For a failure flood of about 200 m^3/s at the bridge site, the method of Blench (1969) predicts a flow depth for a single channel of 20 m width approaching the bridge of $y_{ms} = 4.1$ m. The method of Maza Alvarez and Echavarria Alfaro (1973) predicts an equivalent flow depth of $y_{ms} = 3.5$ m. For $y_{ms} = 4.0$ m and an estimated bend radius of curvature of the order of 60 m, a maximum scoured flow depth in the bend of $y_{bs} = 6.8$-8.3 m is predicted by methods detailed in Melville and Coleman (2000) and Coleman et al. (2000).

Alternatively, if the failure flow is considered to constitute two channel braids (of equal flows and each of 20 m width) meeting at the failed pier, the methods of Blench (1969) and Maza Alvarez and Echavarria Alfaro (1973) predict a braid flow depth of $y_{ms} = 2.6$ m and $y_{ms} = 2.0$ m respectively. For $y_{ms} = 2.5$ m and a confluence angle of about 50°, a maximum scoured flow depth in the confluence of $y_{cs} = 9.5$ m is predicted by methods detailed in Melville and Coleman (2000) and Coleman et al. (2000).

With no degradation or contraction scour evident for the bridge site, the total scour at Pier B is given by the combination of local scour with the general (bend or confluence) scour occurring at the pier.

The local scour depth has an upper limit of $d_s = 4.4$ m for the pier with a projected width of 3.25 m (for the flow at an angle of 84° to the slab-type pier). The total scoured flow depth y_t calculated in this manner ($y_t = y_{bs} + d_s$ or $y_t = y_{cs} + d_s$) is the depth below the water surface for the flood flow, the water surface for the 1998 failure event being estimated at about 0.9 m above the level of the bases of the pile caps.

The present scour analyses are for the purpose of assessment of relative risk of scour at the bridge piers, and not for the design of pile embedment depths, which would require more rigorous analyses. The above analyses are limited by the adoption of an approximate failure flood and approximate river geometries, and the extrapolation of the analyses to the large sediment sizes occurring at the bridge site. Nevertheless, the analyses highlight the large scour depths that can occur at individual piers of the bridge. Such scour may be more critical to bridge stability than scour for larger floods for which the flood flow extends across the entire bridge channel section. Assessment of historical aerial photograph records would reveal whether the 1948 failure of Pier Q was of the same origin as the 1998 failure of Pier B with braid flow focussing at a pier causing undermining of the pier.

It is commonly realised that dramatic channel shift can occur in the course of a single flood for braided rivers. The historical variability of the channel braids at the present bridge site is evidenced in Figures 1 and 2. Based on this variability, it must be recognised that each pier of the Bealey Bridge is subject to the same risk of pier scouring that occurred at Pier B in 1998.

REMEDIAL ACTIONS

After the failure of the bridge, a channel was cut beneath the bridge a few piers away from the failed pier in order to divert some flow away from the failed pier. Within two days of the failure, a single-lane Bailey bridge was installed over the dropped pier and the adjoining spans to facilitate traffic flows across the bridge.

The planned remedial action consisted of jacking Pier B back into position, underpinning the pier, and repairing the damaged spans. Additional piers may also be underpinned depending on assessments of both scour vulnerability for the respective piers and also the overall value of the transit link provided by the bridge. A consideration against significant repairs being carried out at the site is that in 62 years the bridge has only had two problems with respect to scour. In each case, the bridge was readily repairable, especially in terms of quickly restoring traffic flows through the use of a Bailey Bridge.

REFERENCES

1. Blench, T. (1969). "Mobile-bed fluviology." University of Alberta Press, Edmonton, Canada.
2. Coleman, S. E., Melville, B. W., and Lauchlan, C. S. (2000). "Total scour depth at bridge abutments." Proc., International Symposium on Scour of Foundations, Melbourne, Australia, November, 2000.

3. Maza Alvarez, J. A., and Echavarria Alfaro, F. J. (1973). "Contribution to the study of general scour." Proc., Int. Symp. on River Mechanics, IAHR, Bangkok, Thailand, pp. 795-803.
4. Melville, B. W., and Coleman, S. E. (2000). "Bridge scour." Water Resources Publications, Colorado, USA, 550 pp.

ACKNOWLEDGMENTS

The writers wish to thank John Reynolds of Opus International Consultants Ltd., Christchurch, New Zealand, for his discussions and the provision of background information in regard to the present study.

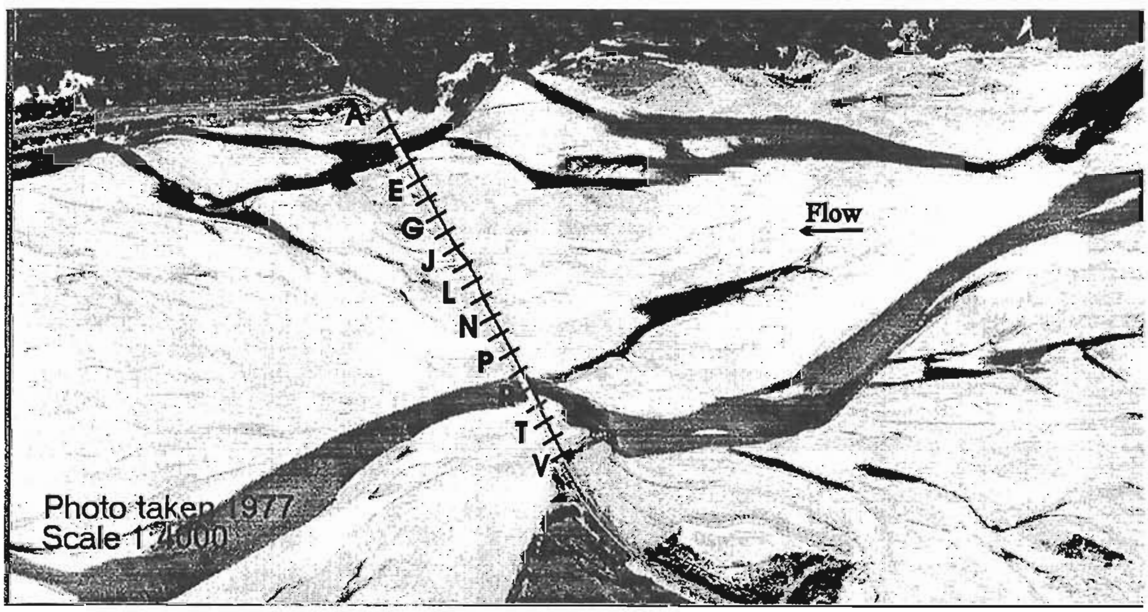

Figure 1. Waimakariri River Planform at Bealey Bridge: 1977.

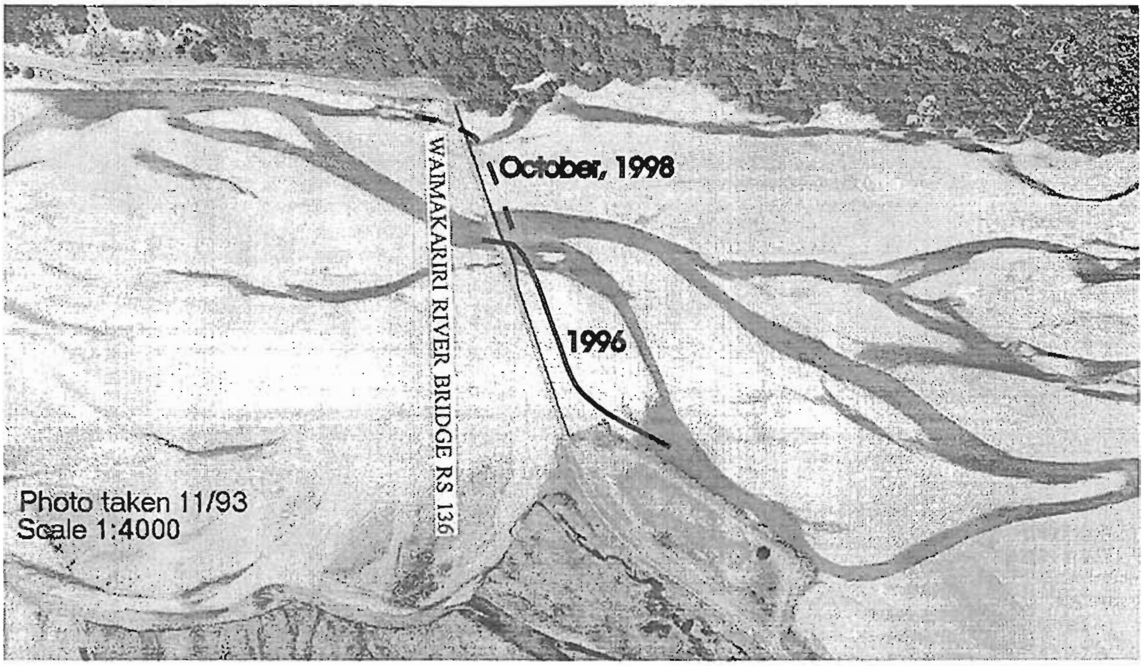

Figure 2. Waimakariri River Planform at Bealey Bridge: 1993-1998.

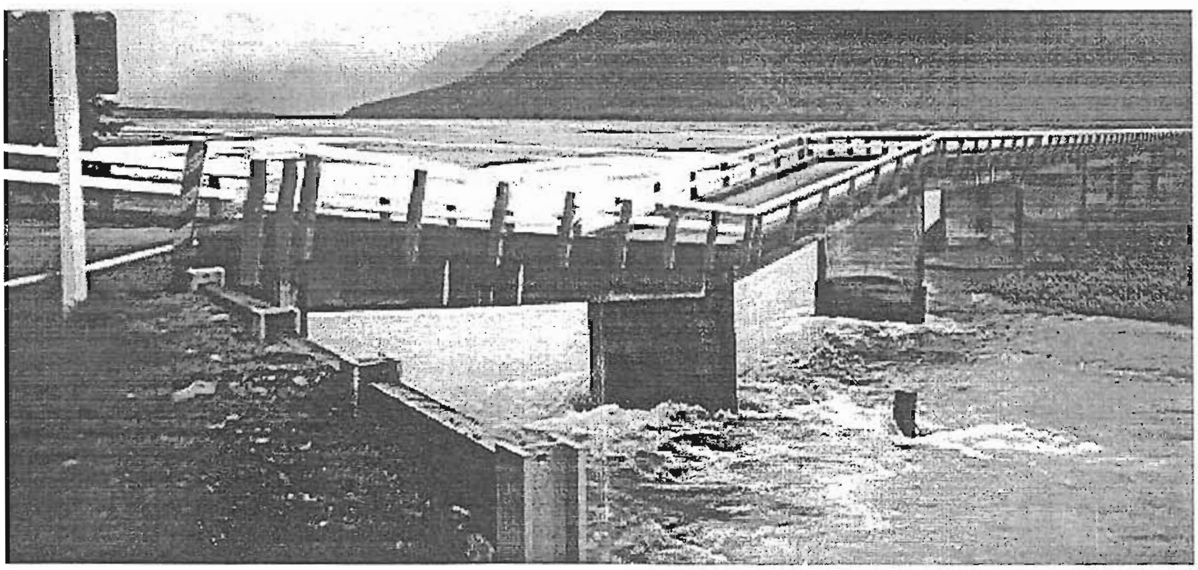

Figure 3. The Bealey Bridge Failure, 20 October, 1998.